Consolidation and other geotechnical properties of shales with respect to age and composition

Smith, Trevor, J.

CONSOLIDATION AND OTHER GEOTECHNICAL PROPERTIES OF SHALES WITH RESPECT TO AGE AND COMPOSITION

by

Trevor J. Smith, B.Sc.

being a thesis presented in fulfilment of requirements for the degree of Doctor of Philosophy at the Department of Geological Sciences in Faculty of Science of the University of Durham.

ABSTRACT

Studies of a wide selection of overconsolidated, weak argillaceous rocks from major formations in the United Kingdom and North America have shown that the compaction history, coupled with the mineralogical composition have a decisive bearing on the nature of the material, both at depth and in the near surface zone.

Current evidence indicates that maximum depths of burial of North American sediments are generally much greater than their British counterparts, infering that overburden does not increase systematically with age. Furthermore major differences have also been observed in the mineralogy and geochemistry of these two groups. In particular, recalculated smectite formulae indicate the onset of the montmorillonite to illite transformation in the former sediments. Preferred orientation studies and electron microscopy have been used to elucidate the clay microstructure, whereas exchangeable cations and pore water chemistry indicate possible interactions between clay minerals.

Consolidation studies to a pressure of 35000kN/m^2 on both undisturbed and remoulded materials have led to a new interpretation of the stress-strain response, and in addition these tests have indicated the presence of diagenetic bonding in unweathered materials the strength of which is dependent upon the maximum depth of burial and mineral species present. Furthermore, since slaking and suction experiments frequently only detect this bonding in the Carboniferous materials, it has been inferred that mineral-mineral welding is present in these and that cationic bonding predominates in younger sediments. Consequently to avoid unforseen engineering complications in the field caused by the subsequent destruction of the latter bond type by weathering agents it has been suggested that a combination of suction and consolidation tests should be performed on the shales in question.

LIST OF CONTENTS

Chapter 3 - Mineralogy and Geochemistry

Chapter 4 - Clay Microstructure and Preferred Orientation

Chapter 5 - Consolidation

LIST OF FIGURES

Chapter 3 - Mineralogy and Geochemistry

Chapter 4 - Clay Microstructure and Preferred Orientation

Chapter 5 - Consolidation

LIST OF TABLES

Chapter 4 - Clay Microstructure and Preferred Orientation

Chapter 5 - Consolidation

Chapter 6 - Soil Suction Characteristics

Chapter 7 - Slaking Behaviour of Overconsolidated Shales

Chapter 8 - Summary and General Conclusions

Chapter One
Introduction

1.1 General Aims of the Investigation

This project involves the study of a selection of 26 overconsolidated, weak, argillaceous rocks from major formations in the United Kingdom and North America. The specimens investigated were largely dictated by the availability of fresh, unweathered borehole material. Although the selection is consequently random, the materials span the stratigraphical sequence Eocene to Westphalian A, i.e. approximately 40 M years B.P. to 310 M years B.P. The materials exhibit various states of induration ranging from clays, quartz-rich clays to shales/mudstones and quartz-rich claystones (siltstones). Many of the North American types contain a high proportion of expandable clay minerals (particularly montmorillonite), whilst these clays minerals in the British materials are very much more restricted stratigraphically.

The investigation is aimed at establishing relationships between depth of burial, geological age, mineralogy, interparticulate bonding, together with the subsequent response of the materials as a consequence of uplift and erosion. Comparisons are made between the rock and clay types from the two areas and inferences are drawn with respect to further material breakdown in the near-surface zone. The overall engineering behaviour of these overconsolidated argillaceous materials can consequently be assessed.

Petrographical studies commonly fail to distinguish between geological age and depth of burial, whereas geotechnical investigations of these argillaceous rock types in the past have tended to ignore mineralogical influences.

Mineralogy, major element geochemistry and cation exchange capacity are used in the present study as controls on composition. Microstructure

and preferred orientation studies have given an indication of the mineral fabrics involved. Fundamental properties are used as a link between mineral composition and compaction studies.

Consolidation tests carried out under high pressures on undisturbed and remoulded materials provide an indirect measure of the depth of burial with respect to geological age. Also, the rebound response and strain energy concepts reflect the likely behaviour of the materials during uplift to the near surface outcrop zone. Investigations of suction and slaking characteristics are a useful indication of the likely problems to be encountered in terms of 'engineering materials', since these effects will be conditioned in the near-surface zones.

1.2 Types of Consolidated Clays and Shales

Terzaghi (1941) suggests that clays can be classified into two groups by reference to their present overburden pressure, i.e.

(a) Normally-consolidated clays*; These are clays which have never been subjected to a pressure greater than their existing overburden load.

(b) Overconsolidated Clays; These are clays where the existing overburden pressure is less than the maximum effective pressure that the clay has ever been subjected to in the past.

The process by which these types of clay are produced is summarised in Figure 1.1, whereby it can be seen that a clay existing at any effective overburden pressure less than the maximum at point (c) will have a different voids ratio depending on whether it is normally - or overconsolidated represented by points (b) and (d) respectively.

1.3 Definition and Nomenclature of Shales

As succintly stated by Underwood (1967) "the geologic literature shows that the terminology used to describe the entire group of

* Underconsolidated clays are not considered because they are mainly found in man-made tailings lagoons & river estuaries.

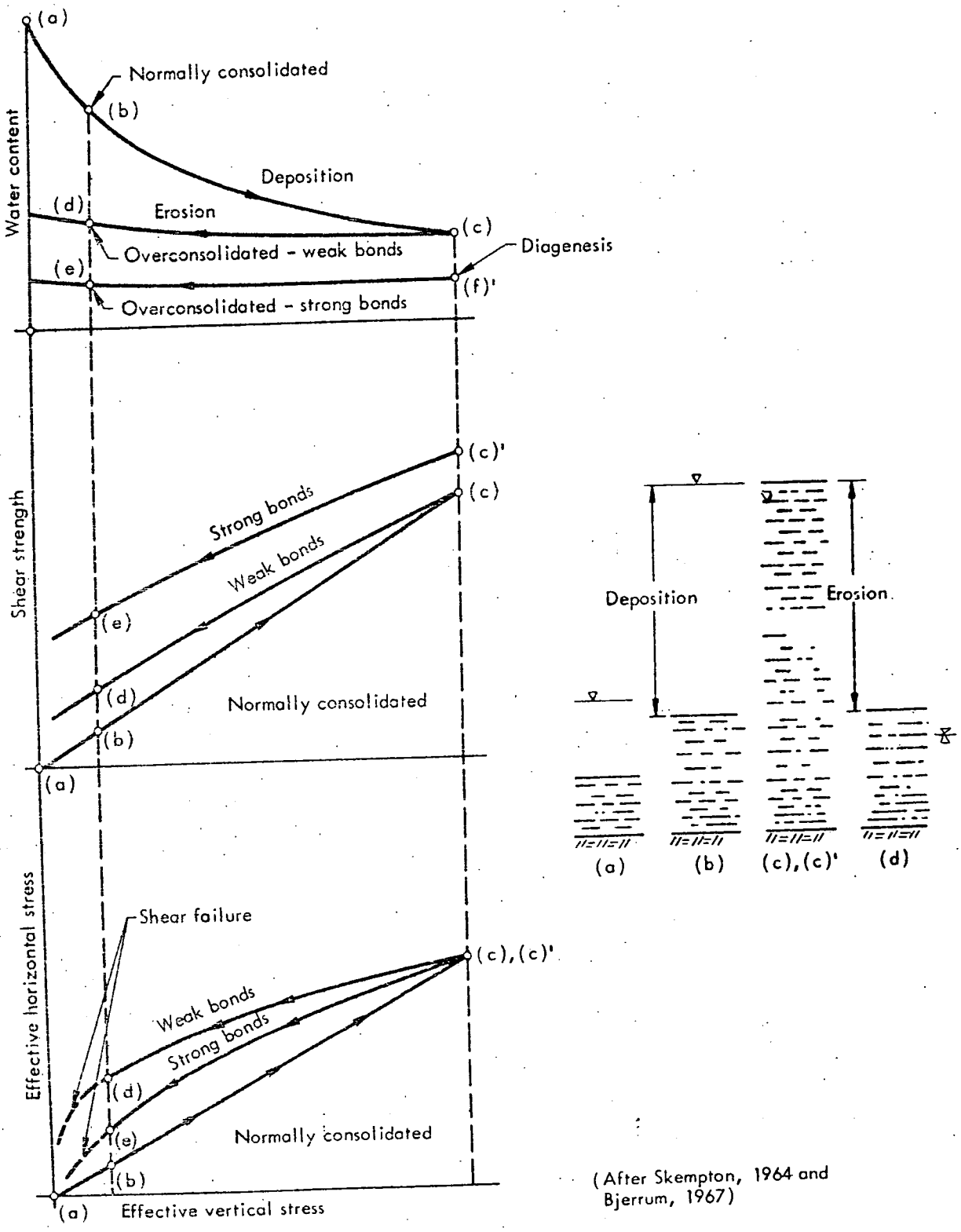

Figure 1.1. Schematic of Geologic History of Overconsolidated Clays (From Fleming et al; 1970).

argillaceous sediments is not standardised and consequently numerous inconsistencies have developed in the classification and nomenclature of shales".

Deo (1972) cites the following definitions given to shales by various authors:-

'A laminated sediment in which constituent particles are prominently of clay grade' (Glossary of Geology, 1957).

'Shales are consolidated fine sediments, usually hardened clay or mud and have a characteristic fracture. Generally dull in appearance shale can be scratched with a fingernail' (Leggett, 1962).

'A product could not be called a shale unless it possesses two properties: when struck with a hammer it should give a clear ring and when immersed in water its volume should remain unchanged' (Terzaghi, 1946).

'Shale includes the indurated, laminated or fissile claystones and siltstones. The cleavage is that of bedding and such other secondary cleavage or fissility that is approximately parallel to the bedding. The secondary cleavage has been produced by the pressure of overlying sediments' (Twenhofel, 1936).

'The term shale is applied to a wide variety of rocks ranging from consolidated clays and silts to rocks which display thin bedding without regard primarily to texture or composition. Shales include siltstones and claystones' (Krumbien, 1947).

'The term shale is used in a general sense to refer to the whole group of silty and clayey rocks. Shale is used in a specific sense for rocks composed primarily of silt and clay with fissility or a tendency to split along fairly close bedding planes' (Deere and Gamble, 1971).

'A fissile rock formed by consolidation of clay, mud or silt, having a finely stratified or laminated structure and unaltered minerals' (Webster Dictionary, 1966).

In the present study, the term shale refers to 'all argillaceous rocks composed largely of silt and clay-sized particles, and which range in composition from clays, quartz-rich clays, to shales/mudstones and quartz-rich mudstones (siltstones). The materials may or may not be slightly cemented by primary and secondary minerals such as iron oxides, silica or calcite, and may be normally- or overconsolidated'. However, only overconsolidated rocks are considered herein and the compositional extremes of materials currently examined range from those containing 100 per cent clay mineral species to those where quartz and other equant habit minerals comprise 60per cent of the total species present.

1.4 Classification of Shales

The classification of shales cited in the literature can be apportioned into two classes depending on whether the materials are considered from a geological or engineering aspect.

1.4.1 Geological Classification

This is based upon the more classical approach of observing the material in its natural state, or by examining its composition.

A fundamental classification is that based on the grain-sized distribution, and accordingly a scale of size which includes gravel, sand, silt and clay has been developed.

Mead (1936) proposes a classification of shales based upon the degree of cementation (Fig.1.2). He suggests two basic categories, i.e. soil-like shales which lack a significant amount of cement, and rock-like shales where cementation or bonding by recrystallisation are evident.

Ingram (1953) proposes a classification based upon the degree of fissility and recognises three categories, i.e.:-

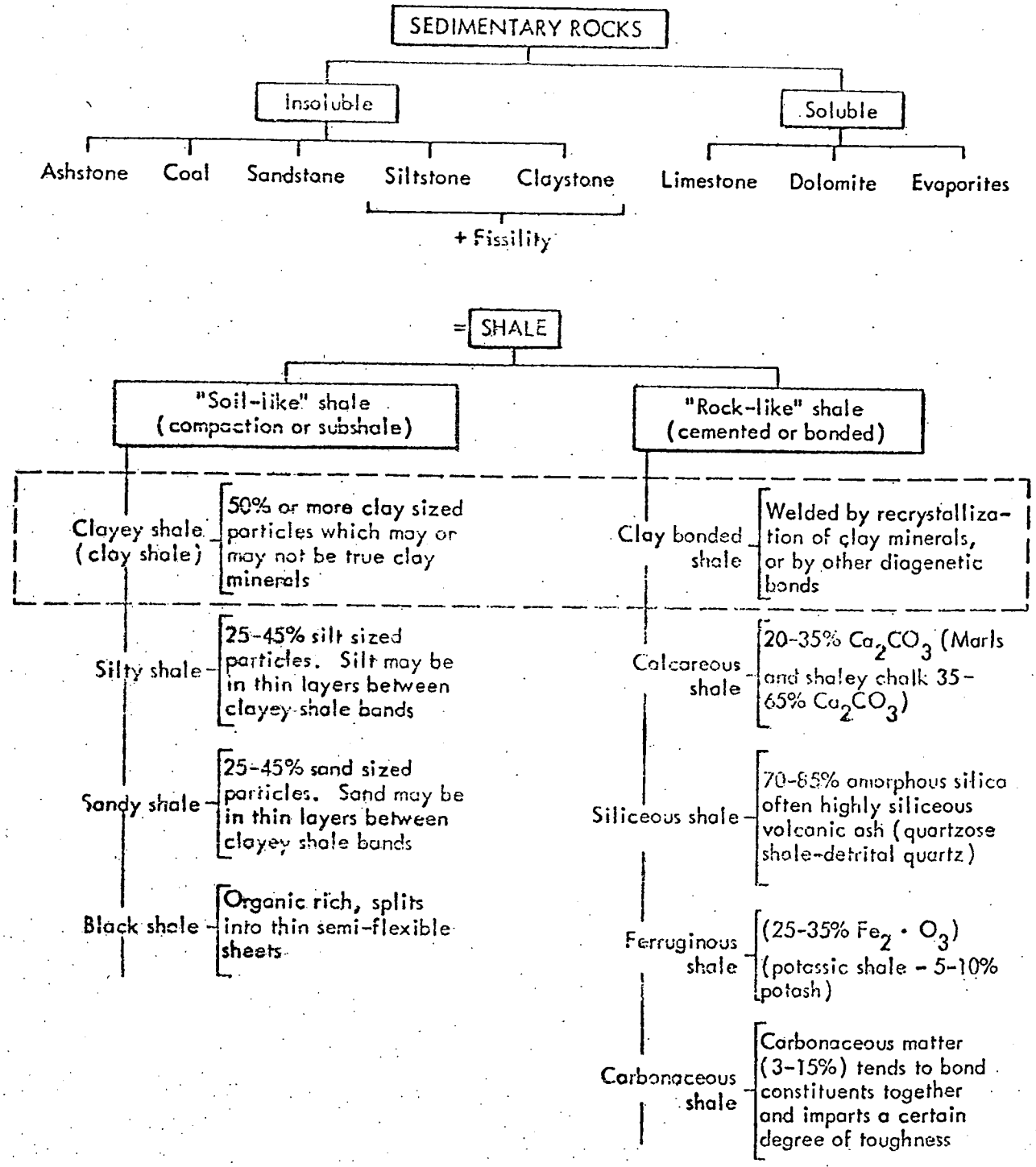

Figure 1.2. A Geological Classification of Shales (After Mead, 1936).

Massive shales which have a random orientation of platy minerals, hence have no preferred direction of cleavage, and which fragment into blocks, few of which are platy in character.

Flaggy shales which split into fragments of varying thickness, but with the width and length many times greater than the thickness and with two flat sides being approximately parallel.

Flaky shales which split along irregular surfaces parallel to the bedding into uneven flakes, thin chips and wedge-like fragments whose length rarely exceeds three inches.

Shales which are not fissile may contain laminations, i.e. bands of colouration or material ranging in thickness from 0.05-1.0m.m. Pettijohn (1957) recognises three types of lamination, i.e. changes of texture, changes of colour and changes of composition.

Twenhofel (1936) proposes a classification which includes indurated clays and silts and their metamorphic equivalents (Fig.1.3).

A classification based upon the chemical composition is discounted by Underwood (1967) because, with the exception of siliceous and calcareous shales, he suggests that the variation is not great enough. However, a classification of shales based upon their mineralogy would be very useful. To this end, significant steps have been taken to identify and quantify the minerals present (e.g. Gibbs 1967; Schultz 1964; Griffin 1954). Other techniques for this purpose such as differential thermal analysis have also been explored (Reeves, 1971).

1.4.2 Engineering Classification

An early attempt at an engineering classification was made by Terzaghi (1936) who proposes three categories of shale, i.e. soft, intact clays free from jointing and fissures; stiff, intact clays free from jointing and fissures, and lastly, stiff fissured clays.

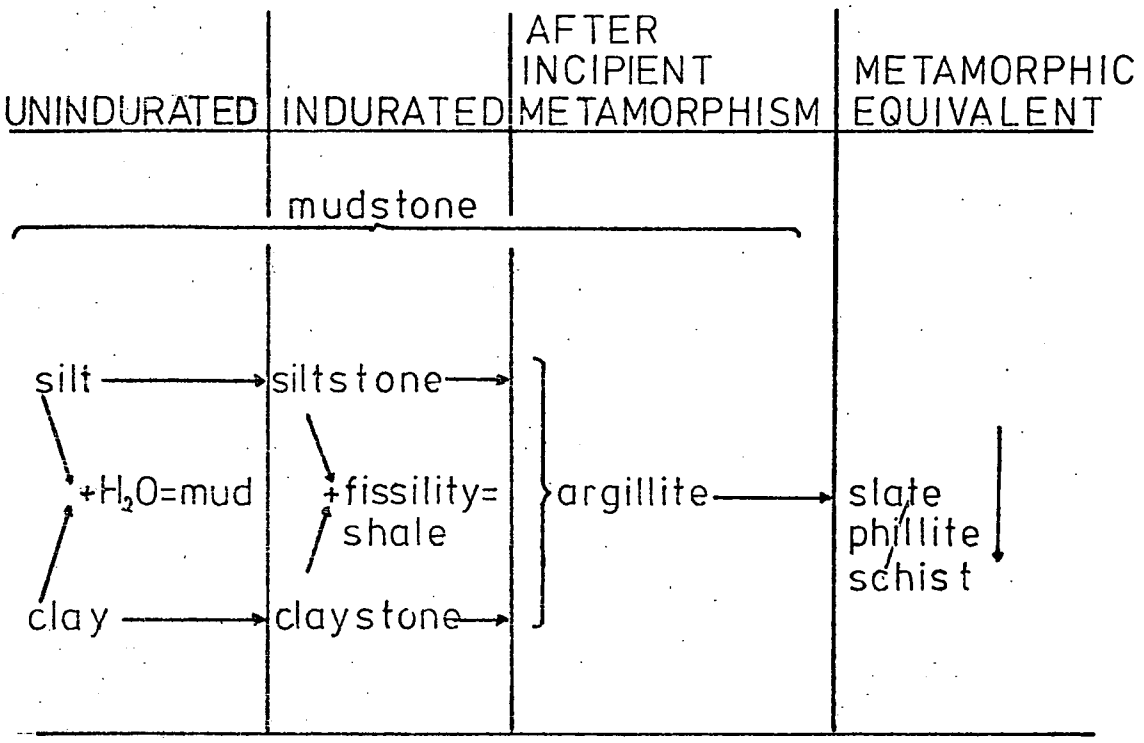

Figure 1.3. A Classification of Shales and Related Rocks (After Twenhofel, 1936).

However, a more exact knowledge of the behaviour of shales is now required by the engineering geologist, especially when dealing with properties such as strength or stability, hence several workers have attempted to classify shales by reference to certain engineering properties.

The Atterberg limits (Atterberg, 1911) are frequently used to classify shales by reference to moisture contents which define transitions between certain consistencies, i.e.:-

Liquid Limit (W_L) which is the moisture content at which the material just begins to flow (i.e. form a slurry) by passing from the plastic to the liquid state. Casagrande (1932b) has designed a mechanical device to standardise this value.

Plastic Limit (W_P) which is the moisture content at which the material passes from the plastic to the solid state. It is obtained in the laboratory by rolling the clay on ground glass until it just begins to crumble.

Shrinkage Limit (W_S) which is the moisture content when all the grains are just in contact, hence further loss of water will not result in a decrease in volume.

Casagrande (1948) combines the liquid and plastic limits on a 'plasticity diagram' whereby he relates the liquid limit to the plasticity index (liquid limit minus plastic limit). The chart is divided into six regions i.e. three above the 'A' line (representing inorganic clays of low, medium and high plasticity) and three below, (representing inorganic silts of low, medium and high compressibility).

Bjerrum (1967a) uses a less formal basis and classifies shales according to whether they possess weak, strong or permanent bonding within the material.

By studying artificial soils, Seed et al (1964) conclude that the 'activity', which Skempton (1953) defines as the ratio of the plasticity

index to the clay-sized fraction, would accurately classify soils.

Underwood (1967) has suggested a classification based on various engineering properties (Table 1.1) for differentiating between 'problem' and 'non-problem' shales with respect to their in-situ behaviour for civil engineering purposes.

Deere and Gamble (1971) and Franklin (1970) have suggested a durability-plasticity classification for shales based upon their relative durability to slaking. Morgenstern and Eigenbrod (1974) have also proposed a classification based on the slaking ability of clays and shales by measuring the rate of increase in the liquidity index during the first drying-wetting cycle to supplement the work of Hamrol (1961). In addition, they also proposed a classification based on the reduction of shear strength after clays have been softened by water (from their natural moisture content) for specified lengths of time.

1.5 Compaction Studies

As a starting point in the formation of the weak rocks under consideration it is important to consider the compaction processes insofar as they affect the sediment after deposition.

As will be seen from Chapter 2 the maximum depths of burial for the most deeply buried shales studied in the project are about 3000 to 3600m, whilst the majority have values which range from 600 to 1800m. In addition, the high pressure consolidation tests performed, simulate depths equivalent to 2100 to 2500m of sedimentation. Therefore it is pertinent to review the various compaction models, applicable to deep burial, which have been advanced by other workers.

1.5.1 Models for Natural Compaction

Skempton (1970) describes compaction as "the result of all processes

Table 1.1. An engineering evaluation of shales[a]

Physical properties			Probable in-situ behavior						
Laboratory tests and in-situ observations	Average range of values		High pore pressure	Low bearing capacity	Tendency to rebound	Slope stability problems	Rapid slaking	Rapid erosion	Tunnel support problems
	Unfavorable	Favorable							
Compressive strength, psi	50 to 300		✓	✓					
		300-5000							
Modulus of elasticity, psi	20,000 to 200,000			✓					✓
		200,000 to 2×10^6							
Cohesive strength, psi	5 to 100				✓	✓			✓
		100 to >1500							
Angle of internal friction, deg	10 to 20				✓	✓			✓
		20 to 65							
Dry density, lb/ft^3	70 to 110		✓					✓(?)	
		110 to 160							
Potential swell, %	3 to 15				✓	✓		✓	✓
		1 to 3							
Natural moisture content, %	20 to 35		✓			✓			
		5-15							
Coefficient of permeability, cm/sec	10^{-5} to 10^{-10}		✓			✓	✓		
		$>10^{-5}$							
Predominant clay minerals	Montmorillonite or illite		✓			✓			
		Kaolinite & chlorite							
Activity ratio = plasticity index / clay content	0.75 to >2.0					✓			
		0.35 to 0.75							
Wetting and drying cycles	Reduces to grain sizes						✓	✓	
		Reduces to flakes							
Spacing of rock defects	Closely spaced			✓		✓		✓(?)	✓
		Widely spaced							
Orientation of rock defects	Adversely oriented			✓		✓			✓
		Favorably oriented							
State of stress	>Existing overburden load				✓	✓			✓
		= Overburden load							

[a] (Underwood, 1967)

causing the progressive transformation of an argillaceous sediment from a soft mud (as originally deposited) to a clay, and finally to a mudstone or shale. These include interparticulate bonding, desiccation, cementation and above all, the squeezing out of pore water under increasing weight of overburden".

Sorby (1908) first presented quantitative data regarding compaction in terms of porosity changes with depth. Later Terzaghi (1923) published the now widely accepted one-dimensional history of consolidation (Chapter 5.2). Rieke and Chilingarian (1974) discuss the other main hypotheses for pressure-depth models, the main points of which are noted herein.

Athy (1930) states that compaction is a simple process of squeezing out of interstial fluids and reducing the porosity, but after sedimentation the pore volume can be modified by deformation and granulation of minerals, cementation, solution, recrystallisation and squeezing grains together.

Hedberg (1936) suggests that compaction occurs in three stages (Fig.1.4):- (a) From 0 - 5500kN/m^2 there is a mechanical rearrangement and dewatering of the clayey mass. Between 90 - 75 per cent porosity, mainly free water is expelled, but from 75 - 35 per cent porosity absorbed water is expelled. Below 35 per cent porosity the particles are pushed closer together. (b) From 5500 - 41200 kN/m^2 (below 35 per cent porosity) the volume is reduced by mechanical deformation of the clay particles, and there is also more expulsion of absorbed water. (c) Recrystallisation occurs at porosities of below 10 per cent.

Weller (1959) proposes a model similar to that of Hedberg. This consists of a compaction process starting at the surface with a porosity of 85 - 45 per cent. As the pressure is increased the interstial fluids are expelled and the porosity decreases to about 10 per cent. The result is that minerals rearrange themselves into a more closely packed structure

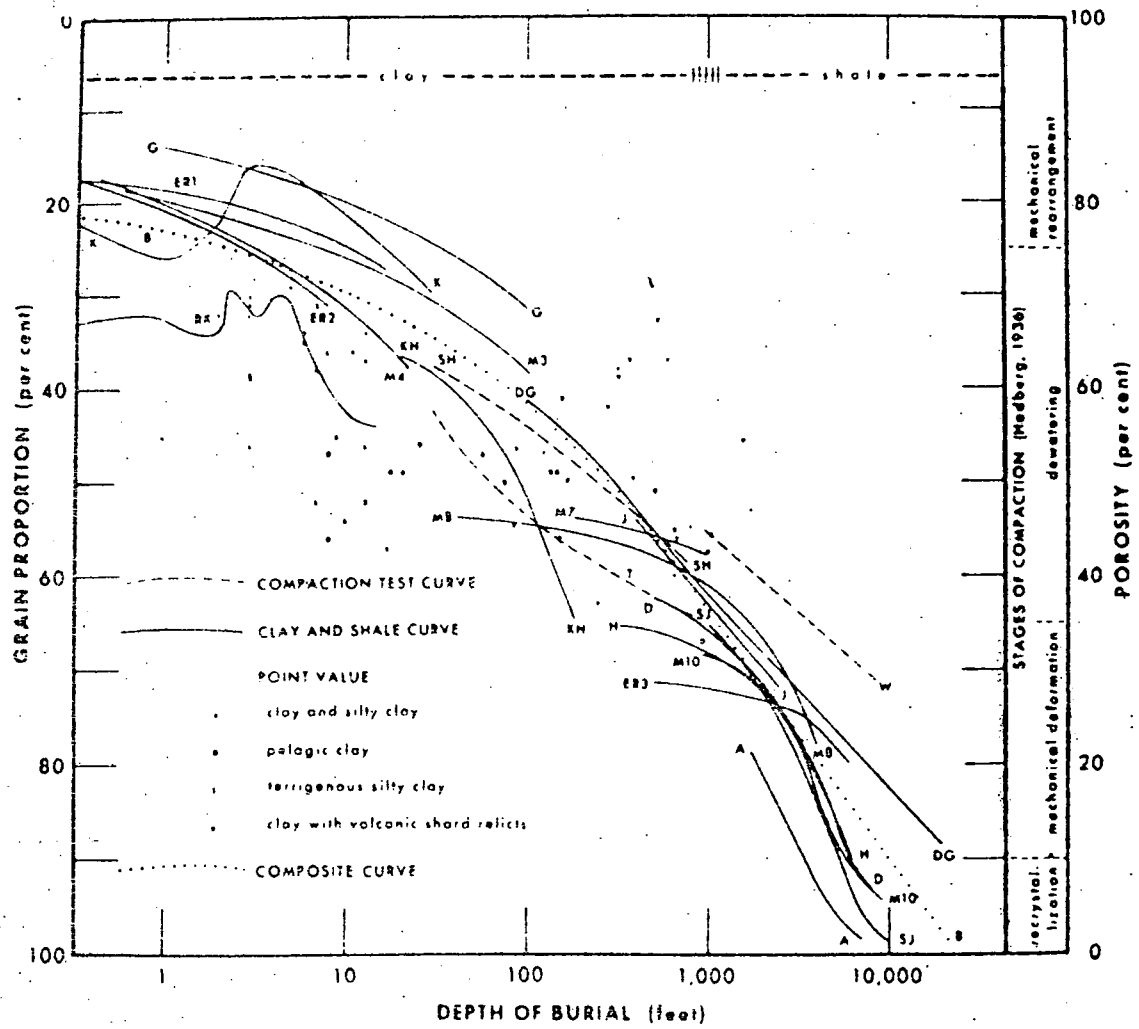

Figure 1.4.

Relationship between depth of burial and grain proportion, showing Hedberg's compaction stages. Composite curve *B* is after Baldwin (1971) – see Fig.42. *A* = composite curve for Oklahoma wells (Athy, 1930, fig.2); *D* = six Venezuelan wells (Dallmus, 1958, figs.17, 18, 22); *DG* = composite curve for Gulf Coast wells (Dickinson, 1953, fig.14); *ER1* = Santa Barbara basin deep-sea core (Emery and Rittenberg, 1952, fig.21C); *ER2* = 13 deep-sea cores off California coast (Emery and Rittenberg, 1952, figs.5–17); *ER3* = five Los Angeles basin wells (Emery and Rittenberg, 1952, fig.30); *G* = seven Lake Mead cores (Gould, 1960, fig.49); *H* = three Venezuelan wells (Hedberg, 1936, fig.2); *J* = generalized curve for JOIDES hole 1 (Beall and Fisher, 1969, fig.3); *K* = fifteen abyssal plain cores (Kermabon et al., 1969, figs.3–8, 17); *KH* = Venezuelan wells (Kidwell and Hunt, 1958, fig.10); *M* = curves *3, 4, 7, 8,* and *10* (Meade, 1966, fig.1A); *RK* = deep-sea core off Nova Scotia (Richards and Keller, 1962, fig.1); *SH* = based on Skempton's compaction test data (Hamilton, 1959, table 1); *SJ* = Skeels' composite for wells (Johnson, 1950, fig.145); *T* = compaction test curve for blue marine clay (Terzaghi, 1925, fig.3, p.743); *W* = curve representing Warner's unpublished compaction test data (Beall and Fisher, 1969, fig.3). (After Baldwin, 1971, fig.2. Courtesy of Society of Economic Paleontologists and Mineralogists).

and compaction at this stage is related to the yielding of clay minerals between the more resistant grains. He postulates that at 10 per cent porosity the non-clay minerals are in contact and the clays are squeezed into the voids space. Further compaction requires deformation and crushing of grains.

By reference to the compaction of the Apsheron horizons in Azerbayjan, Teodorovich and Chernov (1968) propose a three stage compaction model:-

(a) From 0 - 8 to 10m there is a rapid compaction with the porosity decreasing from 66 to 40 per cent (for clays) and 56 to 40 per cent (for silts).

(b) From 10 - 1200 to 1400m there is a rapid decrease in compaction and the porosity decreases to about 20 per cent.

(c) From 1400 - 6000m there is a slow compaction and at 6000m the porosity of silts is 15 - 16 per cent, whilst for shales it is 7 - 8 per cent.

Beall (1970) using data from the JOIDES deep sea drilling project, and from high pressure experiments on muds, proposes the following model:-

(a) From 0 - 1000m compaction principally involves the mechanical expulsion of fluids. Fifty per cent of the total compaction is completed at these depths and the average pore throat diameter is about 6Å.

(b) From 1000 - 2400m approximately 75 per cent of the total compaction is completed and the pore throat diameters are reduced to 1Å. The fluid pressures are still hydrostatic.

(c) As the pressure is further increased, the porosity decreases slowly and the pore throat diameters become less than 1Å. NaCl filtration can take place resulting in progressively less saline fluids being expelled. (To initiate salt filtration requires pressures of 54900 - 85800kN/m^2).

Overton and Zanier (1970) propose a similar model to Beall's but with four zones having different water types.

In the present work porosities are consistent with the above workers and range between 75 - 80 per cent (liquid limit 100 - 135) and 40 per cent (liquid limit 36) at depths equivalent to 0 - 10m, decreasing to between 40 per cent and 7 per cent at depths equivalent to 2500 m. In addition it can also be deduced from Figures 5.1 and 5.2 that up to between 30 and 50 per cent of the compaction has occurred in the first 10m of burial.

1.5.2 Compaction Models based upon Mineralogical and Geochemical Transformations

The present mineralogy of many argillaceous rocks may differ significantly from that of the original sediments, from which they were derived. Weaver (1958a) restricts the term 'diagenesis' to alterations which modify the basic lattice and 'absorbtion' for changes which only affect the interlayer material.

Powers (1959) defines 'hydrogenetic' clays as those which have suffered diagenesis within the depositional environment and 'pedrodiagenetic' clays as those which have suffered post-depositional changes after burial. The equivalent terms used by Weaver (1958a) are 'syngenetic' and 'epigenetic' respectively. It is, however, the consensus of opinion that cation exchange and reconsitution of slightly weathered materials are the major changes which occur in the early stages of deposition.

Kaolinite, illite and chlorite are relatively stable clay minerals, even under large pressures and temperatures. However, the alteration of expanding clays to illite and mixed-layer clay in marine sediments and the associated geochemistry (Fig.1.5) has been described by Powers (1959). Powers attributes these changes to depth of burial and introduces the concept of 'equivalence level', below which potassium is preferentially absorbed over magnesium (and ferrous iron). These latter ions are presumed to move into the octahedral layer and replace Al^{3+}, which in turn replaces

Figure 1.5. Mineralogical Transformations During Compaction (After Powers, 1967).

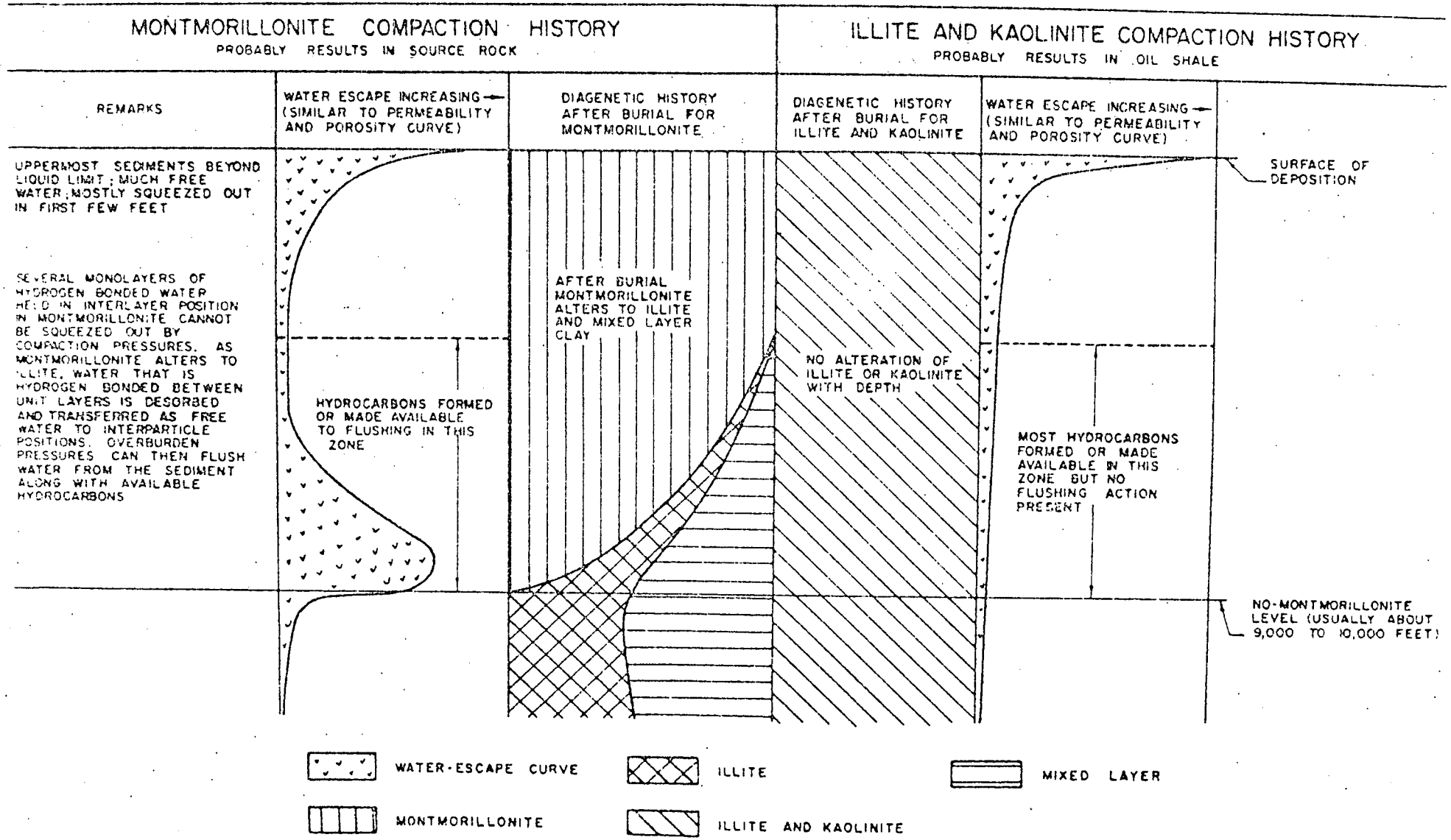

Si^{4+} in the tetrahedral layer. Illite is the resulting mineral and the process only involves beidellite as an intermediate material, and not as a starting point as suggested by Weaver (1959). He cites the possible existence of beidellitic soil (Ross and Hendricks, 1945), although Powers (1959) believes that this would be unstable and quickly fix potassium to form illite.

Keller (1963) suggests four causes for diagenesis of montmorillonite to illite i.e. depth of burial, geothermal gradient, time and activities of the essential ions. Powers (1959) found that the alteration of montmorillonite, in the Texas Gulf Coast, occurs within a small depth range which crosses the entire Tertiary strata, and he suggests that the transformation is not related to geological age, but in some places it may give this appearance because, in general, the older sediments have been more deeply buried.

The transformation of montmorillonite to illite, which requires the removal of the last four layers of orientated water, cannot be accomplished by pressure alone (it requires 550MN/m^2 (24500m of sediments) or 450 MN/m^2 at 50°C) to perform this process. It can, however, be accomplished at relatively low pressures if it is assisted by the electrostatic forces associated with potassium fixation (Powers 1959 and 1967). Potassium fixation is discussed by Weaver (1958b). Nicholls and Loring (1960) also report that there is a general replacement of Na by K in illites after burial.

Powers (1967) proposes the following hypothesis for the transformation of montmorillonite to illite: At about 1000m most of the water has been expelled except for the last few layers of bound water, which comprises 50 per cent of the volume of the deposit. At about 2000m the alteration of montmorillonite to illite begins, and continues at an increasing rate, to a depth, usually of about 3000 - 3500m where there is no discrete

montmorillonite left; the absorbed water becoming free pore water. Burst (1959), Weaver (1959) and Larsen & Chilingar (1967) also agree with these depths. Burst (1969) also offers a compaction model for the transformation of montmorillonite to mixed-layer clay types involving the absorbtion of geothermal heat.

Present results indicate that smectite minerals buried to less than 1000m are 'good' montmorillonites, having Si/Al ratios of approximately 4. However, as the depth of burial increases to 1500 - 1600m, it has been observed that a beidellitic form is developing through the contraction of the lattice, i.e. Si/Al ratio of between 3.6 - 2.9 are encountered with associated high potassium values.

1.5.3 Laboratory Compaction Studies

Compaction studies in the laboratory are usually performed using the one-dimensional consolidation test. Incremental loading techniques are usually applied which can vary greatly in degree, although the majority conform to Terzaghi's theory. However, even the slowest rate of loading (e.g. 10^{-4} kg/cm^2/day as used by Leonards and Altschaeffl (1964)) are far higher than natural rates, hence true conditions are never actually simulated. Constant rate deformation processes have also been used in a limited number of cases (e.g. Smith and Wahls, 1969; Lowe et al, 1969; Wissa et al, 1971) and although useful results such as voids ratio - effective pressure relationships can be obtained, it is doubtful whether certain consolidation parameters(e.g. the coefficient of consolidation (c_v)) as determined experimentally can be extrapolated to the field conditions (Crawford, 1964).

1.5.3.1 Laboratory Studies of Natural Materials

The majority of laboratory studies carried out on natural material appear to have been performed on soft or remoulded clays to maximum pressures of between 1000 - 5000kN/m^2.

For tests performed on undisturbed and remoulded Gosport Clay, Skempton (1944) shows that the e - log P curves do not coincide along the virgin portion in the pressure range 50 - 1000 kN/m^2 although they do tend to merge at higher pressures. He suggests that a type of bonding in the natural material is retaining a more open structure, hence giving a larger voids ratio. Indeed it is the considered opinion of most workers that at low pressures, the remoulded compression curve falls below that of the undisturbed curve. Skempton (1953 and 1970) has compiled data to show the variation between voids ratio and effective pressure for natural normally-consolidated clays and clays compacted in the laboratory from the liquid limit, (Fig.1.6). He points out that although there is close correspondence at low pressures, at pressures equivalent to depths of 1000 - 1600m this agreement disappears because the decrease in the voids ratio of the natural material is more rapid. He suggests that the difference could be due to natural recrystallisation taking place over long periods of time.

With regard to high pressures, Fleming et al (1970) have performed a series of one-dimensional consolidation tests, to a pressure of 35000kN/m^2, on heavily overconsolidated shales from North America. They conclude that the virgin curve was the same regardless of whether or not the shale was tested with the fissility normal to, or parallel to the applied stress, i.e. at these pressures the materials behaved isotropically.

High pressure tests on undisturbed samples of kaolinite to pressures between 14000 - 45500 kN/m^2 have also been performed by Wijeyesekera and De Freitas (1976) to observe changes in the fabric and pore water chemistry.

1.5.3.2 Laboratory Studies of Artificial Sediments

(a) Compression

The relationship between the moisture content and applied effective stress up to 400000psi (2724MN/m2) for pure clays has been studied by

Figure 1.6. Sedimentation Compression Curves for Normally-Consolidated Argillaceous Sediments (After Skempton, 1970).

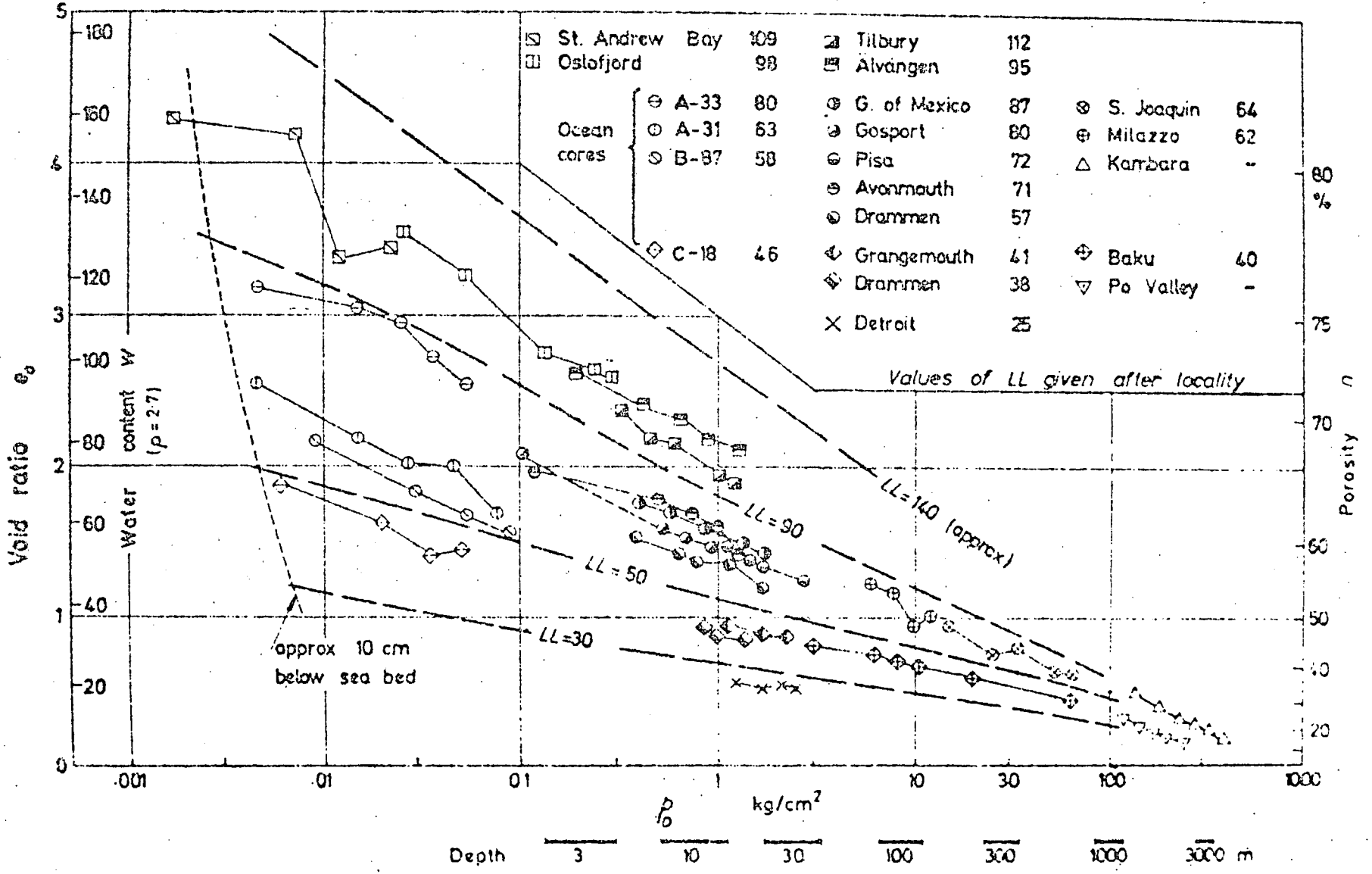

various workers, (e.g. Chilingar and Knight 1960; Chilingarian and Rieke 1968). The order of compressibility is montmorillonite, illite, kaolinite, (Fig.1.7). Rieke and Chilingarian (1974) suggest that this is related to the fact that it is harder to squeeze a given amount of water out of the less plastic clays (which in turn is related to their dimensions and specific surface areas (Table 1.2) and double layer contributions.

It can also be noticed from Figure 1.7 that there is a linear relationship between voids ratio and effective pressure for kaolinite and illite, whereas there is an upwards swing in the early stages of the curve for montmorillonite. Chilingar and Knight (1960) suggest that the break in the curve occurs when only orientated water is being expelled.

Terzaghi was probably the first engineer to make an attempt to understand the mechanisms controlling the compressibilities of clays. He concludes that large voids ratios and high compressibilities of clays are due to 'scale-shaped' mineral particles. Terzaghi also postulates the existence of a semi-solid layer of water on the clay surface to explain the low permeabilities of clays (Terzaghi 1926) and secondary compression (Terzaghi and Frolich, 1936).

Early research into the properties of suspensions by workers in colloid chemistry and related fields, suggested the need for long range electrical forces of attraction and repulsion, in order to explain the physical and chemical effects of such suspensions (Van Olphen 1963). Later these forces were incorporated in soil mechanics research to explain the characteristics of clays. The attractive forces are represented by Van der Waal's forces (Lambe, 1958) i.e. ion-dipole and dipole-dipole links (Lambe likens their effects to those of bar magnets and refers to them as secondary valence forces), and Coulombic forces (Lambe, 1958), i.e. negative surface-positive edge, particle-cation-particle or hydrogen

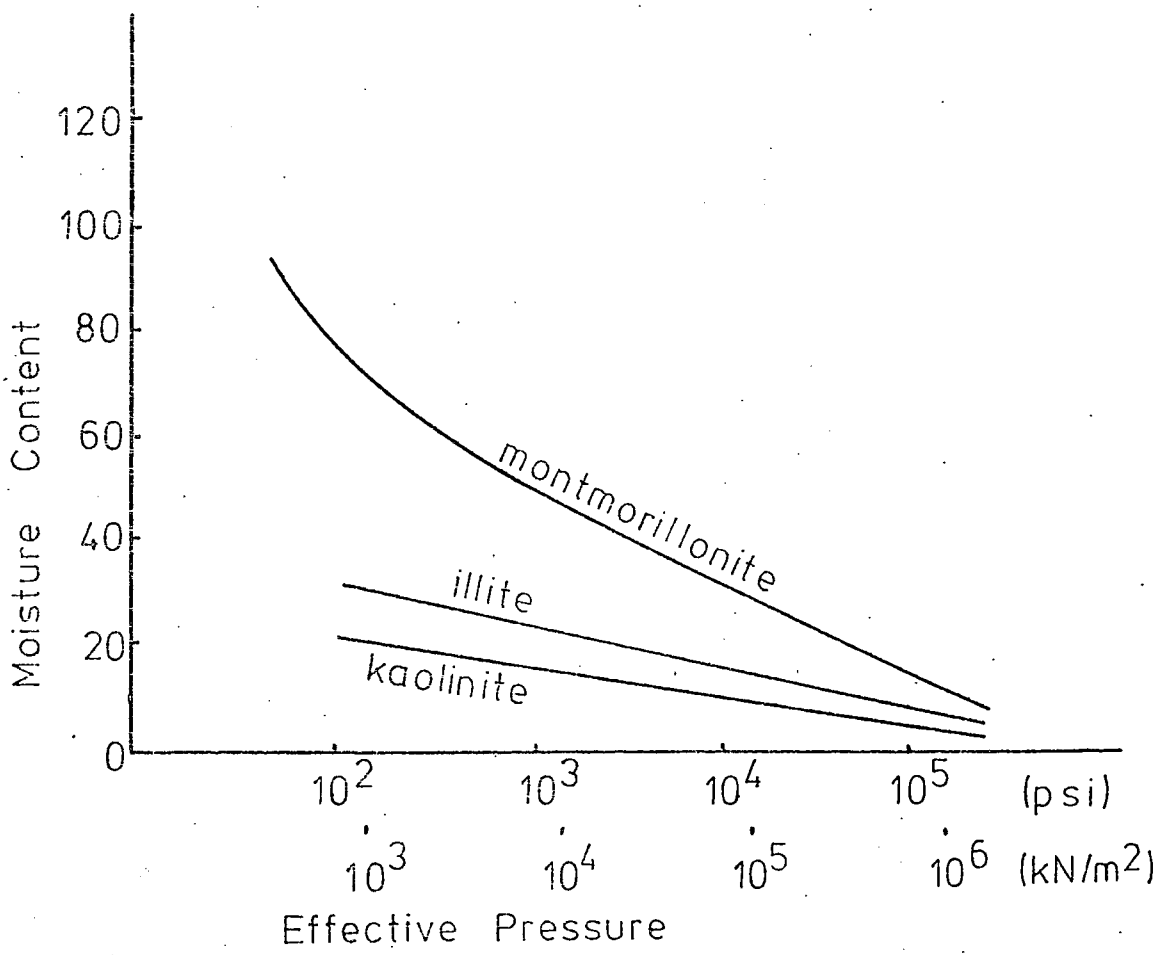

Figure 1.7. Typical Consolidation Compression Curves for Pure Clay Minerals (After Chilingar and Knight, 1960).

	Liquid Limit	Plastic Limit	SG	Surface Area sq m /gm	CEC m.e./litre	Diameter to height	Dimensions
Kaolinite	40 - 50	27 - 31	2.65	14	2.2	2-5	d = 0.3-3μ t = 0.3-0.1d
Illite	83 - 104	31 - 32	2.8	-	28	10-50	d = 0.1-2μ t = 0.1d
Smectite	190 - 1160	31 - 47	2.65-2.8	500-700	100	150 - 500	d = 0.1-1μ t = 0.01d

Table 1.2 Properties of pure clays (after Olson and Mesri, 1970)

bonds. Sridharan and Venkatappa (1973) also propose the Loudon dispersive force as an additional Van der Waal's force. The repulsive forces are primarily due to the osmotic double layer (Bolt, 1956; Lambe, 1958), which is considered to be the most important of the electrical forces and can be shown to increase with an increase in the dielectric constant (Bolt, 1956). It is now the convention to refer to such forces as described above as 'physico-chemical' forces and hence distinguish them from mechanical forces, controlled by the shearing resistance which also operates at the mineral contacts.

Bolt (1956) working on the less than 2μ fraction of pure montmorillonites and Na-illites, regards the repulsive forces acting to keep the particles apart as the difference between the osmotic pressure of the double layer and that of the expelled fluid, the effect being maximum when the particles are parallel. This osmotic pressure extends over distances corresponding to a change in voids ratio of 1-20, depending on the specific surface areas of the minerals. When the plates come close together the pressure may be 4900 - 9800 kN/m^2. As the load is applied, a certain amount of pore fluid is driven out until the osmotic pressure difference equals the applied force. This model does not depend upon mineral to mineral contact.

Experiments performed by Warner (1964), Olsen and Mesri (1970) and Sridharan and Venkatappa (1973) show, that by using pore fluids of different dielectric constants, the amount and nature of the compression is dependent on the minerals present. They conclude that, although both effects must occur simultaneously, the mechanical model is dominant in kaolinite and illite systems, i.e. where the minerals possess a low cation exchange capacity and a low diameter to height ratio, (they can be regarded as stiff elastic plates capable of storing energy)

(see Table 1.2), although the physico-chemical concept is strong in illite systems at low pressures. The physico-chemical concept is dominant in montmorillonite systems where the minerals have high cation exchange capacities and diameter to height ratios of greater than 100. They can be regarded as thin flexible films (see Table 1.2).

Associated with the physico-chemical concept are the nature and size of the exchangeable cations present in the double layer and the concentration of the electrolyte (in aqueous solution), which also govern the compressibility. Olson and Mesri (1970, 1971) and Warner (1964) demonstrate these in Na and Ca systems. The large divalent cations cause a reduction of the double layer, thus causing a reduction in the compressibility, especially in montmorillonites and to a certain extent in illite systems. Kaolinite, having a very low cation exchange capacity (2-10 m.eq/100g) shows only a negligible effect.

An increase in the electrolyte concentration also serves to reduce the effect of the double layer, hence reducing the compression. However, this effect only seems to be of importance in Na-montmorillonites although it occurs in a very minor way in kaolinites. Illites also appear to be almost independent of electrolyte concentration. With regard to Na-montmorillonites, Mitchell (1960) has demonstrated that they do indeed behave in accordance with the predicted double layer theory. Lambe (1958) also considers that a reduction of electrolyte pH will lead to flocculation and hence to a reduction of compression.

(b) Rebound and Expansion

Terzaghi (1929) considers swelling to be 'nothing but the purely elastic extension of the deformable fabric'. However, modern knowledge has revealed that once again both the mechanical and physico-chemical concepts are applicable to swelling and rebound when the applied stress

is removed.

The mechanical concept involves elastic rebound of the plate-like minerals and granules (Lambe and Whitman, 1969) and capillary pressure (Terzaghi and Peck, 1948), which is very significant for randomly orientated clays where the osmotic pressure is small (Yong and Warkentin, 1975). The physico-chemical concept involves the double layer effect (Bolt, 1956) coupled with the exchangable cations present in the double layer and the concentrations of ions in the electrolyte (Olson and Mesri, 1970, 1971). According to Bolt (1956), the osmotic pressure differences within the system will be greater than the stress immediately after a load has been removed, hence swelling will occur and water will enter the system until the internal and external stresses are in equilibrium.

Kaolinite (Olson and Mesri, 1970; Sridharan and Venkatappa, 1973) and granular materials (Lambe and Whitman, 1969) are dominated by the mechanical concept of rebound, with exchangeable cations in aqueous solution having little or no effect. According to Olson and Mesri (1970), illite shows an intermediate effect; the Na form being dominated by the physico-chemical concept, whereas the Ca form tends to show that both concepts are applicable.

As shown by Olson and Mesri (1970 and 1971) and Sridharan and Venkatappa Roa (1973) montmorillonite is dominated by the physico-chemical concept, although only the Na-form expands according to the predicted Guoy-Chapman theory.

This phenomenon can be explained by the fact that Ca-montmorillonite tends to form irreversible domains when squeezed close together (Aylmore and Quirk, 1959) and cannot re-expand to spacings greater than 19-20Å. MacEwan (1948 and 1954) and Norrish and Quirk (1954)

account for this on the basis of strong electrostatic forces existing at these distances in the Ca-forms. These do not develop to any extent in the Na-form because the monovalent ions present allow the double layer to have greater effect.

1.5.4 Microstructure of Clays and Shales

Initially the type of soil structure depends upon the physical and chemical conditions at the time of deposition.

Flocculated clays result when the nett electrical force between adjacent particles is attraction (Lambe, 1958). This requires a small or contracted double layer and implies open structures of edge - edge or face - edge arrangements (Fig. 1.8 a & b). The 'cardhouse' structure for which there is very little support in the literature, refers to an essentially single particle arrangement, whereas the 'bookhouse' structure, consisting of groups of particles has definite supporting evidence (Rosenquist, 1959). A more open or 'honeycombed' structure (Fig. 1.8 c), proposed by Casagrande (1932a) has been confirmed by electron microscope studies of quick clay (Pusch, 1966).

Dispersed clays result when the nett electrical force between particles is repulsion (Lambe, 1958). This requires an expanded double layer and implies a face - face structure (Fig. 1.8 d). A more realistic model, the 'turbostratic' arrangement (Fig.1.8 e) consisting of groups of particles or 'domains' in which clay minerals are approximately parallel, has been proposed by Aylmore and Quirk (1960).

Van Olphen (1963) has proposed seven particle arrangements, although there has been little evidence to support or disprove his hypothesis. In fact Barden (1972) suggests that single particle structures, such as those proposed by Van Olphen are only relevant in dilute colloidal

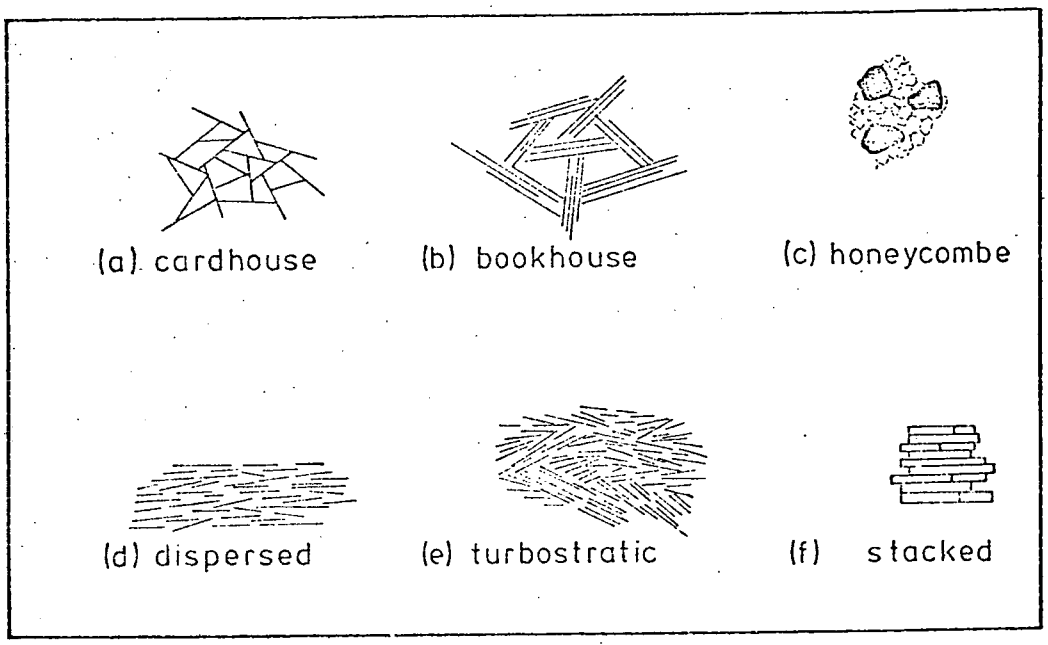

Figure 1.8. Idealised Clay Structures.

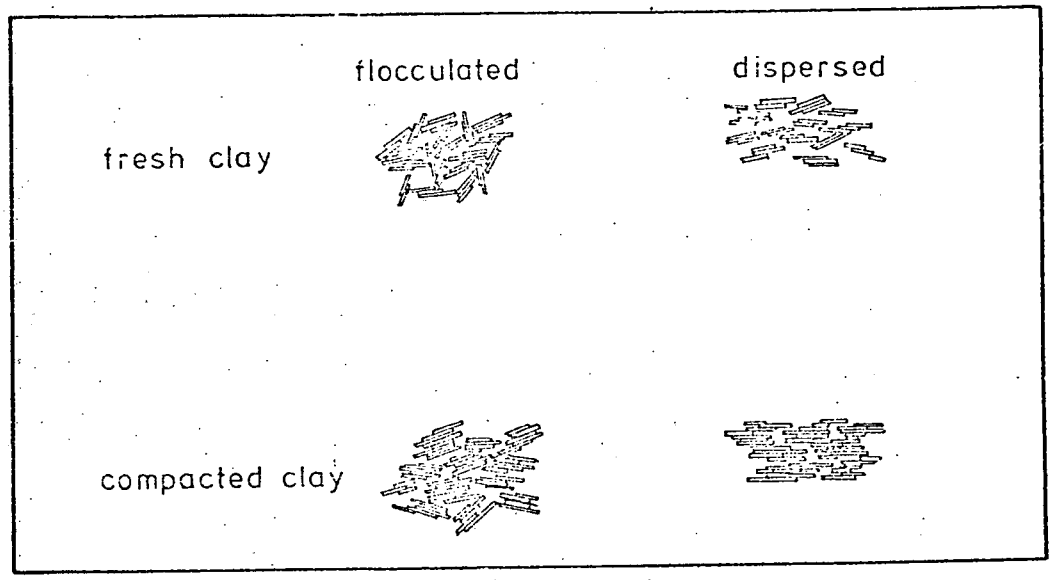

Figure 1.9. A Suggested Scheme for Particle Arrangements in Clay Soils (After Moon, 1972).

suspensions, whereas multiplate structures exist in dense clay systems (i.e. where the proportion of clay is greater than water).

Upon compaction, the initial clay particle structure is destroyed to a certain extent and an increase in the amount of parallelism is produced, especially with respect to the larger particles of kaolinite and illite. Meade (1961b) found that the degree of orientation for the smaller minerals (e.g. montmorillonite) is not related to the superimcumbent load. In fact studies of the structure of lightly compacted pure clays are presented by various authors (e.g. Barden and Sides, 1971a; Sloane and Kell, 1966) whereas studies of naturally compacted clays have been undertaken by such authors as Barden (1972) and Gillot (1969 and 1970).

1.5.5 The Development of Preferred Orientation

The formation of preferred orientation has long been the subject of much research in sedimentary geology, although it is widely accepted that it has a strong association with the degree of fissility. (Odom, 1967).

Until recently, it had been considered that clays existed as single discrete particles and not as packets or 'domains'. Consequently it was thought that preferred orientation (and fissility) must increase with depth of burial. A depth of 350m for the onset of fissility has been suggested by Baldwin (1971 - see Figure 1.4,)whereas Von Engelhardt and Gaida (1963) suggest that shales are formed from clayey sediments in the depth range of 100 - 3000m. Odom (1967), however, did not find any correlation between preferred orientation and depth of burial for illite/kaolinite sediments. In fact White (1961) states that some marine clays are less fissile at depths of 1km. than at depths nearer the surface. Meade (1961b) found no increase in preferred orientation with increasing depth for montmorillonite. He suggests that its compaction

results entirely from the expulsion of pore water in contrast to illite and kaolinite which also combine a certain amount of reorientation.

If the domain concept is considered, the necessity for an increase in preferred orientation with depth is not required because the effect of compression is probably to increase the number of particles in each domain (Blackmore and Miller, 1961) which may still be randomly orientated in a flocculated sediment or parallel in a dispersed sediment. Consequently it is likely that a fissile rock is produced from a dispersed sediment, whereas a massive mudstone is produced from a flocculated clay sediment. Moon (1972) proposes a scheme for the arrangement of particles and packets with increasing compaction (Fig.1.9). Meade (1964) also suggests that for preferred orientation to occur in naturally compacted clays, a partly orientated fabric may be required. This might result from a slow rate of deposition (Meade, 1961b), a high initial moisture content acting as a lubricant (Lambe, 1958; Meade, 1966) or the electrolyte concentration (Lambe, 1958). Meade (1964) also considers that larger particles appear to form domains more rapidly than do smaller particles. However, Moon (1972) states that domains in materials containing extremely small particles, such as montmorillonite, are very difficult to detect, even using the electron microscope. The writer also agrees with Moon's deduction.

Particle size appears to be an important factor in the formation of preferred orientation. Payne (1942) suggests that illitic shales have a greater tendency towards fissility. Alling (1945) tried to correlate fissility with composition and concludes that an increase in the calcareous or siliceous contents greatly reduces the shaliness.

Ingram (1953) concludes that the type of fissility does not correlate with the clay minerals present, although Bolt (1956), Mitchell (1956) and Von Engelhardt and Gaida (1963) report that larger particles of illite and kaolinite develop a preferred orientation more easily than particles such as montmorillonite.

The development of a high degree of preferred orientation has also been attributed to the presence of organic matter in the depositional environment (Odom, 1967; O'Brien 1968; Gipson 1966). This material could quite easily act as a dispersing agent because a few parts per thousand of certain organic ions (O'Brien, 1968) can cause the dispersion of clays by the neutralisation of the surface charges. Gipson (1966) has suggested that the action of benthonic organisms may disorganise some sediment layers and not others, hence resulting in the juxtaposition of strata of preferred and random clay mineral orientations.

1.5.6 Bond Formation in Shales and the Strain Energy Concept

Terzaghi (1941) first postulated the existence of rigid bonds between clay particles and attributed their development to the 'rigid water' which surrounds clay minerals; however, whether bonds result from molecular forces or cementation by deposited matter, their presence is generally deduced from indirect methods, usually involving their effect on various geotechnical properties. This is because of the minute grain size of the material in which bonding occurs. As a consequence, it is frequently only possible to gain a measure of their strength without being able to ascertain what form of bonding predominates.

Bjerrum (1967a) considers the effect of diagenetic bonding (formed from a combination of pressure, pore fluid, temperature,

time and minerals present) upon the rebound characteristics of certain clay-shales. He does not catalogue the bonds genetically but classifies them according to strength i.e. 'weak', 'strong', and 'permanent', (see Fig.1.1). During erosion, due to the presence of 'recoverable strain energy', the clays tend to expand and increase their water contents. However, the amount of expansion is governed by the bond strength. For clays with weak bonds, most of the recoverable strain energy is recovered during expansion; the effect of further weathering on these shales being small, whereas clays with permanent bonds may be considered as indurated soft rocks, strong enough to resist the liberation of strain energy. Clays with strong bonds, which Bjerrum considers to be the most dangerous type, have a large proportion of their recoverable strain energy locked in during unloading, hence limiting the amount of swell. These bonds are gradually destroyed during further weathering, which is accompanied by swelling and an increase in the effective stress parallel to the ground surface. To support this statement he cites the Bearpaw Shale (Cretaceous of North America) as containing strong bonds and by reference to the rebound consolidation curve of the unweathered material (Fig.1.10) he recognises three zones of weathering and increased swelling i.e.:-

(i) 0 - 9m - a zone of complete disintegration

(ii) 9 - 12.5m - a zone of advanced disintegration

(iii) 12.5 - 15m - a zone of medium disintegration

(below 15m the shale is unweathered).

Peterson (1954,1958) had previously noticed that consolidation tests, performed to a maximum pressure of 58 tons/ft^2 (6220kN/m^2) on unweathered Bearpaw Shale (which has a preconsolidation load of approximately 100 tons/ft^2 (10725kN/m^2), yielded a rebound curve which was much flatter than the <u>in situ</u> curve obtained by Casagrande (1949),

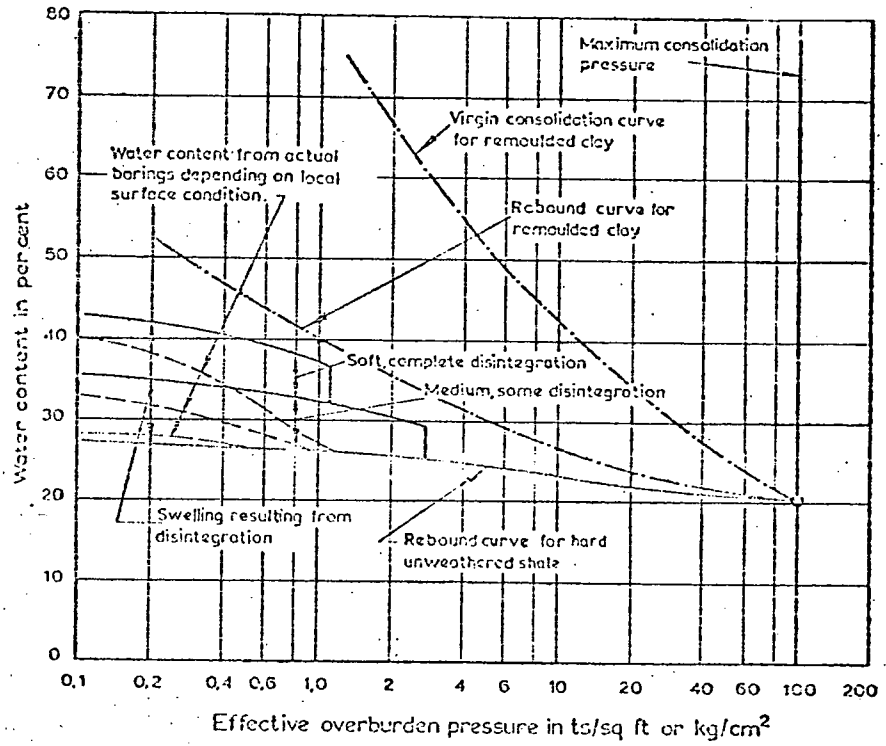

Figure 1.10. Geological History of the Bearpaw Shale.

but he merely attributed this to 'secondary time effects' which had taken place over the centuries.

Bjerrum (1967a) also concludes that the soft, weathered zone near to the surface contains material in which the voids ratio is still slightly lower than that observed from tests performed on the remoulded material and attributes this to groups of particles which are bonded so strongly that weathering agents are unable to separate them.

The concept of strain energy developed by Bjerrum (1967a) provided Brooker (1967) with the basis for a quantitative investigation. In doing this, he performed consolidation tests to a pressure of 2200lb/sq.in. (15169 kN/m^2) on five remoulded materials from a moisture content equivalent to a liquidity index of 0.5. The resulting stress-strain curves are shown in Figure 1.11 whereby it can be seen that the area between the loading and unloading curves (which, according to Brooker represents the 'absorbed strain energy') increases as the plasticity increases (Table 1.3; end column). He suggests that the 'absorbed strain energy' may be accounted for as:-

1. Work expanded in consolidation (partly recoverable)
2. Elastic deformation (recoverable on release of constraint)
3. Work done in the formation of diagenetic bonds (partly recoverable depending upon the strength of the bond)

Upon slaking the consolidated material, Brooker concludes that disintegration is a function of absorbed strain energy (Fig.1.12) and suggests that the absorbed strain energy is dependent upon the clay mineralogy. Brooker also notes that at high overconsolidation ratios, clays with low plasticity give higher values of horizontal pressure than clays with high plasticity and concludes that this must result from the latter materials forming strong diagenetic bonds even after a comparatively short consolidation time.

Figure 1.11. Stress-Strain Relationships for One-Dimensional Consolidation Tests (Brooker, 1967).

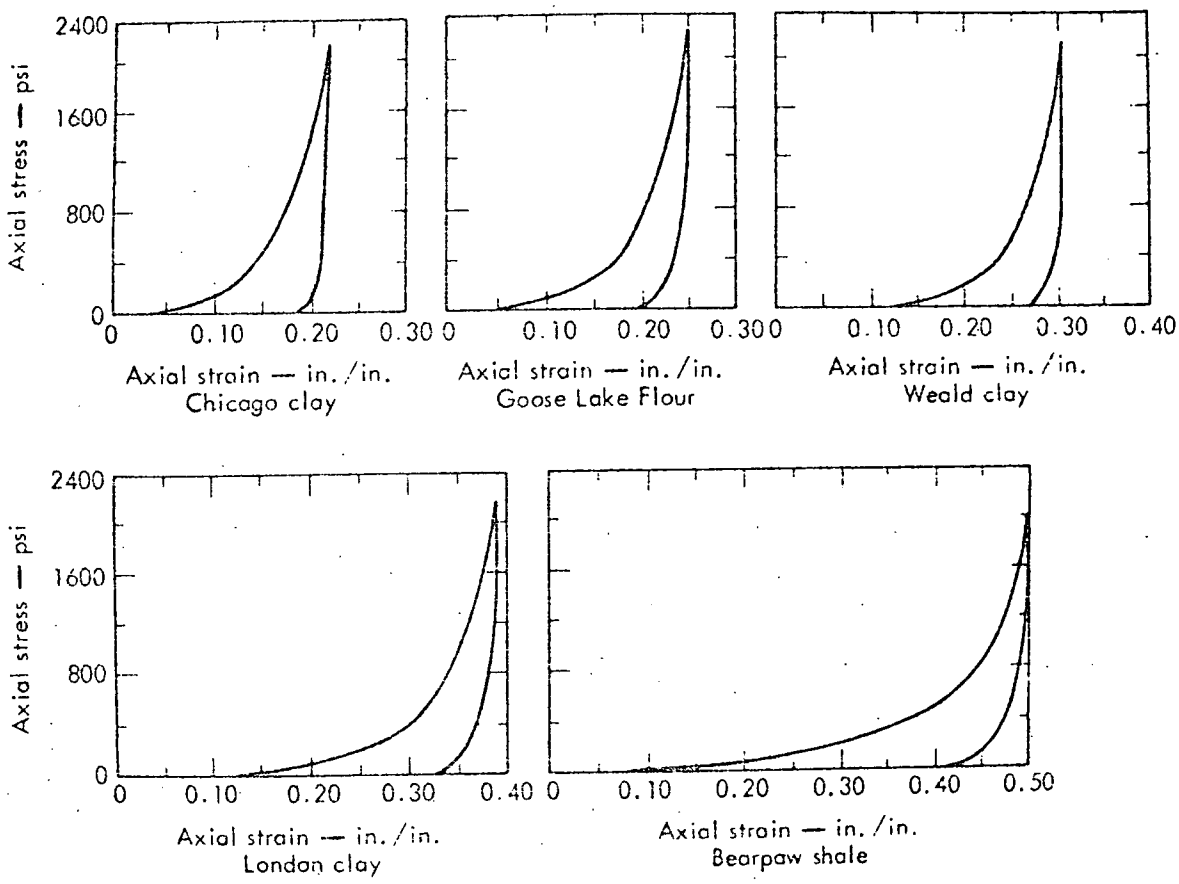

Table 1.3 Characteristics of clays tested by Brooker (1967)

Material	LL[a]	PL[b]	PI[c]	<2 μ[d] (%)	Activity[e]	Mineralogy (%)				Strain Energy (in lb/in³)
						Mont.	Illite	Kaol.	Non-clay	
Chicago clay	28	18	10	36	0.29	5	40	—	55	85
Goose Lake flour	32	16	16	31	0.50	—	15	65	20	85
Weald clay	41	21	20	39	0.53	10	15	15	60	84
London clay	64	26	38	64	0.60	15	35	35	15	100
Bearpaw shale	101	23	78	59	1.53	60	—	5	35	130

[a] LL - liquid limit

[b] PL - plastic limit

[c] PI = LL - PL

[d] Percent, by weight, finer than 2μ

[e] Activity = PI/<2 μ (Skempton, 1953)

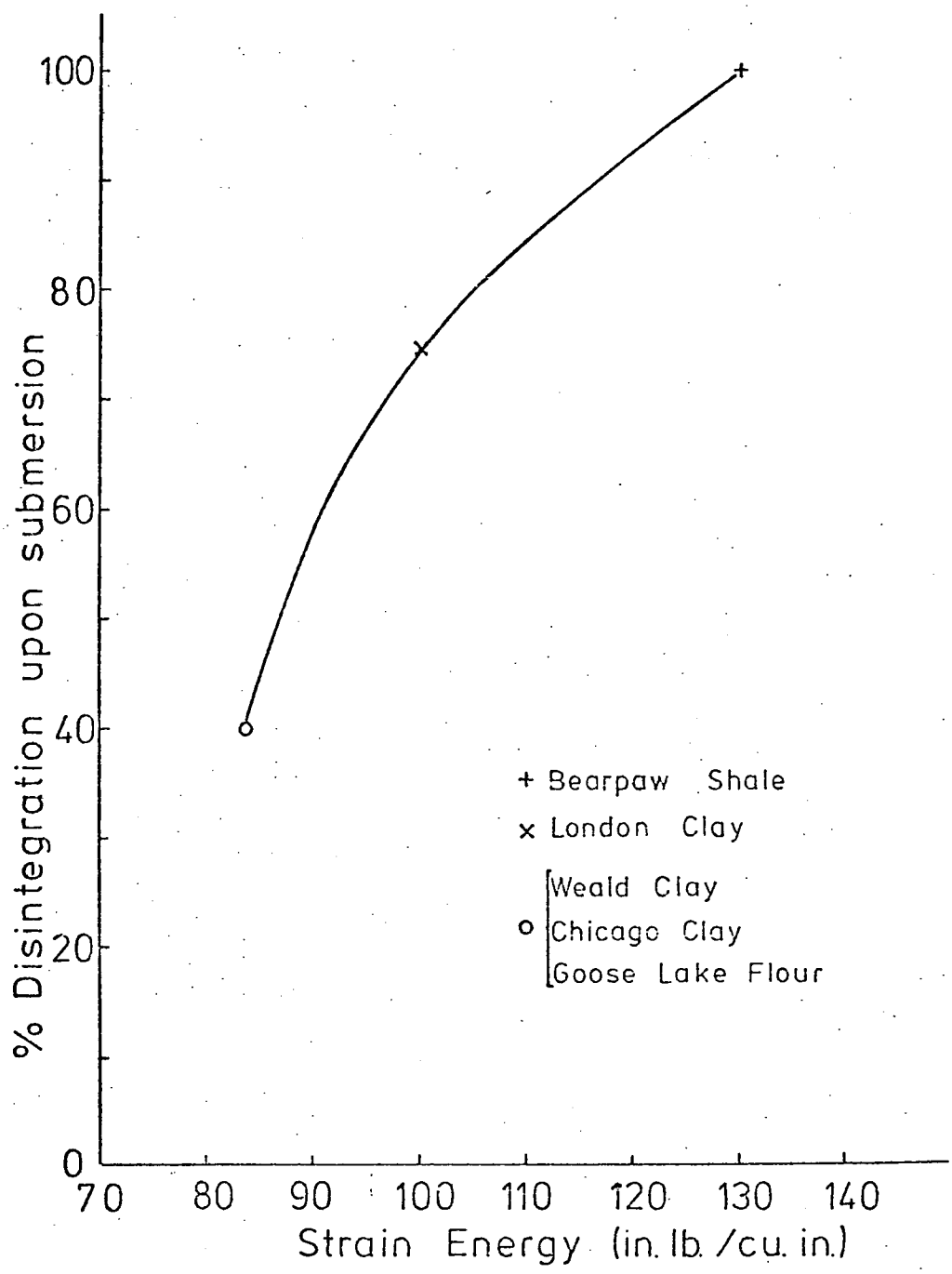

Figure 1.12. Relationship Between Degree of Disintegration and Strain Energy.

The existence of cementation has been demonstrated by Kenney et al (1967). Two specimens of Labrador Clay were initially consolidated to a small overburden pressure. Subsequently one was flushed with water equivalent to the pore fluid, while the other was flushed with EDTA (a disodium salt of ethylene diamine-tetra acetic acid) to remove carbonates, gypsum and iron compounds. Upon continued consolidation they show that the critical pressure had been reduced from 60 tons/m^2 (595kN/m^2) to 25 tons/m^2 (248kN/m^2) in the treated sample.

Bonds existing in natural clay 'with the nature of cementation' have been suggested by Bjerrum and Wu (1960) for certain Norwegian clays. These bonds remain partially intact when the samples were reconsolidated in the laboratory to pressures below their preconsolidation loads, but quickly break down at higher pressures. They suggest that these bonds could be due to particular mineralogical compositions or cementation resulting from carbonation of microfossils and organic matter or supersaturation of pore fluids with chemicals.

With regard to molecular bonding, cold welding of mineral contacts leading to the development of Van der Waal's forces is suggested by Bjerrum (1967a). However, this type of bonding probably exists to a certain extent in all clays but may be very weak and will not affect the compressibility by additional loads.

Diagenetic bonding as proposed by Bjerrum (1967a) forms some kind of molecular interaction between particles. This could take the form of surface fusion, especially in the more deeply buried materials (e.g. Carboniferous shales), but, no direct evidence has been presented to substantiate this idea.

By performing experiments on artificially sedimented clays at very low effective pressures, with rates of loading as low as 10^{-4} grams per cm^2 per day, Leonards and Altschaeffl (1964) offer evidence that the compressibility is much smaller during natural deposition

than in oedometer tests. They suggest that interparticulate bonds are formed which are not equal at all contacts, and that their dispersion plays a decisive role in the stress-strain response. Changes in effective stress cause sliding between contacts, leading to an increase or decrease in the bond strength. If movements result in an overall increase in the bond strength then sliding will decay. However, if the reverse occurs then shear failure will result. Should deposition cease for a given length of time then orientation of water molecules and creep effects will increase the bond strength and thus the strength of the clay. On subsequent loading, again in small steps, a quasi-preconsolidation load is produced, which has also been demonstrated by Leonards and Ramaih (1959). A similar phenomenon was observed by Bjerrum and Lo (1963) when a normally-consolidated Norwegian clay was held at various confining pressures in a triaxial machine for given lengths of time before shearing.

An interesting speculative hypothesis for the nature of interparticulate bonding and its relationship to effective stress and strength was made by Mitchell et al (1969) by studying creep phenomena in soils. They postulate that interparticulate bonds, individually of similar strength, form in response to solid-to-solid contact forces of mineral grains; the number of bonds per contact varying with the compressive force at that contact. For normally-consolidated clays the number of bonds formed is directly proportional to the effective stress. When the applied stress is removed, however, it is not accompanied by a disappearance of all the bonds. Consequently overconsolidated clays are stronger than normally-consolidated clays at the same effective pressure. Mitchell et al also deduce that

compressive strengths are proportional to the number of bonds irrespective of the soil type or state; water only appearing to influence the number of bonds by its effect on the effective pressure. Cohesion results if bonds exist at zero stress.

1.6 Soil Water Phenomena

Following uplift and erosion (e.g. Bjerrum 1967a) soil suction is one of the important processes in the partly-saturated near-surface zone. As a consequence, a brief review of the different mechanisms operatives is currently given. Moreover, in later chapters it will be seen how the compaction history affects suction-moisture content relationships.

1.6.1 The Movement and Distribution of Water in Soils in Relation to Soil Suction

Water will flow from one point to another under the influence of a pressure gradient resulting from hydrostatic pressure, vapour pressure or both (Coleman, 1949). Movement of water under the former process occurs in the form of capillary flow or transfer of moisture films, whereas movement by the latter process occurs by evaporation and condensation.

The surface forces by which water is retained in the soil structure and responsible for the pressure reduction (below atmospheric pressure) are known as the 'soil suction'. This term may be defined as the negative pressure by which water is retained in the pores of a sample of soil when the sample is free from external stress.

To account for the extremely large range of pressures encountered (i.e. from oven dryness to the fully saturated condition) Schofield (1935) developed a scale based on the logarithm of the hydraulic

head (measured in centimetres of water), known as the pF scale (see Table 1.4).

Soil suction is only slightly reduced by an increase in the temperature, but temperature gradients do give rise to significant vapour pressure differences. However, the variation of vapour pressure with moisture content is nevertheless small for soils at the moisture contents likely to be found in practice.

Under isothermal conditions, the effect of suction increases as the soil becomes drier and it can be deduced from Figure 1.13 that only when very dry soils are encountered, where the suction exceeds pF 5, does the pore water vapour pressure differ significantly from that of free water. This infers that only under conditions approaching these suctions will isothermal movements of water take place.

When freezing occurs the soil suction increases; this leads to a redistribution of soil water defined by the equation (Schofield, 1935):-

$$pF = 4.1 + \log_{10} t \quad \ldots\ldots\ldots\ldots\ldots\ldots\ldots\ldots \quad (1)$$

If u is the pre water pressure when an external pressure is applied to a sample, and s is the suction in the material when it is free from external loading, then these quantities can be related by the following equation:-

$$u = s + \alpha p \quad \ldots\ldots\ldots\ldots\ldots\ldots\ldots\ldots \quad (2)$$

where α is the fraction of the applied pressure P which is effective in changing the pressure of the soil water. The value of α, which can be determined by simple experiment (Croney, Coleman and Black, 1958), varies from 0 to 1. For incompressible soils, such as sands, chalk and limestone the value is zero, hence s = -u, but for fully

Table 1.4

Units of Measurement for Suction Pressure

pF	Equivalent Hydraulic Head		Suction		Relative Humidity
	(cm)	(ft)	(kN/m^2)	(lb/in^2)	(%)
0	1	$3.28 * 10^{-2}$	0.0981	$1.42 * 10^{-2}$	-
1	10	$3.28 * 10^{-1}$	0.981	$1.42 * 10^{-1}$	-
2	10^2	3.28 *	9.81	1.42	99.99
3	10^3	3.28 * 10	98.1	1.42 * 10	99.92
4	10^4	$3.28 * 10^2$	981.0	$1.42 * 10^2$	99.27
5	10^5	$3.28 * 10^3$	9810	$1.42 * 10^3$	93.00
6	10^6	$3.28 * 10^4$	98100	$1.42 * 10^4$	48.43
7	10^7	$3.28 * 10^5$	981000	$1.42 * 10^5$	0.07

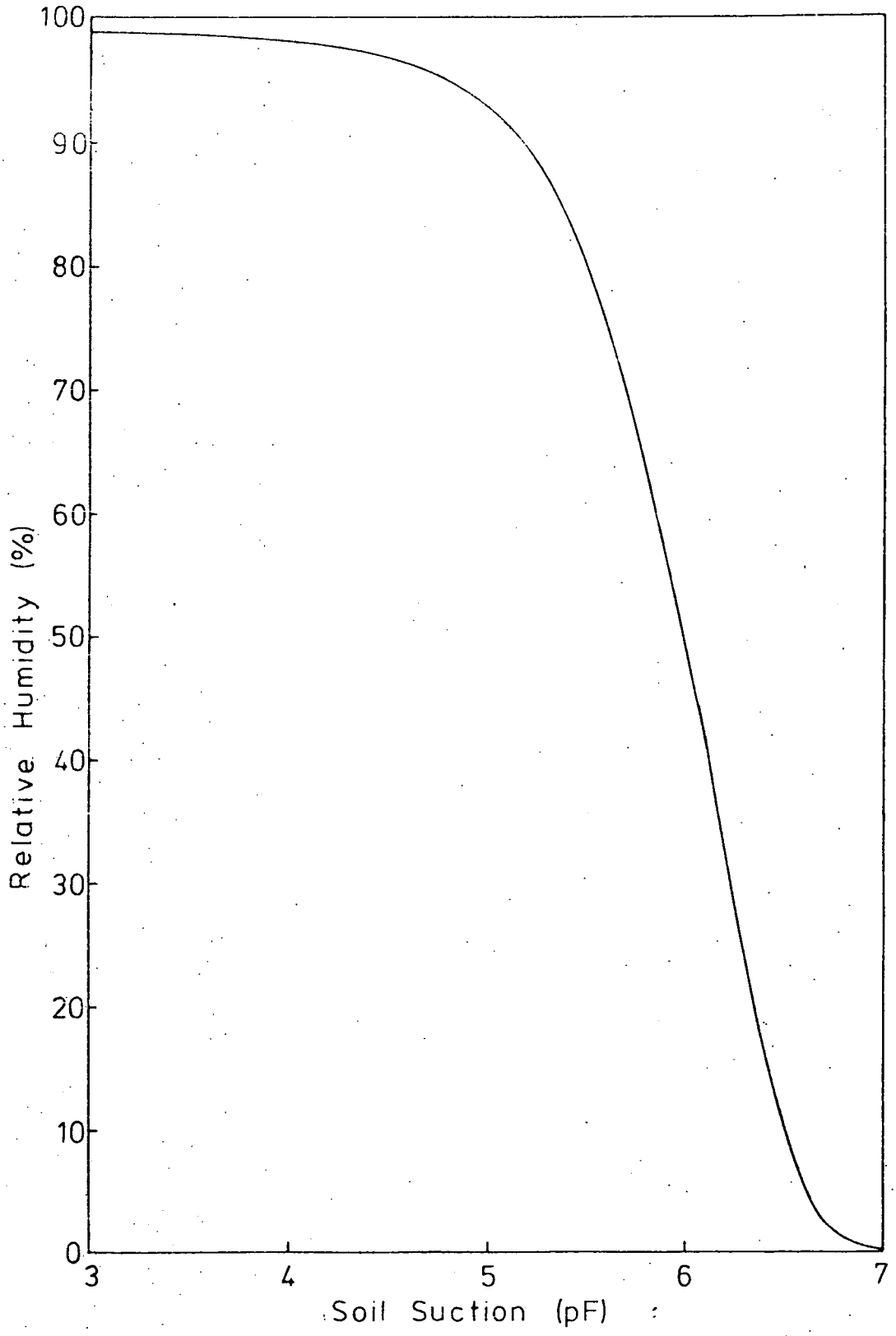

Figure 1.13. The Relationship Between Soil Suction and Relative Humidity.

compressible soils it is essentially 1 since the applied pressure is taken by the water, consequently $u = s + P$. For partially compressible soils (e.g. silts and sandy clays), α varies between the two extremes.

Once the value of α has been determined, equation (2) can be used to derive the distribution of moisture beneath structures and pavements on saturated or unsaturated soils, and the settlements likely to arise from changes in the water table and loading conditions can be determined.

When the water table is near the surface (i.e. in wet climates) this determines the distribution of negative pore pressure and ultimately the distribution of suction and moisture content. Under dry conditions, the moisture content of the ground near the surface can be determined by the atmospheric humidity and suction in these circumstances can be deduced from the average humidity (Croney and Coleman, 1961). A semi-empirical method depending upon the Thornthwaite moisture index (which is a function of the mean air temperature and rainfall at a given site) has been derived by Russam (1959) to deduce the suction between the two extremes (i.e. no water table in the upper 3m of soil).

1.6.2 The Variation of Soil Suction in Compacted Sedimentary Rocks

The way in which moisture content varies with applied suction depends upon the nature of the material, i.e. whether it is incompressible, fully compressible or partly compressible (Croney and Coleman, 1954).

(a) Incompressible soils include all granular materials such as sands, and materials like limestone and chalk, where the internal pressure arising from an overburden is transmitted by the intergranular contacts and does not contribute significantly to the pore water

pressure; the volume of such materials being independent of the moisture content. Typical suction moisture content relationships for incompressible materials are illustrated by studies on the Chalk (Lewis and Croney, 1965) in Figure 1.14a. In incompressible materials the largest proportion of water is retained by surface tension effects around the point contacts of grains and in the soil pores and capillaries. The remaining proportion of water within the soil structure may be regarded as either being chemically combined water in the crystal lattice (which can be regarded as part of the solid, as it cannot be removed by heating at 105°C) or absorbed water (which can be removed by heating at 105°C). The amount of this retained water depends upon the surface area of the material.

Childs (1969) shows that the pressure acting on the surface of water entrapped between grains of soil can be defined by a number of equations depending upon the direction of the two radii of curvature acting through the surface concerned. Since a curved interface can only be maintained by an excess pressure on the concave side then when the two radii of curvature originate from centres on opposite sides of the interface i.e. R_1 (centre on the air side of the interface) and R_2 (centre on the water side of the interface), the nett pressure difference is represented by the equation:-

$$P = A - T\,(1/R_1 - 1/R_2) \quad \ldots\ldots\ldots\ldots\ldots\ldots \quad (3)$$

where T is the surface tension acting in the surface and A and P are the pressures on the sides of the interface which contain R_1 and R_2 respectively.

If both centres of curvature (now represented by R_3 and R_4) originate from the same side i.e. on the side from which A operates, then the nett pressure is represented by the equation:-

$$P = A - T(1/R_3 + 1/R_4) \quad \ldots\ldots\ldots\ldots\ldots\ldots \quad (4)$$

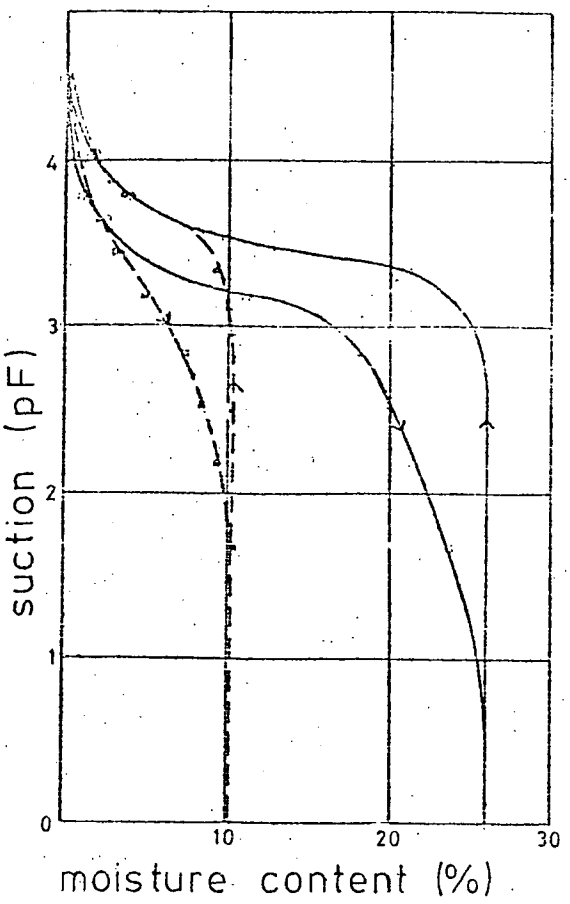

(a) Incompressible soils (After Lewis and Croney, 1965).

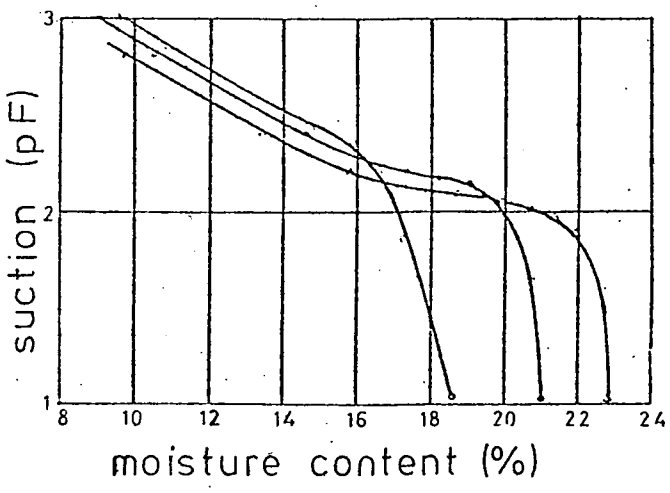

(c) Partially Compressible Soils (After Croney, Coleman and Black, 1958).

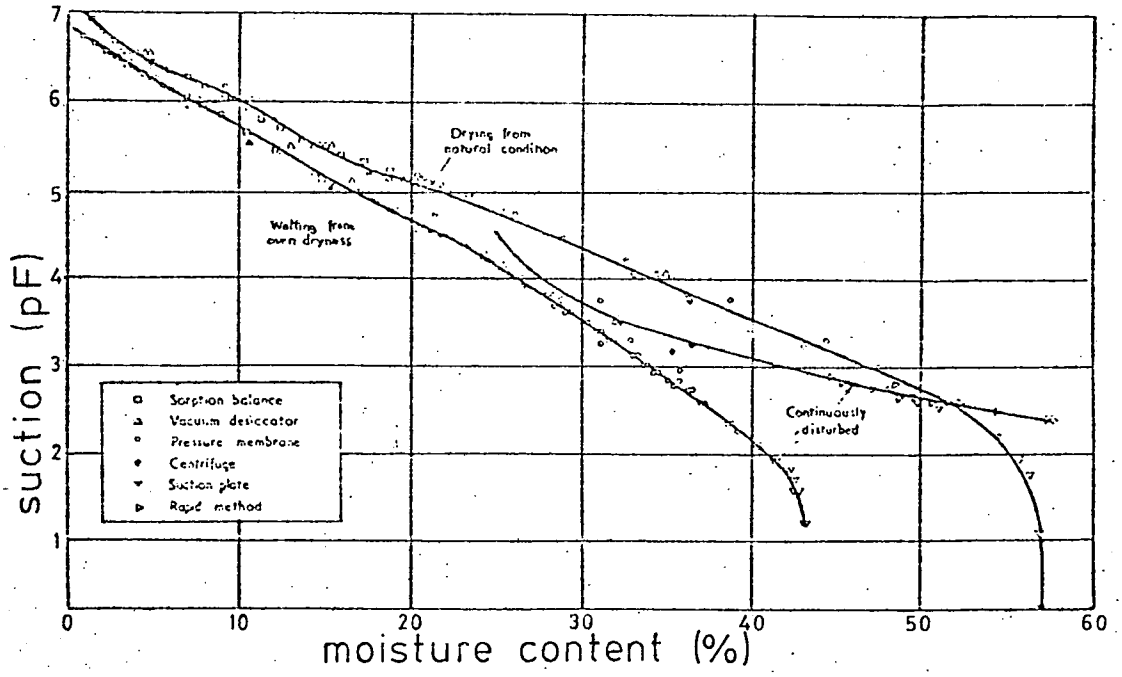

(b) Fully Compressible Soils.
(After Croney, Coleman and Black, 1958).

Figure 1.14. Suction - Moisture Content Relationships.

For a spherical interface (e.g. a small drop of water or an air bubble in water, both radii have the same value (R) and the pressure outside the sphere is represented by:-

$$P = A - 2T/R \quad \ldots\ldots\ldots\ldots\ldots\ldots\ldots\ldots \quad (5)$$

For soils, it is usually found that one side of the interface is in free communication with the atmosphere and consequently is at a constant pressure which can be taken as the datum for measurement of P. Thus if A is zero, then the above formulae become:-

$$P = - T(1/R_1 - 1/R_2) \quad \ldots\ldots\ldots\ldots\ldots\ldots \quad (6)$$

$$P = - T(1/R_3 + 1/R_4) \quad \ldots\ldots\ldots\ldots\ldots\ldots \quad (7)$$

$$P = - 2T/R \quad \ldots\ldots\ldots\ldots\ldots\ldots\ldots\ldots \quad (8)$$

where P is the pressure in the water, which always can be shown to represent a suction. Furthermore, by modifying the geometry it is possible to choose small values of R_1 and R_2 (representing saddles) and large values of R_3 and R_4 (representing cups) to give the same values of suction.

The removal of water from granular soils can best be demonstrated by reference to Figure 1.15 (From Childs, 1969) which is a section through a hypothetical soil specimen. Initially the soil is saturated with the water level above the particle surface (stage 1) and since the interface is planar, the suction just below the surface is zero. If the water is withdrawn from the specimen, then until stage 2 is reached, the suction just under the surface remains zero. As soon as particles cut the air-water interface (stage 3), curvature of the interface is imposed and as the interface withdraws into the specimen the curvature becomes sharper and the suction accordingly increases; being greatest in the narrowest parts of the pore channels (stage 4). At higher suctions the interface retreats into wider channels, i.e. with a

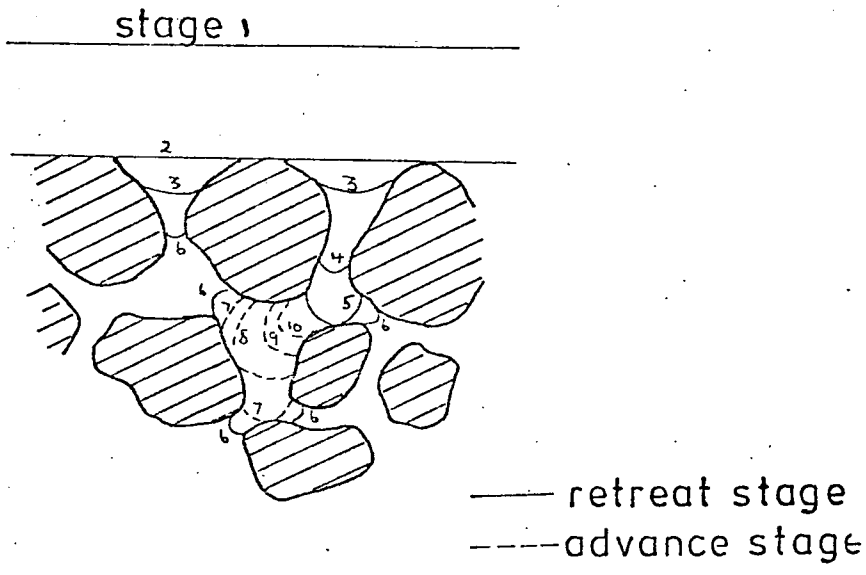

Figure 1.15. Stages of Withdrawal and Reentry of Water Associated With the Pore Space of a Porous Material (After Childs, 1969).

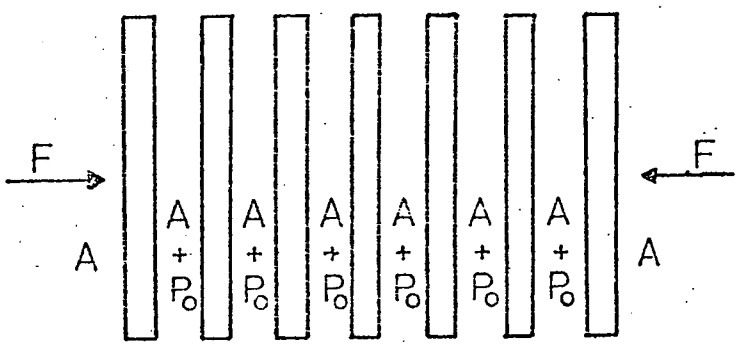

Figure 1.16. A Mass of Parallel Surface-Active Plates in Suspension Experiencing Swell Pressure (After Childs, 1969).

larger curvature (stage 5). Instability results and the interface does not rest until a position in a channel of narrower radius than stage 4 is found (i.e. stage 6). If no suitable channels are found (e.g. in a soil which consists of granules enclosing channels of similar geometry) then almost complete drainage occurs. However, some water does remain at the contacts between grains, and this can only move very slowly either by liquid movement in very thin films left on the particles by molecular attraction, or in the vapour phase.

If the suction is decreased at stage 6, the interface will climb to the widest part (i.e. through stages 7 and 8), after which the interface curvature becomes sharper and requires a greater suction, than at stage 8, to maintain equilibrium. Instability results and the suction is insufficient to prevent the cell refilling until stage 10 is reached. Further uptake of water requires a continued relaxation of the suction.

The hysteresis of the suction/moisture curves is consequently accounted for by the above factors, i.e. the suction required to empty the cell is the relatively high value corresponding to the curvature at stage 4, whilst the suction for refilling is the lower value corresponding to the curvature at stage 8; larger hysteresis effects being produced by a greater size disparity between the pores and channels. Surface tension effects also make a contribution to the difference between the suction for entry and withdrawal, i.e. the radius of curvature is greater for a greater angle of contact. The characteristic moisture content/ suction relationship from the totally saturated condition to that of oven dryness is known as the boundary drying condition, whereas when the reverse occurs the relationship is known as the boundary

wetting condition.

(b) Fully Compressible Soils include clays and colloidal materials. Under field conditions these are normally saturated and pressures are carried exclusively by the pore water. A typical suction-moisture content relationship for these materials is shown in Figure 1.14b (after Croney, Coleman and Black, 1958). These writers also show that the variation in the same relationships when clays of differing Atterberg limits are considered (Fig.1.17). Childs (1969) considers the mineral skeleton as consisting of a large number of parallel plates (Fig.1.16). Repulsion between the plates is due to the hydrostatic pressure between plates being higher than in the region outside the mass. Equilibrium is maintained by the application of either a mechanical pressure or a suction which is equal to the hydrostatic pressure between the plates; any increase in the former quantities causing the plates to move together until the pressures are again equal.

Consequently the previous explanation of hysteresis cannot be applied to colloidal matter. However, assuming that hysteresis is a genuine effect, then a suitable explanation can be put forward. If the clay consists of plates which are non-parallel, then the cavities between them will be larger than in an array of parallel plates, thus the potential energy will be higher. An increase in suction may not only draw the plates closer together but may also reorientate them into nearly parallel positions of lower energy, water being lost in the process. At the same time during rewetting the plates will separate but not necessarily to their original positions, and hence less water will be absorbed. Subsequent cycles of wetting and drying should produce a closed loop.

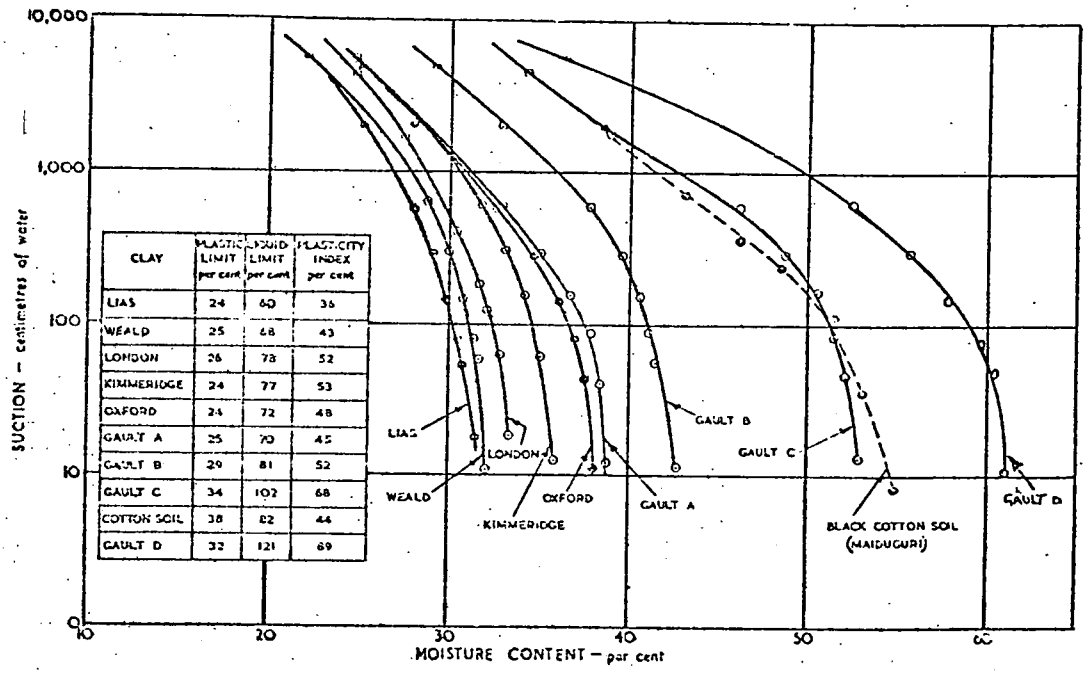

CLAY	PLASTIC LIMIT per cent	LIQUID LIMIT per cent	PLASTICITY INDEX per cent
LIAS	24	60	36
WEALD	25	68	43
LONDON	26	78	52
KIMMERIDGE	24	77	53
OXFORD	24	72	48
GAULT A	25	70	45
GAULT B	29	81	52
GAULT C	34	102	68
COTTON SOIL	38	82	44
GAULT D	32	121	89

Figure 1.17. Relationship Between Suction and Moisture Content for Undisturbed Clay Soils (After Croney, Coleman and Black, 1958).

(c) Water loss by different mechanisms at the same time. In certain circumstances water may be lost with equivalent air entry over part of the suction range and equivalent shrinkage over the remainder. In other cases water loss may occur by both processes simultaneously. Typical suction curves are shown in Figure 1.14c.

If suction is applied to a saturated clay soil consisting of aggregates, then shrinkage of the aggregates will occur simultaneously with the withdrawal of water from the pores between the aggregate. If the aggregates are of commonly occurring sizes ranging from a few millimetres to a few centimetres and are in random array, then the structural pores will be large and empty at low suctions (i.e. a few centimetres of water, and relatively little water is lost from the crumbs. If the plates are of uneven thickness and in random orientation then there will be points of physical contact between some neighbouring plates while there is appreciable separation between others. Shrinkage is consequently limited while there is still large amounts of water left in the pore space and further increases of suction cause curvature of the air-water interface and losses of water by air entry.

1.6.3 The Relationship between Suction and the Mineralogy of Artificially Prepared Soils

An investigation of soil suction (and strength) of artificially prepared remoulded soils has been undertaken by Dumbleton and West (1970). Philpot (1971) uses this data to obtain approximate mineralogical composition from suction curves. An attempt to obtain the liquid limit by a quick suction technique has also been made by Russel and Mickle (1970). Dumbleton and West suggest that, on the basis of suction measurements made on mixtures of kaolinite-

quartz and Ca-montmorillonite-quartz, there is a linear relationship between moisture content and computed liquid limit of the mixture at constant suction pressure.

1.6.4 Determination of the Specific Surface Area

Brunauer, Emmett and Teller (1938) use a molecular model to deduce a theoretical equation for the absorbtion isotherm and from this the surface area (in m^2/g) of the clay minerals present may be calculated. For this model, the surface of the absorbent is visualised as being partially covered with up to n layers of water molecules. The rate of condensation in any layer is proportional to the instantaneous difference in area between the layer and the layer beneath it, and the rate of evaporation is proportional to the difference in area between the layer and the layer above it. At equilibrium the rates of condensation and evaporation are equal, and from these considerations Brunauer, Emmett and Teller produce an equation (the B.E.T. equation) of the form:-

$$\frac{H}{M(1-\frac{H}{100})} = \frac{1}{M_m C} + \frac{C-1}{M_m C} * \frac{H}{100} \quad \ldots\ldots\ldots (9)$$

where M is the moisture content of the soil at a relative humidity H, and M_m is the moisture content when the soil is completely covered by a unimolecular layer of water. The constant C is an exponential function of the latent heat of evaporation of water from the unimolecular layer on the soil surface (E_1 cals/gram), the normal latent heat of evaporation of water (E_L = 538 cals/gram), the molecular weight of water (m = 18.0 grams/mole), the gas content (R = 1.987 cals/mole/^oK) and the absolute temperature (T^oK), i.e.:-

$$C = \exp(E_1 - E_L)\ \frac{m}{RT} \quad \ldots\ldots\ldots\ldots\ldots\ldots\ (10)$$

Equation (9) is of the form $y = mx + c$, thus when $\frac{H}{100}/M(1-\frac{H}{100})$ is plotted against $\frac{H}{100}$ a straight line with an intercept of $\frac{1}{M_m C}$ on the 'y' axis and a slope of $(C-1)/M_m C$ will result. Consequently C and M_m can be calculated knowing that the relative humidity (H) is related to the suction (pF) at 20°C by the following equation derived by Coleman and Farrar (1956):

$$pF = 6.502 + \log_{10}(2 - \log_{10} H) \quad \ldots\ldots\ldots\ldots\ (11)$$

The value of M_m is related to the surface area (A cm^2/g) by the following equation:-

$$A = \frac{\text{area of water mols } (1.05*10^{-15} cm^2)\ M_m/100}{\text{Mol wt water } (18.0) * \text{unit at. mass } (1.66*10^{-24} g)}\ cm^2/g \quad \ldots\ldots(12)$$

(i.e. $A = 35M_m\ m^2/g$)

1.7 Slaking Behaviour

Upon uplift into the zone of weathering, and in particular upon exposure at outcrop or as a result of engineering excavations, materials may disintegrate by slaking through the action of water on the partly saturated or dried fabric. This behaviour is not only controlled by the mineralogy, pore water chemistry and soil fabric, but may also be influenced by the compaction history, especially the presence of diagenetic bonding. Consequently a series of experiments have been performed on the materials currently under consideration in an attempt to delineate the above factors.

1.7.1 Slaking Mechanisms

The most important mechanism operating during the slaking of non-swelling clays (e.g. kaolinite) results from an increase in

the pore air pressure overcoming the tensile strength of the material (Terzaghi and Peck, 1967; Yoder, 1936). According to Henin (1938) and Tschebotarioff (1951) detachment of expansive materials (e.g. montmorillonite) occurs by a shear or tensile stress which is induced by differential swelling. This mechanism may be divided into the osmotic swelling effect (involving forces at distances greater than 20Å) and the surface and cation hydration effect involving short range forces (Mielenz and King, 1955). Slaking by dissolution of cementing agents, which may include diagenetic bonds (Bjerrum, 1967a) has been suggested by Winterkorn (1942).

'Salt heaves', more associated with swelling than slaking, such as the oxydation of pyrrhotite and pyrite (with the former acting as a catalyst for the non-reactive latter) (Bastiansen, et al., 1957) or swelling due to crystallisation and change in hydration state of sulphates has not been considered. The formation of gypsum and jarosite in both in situ and compacted shale infill has posed problems in a number of countries (see Taylor, 1978).

1.7.2 Slaking Behaviour of Pure Clays

General descriptions of the slaking of pure clay minerals are given by Mielenz and King (1955) and general observations have been made by Emerson (1964). Kaolinites and illites disintegrate by spalling until a mass of chips remain, while montmorillonite slakes in different ways depending upon the exchangeable cations present. Air-dried K-forms swell and spall with considerable release of air with each new crack; spalled pieces continuing to disintegrate until only small aggregates remain. The air-dried Ca-form is prone to rapid expansion with simultaneous

disintegration into small aggregates. Air-dried Na-montmorillonite slowly swells and flocculatant growths appear on the surface. Swelling increases the size severalfold, and ultimately the form is lost by slumping.

Slaking of non-expansive kaolinite is prevented by air evacuation prior to immersion, whereas the effect on expansive materials is to cause a more rapid but less complete breakdown (Mielenz and King, 1955). Emerson (1964) concludes that air evacuation only reduces, but does not stop, the slaking of thin flakes of Ca-kaolinite, in the sense that the average size of the debris is greater. His results also indicate that the reduction of slaking due to air evacuation is less for Ca-illites, whereas dried flakes of Ca-montmorillonite swell to the same extent as those not subjected to air evacuation.

With regard to the initial water content, slaking increases as the air-dried condition is approached (Mielenz and King, 1955). Mitchell (1965) produces qualitative evidence in agreement with this statement (see Table 1.5). According to Emerson (1964) the boundary between slaking and non-slaking of Ca-illite occurs at a relative vapour pressure (p/p_o) value of between 0.75 - 0.84 (Table 1.6), and above p/p_o = 0.92 illite flakes are saturated. On the other hand, he reports that at p/p_o = 0.985 only 60 per cent of the pore space of Ca-kaolinite is filled and consequently slaking is complete under these conditions (and is only stopped by slowly wetting the material prior to immersion). He further reports that Ca-montmorillonite flakes do not slake upon immersion, although many transverse cracks occur on the surface and the edges become frayed. Equilibration of dried

Table. 1.5 Effects of Relative Humidity (RH) Equilibration on the Slaking Behaviour of Various Clays (After Mitchell, 1965).

	Degree of Disintegration		
Sample	100% R.H.	(After drying to) 94% R.H.	80% R.H.
Kaolinite	Complete	Complete	Complete
Illite	Severe	Severe— Complete	Complete
Montmorillonite	Moderate	Complete	Complete

Table 1.6 Effects of Relative Vapour Pressure (p/p_o) Equilibration on the Slaking Behaviour of Two Clays (After Emerson, 1964)

	Degree of Disintegration (After 'Wetting' to p/p_o =)			
Sample	0.75	0.84	0.92	0.985
Ca-Kaolinite	—	—	Complete	Complete
Ca-Illite	Slight	None	None	None

samples to higher relative vapour pressures only reduces the amount of swelling subsequent to immersion in water.

The effect of electrolyte concentration upon the dispersion[1] of clays is well known (Van Olphen, 1963) and the existence of a critical salt concentration (CSC) at which 50 per cent of dispersed clay flocculates in 24 hours is recognised. The effect of the exchangeable sodium percentage (ESP)[2] on the dispersion behaviour of illites and montmorillonites is shown in Table 1.7. When the ESP is below 12.5 Ca/Na montmorillonite systems (Rowell, 1963) and Ca/Na illite systems (Rowell et al 1969) behave like the pure Ca material. The equilibrium state of illites and montmorillonites as a function of ESP and electrolyte concentration is shown in Figure 1.18. The dispersion behaviour of kaolinite systems with an ESP higher than 15 per cent is considered to be identical to the pure Na-form (Elgabaly and Elghamry, 1970). These workers also note that the permeability of kaolinite decreases as the ESP increases, and in fact at an ESP of 15 per cent the permeability is 20 times less than that for the Ca-form.

Emerson (1967) reports that the water content for dispersion[3]

1. Dispersion is the separation and suspension of individual particles or domains from the main mass when immersed in a liquid, and is evidenced by a cloudy appearance. It includes deflocculation (Van Olphen, (1963).

2. $ESP = \frac{\text{sodium exchange capacity (m.eq/100g)}}{\text{cation exchange capacity (m.eq/100g)}} * 100\ (\%)$

3 The Water Content for Dispersion is defined as the minimum initial water content of clayey material, usually remoulded, which just exhibit perceptible dispersion when immersed in water.

Table 1.7 Exchangeable Sodium Percentage (ESP) for Dispersion of Air-dry Neutral Clay Flakes in Water (Adapted from Emerson, 1967)

Clay	ESP (%) for Complete Dispersion in Water	ESP (%) for Just Perceptible Dispersion in Water
Ca/Na-illite	13	7
Ca/Na-montmorillonite	12	6

Table 1.8 Water Contents for Dispersion (WCFD) of Clay in Water from Remoulded Silt-Calcium Clay Mixtures (Adapted from Emerson, 1967).

Clay and Measured WCFD for Clay Fraction only	Ratio Silt : Clay	WCFD (%) after Remoulding Measured	Calculated
Ca-illite (WCFD = 52)	1 : 1	26	26
	3 : 1	17	13
Ca-montmorillonite (A) (WCFD = 150)	1 : 1	78	75
	3 : 1	48	39
Ca-montmorillonite (B) (WCFD = 350)	1 : 1	180	175

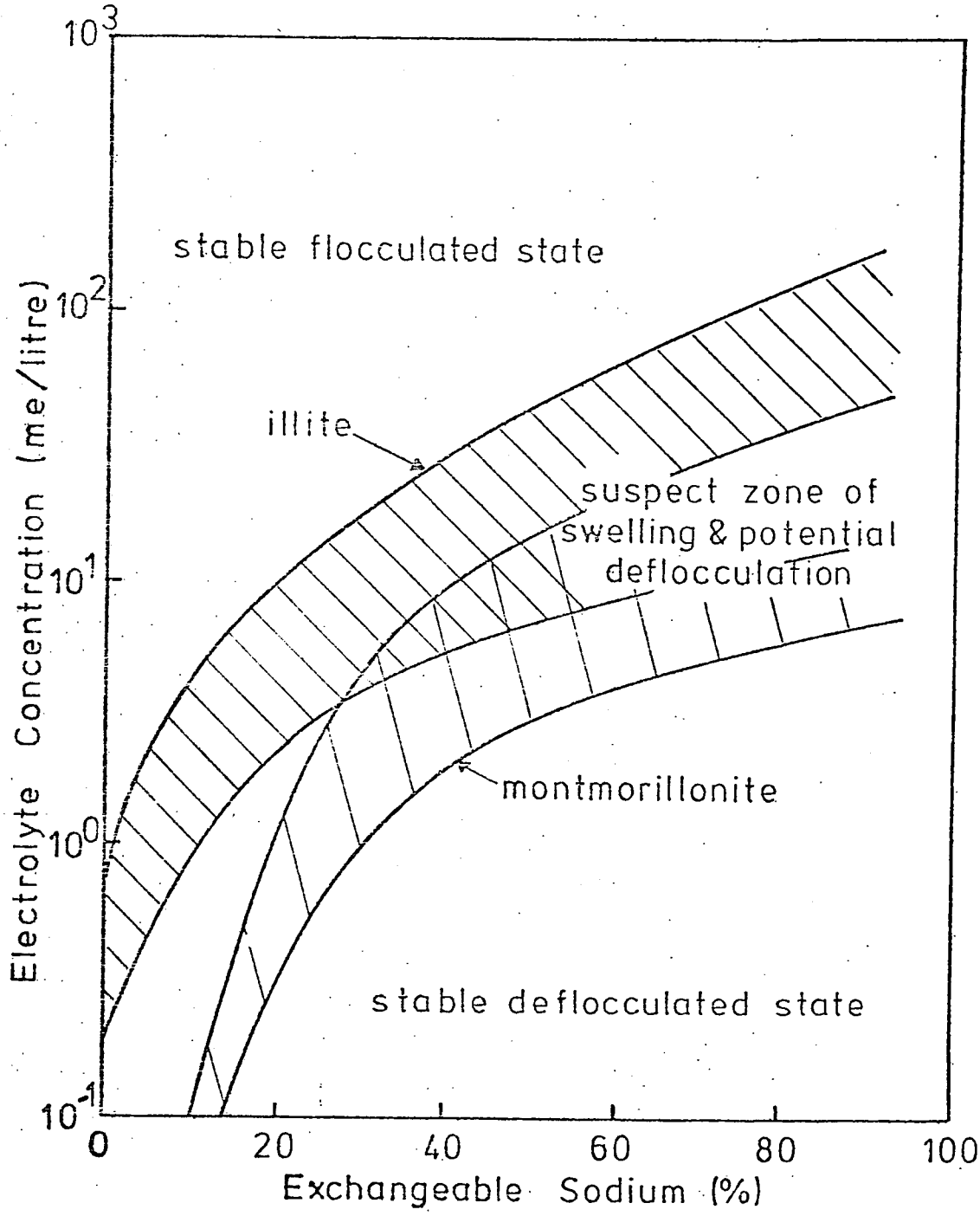

Figure 1.18. Influence of Exchangeable Sodium in Soil Structural Equilibrium - Electrolyte Concentration Relationships (After Inges, 1968 and Moriwaki, 1974).

(WCFD) to be 52 per cent for Ca-illite and 150 and 350 per cent for two different Ca-montmorillonites tested. However, the latter two values correspond to basal spacings of 28Å and 53Å respectively (assuming a specific surface area of $800m^2/g$) which are much higher than the 19Å maximum basal spacing reported by Norrish and Quirk (1954). Consequently he concludes that the excess must be associated with the inter-domain pore space. On the other hand, Ca-kaolinites flocculate in water (Schofield and Samson, 1954) and aggregates cannot be dispersed by increasing the water content (Emerson, 1967).

The effect of silt upon the WCFD is summarised in Table 1.8 and the good agreement between measured and calculated values possibly implies that the silt is merely acting as a dilutant. Water contents for dispersion of mixtures of Ca-illite and Ca-kaolinite indicate that the presence of kaolinite up to 50 per cent does not alter the WCFD of the illite (see Fig.1.19). By considering the work of Sills et al (1973) the shape of the curves may be explained by assuming an inert kaolinite structure dominated by active illite particles which fill the voids surrounding the former.

Schofield and Samson (1953) demonstrate that Na-kaolinite (flocculated at pH 4) deflocculates upon increasing the alkalinity by the addition of NaOH. A similar, but lesser effect is observed in Na-montmorillonites (Emerson, 1963). Arora (1969) reports that, in general, the CSC for pure Na-clays increases from pH 7 to a maximum at about pH 8.3 and then decreases at about pH 9.5. Clays containing divalent cations are only affected in a small way by changes in pH and CSC values are generally low (i.e. in the order

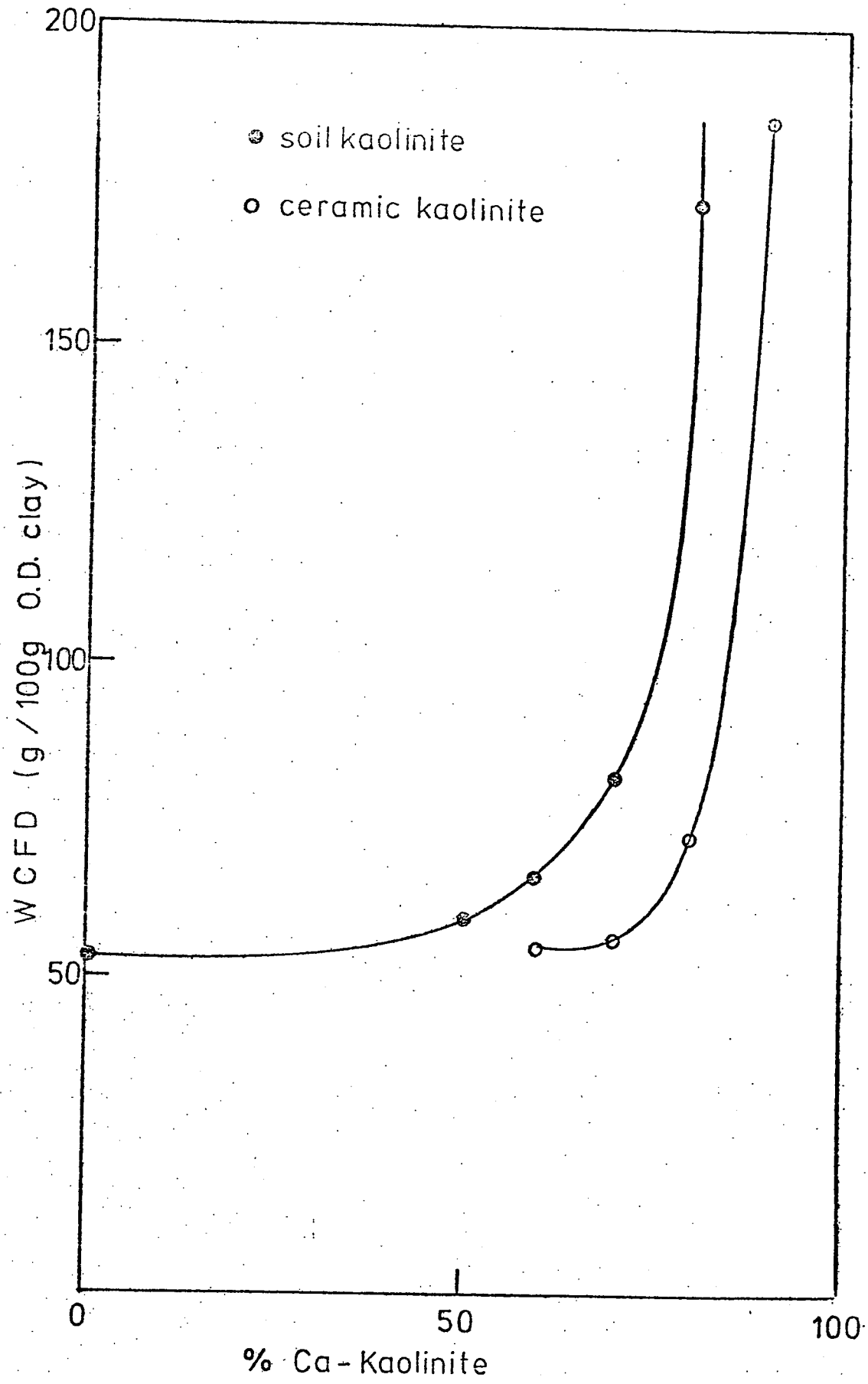

Figure 1.19. Water Contents for Dispersion of Ca-Kaolinite-Illite Mixtures (Adapted from Emerson, 1968).

of 1 me/litre). The effect of CSC values on heterionic Na/Ca and Na/Mg clays is summarised in Figure 1.20.

The effect of particle size on dispersion behaviour has been studied by Arora (1969) whilst the effect of soluble silicates on the aggregation behaviour of bentonite and kaolinite has been reported by Dutt (1948).

With regard to clay microstructure and fabric, Lambe (1958) suggests that dispersed structures in compacted clays resulted in faster slaking than for corresponding flocculated structures, but he doesnot elaborate on this except to mention that differences in permeability may be a complicating factor. Studies with a scanning electron microscope and other methods (Barden and Sides, 1971a) indicate that the structure of kaolinite contains large domains with ill-defined boundaries showing gradual changes in orientation regardless of being flocculated or deflocculated (Smart, 1967). Emerson (1964) further concludes that rearrangement of kaolinite crystals upon immersion is not a major cause of slaking for this material. Illite, on the other hand, shows a marked change in fabric (i.e. dispersed or salt flocculated) depending upon the physico-chemical conditions (Barden and Sides, 1971a). At present the resolution limit of the scanning electron microscope prevents any conclusion on the fabric of montmorillonite.

Swelling phenomena in clay minerals occur by either intramicellar (intracrystalline) swelling, involving the expansion of the clay mineral itself, or intermicellar (intercrystalline) swelling, involving expansion due to the water between the clay minerals (Barshad, 1955). Intracrystalline swelling to unlimited basal spacings occurs in Na-montmorillonites whereas a maximum value

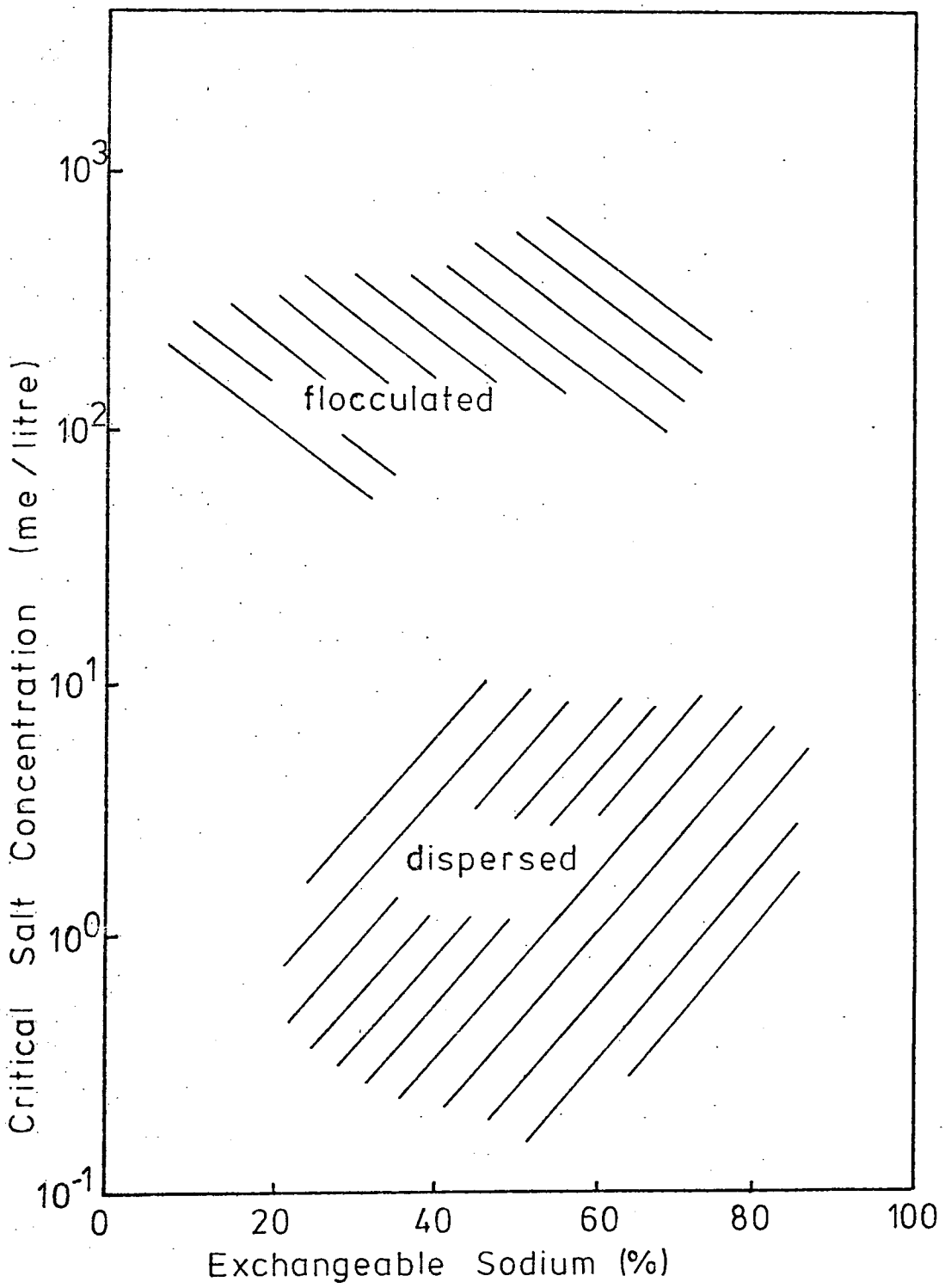

Figure 1.20. Influence of Exchangeable Sodium on Critical Salt Concentration Values in Ca/Na Clay Systems (After Arora,1969; Moriwaki, 1974).

of 19Å occurs in the Ca-form (Norrish and Quirk, 1954). By studying Na/Ca montmorillonite systems, this behaviour can be accounted for by the domain concept (Aylmore and Quirk, 1959) and the concept of demixing of cations (Fink et al, 1971). According to the latter authors, with an ESP 50 per cent random mixing of Na and Ca cations occurs and there is unlimited swelling between all the plates when water is added. As the ESP is reduced from 50 to 10 per cent there is progressively more demixing on the interlayer exchange sites with progressively more sets of plates collapsing to a 20Å repeat spacing. With an ESP of 10-15 per cent the interlayer exchange sites are predominantly Ca saturated and Na ions occupy external planar and edge sites.

Physico-chemical aspects of swelling have been reviewed by Mitchell,(1973). By varying the electrolyte concentration and ESP the effect on the swelling potential of illite (Rowell et al, 1969) and montmorillonite (Rowell, 1963) are shown in Figures 1.21 and 1.22 respectively. In both cases the pure Ca-form appears to be nearly independent of the former variable.Emerson (1962), however, concludes that the swelling of orientated Ca-montmorillonite gradually increases as the electrolyte concentration is reduced.

Emerson (1964) has suggested that on a macroscopic scale the pressure of entrapped air will be lower in swelling materials (than in non-swelling materials) because a larger amount of additional water absorbed is used to swell the already wet regions and not in occupying new pore space. Consequently, montmorillonite, with small flexible plates, should have a lower entrapped air pressure than either illite or kaolinite.

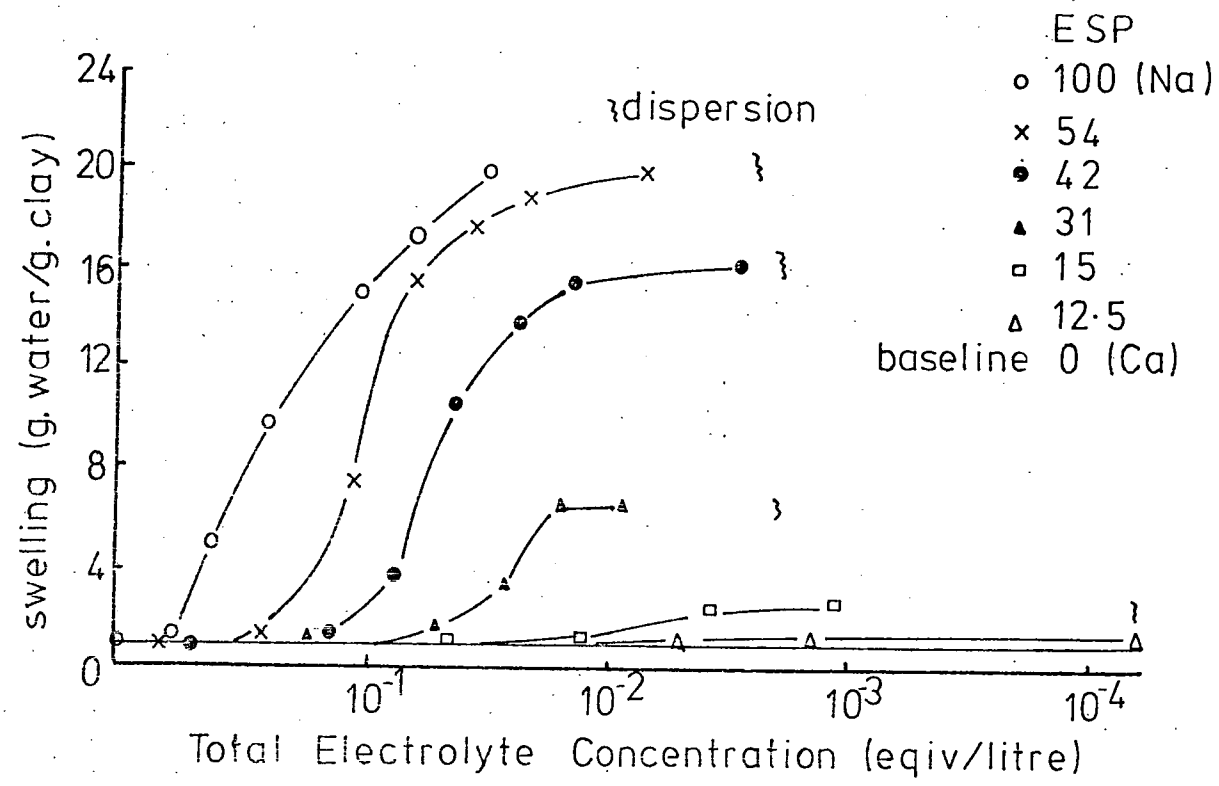

Figure 1.21. Effect of Total Electrolyte Concentration on the Swelling of Mixed Na-Ca Montmorillonite Aggregates (After Rowell, 1963).

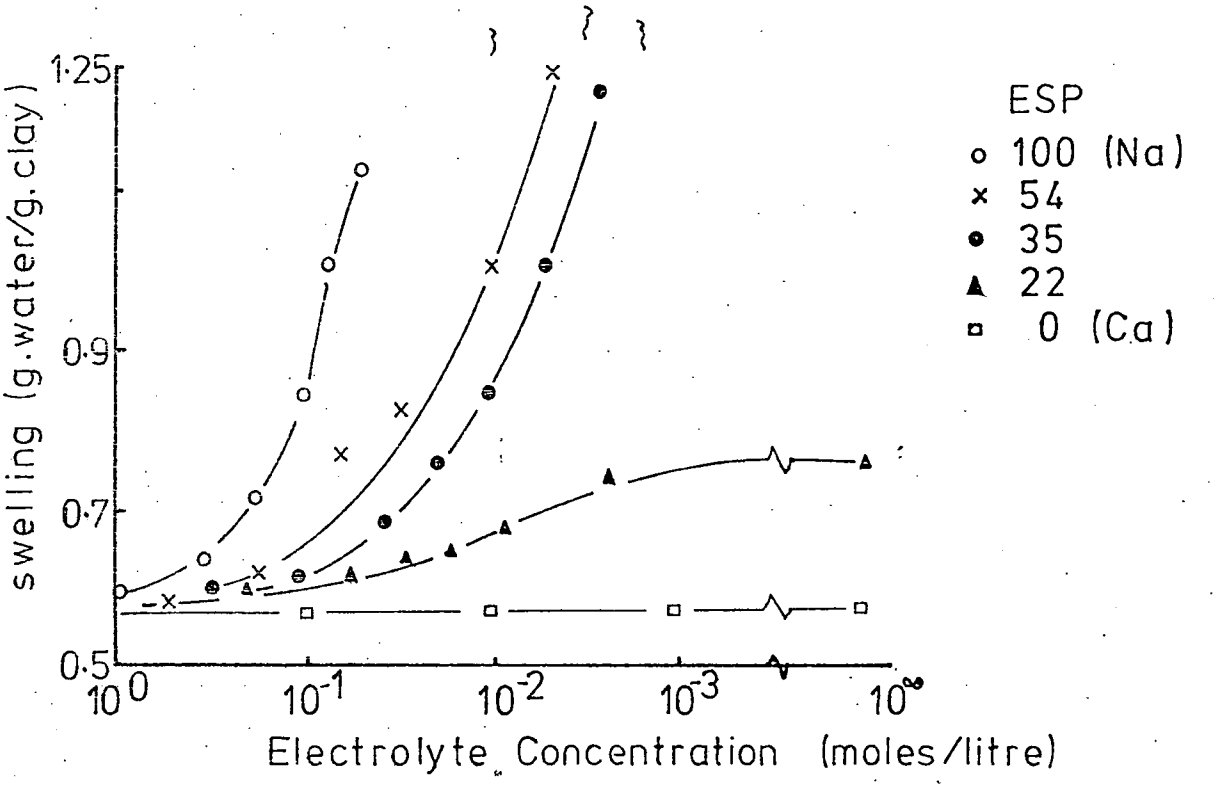

Figure 1.21. Effect of Electrolyte Concentration on the Swelling of Mixed Na-Ca Illitic Aggregates (After Rowell et al, 1969).

1.7.3 Slaking Behaviour of Natural Clays and Shales

Natural clays and shales, in addition to being polymineralic, have additional complicated structural features such as fissility, jointing and slikensiding and diagenetic bonding which makes studying their slaking behaviour a fairly difficult task. As a consequence of this a suitable classification based on their engineering properties has not yet been well established (Underwood, 1967; Morgenstern and Eigenbrod,1974).

According to many workers (e.g. Nakano, 1967; Nordquist and Bauman, 1967; Kennard et al, 1967; Grice, 1968) natural materials at in situ moisture contents do not slake in water; a fact which has also been noticed by the present writer. Nakano (1967) has indicated the existence of a critical relative humidity (CRH) as he found that samples did not slake if they were kept at a relative humidity of greater than 94 - 98 per cent before immersion. Furthermore when equilibrated to drier conditions than their natural state, all the materials had a greater tendency to disintegration in water which may be attributed to air breakage and clay mineralogy (Taylor and Spears, 1970). Van Eeckhout (1976) shows that the strength of coal mine shales is severely lowered by humidity fluctuations, and results from expansion-contraction characteristics lengthening internal cracks and from the lowering of fracture energy with increased moisture. In fact Johns et al (1963) have actually used humidity control in the field to prevent disintegration. However, when studying the storage and drying effect of samples of Oxford and Weald Clays on slaking durability values, Franklin and Chandra (1972) found that slaking was reduced for samples with lower initial moisture content. In addition, oven-drying did not change the effect of moisture content variation on the slaking behaviour. Van Eeckhout (1976) further

shows that at humidities of less than 60 per cent, the strength of coal mine shales is kept relatively high. Aughenbaugh (1974) suggests that it is not possible to correlate slaking behaviour of shales to their moisture content changes under various relative humidity conditions.

The effect of air evacuation on the slaking behaviour of illitic shales associated with British coal seams has been explored by Badger et al (1956), (Table 1.9). They report that slaking of the majority of shales tested increased with air evacuation and attribute this to the fact that removal of air from the pores permits more water to reach and attack a greater surface area by the use of the 'ionic dispersive force'. Only one sample, containing a relatively large amount of kaolinite showed a large reduction of slaking, particularly of the minus 10 μm and minus 5 μm particle sizes. Consequently they consider air breakage important in mechanically weak shales. However, no mention is made of the effect of reduction of initial moisture content as previously discussed. Taylor and Spears (1970) also note that breakdown is partially reduced in materials which contain relatively large amounts of kaolinite and chlorite.

A montmorillonitic mudstone, studied by Nakano (1967) showed a significant change in slaking behaviour upon air evacuation, although the percentage of small grains remained lower after slaking in vacuo.

By studying the physico-chemical factors associated with slaking behaviour, Badger et al (1956) show some correlation between exchangeable sodium and the degree of disintegration, (Table 1.10). They also note that high electrolyte concentrations of Na Cl and $CaCl_2$ significantly reduced slaking in the samples

Table 1.9. Effect of Air Evacuation on Slaking of Coal Shales (After Badger et al., 1956).

Shale	Kaolinite in shale, percent by weight	Percentage shale disintegration						Assessment of t test**
		-36 B.S. mesh		-10 μm		-5 μm		
		NE*	AE*	NE	AE	NE	AE	
Ryder	10 15	82.5	76.2	40.5	19.7	29.5	14.6	At all sizes there is a significant decrease after evacuation
Kingsbury	5	41.5	59.2	31.5	38.3	21.1	23.3	A significant increase after evacuation except at 5μ
Flaggy Delf	5	32.3	28.2	11.7	7.7	8.1	6.5	A significant decrease after evacuation at all sizes
Denby	5	19.7	22.0	6.7	12.1	--	10.3	No difference at -36 B.S. mesh; a significant increase at -10μ
Linby	5	11.7	15.6	8.0	8.3	6.6	6.6	No significant difference in the two sets of results except at -36 B.S. mesh
Llanharan	5	9.7	10.7	3.9	4.4	--	2.7	No significant difference
Rushy Park	5	5.4	6.2	3.2	4.4	2.9	3.5	In both shales there is a small significant increase at -10μ but at other size the NE and AE results are similar
Penalita	0	4.4	5.9	1.4	3.0	--	2.1	

note: * = The columns marked NE give the disintegration results without air evacuation. The values are a mean of 8 or 9 determinations. The columns marked AE give results of shale disintegration after air has been evacuated. The results are based on two determinations.

** = t test is a method of standard statistical hypothesis testing and is quite useful when comparing two means. Comparison of means of two normally distributed random variables, m_1 and m_2, can be done by testing:

H_0: $m_1 - m_2 = \Delta = 0$ against $H_1 = m_1 - m_2 = \Delta > 0$. (For details, e.g. Ehrenfeld and Littauer, 1964)

Table 1.10 Correlation of Exchangeable Ions and Disintegration (After Badger et al 1956)

Shale	Ion concentration, milli-equivalents per 100 g. shale		Percentage of $\frac{1}{4}$ in. to $\frac{1}{6}$ in. shale disintegrating.	
	Na^+	K^+	-36 B.S. mesh	-10 um
Ryder	15.0	5.0	82.5	40.5
Kingsbury	12.2	4.5	31.9	26.2
Flaggy Delf	9.5	7.2	32.3	11.7
Denby	9.0	6.4	19.7	6.7
Linby	8.5	4.8	11.7	8.0
Llanharan	6.2	5.1	9.7	3.9
Rushy Park	5.5	4.9	5.4	3.2

tested, although they conclude that the concentration necessary to completely suppress slaking is so large that no practical significance can be placed upon the results.

In general, liquids which have a high dielectric constant tend to give higher degrees of disintegration (Denisov and Reltov, 1961; Badger et al, 1956). Nakano (1967) concludes however, that because no reaction was observed with nitrobenzene (dielectric constant 36), it is the ability of a liquid to form hydrogen bonds with water which is important in slaking behaviour rather than the dielectric constant itself. He also establishs a relationship between swelling and slaking behaviour and suggests that the latter involves hydrogen bonding with the clay surfaces which releases excess free energy of the liquid ultimately causing destruction of the material.

Taylor and Spears (1970) conclude that breakdown of sandstones and siltstones is slow and is controlled by structures such as joints and stratification. They also note that mudstones and shales (including seatearths) breakdown rapidly, structure again playing an important role, although a simple pattern cannot be applied because of the range of mineralogy etc.; extreme members literally exploding when water is added to the desiccated material. They also conclude that a highly preferred orientation does not necessarily reduce breakdown in argillaceous shales whereas White (1961) suggests that non-fissile materials tend to disintegrate more in water.

Disintegration of shales by the formation of a polyagonal cracking pattern perpendicular to the bedding upon drying has been reported by Kennard et al (1967), who conclude that the feature is

formed as a result of tensile stresses created due to negative pore pressures.

The destruction of diagenetic bonding (Bjerrum, 1967a) leading to the release of locked in strain energy results in the slaking of overconsolidated shales after stress release. Under natural conditions these bonds are destroyed by weathering agents over long periods of time (Peterson, 1958), at rates which are dependent upon their own strength; a process which ultimately leads to an increase in swelling and associated higher moisture contents. Strong diagenetic bonding may only break down to a certain extent when the material is rapidly consolidated and rebounded in the laboratory under test conditions (Bjerrum 1969). However, when subjected to repeated cycles of loading and unloading (Bjerrum, 1969) or to repeated cycles of drying and wetting (Morgenstern and Eigenbrod, 1974), then it is quite possible that these bonds can be broken down and the resulting increase in moisture content can be measured. Consequently it is not surprising that cycles of wetting and drying generally cause a rapid breakdown of shales (Underwood, 1967) and that samples which do not break down appreciably upon the first cycle of the slaking durability test tend to fall apart after a number of cycles (Gamble, 1971).

Chapter Two

Geological Nature and Characteristics of the Samples Studied

2.1 General Information

Details of sample localities, present depths of burial, water table levels and how the samples were obtained, in addition to their coding (for future reference), are given in Tables 2.1 and 2.2. Areal distributions of the samples are shown in Figures 2.1 and 2.2.

2.2 Stratigraphy and Lithology

Stratigraphical distributions along with correlations of the British and North American strata are presented in Figure 2.3; local geological conditions being shown in Figures 2.4 and 2.5.

The general stratigraphical details for the British Isles were obtained from Rayner (1967) whilst for the North American materials, Dunbar and Waage (1969) was consulted.

The rock materials investigated are briefly described below on a lithological basis starting with the oldest types sampled in the respective geological successions of the two countries.

2.2.1 British Materials

2.2.1.1. Carboniferous Deposits

Swallow Wood roof	(Westphalian B)	(sample SWR, Table 2.1)
Flockton Thin roof	(Westphalian A)	(sample FTR, Table 2.1)
Flockton Thin seatearth	(Westphalian A)	(sample FTS, Table 2.1)
Widdringham roof	(Westphalian A)	(sample WR, Table 2.1)

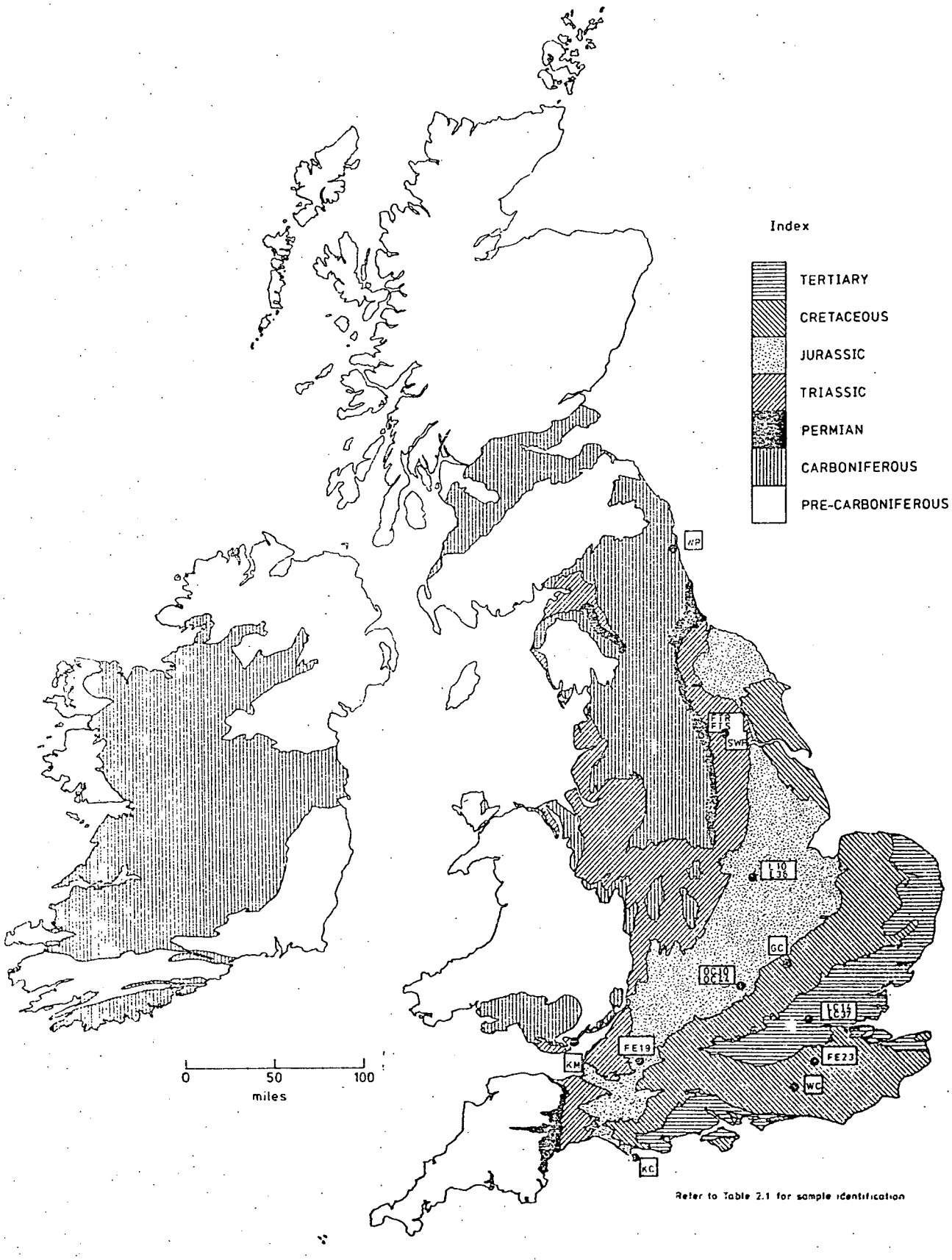

Figure 2.1. Areal Distribution of British Samples.

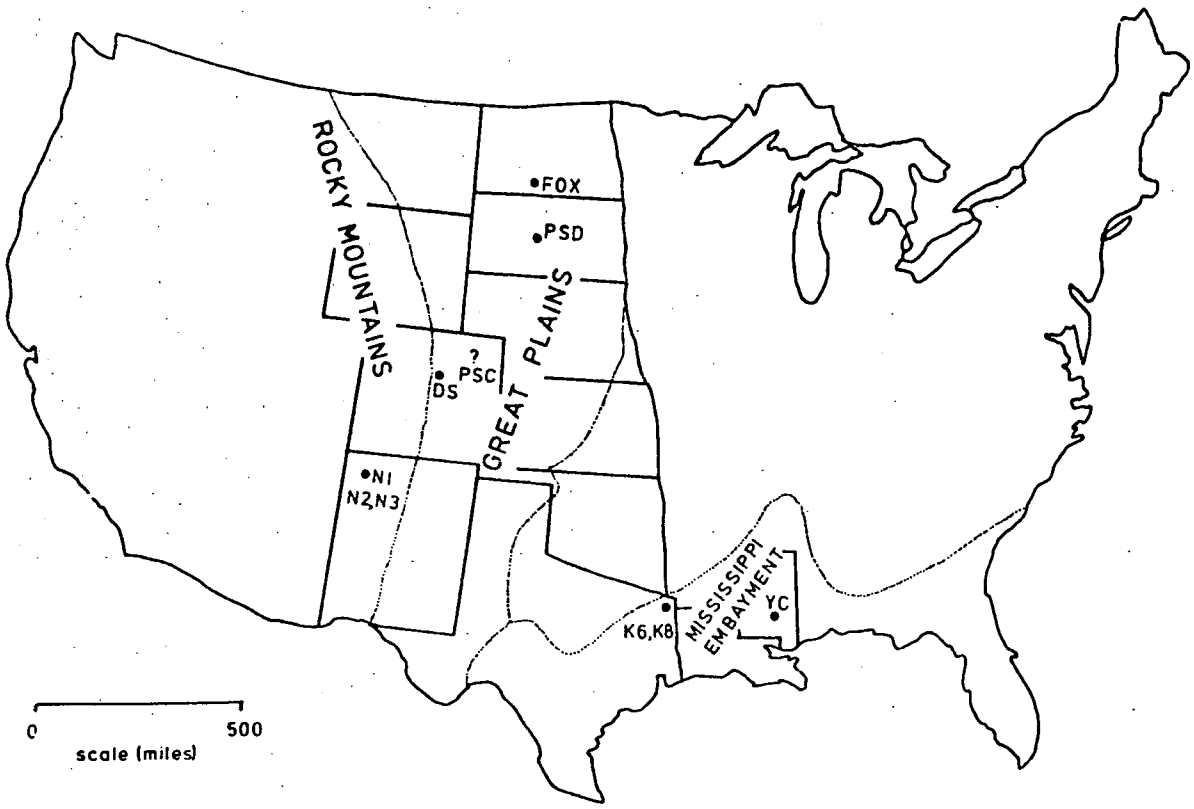

Refer to Table 2.1 for sample identification

Figure 2.2. Areal Distribution of North American Samples.

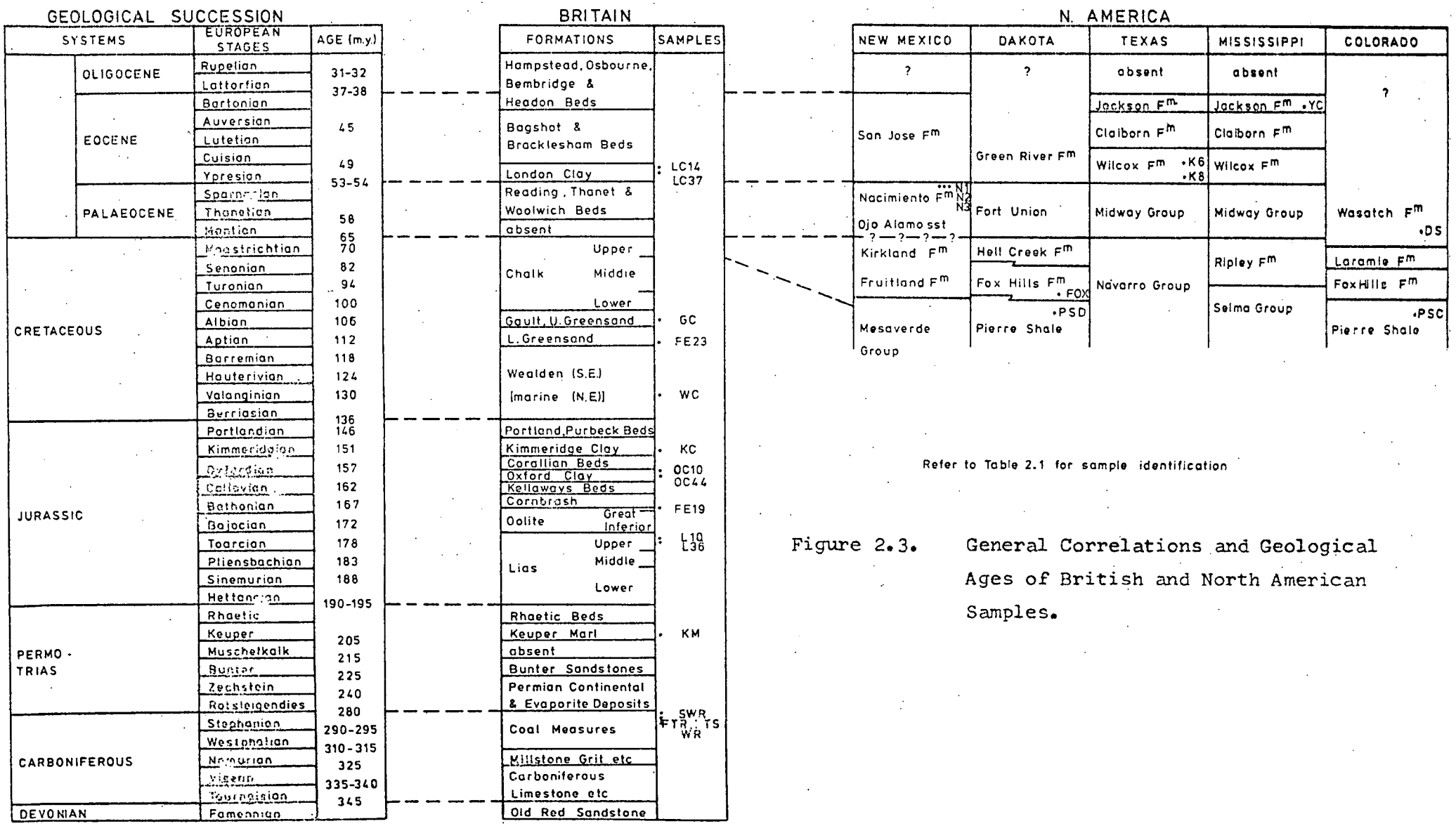

Refer to Table 2.1 for sample identification

Figure 2.3. General Correlations and Geological Ages of British and North American Samples.

These are the oldest rocks investigated and are the products of deposition in low-lying, non-marine, paralic conditions, which tended to produce cyclic deposits in the general sequence: mudstone-siltstone -sandstone-seatearth-coal.

The three roof shales are hard and mildly indurated, commonly showing a marked fissility. The Widdringham roof (sample WR) is the weakest by virtue of the fact that it contains carbonaceous partings.

Highly polished listric surfaces together with occasional root remains, are present throughout the seatearth, endowing the specimen with a relatively weak strength and the facility to crumble easily.

2.2.1.2 Triassic Deposits

Keuper Marl (sample KM, Table 2.1)

The Keuper Marl was laid down in saline basins of inland drainage under hot, arid, oxidising conditions such that haematite gives the rock a general red colouration. Local green patches are probably the result of later periods of reduction, rather than local variations in the conditions of deposition. The material itself is composed of a silty-clayey matrix surrounding angular, non-uniform grains of quartz, carbonate and (?) evaporite.

2.2.1.3 Jurassic Deposits

Kimmeridge Clay	(Kimmeridgian)	(sample KC, Table 2.1)
L. Oxford Clay	(Oxfordian/ Callovian)	(samples OC10, and OC44). Table, 2.1)
Fuller's Earth	(Bathonian)	(sample FE19, Table 2.1)
U. Lias Clay	(Toarcian)	(sample L10, and L36, Table 2.1)

The Kimmeridge Clay, Oxford Clay and Lias Clay are typical of the heavy clays which were deposited under the widespread shelf sea conditions which prevailed throughout most of the period, particularly in the southern part of Britain.

The deeper samples of the Oxford and Lias Clays (i.e. samples OC44 and L36 (Table 2.1) respectively) are very firm and fine grained, although the former is noticeably coarser. They also show a marked fissility by splitting along well developed planes, sub-parallel to the bedding. The samples of Oxford and Lias Clay from shallow depth (i.e. samples OC10 and L10 (Table 2.1) respectively) and the Kimmeridge Clay (sample KC, Table 2.1) which is from 10m depth, are noticeably softer, although the Lias Clay has still retained a moderate fissility. The Oxford Clay shows traces of iron staining, highly disturbed bedding and occasional listric surfaces indicating that it is in an advanced state of weathering. The Kimmeridge Clay contains occasional faintly polished surfaces.

The Fuller's Earth, (sample FE19, Table 2.1) from the Retrocostatum Zone of the Middle Jurassic Bathonian beds probably represents a devitrified volcanic ash deposit (Hallam & Sellwood, 1968) laid down under marine conditions. It occurs as a band 2m in thickness in the Fuller's Earth Clay of the Coombe Hay area near Bath. The lower 1.6m, from which the sample was taken, is nearly pure calcium montmorillonite. In the unweathered condition it is blue-grey in colour but quickly weathers to a yellow colour upon exposure to air. The material has a soapy texture, with laminations and a conchoidal fracture.

2.2.1.4 Cretaceous Deposits

U. Gault Clay (Albian) (sample GC, Table 2.1)

Fuller's Earth (Aptian) (sample FE23, Table 2.1)

U. Weald Clay (Barremian) (sample WC, Table 2.1)

The Cretaceous Period is characterised initially by non-marine conditions to the south of the London Platform and marine conditions in Yorkshire. Subsequently widespread marine conditions were established over the whole of Britain under which the Chalk was deposited.

The Weald Clay specimen (sample WC, Table 2.1) was laid down as a fresh water deposit (Allen, 1959) at the top of a rhythmic series of sediments involving the interaction of lacustrine and deltaic conditions. The material itself is very hard, silty clay containing very thin, irregularly spaced, non-uniform bands of hard and soft material, the former containing large quantities of quartz, often in lenticular masses.

The Gault Clay (sample GC, Table 2.1) is a stiff, unbedded clay from 30m below the base of the Chalk and contains up to 30 per cent calcium carbonate which appears to be present in the form of coccoliths.

The Cretaceous Fuller's Earth, (sample FE23, Table 2.1) from the Sandgate Beds in the Redhill-Reigate area, has the same characteristics as the Jurassic deposit, and is probably of similar origin. It has been described by various authors (e.g. Hallam & Sellwood, 1968; Dines & Edmunds, 1933). The deposit consists of several seams of nearly pure calcium montmorillonite alternating with sandy glauconitic limestones in a lenticular mass, up to 21.5m thick, of which the principal seam is nearly 2.5m thick.

2.2.1.5 Tertiary Deposits

London Clay (Ypresian) (samples LC14 and LC37, Table 2.1)

Tertiary deposits in mainland Britain are limited to the London

and Hampshire basins; the London Clay being laid down as the second marine transgression into these areas. The deposit is relatively uniform in character, being a brown clay with sandy partings.

The specimen from 37m depth (sample LC37, Table 2.1) is a stiff fissured clay from the unweathered "blue" London Clay zone. It has frequent sandy partings and a gritty texture, indicating a high quartz content. The specimen from 14m depth (sample LC14, Table 2.1) is from the transition zone between the "blue" and "brown" (weathered) London Clay. It is moderately stiff with a very fine-grained texture.

2.2.2 North American Materials

2.2.2.1 Cretaceous Deposits - Western Interior

Pierre Shale (Campanian) (samples PSD & PSC, Table 2.2)

Fox Hills Shale (Maastrictian) (sample FOX, Table 2.2)

The Cretaceous deposits of the Western Interior (Fig.2.2) were laid down in the Rocky Mountain geosyncline which was occupied by a vast epicontinental sea covering the whole of North America from the Gulf Embayment to the boreal sea in the Mackenzie Delta region of Canada. The deposits are characterised by decreasing amounts of non-marine, and relatively coarse-grained material in an easterly direction from the foothills of the Rocky Mountains (Tourtelot, 1962).

The Pierre Shale(which correlates with the Bearpaw and Claggett formations from other areas)is the most widespread deposit in this region. The sample from South Dakota, from the Verendyke member (sample PSD, Table 2.2), is a very fine-grained material containing a high proportion of montmorillonitic minerals which were derived from the volcanic activity in the western highlands according to

Tourtelot (1962). The material may be identified with the eastern facies of shales and marlstones.

The Pierre Shale from Colorado (sample PSC, Table 2.2) is a coarser, silty material which may be identified with the western facies of alternating marine shales and sands (Tourtelot, 1962). Weimer and Land (1975) suggest that the deposits in Colorado are either those of a pro-delta or deeper neritic facies, depending upon the area of deposition.

Sample (FOX) shown in Table 2.2, is from the Fox Hills Shale from North Dakota. It is a non-fissile, moderately stiff, dark brown clay containing abundant organic matter, coming from a non-marine deltaic sequence which is characterised by cross-bedded sandstones and dark coloured shales (Weimer and Land, 1975).

2.2.2.2 Tertiary Deposits - Eastern Rockies

Dawson Shale	(Palaeocene)	(sample DS, Table 2.2)
L. Nacimiento Shale	(Palaeocene, Puerco Unit)	(samples N1, N2 & N3 Table 2.2)

These deposits from the Eastern Rockies occur in basins of rapid deposition and erosion as a result of the orogenic phase which produced the Rocky Mountains.

The Dawson Shale occurs in the Denver Basin of Colorado (Brown, 1943) and has a lithology which is very variable, but is broadly that of a terrestial river or stream-laid arkosic deposit of sandstones, siltstones and claystones containing andesitic lenses. Correlation is difficult because of the lack of marker bands, but it is believed that the lower 170m are of Cretaceous age whilst the remainder are Palaeocene.

The Nacimiento Shale occurs in the San Juan Basin, New Mexico

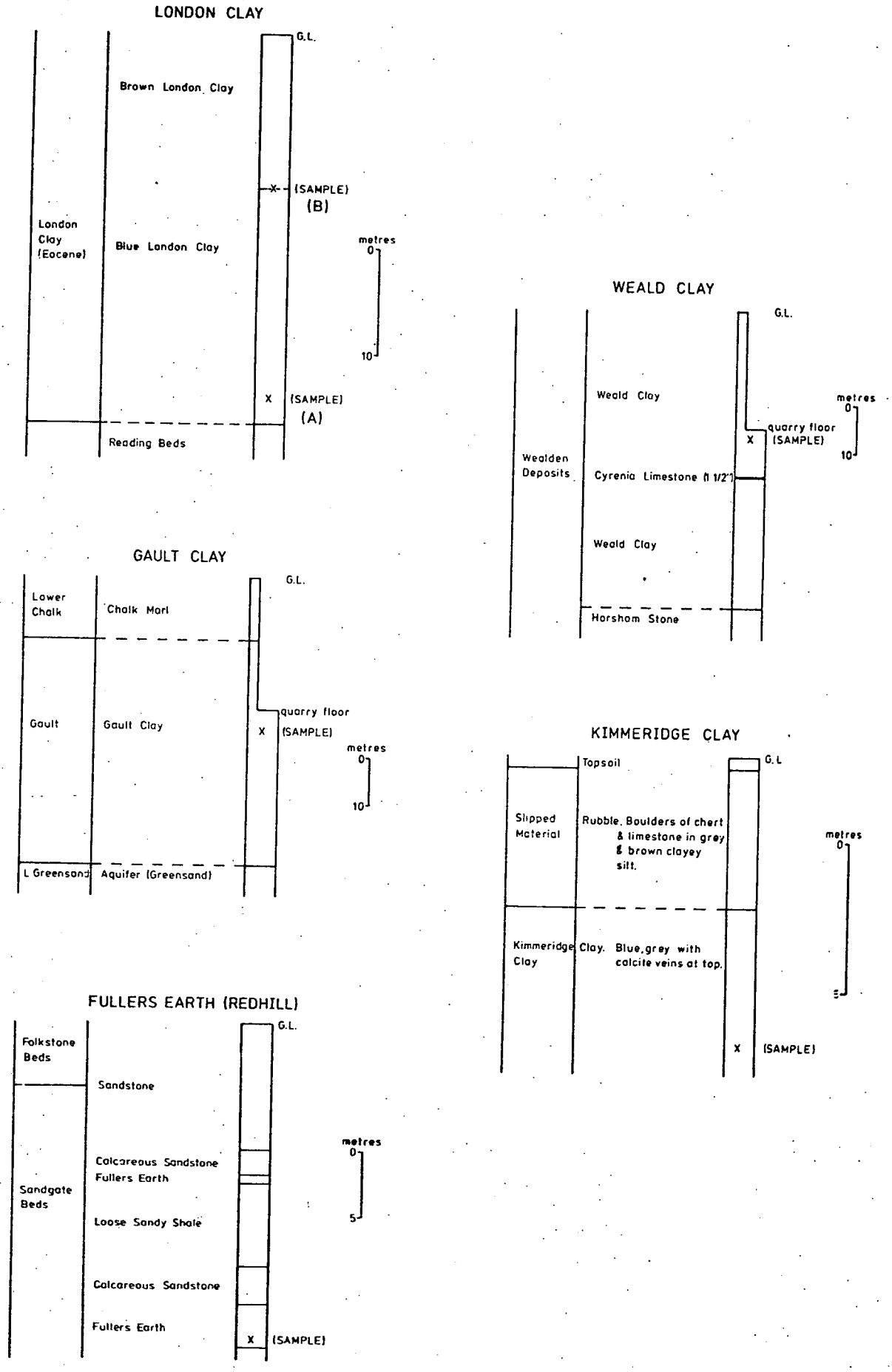

Figure 2.4. Local Geology Surrounding British Samples.

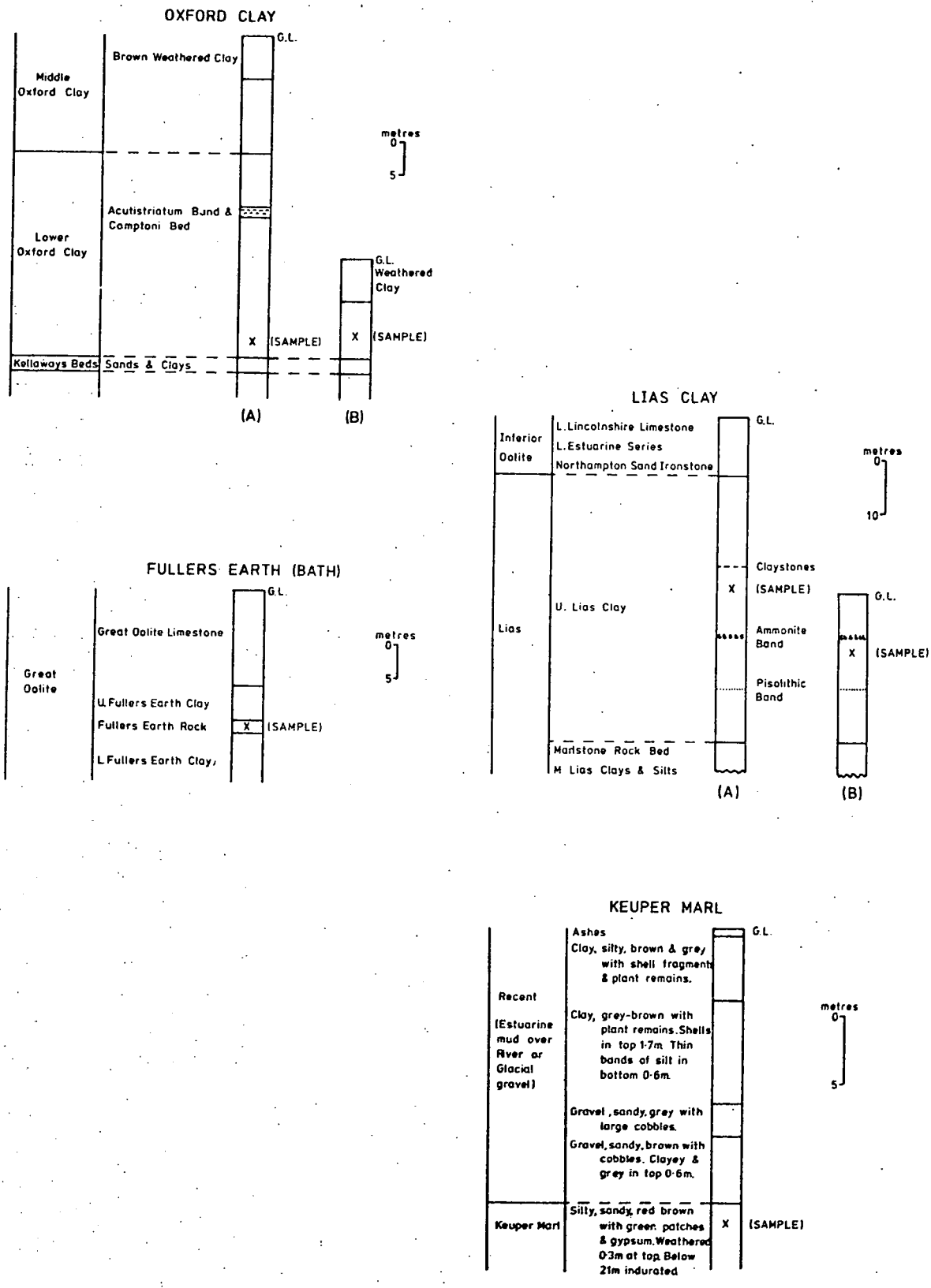

Figure 2.4. continued.

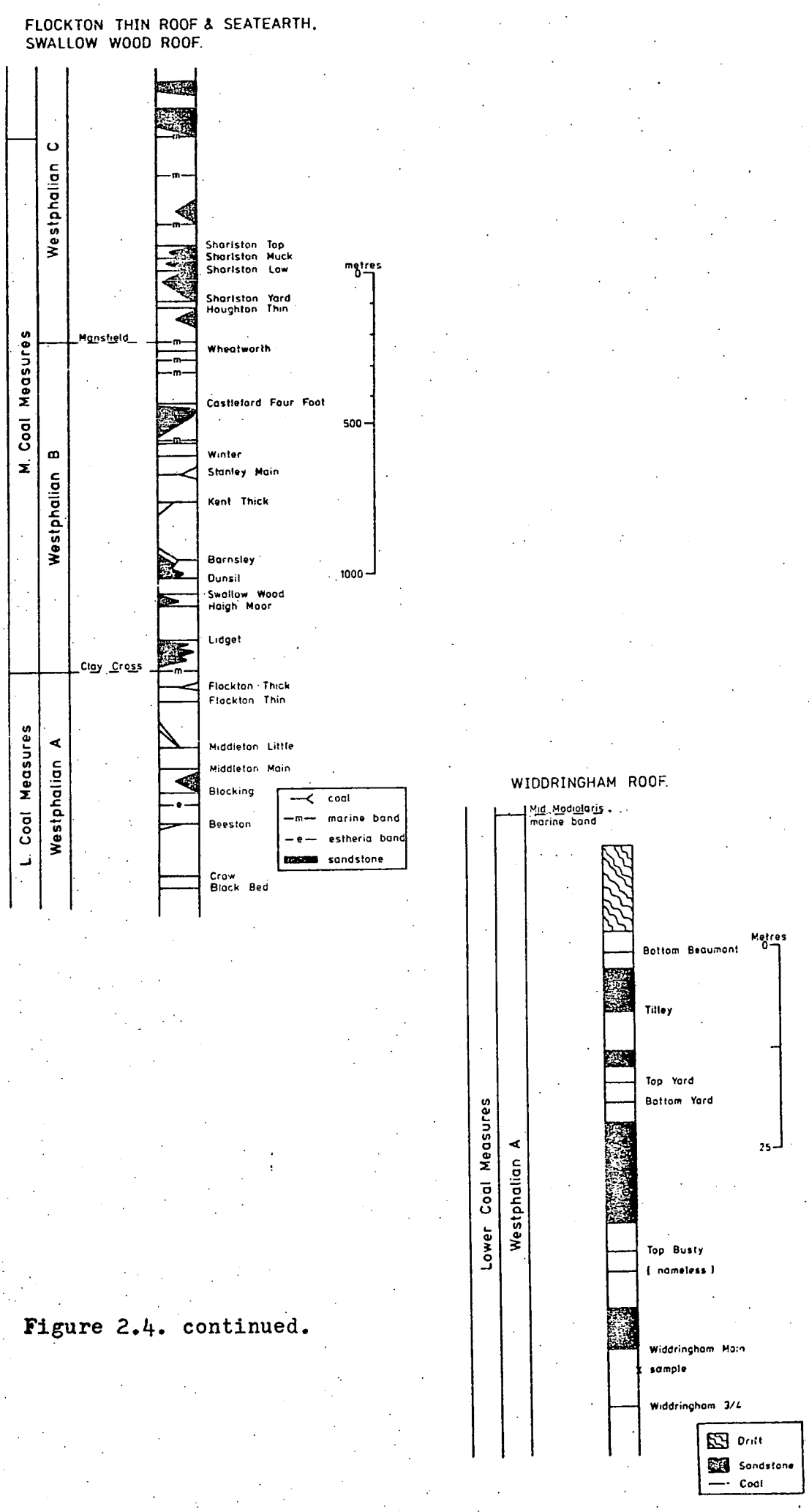

Figure 2.4. continued.

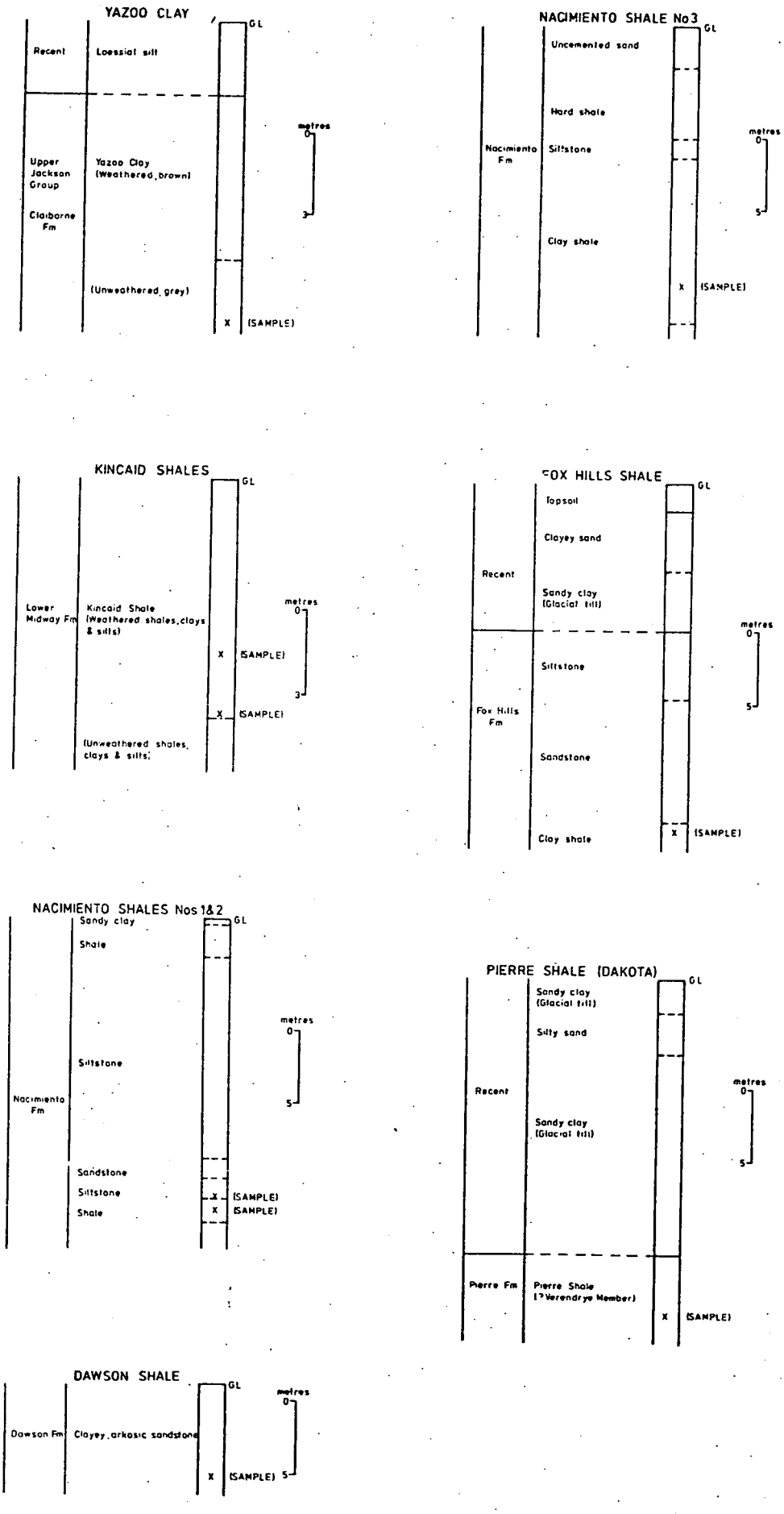

Figure 2.5. Local Geology Surrounding North American Samples.

(Baltz, 1967) and also consists of terrestial stream-laid sandstones and siltstones with interbedded shales containing much volcanic debris. Specimens N1 and N2 consist of hard, clayey siltstones whereas specimen N3 is a stiff, dark clay.

2.2.2.3 Tertiary Deposits - Mississippi Embayment

Yazoo Clay (Jackson Formation) (sample YC, Table 2.2)

Kincaid Shale (Midway Formation) (samples K6 & K8, Table 2.2)

A shallow sea has occupied this area since the late Jurassic Period and thick deposits have been laid down in a slowly sinking basin which has a central axis running in a north-south direction through the states of Mississippi and Louisiana.

The Kincaid Formation, from the base of the Midway Formation (Cushing et al, 1964) consists of glauconitic sands, clays and limestones, all of marine origin. The two samples investigated (samples K6 and K8, Table 2.2) are both weak, silty, weathered clays having a yellowish colouration with interdispersed greyish areas. Fossil debris is common throughout both materials.

The Yazoo Clay, from the Jackson Formation, is considered by Monroe (1954) to be a marine deposit laid down fairly close to the shore in a region where large amounts of material were brought into the sea by a large river, or several rivers. The material (i.e. sample YC, Table 2.2) itself is a soft, blue-grey fat clay with patches of brown colouration.

2.3 Estimation of the Maximum Overburden Thicknesses of Strata

Three methods were used to estimate the maximum probable thicknesses of strata which have overlain the samples studied in this project, the results of which are summarised in Tables 2.3 and 2.4. No account has been taken of the weight of ice cover during the

Table 2.1 General Location Details for British Samples

Sample	Location	Grid Ref.	Depth (m)	How Obtained	Water Level (m)	Overburden Pressure (kN/m^2)	Sample Ref.
London Clay 14m	Regent Park, London.	280830	14.5	Borehole	3 - 5m	194.1	LC37
London Clay 37m	Regent Park, London.	280830	37.0	Borehole	3 - 5m	433.0	LC14
Gault Clay	Nr. Letchworth, Herts.	185350	4.0	Quarry	-	81.4	GC
Fuller's Earth(Redhill)	Redhill, Surrey.	29955005	23.0	Quarry	-	(?)399.1	FE23
Weald Clay	Warnham, Nr. Horsham, Sussex.	352174	3.0	Quarry	-	71.2	WC
Kimmeridge Clay	Portland Naval Base, Dorset.	696740	9.5	Borehole	-	195.2	KC
Oxford Clay 10m	Calvert, Bucks.	685235	10.6	Borehole	6.1	151.0	OC10
Oxford Clay 44m	Calvert, Bucks.	685235	44.0	Borehole	6.1	507.0	OC44
Fuller's Earth (Bath)	Coombe Hay, Nr. Bath, Avon	734615	19.5	Mine	-	380.5	FE19
Lias Clay 10m	Empingham, Leics.	023058	10.0	Tunnel	1.0	114.7	L10
Lias Clay 36m	Empingham, Leics.	053033	36.0	Tunnel	10.0	493.2	L36
Keuper Marl	Cardiff Docks, Gwent	194745	22.0	Borehole	5.79		KM
Swallow Wood roof	Scalm Park, Selby, Yorks.	565328	317.0	Borehole	3.0	4352.3	SWR
Flockton Thin roof	Selby Common, Yorks.	5893933405	593.0	Borehole	3.0	8141.7	FTR
Flockton Thin seat	Selby Common, Yorks.	5893933405	595.0	Borehole	3.0	8169.2	FTS
Widdringham roof	Chesterhouse Farm, Northumberland.	424130602394	63.0	Borehole	10 - 12	913.0	WR

Table 2.2 General Location Details for North American Samples

Sample	Location	Grid Ref.	Depth (m)	How Obtained	Water Level (m)	Overburden Pressure (kN/M^2)	Sample Ref.
Yazoo Clay	Clinton Inst., Jackson Mississippi.	BH No.1	10.0	B/H	Not known	176.5	YC
Kincaid Shale 6m	Cooper Dam, Texas.	BH No.U-24	5.79	B/H	Not known	110.6	K6
Kincaid Shale 8m	Cooper Dam, Texas.	BH No.U-24	7.92	B/H	Not known	149.9	K8
Nacimiento Shale	Navajo Indian Res., Tunnel No.5, San Juan, New Mexico.	N.2032910 E.392444	18.5	B/H	-	399.1	N1
Nacimiento Shale	As above.	N.2032910 E.392444	19.2	B/H	-	420.7	N2
Nacimiento Shale	As above.	N.2037474 E.387839	17.0	B/H	-	366.7	N3
Fox Hills Shale	Lontree Damsite, N. Dakota.	N.250953 E.2125596	23.1	B/H	4.6	224.5	FOX
Dawson Shale	Chatfield Damsite, Littleton, Colorado.	DH.174	6.09	Cutting	-	129.4	DS
Pierre Shale	Medicine Creek Siphon, Oahe Dam, S. Dakota	DH.72-273(DN)	23.16	B/H	2.5	228.5	PSD
Pierre Shale	Fort Carson, Colorado	BH BOQ-3	11.0	B/H	Not known	257.8	PSC

Pleistocene, tectonic forces, groundwater fluctuations and the stresses due to freeze-thaw cycles, as these factors cannot be quantified. The three methods employed were:-

2.3.1 Summation of Thicknesses from the Literature

The probable thicknesses overlying the British strata (Table 2.5) were obtained from Strahan et al (1916), Dines and Edmunds (1933), Welsh and Crookall (1935), Arkell (1947), Sherlock (1947), Chatwin (1947), Edmunds (1947), Wilson (1948), Chatwin (1948), Larwood and Funnel (1970), Rayner and Hemingway (1974). The estimates for the samples from North America (Table 2.6) were obtained from Brown (1943), Bass and Northrop (1963), Cushing et al (1964), Robinson et al (1964), Underwood et al (1964), Baltz (1967), Varnes and Scott (1967), Hail (1968), Cooley et al (1969), Hilpert (1969), Fleming et al (1970), Shawe (1970) and Fasset and Hinds (1971).

2.3.2 Casagrande Construction

Where possible, the construction proposed by Casagrande (1936) has been used on the e - log P curves (Fig. 2.6) to estimate the preconsolidation loads (See Tables 2.3 and 2.4). To do this, the point of maximum curvature on the compression limb was located visually (point C) and through this point a tangent (AB) and a line parallel to the pressure axis CD were inserted. The intersection of the bisectrix of the acute angle, formed by this pair of lines, and the projection of the virgin consolidation curve was considered to represent the preconsolidation load (P_c).

Although the oedometers used could simulate depths equivalent to 2100 - 2500m of sedimentation (35000kN/m^2), a limiting value for

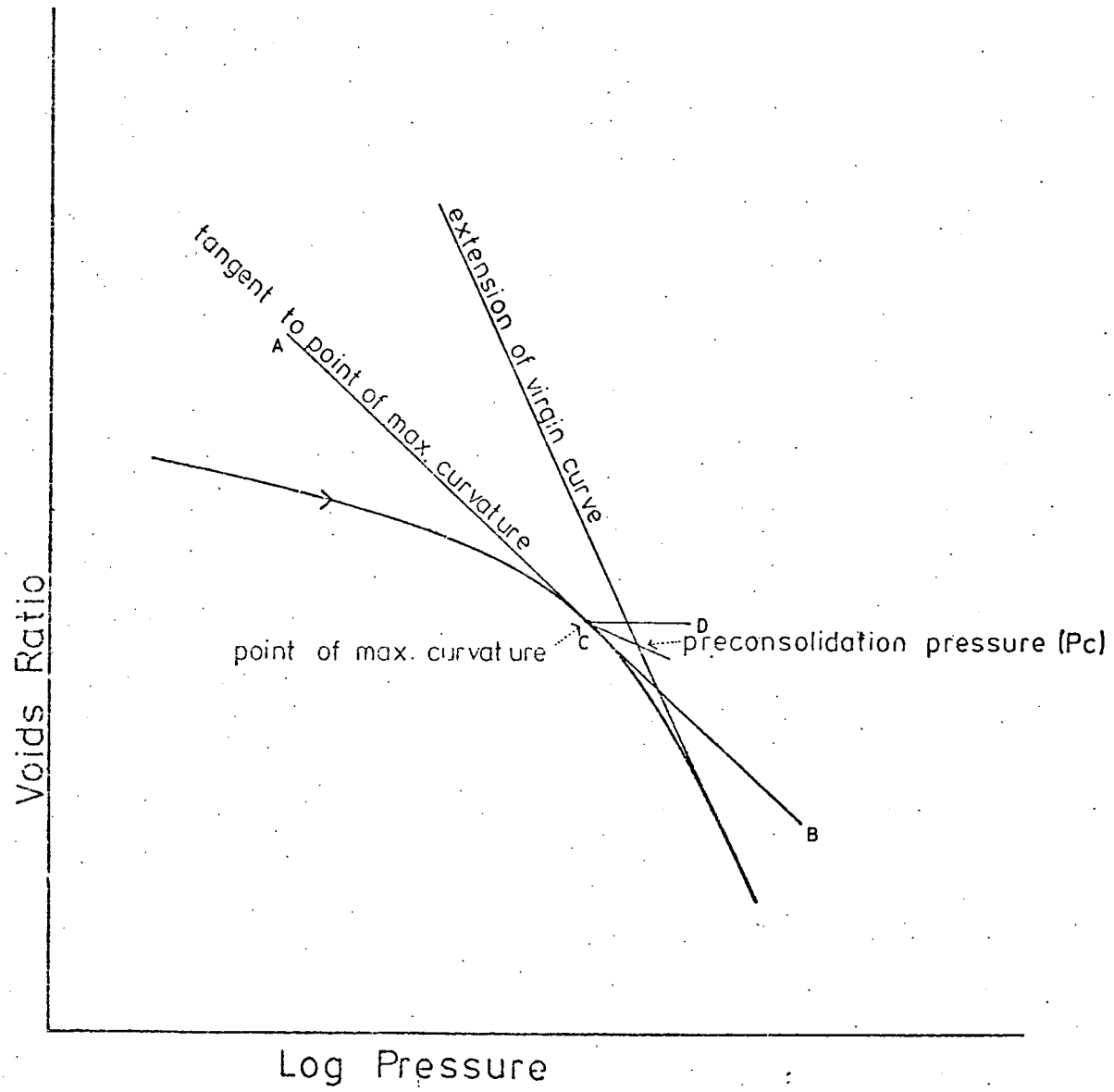

Figure 2.6. Casagrande Construction.

Figure 2.7. Interpretation of the Maximum Burial Depth from Rebound Characteristics.

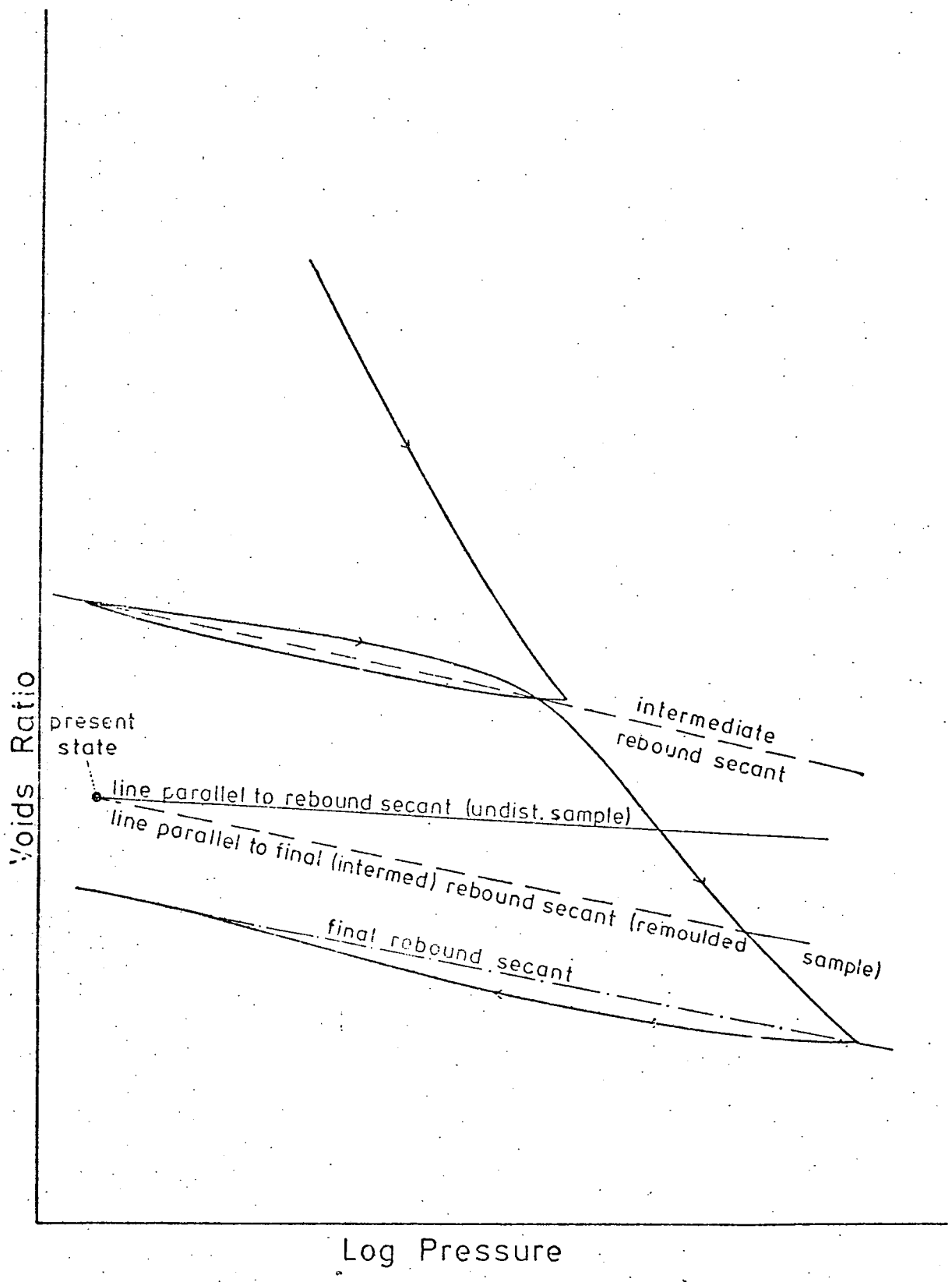

the preconsolidation load of 1050 - 1200m (14000 - 15000kN/m^2) was found to operate[1]. Hence the maximum depths of clays buried to greater depths were not estimated by this method.

2.3.3 Rebound Characteristics using Undisturbed Samples

From the consolidation test data for undisturbed specimens a line whose gradient was equivalent to the average swelling index was projected through the point which represents the present day overburden/voids ratio of the sample, i.e. calculated for the location and present topography from which the sample was taken. Where this projected line met the corrected[2] e - log P compression curve for the same specimen in its remoulded state, the intersection was taken as being equivalent to the preconsolidation pressure (See Fig.2.7). The maximum overburden pressures obtained are recorded in Tables 2.3 and 2.4 and further details relating to the technique are given in Chapter 5.

Altschaeffl and Harrison (1959) use a somewhat similar technique by projecting a line with a slope equivalent to the average remoulded swelling index and consider that the intersection of this with the remoulded compression curve represents the preconsolidation load. However, by reference to Chapter 5, it can be concluded that remoulding can sometimes enhance the swelling properties of the material, implying that the slope of the rebound

(1) As the applied pressure is doubled for each load increment, a preconsolidation load of less than 1200m allows at least two points to be plotted on the virgin curve.

(2) Correction of the remoulded e-log P curve necessitates adjusting the curve so that the voids ratios at the high pressures coincide with those of the virgin curve for the undisturbed sample. (See Section 5.8).

Table 2.3 Estimated Maximum Burial Depths of British Materials

Sample	Sample Ref.	Per Casagrande Construction	Per Literature		Per Rebound Characteristics		
					Undisturbed Samples	Remoulded Samples	
						Intermediate unloading stage	Final unloading stage
		P_c	(m)	(kN/m^2)	(kN/m^2)	(kN/m^2)	(kN/m^2)
London Clay 14m	LC14	5146	190 - 396	2048 - 4272	3814	3728	3814
London Clay 37m	LC37	6784	210 - 396	2264 - 4272	5774	5388	7789
Gault Clay	GC	8346	425 - 520	4582 - 5606	10148	7104	8157
Fuller's Earth (Redhill)	FE23	7104	610 - 760	6576 - 8193	7638	4932	7104
Weald Clay	WC	13229	1220 - 1370	13153 - 14770	15906	15191	15200
Kimmeridge Clay	KC	13229	1070 - 1220	11535 - 13152	10748	8541	12631
Oxford Clay 10m	OC10	9536	850 - 945	9164 - 10188	6478	5030	4586
Oxford Clay 44m	OC44	14504	850 - 945	9164 - 10188	14847	16279	24635
Fuller's Earth (Bath)	FE19	9583	760 - 885	8194 - 9541	10032	14847	35609
Lias Clay 10m	L10	14847	885 - 975	9541 - 10511	11003	7612	8943
Lias Clay 36m	L36	14847	885 - 975	9541 - 10511	17436	26400	31009
Keuper Marl	KM	-	1100 - 1990	11859 - 21454	-	-	-
Swallow wood roof	SWR	-	3050 - 3810	38860 - 48544	87575	214577	514671
Flockton thin roof	FTR	-	3050 - 3810	38860 - 48544	77897	135336	186823
Flockton thin seat	FTS	-	3050 - 3810	38860 - 48544	40000	59096	77897
Widdringham roof	WR	-	3050 - 3810	38860 - 48544	63323	112584	151910

Table 2.4 Estimated Maximum Burial Depths of North American Materials

Sample	Sample Ref.	Per Casagrande Construction	Per Literature		Per Rebound Characteristics		
					Undisturbed Samples	Remoulded Samples	
						Intermediate unloading stage	Final unloading Stage
		P_c (kN/m^2)	(m)	(kN/m^2)	(kN/m^2)	(kN/m^2)	(kN/m^2)
Yazoo Clay	YC	1868	120 - 150	1293 - 1617	1591	1322	1322
Kincaid Shale6m	K6	3479	420 - 550	4528 - 5929	53883	2691	3995
Kincaid Shale8m	K8	6046	420 - 550	4528 - 5929	3400	2246	3400
Nacimiento Shale	N1	-	1220 - 1530	13152 - 16495	26400	32470	41836
Nacimiento Shale	N2	-	1220 - 1530	13152 - 16495	24076	25792	39041
Nacimiento Shale	N3	-	1220 - 1530	13152 - 16495	22987	35609	44827
Fox Hills Shale	FOX	6332	460 - 610	4959 - 6576	5387	3814	4380
Dawson Shale	DS	-	(?) 530	16495	22987	28283	53889
Pierre Shale (Dakota)	PSD	12062	760 - 915	8193 - 9864	10267	34795	34000
Pierre Shale (Colorado)	PSC	14504	?	-	18260	28283	64794

curve will be increased. Consequently, Altschaeffl and Harrison's intersection point will lead to enhanced values of the preconsolidation load.

The preconsolidation loads obtained by using the undisturbed swelling characteristics agree reasonably well with the values obtained by other methods (Tables 2.3 and 2.4). However, when the values determined from remoulded swelling characteristics are considered, it can be seen that for the final unloading stage only 11 out of the 25 samples have results which are in agreement with other methods; the remainder give higher values (Table 2.3 and 2.4). Values obtained using the intermediate unloading stage (See Fig. 2.7) during the tests on remoulded material follow the same pattern, (Tables 2.3 and 2.4), although their swelling characteristics tend to be less than those of the final stage, which is probably a reflection of the states of particle packing at the different pressures (i.e. the elastic and physico-chemical effects being greater at the higher pressure).

2.4 Assessment of the Accuracy of Estimated Maximum Depths of Burial

2.4.1 British Materials

Documentary evidence for the thicknesses of British strata is fairly complete, hence comprehensive compilations of overlying strata were readily obtained (Tables 2.5). However, possible inaccuracies arise where deep erosion has removed large amounts of strata.

The maximum recorded thicknesses of Tertiary and Recent strata down to the base of the London Clay, in the London basin, is about 244m (Strahan et al, 1916), whereas in the Hampshire basin the

thickness to the same horizon is over 610m. At the end of the Eocene epoch the S.E. corner of England was subjected to uplift and erosion, thus a considerable thickness of sediments may have been removed. From consolidation tests on the London Clay, maximum depths of about 420m (for the shallow sample, LC14) to 520m (for the deep sample, LC37), are indicated, which are confirmed by the rebound characteristics (Table 2.3). These depths are considerably greater than the measured thicknesses, but are supported by Bishop et al (1965), where a maximum depth of 366-396m was calculated, also using geotechnical methods. Fookes (1966) suggests that although these depths cannot be substantiated directly, it is possible that the Barton Beds at the top of the Eocene, which form the erosion surface, could have been considerably thicker than the present maximum of 15m (compared to 120m in the Hants Basin). Dr. G. Larwood (Durham University, personal communication) agrees with this statement and suggests that evidence of deep erosion may be found in the abnormal direction of the local rivers in the S.E. of England.

Because of deep erosion at the end of the Upper Cretaceous Period, large thicknesses of Chalk have been removed, thus making the estimation of burial depths of older strata uncertain. However, Dr. G. Larwood (personal communication) believes that a thickness of at least 300-360m has probably been removed from the Midlands and up to 600m from the West Country. These figures are confirmed by Jackson and Fookes (1974).

Measured thicknesses of strata from the Lower Jurassic Period to the Chalk in the Midlands and West Country are considered to be representative of the actual thicknesses of strata laid down. Therefore by assuming a thickness for the Chalk, reasonable estimations of the maximum depths of burial can be made for all the Mesozoic strata studied.

Depths obtained from Rayner (1967) indicate that maximum thicknesses to the base of the Jurassic are found in the Weald and Wessex basins where they are of the order of 2400 - 3000m (450 - 700m of Tertiary, 1200 - 1500m of Cretaceous, and 1200 - 1500m of Jurassic). Elsewhere the beds tend to be much thinner; the accumulated thicknesses of strata in the Midlands and West Country averaging about 900m to the base of the Middle Jurassic (1200m to the base of the Lower Jurassic). Even in the Yorkshire Basin, Attewell and Taylor (1970) only record a thickness of 1067m to the top of the Lower Lias.

The maximum recorded depths for these materials studied (i.e. samples from the L. Jurassic to the Chalk) using the consolidation parameters are in general consistent with the results obtained from the summation technique. In certain cases, however, (e.g. Gault Clay (GC), Oxford Clay (OC44) and Lias Clay (L36))geotechnical information indicates a greater depth than summated thicknesses, which may be caused by a possible underestimation of the assumed Chalk thickness in the Midlands. The slightly low results obtained from the consolidation parameters for the Oxford Clay (OC10) and the Kimmeridge Clay (KC) may be explained by the fact that these samples are from shallow depths and show some signs of disturbance (See Chapter 2.2.1.3.)

The total thickness of strata which existed above the Coal Measures rarely exceeded 2400 - 3050m in the British Isles (Rayner, 1967). This is indeed the case when considering the strata of Yorkshire where between 1370 - 2740m have been recorded (Table 2.5). In addition, the Carboniferous materials tested have also had between 850 - 1000m of Upper Carboniferous strata above them. However, as no exact figure could be arrived at for the maximum depths of burial, an average figure of 3800m (Table 2.5) has been proposed, which is

considered by the writer to be quite reasonable.

Because of the great depth of burial of the Carboniferous shales, preconsolidation loads, using the Casagrande construction could not be obtained. Nevertheless, by considering the rebound characteristics an indication of their values could be deduced, although only that of Flockton Thin seatearth (FTS) is in accordance with the measured depths. The remaining three samples give results of 4900m (for the Widdringham roof (WR)) and 6100 - 6700m (for the Flockton Thin roof (FTR) and Swallow Wood roof (SWR)), which are obviously far higher than could be reasonably expected. When the physical properties are considered, those of the seatearth, being crumbly and readily susceptible to slaking (Chapter 7) may be associated with the fact the coal directly above is often a good aquifer (Taylor and Spears, 1970), whereas, those of the roof are more akin to undurated sediments.

2.4.2 North American Materials

Documentary evidence relating to the thicknesses of the North American strata was not always readily to hand for the actual sample locations, therefore estimations often involved extrapolations from adjacent areas (Table 2.6).

Thicknesses of strata which once overlaid the American material tend to be very variable but on the whole are much greater than thicknesses overlying the British materials. In the Great Plains region and the Eastern Rockies, the Cretaceous strata forms an eastwards sloping wedge 6100m thick in the west which tapers off to 600m on the eastern side, whilst in the Mississippi Embayment, up to 2150m of strata were laid down. Tertiary strata occurring on the eastern slopes of the Rockies forms basin and apron deposits up to 3650m thick, whereas in the Great Plains, thicknesses are generally of the order of 600 - 950m. From a boring in Louisianna,

in the Gulf of Mexico, thicknesses of Tertiary strata in the Mississippi Embayment extend to depths of 7600 - 9100m.

The above thicknesses are reflected in the Tertiary and Cretaceous sediments studied. Preconsolidation loads and rebound characteristics (Table 2.4) indicate a maximum depth of burial of 760 - 910m for the Pierre Shale (Dakota, Sample PSD), and 460 - 610m for the Fox Hills Shale (sample FOX), which are both similar to the values obtained by Underwood et al (1964) and Fleming et al (1970). Data regarding measured thicknesses for these materials is not considered to be reliable because erosion has stripped material from vast areas of the central plains. In fact Fleming et al (1970) record a maximum measured thickness overlying the Pierre Shale of only 250m.

Although no information regarding the depth of burial was obtained for the Pierre Shale from Colorado (Sample PSC) the preconsolidation load and rebound characteristics suggest a maximum depth of burial of about 1050 - 1350m (Table 2.4).

Available literature concerning the N.W. area of the San Juan basin in New Mexico shows that at least 730 - 1530m of sediments (Table 2.6) have been recorded as occurring above the base of the Nacimiento Formation, from which horizon the samples were taken (Cooley et al 1969; Baltz, 1967; Fasset and Hinds, 1971). However, although no preconsolidation pressures were obtained to confirm this figure, the rebound characteristics indicate that a maximum thickness of 1650m may once have been present (Table 2.4).

No conclusive evidence was obtained from the literature regarding the maximum measured overburden on the Dawson Shale from the Denver basin because this deposit is the youngest remaining formation in the

area, and only 610m have been recorded by Brown (1943) and Varnes and Scott (1967). However in adjacent basins, thicknesses of equivalent formations ranging from 1520m (Bass & Northrop, 1963) to 3650m (Hail, 1968) have been recorded. Again, although no preconsolidation load could be determined (which indicates that a large thickness of overlying strata has been removed), the rebound characteristics imply a maximum possible thickness of 1500m (Table 2.4) which in the light of the above evidence does not seem unreasonable.

The preconsolidation load and rebound characteristics for the Yazoo Clay (YC) and Kincaid Shales (K6 and K8) from the Mississippi Embayment indicate maximum thicknesses of 120 - 150m and 430 - 550m respectively, which are in line with the recorded depths (Table 2.6) of other workers (e.g. Cushing et al, 1964).

2.5 Conclusions

(1) The maximum depth of burial for each sample has been assessed by up to three methods which involved:-

(a) A literature review.

(b) The use of the Casagrande construction on the compression e - log P curve of undisturbed samples.

(c) The use of rebound characteristics.

(2) In general, the thicknesses of British strata are much thinner than those of equivalent strata from the Eastern Rockies, Great Plains and Mississippi Embayment regions of North America. This is illustrated by a simple table, i.e.:-

	Britain	North America		
	Weald & Wessex Basins (m)	Rockies (m)	Great Plains (m)	Mississippi Embayment (m)
Tertiary	400 - 700	up to 3650	600 - 950	up to 9100
Cretaceous	1200 - 1500	-	600 - 6000	up to 2100
Jurassic	1200 - 1500			

(Max. thickness overlying Carb. strata is about 4000m.)

(3) In general, the greater thicknesses overlying the American samples are reflected in their maximum depths of burial, although certain samples have maximum depths which are compatible with British sediments.

(4) As a consequence of conclusions (2) and (3) it can be concluded that in general, that overburden does not increase systematically with age, although on a local scale this may be true if deposition is uninterrupted.

Table 2.5. Recorded Thicknesses of Strata Over British Materials.

London Clay

	m
Superficial	15 - 30
Barton Beds	12 - 15
Bracklesham Beds	12 - 20
Bagshot Beds	30 - 36
Claygate Beds	15 - 17
London Clay	106 - 137
	190 - 255

Geotechnical evidence, eg, Bishop et al, 1965) suggests 365-396m.

Gault Clay

Tertiary and Recent	30 - 91
Chalk	274 - 365
U. Greensand	0 - 6
Gault Clay	45 - 91
	349 - 553

Probable thickness 425-520m

Fuller's Earth (Redhill).

Recent	0 - 45
Bracklesham Beds	0 - 137
Bagshot Beds	18 - 24
Claygate Beds	8 - 9
London Clay	100 - 121
Reading Beds	15 - 20
Thanet Sands	3 - 4
Chalk	304 - 457
U.Greensand	9 - 18
Gault Clay	45 - 103
Folkstone Beds	37 - 76
Sandgate Beds	0 - 24
	539 -1038

Probable thickness 610-760m

Weald Clay

	m
Recent	0 - 45
Bracklesham Beds	15 - 24
Bagshot Beds	0 - 24
Claygate Beds	0 - 9
London Clay	91 - 146
Reading Beds	9 - 27
Thanet Sands	0 - 10
Chalk	304 - 457
U. Greensand	9 - 61
Gault Clay	45 - 91
Folkstone Beds	48 - 79
Sandgate Beds	15 - 45
Hythe Sands	30 - 91
Atherfield Beds	6 - 18
Weald Clay	121 - 426
	693 -1553

Probable thickness 1220-1370m

Kimmeridge Clay

Recent and Tertiary	31 - 243
Chalk	426 - 548
U. Greensand & Gault Clay	31 - 62
L. Greensand	15 - 62
Wealden	62 - 121
Purbeck	58 - 121
Portland	62 - 76
Kimmeridge Clay	457 - 487
	1142 -1720

Probable thickness 1070-1220m

Oxford Clay

Recent and Tertiary	30 - 106
Chalk	274 - 457
U. Greensand	0 - 6
Gault Clay	45 - 70
L. Greensand	21 - 67
Wealden	0 - 15
Purbeck	6 - 9
Portland	12 - 18
Kimmeridge Clay	30 - 38
Corallian	6 - 12
Oxford Clay	121 - 152
	545 - 950

Probable thickness 850-945m

Fuller's Earth (Bath)

	m
Recent and Tertiary	0 - 30
Chalk	426 - 548
U.Greensand	30 - 55
Gault Clay and L. Greensand	0 - 27
Wealden	-
Purbeck	-
Portland	-
Kimmeridge Clay	45 - 91
Corallian	0 - 36
Oxford Clay and Kellaways Beds	121 - 152
Cornbrash	6 - 8
Forest Marble	27 - 39
Great Oolite	0 - 33
Fuller's Earth Clay	39 - 128
	694 -1147
Inferior Oolite	6 - 15
U. Lias	9 - 82
M. Lias	30 - 76
L. Lias	0 - 152
Rheatic	0 - 30
Keuper Marl	365 - 487
	1104 -1989

Probable thickness to:
(a) Fuller's Earth 760-885m
(b) Keuper Marl 1100-1990m

Lias Clay

	m
Recent and Tertiary	30 - 61
Chalk	304 - 426
L. Cretaceous	76 - 106
Purbeck	-
Portland	-
Kimmeridge Clay	0 - 91
Corallian (Amphill)	0 - 6
Oxford Clay and Kellaways Beds	91 - 106
Cornbrash	0 - 3
Great Oolite	16 - 30
Inferior Oolite	15 - 70
U. Lias	6 - 76
	538 - 975

Probable thickness 885-975m

Carboniferous Samples

Tertiary and Recent	30 - 61
Chalk	426 - 548
L. Cretaceous	121 - 137
Kimmeridge Clay	182 - 213
Corallian	61 - 91
Oxford Clay	15 - 45
Callovian	12 - 55
M. Jurassic	91 - 243
U. Lias	45 - 128
M. Lias	0 - 43
L. Lias	24 - 243
Trias	365 - 670
Permian	304 - 609
Carboniferous	853 -1006
	2529 -4092

Probable thickness 3050-3810m

Table 2.6 Recorded Thicknesses of Strata Overlying North American Materials

Yazoo Clay

	m
Quaternary	31 - 62
Oligocene	45 - 62
Eocene	91 - 106
	167 - 230 Probable thickness 120-150m

Kincaid Shale

	m
Eocene	
Claibourne Group	
Sparta Sand	91
Mt. Selma Fm.	91
Carrizo Sand	62
Wilcox Fm.	152
Palaeocene	
Midway Group	
Wills Point Fm.	152
Kincaid Shale	9
	557 Probable thickness 420-550m

Nacimiento Shale

	m
Quaternary	0 - 91
Eocene	
San Jose Fm.	426 - 914
Palaeocene	
Nacimiento Fm.	304 - 548
	730 - 1553 Probable thickness 1220-1530m

Fox Hills Formation

	m
Oligocene	45
Eocene	91
Palaeocene	
Fort Union Gp.	365
U. Cretaceous	
Lance Fm.	152
Fox Hills Fm.	45
	698 Probable thickness 460-610m

Chapter Three
Mineralogy & Geochemistry

3.1 Mineralogy

A Phillips 2kw X-ray diffractometer was used to analyse all of the samples studied in this project for the major clay mineral components (illite, kaolinite, montmorillonite, mixed-layer clay and chlorite) as well as other detrital and non-detrital minerals (quartz, feldspar, calcite, dolomite and pyrite). The resulting X-ray traces of all the specimens analysed are presented in Figures 3.1 and 3.2.

Quantitative analyses* reported in Appendix A 1.1 were carried out using boehmite as an internal standard (Griffin, 1954; Gibbs, 1967) by reference to standard minerals listed in Table 3.1. However, for chlorite and feldspar, which occur in small quantities, estimates were derived by spiking the relevant samples with penninite and orthoclase respectively. Because of variations in crystallinity and chemical composition (Brown, 1961) it was found necessary to use several standards to cover the range of diagnostic X-ray reflection shapes encountered for the three main clay mineral types.

All uncorrected total mineral concentrations lay between 90 - 110 per cent, indicating that the method used gave reasonable results. However, for the purposes of the following discussion, all results have been normalised to 100 per cent and are presented in Table 3.2.

* Mineralogical analyses of rocks containing a high proportion of silt and clay size minerals (plus colloidal matter) are strictly semi-quantitative.

Table 3.1 Minerals used to Prepare Semi-quantitative Calibration Curves

Mineral	Source	Impurities
Quartz	Madagascar	None
Cornish Kaolinite	Cornwall, England	5% quartz
Kaolinite, A.P.I. ref.	Bath, S. Carolina	5% quartz
Kaolinite, A.P.I. ref. (crushed)	Bath, S. Carolina	5% quartz
Fithian Illite, A.P.I. ref.	Illinois	20% quartz 5% other
Morris Illite, A.P.I. ref.	Illinois	12% quartz 3% other
French Illite	Puy-en-Valey, France	5% quartz
Montmorillonite, A.P.I. ref.	Otay, California	None
Montmorillonite, Fuller's Earth	Coombe Hay, England	2% quartz 6% feldspar 7% calcite 3% pyrite
Calcite	Unknown (Durham Univ. Geol. Dept.)	None
Dolomite	N. Nottingham, England	None
Pyrite	Hopa, N.E. Turkey	None

Table 3.2 Mineralogy of British & North American Shales

	Sample Ref.	Smectite	Illite	Mixed Layer	Kaol	Chl	Qtz	Cal	Dol	Pyr	Fels	C	Total
British Shales													
x London Clay 14m	LC14	12.5	34.5	11.0	19.5	0.0	18.5	0.0	3.0	1.0	Trace	0.0	100.0
x London Clay 37m	LC37	7.0	22.5	7.5	10.5	Trace	41.5	0.0	3.0	0.0	6.0	0.0	100.0
Gault Clay	GC	7.0	23.0	1.5	19.0	0.0	14.0	34.5	0.0	1.0	0.0	0.0	100.0
Fuller's Earth(REDL)	FE23	99.0	0.0	0.0	0.0	0.0	1.0	Trace	0.0	Trace	0.0	0.0	100.0
Weald Clay	WC	0.0	25.5	1.5	18.0	0.0	55.0	0.0	0.0	Trace	Trace	0.0	100.0
Kimmeridge Clay	KC	0.0	21.0	26.5	18.5	Trace	23.0	7.0	0.0	4.0	0.0	0.0	100.0
Oxford Clay 10m	OC10	0.0	22.5	26.0	21.0	0.0	21.5	3.0	0.0	3.0	0.0	3.0	100.0
Oxford Clay 44m	OC44	0.0	23.0	15.5	20.0	1.0	29.5	3.0	0.0	5.0	Trace	3.0	100.0
Fuller's Earth(Bath)	FE19	82.0	0.0	0.0	0.0	0.0	2.0	6.0	Trace	3.0	7.0	0.0	100.0
Lias Clay 10m	L10	0.0	25.5	17.0	34.0	2.0	15.5	3.0	0.0	3.0	Trace	0.0	100.0
Lias Clay 36m	L36	0.0	25.5	17.5	35.0	1.0	13.0	3.0	0.0	5.0	0.0	0.0	100.0
Keuper Marl	KM	0.0	33.0	2.0	4.0	6.00*	34.0	13.0	7.0	Trace	0.0	1.0	100.0
Swallow Wood roof	SWR	0.0	54.5	15.5	16.0	2.0	12.0	Trace	0.0	Trace	Trace	0.0	100.0
Flockton Thin roof	FTR	0.0	37.0	13.0	17.0	3.0	24.0	Trace	0.0	Trace	5.0	1.0	100.0
Flockton Thin seat	FTS	0.0	16.0	45.0	34.0	2.0	2.0	Trace	0.0	Trace	0.0	1.0	100.0
Widdringham roof	WR	0.0	16.5	9.5	54.5	2.0	14.5	Trace	0.0	Trace	0.0	3.0	100.0
North American Shales													
Yazoo Clay	YC	49.0	0.0	0.0	31.0	0.0	12.0	8.0	0.0	Trace	0.0	0.0	100.0
x Kincaid Shale 6m	K6	13.0	0.0	0.0	28.0	0.0	46.0	10.0	1.0	Trace	2.0	0.0	100.0
Kincaid Shale 8m	K8	14.5	0.0	0.0	26.0	0.0	54.0	0.0	5.5	Trace	0.0	0.0	100.0
Nacimiento Shale	N1	17.0	19.0	1.0	27.0	0.0	28.0	Trace	0.0	Trace	8.0	0.0	100.0
Nacimiento Shale	N2	15.0	16.0	1.5	21.0	0.0	35.0	Trace	0.0	Trace	11.5	0.0	100.0
Nacimiento Shale	N3	49.5	0.0	0.0	28.0	0.0	22.5	Trace	0.0	Trace	Trace	0.0	100.0
Fox Hills Shale	FOX	54.0	7.5	1.5	6.0	0.0	26.0	1.0	0.0	1.0	Trace	3.0	100.0
Dawson Shale	DS	40.0	0.0	.0.0	7.0	0.0	49.0	Trace	0.0	Trace	4.0	0.0	100.0
Pierre Shale(DAK)	PSD	44.0	14.0	11.5	5.0	0.0	22.5	1.0	2.0	Trace	Trace	0.0	100.0
Pierre Shale (COL)	PSC	8.0	25.0	15.0	11.0	0.0	29.0	0.0	4.0	Trace	8.0	0.0	100.0

x Possible Akerite present

* Swelling chlorite

NB Carbon is only recorded where measured amounts exceeded 1%

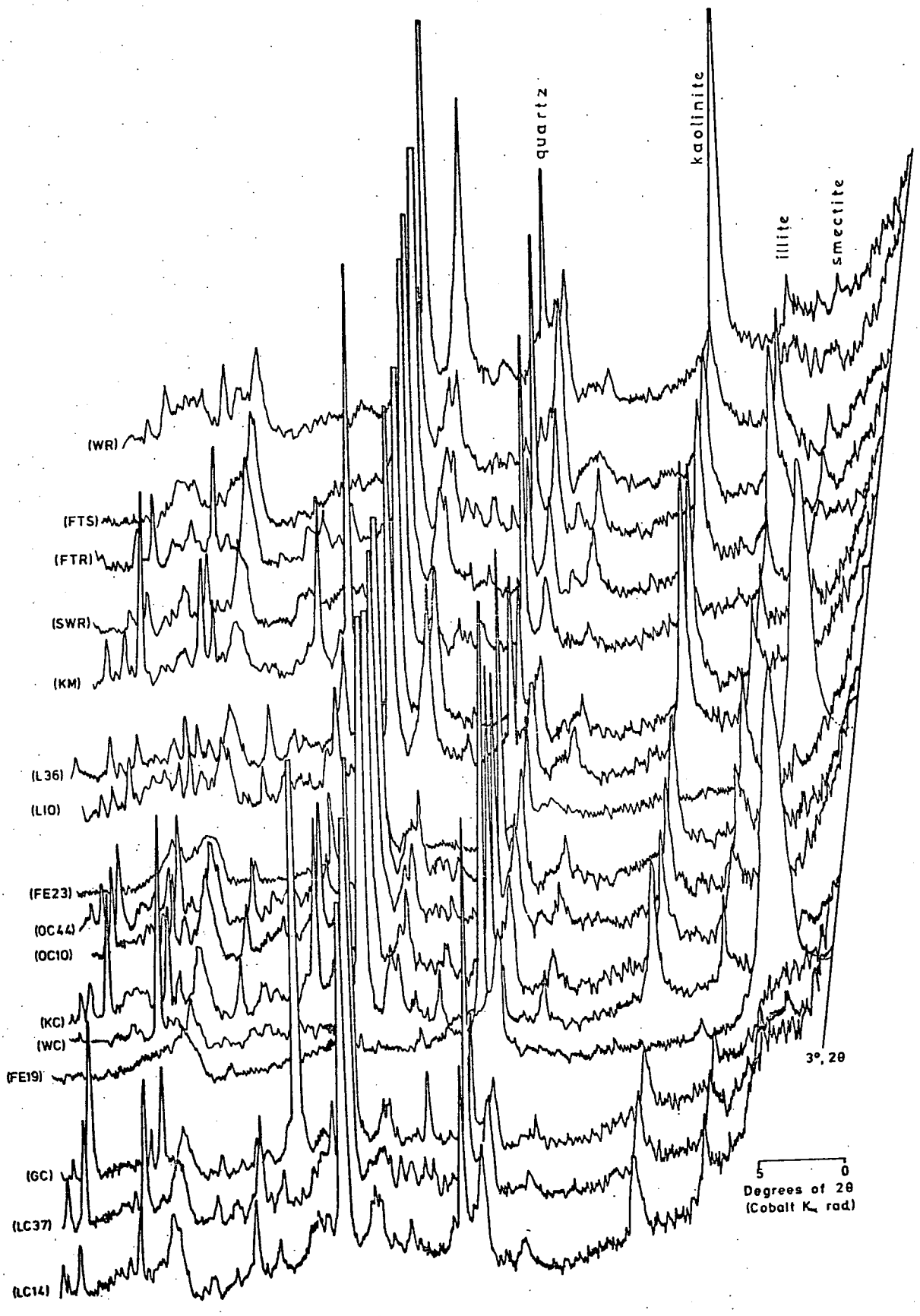

Figure 3.1. X-Ray Traces of British Samples.

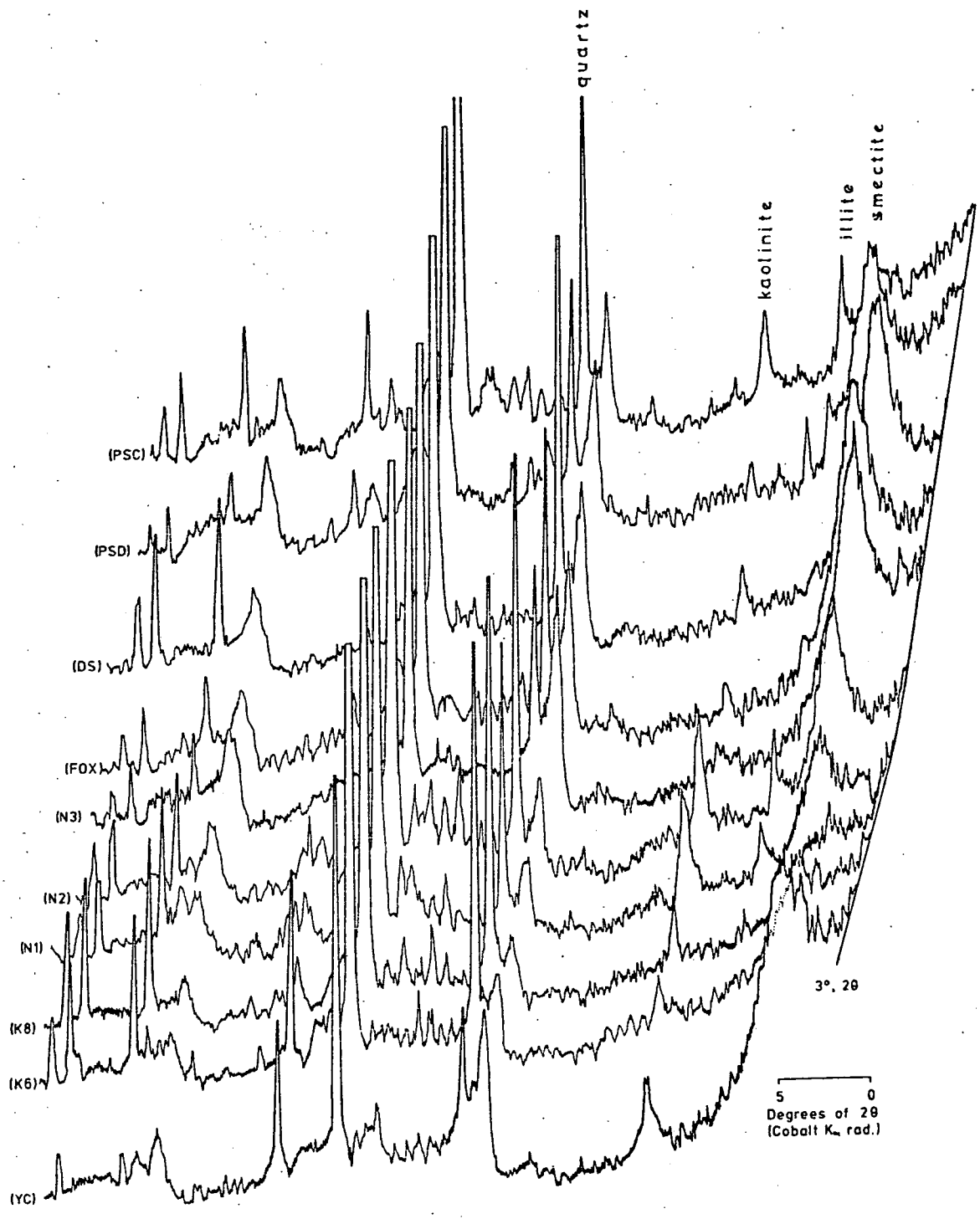

Figure 3.2. X-Ray Traces of North American Samples.

3.1.1 Clay Minerals

3.1.1.1 Illite and Mixed-layer Clay

All micaceous minerals with a basal spacing of 10Å have been placed in this group and the term 'illite' has been adopted to identify them. These minerals usually contain an expanding mixed-layer component which occurs as a 'tail' on the low 2θ side of the 10Å peak. Consequently this component has been included in the illite group for the purposes of quantitative analysis and the discussion which follows.

Quantitative estimation of illite minerals proved difficult because the shape of the reflection varies greatly depending upon the crystallinity of the illite and the quantity of mixed-layer clay present (a selection of typical shapes is presented in Figure 3.3). Consequently three reference illites were chosen (see Figure 3.3) whose shapes approximately covered the range of shapes shown by the illites in the samples studied, and calibration curves for quantitative analyses were prepared using these species. The concentration of mixed-layer clay present was determined by estimating the reduction of the area of the untreated illite peak, after glycolation had expanded the mixed-layer component to a higher angstrom spacing. (see Appendix A1.1).

The shape of the 10Å reflection is indicative of the type of illite. Griffin (1954) uses a 'shape factor', which he defines as the ratio of the width at half peak height of the mineral to that of boehmite, (the internal standard), for selecting the appropriate calibration curve. Taylor (1971) expresses the 'shape factor' as the ratio of the height of the illite reflection to its width at half height. The shape factors of the reference illites are:-

	After Griffin	After Taylor
French Illite	3.2 - 4.5	0.13
Fithian Illite	8.2 - 10.9	0.35
Morris Illite	15.0 - 18.1	0.59

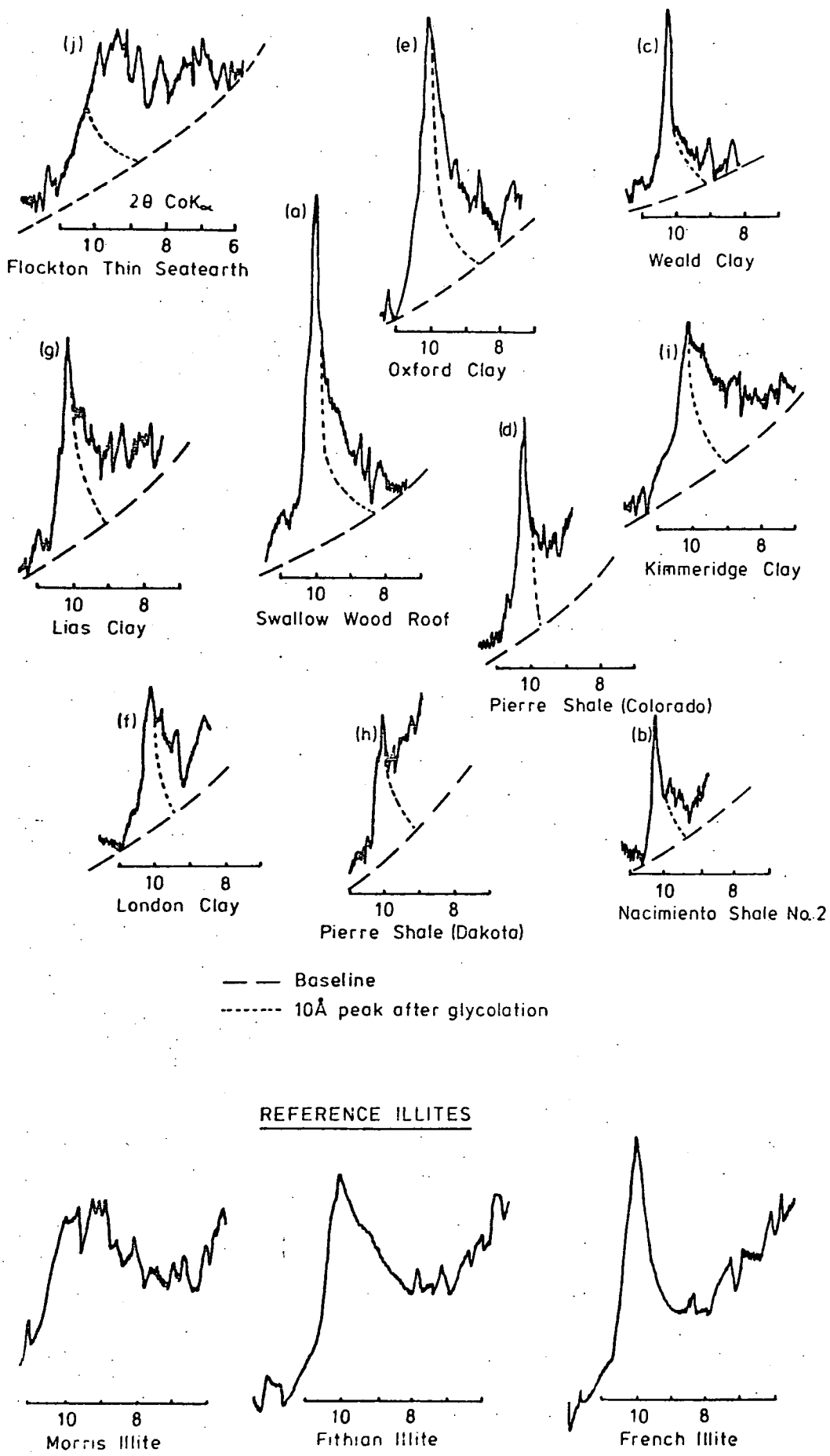

Figure 3.3. Typical 'Illite' X-Ray Traces.

Share factors and the calibration curves used to determine quantities of illites currently identified are presented in Table 3.3.

Two of the Carboniferous roof shales, namely the Flockton Thin and Swallow Wood, contain a 10Å illite with a tall narrow peak (similar to hydromuscovite) which does not correspond to any of the reference samples. (Fig.3.3). However, by ignoring the narrow portion at the top of the reflection, a shape similar to that of the Fithian Illite was obtained, hence this calibration curve was used for their estimation.

The shape factor can be used as a measure of the crystallinity state of the mica present. Taylor (1971) using CuK_{α} radiation and a shape factor of height to width at half peak height, shows that the ratio of a highly crystalline mica (the Miami Muscovite) to be 0.001, and illites with a mixed-layer mineral 'tail' on the low 2θ side of the basal reflection to have higher values (the Morris Illite ratio being 0.134). In the present study, using Taylor's shape factor and the same rate of scan, the ratios calculated (see Table 3.3) for Cobalt radiation, appear to be of a higher order (the Morris Illite ratio is 0.59), but the same trend is observed. A similar trend is also observed when the Griffin shape factors are considered.

Referring to Figure 3.2, illites of type (a) (from the Carboniferous roof shales) and possibly those of types (b) and (c) have sharp, narrow peaks with a relatively small tail, and can be interpreted as hydromicas.

Illites of types (d) and (e) have tall, broader peaks and a more pronounced tail and these are identified as being intermediate between hydromicas and typical illites.

Illites of types (f), (g), (h) and (i) have low, broad peaks with long tapering tails and are interpreted as typical illites.

Table 3.3

Shape Factors of Clay Minerals

British Shales	Sample Ref.	KAOLINITE Shape Factor	KAOLINITE Curve Used	ILLITE Shape Factor (After Griffin)	ILLITE Shape Factor (After Taylor)	ILLITE Curve Used	MONTMORILLONITE Shape Factor	MONTMORILLONITE Shape Factor (Glycolated)	MONTMORILLONITE Curve Used
London Clay 14m	LC14	2.72	C.K.	2.72	0.10	French	-	8.63	Glycolated
London Clay 37m	LC37	2.27	C.K.	4.54	0.20	French	-	7.72	Glycolated
Gault Clay	GC	2.72	C.K.	2.27	0.14	French	-	-	Glycolated
Fuller's Earth (Redhill)	FE23	-	-	-	-	-	6.36	3.86	Glycolated
Weald Clay	WC	2.27	C.K.	1.81	0.10	French	-	-	-
Kimmeridge Clay	KC	2.50	C.K.	10.90	0.43	Fithian	-	-	-
Oxford Clay 10m	OC10	2.27	C.K.	6.81	0.21	Fithian	-	-	-
Oxford Clay 44m	OC44	1.81	C.K.	5.00	0.17	Fithian	-	-	-
Fuller's Earth (Bath)	FE19	-	-	-	-	-	5.90	3.40	Glycolated
Lias Clay 10m	L10	2.04	C.K.	10.00	0.33	Fithian	-	-	-
Lias Clay 36m	L36	2.04	C.K.	10.90	0.39	Fithian	-	-	-
Keuper Marl	KM	2.04	C.K.	2.72	0.10	French	-	-	-
Swallow Wood roof.	SWR	2.27	C.K.	2.68	0.05	Fithian	-	-	-
Flockton Thin roof.	FTR	2.27	C.K.	2.27	0.05	Fithian	-	-	-
Flockton Thin seat.	FTS	3.18	C.K.	20.40	0.84	Morris	-	-	-
Widdringham roof.	WR	2.04	C.K.	8.18	0.42	Fithian	-	-	-
North American Shales									
Yazoo Clay	YC	3.18	C.K.	-	-	-	14.09	7.72	Glycolated
Kincaid Shale 6m	K6	4.09	D.K.	-	-	-	-	7.27	Glycolated
Kincaid Shale 8m	K8	3.86	D.K.	-	-	-	-	7.72	Glycolated
Nacimiento Shale	N1	2.72	C.K.	3.40	0.22	French	13.60	6.81	Glycolated
Nacimiento Shale	N2	2.27	C.K.	2.27	0.11	French	6.13	4.54	Glycolated
Nacimiento Shale	N3	5.00	D.K.	-	-	-	7.50	9.09	Glycolated
Fox Hills Shale	FOX	2.27	C.K.	7.50	0.58	Fithian	10.22	5.90	Glycolated
Dawson Shale	DS	2.04	C.K.	-	-	-	8.18	5.90	Glycolated
Pierre Shale (Dakota)	PSD	2.04	C.K.	10.00	0.50	Fithian	15.90	6.81	Glycolated
Pierre Shale (Colorado)	PSC	2.04	C.K.	2.27	0.07	French	-	7.27	Glycolated

C.K. - Crushed Kaolinite

D.K. - Disordered Kaolinite

Illites of type (j) from the Carboniferous Flockton Thin seatearth have very broad peaks with a large, well developed tail on the low 2θ side of the peak and a ragged tapering edge on the high 2θ side. This suggests that a large amount of disordering is present (Brown, 1961). A small, broad, diffuse peak is also visible at 17Å indicating that montmorillonite is present in the mixed-layer component. This mineral has the characteristics of a typical degraded illite.

In all cases where the 060 reflection was identified, it was close to 1.5Å implying that the 10Å minerals are dioctahedral, but because of peak interference from quartz, calcite and boehmite in the 2.6 - 4.4Å region it was not always possible to identify the type of polymorph present. However, the illites from the Carboniferous roof shales, the Oxford Clay 44m (sample ref.OC44) and the Weald Clay were all identified as 2M polymorphs, although that of the seatearth could be closely related to the 1Md polymorph described by Yoder & Eugester (1955). It was not possible to positively identify the state of any other illites.

3.1.1.2. Kaolinite

Kaolinite is the most stable of the clay minerals and is identified by its 001 reflection which occurs at 7Å.

A selection of typical 7Å reflections is presented in Figure 3.4, and again, as with the illites, it can be seen that quantitative estimation is difficult because of the variation in peak shapes. These variations, which are represented by broadening of, and the development of a tail on the peak, are caused by differences in crystal size and random displacements of b/3 parallel to the 'b' axis (Brindley and Robinson, 1947) respectively. They are nevertheless unlikely to be greatly affected by chemical changes. Disordered kaolinites are common

in Carboniferous seatearths (Schultz, 1958) and are typically represented by the Flockton Thin seatearth. Several North American kaolinites, however, also show signs of disorder, which may reflect their conditions of deposition.

Murray & Lyons (1956) list the important differences between ordered and disordered kaolinites, the most useful of which are:-

(i) Non-resolution of the 4.12 - 4.17Å doublet in disordered kaolinites.

(ii) A broad 2.5Å peak replaces the 2.55 - 2.52 - 2.49Å triplet of the ordered form.

(iii) A broad 2.3Å peak replaces the 2.37 - 2.33 - 2.28Å triplet of the ordered form.

In the present study the triplets could only be resolved in samples where a sufficient quantity of kaolinite was present and line interference from other minerals was not too great. In the case of the Flockton Thin seatearth, a disordered form was implied by the presence of two broad bands which replaced the two triplets. The doublet could only be resolved in the Widdringham roof shale, the Lias Clay, the Swallow Wood roof shale and the Flockton Thin roof shale.

Hinkley (1963) uses the $I\bar{1}0$ (4.35Å) and the $II\bar{1}$ (4.17Å) planes to obtain a measure of the crystallinity state. Firstly a background baseline is drawn on the trace and then another baseline is drawn from the low 2θ side of the $I\bar{1}0$ reflection to the high 2θ side of the $II\bar{1}$ reflection. The crystallinity factor is:- $\frac{A + B}{A_t}$

where, A is the height of the $I\bar{1}0$ peak above the secondary baseline,

B is the height of the $II\bar{1}$ peak above the secondary baseline,

and A_t is the height of the $\bar{1}10$ peak above the primary baseline.

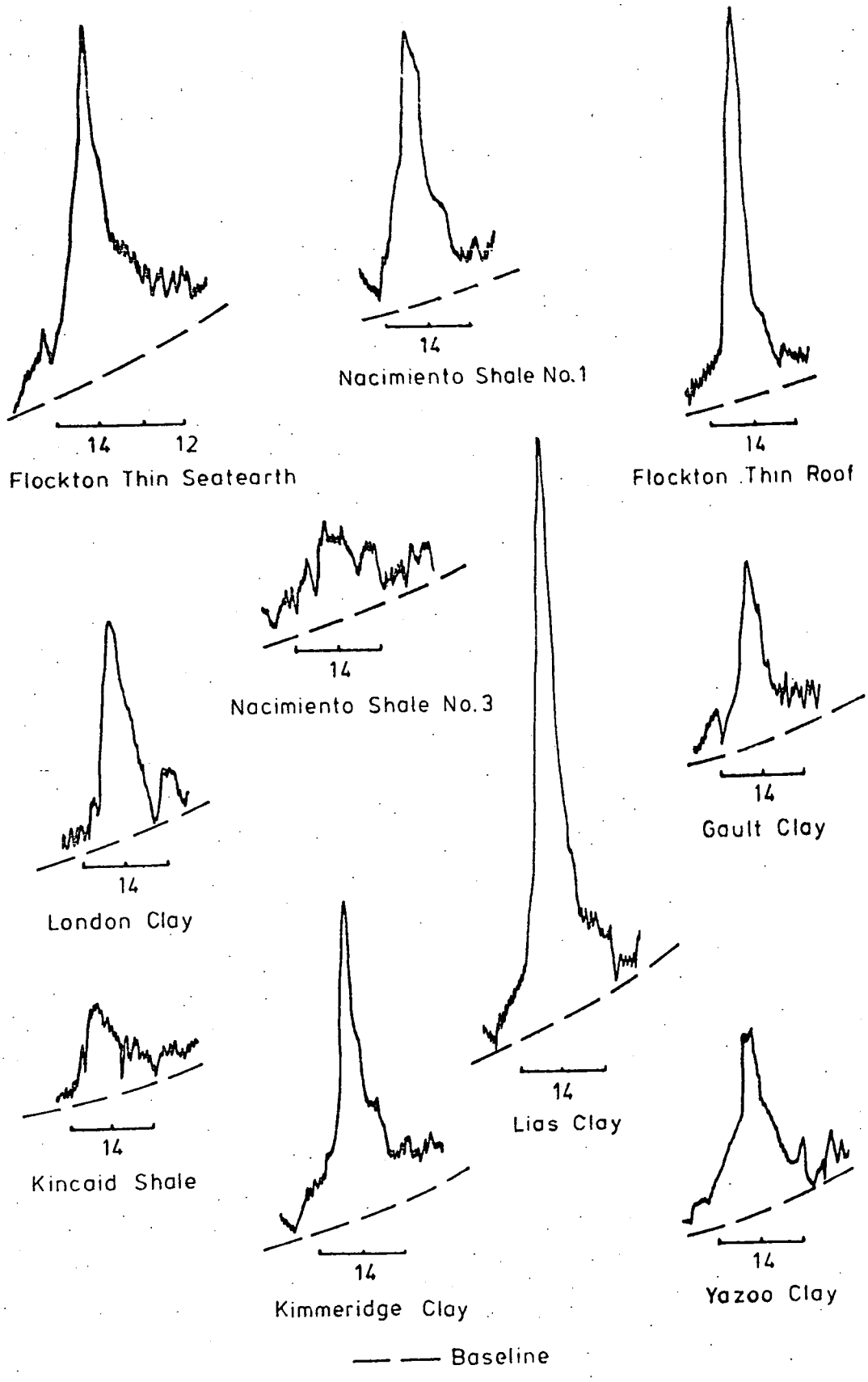

Figure 3.4. Typical Kaolinite X-Ray Traces.

Hinkley quotes 1.284 for the crystallinity factor of a well ordered kaolinite and 0.25 for that of a poorly crystalline kaolinite. Taylor (1971) obtains a value of 0.973 for the Cornish kaolinite used for calibration in this project. A value of 0.710 was obtained by the writer for the reference kaolinite from Bath, South Carolina, indicating a lower degree of crystallinity (which is borne out by reference to the shape factor - see later). However, owing to interference from the 4.26Å reflection of quartz, and also a lack of kaolinite concentration, only six crystallinity factors for the samples studied could be obtained. These were 0.652 for the Widdringham roof, 0.473 for the Flockton Thin seatearth, 0.611 for the Lias Clay, 0.500 for the London Clay, 0.584 for the Flockton Thin roof and 0.625 for the Swallow Wood roof.

Griffin (1954) uses the 'shape factor', i.e. the ratio of the width at half peak height of kaolinite to that of boehmite (see also Illites and Mixed-Layer Clay) as a measure of the crystallinity state, with low values representing higher degrees of crystallinity. The shape factors for the reference kaolinites are:-

Cornish Kaolinite	1.4
Kaolinite, South Carolina	1.6
Crushed Kaolinite, South Carolina	1.95
Disordered Kaolinite	4.5 (approx.)

The shape factors for the kaolinites in the samples studied (Table 3.3) are, in general, much higher than those of the two crystalline kaolinites. However, by heavily crushing the kaolinite from South Carolina for 10 minutes in an agate mortar and pestle, the 7Å peak height can be greatly reduced and the peak width broadened so increasing the shape factor to a level which is comparable with those of the majority of kaolinites studied, due to distortion of

the structure (Grim, 1968). Consequently the crushed kaolinite was used for the majority of semi-quantitative estimations. Miller and Oulton (1970) discuss the effect of progressive grinding on kaolinites and Brindley (1961a) states that crystals much smaller than one micron give appreciably broadened reflections with correspondingly smaller peak heights.

The kaolinites from the Kincaid Shales and Nacimiento Shale (M3) appear to have shape factors which are more akin to the disordered kaolinite and their quantities have been estimated using this curve. The kaolinites of the Yazoo Clay and Flockton Thin seatearth have shape factors which are intermediate between those of the disordered kaolinite and the crushed kaolinite, but as no comparable standard was available, their estimates were based on the crushed kaolinite curve, and hence they may be slightly underestimated.

When chlorite is present, the 7Å (002) reflection coincides with and tends to broaden the 7Å (001) basal reflection of kaolinite, thus increasing the shape factor, as well as adding to the area of the kaolinite peak. The correction procedure for removing this component from the kaolinite peak is reported in Appendix A 1.1.

3.1.1.3 Smectite

Smectites are identified by their 001 basal reflection which occurs between 12.5 - 15Å (see Table 3.4), depending on the state of hydration of the mineral (Grim, 1968). Grim states that "the 'c' axis spacing, the diffuseness of the reflection, and the number of orders shown, vary from sample to sample, depending on the thickness of the water layers and their regularity, which factors in turn are dependent on the exchangeable cations present and the conditions, e.g. water-vapour pressure, under which the sample has been prepared".

Bradley et al (1937) found that the water occurring between the silicate layers is an integral number of layers, and for naturally occurring smectites with Na as the exchangeable cation, generally only one layer of water molecules is present giving a 'c' axis spacing of about 12.5Å. If Ca is the exchangeable cation, two layers of water molecules are present and the 'c' axis spacing is 14.5 - 15.5Å depending on the relative humidity. Cation exchange determinations shown in Table 3.12 revealed that the majority of smectites have Ca as the dominant interlayer cation. The Pierre Shales from Dakota and Colorado, however, were found to contain moderate Na levels and from Table 3.4 it can be seen that these two clays have lower untreated basal 001 spacings.

It is necessary to distinguish between smectites and vermiculites, because both minerals have a basal spacing of about 14Å. The most commonly occurring variety of vermiculite is the Mg-form which has a basal spacing of 14.4Å. However, unlike that of smectites, this spacing does not vary with relative humidity (Walker, 1961). Upon treatment with ethylene glycol (Brunton, 1955; Brown and Farrow, 1956) the basal spacing of smectites expands to about 17Å, because two layers of glycol are taken into the structure to replace the water molecules (see Table 3.4); the resulting complex having a higher degree of regularity (Bradley, 1945) with the 001 reflection becoming taller and narrower. On the other hand, glycolation of Mg-vermiculites results in a one layered organic complex (Walker, 1950; Barshad, 1950) with a basal spacing of 14.3Å, which is approximately the same as the untreated sample. However, the double-layered complexes can be occasionally formed (Walker, 1957) depending on the lattice charge and the size of the vermiculite particles.

He states that expansion to approximately 16Å may be observed with some Ca, Sr, and Ba-vermiculites. Mg-vermiculites with a low layer charge may also expand to 'd' spacings greater than 14.3Å. Therefore, glycolation cannot be used as an absolute diagnostic test for the distinction between smectites and vermiculites. However, overall the results infer the presence of smectite rather than vermiculite because the large degree of swelling of the 001 reflection to 17Å is in line with the swelling characteristics of smectites, since vermiculites rarely swell to spacings greater than 16Å. The geochemistry also implies that smectite is present (see Section 3.2).

Semi-quantitative estimates of the smectite content were performed using the glycolated peak areas because their 'shape factors' (see Illites and Kaolinites) were more consistent than those of untreated peaks as a result of the increase in regularity of the crystal structure as previously discussed (see Table 3.3).

Where the 060 reflection was distinguished it was always close to 1.495 - 1.500Å, showing that the mineral species present are dioctahedral, but the type was difficult to ascertain. However, geochemical evidence (Section 3.2), particularly the combined silica to alumina ratio tentatively suggests that the smectites belong to the montmorillonite-beidellite series.

Because the smectites have an important bearing on the engineering properties of shales, an attempt was made to derive the basic formula units present using geochemical data presented in Table 3.10. However, this was only possible when the only other minerals present in the shale were quartz, kaolinite, calcite or feldspar, because these minerals have reasonably constant compositions, thus enabling a fairly accurate correction to be made to the major element geochemistry (see Appendix A 1.2). No recalculation was attempted when illite was present

Table 3.4 'D' Spacings of Smectites Before & After Glycolation

	Sample	Untreated		Treated	
British Samples	Ref.	2θ	Å	2θ	Å
London Clay 14m	LC14	6.80	15.09	5.80	17.69
London Clay 37m	LC37	7.10	14.45	5.80	17.69
Gault Clay	GC	No measurable peaks before or after glycolation			
Fuller's Earth (Redhill)	FE23	7.00	14.66	6.00	17.10
Fuller's Earth (Bath)	FE19	7.10	14.45	6.00	17.10
Keuper Marl *	KM	7.20	14.25	6.00	17.10
North American Samples					
Yazoo Clay	YC	6.70	15.31	5.95	17.24
Kincaid Shale 6m	K6	6.40-7.00	14.66-16.03	5.90	17.39
Kincaid Shale 8m	K8	No measurable peak		5.70-5.90	17.39-18.00
Nacimiento Shale	N1	7.00	14.66	5.95	17.24
Nacimiento Shale	N2	7.00	14.66	5.90-6.05	16.96-17.39
Nacimiento Shale	N3	6.80	15.09	6.00-6.05	16.96-17.10
Fox Hills Shale	FOX	7.20-7.60	13.50-14.25	5.95-6.05	16.96-17.24
Dawson Shale	DS	6.60-7.10	14.45-15.54	5.80-6.10	16.82-17.69
Pierre Shale (Dakota)	PSD	7.50-8.00	12.38-13.86	5.95-6.05	16.96-17.24
Pierre Shale (Colorado)	PSC	7.20-8.10	12.67-14.25	5.90-6.00	17.10-17.39

* After heat treatment a peak still remains at 14Å suggesting that the mineral present could be a swelling chlorite.

because of the very complex and variable nature of the composition of this mineral.

The method of recalculation used is based on Nagelschmidt (1938), whereby the basic structure has been reduced from $Al_2Si_4O_{10}(OH)_2 \cdot mH_2O$ to $Al_2Si_4O_{11}$ i.e. basing the structural composition on eleven oxygen atoms and removing the uncertainty about the number of hydroxyl groups present in the lattice. The actual recalculations are given in Appendix A 1.2.1 - A 1.2.5, and a summary of the results presented in Table 3.5. Only oxides which are considered likely to be present in the smectite are used in the recalculation. Hence, titanium, phosphorus, sulphur, carbon and carbon dioxide have been excluded in addition to the water content. The structural formula for the montmorillonite from Otay, California (Oligocene) has also been recalculated (Appendix A 1.2.6) and included in Table 3.5. In addition, the composition of the two samples of Fuller's Earth, as recalculated by Kerr & Hamilton (1949) are also presented, and are seen to agree exceedingly well with the writers own results.

Because of the assumption made and the correction procedures used, the results obtained are used primarily to portray differences in the smectite lattice structure rather than as absolute values. A principal source of error when the smectite is derived from volcanic material is the presence of amorphous material, particularly silica and alumina, which are not easily estimated (Weaver & Pollard, 1973).

MacEwan (1961) discusses the ranges of Si and Al ratios in the montmorillonite-beidellite series and concludes that the maximum ratio representing the idealised montmorillonite mineral with the tetrahedral layer having Si = 4, and in which magnesium was the only other major constituent, would be 5 : 2. The maximum ratio representing the

idealised beidellite would be 3 : 2. However, it will be noticed that iron is present to a moderate degree in the octahedral layer, thus complicating the above statements. Nevertheless, important variations in the silicon and aluminium content of the tetrahedral layer, which are implied from the above statements can be used as a guide to the type of mineral present.

The Fuller's Earth from Redhill (sample FE23) and the montmorillonite from Otay, California both have an Si value of 4 in the tetrahedral layer, which probably indicates that these are 'good' montmorillonites. In addition, the Fullers Earth from Bath (sample FE19), having an Si value of 3.94 must also be considered a typical montmorillonite-type mineral.

The remaining three minerals all have lower amounts of silicon, and more aluminium in the tetrahedral layer, particularly the Dawson Shale where the Si value is only 2.91, and it must be inferred from this that the mineral present is more akin to a beidellite. The smectites from the Nacimiento Shale (N3) and the Yazoo Clay have intermediate Si values of 3.62 and 3.83 respectively and may represent a transitional type of mineral, although that from the former may be approaching a typical beidellite mineral. Another indication that the latter three smectites are beidellitic in character is reflected in their high potassium contents. Weaver & Pollard (1973) state that beidellitic smectites can have a sufficiently high layer charge to fix potassium in the interlayer position, causing layers to contract to 10Å. However, no discrete 10Å peaks were recorded on the X-ray charts, although the low angstrom side of the smectite peaks was far more ragged and extended farther towards the 10Å area than that seen on the traces for the Fuller's Earths or montmorillonite from Otay, California, (See Fig. 3.1 and 3.2). Weaver (1958a) however,

Table 3.5 Recalculated Smectite Formulae

British Shales

(a) Fuller's Earth (Redhill)

$(Al_{1.10}Fe_{0.41}Mg_{0.38})(Si_{4.04})O_{10}(OH)_2(Ca_{0.24}Na_{0.03}K_{0.04})$

$(Al_{1.48}Fe_{0.33}Mg_{0.42})(Al_{0.06}Si_{3.94})O_{10}(OH)_2(Ca_{0.55}Na_{0.03})$ After Kerr & Hamilton(1949)

(b) Fuller's Earth (Bath)

$(Al_{1.30}Fe_{0.28}Mg_{0.39})(Al_{0.05}Si_{3.94})O_{10}(OH)_2(Ca_{0.20}Na_{0.06}K_{0.04})$

$(Al_{1.51}Fe_{0.20}Mg_{0.32})(Al_{0.11}Si_{3.89})O_{10}(OH)_2(Ca_{0.57}Na_{0.11})$ After Kerr & Hamilton (1949)

North American Shales

(a) Nacimiento Shale No. 3

$(Al_{0.75}Fe_{0.86}Mg_{0.30})(Al_{0.38}Si_{3.62})O_{10}(OH)_2(Ca_{0.22}Na_{0.05}K_{0.46})$

(b) Dawson Shale

$(Al_{1.33}Fe_{0.51}Mg_{0.41})(Al_{1.09}Si_{2.91})O_{10}(OH)_2(Ca_{0.19}Na_{0.05}K_{0.31})$

(c) Yazoo Clay

$(Al_{1.03}Fe_{0.57}Mg_{0.44})(Al_{0.16}Si_{3.83})O_{10}(OH)_2(Ca_{0.04}Na_{0.06}K_{0.31})$

REFERENCE CLAY

Montmorillonite (Otay, California)

$(Al_{1.15}Fe_{0.10}Mg_{0.81})(Si_{4.04})O_{10}(OH)_2(Ca_{0.10}Na_{0.16}K_{0.03})$

$(Al_{1.43}Fe_{0.03}Mg_{0.64})(Al_{0.01}Si_{3.99})O_{10}(OH)_2(Ca_{0.07}Na_{0.12})$ After Kerr & Hamilton (1949)

points out that the relationship between potassium fixation and contracted layers is still not clear.

The relationships of these findings to the age and depth of burial of the shales is discussed in Section 3.4.

3.1.1.4 Chlorite

Chlorite is recognised by its 001 basal reflection which occurs at 14.3Å.

To distinguish chlorite from vermiculite, which also has a reflection at 14Å, the samples were heated at 550°C for one hour. At this temperature vermiculite (and also kaolinite) are removed by dehydration and the chlorite peaks remain unaltered. Schultz (1958) uses a dual procedure for the separation of these minerals. Firstly, by heating at 450°C any vermiculites present (and montmorillonites) undergo dehydration and the disappearance of the 14Å peak would indicate their presence. Secondly, the samples are reheated at 550°C, whereby any kaolinite present is removed and any 14.7Å and 4.7Å reflections represent chlorite minerals.

Brindley (1961b) uses the relative intensities of basal reflections to determine whether the chlorites are Mg- or Fe-rich. For Fe-rich chlorites the odd intensities (001,003) tend to be relatively low compared to the Mg-rich chlorites. Measurement of the basal reflections before and after heating showed that the chlorites from the Flockton Thin roof, the Swallow Wood roof and the Oxford Clay (sample OC44) produced large increases in their odd reflections (particularly the 001 peak) after heating, suggesting that they were of the Mg-rich variety; the 002 reflections were completely absent. Other chlorites were more problematical as the peaks were very small before and after heating. Small increases were noticed in the intensities of the odd reflections, but no attempt was made to classify them.

A broad 14Å peak in the Keuper Marl, which moved to 17.1Å after glycolation was suspected of being a smectite. However, after heating at 550°C, a 13.87Å peak was present and a swelling chlorite similar to one described by Honeybourne (1951) for the Keuper Marl is a more logical diagnosis.

A further test to confirm the presence of chlorite was performed by warming the samples with dilute hydrochloric acid at 80°C for 12 hours. The destruction of the 14Å peak confirmed that chlorite was present. If this peak had been unaffected then the mineral present may have been vermiculite.

3.1.1.5. Vermiculite

Vermiculite was not detected in any of the samples examined. All tests performed indicated that minerals occurring with a reflection at 14Å were either smectites or chlorites. Perrin (1971) records that various workers have found traces of vermiculite throughout the British succession but there is no confirmation of this from the present work.

3.1.2. Relative Abundances of Clay Minerals

The average concentrations of the clay minerals present, including their standard deviations have been computed in two groups; one based on 15 British materials and the other based on 10 American materials (see Table 3.6). The mineralogy of the Keuper Marl has been excluded from the computation because it is not a true shale and also because of the abnormal chlorite which is present. Materials with high quartz contents have been included because in subsequent discussions they are used as mineralogical extremes. For comparison, average shale compositions (Clark, 1924; Yaalon, 1962; Shaw and Weaver, 1965) have also been included.

Table 3.6 Average Mineralogy and Geochemistry of Shales

	N. American Shales		British Shales		Clark
	Aver.	SD	Aver.	SD	(1924)
SiO_2	62.65	4.83	53.58	7.34	58.10
Al_2O_3	15.26	1.51	19.14	5.09	15.40
Fe_2O_3	4.84	1.38	5.10	1.36	6.46
MgO	1.66	0.51	2.06	0.79	2.44
CaO	1.70	0.97	2.94	4.16	3.11
Na_2O	0.76	0.49	0.49	0.27	1.30
K_2O	2.47	0.59	2.82	0.96	3.24
TiO_2	0.67	0.10	0.92	0.19	0.65
S	0.62	0.66	1.16	1.10	-
P_2O_5	0.10	0.02	0.12	0.04	0.17
CO_2	0.99	0.96	1.86	3.23	2.63
C	0.76	0.85	1.14	1.05	0.80
H_2O	7.46	2.16	8.62	3.11	5.00

	N.Americ. Shales			Brit. Shales			Clark	Yaalon	Shaw & Weaver
	Aver.	SD		Aver.	SD		(1924)	(1962)	(1965)
Mont.	30.46	17.31)		13.81	30.45)	)			
Ill.	8.10	9.06)	Total	23.13	12.92)	Total)			
Mixed	3.06	5.11)	Clay	13.81	11.84)	Clay)			
Kaol.	18.98	9.86)	60.61	21.21	13.45)	72.84)	25.0	59.0	66.9
Chl.	-	-)	SD = 14.23	0.86	1.02)	SD = 15.73)			
Qtz.	32.40	12.79		19.17	14.15		22.3	20.0	36.8
Cal.	1.97	3.72		3.91	8.42)				
Dol.	1.21	1.80		0.40	1.02)		5.7	7.0	3.6
Pyr.	0.20	0.40		1.75	1.76		-	-	-
Fel.	3.28	4.02		1.18	2.40		30.0	8.0	4.5
C.	0.76	0.85		1.14	1.05		-	-	1.0
Lim.	-	-		-	-		5.6	3.0	0.5
Misc.	-	-		-	-		11.4	3.0	0.2

The average total clay mineral content of the British shales of 72.8 per cent, compared with 60.6 per cent for the samples from North America is a reflection of the variation in the conditions of deposition (see Chapter 2), i.e. generally slow deposition for the former and comparatively rapid deposition for the latter.

Relative abundances of clay minerals species expressed in terms of illite, kaolinite (plus chlorite) and expandable clays (montmorillonite plus mixed-layer clay) are presented in Figure 3.5, whilst the relative proportions of non-expandable clay to expandable clay in relation to the ratio of quartz to total clay content are presented in Figure 3.6 (See also Tables A1.1 to A1.3).

3.1.2.1 British Materials

A guide to the clay mineralogy of British sediments is given by Perrin (1971).

For the materials currently being examined, semi-quantitative estimations show that, illite, having a mean concentration of 23.1 per cent is the most common clay mineral, followed closely by kaolinite, having a mean concentration of 21.2 per cent. Both of these clay minerals being of detrital origin, occur in all of the samples, except for the Fuller's Earths from Bath (sample FE19) and Redhill (sample FE23) which may be considered as atypical deposits because they result from devitrifed volcanic fallout (Hallam & Sellwood, 1969) and contain calcium montmorillonite as the only clay mineral phase (Table 3.2). Montmorillonite is only present in three other British samples, i.e. the London Clay 14m, sample LC14, (12.4 per cent), the London Clay 37m, sample LC37 (6.8 per cent) and the Gault Clay(7.1 per cent), and in these samples it is probably detrital in origin.

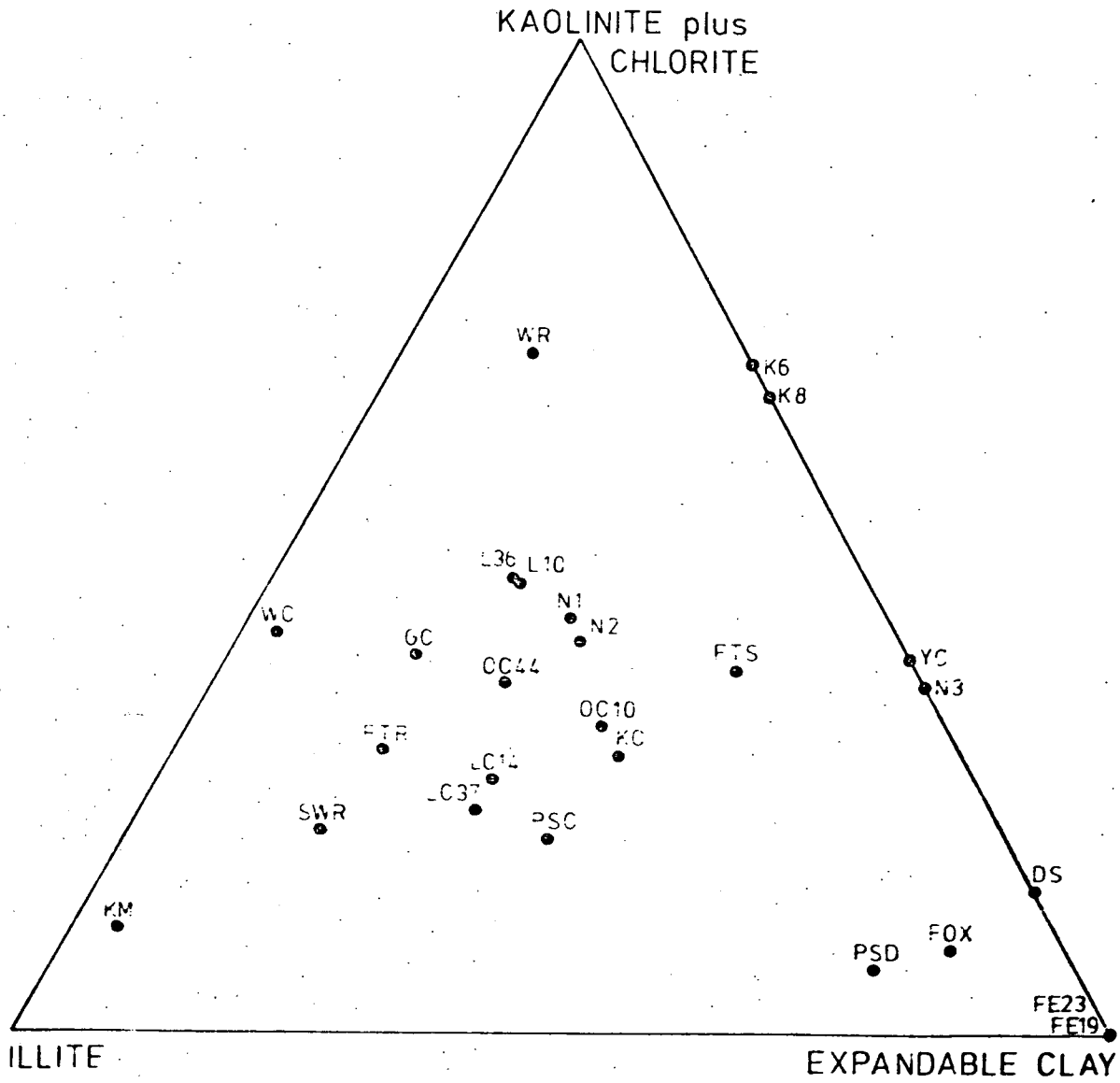

Figure 3.5. Relative Abundance of Clay Mineral Species.

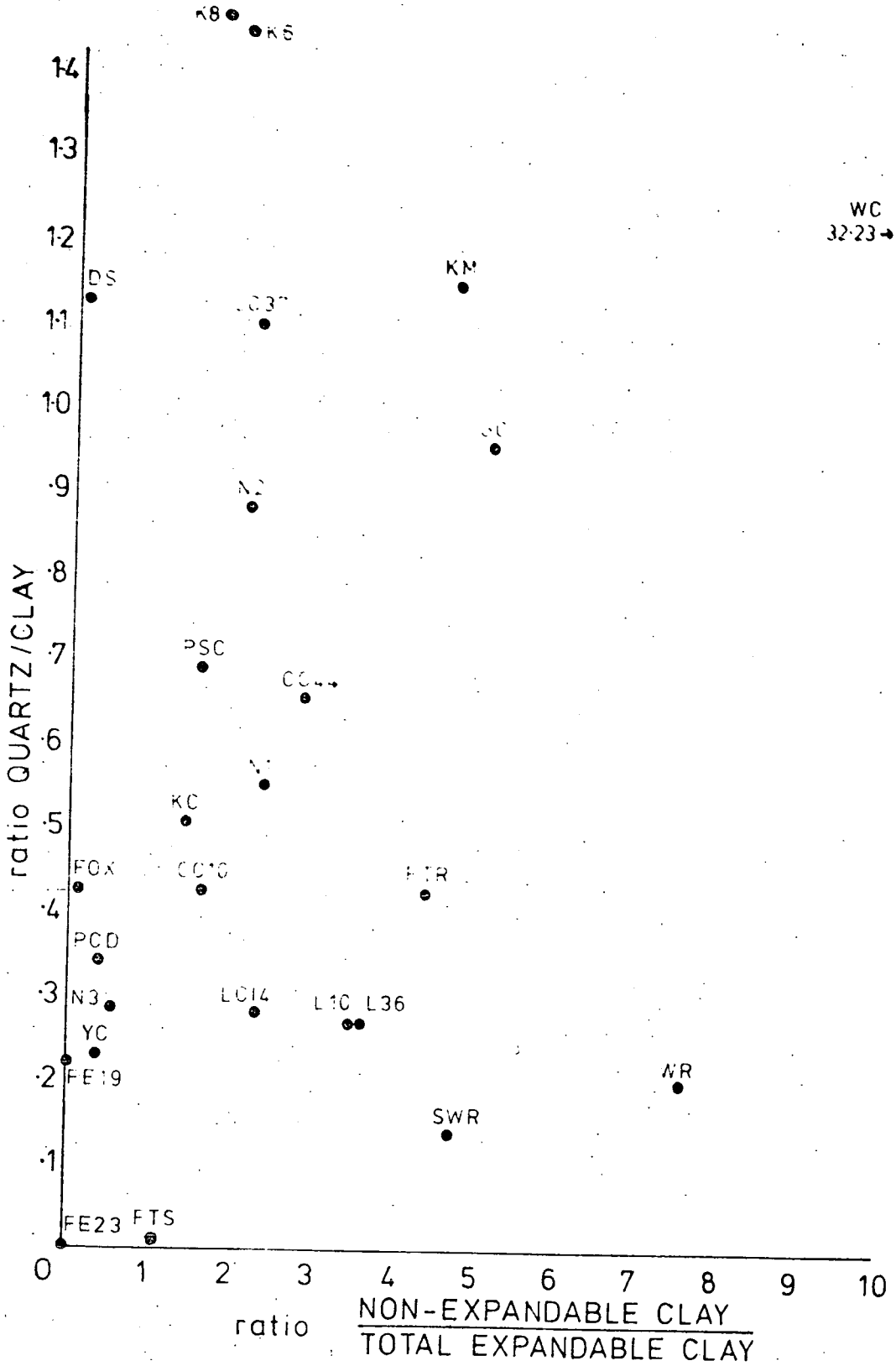

Figure 3.6. Relative Proportions of Non-Expandable Clay to Expandable Clay in Relation to Quartz Content.

Burnett & Fookes (1974) record a zonation in the montmorillonite content of the London Clay from 10 - 35 per cent in a south-easterly direction away from the south-east shoreline of the London Platform. Perrin (1971) records the presence of smectite from the Tertiary Period to the Jurassic Period, after which it becomes very rare, the disappearance being related to the removal of this mineral with deep burial (see Section 3.4).

Mixed-layer clay occurs to a varying degree in all of the British shales, except for the two samples of Fuller's Earth, and has a mean value of 13.8 per cent. It has an exceptionally high concentration (45.3 per cent) in the Flockton Thin seatearth where it probably results from the degradation of illite in a manner described by Taylor & Spears (1970).

Chlorite is present in minor amounts in eight of the British samples. The chlorite from the Keuper Marl is of a swelling variety (see Chlorites) and has a concentration of about 6 per cent, but the remaining samples in which it occurred contained normal varieties which range in concentration from 0.9 - 3.0 per cent. The origin of this mineral is probably detrital (Taylor, 1971; Reeves, 1971).

3.1.2.2. North American Shales

Montmorillonite is the most common clay mineral in the North American samples, having a mean value of 30.4 per cent and occurs in all of the samples studied. Its occurrence in the Late Cretaceous and Tertiary strata of the Western Interior is associated with the uplift of the Rocky Mountains. Some of this material underwent terrestial accumulation and transportation to the site of deposition, but the majority was probably the result of volcanic ash fallout (Tourtelot, 1962).

Kaolinite is the next most common clay mineral and also occurs in all of the samples studied; having a mean value of 18.8 per cent.

Illite, averaging 8.1 per cent, and mixed-layer clay, averaging 6.1 per cent are the least abundant of the clay minerals studied. Schultz (1964), records large quantities of mixed-layer material in the Pierre Shale. However, only minor amounts were recorded in the two samples studied in this project.

Chlorite was not recorded in the samples analysed.

Therefore it can be concluded that major differences do exist between the clay mineral contents of the British and North American shales. These differences are in exceedingly good agreement with the results obtained from a similar study of Attewell & Taylor (1973) and will also have a decisive bearing on the engineering properties of the particular shales studied, as will be seen in the following Chapters.

3.1.3 Other Detrital Minerals

3.1.3.1 Quartz

Quartz is identified by its principal (101) reflection which occurs at 3.31Å. However, quantitative analysis was performed on the 4.26Å reflection because this peak varies in a uniform manner with concentration, which is easily comparable with the boehmite 6.18Å peak. Taylor (1971) found that the quartz content, as determined quantitatively, compared exceedingly well with the more precise wet chemical method of Trostel & Wynne (1940).

In the present study, quartz is the dominant massive mineral in both the British and the North American samples. In the former

it varies from 1 - 55 per cent and has a mean value of 21.8, whilst in the latter it varies from 11 - 54 per cent and has a mean value of 32.4.

Thin section examination revealed that the shape and size of the grains was very variable. The Weald Clay, having the largest quartz content (55 per cent), has grains which are present in two principal size ranges, i.e. very small grains dispersed in the matrix and larger, angular and subrounded grains up to 0.3 - 0.5mm in diameter, often occurring in clusters. The Dawson Shale, an arkosic deposit, generally consists of large angular and subrounded grains up to 0.5mm in diameter, distributed with occasional feldspars in a matrix of smectite. The Kincaid Shale has angular grains up to 0.1mm in diameter distributed throughout the shale. The remaining shales have a random distribution of very small grains (approximately up to 0.03mm in diameter) within the clay matrix.

3.1.3.2 Feldspar

In the present study, orthoclase, microcline and plagioclase were identified by a series of peaks occurring between 3.23 and 3.18Å. An estimation of the quantities in the shales was based on spiking with 5 and 10 per cent orthoclase.

Feldspar species occur in eight out of ten North American shales, varying from trace amounts (in three) to 11.4 per cent in others. They have an average value in the shales of 3.28 per cent and are probably associated with the vulcanism which gave rise to the parental material which subsequently degraded to montmorillonite. They also occur in eight of the British samples, but only as trace amounts in five, and up to 7 per cent in the Fuller's Earth from Bath (sample FE19)

where they are also associated with vulcanism in a similar manner to those from North America. No feldspars were detected in the Redhill Fuller's Earth, (sample FE23), although Hallam & Sellwood (1968) record traces of albite and sanadine in this deposit.

3.1.4 Non Detrital Minerals

3.1.4.1 Carbonates

The major carbonate phases identified were calcite (peak at 3.03Å), dolomite (peak at 2.88Å), siderite (peak at 2.79Å) and (?)ankerite (peak at 2.90Å).

Calcite occurs throughout the British and North American samples, but chiefly in the marine strata where it is present in the form of fossil debris, averaging 3.9 per cent for the former and 1.9 per cent for the latter. In the Gault Clay calcite occurs in the form of coccoliths which constitute 35 per cent of the mineralogy of the sample. In the Keuper Marl 13.3 per cent is present, although this is formed as a result of precipitation caused by evaporation of basins of inland drainage. Dolomite is present in small quantities (in marine samples), ranging from 1 - 7 per cent in three British shales and 1 - 5 per cent in four North American shales.

The percentages of calcite and dolomite were determined by the use of semi-quantitative calibration curves (see Appendix A1.). These values are compared in Table 3.7 with quantitative estimates of the carbonate contents expressed as (a) all calcite and (b) all dolomite, obtained by recalculation of the CO_2 percentages (Table 3.10).

However, only moderate agreement appears to exist. This may be accounted for on the basis that the majority of the carbonates are present in the form of fossil debris, as previously mentioned (which is not evenly distributed throughout the specimens) and also by the fact that other carbonates (e.g. siderite and ankerite) may be

Table 3.7 Measured and Calculated Carbonate & Pyrite Concentrations

	Sample Ref.	Pyrite measured(%)	Pyrite calculated(%)	Carbonate Measured(%) calcite	Carbonate Measured(%) dolomite	Carbonate Measured(%) total	Carbonate Calculated(%) calcite	Carbonate Calculated(%) dolomite
British Shales								
*London Clay 14m	LC14	1	1.03	-	3	3	1.77	1.56
*London Clay 37m	LC37	2	1.96	-	3	3	0.04	0.04
Gault Clay	GC	1	0.82	34	-	34	30.13	26.52
Fuller's Earth (Redhill)	FE23	-	0.69	-	-	-	0.61	0.54
Weald Clay	WC	-	0.39	-	-	-	-	-
Kimmeridge Clay	KC	4	4.18	7	-	7	1.06	0.94
Oxford Clay 10m	OC10	3	5.51	3	-	3	9.38	8.26
Oxford Clay 44m	OC44	5	5.60	3	-	3	3.93	3.46
Fuller's Earth (Bath)	FE19	3	1.89	6	-	6	2.68	2.36
Lias Clay 10m	L10	3	2.96	3	-	3	5.27	4.64
Lias Clay 36m	L36	5	6.00	3	-	3	1.68	1.48
Keuper Marl	KM	-	0.45	13	7	20	23.99	21.12
Swallow Wood roof	SWR	-	0.20	-	-	-	4.54	4.00
Flockton Thin roof	FTR	-	0.97	-	-	-	0.02	0.02
Flockton Thin seat	FTS	-	0.15	-	-	-	2.34	2.06
Widdringham roof	WR	-	0.24	-	-	-	0.11	0.10
North American Shales								
*Yazoo Clay	YC	-	2.66	8	-	8	5.81	5.12
*Kincaid Shale 6m	K6	-	0.15	10	1	11	5.27	4.64
Kincaid Shale 8m	K8	-	2.68	-	5	5	4.63	4.08
Nacimiento Shale	N1	-	0.09	-	-	-	0.02	0.02
Nacimiento Shale	N2	-	0.26	-	-	-	-	-
Nacimiento Shale	N3	-	0.05	-	-	-	0.18	0.16
Fox Hills Shale	FOX	1	3.56	1	-	1	1.02	0.90
Dawson Shale	DS	-	0.13	-	-	-	0.22	0.20
Pierre Shale (Dakota)	PSD	1	0.97	-	2	2	2.81	2.48
Pierre Shale (Colorado)	PSC	-	1.03	-	4	4	2.68	2.36

* possible ankerite present

present which have not been accounted for.

On the basis of a trace run with 5 per cent siderite present, the peaks identified for this mineral represented only about 0 - 1 per cent by weight, hence siderite was considered to be merely a trace mineral.

The possible presence of ankerite was detected in the samples of London Clay and the Kincaid Shale as a kink on the low 2θ side of the dolomite 2.88Å peak. No attempt was made to estimate its concentration.

3.1.4.2. Pyrite

Pyrite is identified by an X-ray peak at 2.71Å and the semi-quantitative estimation made for this mineral (see Appendix A 1) agrees reasonably well with the values obtained by recalculation of the sulphur content in terms of FeS_2 (Table 3.7).

This early diagenetic mineral is more common in the British samples, where it occurs in nine specimens and varies in concentration from 1 - 4.7 per cent, than in the North American samples where it is only recorded in the Fox Hills Shale. Its concentration in sediments is dependent on a suitable type and source of organic matter to support the sulphate reducing bacteria and also on the rate of sulphate diffusion from the overlying water.

3.1.5 Carbonaceous Material

The organic carbon contents were determined by wet chemical analysis (see Appendix A 1.4). Carbonaceous matter was visible as coaly partings in the Widdringham roof shale, as lignitic material in the Fox Hills Shale and as occasional rootlets in the Flockton Thin seatearth. Both samples of Oxford Clay contain over 3 per cent organic carbon, but this is in a finely disseminated form since

none was visible in hand specimen. The organic carbon in the remaining samples is below 1 per cent (Table 3.10).

3.1.6 Mineral Relationships

Two correlation matrices were set up to determine whether any significant mineralogical (and geochemical) relationships existed within the groups of shales studied; the British group containing 15 samples (excluding the Keuper Marl) and the North American group containing 10 samples. The resulting levels of significance (presented in Tables 3.9 and 3.10 respectively), i.e. 99.9 and 99 per cent - highly significant, and 95 per cent - probably significant, were determined by reference to statistical tables presented by Fisher & Yates (1974).

In a closed system where all the components total 100 per cent (as in the case of the present mineralogy), an increase in one leads to a reduction in the others, which means that the presence of a strong negative correlation (e.g. quartz and total clay mineral content) is not, by itself, of particular relevance. However, a strong positive correlation may indicate co-existence between mineral pairs, particularly when other evidence such as geochemical data supports the relationship.

Correlations are also very dependent on the amount and type of data analysed. In the present instance, the samples analysed are from two principal global locations, i.e. Britain and North America. In addition, the samples from each are not from within particular suites of sediments, but randomly selected, therefore only broad mineral relationships can be expected from the present work, although more sensitive correlations would be expected when the geochemical correlations are included.

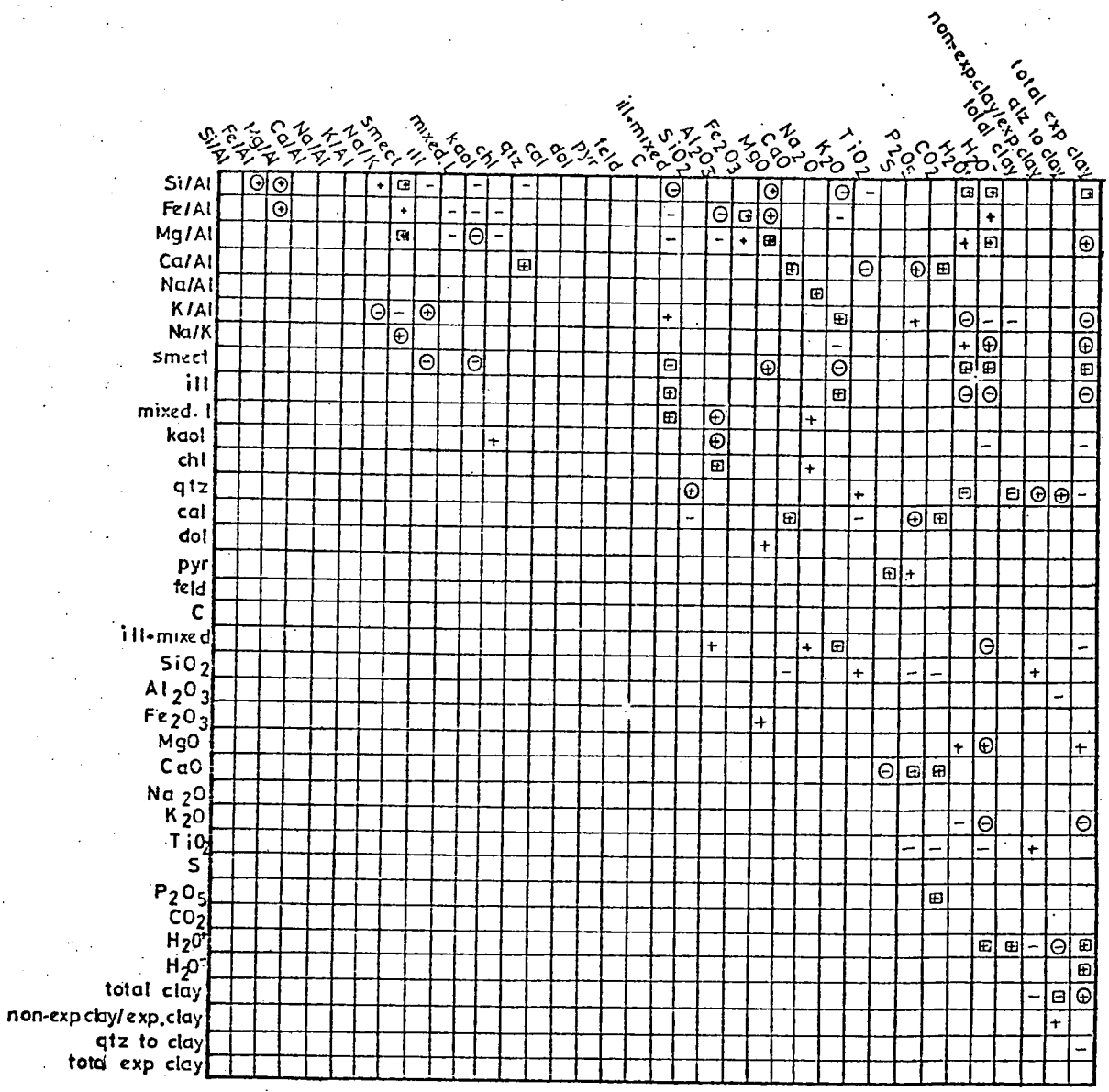

\+ - 95.0% - probably significant

⊕ ⊖ 99.0%
⊞ ⊟ 99.9% } - highly significant

Table 3.8. Significant Correlations Arising Within the Mineralogy and Geochemistry of 15 British Samples.

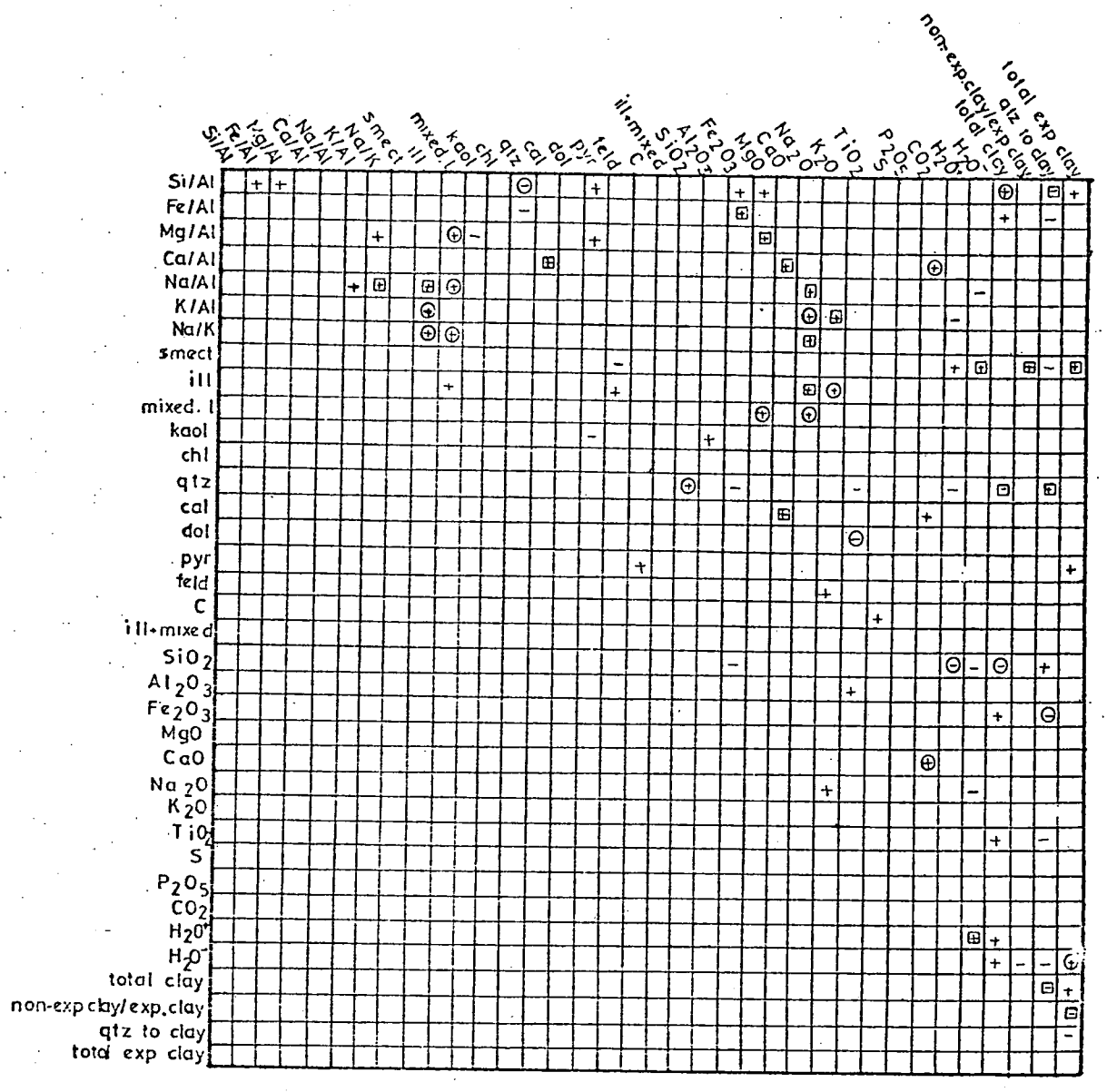

+ - 95.0% - probably significant

⊕ ⊖ 99.0%

⊞ ⊟ 99.9%

highly significant

Table 3.9. Significant Correlations Arising Within the Mineralogy and Geochemistry of the North Americam Samples.

For the 15 British samples in the present study, the only significant positive correlation is between kaolinite and chlorite (at the 95 per cent level). But since both of these minerals are believed to be detrital in origin, their co-existence is probably more symptomatic of the source material from which they were derived, and is unlikely to represent any geochemical affiliation such as the transformation of kaolinite to chlorite during sediment diagensis (see Fig. 1.5)

In the North American group, a positive correlation exists between feldspar and illite (at the 95 per cent level). However, this again can only be regarded as evidence of a detrital origin of these materials.

3.2 Geochemistry

3.2.1 Method of Analysis

Geochemical analyses were performed with a Philips PW 1212 Automatic Sequential Analyser X-ray Fluorescence (XRF) machine. The data from which, were processed using standard programmes with an IBM 360/67 computer, listing the elemental compositions in terms of their oxides (except for sulphur). Ten major elements were analysed by this technique, viz: Si, Al, Fe, Mg, Ca, Na, K, Ti, P and S. The normalised results are presented in Table 3.10.

Carbon, carbon dioxide and total water contents were analysed by conventional wet chemical methods. (See Appendix A1.4).

To aid analysis of the geochemistry, and to highlight any trends which can be related to the clay minerals, the oxide/alumina ratios of combined silica (total silica minus quartz), Fe_2O_3, MgO, CaO, Na_2O, K_2O have been computed along with the Na_2O/K_2O ratio and are presented in Table 3.11. Ratios of TiO_2, S and P_2O_5 are not included since

these elements are generally unimportant with respect to clay minerals.

Significant relationships between major elements or between major elements and mineralogy were determined with the aid of two correlation matrices (See Section 3.1.6).

3.2.2 Geochemical Relationships

The total silica content is composed of free silica (quartz) and combined silica. Combined silica, along with alumina, occurs as a major constituent of silicates. Except where feldspar is present, these two oxides are dominantly represented by clay minerals.

The average total silica contents for the British and North American shales in the present study are 53.5 and 62.5 per cent respectively, which favourably reflects the difference between the average quartz contents, since the combined silica contents for both groups are approximately the same, i.e. 33 and 30 per cent respectively.

The ratio of combined silica to alumina can be used as a measure of the variation in clay mineral species in sedimentary rocks provided that they are relatively free from other silicates. Typical combined silica to alumina ratios for clay minerals are:-

(a) Kaolinite	1.06 - 1.37	(Values for (a), (b) and (c) are average values from Weaver and Pollard, 1973)
(b) Illite	1.45 - 2.40	
(Fithian Illite 2.02)		
(c) Montmorillonite	2.14 - 3.45	
(Fuller's Earth 4.32)		

Hydromicas and beidellites have smaller values than illites and montmorillonites respectively.

The combined silica to alumina ratio in the British samples currently studied shows a significant positive correlation with the montmorillonite content indicating the dominance of Si over Al in the smectite lattice. This is further supported by a negative relationship (at the 95 per cent level) with the kaolinite and illite. Unfortunately, owing to the more uniform nature of the samples from North America, this relationship falls below the 95 per cent level, but can be inferred from the high combined silica to alumina ratios in Table 3.11.

Referring to the British samples, the mean value for the combined silica to alumina ratio is 1.903, but this is drastically reduced to 1.599 when the two samples of Fuller's Earth are excluded, and clearly reflects the dominance of illite and kaolinite in these materials (the Fuller's Earth rocks have values of 4.32 and 4.43 which are consistent with their compositions as almost pure montmorillonites, See Table 3.5.

The mean value for the combined silica to alumina ratio for the samples from North America is 2.005 which reflects the high smectite content, although the value is somewhat depressed by the presence of other clay minerals and beidellitic species of smectite (see Table 3.2).

The lower alumina content in the North American samples (i.e. 15.2 per cent compared with 19.1 per cent for the British samples) must be taken as further evidence for the dominance of smectite in these shales, although part of this difference may be explained by the lower total clay mineral content (60 per cent as opposed to 73 per

cent in the British shales). The small standard deviation observed for the alumina content in the North American shales indicates that a smaller variation in the clay mineral types might be expected, and this is indeed the case.

The higher level of alumina in the lattices of kaolinite and chlorite is confirmed by significant positive correlations between these two minerals and alumina in both groups of sediments. A strong positive correlation also exists between alumina and mixed-layer clay in the British samples.

The strong positive correlation between MgO and Fe_2O_3 and between MgO/Al_2O_3 and Fe_2O_3/Al_2O_3 observed in the British samples shows the high degree of inter-relationship between iron and magnesium in the silicate lattices, particularly of smectite (and illite), (see Table 3.5). This relationship is not shown by the samples from North America. However, the strong positive relationship between these latter two ratios and the combined silica to alumina ratio, which is shown in both the British and North American shales, and the positive relationship between the oxide (MgO and Fe_2O_3) to alumina ratios and smectite content for the British samples, indicates their association with the octahedral layer of smectite minerals where they replace alumina (See Table 3.5). This is supported by the negative correlations for the ratios of MgO/Al_2O_3 and Fe_2O_3/Al_2O_3 with alumina, kaolinite, chlorite and mixed-layer clay in the British samples. In addition, the positive correlation of MgO and Fe_2O_3 with the combined silica to alumina ratio in the North American samples and MgO with the combined silica to alumina ratio in the British samples may indicate their relative importance within the smectite minerals (see Table 3.5). The relationship between MgO and smectite in the

British samples is partly explained by the high MgO to alumina ratios found in the Fuller's Earths, but also by the fact that dolomite is present in both the London Clays (which also contain smectite) thus enhancing the previously mentioned ratio.

In addition to their clay mineral association, iron and magnesium are also associated with other minerals found in sediments. Iron is found in the reduced ferrous state combined with sulphur in pyrite. However, although this mineral was recorded in many of the samples no significant correlations were recorded between iron and sulphur or between iron and pyrite, which suggests that most of the iron is probably held within the silicate lattices. A strong relationship between sulphur and pyrite does, however, exist in the British samples. Magnesium is often present in carbonates in the form of dolomite (calcium magnesium carbonate), as evidenced by its correlation with this mineral in the British samples. The Keuper Marl, which has been excluded from the statistical analysis, contains 7.14 per cent dolomite, accounting for the high magnesium oxide content of 7.91 per cent.

CaO is present in the form of calcite as evidenced by its strong correlation to this mineral, and also to carbon dioxide in both the British and North American shales. The significance of these remarks is demonstrated by the large occurrence of both CaO and CO_2 in the Gault Clay (17.5 and 13.2 respectively) and in the Keuper Marl (12.5 and 10.5 per cent respectively). CaO does not show any significant relationships with MgO but their presence together can be inferred from the presence of dolomite in some of the samples tested.

The relationship of Na_2O within the clay minerals is partly obscured by the presence of feldspar, hence no degree of certainty

can be placed upon the correlations obtained, especially those for the North American shales where feldspar is very common. However, as sodium is mainly an interlayer cation, it is possible to obtain a more accurate measure of its presence in the clay minerals by reference to the cation exchange capacities, (see Section 3.3). From these it can be seen that the Pierre Shale (Dakota) and the Flockton Thin seatearth have reasonably high Na exchange values which are reflected in the high Na_2O/K_2O values (0.51 and 0.33 respectively) and the high Na_2O/Al_2O_3 values (0.1 and 0.03 respectively).

Potassium is fixed by the illites, as evidenced by a highly significant positive correlation between K_2O and illite in both groups of shales. This is further confirmed by the positive relationship between the K_2O/alumina ratio and illite. Potassium is also present in feldspars as evidenced by its correlation with this mineral in the North American samples (the correlation between Na_2O and feldspar falls just below the acceptable confidence level). Hence it is possible that some of the relationships involving potassium may have arisen because of this fact, and also because feldspar and illite are seen to be associated, since they are both detrital minerals. The relationship between Na_2O and K_2O is also probably related to the high feldspar content of these samples as it would not normally be expected for these two oxides to follow the same trends within clay minerals (Attewell and Taylor, 1973).

Water is present in all clay minerals in the form of 'lattice water' (which is removed at 1100°C) and 'absorbed water' (which is removed at 105°C). These two types have been combined to form the 'total water' content presented in Table 3.10.

All indications from the correlation matrices are that the total water content is related to the total expandable clay mineral content, especially that of the smectite. This is confirmed by reference to the chemical analyses of workers such as Kerr and Hamilton (1949) and Weaver and Pollard (1973).

The remaining major elements i.e. organic carbon, sulphur, phosphorus and titanium occur in minor amounts and are not associated with the clay mineralogy.

Organic carbon and sulphur are often found in close association under reducing conditions, which are suitable for the formation of pyrite. Phosphorus, analysed as P_2O_5, has strong affiliations with carbonates as evidenced by its relationships with calcite, carbon dioxide and CaO in the British samples. This is indicative of its presence in fossil debris, possibly as a phosphate mineral and consequently this association infers mainly marine conditions for the palaeosalinity.

Titanium, (as TiO_2) is commonly found as rutile inclusions in clay minerals and hence may follow the clay mineral trends, particularly kaolinite with which it is commonly associated. This statement is supported by the fact that there is a strong association between TiO_2 and Al_2O_3 in the North American samples. This is not shown by the British samples as the correlation coefficient falls below the acceptable level of significance. However, by inspection, the TiO_2 value does tend to follow kaolinite and alumina. An interesting relationship does come to light in the British samples, and that is the positive association between TiO_2 and quartz, which may well indicate a detrital origin for the oxide as proposed by Goldschmidt (1954) and Spears (1964).

Table 3.10 Geochemistry of British & North American Samples

British Shales	Sample Ref.	SIO2	AL203	FE203	MGO	CAO	NA20	K20	TIO2	S	P205	CO2	C	H20
London Clay 14m	LC14	55.02	17.32	7.94	3.51	1.09	0.27	3.37	1.11	0.55	0.12	0.78	0.48	8.44
London Clay 37m	L37	62.48	15.55	5.09	3.04	1.29	0.38	2.99	0.97	1.05	0.14	0.02	0.68	6.31
Gault Clay	GC	39.81	12.28	3.10	1.47	17.52	0.16	2.71	0.54	0.44	0.23	13.26	0.74	7.76
Fuller's Earth (Redhill)	FE23	55.14	12.53	7.20	3.39	3.45	0.24	0.45	0.67	0.37	0.10	0.27	0.28	15.91
Weald Clay	WC	72.10	14.68	4.87	0.92	0.31	0.44	1.94	1.36	0.21	0.06	0.00	0.00	3.10
Kimmeridge Clay	KC	56.39	18.58	5.23	1.29	3.32	0.35	2.89	0.90	2.23	0.13	0.47	0.69	7.53
Oxford Clay 10m	OC10	48.34	17.13	4.39	1.72	5.21	0.46	3.15	0.80	2.94	0.17	4.13	3.71	7.83
Oxford Clay 44m	OC44	54.10	18.33	4.61	1.63	1.63	0.81	3.10	0.88	2.99	0.13	1.73	3.12	6.94
Fuller's Earth (Bath)	FE19	54.07	15.14	4.54	3.20	3.83	0.44	1.62	0.66	1.01	0.11	1.18	0.43	13.78
Lias Clay 10m	L10	49.64	21.59	6.52	2.20	2.57	0.43	3.29	1.01	1.58	0.16	2.32	0.71	7.97
Lias Clay 36m	L36	48.45	21.66	6.45	1.98	2.39	0.55	3.01	0.96	3.20	0.16	0.74	0.70	9.75
Keuper Marl	KM	46.89	8.82	3.21	7.91	12.55	0.51	3.02	0.38	0.24	0.20	10.56	1.03	4.68
Swallow Wood roof	SWR	53.00	23.58	4.73	2.01	0.44	0.62	4.70	0.88	0.11	0.09	2.00	0.92	6.91
Flockton Thin roof	FTR	58.81	21.20	4.73	1.80	0.39	1.10	3.97	0.92	0.52	0.09	0.01	0.80	5.66
Flockton Thin seat	FTS	44.31	31.93	2.69	1.28	0.41	0.99	3.03	1.07	0.08	0.07	1.03	1.34	11.77
Widdringham roof	WR	51.99	25.64	4.44	1.60	0.38	0.12	2.17	1.11	0.13	0.07	0.05	2.56	9.73
North American Shales														
Yazoo Clay	YC	51.53	17.60	5.50	2.16	3.57	0.25	1.78	0.80	1.42	0.13	2.56	0.58	12.14
Kincaid Shale 6m	K6	64.24	14.09	4.45	1.10	3.47	0.45	1.90	0.61	0.08	0.12	2.32	0.09	7.09
Kincaid Shale 8m	K8	67.48	14.30	2.62	1.08	1.47	0.66	2.29	0.47	1.43	0.10	2.04	0.40	5.67
Nacimiento Shale	N1	63.80	15.75	5.96	1.37	0.90	1.00	3.61	0.77	0.05	0.10	0.01	0.33	6.35
Nacimiento Shale	N2	65.21	17.37	2.83	1.44	0.89	1.28	3.44	0.80	0.14	0.17	0.00	0.60	5.83
Nacimiento Shale	N3	58.25	17.06	7.13	1.27	1.39	0.18	2.28	0.79	0.03	0.08	0.08	0.30	11.17
Fox Hills Shale	FOX	61.77	13.58	5.88	1.83	0.73	0.72	2.18	0.70	1.90	0.07	0.45	3.24	6.93
Dawson Shale	DS	70.06	14.29	3.55	1.45	1.07	0.14	1.92	0.62	0.07	0.08	0.10	0.41	6.24
Pierre Shale (Dakota)	PSD	62.57	13.43	5.29	2.41	1.78	1.34	2.63	0.60	0.52	0.12	1.24	0.79	7.30
Pierre Shale (Colorado)	PSC	61.64	15.16	5.25	2.52	1.78	1.59	2.69	0.63	0.55	0.12	1.18	0.93	5.97
Reference Samples														
Kaolin		44.64	38.39	0.69	0.13	0.29	0.03	0.15	1.64	0.02	0.08	0.00	0.00	13.95
French Illite		51.29	18.37	6.39	3.97	1.07	0.30	8.37	0.73	0.02	0.21	0.00	0.00	9.28
Fithian Illite		57.13	18.32	5.74	2.06	0.56	0.52	4.87	0.89	1.07	0.14	0.00	0.00	8.69
Morris Illite		54.77	18.02	8.90	2.28	0.93	0.26	5.00	0.63	2.02	0.09	0.00	0.00	7.10
Otay Mont.		56.06	13.66	1.88	7.61	1.33	1.13	0.35	0.32	0.03	0.07	0.00	0.00	17.56

Table 3.11

Geochemical Ratios

British Shales	Sample Ref.	SIO2/AL203	FE203/AL203	MGO/AL203	CAO/AL203	NA20/AL203	K20/AL203	NA20/K20
London Clay 14m	LC14	2.10	0.45	0.20	0.06	0.01	0.19	0.08
London Clay 37m	LC37	1.33	0.32	0.19	0.08	0.02	0.19	0.12
Gault Clay	GC	2.08	0.25	0.11	1.42	0.01	0.22	0.05
Fuller's Earth (Redhill)	FE23	4.32	0.57	0.27	0.27	0.01	0.03	0.54
Weald Clay	WC	1.16	0.33	0.06	0.02	0.03	0.13	0.22
Kimmeridge Clay	KC	1.78	0.28	0.06	0.17	0.01	0.15	0.11
Oxford Clay 10m	OC10	1.57	0.25	0.10	0.30	0.02	0.18	0.14
Oxford Clay 44m	OC44	1.36	0.25	0.08	0.08	0.04	0.16	0.25
Fuller's Earth (Bath)	FE19	3.43	0.29	0.21	0.25	0.02	0.10	0.26
Lias Clay 10m	L10	1.58	0.30	0.10	0.11	0.02	0.15	0.13
Lias Clay 36m	L36	1.62	0.29	0.09	0.11	0.02	0.13	0.18
Keuper Marl	KM	1.49	0.36	0.89	1.42	0.05	0.34	0.16
Swallow Wood roof	SWR	1.73	0.20	0.08	0.01	0.02	0.19	0.13
Flockton Thin roof	FTR	1.64	0.22	0.08	0.01	0.05	0.18	0.27
Flockton Thin seat	FTS	1.32	0.08	0.04	0.01	0.03	0.09	0.32
Widdringham roof	WR	1.46	0.17	0.06	0.01	0.01	0.08	0.05
North American Shales								
Yazoo Clay	YC	2.26	0.31	0.12	0.20	0.01	0.10	0.14
Kincaid Shale 6m	K6	1.36	0.31	0.07	0.24	0.03	0.13	0.23
Kincaid Shale 8m	K8	1.08	0.18	0.07	0.10	0.04	0.16	0.28
Nacimiento Shale	N1	2.28	0.37	0.08	0.05	0.06	0.22	0.27
Nacimiento Shale	N2	1.72	0.16	0.08	0.05	0.07	0.19	0.37
Nacimiento Shale	N3	2.09	0.41	0.07	0.08	0.01	0.13	0.07
Fox Hills Shale	FOX	2.63	0.43	0.13	0.05	0.05	0.16	0.33
Dawson Shale	DS	1.47	0.24	0.10	0.07	0.01	0.13	0.07
Pierre Shale (Dakota)	PSD	2.98	0.39	0.17	0.13	0.09	0.19	0.50
Pierre Shale (Colorado)	PSC	2.14	0.34	0.16	0.11	0.10	0.17	0.59
Reference Samples								
Kaolin		1.03	0.01	0.00	0.00	0.00	0.00	0.20
French Illite		2.52	0.34	0.21	0.05	0.01	0.45	0.03
Fithian Illite		2.02	0.31	0.11	0.03	0.02	0.26	0.10
Morris Illite		2.37	0.49	0.12	0.05	0.01	0.27	0.05
Otay Mont.		4.10	0.13	0.55	0.09	0.08	0.02	3.28

3.3 Cation Exchange Capacity

3.3.1 Method of Analysis

Two methods (reported in Appendix A1.3) were used to obtain the cation exchange capacity of the shales studied:-

(i) The individual concentration of exchangeable Na^+, K^+, Ca^{++} and Mg^{++} cations (in milliequivalents per 100 grams of clay) were determined by leaching with ammonium acetate (Chapman, 1965; Spears, 1973), see Table 3.12. Although this method is suitable for analysis of all mineralogical species, enhanced values for exchangeable Ca are obtained if calcite is present to any degree (clays for which this situation arises are marked by an asterisk in Table 3.12).

(ii) The total cation exchange capacity (Table 3.13) was determined (in milliequivalents per 100 grams) for certain materials using methylene blue absorption (Taylor, 1967). This method is, however, only suitable for analysing shales containing mixtures of illite and kaolinite because the large methylene blue molecule cannot enter the smectite lattice (e.g. Fuller's Earth from Bath, Table 3.13). Therefore this method was used to obtain true total exchange capacities for illite-kaolinite shales where calcite had affected the result. This enabled a corrected calcium value to be obtained. Three control samples, i.e. two Carboniferous shales and the London Clay (LC37) were also analysed for comparison with acetate leaching.

3.3.2 Exchangeable Cation Relationships

Typical values given by Weaver and Pollard (1973) for the exchange capacity of pure clays are:-

Kaolinite	3.6 - 18 meq/100g
Illite	10.0 - 40 "
Montmorillonite	70.0 -130 "

The majority of recorded values are in line with the values quoted above (See Tables 3.2 and 3.12); a notable exception being the Fox Hills Shale which contains 3 per cent carbonaceous material.

Unlike the relationships existing between geochemistry and mineralogy, which follow certain rigid trends, the exchangeable cations are controlled by a variety of factors, e.g. the composition of the water in environment of deposition, post-depositional leaching and diagenesis, depth of burial, and to a certain extent, the time in which the particular events took place. Therefore it is possible for the same mineral to contain different cations depending on these variables.

Spears (1973) shows that the variation in the exchangeable cations from a sequence of Carboniferous strata could be related to changes in the palaeosalinity (i.e. in marine shales the exchangeable Mg is higher than in shales deposited under brackish conditions, and the concentrations of exchangeable Ca and Na , and K are lower; the same relationships being recorded in modern sediments). Other workers have commented on the effect of burial upon the cations present. Weaver and Beck (1971), show that the order of exchangeable cations (from a borehole in the Gulf of Mexico) changes with depth from Na , Ca , Mg , K at the surface to Ca , Mg , K , Na at a depth of 5200 metres.

In the present range of shales, Ca , followed by Mg are the dominant exchange cations, although Na is an important constituent of the Flockton Thin seatearth and the Pierre Shale from Dakota. Unfortunately the samples studied are not from related suites, therefore it is not possible to fully equate the cation values, or their ratios (Table 3.14) to the above findings. Nevertheless, a number of significant relationships are observed(Table 3.16).

Table 3.12 Cation Exchange Capacities from Acetate Leaching (m.eq/100g Clay)

	Sample Ref.		Na	K	Mg	Ca	Total
British Shales							
London Clay 14m	LC14		0.44	0.34	12.63	18.87	32.28
London Clay 37m	LC37	*	0.36	0.30	10.30	15.32	26.28
Gault Clay	GC	*	1.62	0.19	3.81	133.03	138.65
Fuller's Earth (Redhill)	FE23		1.09	0.40	3.76	93.41	98.06
Weald Clay	WC		-	-	-	-	-
Kimmeridge Clay	KC	*	0.48	0.23	4.36	22.18	27.25
Oxford Clay 10m	OC10	*	1.06	0.29	4.67	121.95	127.97
Oxford Clay 44m	OC44	*	0.49	0.22	2.30	31.88	34.89
Fuller's Earth (Bath)	FE19		0.67	0.23	10.60	103.16	114.66
Lias Clay 10m	L10	*	0.73	0.20	3.30	54.80	59.03
Lias Clay 36m	L36	*	0.70	0.29	3.08	59.04	63.11
Keuper Marl	KM	*	0.79	0.34	6.12	99.55	106.80
Swallow Wood roof	SWR		2.57	1.36	2.70	3.90	10.53
Flockton Thin roof	FTR		1.63	1.06	1.44	3.04	7.17
Flockton Thin seat	FTS		10.59	1.28	1.62	5.20	18.69
Widdringham roof	WR		0.40	0.28	2.86	3.54	7.08
North American Shales							
Yazoo Clay	YC	*	0.90	0.31	10.61	87.37	99.19
Kincaid Shale 6m	K6		0.97	0.11	0.99	69.81	71.88
Kincaid Shale 8m	K8		0.40	0.06	0.22	14.37	15.05
Nacimiento Shale	N1		1.16	0.55	1.84	22.53	26.08
Nacimiento Shale	N2		0.55	0.31	0.51	14.08	15.45
Nacimiento Shale	N3		0.60	1.21	5.37	39.22	46.60
Fox Hills Shale	FOX		1.51	1.71	7.40	9.37	19.99
Dawson Shale	DS		0.71	0.28	3.53	60.15	64.67
Pierre Shale (Dakota)	PSD		6.23	4.10	5.38	30.57	46.28
Pierre Shale (Colorado)	PSC		0.57	0.29	6.85	19.18	26.89

* Enhanced calcium concentration because of calcite concentration

Table 3.13 Total Exchangeable Cation Capacity (From Methylene Blue Absorption)

	Sample Ref.	Total C.E.C. (m.eq/100g)	Corrected Calcium (where applicable) (m.eq/100g)
London Clay 37m	LC37	17.90	6.94
Gault Clay	GC	14.76	9.14
Kimmeridge Clay	KC	12.07	7.00
Oxford Clay 10m	OC10	14.06	8.04
Oxford Clay 44m	OC44	11.33	8.32
Fuller's Earth (Bath)	FE19	7.75	-* pure montmorillonite
Lias Clay 10m	L10	12.16	7.93
Lias Clay 36m	L36	13.66	9.59
Flockton Thin seat	FTS	13.25	-
Widdringham roof	WR	6.71	-
Reference Clays			
Morris Illite (A.P.I. No.36)		21.05	
"		21.10	
Calcite		0.18	

Table 3.14 Cation Ratios

	Sample Ref.	Na/K Water Soluble Cations	Na/K Exchangeable Cations	Mg/Ca Water Soluble Cations	Mg/Ca Exchangeable Cations
London Clay 14m	LC14	0.36	1.29	2.05	0.67
London Clay 37m	LC37	1.16	1.20	2.40	0.67
Gault Clay	GC	0.22	8.52	0.37	0.41
Fuller's Earth (Redhill)	FE23	0.48	2.72	0.18	0.04
Weald Clay	WC	-	-	-	-
Kimmeridge Clay	KC	0.85	2.08	0.32	0.63
Oxford Clay 10m	OC10	1.89	3.65	0.35	0.58
Oxford Clay 44m	OC44	3.34	2.23	0.29	0.28
Fuller's Earth (Bath)	FE19	0.30	2.91	0.27	0.10
Lias Clay 10m	L10	1.49	3.50	0.32	0.42
Lias Clay 36m	L36	3.95	2.41	0.25	0.32
Keuper Marl	KM	5.05	2.32	0.62	3.45
Swallow Wood roof	SWR	2.03	1.88	2.33	0.69
Flockton Thin roof	FTR	4.80	1.53	2.20	0.47
Flockton Thin seat	FTS	12.49	8.27	1.58	0.31
Widdringham roof	WR	0.32	1.42	0.87	0.81
Yazoo Clay	YC	2.66	2.90	0.46	0.12
Kincaid Shale 6m	K6	2.80	8.81	0.09	0.01
Kincaid Shale 8m	K8	3.23	6.66	0.04	0.02
Nacimiento Shale	N1	11.68	2.10	0.97	0.08
Nacimiento Shale	N2	7.30	1.61	0.22	0.03
Nacimiento Shale	N3	2.68	0.49	0.44	0.13
Fox Hills Shale	FOX	4.74	0.88	1.16	0.78
Dawson Shale	DS	0.95	2.53	0.44	0.05
Pierre Shale (Dakota)	PSD	14.61	1.52	1.02	0.17
Pierre Shale (Colorado)	PSC	9.31	1.97	1.43	0.35

3.3.3 Water-Soluble Cations

Spears (1974) suggests that the water-soluble cations in non-marine and brackish conditions are characterised by high Na^+ and K^+ concentrations and low Ca^{++} and Mg^{++} concentrations; the reverse situations prevailing for marine conditions. Weaver and Beck (1971) and Van Moort (1971) report that from deep boreholes Na^+ is the major cation, followed by K^+, Mg^{++} and Ca^{++}, and suggest that Ca^{++} is selectively retained during burial. Spears (1974) shows that the water soluble-cations from a sequence of Carboniferous strata do not bear any relationship to the original pore water, but instead are the result of diagenetic alterations causing the removal of exchange sites by the transformation of montmorillonite layers to illite. Drever (1971) accounts for post-depositional changes in the exchange characteristics of marine sediments in the Rio Ameca Basin by the action of anaerobic bacteria.

Water-soluble cations from the current shales (Table 3.15), determined in association with ammonium acetate leaching (Appendix A1.3) show that Ca^{++} and Na^+ are the dominant species. Those of the Swallow Wood roof, Flockton Thin roof and seatearth, which are all non-marine in origin, conform to the argument of Spears (1974). The Widdringham roof also of non-marine origin, does not, however, agree with his hypothesis, but as the sample is from relatively shallow depth, compared with the other Carboniferous materials, it is possible that the pore waters have been substantially altered. Of the non-marine shales from North America, the Nacimiento samples also tend to agree with Spear's findings although the Dawson and Fox Hills shales do not. In complete contrast, pore waters from the Pierre Shales are sodium-rich, although both of these materials

Table 3.15 Water-Soluble Cations (m.eq/100g Clay)

	Sample Ref.	Na	K	Mg	Ca	Total
British Shales						
London Clay 14m	LC14	1.26	3.52	9.79	4.77	19.34
London Clay 37m	LC37	2.96	2.56	5.82	2.42	13.76
Gault Clay	GC	0.63	2.75	4.99	13.22	21.59
Fuller's Earth (Redhill)	FE23	0.44	0.90	2.32	12.46	16.12
Weald Clay	WC	-	-	-	-	-
Kimmeridge Clay	KC	0.67	0.78	1.25	3.88	6.58
Oxford Clay 10m	OC10	5.69	2.01	2.80	7.96	19.46
Oxford Clay 44m	OC44	7.91	2.37	3.02	10.35	23.65
Fuller's Earth (Bath)	FE19	0.33	1.10	2.41	8.96	12.80
Lias Clay 10m	L10	5.30	3.54	3.44	10.80	23.08
Lias Clay 36m	L36	8.94	2.26	2.16	8.45	21.81
Keuper Marl	KM	6.02	1.19	5.57	8.93	21.71
Swallow Wood roof	SWR	5.63	2.76	1.05	0.45	9.89
Flockton Thin roof	FTR	8.32	1.73	1.10	0.50	11.65
Flockton Thin seat	FTS	10.12	0.81	0.60	0.38	11.91
Widdringham roof	WR	0.25	0.78	0.70	0.80	2.53
North American Shales						
Yazoo Clay	YC	4.32	1.62	5.80	12.57	24.31
Kincaid Shale 6m	K6	1.26	0.45	1.00	10.85	13.56
Kincaid Shale 8m	K8	1.26	0.39	1.39	39.67	42.71
Nacimiento Shale	N1	4.09	0.35	0.73	0.75	5.92
Nacimiento Shale	N2	3.36	0.46	0.25	1.12	5.19
Nacimiento Shale	N3	2.82	1.05	0.79	1.79	6.45
Fox Hills Shale	FOX	2.42	0.51	8.63	7.40	18.96
Dawson Shale	DS	3.63	3.79	3.46	7.75	18.63
Pierre Shale (Dakota)	PSD	15.49	1.06	2.70	2.64	21.89
Pierre Shale (Colorado)	PSC	13.97	1.50	3.07	2.14	20.68

British Materials

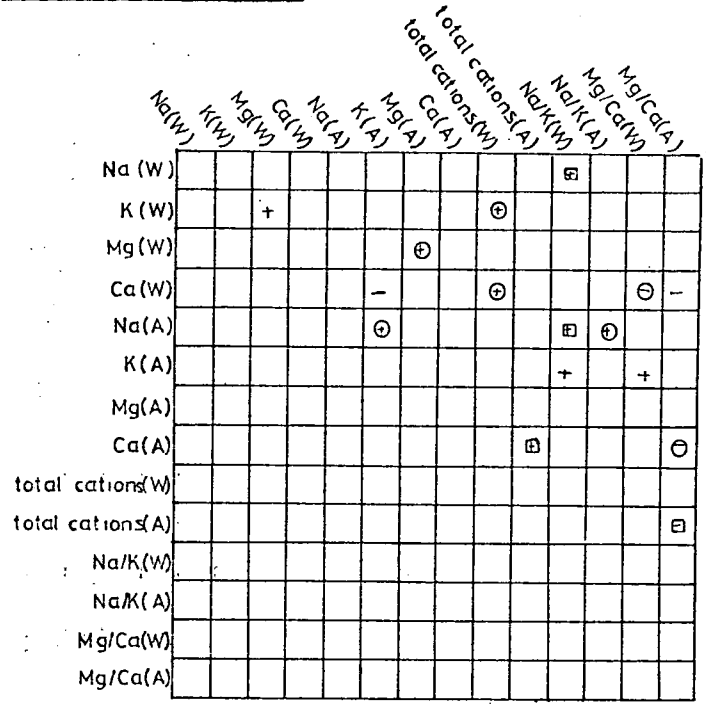

A - leached with acetate
W- water-soluble

North American Materials

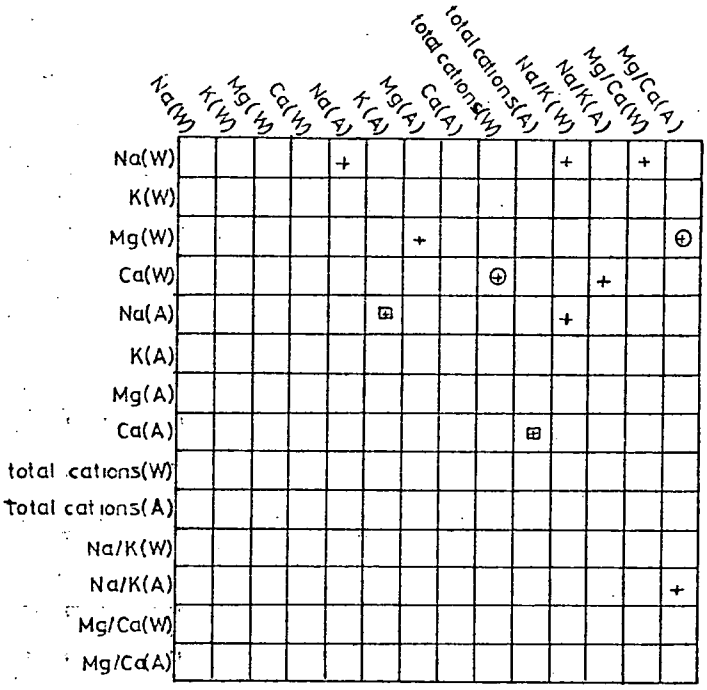

\+ – 95.0% - Probably Significant

⊕ ⊖ 99.0%

⊞ ⊟ 99.9% - Highly Significant

Table 3.16. Significant Correlations Arising Amongst Exchangeable and Water-Soluble Cations.

are marine in origin. No other definite conclusions regarding palaeosalinity could be found.

3.4 The Effect of Age and Depth of Burial upon the Mineralogy and Geochemistry

In the present study, the British shales from the Tertiary to the Lias have been buried to a maximum depth of about 1250m (see Chapter 2) and hence are above the level at which the mineralogical transformations begin, (Powers, 1967). Even the most deeply buried shales in the above age range have preconsolidation loads equivalent to only 2500m. From the recalculation of the smectite chemical structure from the Fuller's Earth from Bath (which is Great Oolite in age and consequently among the oldest of the sediments in Britain which have not been affected by orogenic phases), the mineral present is shown to be an almost pure montmorillonite (Si/Al = 3.94). This implies that the age alone does not alter the mineralogy. Powers (1967) suggests that this may be the case but did not have clear evidence because all of his samples were relatively young. Bradshaw (1975) shows that the ratio of mixed-layer clay to montmorillonite in the Esturine Series of the Middle Jurassic is not constant and concludes that the mixed-layer material is of detrital origin because if it had been derived from the montmorillonite, the above ratio would have been constant throughout the section.

The British Carboniferous shales, which are the result of over 3500m of sedimentation, have a simple mineralogy of illite, mixed-layer clay, kaolinite and chlorite. Perrin (1971) shows that montmorillonite is notably absent (or very rare) in the Carboniferous or older rocks and this conforms to the depth argument of Powers.

However, evidence of ash bands in these older rocks is presented by several workers. Spears (1971) suggests that the Stafford tonstein, where the principal clay mineral is a mixed-layer mica-montmorillonite comparable to a K-bentonite, is the product of an ancient volcanic ash band. Bands containing K-bentonite material in the mixed-layer component have also been noted by Trewin (1968) and Gilkes and Hodson (1971).

With regard to the North American shales, which are from the Late Cretaceous and Tertiary, all are seen to contain smectite which suggests that the distribution of this mineral is much greater than in the British shales, presumably because of the volcanism associated with the formation of the Rocky Mountains (Tourtelot, 1962).

From the estimates of the maximum depth of burial, it can be concluded from the present work, that the North American strata have been, in general, more deeply buried than much of the older British strata. In the present study several samples have had a maximum overburden pressure equivalent to 1650 - 1800m of sediments, although the maximum thicknesses of Tertiary and Upper Cretaceous strata in North America can reach 7500 - 9000m (Dunbar & Waage, 1969). The recalculation of smectites (Table 3.5) shows that the most deeply buried North American samples have low Si/Al ratios of 2.9 - 3.6 and high potassium contents, and are consequently beidellitic in character. These shales may therefore show the initial stages of the montmorillonite to illite conversion with associated potassium fixation.

The Si/Al ratio for the smectite of the Yazoo Clay is 3.83, and the potassium content is also moderately high, which would suggest that a certain degree of degradation has occurred. However, as the

smectite is of detrital origin and as this deposit is not deeply buried it is likely that this degradation may have occurred before deposition and is not associated with the history of the Yazoo Clay.

To conclude, it appears that the depth of burial is the most important factor which influences the diagenetic alteration of clay minerals, particularly the smectite species. Age alone does not appear to greatly affect the transformation process as may be deduced from the sample of Fuller's Earth from Bath.

3.5 The Relationship between Mineralogy, Atterberg Limits and Clay-Sized Fraction

The Atterberg Limits* are used as a means of classification in soils engineering and because of their dependency on mineralogical composition, it is pertinent to consider them at this point.

Two series of tests were conducted, the first (Table 3.17) was under the conditions specified by British Standard 1377 (1967), while the second was after the material had been slaked, mechanically disintegrated, dried and powdered to pass a B.S. 200 mesh. The results, which are presented on plasticity diagrams (Fig.3.7), after Casagrande (1948) indicate that there is a general increase in the liquid limit (of up to 87 per cent in the more indurated materials) and decrease in the plastic limit when the slaking technique is used. Furthermore, it is considered that the results obtained, after using the slaking technique are more representative of the properties of the shales studied since they probably reflect the behaviour of individual particles and not aggregates, (as suggested by the indurated sediments).

The liquid limits vary from 35 - 135, with the higher values (i.e. greater than 75) being associated with smectite concentration.

* Atterberg Limits are defined in Section 1.4.2

Even small quantities of this mineral in shales containing large quantities of quartz tends to enhance the value (e.g. Dawson Shale and Kincaid Shale). The two samples of Fuller's Earth, being principally Ca montmorillonites, have values of 100 and 117 which, although low when compared with a number of values for multi-component systems, are in good agreement, however, with those of other workers (Dr. A.B. Hawkins, Bristol University, personal communication). The presence of exchangeable sodium to any degree in the smectites greatly enhances the liquid limit (e.g. Pierre Shale, Dakota (sample PSD)), conversely a relatively high carbonaceous content, even in smectite rich sediments, appears to depress the aforementioned value (e.g. Fox Hills shale).

Moderate liquid limits (50 - 80) are typical of shales containing illite, mixed-layer clay, kaolinite and quartz (e.g. the majority of British sediments).

Liquid limits of 35 - 45 are characteristic of shales where quartz or kaolinite are the major mineral species (e.g. Weald Clay-high quartz, Widdringham roof shale - high kaolinite).

The plastic limit appears to increase as the smectite content increases, provided that Ca is the dominant exchangeable cation. Conversely the presence of exchangeable sodium appears to maintain a depressed value for the plastic limit (e.g. Pierre Shale, Dakota).

Seed et al (1964) have suggested that the activity* (Skempton, 1953) will accurately classify artificially prepared soils. Therefore the clay-sized fraction was determined for the materials tested (table 3.18). However, although a general increase is associated with the higher liquid limits, these results, and those of the associated activity (Table 3.18) are not considered to be entirely accurate because difficulties were encountered with flocculation

* Activity is defined in Section 1.4.2

Table 3.17 Atterberg Limits of the Shales Tested

	Sample Ref.	Slaked 200 mesh			Crushed 36 mesh		
		LL	PL	PI	LL	PL	PI
British Samples							
London Clay 14m	LC14	84	31	53	84	31	53
London Clay 37m	LC37	63	25	38	65	25	40
Gault Clay	GC	75	27	48	76	30	46
Fuller's Earth (Redhill)	FE23	117	54	63	117	61	56
Weald Clay	WC	36	25	11	37	25	12
Kimmeridge Clay	KC	70	24	46	58	22	36
Oxford Clay 10m	OC10	76	26	50	63	32	31
Oxford Clay 44m	OC44	58	29	29	51	29	22
Fuller's Earth (Bath)	FE19	100	39	61	100	37	61
Lias Clay 10m	L10	68	23	45	60	28	32
Lias Clay 36M	L36	65	28	37	50	30	20
Swallow Wood roof	SWR	58	26	32	33	20	13
Flockton Thin roof	FTR	46	24	23	31	20	11
Flockton Thin seat	FTS	61	26	35	34	20	14
Widdringham roof	WR	45	23	22	29	19	10
North American Samples							
Yazoo Clay	YC	117	32	85	101	37	64
Kincaid Shale 6m	K6	72	19	53	61	20	41
Kincaid Shale 8m	K8	58	19	37	48	23	25
Nacimiento Shale	N1	37	24	13	35	24	11
Nacimiento Shale	N2	39	25	14	42	21	21
Nacimiento Shale	N3	94	33	61	65	31	34
Fox Hills Shale	FOX	61	40	21	57	37	20
Dawson Shale	DS	75	24	51	49	23	26
Pierre Shale (Dakota)	PSD	135	29	106	115	36	79
Pierre Shale (Colorado)	PSC	62	17	45	53	20	33

Table 3.18 Clay-sized Fraction & Activity Values & Specific Gravity

British Materials	Sample Ref.	Clay-Sized Fraction	Activity	S.G.
London Clay 14m	LC14	65	0.82	2.77
London Clay 37m	LC37	53	0.72	2.72
Gault Clay	GC	60	0.80	2.71
Fuller's Earth (Redhill)	FE23	69	0.91	2.80
Weald Clay	WC	32	0.34	2.69
Kimmeridge Clay	KC	57	0.81	2.68
Oxford Clay 10m	OC10	37	1.35	2.49
Oxford Clay 44m	OC44	46	0.63	2.53
Fuller's Earth (Bath)	FE19	68	0.90	2.70
Lias Clay 10m	L10	62	0.73	2.67
Lias Clay 36m	L36	65	0.57	2.65
Keuper Marl	KM	43	0.33	2.75
Swallow Wood roof	SWR	35	0.94	2.75
Flockton Thin roof	FTR	48	0.46	2.75
Flockton Thin seat	FTS	42	0.83	2.66
Widdringham roof	WR	64	0.34	2.50
North American Materials				
Yazoo Clay	YC	85	1.00	2.73
Kincaid Shale 6m	K6	68	0.78	2.71
Kincaid Shale 8m	K8	16	2.44	2.66
Nacimiento Shale	N1	21	0.62	2.69
Nacimiento Shale	N2	54	0.26	2.67
Nacimiento Shale	N3	34	1.79	2.76
Fox Hills Shale	FOX	61	0.34	2.57
Dawson Shale	DS	63	0.81	2.62
Pierre Shale (Dakota)	PSD	71	1.49	2.64
Pierre Shale (Colorado)	PSC	47	0.96	2.67

Figure 3.7. Relationships Between Liquid Limit and Plasticity Index.

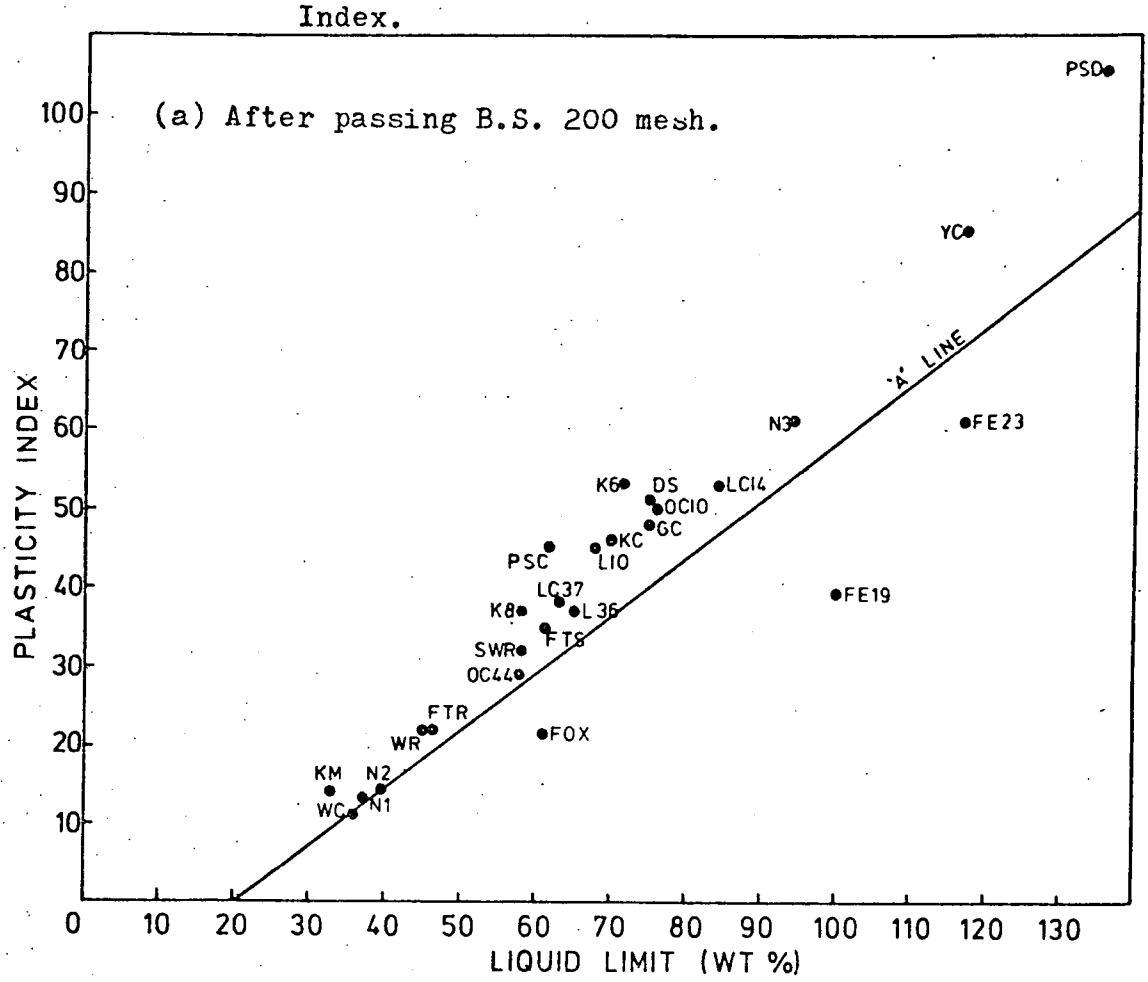

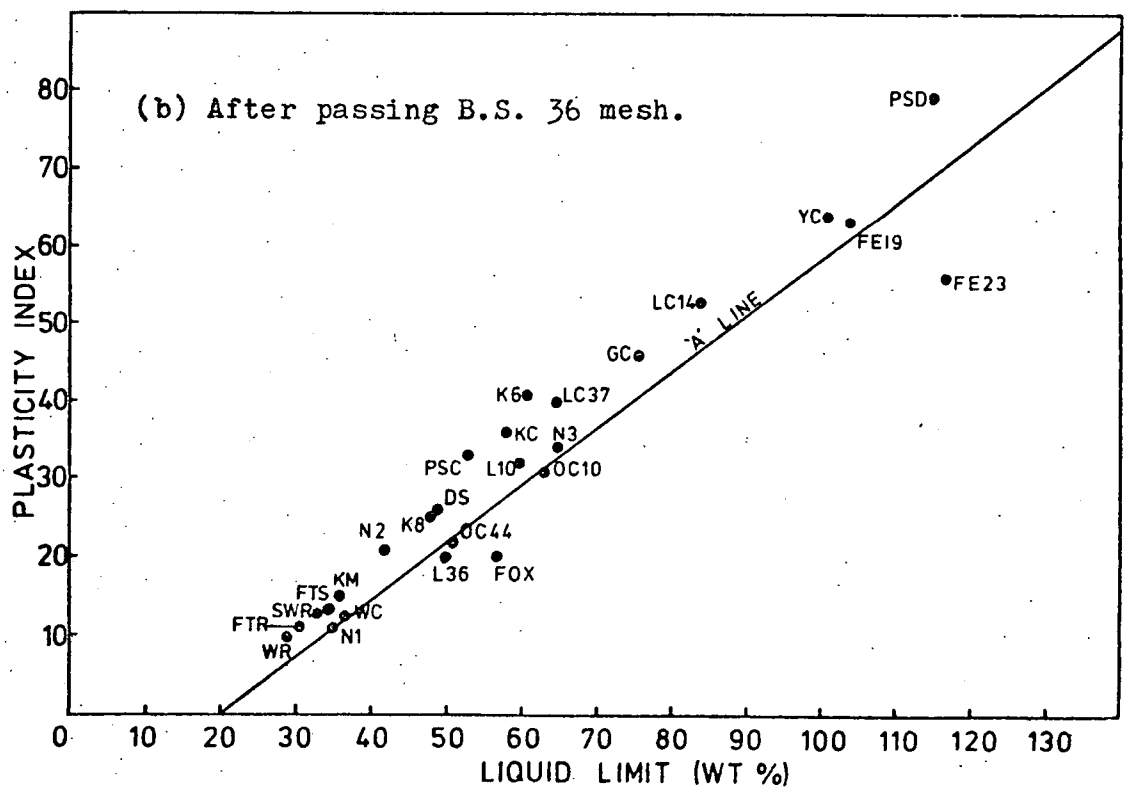

during the course of testing. Consequently, the results have, in the main, been excluded from further analysis.

3.6 Conclusions

From a detailed analysis of the mineralogy (obtained by X-ray diffraction) and geochemistry of 16 British shales (ranging in age from the Carboniferous Period to the Tertiary Period) and 10 North American shales (from the Late Cretaceous and Tertiary Periods), major differences were found in the relative abundances of mineral species present in each group, and as a consequence, the engineering properties of the shales in each will be very different. In addition, further evidence is presented to confirm that the depth of burial, and not the age, is the most important factor controlling the transformation of montmorillonite to illite during diagenesis of sediments. This evidence is based on the recalculation of the structural formulae of several smectite minerals from both groups of shales.

The following are the major points which arise from the mineralogy and geochemistry to justify the above statements:-

(1) Smectite is the dominant mineral in the North America shales, occurring in every sample, whereas its occurrence in the British shales is restricted to 5 samples (i.e. the two samples of Fuller's Earth where it is the only clay mineral and 3 others where it is a minor constituent).

(2) By recalculating the structural formulae of smectites from 5 samples it was concluded that the depth of burial was the most important control in the transformation of montmorillonite to illite. The two samples of Fuller's Earth, which have not been deeply buried (less than 1000m) contained good montmorillonite which showed no signs of degrading to illite, even though the sample from Bath is of Great

Oolite age . The smectites from the Dawson Shale and the Nacimiento Shale No.3, having been buried to depths of about 1800m were much more beidellitic in character and could be interpreted as being in the initial stages of the transformation process. No conclusions were drawn for the smectite from the Yazoo Clay because of the detrital origin of the deposit.

(3) Illite is the dominant clay mineral in the British samples, whereas, it is the least important clay mineral species in the North American suite. All the illites were found to be dioctahedral, and where identification was possible, the 2M polymorph prevailed except in the Flockton Thin seatearth where the 1Md polymorph was suspected.

(4) Kaolinite is the second most abundant clay mineral in both groups, although it is more common in the British shales. The variations in the kaolinites are primarily caused by differences in the crystallinity states or by 'b' axis disordering of the lattice.

(5) Expandable mixed-layer clay occurs to a varying degree in both groups of shales. However, as the material identified is more closely related to the illites in the present study; the higher concentrations are found in the British samples. Evidence is also presented to confirm that the mixed-layer component is detrital in origin and does not arise from the transformation of montmorillonite.

(6) Chlorite is present as a minor detrital clay mineral in the British samples only. None was detected in the North American samples.

(7) Quartz is the dominant massive mineral in both groups of shales although it has a significantly higher concentration in the North American samples, which is probably associated with higher rates of deposition.

(8) Feldspar is found in both groups of shales but again its occurrence is far more frequent in the North American material. This is associated with the vulcanicity which was present during the Late

Cretaceous and Tertiary times in the United States.

(9) The non-detrital minerals i.e. carbonates and pyrite were found to be present in both the British and North American shales. Pyrite occurs with greater frequency in the British shales, whereas the carbonates are evenly distributed between the two groups. Their presence reflects marine conditions of deposition.

(10) The trends observed from the geochemical analyses, in terms of ten major elements, have proved a useful guide to clarify and elucidate the mineralogy and the results obtained are in good agreement with other workers.

(11) Cation exchange capacities were determined by two methods and the results indicate that Ca^{++} is the dominant exchangeable cation, although Na^{+} was present in significant amounts in several samples. In addition, the concentration of water-soluble cations were also determined, and in conjunction with the exchangeable cations an attempt was made to relate their values to the palaeosalinities etc., although this was obscured by anomalous Ca^{++} values caused by the presence of calcite.

Chapter Four

Clay Microstructure and Preferred Orientation

4.1 Introduction

Soil structure presents a complex picture which is often difficult to quantify. It exists at a wide variety of levels from the micro to the macro (Barden, 1972). Macrostructure includes such features as horizontal bedding, laminations, varves, vertical root channels, tension cracks, fissures and joints, whereas the microstructure, which forms the basis of this chapter, embraces the distribution and forms of the particles which constitute the sediment.

Early studies of clay microstructure, mostly based on speculation were undertaken by for example Terzaghi (1925), Casagrande (1932) and Lambe (1953 and 1958). However, later research using techniques of scanning electron microscopy, X-ray diffraction and the polarising microscope have lead to a greater understanding of the basic engineering behaviour of soils, although only the electron microscope allows examination at the scale of individual particles because even with high powered microscopes it is never possible to be certain whether it is single particles or aggregates that are being viewed (Tchalenko, 1968). Nevertheless, the polarising microscope and X-ray diffraction have proved useful tools for obtaining quantitative evaluations of the degree of orientation of the clay minerals over scanning areas of varying size.

4.2 Preferred Orientation Studies

4.2.1 Methods of Analysis

Quantitative evaluations have been performed by optical means and X-ray analysis (Appendix A.2). The degree of preferred orientation

has subsequently been calculated in terms of 'orientation ratio', which is on a scale of 0 to 1 (i.e. 0 implying perfect orientation and 1 implying random distribution).

If the study of preferred orientation is to lead to representative results, then it is essential that no significant alterations occur to the original fabric during preparation of the sample for analysis. Consequently impregnation of the material with a binding agent is often necessary to prevent shrinkage during drying to provide sufficient hardness to allow grinding.

Freeze drying avoids large volume changes but is only effective to shallow depths (0.2 cms.) within the sample (Brewer, 1964). An impregnation technique has been devised by Mitchell (1956). This involves submerging a sample, at it natural moisture content, for one week, in melted Carbowax at 60°C, which being soluble in water in all proportions, gradually replaces the water. Shrinkage in Carbowax is however, not totally eliminated. Quigley and Thompson (1966) quote linear shrinkages of 7.2 per cent in the horizontal direction and 8.8 per cent in the vertical direction for undisturbed samples of Leda Clay. Morgenstern and Tchalenko (1967) obtain a value of 8.8 per cent for the vertical direction and about half this value for directions orthogonal to this.

Typical air-dried shrinkages for the clays presently under consideration are presented in Table 4.1. The majority have values in the range of 0.1 - 9.1 per cent for the vertical direction and 0.1 - 6.0 per cent for the horizontal direction. The Yazoo Clay and Fuller's Earth from Redhill (sample FE23), having very high initial moisture contents compared with the other materials show larger shrinkages (i.e. 20.7 and 12.8 per cent respectively for the vertical direction and 8.6 to 10.1 per cent respectively for the horizontal direction). Consequently, since these values, with the exception of the last two clays, are well within the limits of

shrinkage accepted by other workers, it was decided that total impregnation was not required. However, a surface impregnation technique was adopted during the preparation of thin sections for visual analysis. Material examined by X-ray diffraction was merely air-dried before orientated samples were prepared.

4.2.1.1 An Optical Method for the Determination of Preferred Orientation

An optical method which led to three relationships between orientation ratio and birefringence ratio (i.e. minimum to maximum birefringence) for clay particles has been developed by Morgenstern and Tchalenko (1967a & b), (Appendix A.2.1). The linear model (Fig.4.1), which they consider to be unrealistic, assumes that the clay particles are either in domains with a random structure or domains with perfect parallelism and having a common direction of preferred orientation. The two dimensional model, (Fig.4.1) which they consider to be best suited for the determination of the orientation ratio, and the one adopted by the writer, assumes that all clay particles lie with their basal sections orthogonal to the plane of the section, whereas the three dimensional model (Fig.4.1) assumes that the particles do not have their basal sections orthogonal to the plane of section.

The method is independent of sample thickness but has been developed for use on monomineralic aggregates. Nevertheless, in the present study orientation ratios (which compare very favourably with those obtained by X-ray methods) have been found for five materials (Table 4.2) which contain either relatively small amounts of granular material, or where granule free areas could be scanned. No results were obtained from materials which contained large quantities of

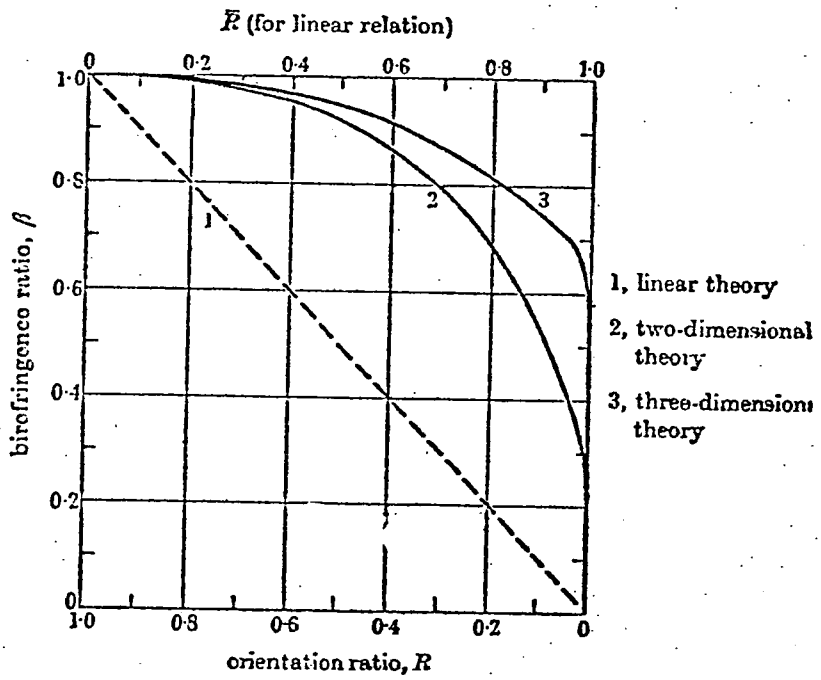

Figure 4.1. Relationship Between Orientation Ratio and Birefringence Ratio (After Morgenstern and Tchalenko, 1967a).

Table 4.1 Air-Dried Shrinkage Values

British Clays	Sample Ref.	Vertical Direction (%)	Horizontal Direction (%)
London Clay 14m	LC14	5.5 - 6.7	3.2 - 4.5
London Clay 37m	LC37	5.2 - 5.3	2.1 - 2.3
Gault Clay	GC	1.9 - 2.0	0.3 - 0.4
Fuller's Earth (Redhill)	FE23	12.8	10.1
Weald Clay	WC	0.5	0.1
Kimmeridge Clay	KC	4.1 - 4.6	2.3 - 2.9
Oxford Clay 10m	OC10	9.1 - 9.4	3.8 - 4.1
Oxford Clay 44m	OC44	3.1 - 3.6	0.7 - 0.9
Fuller's Earth (Bath)	FE19	8.3	6.0
Lias Clay 10m	L10	5.8	1.4
Lias Clay 36m	L36	3.0 - 3.4	0.1 - 0.2
Keuper Marl	KM	N/A	N/A
Swallow Wood roof	SWR	0.3	0.1
Flockton Thin roof	FTR	0.3	0.1
Flockton Thin seat	FTS	1.7	0.7
Widdringham roof	WR	0.5	0.2
North American Clays			
Yazoo Clay	YC	20.7 - 22.3	8.5 - 9.2
Kincaid Shale 6m	K6	3.5 - 3.8	2.3 - 3.2
Kincaid Shale 8m	K8	4.1	3.6
Nacimiento Shale	N1	0.6	0.2
Nacimiento Shale	N2	0.6	0.2
Nacimiento Shale	N3	N/A	N/A
Fox Hills Shale	FOX	4.4 - 4.7	4.5 - 4.5
Dawson Shale	DS	0.1	0.1
Pierre Shale (Dakota)	PSD	5.4 - 5.6	2.1
Pierre Shale (Colorado)	PSC	0.4	0.2

Table 4.2 Optical Orientation Ratios *

	Sample Ref.	Orientation Ratio
London Clay 37m	LC37	0.20 - 0.28
Kimmeridge Clay	KC	0.10 - 0.18
Oxford Clay 44m	OC44	0.10 - 0.18
Lias Clay 36m	L36	0.02 - 0.06
Flockton Thin roof	FTR	0.01 - 0.02

* Based on the two dimensional model of Morgenstern and Tchalenko, (1967a).

Table 4.3 **Calculation of Orientation Ratio from X-Ray Analysis**

	Intensity Ratio	Equivalent Orientation Ratio
Bates, 1947	$\frac{(002) / (110)H}{(002) / (110)V}$	$\frac{1}{R^2}$
Kaarsberg, 1959	$\frac{(002) / (110)H}{(002) / (110)V}$	$\frac{1}{R^2}$
Meade, 1961a	$\frac{(001) / (020)H}{\frac{(001) + (001)}{(020) + (020)}V}$	$\frac{1}{R^2}$
O'Brien, 1964	$\frac{\frac{(001)K + (002)I}{(020)K + (110)I}H}{\frac{(001)K + (002)I}{(020)K + (110)I}V}$	$\frac{1}{R^2}$
Gipson, 1966	$\frac{(002) / (020)H}{\frac{(002) + (002)}{(020) + (020}V}$	$\frac{1}{R^2}$
Odom, 1967	$\frac{(00L)V}{(00L)V + (00L)H}$	$\frac{R}{R + 1}$

H = Horizontal (at right angles to the vertical direction)

V = Vertical (parallel to the vertical direction)

K = Kaolinite

I = Illite

smectite, even when the granular content was low, because the presence of this mineral caused the slide, no matter how thinly ground, to have a brown, muddy appearance which obliterated all traces of birefringence under crossed nicols.

4.2.1.2 X-Ray Diffraction Methods for the Determination of Preferred Orientation

X-ray diffraction methods rely on a comparison of the basal 'c' axis reflections (and also reflections at right angles to these) when the material is orientated parallel to and at right angles to the bedding. Various methods for calculating the preferred orientation, as used by other workers are given in Table 4.3. Bates (1947), Kaarsberg (1959) and Gipson (1966) have used illite peaks only, as this was the dominant mineral in their specimens. O'Brien (1964) combines the illite and kaolinite peaks to account for the reflections in the 4.4Å clay wedge. Meade (1961a), in his study of the orientation of montmorillonite, uses a similar ratio to Gipson (1966), and in both these cases, three orthogonal sections have been chosen, i.e. two parallel to the vertical direction and one at right angles to it. Odom (1967) uses the ratio of the principal 'c' axis reflections and consequently his formula is applicable to each of the clay minerals separately, making it possible to compare their orientations and hence their behaviour.

Two different methods have been employed by the writer to obtain a measure of the degree of preferred orientation of the clay minerals. For each, an orientation ratio has been calculated on a peak height and a peak area basis, and in all cases the near coincidence of the results suggests that either method can be used with a high degree of confidence.

(i) The method of Odom (1967) has been applied separately to the illite 002 reflection, the kaolinite 001 reflection and the montmorillonite 001 reflection (Table 4.4).

(ii) An overall measure of the orientation for each clay has also

Table 4.4 Orientation Ratios of Individual Minerals *

British Materials	Sample Ref.	Illite peak ht.	Illite peak area	Kaolinite peak ht.	Kaolinite peak area	Montmorillonite peak ht.	Montmorillonite peak area
London Clay 37m	LC37	0.49	0.45	0.47	0.47	0.63	0.61
Gault Clay	GC	0.53	0.41	0.52	0.49	-	-
Fuller's Earth (Redhill)	FE23	-	-	-	-	1.00	0.96
Kimmeridge Clay	KC	1.04	0.58	0.47	0.49	-	-
Oxford Clay 44m	OC44	0.16	0.16	0.11	0.16	-	-
Fuller's Earth (Bath)	FE	-	-	-	-	1.00	1.00
Lias Clay 36m	L36	0.19	0.20	0.12	0.11	-	-
Flockton Thin roof	FTR	0.07	0.08	0.15	0.15	-	-
Flockton Thin seat	FTS	0.61	0.75	0.47	0.52	-	-
North American Materials							
Yazoo Clay	YC	-	-	0.13	0.04	0.17	0.15
Kincaid Shale 6m	K6	-	-	0.69	0.52	0.75	0.69
Nacimiento Shale	N2	0.41	0.22	0.25	0.19	0.37	0.25
Nacimiento Shale	N3	-	-	0.81	0.81	0.85	0.88
Fox Hills Shale	FOX	-	-	-	-	1.00	1.00
Dawson Shale	DS	-	-	1.00	0.78	0.78	0.66
Pierre Shale (Dakota)	PSD	0.45	0.30	0.85	0.38	0.78	0.61
Pierre Shale (Colorado)	PSC	0.54	0.61	0.72	0.75	0.92	0.81

* Based on Odom, (1967)

Table 4.5 Combined Orientation Ratios

	Sample Ref.	Kaolinite + Illite[1]		Kaolinite + Mont + Illite[2]	
		Peak ht.	Peak Area	Peak Ht.	Peak Area
British Materials					
London Clay 37m	LC37	0.40	0.39	0.42	0.36
Gault Clay	GC	0.53	0.49	-	-
Fuller's Earth (Redhill)	FE23	-	-	0.85	0.79
Kimmeridge Clay	KC	0.64	0.52	-	-
Oxford Clay 44m	OC44	0.19	0.19	-	-
Fuller's Earth (Bath)	FE19	-	-	0.83	0.88
Lias Clay 36m	L36	0.13	0.11	-	-
Flockton Thin roof	FTR	0.19	0.23	-	-
Flockton Thin seat	FTS	0.46	0.44	-	-
North American Materials					
Yazoo Clay	YC	0.28	0.16	0.31	0.26
Kincaid Shale 6m	K6	0.73	0.67	-	0.78
Nacimiento Shale	N2	0.57	0.49	0.61	0.42
Nacimiento Shale	N3	0.82	0.75	0.84	0.77
Fox Hills Shale	FOX	-	-	1.00	1.00
Dawson Shale	DS	0.83	0.68	0.72	0.63
Pierre Shale (Dakota)	PSD	0.39	0.24	0.42	0.31
Pierre Shale (Colorado)	PSC	0.56	0.65	0.58	0.71

(1) Based on O'Brien (1964)

(2) Based upon modified O'Brien formula, i.e.:-

$$\frac{\dfrac{(001)K + (002)I + (001)M}{(020)K + (110)I + (020)M}\,H}{\dfrac{(001)K + (002)I + (001)M}{(020)K + (110)I + (020)M}\,V}$$

been obtained using the equation proposed by O'Brien (1964). In addition, to account for the presence of montmorillonite, a modified version of this equation has also been used (see Table 4.5).

4.2.2 The Relationship of Preferred Orientation to Mineralogy and Depth of Burial

Upon inspection of the preferred orientation ratios for the individual clay minerals (Table 4.4), it is observed that when illite and kaolinite occur together their orientation ratios are approximately identical. This would suggest that under natural conditions they behave in approximately the same fashion under compaction. Barden and Sides (1970) have, however, concluded that, from tests performed on artificially prepared clays, chemical additives have little effect on the structure of kaolinite whereas their presence is apparent in illitic clays. Montmorillonite on the other hand, frequently has a more random degree of preferred orientation than either illite or kaolinite which may be present in the same material, thus confirming that the larger minerals develop an orientated fabric more easily (Von Engelhardt and Gaida, 1963; Mitchell 1956), although these findings are not depth dependent, (see later).

In general the current results confirm the findings of other workers (see Chapter 1.5.5) in that there is no significant relationship between preferred orientation and depth of burial (Fig.4.2), consequently it can be inferred that it is the initial conditions which govern the formation of the said parameter (Meade, 1961b, 1964, 1966; Lambe, 1958). This is particularly well illustrated by two instances. Firstly by reference to the two deeply buried Carboniferous Shales where the Flockton Thin seatearth has a very much more random structure

Figure 4.2. Relationship Between Orientation Ratio and Depth of Burial.

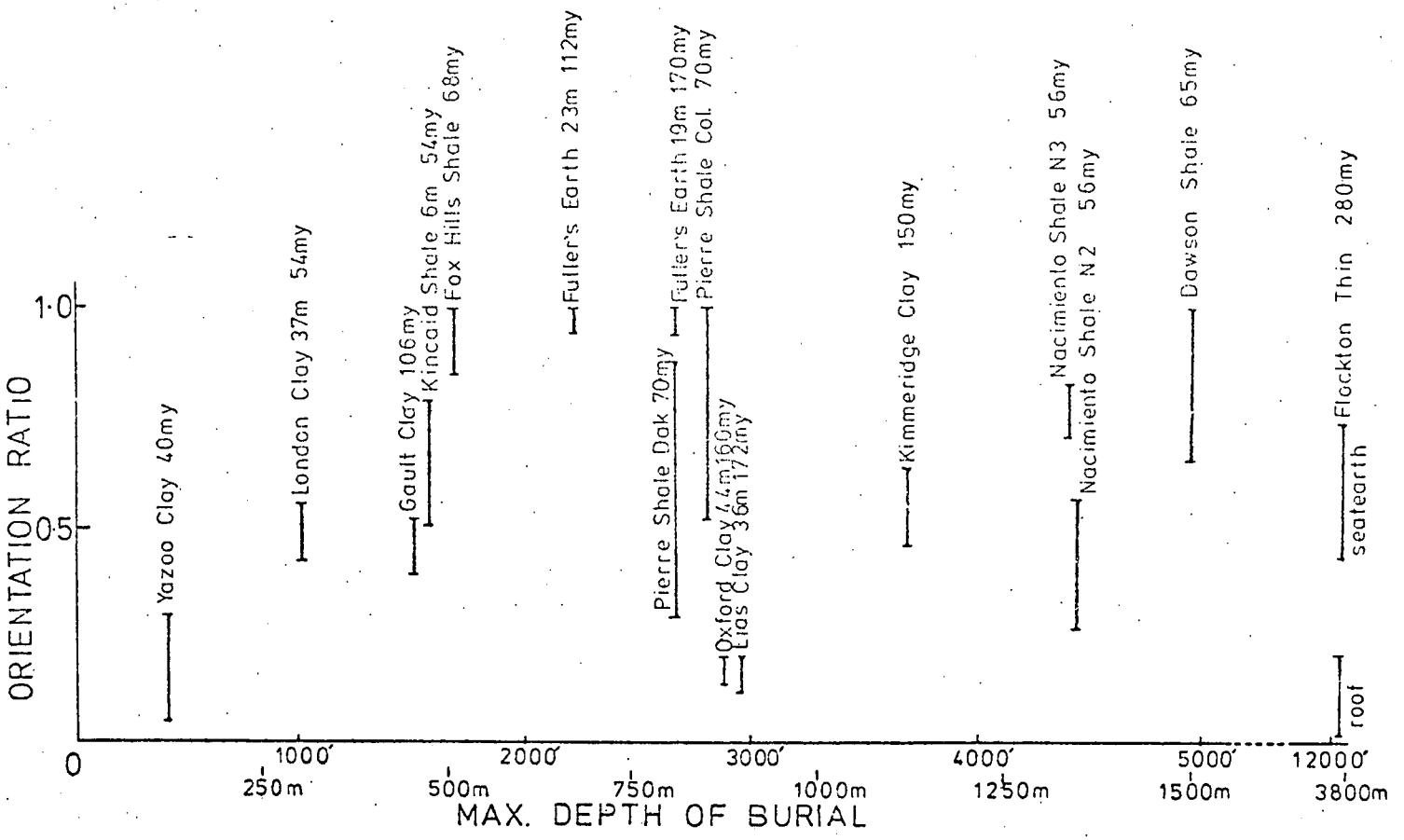

than the associated fissile roof shale. Secondly, by reference to the fact that the smectite minerals only show any tendency towards an orientated fabric in the Yazoo Clay, which is considered to have been deposited in a dispersing environment.

With regard to the relationship with fissility, of the shales examined in the present study, four exhibit a high degree of preferred orientation. Of these, the Oxford Clay (OC44), Lias Clay (L36) and the Flockton Thin roof, show a marked fissility by splitting with a sub-parallel fracture. These are all hard, or stiff materials with a clay mineralogy consisting predominantly of the larger particles of illite and kaolinite (Table 3.2). The Yazoo Clay, a fat, soft clay with smectite as the major clay mineral phase also shows some degree of fissility but this is less obvious than in the other three and may be attributed to its softer nature and overall smaller grain size.

4.3 Clay Microstructure

4.3.1 Method of Analysis

A scanning electron microscope, embracing magnifications in the range of x20 to x12000 has been employed to study the clay microstructure, and with its large depth of focus an almost three dimensional build-up was obtained. The clay samples which were used were prepared by a simple technique reported in Appendix A2.3.

A standard magnification of x2500 has ultimately been chosen for the general presentation of the results, although other magnifications have been used to illustrate specific features.

4.3.2 Microstructure of the samples studied

An introductory review of the development of clay microstructure is presented in Chapter 1.5.4. However, before discussing the microstructure of the rocks presently under consideration it is pertinent to note that all have been heavily overconsolidated, although their conditions have been very varied (Chapter 2). Barden (1972) concludes that a predominantly dispersed structure, portrayed by six heavily overconsolidated marine clays, results from the collapse of an originally flocculated arrangement, and consequently a true representation of this original structure can only be inferred by considering all of the facts. With regard to the development of preferred orientation within this type of deposit, Tchalenko (1968) has shown that the degree of horizontal orientation, deduced from the birefringence ratio of the London Clay can be reproduced in the laboratory by compressing a flocculated sediment containing 35 grams per litre of NaCl. Chandler (1971) has also noticed a similar birefringence ratio in the Lias Clay. Had the sedimentation conditions been dispersing, then the mineral orientations in the natural sediment may be expected to be higher, even approaching the C.P.O. (complete preferred orientation) of Smart (1969).

This dispersed turbostratic structure as evidenced by a preponderance of edges in the vertical section, is currently displayed by clays containing large clay minerals, i.e. the Oxford Clay (OC 4-4), (Fig.4.12), and the Lias Clay (L36), (Fig.4.13). The Kimmeridge Clay (Figs.4.10 and 4.11), the London Clay (Figs.4.3 and 4.4) and the Gault Clay (Fig.4.5) also show a turbostratic arrangement of minerals although their structures are somewhat more random, as shown by the greater number of flat surfaces which are visible. Reorientation of the clay minerals along micro-shear planes, as a result of stress

release, is clearly indicated in the Kimmeridge Clay (Fig.4.10).

A dispersed turbostratic arrangement is also shown by the Yazoo Clay (Fig.4.19) although in this case montmorillonite forms a major proportion of the clay mineral content. Because this mineral does not reorientate under pressure (Meade, 1961), the writer considers that this structure is symptomatic of the conditions of deposition producing a dispersing environment.

A factor common to the granular minerals in the turbostratic structure also observed by Barden (1972) and confirmed by polarising microscope observations (Mitchell, 1956) is that they do not appear to touch one another, but are surrounded by a skin of clay particles (e.g. Kimmeridge Clay, Fig.4.10). When the silt particles have been plucked out, a hole is often in evidence in the surrounding clay structure, (e.g. Fig.4.12). A general observation with reference to the calcareous content of the Gault Clay is that the presence of this material is in the form of coccoliths, i.e. the 'button shaped' particles identified in Figure 4.5.

Flocculated clay mineral structures shown by an overall random distribution with large numbers of edges, flats and cavities visible are identified in materials where smectite and other expandable clay minerals form a large proportion of the constituents (e.g. Figs. 4.20, 4.21, 4.22, 4.23, 4.24, 4.25, 4.26). These minerals are very small and are generally represented by a somewhat crinkled appearance, but unfortunately even at higher magnifications no greater detailed structure is visible. However, a type of domain structure, involving the parallel alignment of particles is visible in the Fuller's Earth materials (Fig. 4.6 and 4.7).

Certain evidence for an edge-to-face flocculated structure can be identified in the Weald Clay (Figs.4.8 and 4.9), which is an illite, kaolinite quartz-rich sediment of freshwater origin. However

it must be added that as the material contains over 50 per cent quartz, this structure could result from entrapped clay minerals. Another characteristic of this sediment is that it contains clusters of quartz surrounded by a matrix of clay minerals and smaller granules, (Fig.4.9), a feature which was also evident under the polarising microscope.

Electron microscope photographs of the Carboniferous material i.e. the Flockton Thin roof shale (Figs.4.15 and 4.16) and the Flockton Thin seatearth (Figs.4.17 and 4.18) do not resemble any of the other sediments, which probably reflects their indurated nature. The photograph of the roof shale was taken at an orientation of 45° to the bedding, hence the structure is not altogether clear. Nevertheless, on close inspection a face-to-face orientation of minerals can be detected (which is supported by a high degree of preferred orientation - see Table 4.5). A contorted structure of twisted clay minerals with a (?) face-to-face structure is shown by the seatearth. Preferred orientation studies suggest a random particle arrangement exists and consequently it is considered that this must result from the above mentioned structure rather than from a truly flocculated clay structure.

4.4 The Relationship Between Clay Microstructure and Preferred Orientation

From the S.E.M. photographs it is not always possible to relate the observed structure to the preferred orientation (as determined by X-ray and optical techniques). Nevertheless by reference to the previous section it can be concluded that a preponderance of edges in vertical section, showing parallel alignment would indicate a highly preferred orientation. In fact this situation is particularly well demonstrated by the illite/kaolinite clays of the Oxford Clay

(OC44) in Figure 4.12 (preferred orientation 0.19), the Lias Clay (L36) in Figure 4.13 (preferred orientation 0.13) and the Flockton Thin roof in Figure 4.16 (preferred orientation 0.19). A less well developed edge-facing structure is also developed in the smectite-rich Yazoo Clay (Fig.4.19) which has a preferred orientation ratio of 0.28.

As the degree of preferred orientation is decreased then there will be a gradual decrease in the areas of dispersed structure and an increase in the number of top surfaces of clay minerals (or 'flats') visible in vertical section. The Kimmeridge Clay, (Fig. 4.11), the London Clay (LC37), Figure 4.4, and Gault Clay (Fig.4.5), having moderate orientation ratios (0.64, 0.40 and 0.53 respectively) show such an arrangement where areas of dispersion are interspersed with areas where only flats are visible. No orientation ratios were obtained for the remoulded samples, however, the SEM photograph of the remoulded Lias Clay (Fig.4.14) clearly indicates that a partial alignment of clay minerals has been produced, even after rapid consolidation.

A random distribution of clay minerals is associated with the flocculated structure and is demonstrated in SEM photographs by a situation whereby large numbers of edges, flats and cavities are visible. Such features are clearly indicated in materials which contain large quantities of expandable clay minerals (e.g. Fuller's Earth (Fig.4.6), Kincaid Shale 6m (Fig.4.20), Nacimiento Shales Nos. 2 and 3 (Fig.4.21 and 4.22), Fox Hills Shale (Fig.4.23), Dawson Shale (Fig.4.24) and the Pierre Shales (Figs. 4.25 and 4.26).

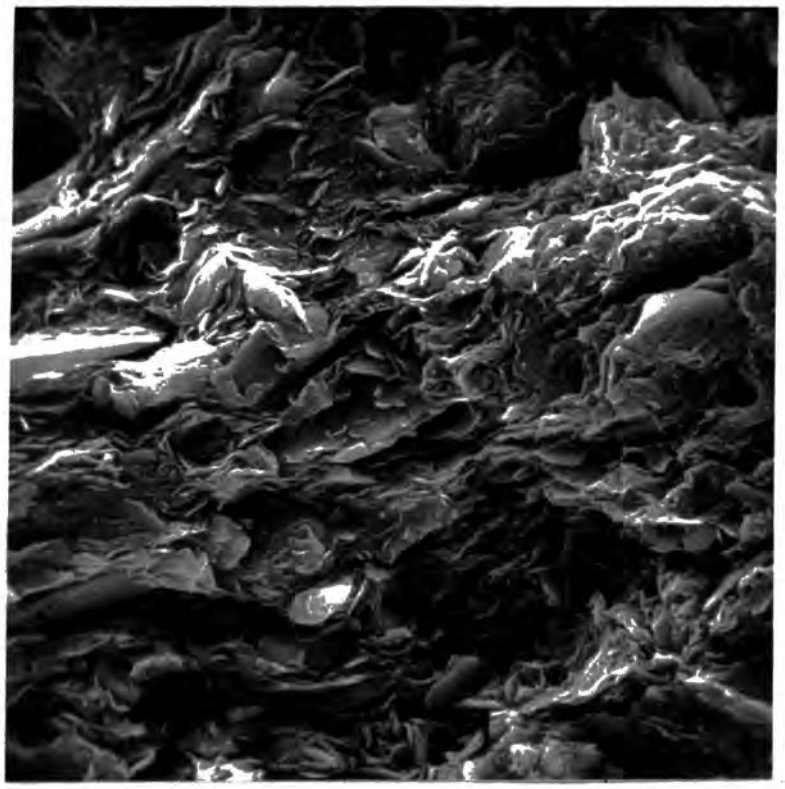

Figure 4.3. S.E.M. Photograph of London Clay 37m., x2400.

Figure 4.4. S.E.M. Photograph of London Clay 37m., x2400.

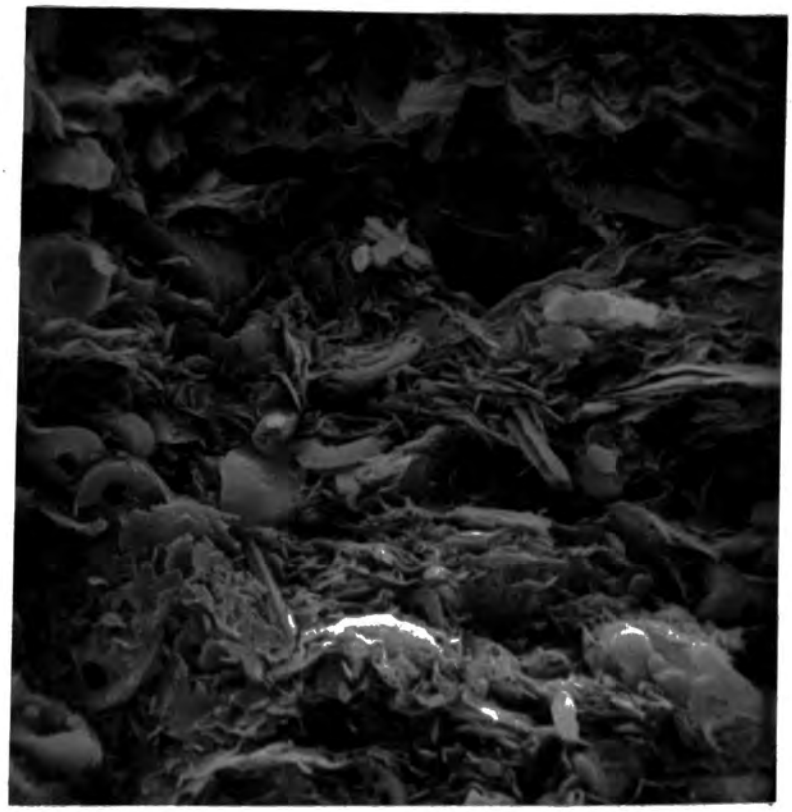

Figure 4.5. S.E.M. Photograph of Gault Clay, x2480.

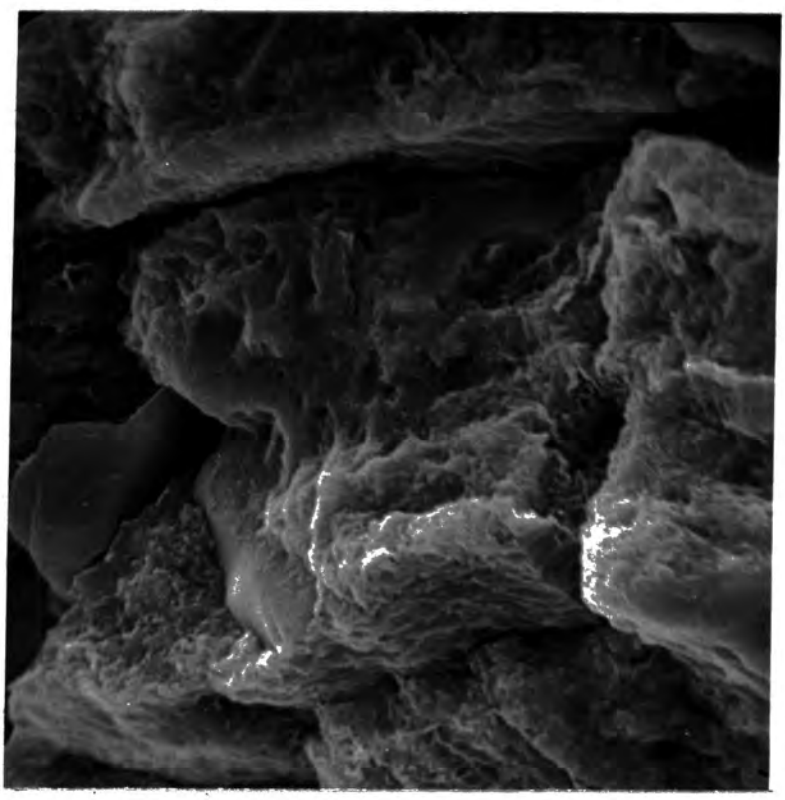

Figure 4.6. S.E.M. Photograph of Fullers Earth from Redhill, x2300.

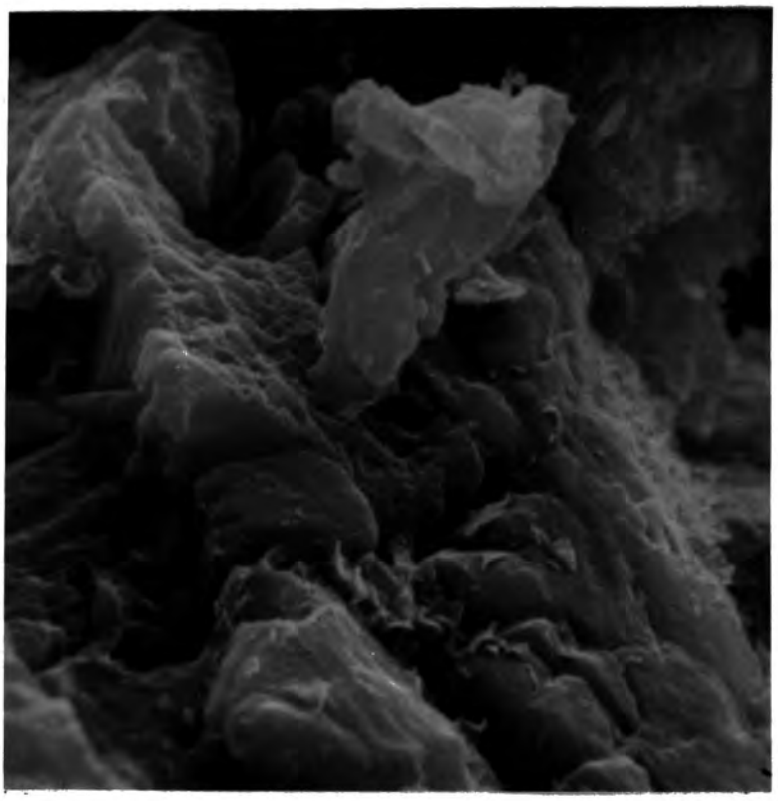

Figure 4.7. S.E.M. Photograph of Fullers Earth from Redhill, x6400.

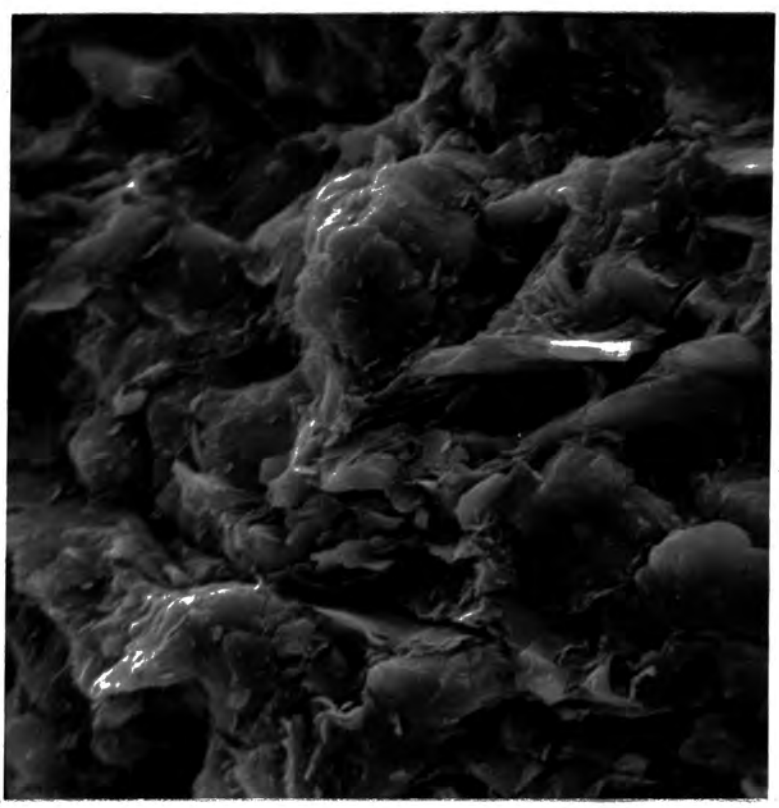

Figure 4.8. S.E.M. Photograph of Weald Clay, x2440.

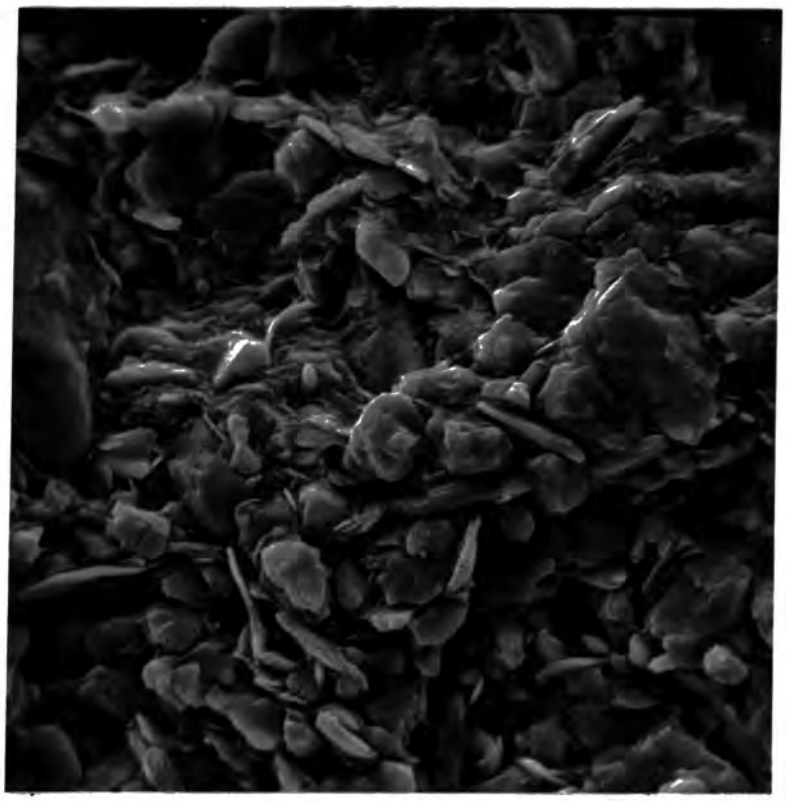

Figure 4.9. S.E.M. Photograph of Weald Clay, x1220.

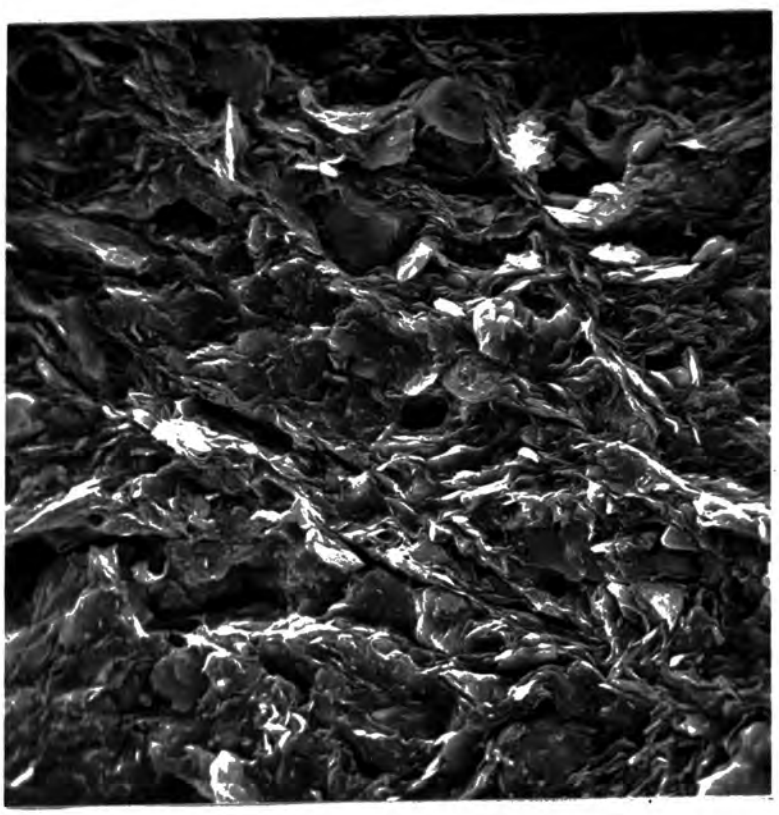

Figure 4.10. S.E.M. Photograph of Kimmeridge Clay, x1200.

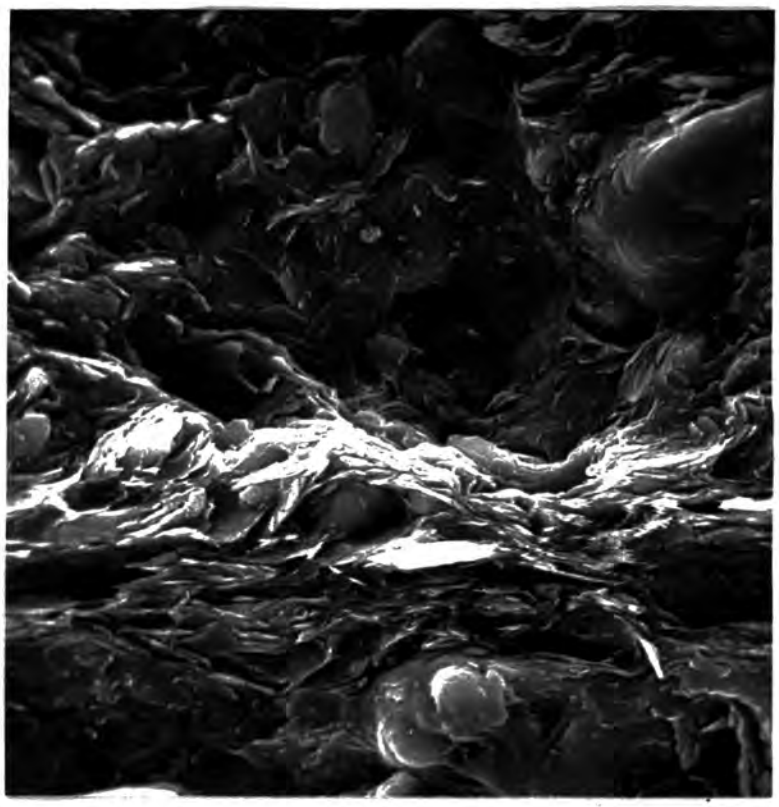

Figure 4.11. S.E.M. Photograph of Kimmeridge Clay, x2400.

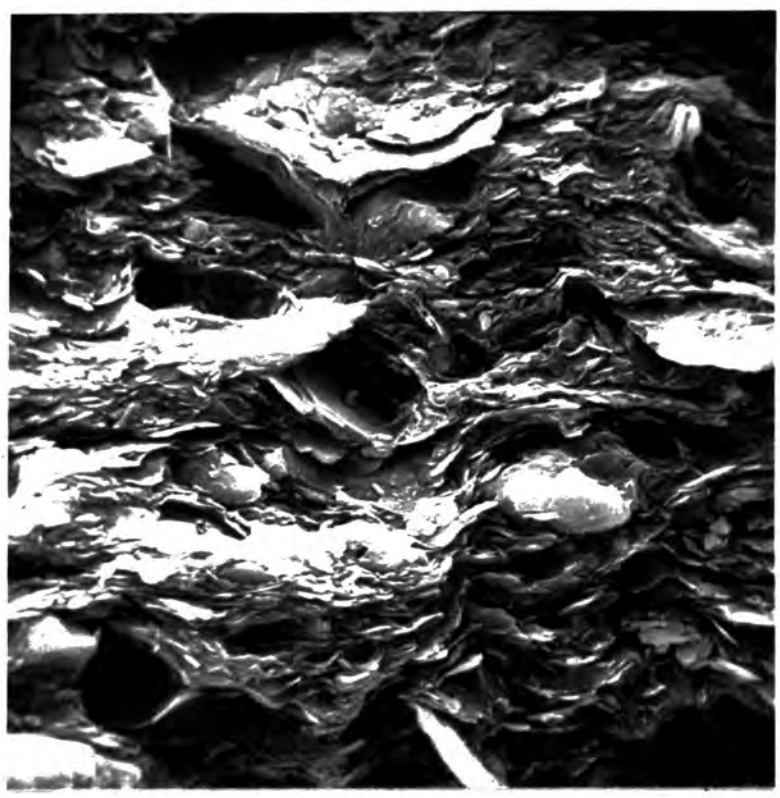

Figure 4.12. S.E.M. Photograph of Oxford Clay 44m, x2400.

Figure 4.13. S.E.M. Photograph of Lias Clay 36m, x2450.

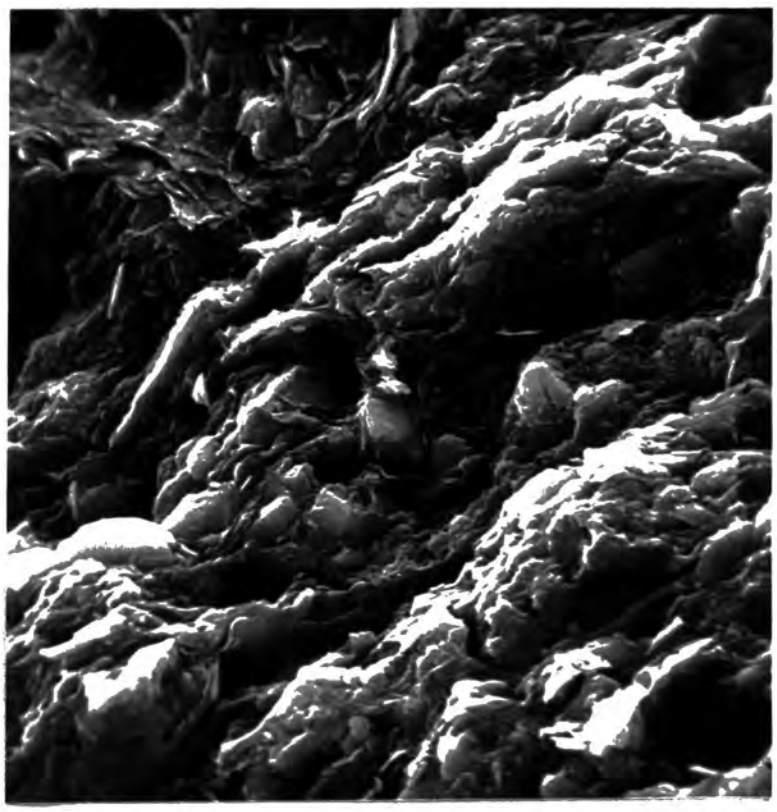

Figure 4.14. S.E.M. Photograph of Lias Clay 36m (remoulded), x2500.

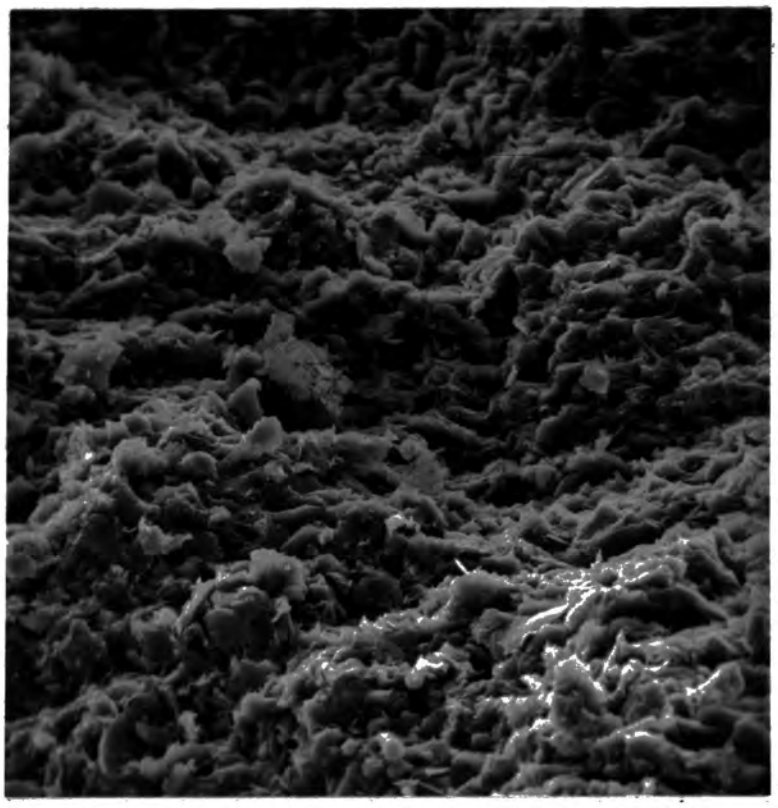

Figure 4.15. S.E.M. Photograph of Flockton Thin roof, x610.

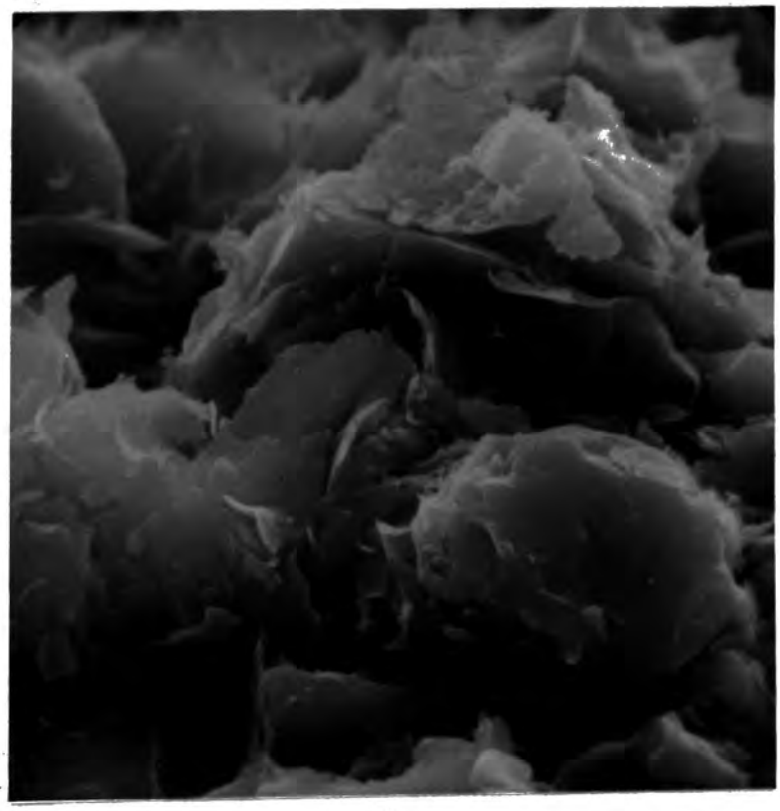

Figure 4.16. S.E.M. Photograph of Flockton Thin roof, x6100.

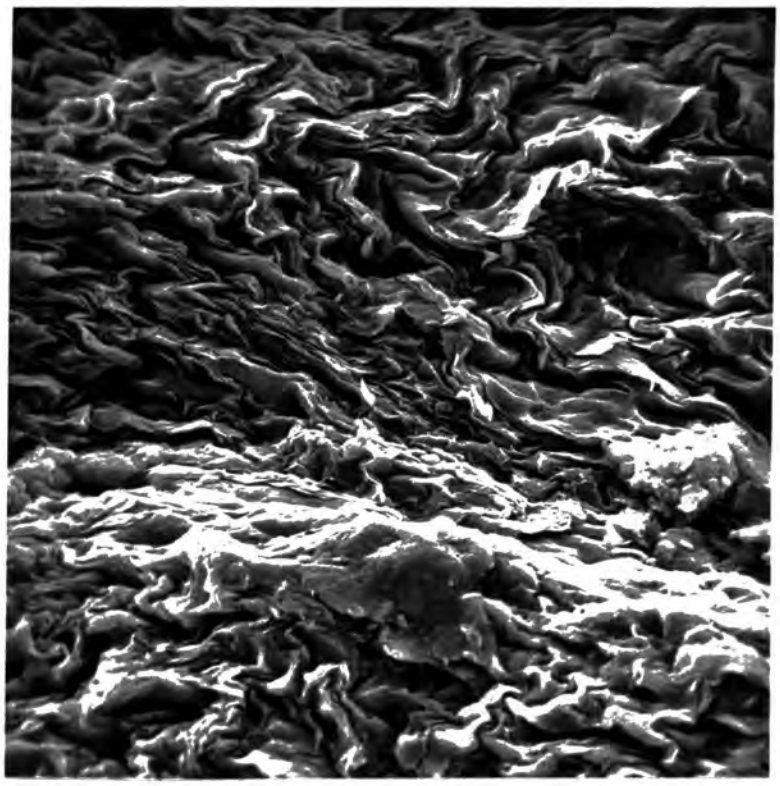

Figure 4.17. S.E.M. Photograph of Flockton Thin seatearth, x1150.

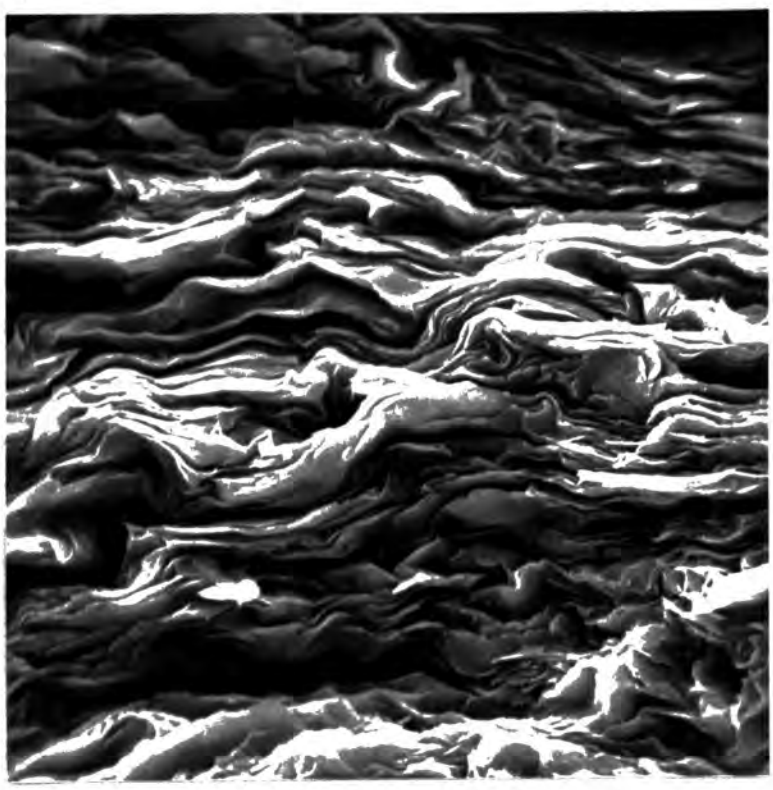

Figure 4.18. S.E.M. Photograph of Flockton Thin seatearth, x2390.

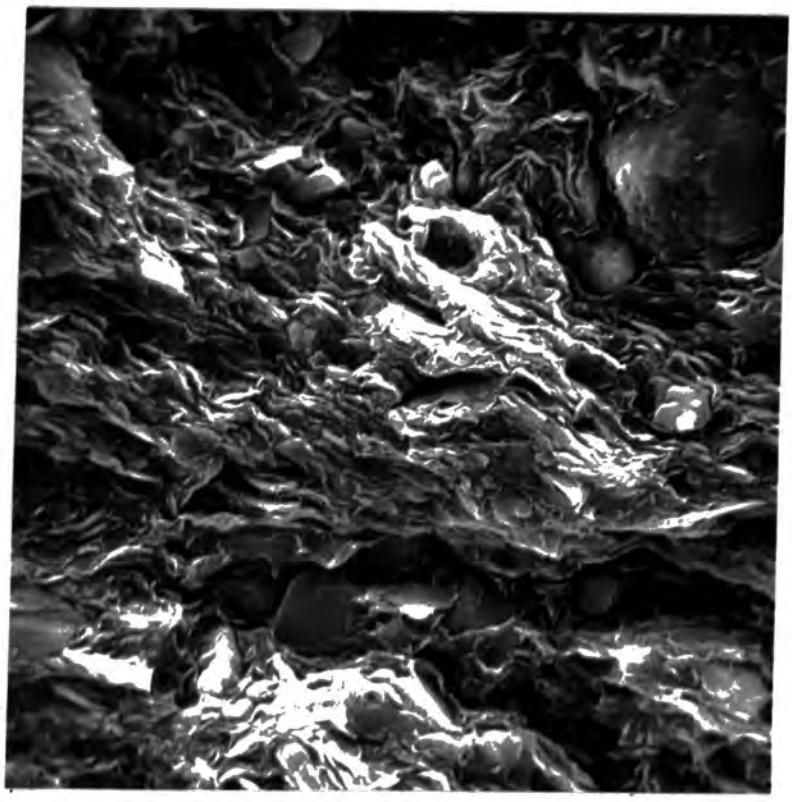

Figure 4.19. S.E.M. Photograph of Yazoo Clay, x2500.

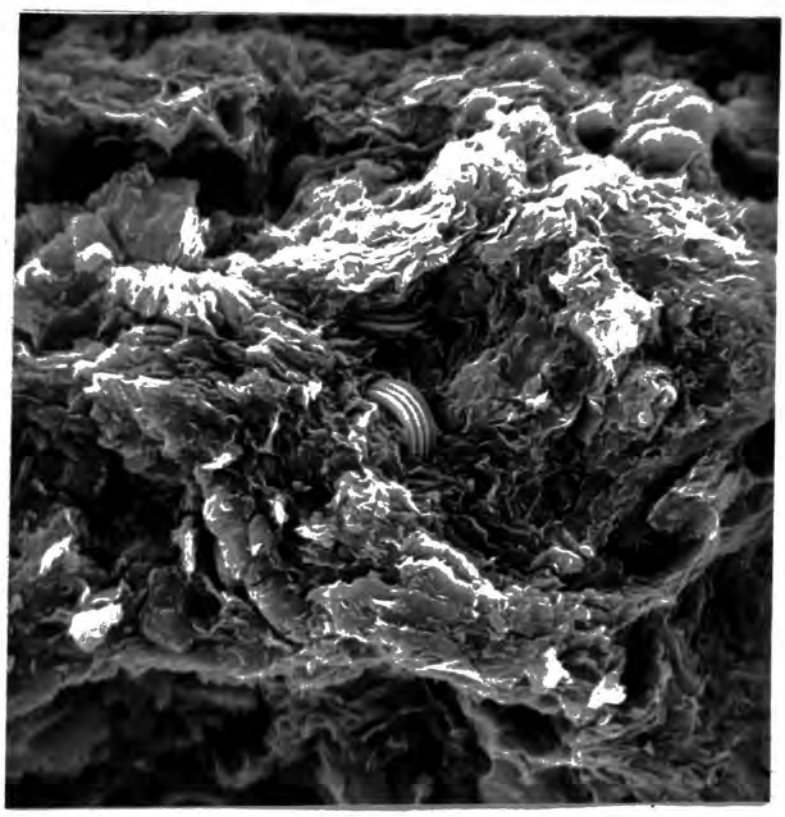

Figure 4.20. S.E.M. Photograph of Kincaid Shale 6m, x2500.

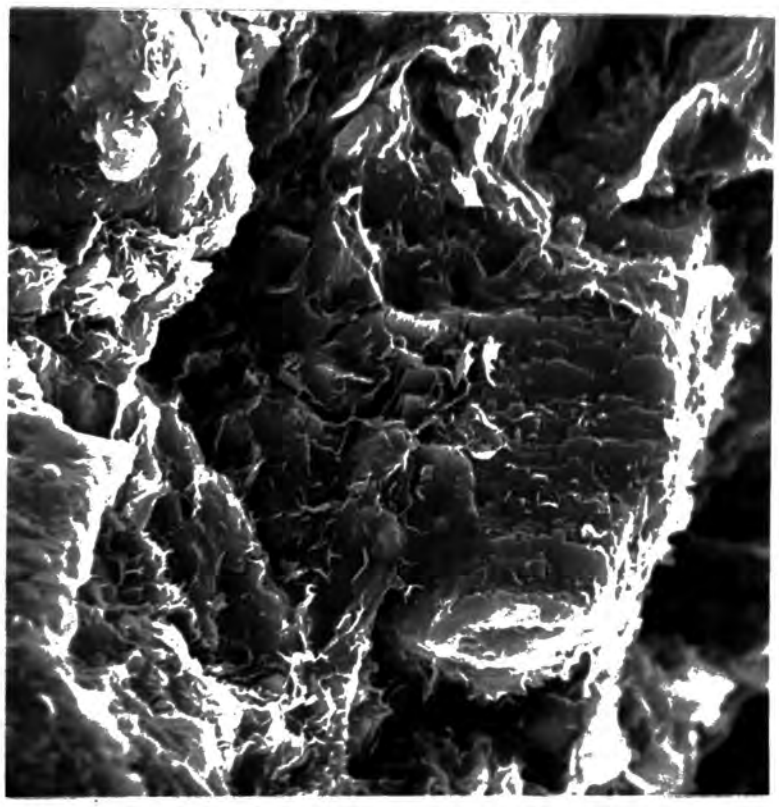

Figure 4.21. S.E.M. Photograph of Nacimiento Shale N2, x2350.

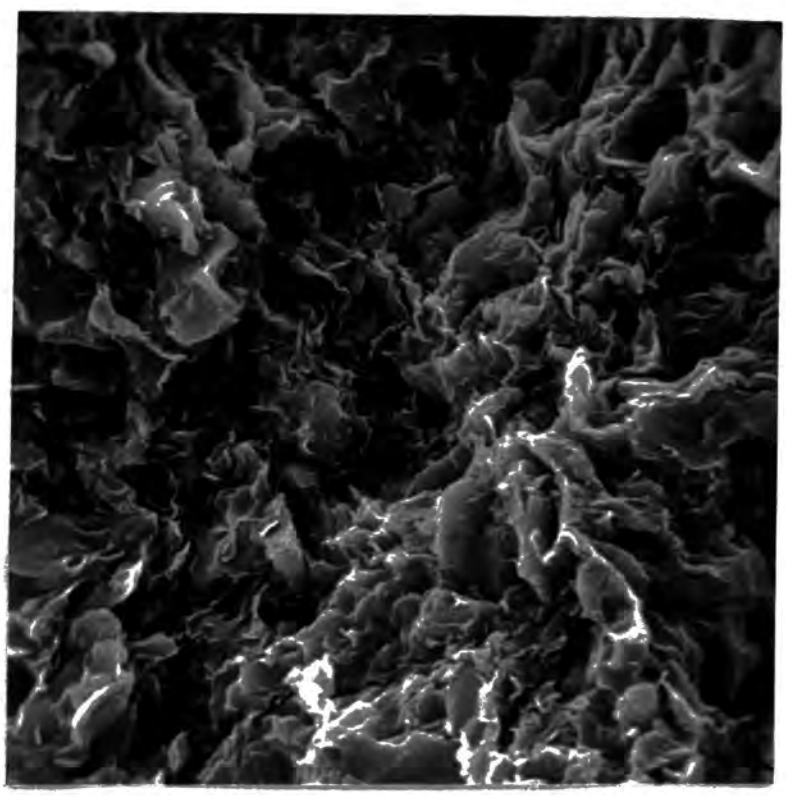

Figure 4.22. S.E.M. Photograph of Nacimiento Shale N3, x2500.

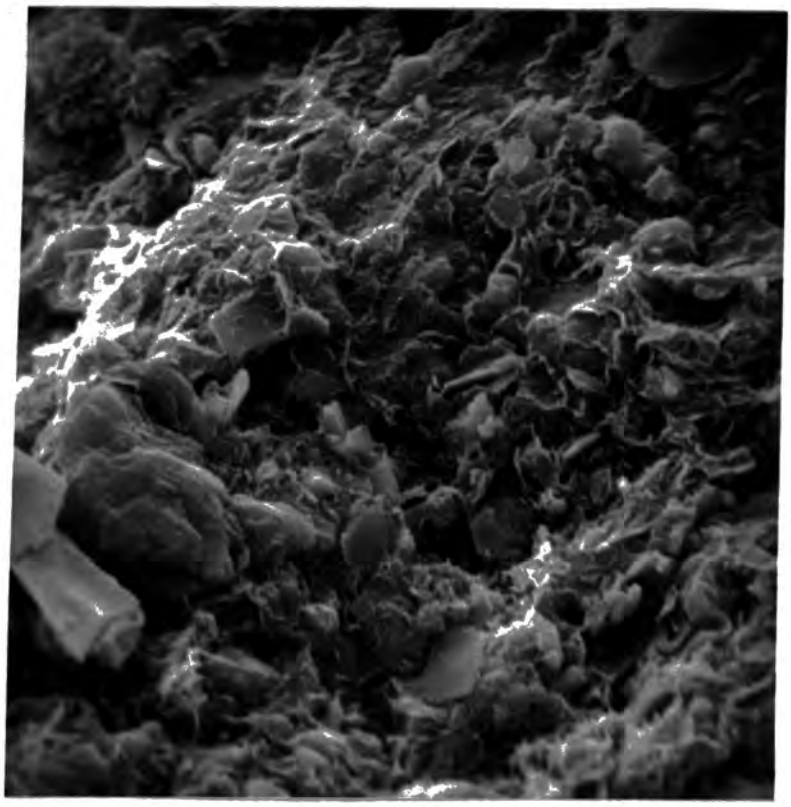

Figure 4.23. S.E.M. Photograph of Fox Hills Shale, x2400.

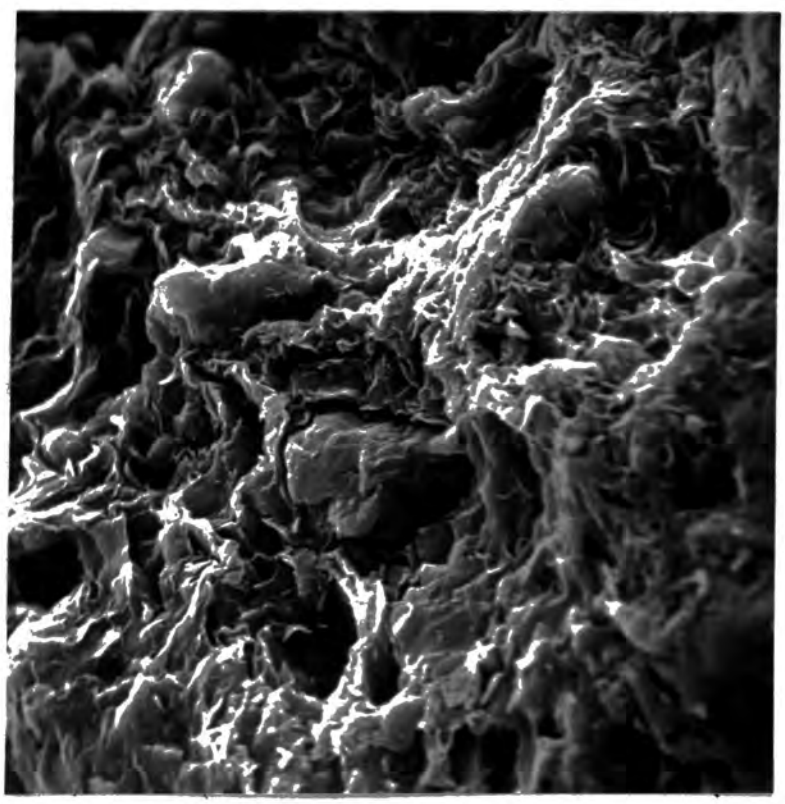

Figure 4.24. S.E.M. Photograph of Dawson Shale, x2600.

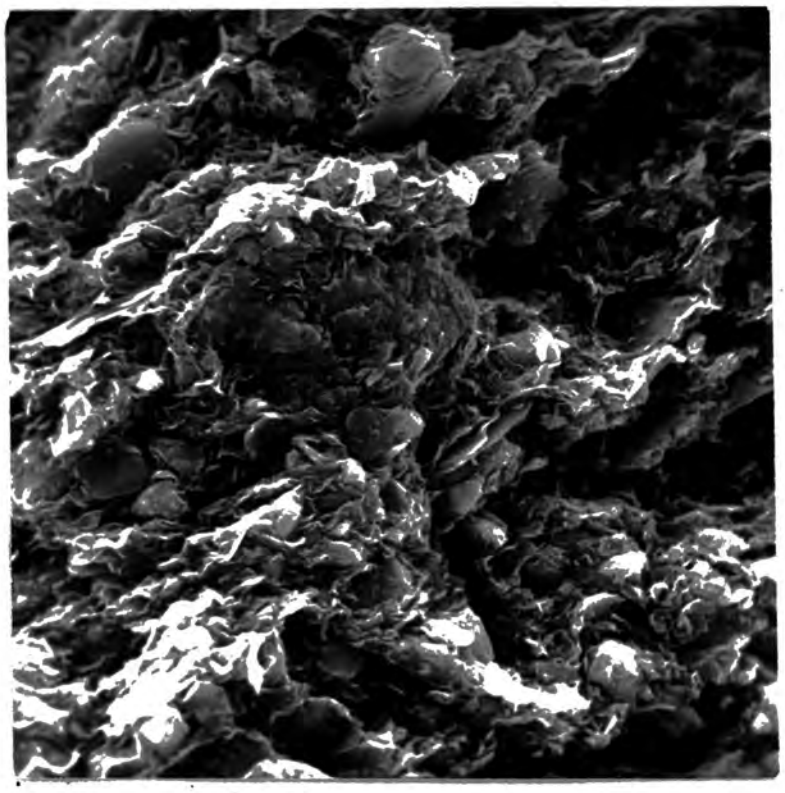

Figure 4.25. S.E.M. Photograph of Pierre Shale (Dakota), x2300.

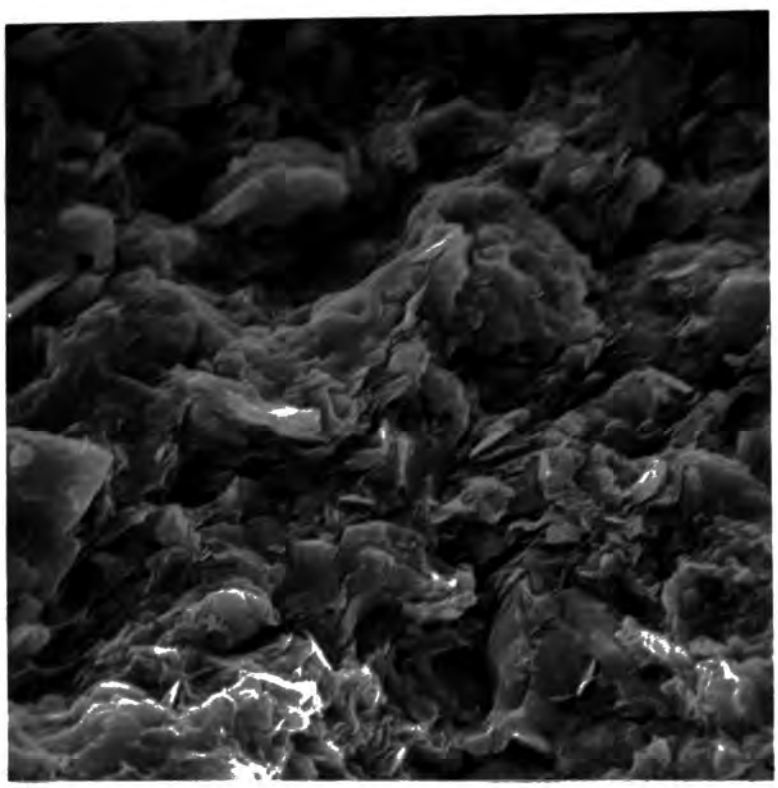

Figure 4.26. S.E.M. Photograph of Pierre Shale (Colorado), x2400.

Chapter Five
Consolidation

5.1 Introduction

A standard oedometer, modified to accommodate high pressures has been used to compress a series of overconsolidated shales (see Chapter 2) in both the undisturbed state and remoulded at their liquid limit, to a pressure of 35000kN/m^2. In the majority of cases this was found to be above the original preconsolidation loads. Experimental details are reported in Appendix A.3. In addition, a series of tests were conducted on four materials remoulded at various initial moisture contents in a conventional oedometer to a pressure of 8400 kN/m^2.

The resulting consolidation parameters c_v, m_v, k. C_c and C_s, have been reviewed in the light of the mineralogical composition and the induration state of the shales, and by reference to the swell index (C_s) the presence of diagenetic bonding has been deduced in certain cases.

Statistical methods involving the use of correlation matrices (c.f. mineralogical analysis - Chapter 3) have been used to analyse the stress-strain response of the clays tested and a new concept for this behaviour has been put forward based on these findings.

5.2 The One-Dimensional Theory of Consolidation

The equation governing the one-dimensional theory of consolidation, is of the form:-

$$c_v \cdot \frac{d^2u}{dz^2} = \frac{du}{dt} \quad \ldots\ldots\ldots\ldots\ldots\ldots (13)$$

derived by Terzaghi in 1923. In formulating this equation Terzaghi adopted the following assumptions:-

(1) The soil is homogeneous and isotropic.

(2) The soil is fully saturated.

(3) The compressional stress and pore water flow are in one direction only.

(4) Both the soil and water are incompressible.

(5) The flow of water is governed by Darcy's Law:-

$$V = k.\frac{du}{dx} \quad \ldots\ldots\ldots\ldots\ldots\ldots \quad (14)$$

(6) The temperature remains constant.

(7) The coefficient of volume compressibility and permeability remain constant over the interval of consolidation.

(8) The weight of the sample is negligible compared with the weight of the load.

(9) The compressional strain during the interval of consolidation is sufficiently small so that an element of space through which pore water flows, and whose dimensions do not change with time, can be used interchangeably with an element of the soil skeleton, which is compressing with time.

(10) Only hydrodynamic time lag is considered.

5.3 A Review of Research into the Validity of the Terzaghi Theory

According to the Terzaghi theory, the degree of consolidation should be numerically equal to the degree of pore pressure dissipation at any given time during each compression stage. This implies that compression should be completed at the end of 'primary consolidation' (which is defined as that which occurs when excess pore pressure is being dissipated, and which proceeds according to the Terzaghi theory). However, it has been found that experimental compression time curves usually depart from the theoretical model in the later stages of compression. This deviation is known as 'secondary consolidation' and is represented by colloid chemistry

processes (e.g. stressed moisture films around grains, surface tension effects in the corners between grains, density and viscosity changes in the stressed moisture films and absorbed ionic bonds) and reorientation effects.

Newlands and Allely (1960), Taylor (1942) and Leonards and Girault (1961) have shown that with step loading, the ratio of secondary to primary compression decreases as the load increment ratio is increased. This ratio becomes zero when the load increment ratio reaches a factor of ten or above (Newlands and Allely, 1960).

Work done by Leonards and Ramaih (1959) on remoulded clays to supplement the work of Taylor (1942), Van Zelst (1948), Lewis (1950) and Northely (1956) on the effect of load increment durations, suggests that e - log P relationships are insensitive to load increment duration provided that: sufficient time has elapsed to allow the dissipation of pore pressure, the load increment ratio is large enough and the soil does not exhibit inherently large secondary compression effects (e.g. peat). They did, however, conclude that the coefficient of consolidation, c_v, is dependent on the soil type, consolidation pressure and the magnitude and duration of the pressure increments. Therefore the value of c_v calculated in the laboratory may bear no relationship to that found under natural conditions, but used on a comparative basis, can be a useful guide to the mineralogy of the clays tested.

Langer (1936) found that soil is less compressible under small load increments and attributes this to the fact that, firstly, large load increments cause a shock to the soil structure and, secondly, that the induced pore pressure gradients cause internal rupture to the structure.

Crawford (1964) working on undisturbed, sensitive clays shows that the e - log P curve and the preconsolidation pressure vary according to the length of time that secondary compression is allowed to proceed.

Various models have been suggested to accommodate the time-compression curves. Terzaghi's model is represented by a linear spring whereby the volumetric strain is proportional to the effective stress. Taylor (1942) proposes a modification to this by suggesting that the mineral skeleton might be represented by a spring and a linear dashpot proportional to the time rate of compression. Both of these models imply that only primary consolidation is represented because compression ceases when the pore pressure is dissipated. Tan (1957), Murayama and Shibata (1959), Gibson and Lo (1961) and Lo (1961) have since attempted to modify Taylor's model by using springs, dashpots and sliders to simulate measured time-compression curves. Leonards and Altschaeffl (1964) have attempted to observe the effect of sample thickness on the rate of compression by using multiples of the simple linear models.

The validity of Darcy's law at small hydraulic gradients has been questioned by several workers. Hansbo (1960) has found that at small velocities the equation is better represented by the equation $v = k(i)^n$ where $n = 1.5$. However, for a wide range of medium velocities $n = 1$. Leonards and Girault (1961) have shown that variation of the load increment ratio has a great influence on the consolidation properties. They show that for small or medium load increment ratios (i.e. $P/P = 0.1 - 0.3$) or for the load increment which straddles the preconsolidation load, the pore pressure dissipation (hence rate of consolidation) does not follow the Terzaghi theory, even approximately. However, for larger load

increment ratios (i.e. $P/P = 1$) consolidation proceeds according to Terzaghi's theory.

A one-dimensional model has been produced by Gibson et al (1967) which does not impose the limitations on large strains and in which Darcy's law has to be recast in a form whereby the relative velocity of the soil skeleton and the pore fluid are related to the excess pressure gradient.

Barden (1965a) assumes that at small stresses, variations from Terzaghi's theory are unlikely to be caused by variations in permeability but more likely as a result of creep effects. He therefore has produced a theory of consolidation which involves non-linear viscosity and concludes that it provides a method for extrapolating pore pressure-time curves, obtained in the laboratory, to the field scale, which also incorporates the effects of sample thickness and load increment ratio.

Other workers (e.g. Davis & Raymond, 1965; Barden & Barry, 1965) have attempted to produce theories of consolidation whereby the decreases in compressibility and permeability during compression have been taken into consideration.

The non-linear theory produced by Davis and Raymond (1965), which is for normally-consolidated clays, assumes that the coefficient of consolidation remains constant and that Darcy's law is obeyed. Their results show that for high ratios of final to initial effective pressure, the pore pressure is higher at any given time than that predicted by the Terzaghi theory, but the degree of settlement is independent of load increment ratio and is the same as that predicted from the Terzaghi theory.

Schiffman (1958) assumes that the coefficient of volume compressibility remains constant during a loading stage, and that the permeability decreases. However, this treatment leads to a reduction

in the coefficient of consolidation with increasing pressure, whereas it is the reverse situation which usually occurs.

Lo (1961) attempts to take account of the variation in the permeability and the coefficient of consolidation.

Barden (1965b) has produced a theory to account for partially saturated material which includes the effects caused by non-linear variations of permeability and compressibility.

5.4 Concept of Effective Stress

Terzaghi (1923) proposes the following relationship between total stress, σ, and pore water pressure, u :-

$$\sigma = \sigma' + u \quad \ldots\ldots\ldots\ldots\ldots\ldots \quad (15)$$

He recognises that in a saturated material, the all-round pressure, u, can not have any influence on the mechanical properties, and that compaction must be a function of the pressure, σ', which he defines as the 'effective pressure'.

With regard to consolidation, at the instant of application of load, the total pressure increment is carried by the pore water. However, if the facility for drainage is present, as in laboratory experiments, the load is gradually transferred to the mineral skeleton as the water is expelled. Ultimately the excess pore pressure is zero and the total stress becomes equal to the effective stress.

To account for low porosities, Skempton (1970) suggests a more accurate form of the Terzaghi effective stress equation would be of the form:-

$$\sigma = \sigma' - \left(1 - \frac{C}{C_s}\right). u \quad \ldots\ldots\ldots\ldots \quad (16)$$

where C_s and C are the compressibilities of the clay particles and the clay structure respectively, hence accounting for the wide range of

porosities encountered. However, even at low porosities (15 per cent) the ratio of C_s/C is still only about one per cent, implying that the Terzaghi equation is still applicable.

Sridharan & Venkatappa (1973) have also proposed a modification to the Terzaghi effective stress equation, because it does not account for electrical forces of attraction and repulsion which are discussed in Chapter 1.5.3.2. The modified equation is of the form:-

$$c = \sigma' - u_w - R + A \quad \ldots\ldots\ldots\ldots\ldots\ldots \quad (17)$$

where c = the effective contact stress, u_w and u_a are the effective pore water and pore air pressures respectively and R and A are the total repulsive and attractive forces respectively divided by the total interparticulate areas.

An alternative to Terzaghi's effective stress concept has been proposed by Bjerrum (1967b). He introduces the concept of 'instant' and 'delayed' compression as being applicable to natural sediments. Instant compression occurs simultaneously with an increase in the effective stress and causes a reduction of the voids ratio until an equilibrium value is reached when the structure effectively supports the overburden pressure. Delayed compression represents the reduction in volume at unchanged effective stress. This process requires the incorporation of time lines on the diagram relating voids ratio to logarithms effective pressure, each representing the equilibrium voids ratio for different values of effective overburden at specific times of sustained load. These lines are approximately parallel (Taylor, 1942).

5.5 Consolidation Tests - Method of Analysis

5.5.1 Apparatus

A conventional floating head oedometer has been modified so that

pressures of approximately 35000kN/m^2 (equivalent to 2500 - 3000m of sedimentation) could be applied to the specimens (See Fig.A3.1). This was accomplished by:-

(1) Extending the lever arm so that the loading ratio was increased from 10:1 to 20:1.

(2) Reducing the cross-sectional area of the sample container to 10.75cm^2 (i.e. using a diameter of 3.7cm).

(3) Replacement of the porous drainage platons by sintered bronze discs.

5.5.2. Experimental Procedures

(1) A series of consolidation tests were performed on materials in both the undisturbed condition and from a remoulded condition using an initial moisture content equal to the liquid limit (a detailed account of which is given in Appendix A.3)

(2) An additional series of consolidation tests were performed to a maximum pressure of 8400 kN/m^2 in a conventional floating head oedometer on four remoulded materials to investigate the effect of variation of the initial moisture content (see Appendix A.3).

5.6 Comparison of the Performance of the High Pressure Cell with a Standard Oedometer

By reference to tests carried out on four remoulded materials (with initial moisture contents equal to their liquid limit), it was possible to compare the performance of the high pressure oedometer with standard laboratory equipment containing a 50mm diameter cell, and hence assess the acceptability of the results, which form the basis of this thesis.

5.6.1. Voids Ratio - Pressure Relationships

The large size of the lever arm endowed the oedometer with a slightly unbalanced nature which made seating on top of the plunger

quite difficult. However, this was overcome by applying a small load of 20kN/m^2 to the specimen before the test was commenced. Consequently the initial voids ratios are slightly reduced in all cases (Table 5.1).

The e - log P curves produced by the standard oedometer are uniformly curved and slightly concave upwards over their entire length (e.g. Fig. 5.3), whereas those from the high pressure cell tend to show an irregular response in the 20-100kN/m^2 pressure range. This behaviour could well be the result of incorrect pressure assumptions, caused by the effect of the large lever arm. However, above 200kN/m^2 this effect seems to be insignificant and is considered to be unimportant because the principal areas of interest are in the high pressure range. At higher pressures the e - log P curves become parallel to those from the standard oedometer. Small displacements between the curves which are reflected by the difference at 8400 kN/m^2 (Table 5.1), are attributed to errors in sample measurement at the end of the tests.

5.6.2. Stress-Strain Response

The fact that a small load was imposed upon the samples before measurements commenced (causing consolidation), is not only reflected by the initial voids ratio, but also by the lower total percentage strain: the differences for which have been calculated at pressures of 500kN/m^2 and 8400kN/m^2 (Table 5.1).

With the exception of the London Clay, the total strain at the lower pressure is between 4.1 - 4.8 per cent smaller for the high pressure cell and this difference, although slightly reduced to between 3.1 - 4.0 per cent, is maintained to the higher pressure.

Table 5.1 A Comparison of the Consolidation Parameters from the High Pressure Cell with those from a Conventional Oedometer

	c_v (m^2/y)		m_v (m^2/MN)		k ($m/s \times 10^{-10}$)		C_c		C_s	
	conventional cell 8400kN/m^2	HP cell 9350kN/m^2	conventional cell 8400kN/m^2	HP cell 9350kN/m^2	conventional cell 8400kN/m^2	HP cell 9350kN/m^2	conventional cell 8400kN/m^2	HP cell 9350kN/m^2	conventional cell 8400kN/m^2	HP cell 9350kN/m^2
London Clay 37m	0.28	0.30	0.017	0.012	0.01530	0.01175	-0.329	-0.273	0.108	0.094
Fuller's Earth, (Bath)	0.03	0.01	0.020	0.017	0.00173	0.00078	-0.489	-0.467	0.187	0.178
Widdringham roof	9.54	6.08	0.015	0.011	0.45660	0.21537	-0.267	-0.228	0.068	0.048
Pierre Shale, Dak.	0.09	0.04	0.026	0.018	0.00707	0.00229	-0.533	-0.459	0.252	0.179

	Percentage Strain at 8400kN/m^2			Percentage Strain at 500kN/m^2			Initial Voids Ratio		Voids Ratio at 8400kN/m^2	
	conventional cell	HP cell	difference	conventional cell	HP cell	difference	conventional cell	HP cell	conventional cell	HP Cell
London Clay 37m	50.9	49.4	1.5	33.8	32.9	0.9	1.87	1.70	0.49	0.53
Fuller's Earth (Bath)	59.9	56.6	3.3	43.6	38.8	4.8	3.40	2.89	0.76	0.69
Widdringham roof	39.9	35.9	4.0	25.1	20.8	4.3	1.15	0.97	0.29	0.32
Pierre Shale, (Dakota)	69.4	66.3	3.1	51.1	47.0	4.1	3.86	3.61	0.49	0.53

Table 5.2(a) A Comparison of the Teflon and Aluminium Cells using the London Clay (sample LC37)

Pressure (kN/m²)	Percentage Strain		Compression Index	
	Aluminium cell	Teflon cell	Aluminium cell	Teflon cell
158 - 279	7.44	6.37	- 0.73	- 0.52
279 - 574	5.30	5.45	- 0.50	- 0.48
574 -1128	4.41	5.18	- 0.40	- 0.38
1128 -2426	4.37	4.65	- 0.35	- 0.36
2426 -4675	3.72	3.81	- 0.29	- 0.19
4675 -9349	3.05	4.48	- 0.27	- 0.28
9349 -18697	2.55	3.85	- 0.22	- 0.35
18697 -34967	2.44	4.86	- 0.24	- 0.48
34967 -2	11.63	13.75		

Voids Ratio at Max.Pres.		Voids Ratio after consol.	
Aluminium cell	Teflon cell	Aluminium cell	Teflon cell
0.21	0.16	0.53	0.52

Table 5.2(b) A Comparison of the Teflon and Aluminium Cells using the Oxford Clay (sample OC44)

Pressure (kN/m²)	Percentage Strain		Compression Index	
	Aluminium cell	Teflon cell	Aluminium cell	Teflon cell
158 - 279	7.04	4.67	- 0.83	- 0.41
279 - 574	4.34	6.90	- 0.22	- 0.57
574 -1128	4.44	4.80	- 0.38	- 0.39
1128 -2426	4.49	4.77	- 0.34	- 0.34
2426 -4675	3.65	4.26	- 0.27	- 0.32
4675 -9349	2.99	3.54	- 0.25	- 0.28
9349 -18697	3.24	4.14	- 0.27	- 0.32
18697 -34967	2.94	4.23	- 0.27	- 0.37
34967 -2	11.49	17.51		

Voids Ratio at Max.Pres.		Voids Ratio after consol.	
Aluminium cell	Teflon cell	Aluminium cell	Teflon cell
0.18	0.09	0.48	0.51

Table 5.3 A Comparison of the Voids Ratios at 35000kN/m^2 for Undisturbed & Remoulded Samples

	Sample Ref.	Undisturbed Material	Remoulded Material	Difference	
British Material					
London Clay 14m	LC14	0.349	0.392	- 0.043	
London Clay 37m	LC37	0.308	0.216	0.092	
Gault Clay	GC	0.296	0.28°	0.008	
Fuller's Earth (Redhill)	FE23	0.702	0.707	- 0.005	
Weald Clay	WC	0.083	0.088	- 0.005	
Kimmeridge Clay	KC	0.256	0.221	0.035	
Oxford Clay 10m	OC10	0.279	0.262	0.017	
Oxford Clay 44m	OC44	0.235	0.186	0.049	
Fuller's Earth (Bath)	FE19	0.404	0.419	- 0.015	
Lias Clay 10m	L10	0.247	0.277	- 0.03	
Lias Clay 36m	L36	0.249	0.264	- 0.015	
Keuper Marl	KM	-	0.242	-	not over preconsolidated load
Swallow Wood roof	SWR	-	0.205	-	
Flockton Thin roof	FTR	0.073	0.196	-	
Flockton Thin seatearth	FTS	0.147	0.185	-	
Widdringham roof	WR	0.041	0.130	-	
North American Material					
Yazoo Clay	YC	0.342	0.330	0.012	
Kincaid Shale 6m	K6	0.316	0.261	0.055	
Kincaid Shale 8m	K8	0.304	0.214	0.090	
Nacimiento Shale	N1	0.194	0.203	- 0.009	
Nacimiento Shale	N2	0.202	0.195	0.007	
Nacimiento Shale	N3	0.372	0.321	0.051	
Fox Hills Shale	FOX	0.430	0.346	0.084	
Dawson Shale	DS	0.208	0.219	- 0.011	
Pierre Shale (Dakota)	PSD	0.390	0.315	0.075	
Pierre Shale (Colorado)	PSC	0.151	0.171	- 0.020	

With regard to the strain energy, although there does not appear to be a simple mathematical relationship between the results encountered at different pressures, similar trends are observed for both oedometers when the maximum pressures are considered. These are discussed in detail in Section 5.11.

5.6.3. Consolidation Parameters

The differences in the low pressure range are also reflected, to a certain extent by the consolidation parameters. However, as higher pressures are encountered ($4000kN/m^2$ upwards), the behaviour of both machines becomes nearly identical, (Table 5.1). The main difference is that there is a tendency for those from the high pressure machine to be slightly lower, although this may be partially accounted for by the higher pressure used in each case.

5.7 Experiments with a Teflon Oedometer Cell

Initially a pure teflon cell was produced for performing tests on remoulded materials, essentially to reduce the effects of side friction on the metal plunger. The very stiff nature of the natural clays ruled out its use in the tests on these materials because of the difficulty encountered in getting the samples into the cell.

From tests conducted on remoulded samples of London Clay (LC37) and Oxford Clay (OC44) (see Table A3.62 and A3.63). It was discovered that in the high pressure range (i.e. 2426 - $34967kN/m^2$), the incremental strains were much larger than those obtained when a silicone greased aluminium cell was used (Tables 5.2 a & b). This is reflected in the larger values of C_c and smaller values of voids ratio (Table 5.2 a & b). Similarly when the load was removed, larger expansive strains were produced from the teflon cell, (Table 5.2 a & b) resulting in final voids ratios which were comparable with those

obtained from the aluminium cell.

Therefore it was concluded that the teflon cell was compressing elastically at the higher pressures, thus increasing the cross-sectional area and consequently affecting the results (which are considered on a one-dimensional basis). Consequently it was decided that the teflon cell could not be used and no further tests were performed with this material.

5.8 Voids Ratio Correction for the Remoulded Consolidation Curve

When the voids ratio-pressure relationships are compared for the undisturbed and remoulded states at the highest pressure for clays where the preconsolidation load has been exceeded, certain relative displacements of the curves are noticed. From Table 5.3 it can be seen that for some samples the undisturbed voids ratio is larger (the difference being expressed as a positive notation) whilst in others the reverse situation occurs; in some the results are nearly identical.

These differences in the voids ratio at the highest pressure are either due to actual differences in the clay fabric or to errors in the measurement of the final thickness of the remoulded samples (because of the small sample size). However, because the e - log P curves for the undisturbed materials have been confirmed by independent initial voids ratio determinations, it has been assumed that errors in measurement are the chief causes of these discrepancies (e.g. an 0.051mm difference can alter the voids ratio by 0.015). Errors in measurement are also suspected because although the curves are parallel for the majority of clays tested, the remoulded curve should always lie beneath that of the undisturbed specimen. Nevertheless since the pressures concerned are reasonably large, the difference will be negligible. To support this latter statement, Fleming et al

(1970), attribute the coincidence of the e-log P curves, in the pressure range 9000 - 35000kN/m^2 for materials consolidated from positions normal to, and parallel to the bedding, to isotropic behaviour of clays beyond their preconsolidation loads.

The relative positions of the e - log P curves do not materially affect the consolidation parameters of c_v, m_v, k, C_c and C_s but can cause significant errors in the depth estimations when the method utilising the rebound characteristics is considered, (Chapter 2).

Therefore for the purpose of calculating the maximum depths of burial from the rebound characteristics, this discrepancy has to be minimised by making the remoulded and undisturbed curves coincide by adjusting the former by the difference in the voids ratio at the highest pressure.

5.9 Consolidation Test Results

5.9.1. Voids Ratio - Pressure Relationships

During each stage of consolidation tests on both remoulded and undisturbed materials, the voids ratio has been calculated in accordance with methods laid down in standard soils texts, for each clay the values so obtained have been presented graphically against the logarithm to the base ten of effective pressure (Figs.5.1.1-5.1.5 0). To ensure the highest degree of accuracy, the initial voids ratio for each clay in the undisturbed state has been independently checked by additional tests (Appendix A3.2).

Since all the materials are heavily overconsolidated, where increased curvature is present in the compression curve, the Casagrande construction (Figure 2.6) has been used to assess the maximum overburden pressures (Tables 2.3 and 2.4). In certain cases, to enable another construction method (Section 2.3) to be used to calculate the maximum depth of burial an additional line, which represents the adjusted

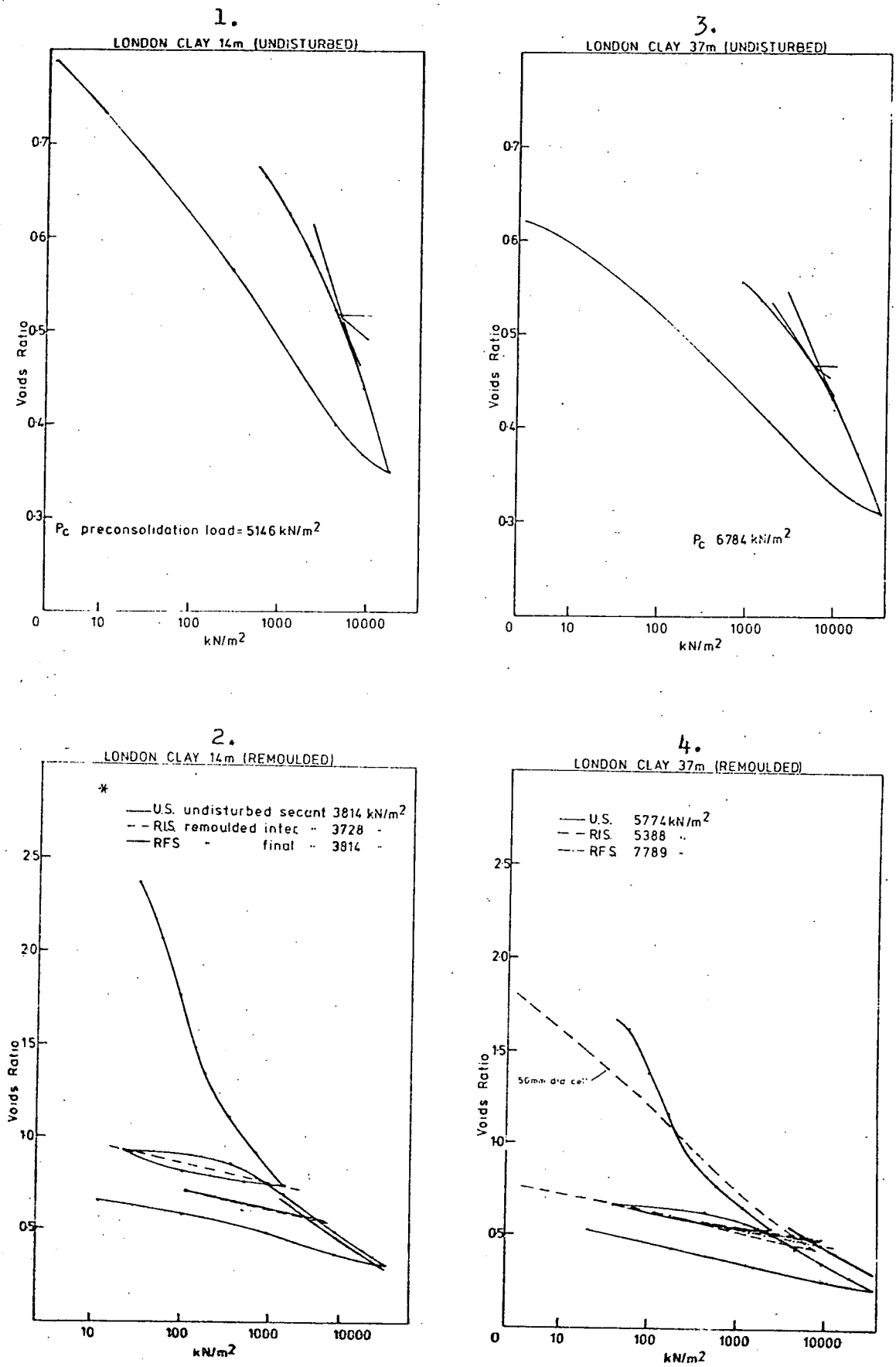

Figure 5.1. Voids Ratio - Effective Pressure Relationships for the Samples Tested.

* Values indicate the estimated maximum depth of burial using rebound characteristics (Chapter 2.3.).

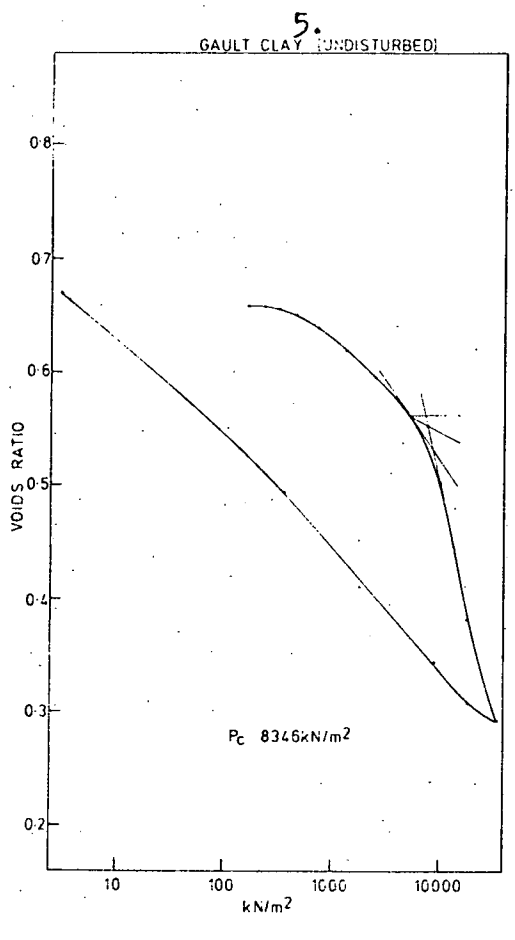

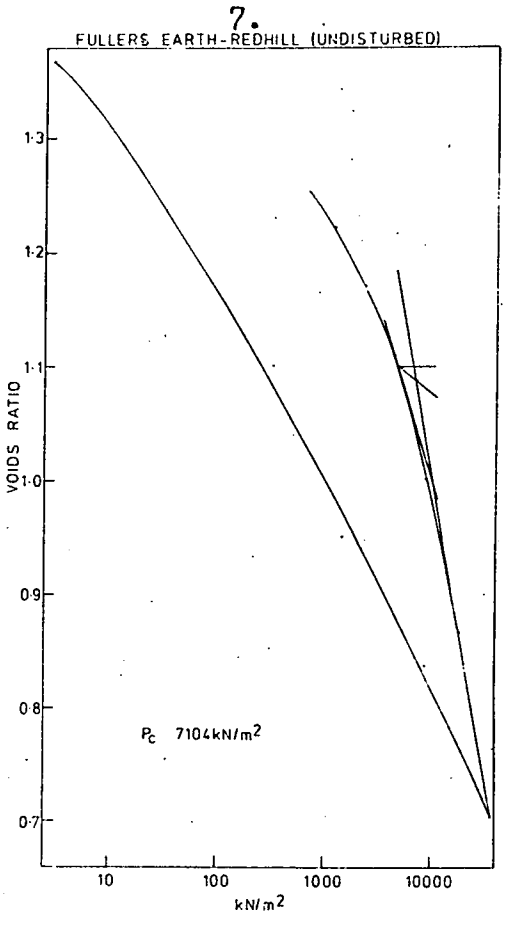

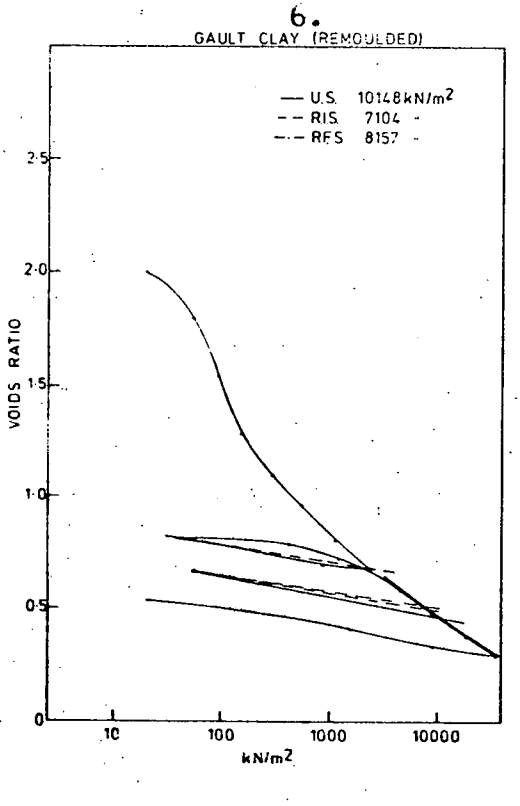

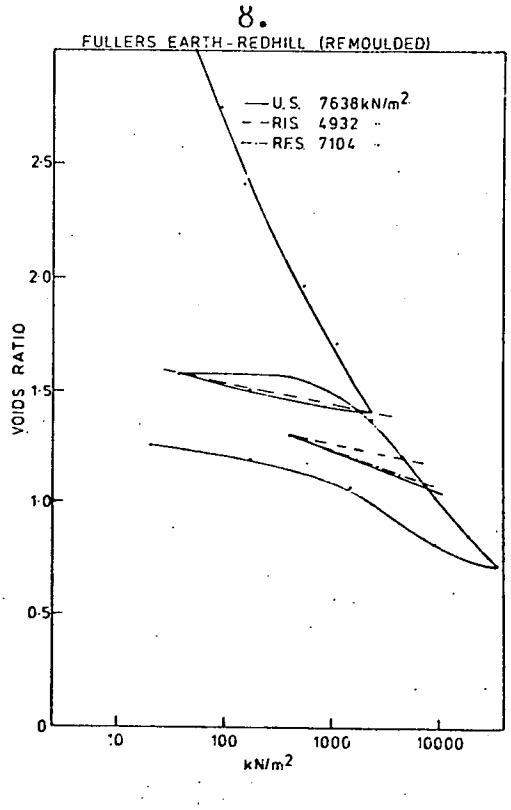

Figure 5.1. cont.

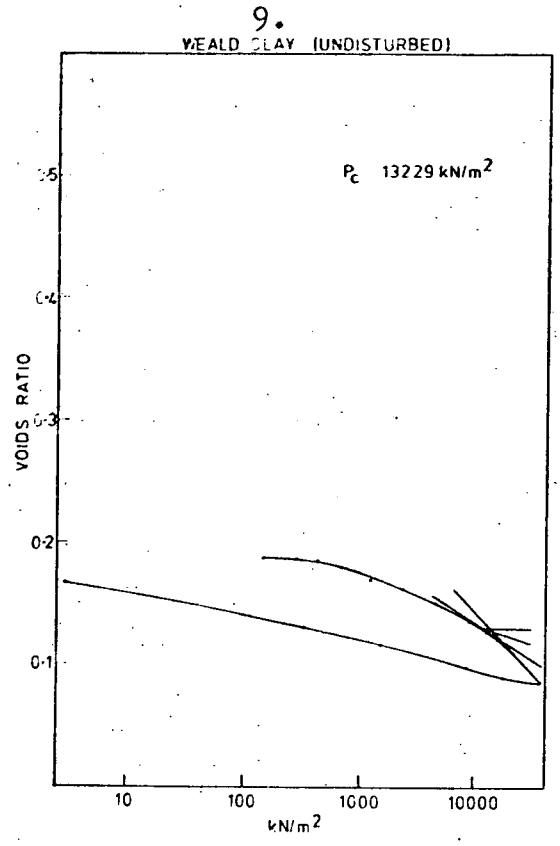

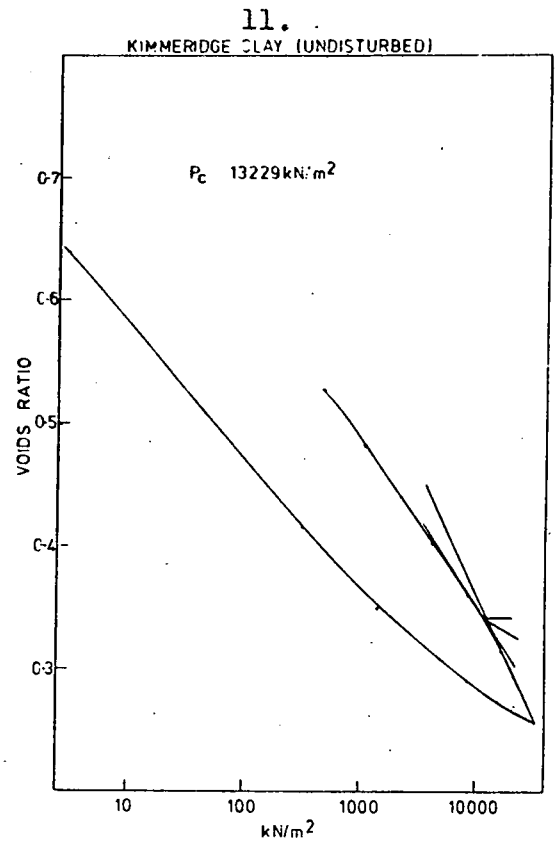

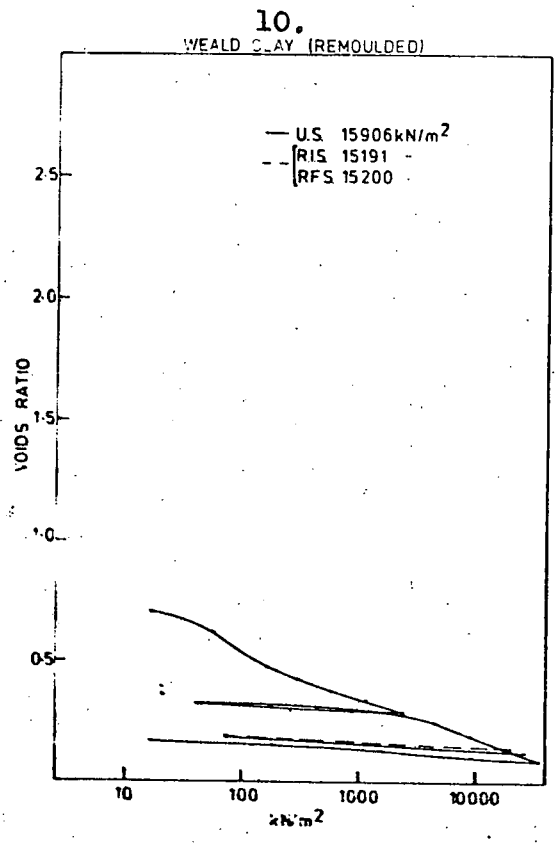

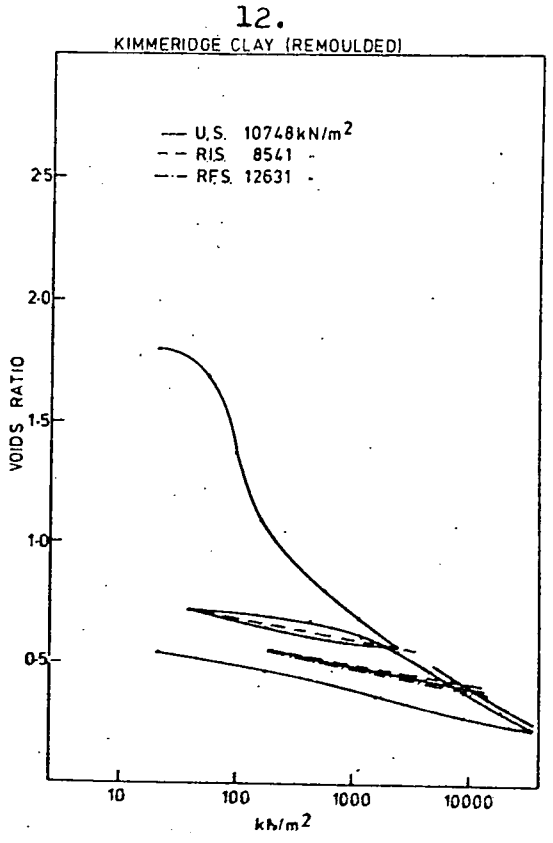

Figure 5.1. cont.

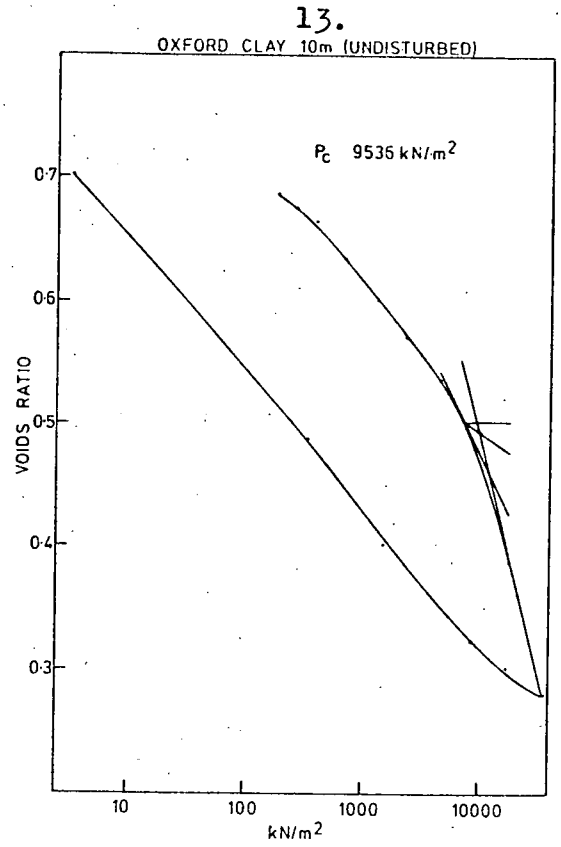

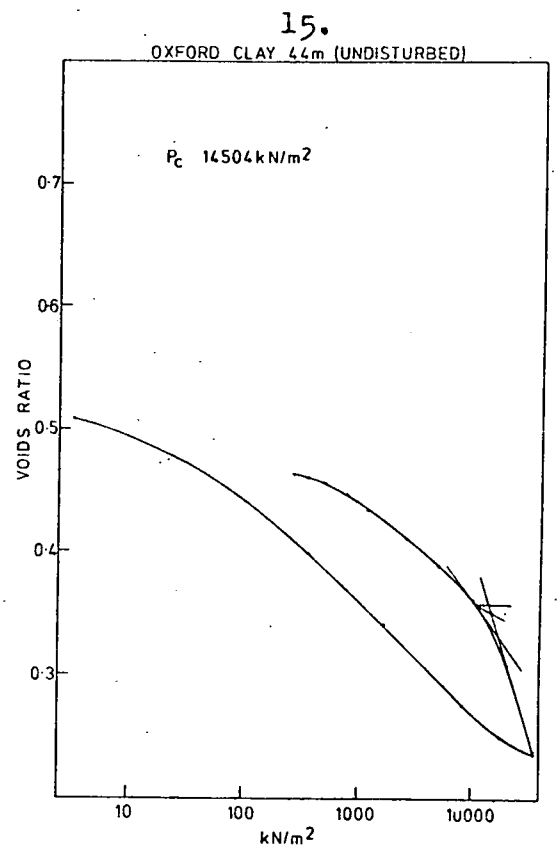

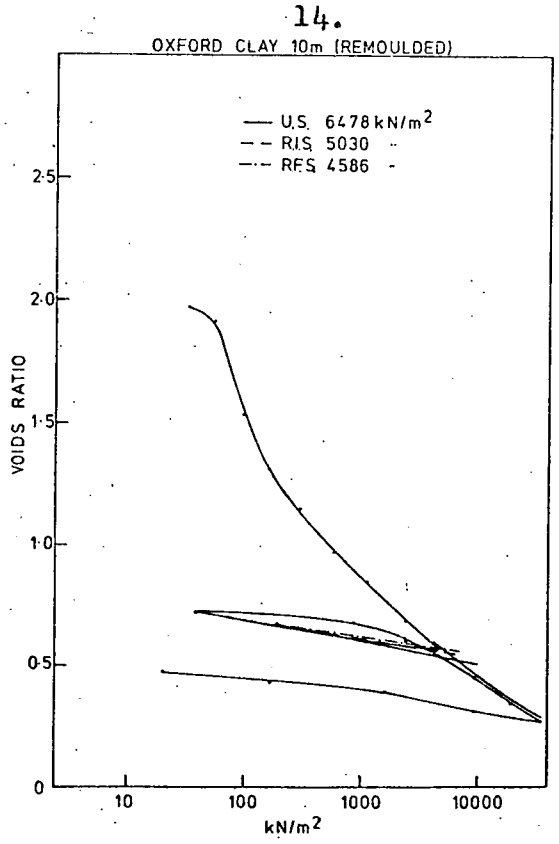

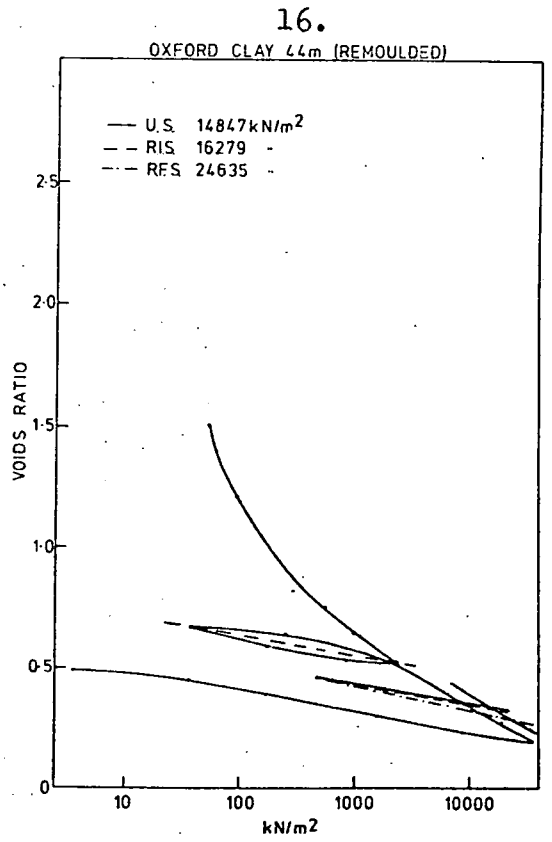

Figure 5.1. cont.

17.

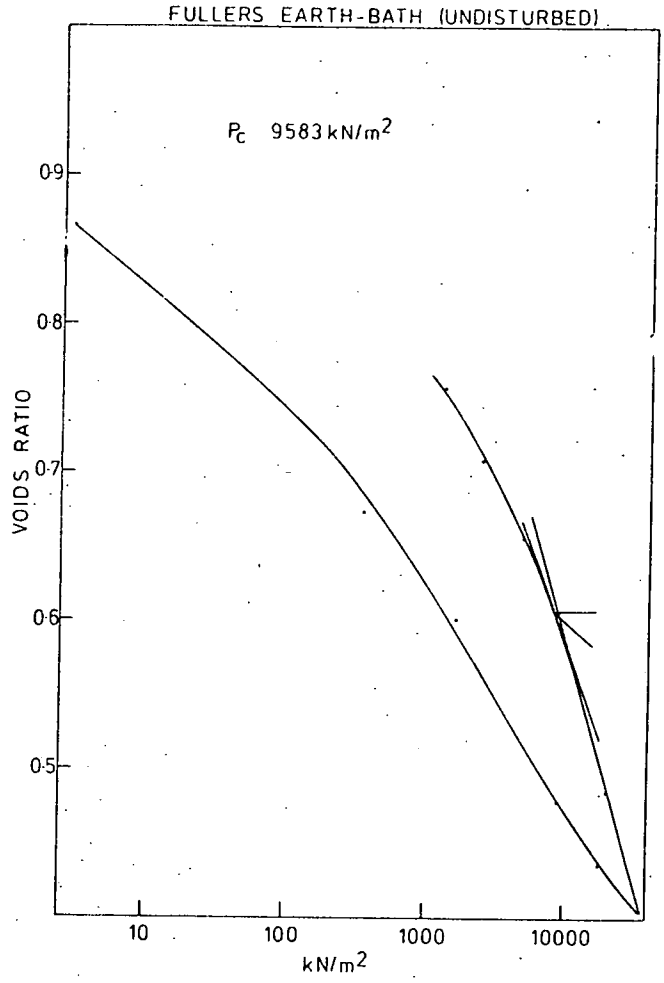

18.

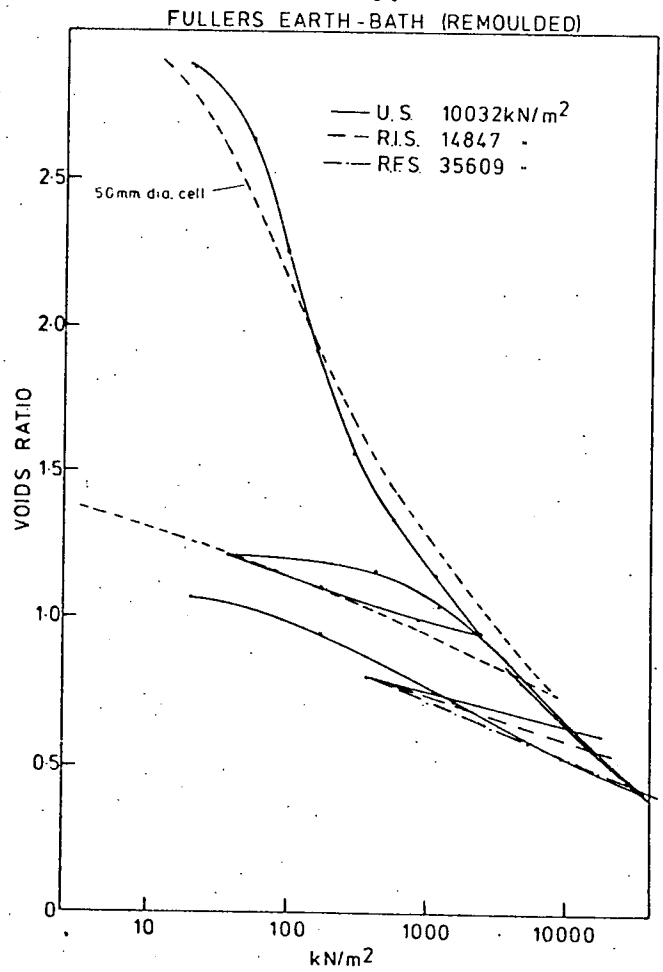

Figure 5.1. cont.

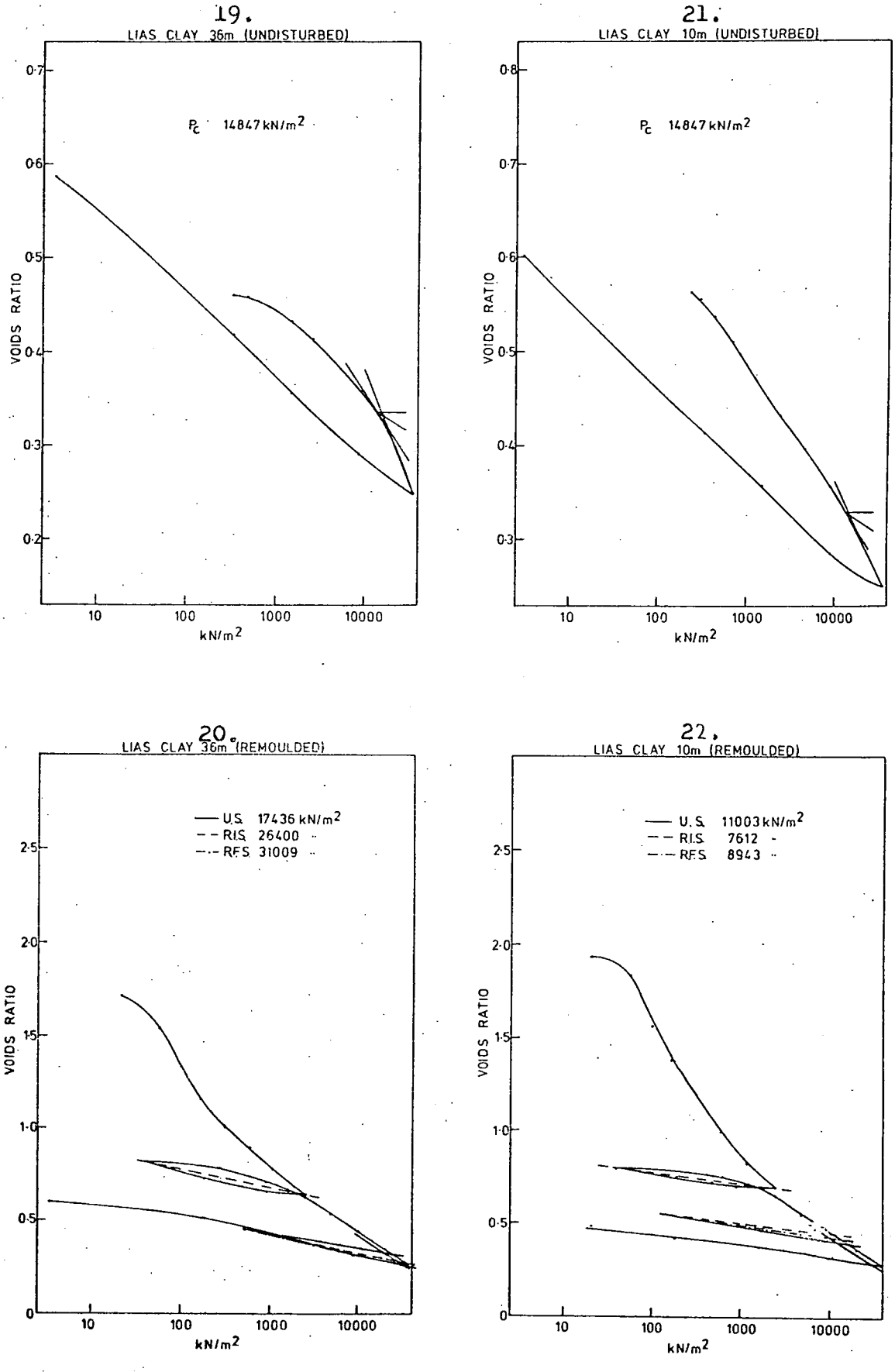

Figure 5.1. cont.

23.

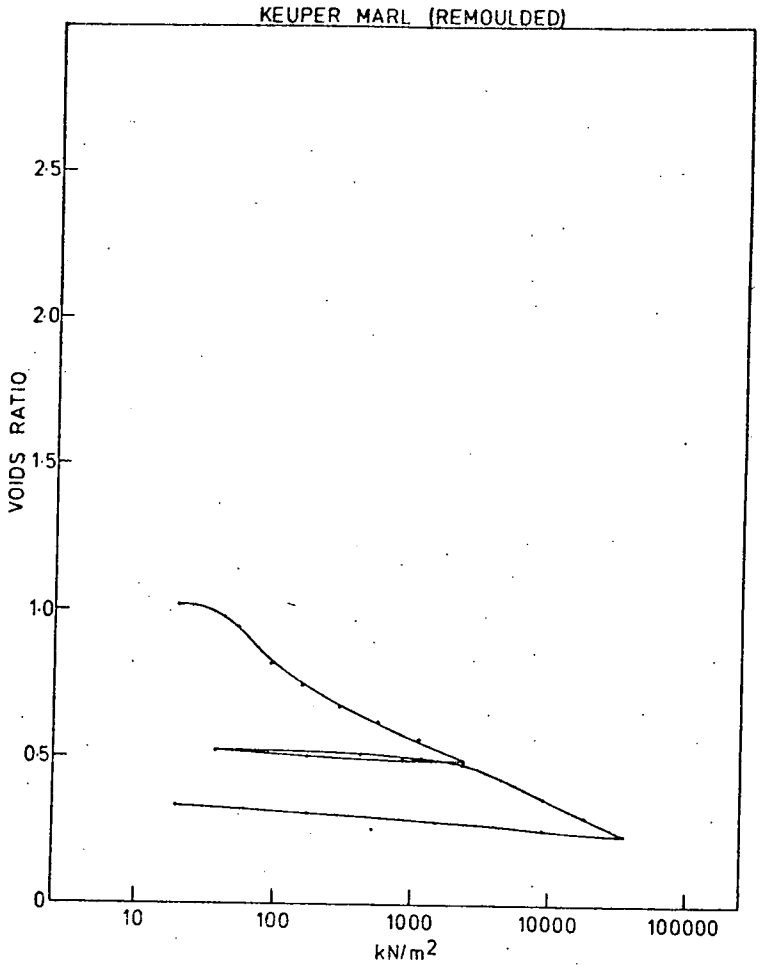

24.

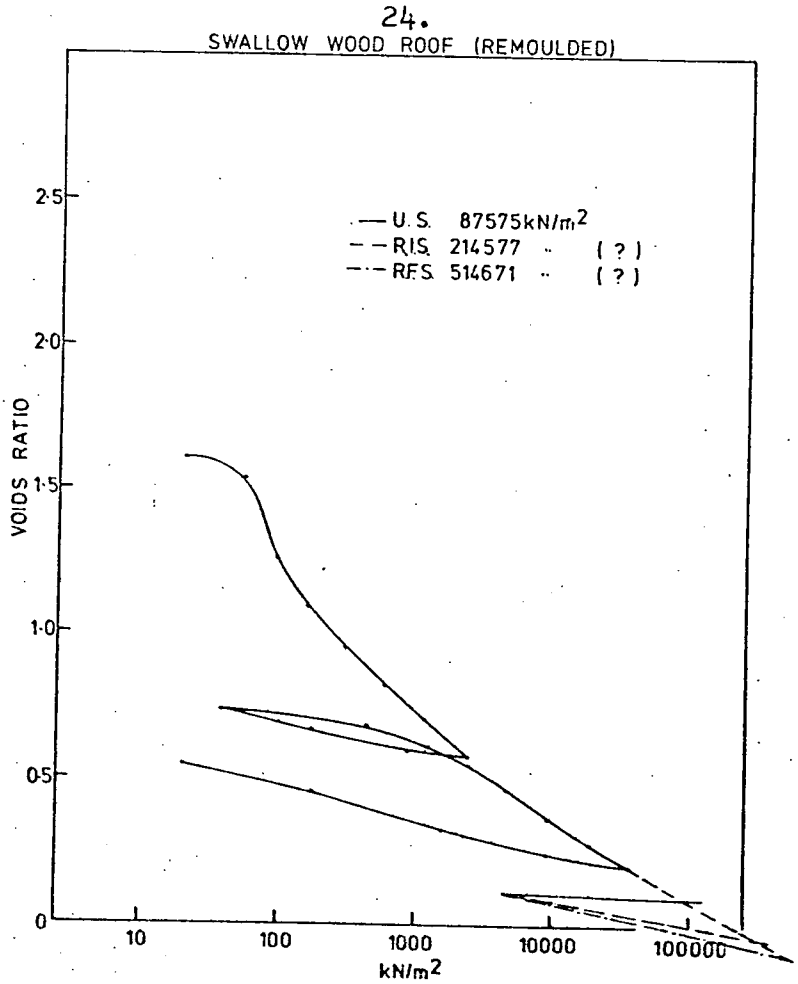

Figure 5.1. cont.

25.

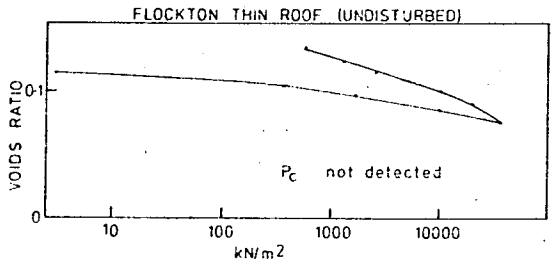

26.

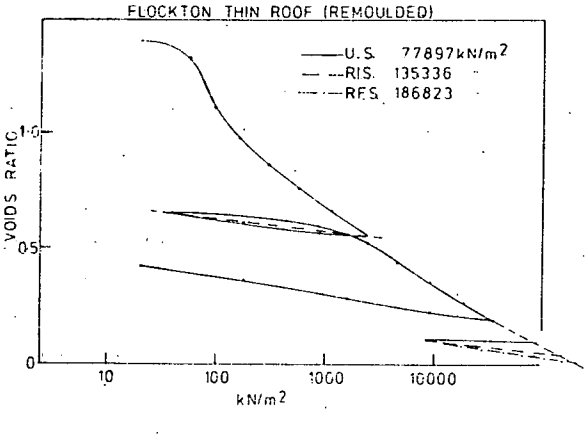

27.

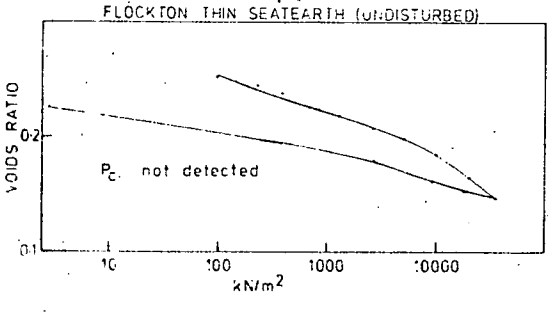

28.

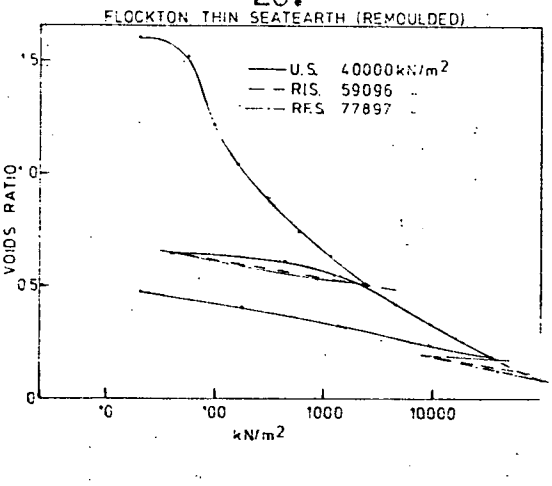

29.

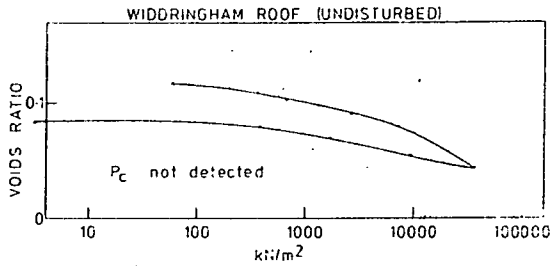

30.

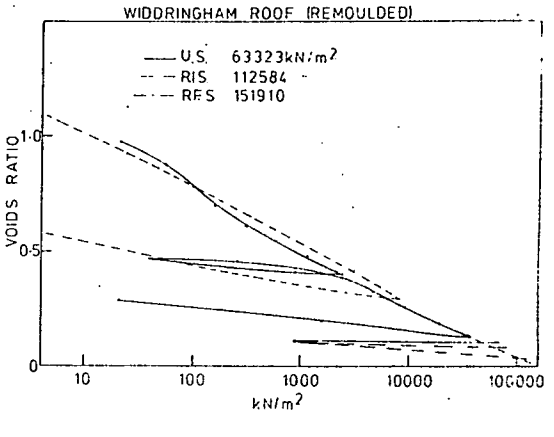

Figure 5.1. cont.

31.

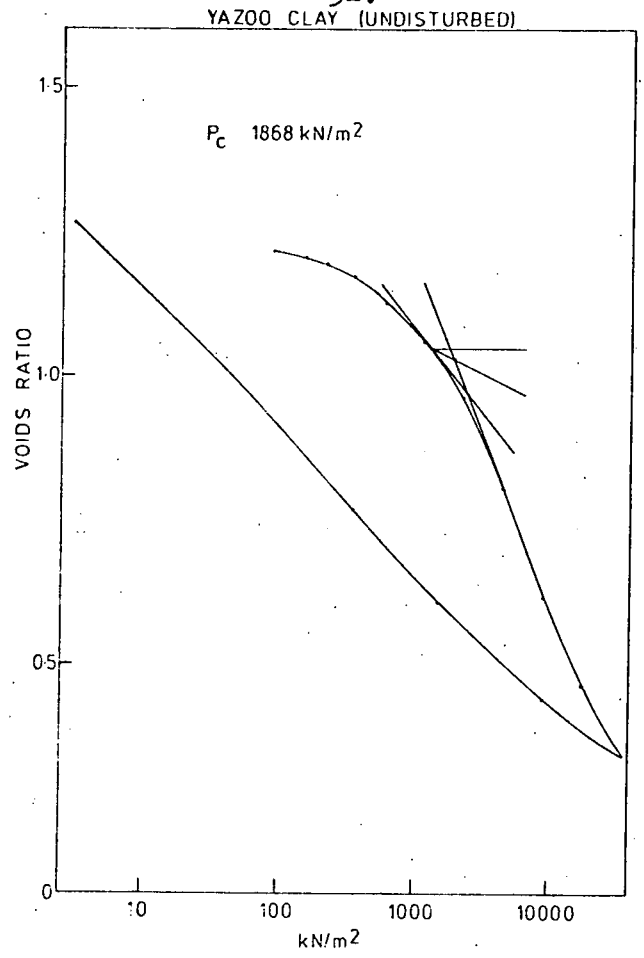

32.

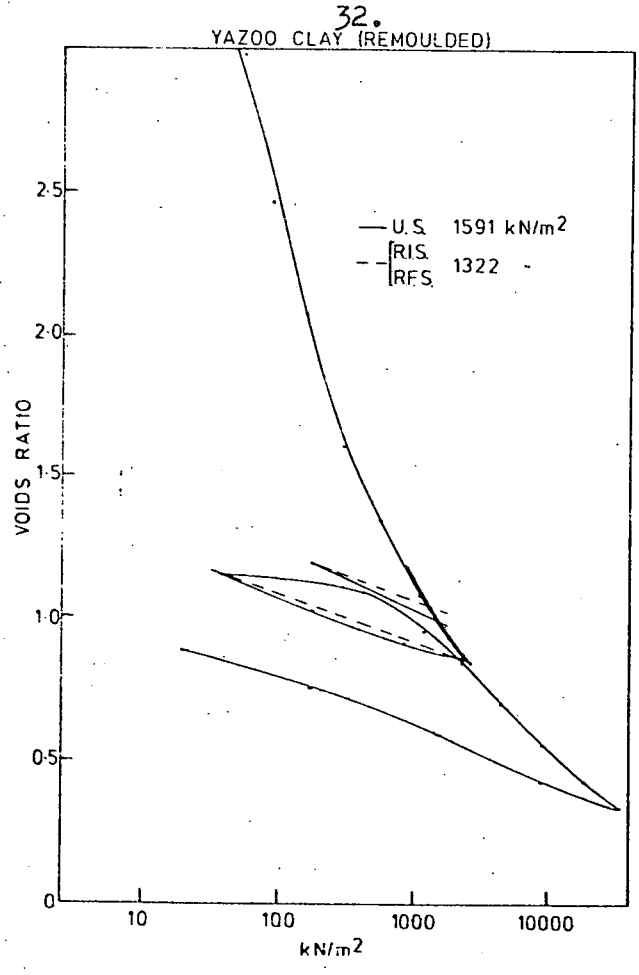

Figure 5.1. cont.

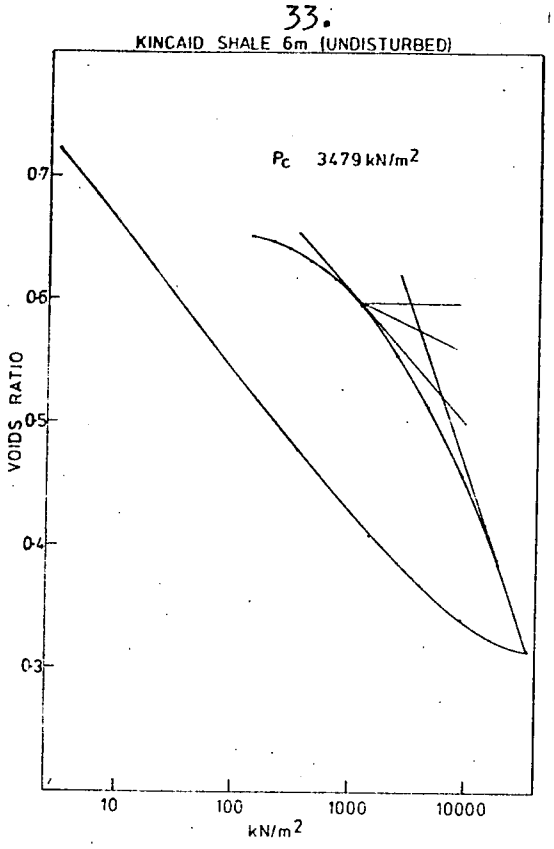

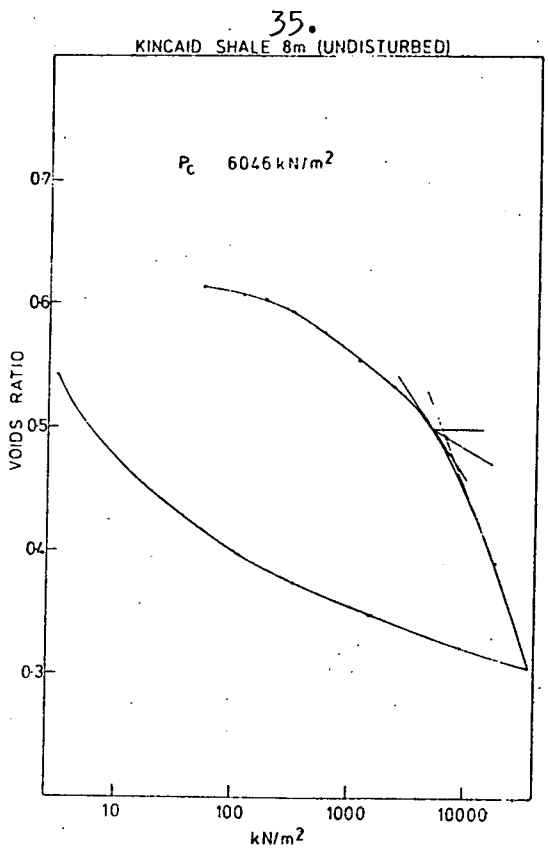

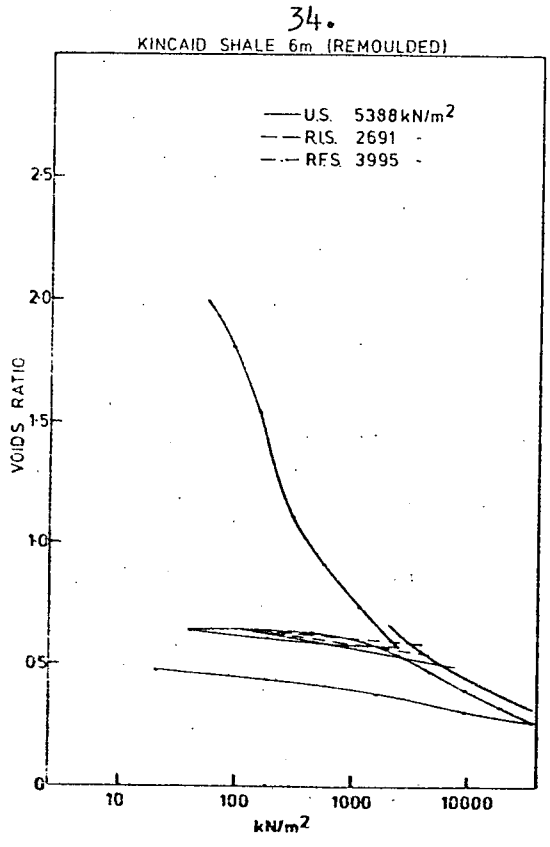

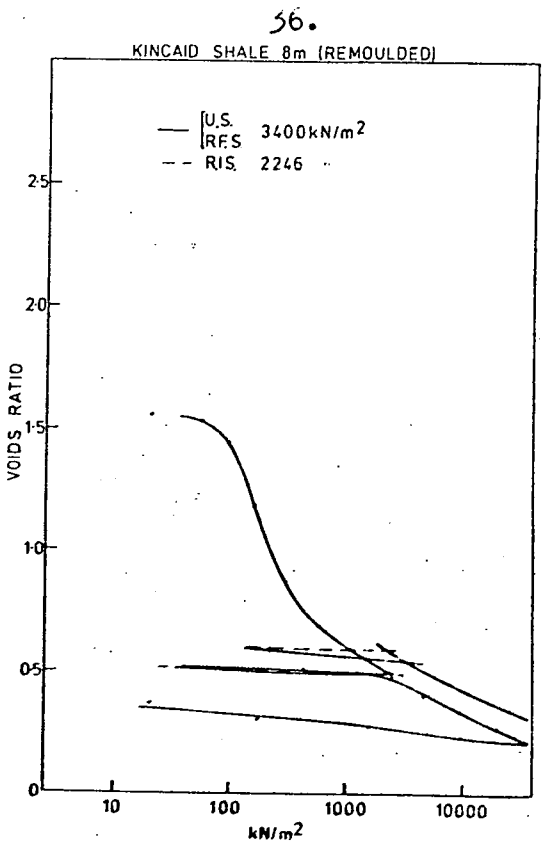

Figure 5.1. cont.

37.

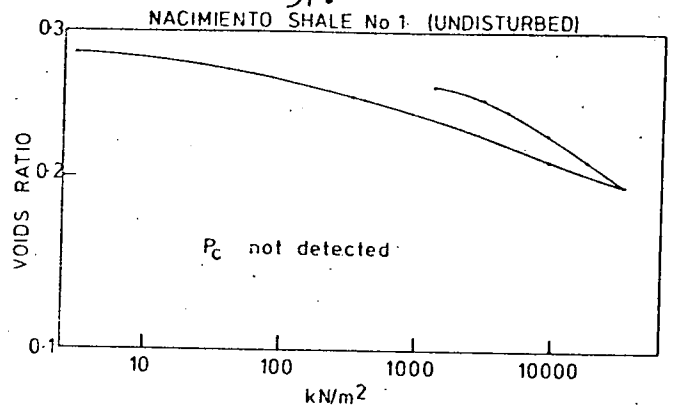

38.

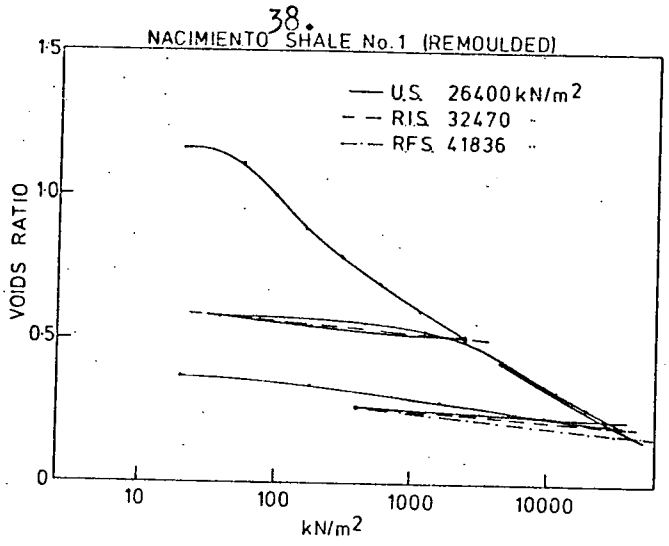

39.

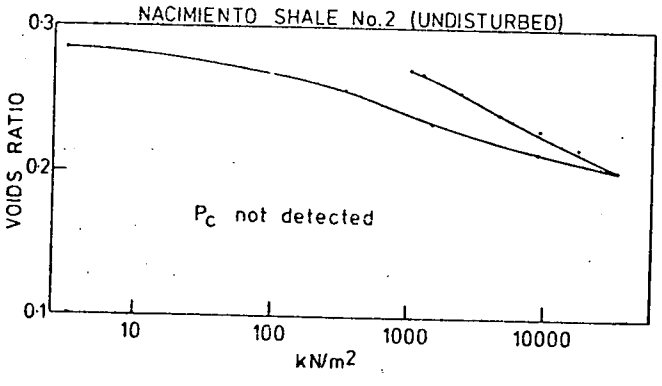

40.

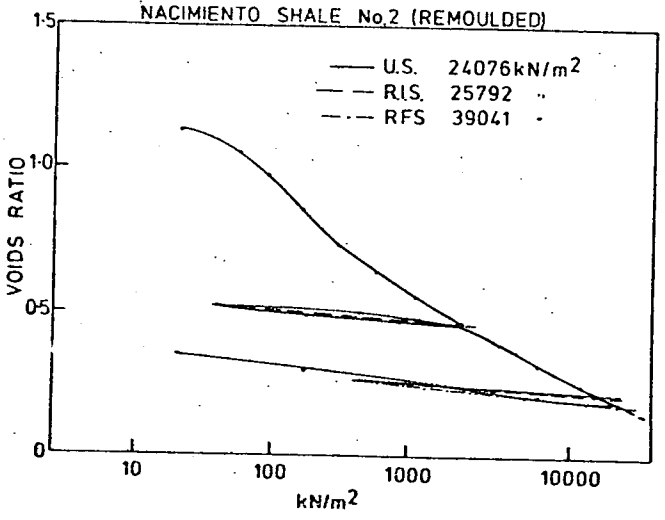

Figure 5.1. cont.

41.

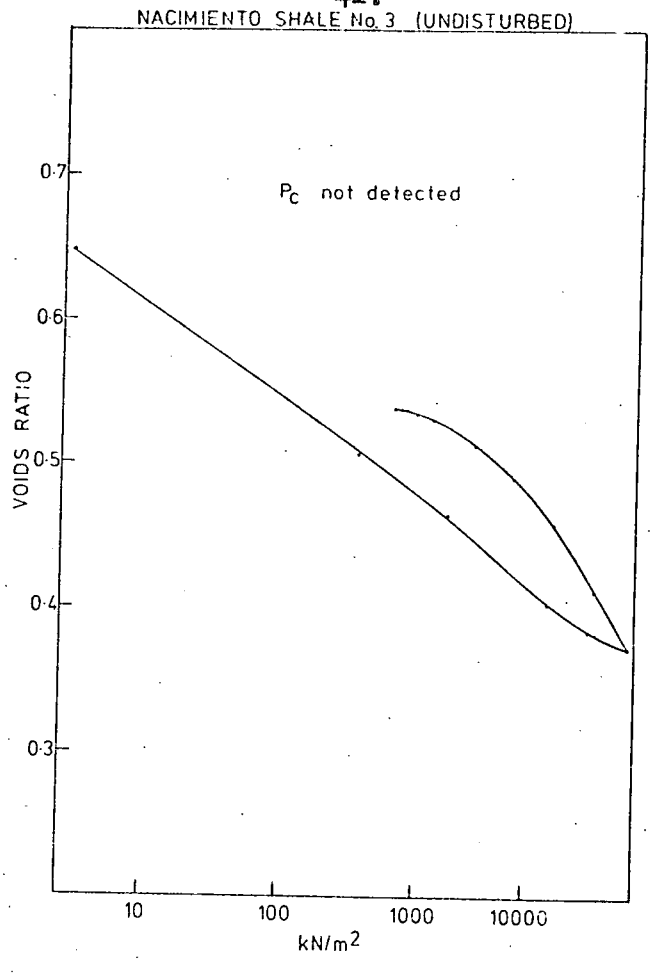

42.

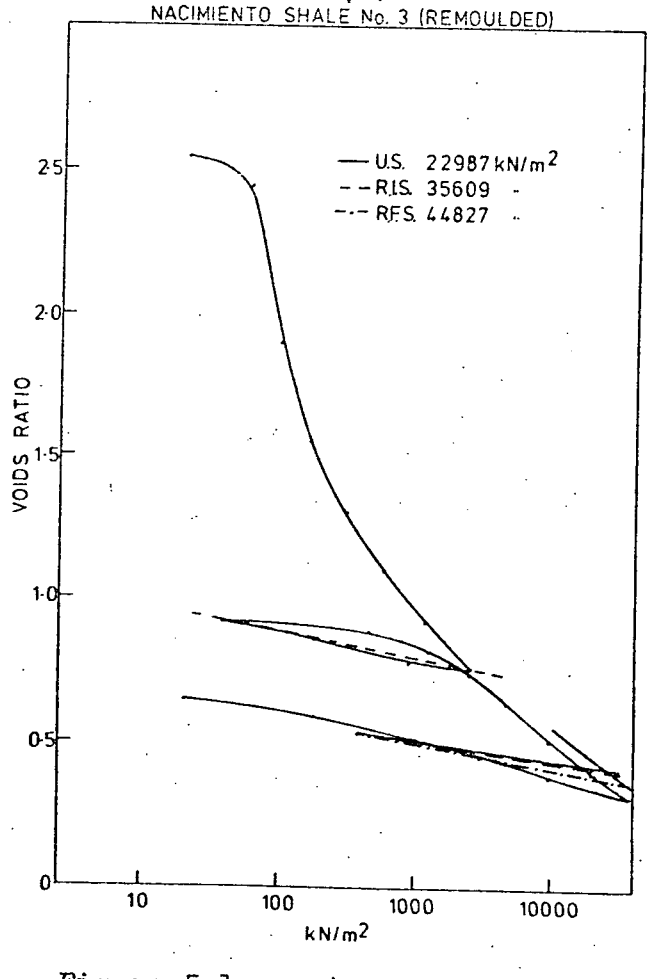

Figure 5.1. cont.

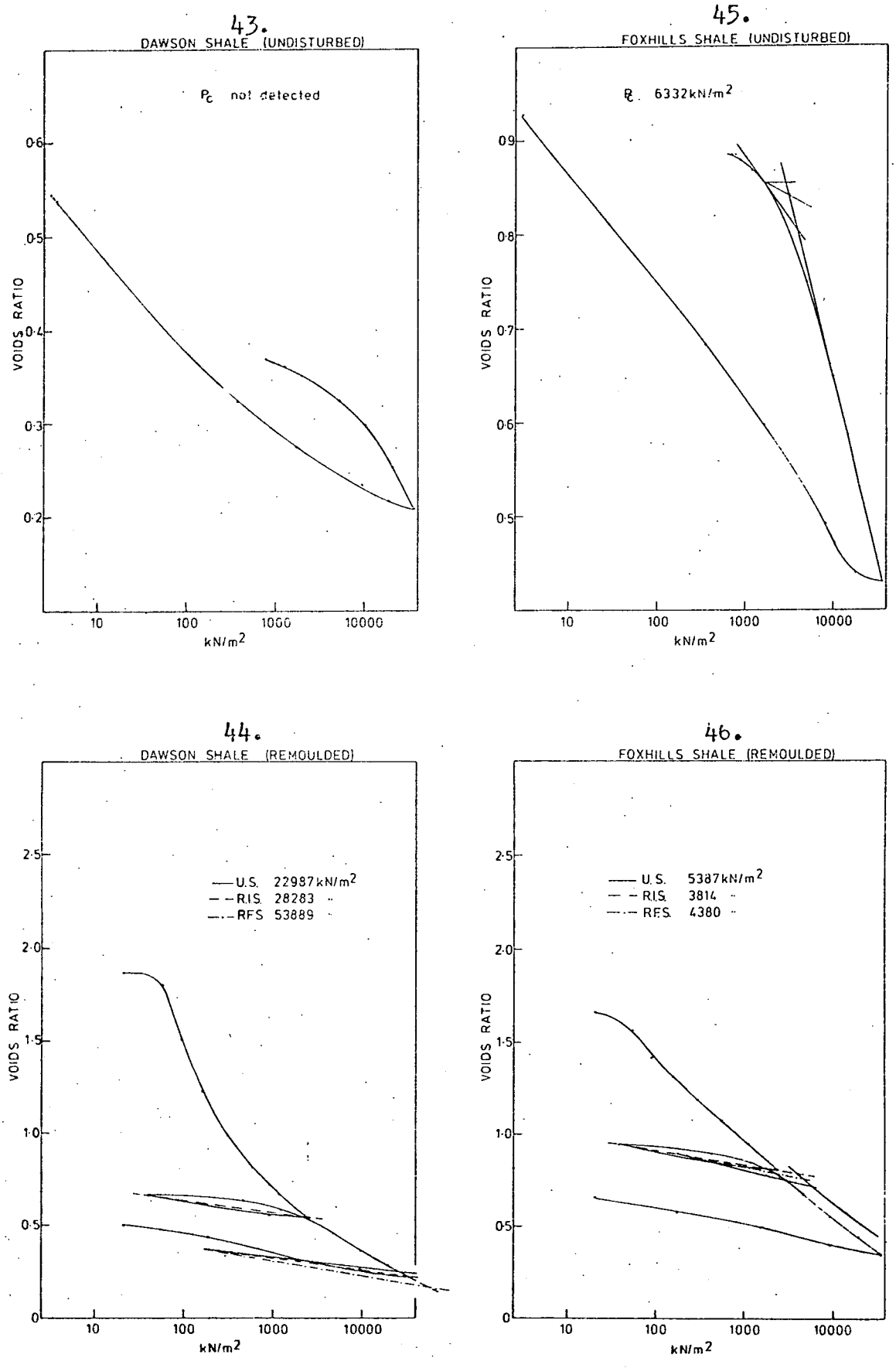

Figure 5.1. cont.

47.

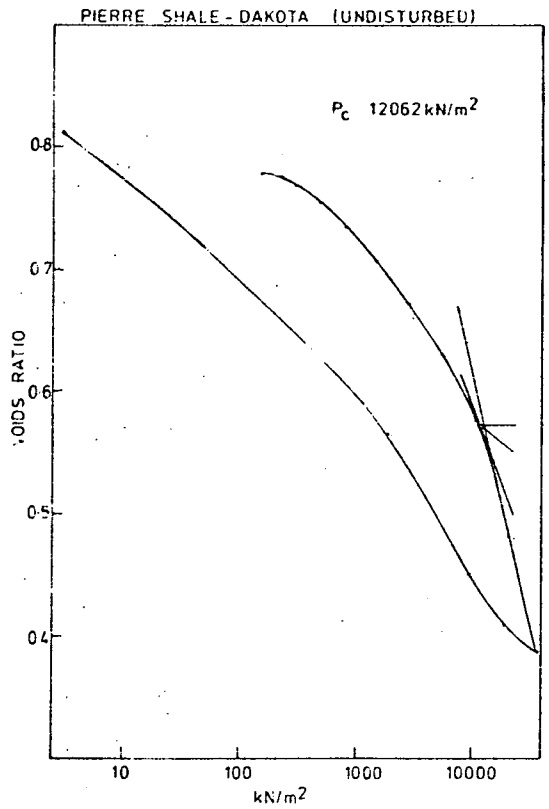

49.

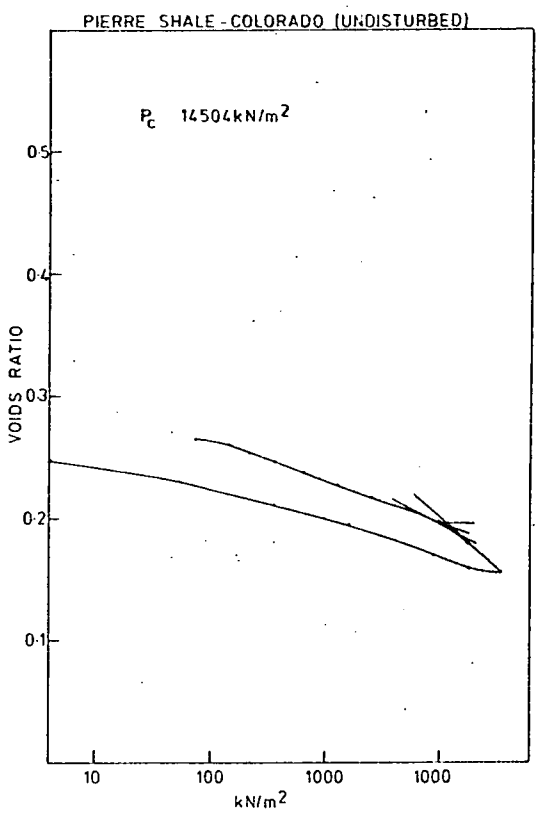

48.

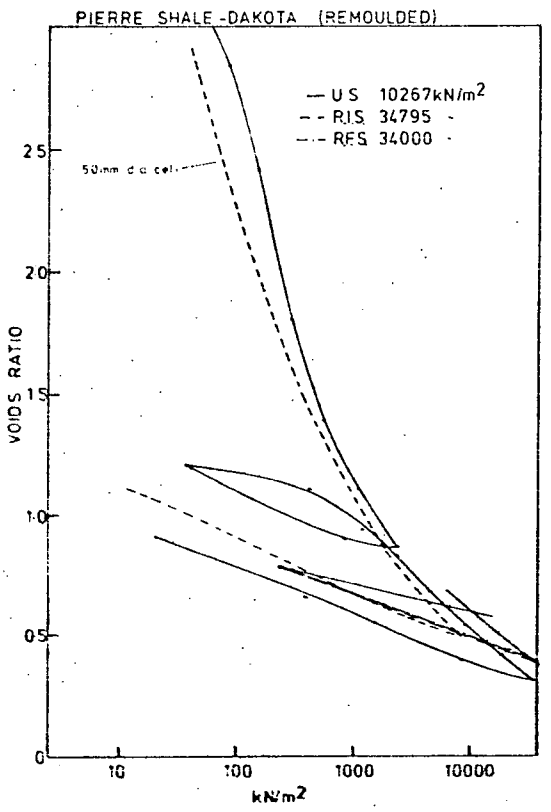

50.

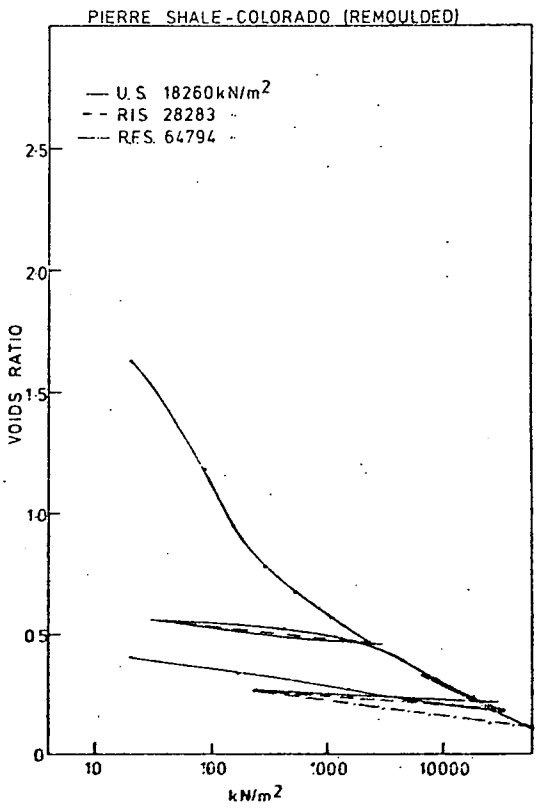

Figure 5.1. cont.

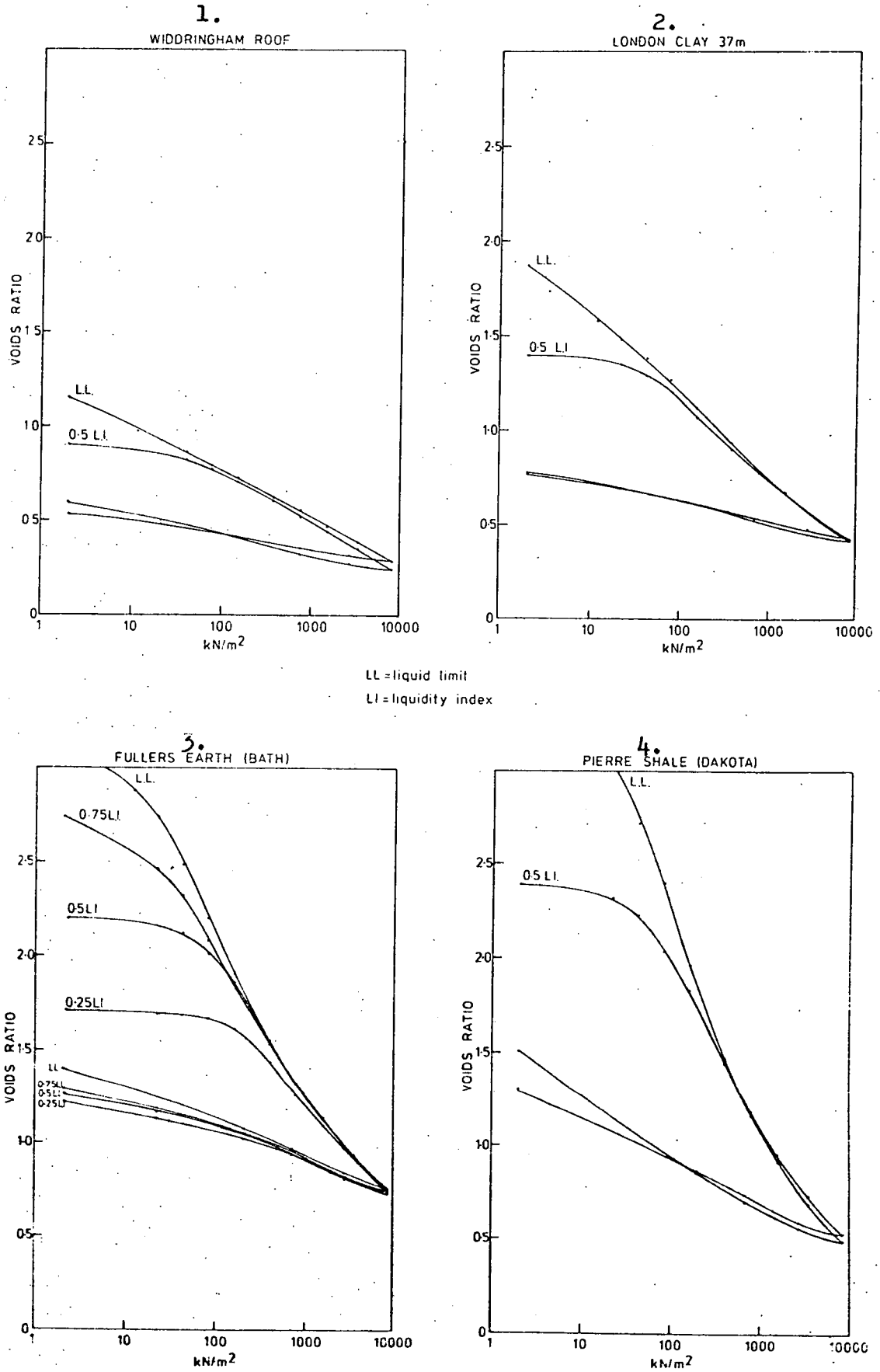

Figure 5.2. E - LogP Relationships Using a Conventional Oedometer and the Associated Effect of Initial Moisture Content.

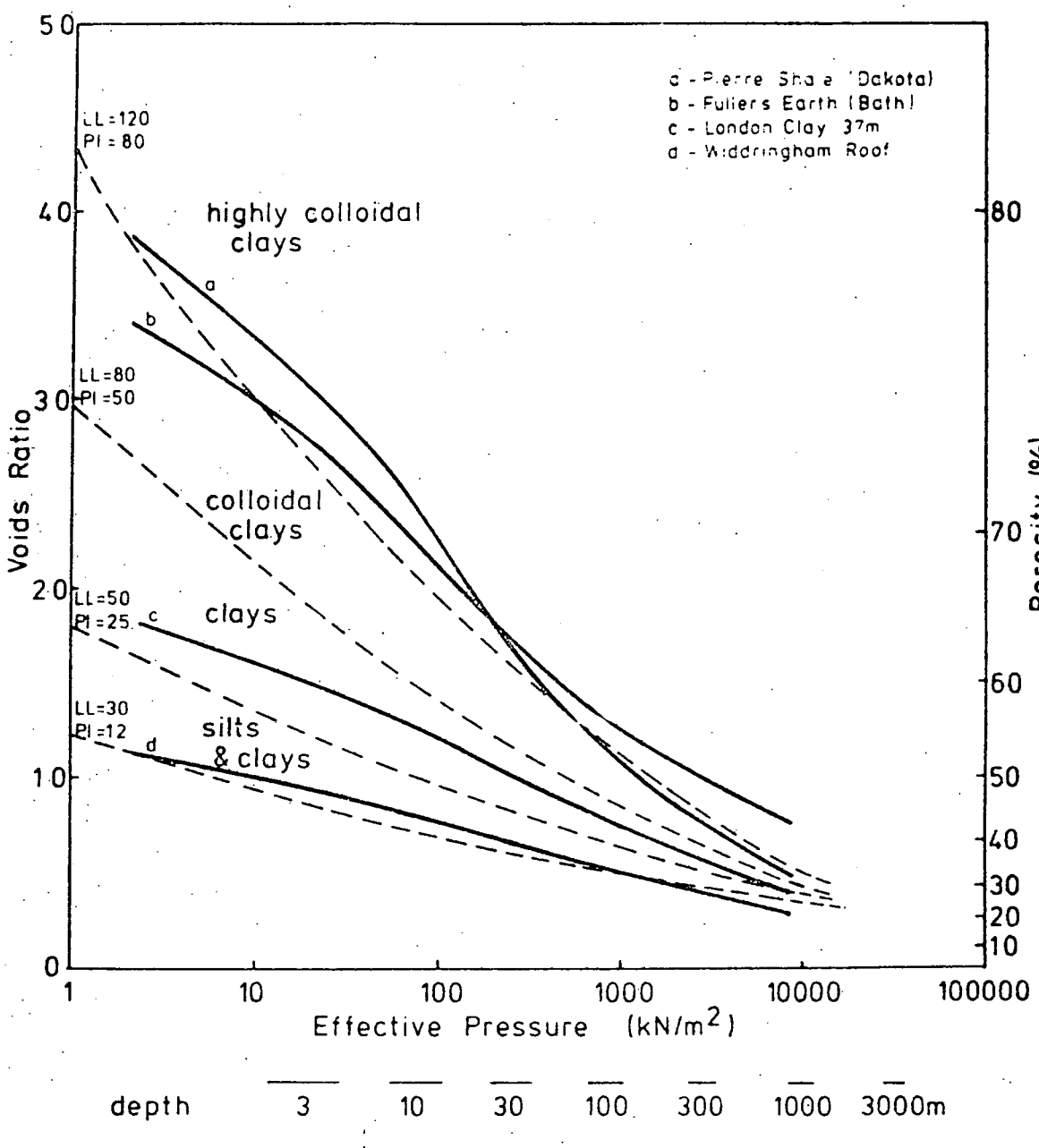

Figure 5.3. Compression Curves for Certain Remoulded Clays in Relation to the Sedimentation Curves of Skempton (1953).

position of the remoulded curve (see Section 5.8) has been added to the e - log P relationships for these materials.

Remoulded e - log P relationships from the low pressure tests at various initial moisture contents are presented in Fig.5.2 where it can be seen that an effect similar to the preconsolidation condition is produced in the 80-150kN/m^2 region when the initial moisture content is reduced from the liquid limit. This effect is assumed to be associated with the way the material is paddled into the oedometer cell. In addition, the e - log P relationships for the condition starting from the liquid limit have been incorporated in one diagram (Fig.5.3) where a close correspondence is noticed with trends suggested by Skempton (1944, 1953).

5.9.2. Coefficient of Consolidation (c_v)

This is dependent upon the thickness of the sample and upon the rate of loading. It relates the decrease in volume of a sediment to the applied pressure and time, thus enabling the rate of settlement to be predicted and has been calculated in the present study by reference to the T_{90} value obtained from the compression - root time curves (Taylor, 1948) i.e. -

$$c_v = \frac{0.848H^2}{T90} \quad \text{..... (18)}$$

where H is the average thickness during the loading increment. The value of c_v has the dimensions of L^2T^{-1} (e.g. m^2/yr).

The values of c_v for the undisturbed samples, beyond the preconsolidation load, are presented in Table 5.4, column (a), whilst the average values for the remoulded samples between the pressures of 4675 - 34967 kN/m^2 and 297 - 2426 kN/m^2 are presented in columns (b) and (c) respectively. Average values obtained from

Table 5.4 Average Coefficient of Consolidation (c_v) Values (m^2/y)

	Sample Ref.	Undisturbed Samples (a)	Remoulded Samples 4675-34967kN/m² (b)	Remoulded Samples 297-2426kN/m (c)
British Samples				
London Clay 14m	LC14	0.28	0.27	0.10
London Clay 37m	LC37	0.31	0.24	0.48
Gault Clay	GC	0.91	0.64	0.55
Fuller's Earth (Redhill)	FE23	0.02	0.01	0.03
Weald Clay	WC	25.10	10.90	3.54
Kimmeridge Clay	KC	0.25	0.43	0.47
Oxford Clay 10m	OC10	0.49	0.92	0.15
Oxford Clay 44m	OC44	0.57	0.90	1.09
Fuller's Earth (Bath)	FE19	0.02	0.02	0.08
Lias Clay 10m	L10	0.42	0.26	0.13
Lias Clay 36m	L36	0.67	0.85	1.15
Keuper Marl	KM	-	7.18	4.56
Swallow Wood roof	SWR	-	1.01	0.51
Flockton Thin roof	FTR	-	1.76	0.75
Flockton Thin seat	FTS	-	0.56	0.67
Widdringham roof	WR	-	6.72	9.67
North American Samples				
Yazoo Clay	YC	0.03	0.03	0.08
Kincaid Shale 6m	K6	0.55	0.13	0.18
Kincaid Shale 8m	K8	47.47	0.62	0.52
Nacimiento Shale	N1	?9.13	2.14	4.38
Nacimiento Shale	N2	?32.39	0.53	1.28
Nacimiento Shale	N3	?0.04	0.12	0.47
Fox Hills Shale	FOX	0.10	0.18	1.07
Dawson Shale	DS	?0.04	0.08	0.22
Pierre Shale (Dakota)	PSD	0.10	0.04	0.04
Pierre Shale (Colorado)	PSC	24.39	0.32	0.30

Table 5.5 Coefficient of Consolidation for Pure Minerals (after Hough, 1957)

Mineral	Liquid Limit	Coefficient of consolidation (m^2/yr)
Kaolinite	45	9.45
Illite	100	3.1×10^{-2}
Montmorillonite	210	9.4×10^{-3}

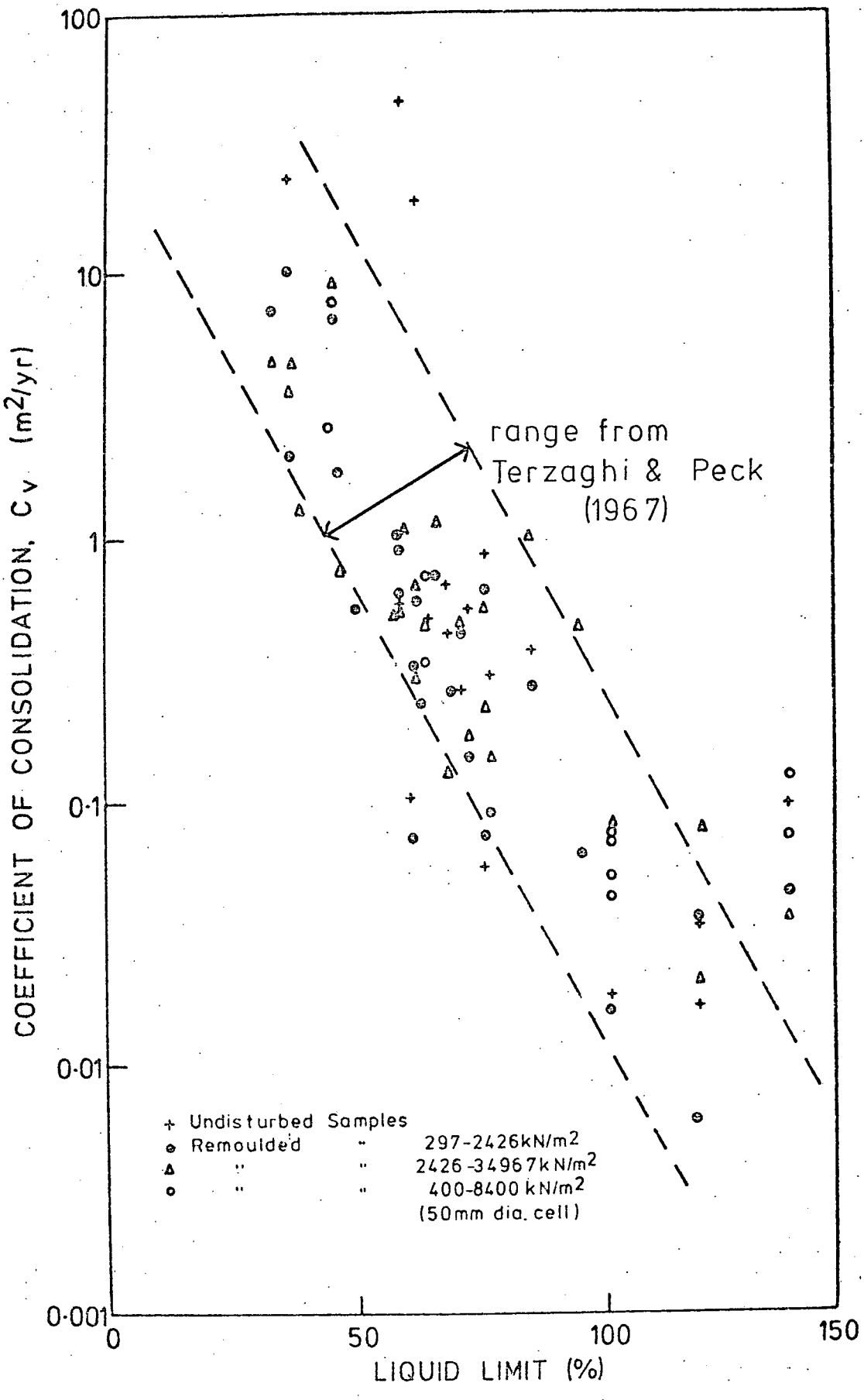

Figure 5.4. Variation of the Coefficient of Consolidation (c_v) with Liquid Limit.

tests conducted on four remoulded specimens in the conventional oedometer between 400 - 8400 kN/m^2 are presented in Table 5.11.

The values obtained for c_v decrease as the liquid limit increases in accordance with the trend observed by Terzaghi and Peck (1967), (see Fig.5.4), and currently range from 47.47m^2/yr at a liquid limit of 36, to 0.01 m^2/yr at a liquid limit of 117. This trend is associated with the reduction in the permeability of highly colloidal clays due to their extremely small particle size. However, there is no significant difference between those values obtained from the tests performed on the undisturbed materials and those from tests performed on both the high and low pressure ranges of the remoulded samples. Values of c_v for pure kaolinite and illite (Hough, 1957; Table 5.5) agree exceedingly well with the range proposed by Terzaghi and Peck (1967), although the values for montmorillonite show that at very high liquid limits the c_v decreases much less rapidly than in the range between 20 - 100 per cent.

Typical variations of c_v with increasing pressure obtained from tests performed on four remoulded clays up to pressure of 8400kN/m^2 (Fig.5.10(b)) indicate that at low pressures the value is dominantly controlled by the liquid limit, but at higher pressures the particle size and mineralogy play an important role (e.g. the c_v for the Fuller's Earth from Bath, (sample FE19), having a liquid limit of 100, falls below that of the Pierre Shale from Dakota, (sample PSD), which has a liquid limit of 136).

5.9.3. Compression Index (C_c)

The compression index, which is a dimensionless quantity, is a measure of the compressibility of the material and is defined

by the equation:-

$$C_c = \frac{e_o - e}{\log_{10}P_o - \log_{10}P} \quad \ldots\ldots\ldots\ldots\ldots\ldots (19)$$

where e_o and P_o are the voids ratio and pressure at the beginning of a pressure increment and e and P are the corresponding values at the end of the loading stage (both defining points on the virgin compression curve).

Average values for the compression index (beyond the preconsolidation load) for the undisturbed material are presented in Table 5.6, column (a) whilst average values for the remoulded samples between pressures of 4675 - 34967 kN/m^2 and 297 - 2426 kN/m^2 are presented in columns (b) and (c) respectively. Average values obtained during the consolidation of remoulded clays to a pressure of 8400 kN/m^2, in the conventional oedometer, are presented in Table 5.11.

Terzaghi and Peck (1948), citing the work of Skempton (1944) - where a strong relationship between C_c and liquid limit was obtained - propose an expression relating these quantities for remoulded clays, i.e.:-

$$C_c = 0.009\ (LL - 10\%) \quad \ldots\ldots\ldots\ldots (20)$$

and for remoulded clays having a medium or low sensitivity they propose the expression:-

$$C_c = 0.007\ (LL - 10\%) \quad \ldots\ldots\ldots\ldots (21)$$

From the present study it can be seen (Fig.5.5) that the results obtained in the low pressure range (297 - 2424 kN/m^2) and those from the tests performed in the conventional oedometer are in agreement with such relationships. However, the results at higher pressures (2426 - 34967 kN/m^2) on remoulded samples and those from beyond the preconsolidation load in the case of undisturbed samples are better expressed by an equation of the form (Fig.5.5)

$$C_c = 0.004\ (LL - 10\%) \quad \ldots\ldots\ldots\ldots (22)$$

Current values of C_c range from 0.1 for silts (LL = 33) to 0.34 - 0.54 for highly colloidal clays (LL = 136), with a value of 0.2 - 0.3 for clays of intermediate liquid limit (i.e. 60 - 75). According to Skempton (1944) the average value for the compression index of natural clays between pressures of 50 - 100 kN/m^2 varies from 0.08 (LL = 24) to 0.91 (LL = 127) and is about 0.35 - 0.45 for clays where the liquid limit is between 60 - 75. Fleming et al (1970) offer several values for the compression index from tests carried out on North American shales (see Fig.5.5). Although these are of the same order as those from the high pressure range, they do not appear to have quite the same consistency with regard to the liquid limit. However, it is not clear if they represent particular load increment values or whether they have been averaged over a certain pressure range.

Typical values of C_c from low pressure tests on illites, collated by Lambe and Whitman (1969) follow the trend, defined by Equation (20), see also Figure 5.5, whilst those for kaolinites, which have low liquid limits, conform equally well to either equations (20) or (21) and are also similar to values currently obtained (e.g. Widdringham roof shale - 53% kaolinite). On the other hand, the values of C_c for montmorillonite (which have extremely high liquid limits) appear to be more in accordance with the equation currently proposed i.e. equation (22). A similar series of results was also found by Olson & Mesri (1970) - see Table 5.8.

When the values obtained for the compression indic es of both the high pressure and low pressure regions of the remoulded curves and those from the undisturbed curves (above the preconsolidation loads) are plotted against the average voids ratio over the corresponding pressure range (Fig.5.6), then all the results define

Table 5.6 Average Compression Index (C_c) Values

	Sample Ref.	Undisturbed Material (a)	Remoulded Materials 4675-34967kN/m² (b)	Remoulded Materials 297-2426kN/m² (c)
British Samples				
London Clay 14m	LC14	0.281	0.334	0.675
London Clay 37m	LC37	0.216	0.260	0.500
Gault Clay	GC	0.322	0.322	0.512
Fuller's Earth (Redhill)	FE23	0.547	0.568	0.847
Weald Clay	WC	0.116	0.162	0.161
Kimmeridge Clay	KC	0.210	0.277	0.454
Oxford Clay 10m	OC10	0.338	0.288	0.475
Oxford Clay 44m	OC44	0.289	0.273	0.451
Fuller's Earth (Bath)	FE19	0.322	0.449	0.830
Lias Clay 10m	L10	0.208	0.320	0.593
Lias Clay 36m	L36	0.245	0.311	0.433
Keuper Marl	KM	-	0.210	0.211
Swallow Wood roof	SWR	-	0.292	0.433
Flockton Thin roof	FTR	-	0.289	0.356
Flockton Thin seat	FTS	-	0.266	0.451
Widdringham roof	WR	-	0.218	0.257
North American Samples				
Yazoo Clay	YC	0.536	0.431	1.050
Kincaid Shale 6m	K6	0.258	0.246	0.606
Kincaid Shale 8m	K8	0.266	0.222	0.420
Nacimiento Shale	N1	?0.067	0.250	0.318
Nacimiento Shale	N2	?0.060	0.223	0.328
Nacimiento Shale	N3	?0.158	0.365	0.674
Fox Hills Shale	FOX	0.374	0.373	0.427
Dawson Shale	DS	?0.176	0.267	0.595
Pierre Shale (Dakota)	PSD	0.344	0.441	1.054
Pierre Shale (Colorado)	PSC	0.077	0.238	0.422

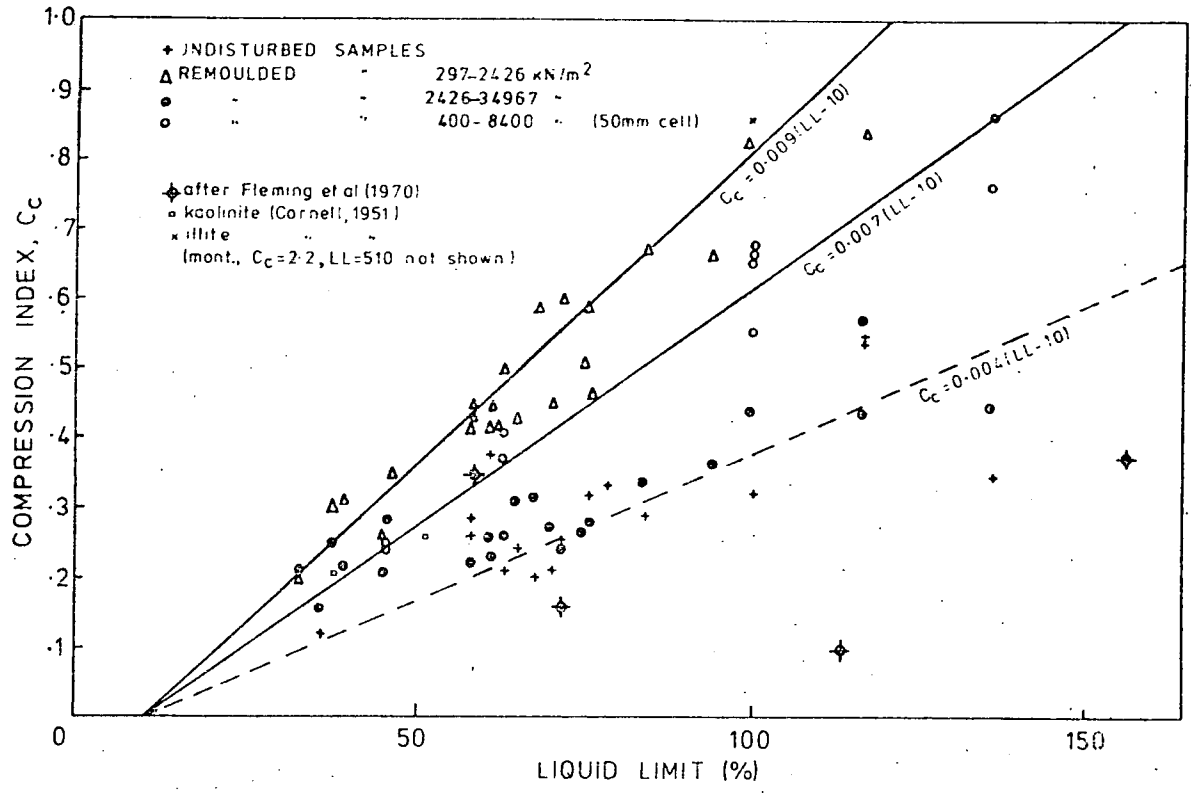

Figure 5.5. Variation of Compression Index with Liquid Limit.

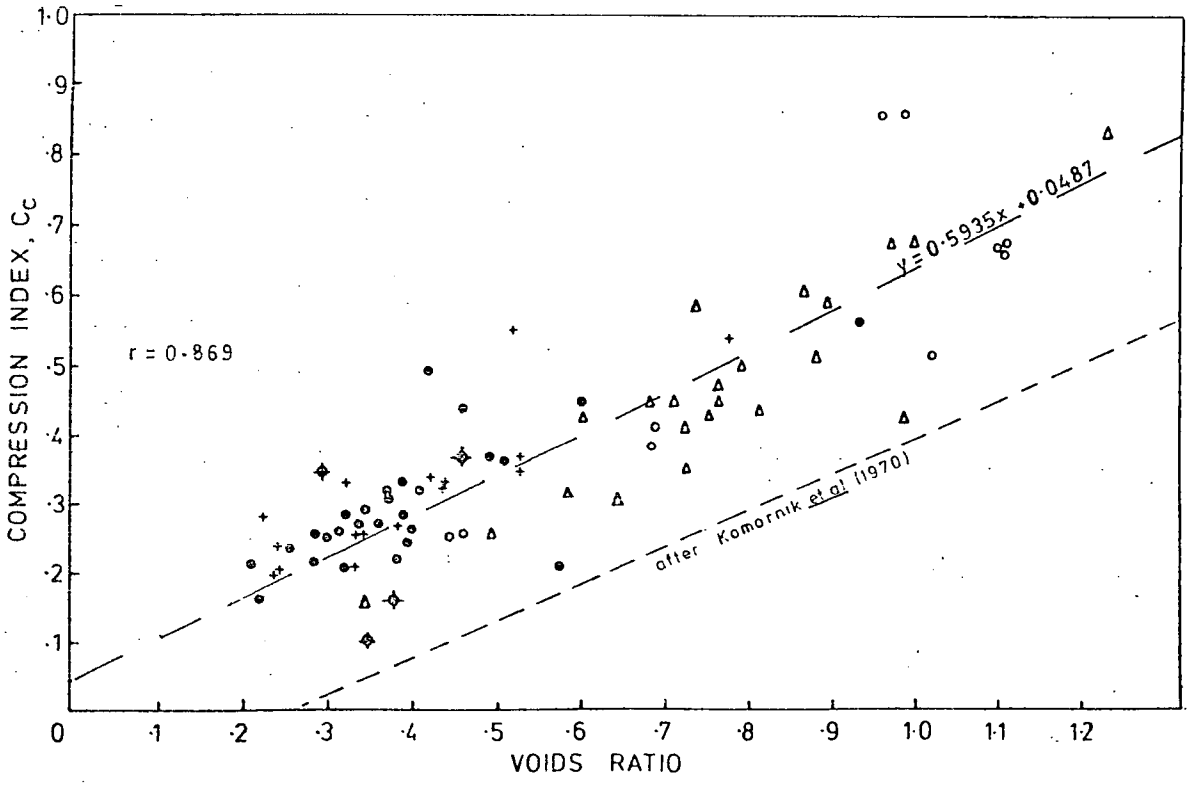

Figure 5.6. Variation of Compression Index with Average Voids Ratio.

one trend, similar to, but above that of Komornik et al (1970). This relationship is ultimately governed by the mineralogy, and at any given pressure the presence of a large expandable mineral content will exert a strong physico-chemical effect thus increasing the voids ratios, and as a consequence those clays are more compressible (Chilingar and Knight, 1960). Alternatively within certain limits, as the pressure is increased, the voids space and C_c will be reduced in accordance with Figure 5.6.

The coincidence of the compression index for the undisturbed and remoulded materials (Figs.5.5 and 5.6) indicates that at high pressure the history of the shale does not influence the results provided that the values are beyond the preconsolidation load.

Tests conducted on four remoulded materials to a pressure of 8400kN/m^2 (Fig.5.10c) indicate that the compression index becomes less sensitive to applied pressure as the liquid limit decreases.

5.9.4. Swell Index (C_s)

The swelling characteristics of the materials have been studied by reference to the Swell Index (C_s) i.e.

$$C_s = \frac{e_o - e}{\log_{10}P_o - \log_{10}P} \quad \ldots\ldots\ldots\ldots\ldots (23)$$

where e and P are the voids ratio and pressure before a load increment is removed and e_o and P_o are the corresponding values at the end of the unloading stage.

Average swell index values obtained from tests performed on undisturbed material are presented in Table 5.7, column (a), whilst average value for the final and intermediate rebound stages (see Fig.2.7) obtained from tests performed on remoulded material are

presented in columns (b) and (c) respectively. Average rebound values obtained for tests conducted on four remoulded specimens in a conventional oedometer are given in Table 5.11.

By considering the same pressure range, it has been found that the swell index value of undisturbed material is often lower than that found in the remoulded counterpart (Table 5.7, column (d)). This phenomenon is attributed to the effect of diagenetic bonding and is discussed in this context in Section 5.10. However, when the swell index values for both of these conditions are plotted against the liquid limit of the material (Fig.5.7), exceedingly good agreement is obtained with the results of Lambe and Whitman (1969).

The results from the present materials, which are all multi-component systems (Table 3.2), appear to be lower than those of pure clays (Table 5.8), as obtained by Olson and Mesri (1970) when these were remoulded and consolidated to a pressure of 3026 kN/m^2 (64000psf). Nevertheless, for remoulded shales (free from diagenetic bonding), when the mineralogy is considered, the same general trend is observed (Fig.5.7) whereby the swell index increases from clays where quartz (Weald Clay) and kaolinite (Widdringham roof) are dominant to clays where montmorillonite is dominant (e.g. Fuller's Earths and Pierre Shale (Dakota). This variation is also shown clearly in Figure 5.10d where the low pressure tests on four remoulded shales are considered. There is, moreover, a general increase in the swell index from the intermediate to the final unloading stage (which may result from tighter packing affecting the swelling characteristics).

Table 5.7 Average Swell Index (C_s) Values

	Sample Ref.	Undisturbed Material (a)	Remoulded Material: Final Unloading (b)	Remoulded Material: Intermediate Unloading (c)	(b)-(a) (d)
British Materials					
London Clay 14m	LC14	0.107	0.108	0.097	0.001
London Clay 37m	LC37	0.077	0.094	0.070	0.017 *
Gault Clay	GC	0.095	0.077	0.068	(0.018)
Fuller's Earth (Redhill)	FE23	0.184	0.178	0.094	(0.006)
Weald Clay	WC	0.024	0.025	0.019	0.001
Kimmeridge Clay	KC	0.086	0.095	0.078	0.009
Oxford Clay 10m	OC10	0.098	0.068	0.070	(0.030)
Oxford Clay 44m	OC44	0.071	0.099	0.074	0.028 *
Fuller's Earth (Bath)	FE19	0.123	0.199	0.140	0.076 *
Lias Clay 10m	L10	0.083	0.064	0.054	(0.019)
Lias Clay 36m	L36	0.080	0.110	0.086	0.030 *
Keuper Marl	KM	-	0.026	0.013	-
Swallow Wood roof	SWR	-	0.012	0.080	-
Flockton Thin roof	FTR	0.013	0.070	0.047	0.057 *
Flockton Thin seat	FTS	0.027	0.087	0.069	0.060 *
Widdringham roof	WR	0.016	0.048	0.036	0.032 *
North American Materials					
Yazoo Clay	YC	0.218	0.172	0.156	(0.046)
Kincaid Shale 6m	K6	0.089	0.067	0.032	(0.022)
Kincaid Shale 8m	K8	0.046	0.046	0.010	(0.000)
Nacimiento Shale	N1	0.027	0.051	0.033	0.024 *
Nacimiento Shale	N2	0.023	0.046	0.023	0.023 *
Nacimiento Shale	N3	0.064	0.109	0.063	0.045 *
Fox Hills Shale	FOX	0.117	0.096	0.067	(0.021)
Dawson Shale	DS	0.064	0.085	0.065	0.021 *
Pierre Shale (Dakota)	PSD	0.116	0.179	0.177	0.063 *
Pierre Shale (Colorado)	PSC	0.026	0.068	0.042	0.042 *
Oxford Clay 44m ($6245 kN/m^2$)	OC44	0.044			

(Bracketed figures in column (d) indicate that the remoulded swell index is greater than that for the undisturbed sample).

Table 5.8 Swell and Compression Indices for Pure Clays *

	C_s	C_c 1000 - 10000psf	C_c 10000 - 64000psf
Kaolinite			
Water, Ca 1N	0.07	0.3	0.2
Water, Ca $1*10^{-4}$N	0.07	0.3	0.2
Water, Na 1N	0.08	0.25	0.25
Water, Na $1*10^{-4}$N	0.08	0.25	0.25
Illite			
Water, Ca 1N	0.28	1.0	0.375 - 0.5
Water, Ca $1*10^{-3}$N	0.31		
Water, Na 1N	0.37	1.6	0.5
Water Na $1*10^{-3}$N	0.65		
Smectite			
Water, Ca 1N	0.26	1.4 - 1.5	0.675
Water, Ca $1*10^{-3}$N	0.34		
Water, Na $1*10^{-1}$N	1.53	7.0	1.875
Water, Na $5*10^{-4}$N	3.60	13.0	3.125
Sand	0.01 - 0.03		

* After Olson and Mesri (1970)

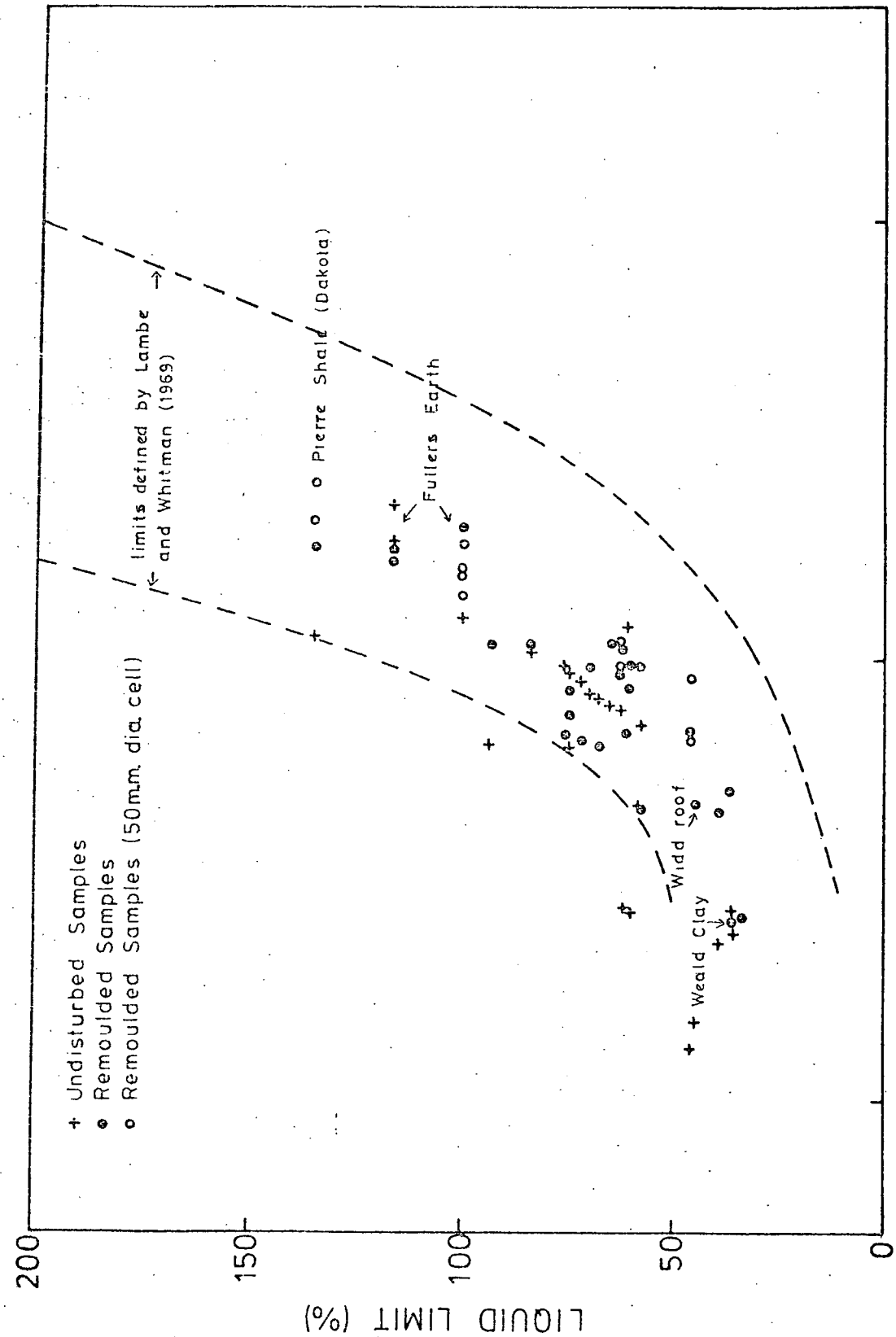

Figure 5.7. Variation of Swell Index with Liquid Limit.

5.9.5 Permeability (k)

Permeability is a measure of the flow of liquid through a medium (which in this case consists of granular and plate-like minerals) and is governed by the particle size, voids ratio , fabric, composition and degree of saturation.

When dealing with one-dimensional consolidation tests, permeability is commonly calculated from the following relationship:

$$k = c_v \times m_v \times x_w \quad \ldots\ldots\ldots\ldots\ldots\ldots \quad (24)$$

where x_w is the unit weight of water.

Average values for the permeability of the undisturbed material beyond the preconsolidation load are presented in Table 5.9, column (a), whilst average values for the remoulded samples, between pressures of 4675 - 34967 kN/m^2 and 297 - 2426 kN/m^2 are presented in columns (b) and (c) respectively. Average values for the four remoulded clays consolidated in the larger oedometer between pressures of 400 - 8400 kN/m^2 are presented in Table 5.11.

The permeability as with the compression index, is dependent on the voids ratio (Fig.5.8) but is independent of the consolidation and induration state of the shale. (This is evidenced by the coincidence of the values from the high pressure range of the remoulded samples with those of the undisturbed shales).

Typical permeability - voids ratio relationships have also been presented in Figure 5.8 for pure minerals in calcium electrolyte (Olson and Mesri, 1971), various pure kaolinites* (Warner, 1964; Olsen, 1966); pure illites* (Warner, 1964), the Wyoming bentonite* (Warner, 1964), the Pierre Shale* (Kemper, 1961) and a typical sandy clay (Lambe and Whitman, 1969).

* As cited in Rieke and Chilingarian (1974).

Table 5.9 Average Permeability (k) Values ($m/s*10^{-10}$)

	Sample Ref.	Undisturbed Samples	Remoulded Samples 4675-34967kN/m^2	Remoulded Samples 297-2426kN/m^2
		(a)	(b)	(c)
British Materials				
London Clay 14m	LC14	0.0081	0.0069	0.1091
London Clay 37m	LC37	0.0038	0.0093	0.5224
Gault Clay	GC	0.0224	0.0268	0.3647
Fuller's Earth (Redhill)	FE23	0.0004	0.0002	0.3742
Weald Clay	WC	0.1623	0.2283	0.6907
Kimmeridge Clay	KC	0.0022	0.0166	0.3555
Oxford Clay 10m	OC10	0.0095	0.0032	0.0544
Oxford Clay 44m	OC44	0.0053	0.0382	0.5008
Fuller's Earth (Bath)	FE19	0.0002	0.0007	0.1362
Lias Clay 10m	L10	0.0036	0.0104	0.0810
Lias Clay 36m	L36	0.0068	0.0376	0.6565
Keuper Marl	KM	-	0.1969	0.9401
Swallow Wood roof	SWR	-	0.0364	0.2559
Flockton Thin roof	FTR	-	0.0627	0.3502
Flockton Thin seat	FTS	-	0.0229	0.3153
Widdringham roof	WR	-	0.2621	4.8910
North American Materials				
Yazoo Clay	YC	0.0025	0.0019	0.1297
Kincaid Shale 6m	K6	0.0079	0.0048	0.2431
Kincaid Shale 8m	K8	0.6896	0.0194	0.4829
Nacimiento Shale	N1	?0.0272	0.0998	2.0491
Nacimiento Shale	N2	?0.0853	0.0200	Q.6953
Nacimiento Shale	N3	?0.0002	0.0063	0.4723
Fox Hills Shale	FOX	0.0024	0.0108	0.6739
Dawson Shale	DS	?0.0002	0.0034	0.2634
Pierre Shale (Dakota)	PSD	0.0016	0.0024	0.0562
Pierre Shale (Colorado)	PSC	0.1141	0.0117	0.2016

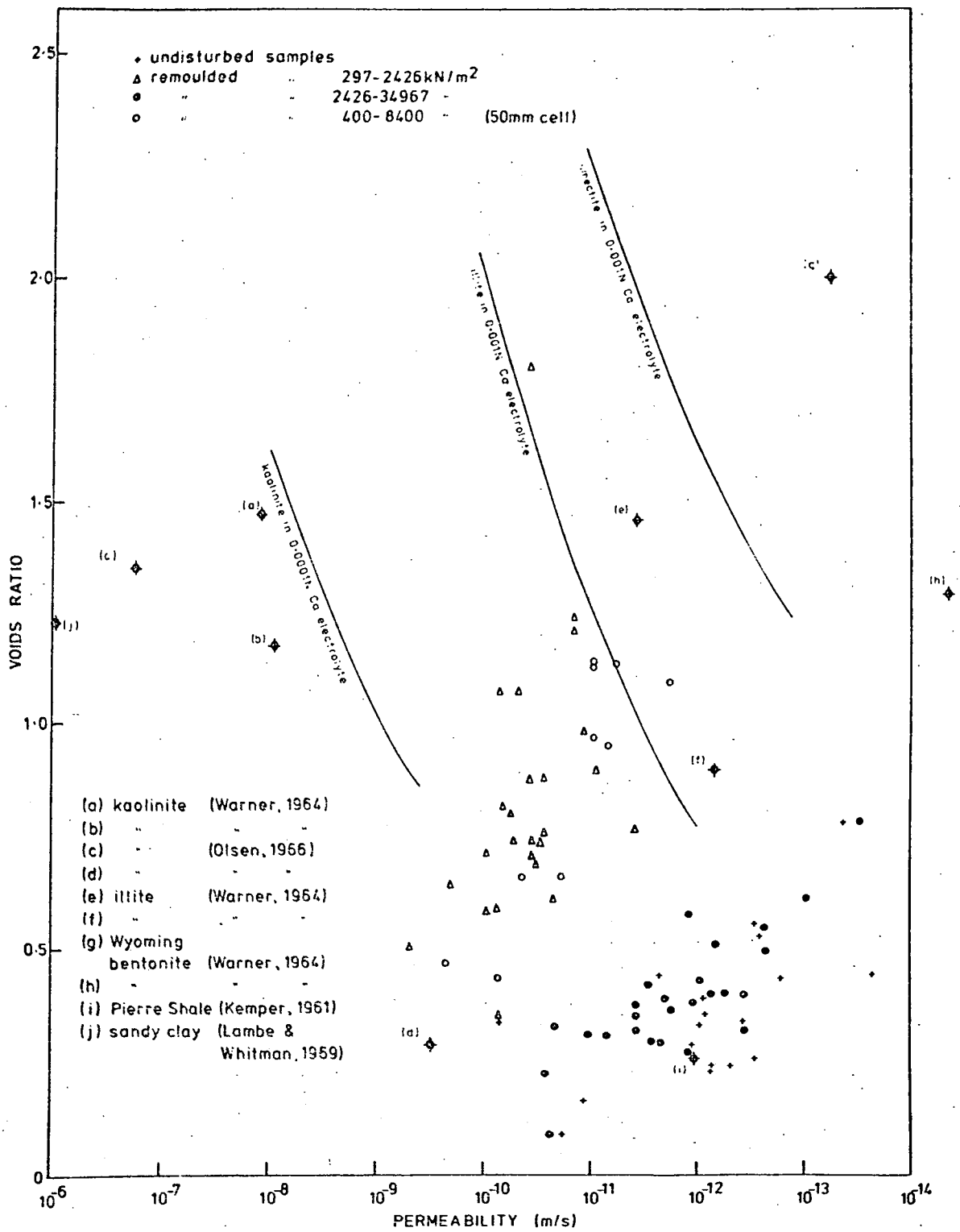

Figure 5.8. Variation of Permeability with Voids Ratio.

The variation of permeability with voids ratio for four remoulded clays is displayed in Figures 5.10e, where a regular decrease with decreasing voids ratio is noticed (although an irregular reponse is sometimes noticed (Waidelich, 1958)). The relative positions of the curves appear to be controlled by the mineralogical composition and the writer considers that the explanation given by Olson and Mesri (1971) adequately explains this behaviour. These authors conclude that the reduction of permeability from kaolinite to illite to smectite at constant voids ratio is largely the result of size reduction of the individual flow channels, causing an increase in tortuosity of the flow paths, coupled with the relative effects of dispersion and flocculation caused by physico-chemical variables associated with the double layer.

5.9.6. Coefficient of Volume Compressibility (m_v)

The coefficient of volume compressibility (m_v) represents the compression of a soil per unit of original thickness due to unit increase in pressure, i.e.:-

$$m_v = \frac{\Delta e}{(1+e)\,\Delta p} \quad \ldots\ldots\ldots\ldots\ldots\ldots\ldots\ldots \quad (25)$$

where Δe and Δp are changes in voids ratio and applied pressure and e is voids ratio before the pressure is applied. The value of m_v has the dimensions $L^2\,M^{-1}$ (i.e. m^2/MN).

Average values for m_v (beyond the preconsolidation load) for the undisturbed materials are presented in Table 5.10, column (a) whilst average values for remoulded samples between pressures of 4675 - 34967kN/m^2 and 297 - 2426kN/m^2 are presented in columns (b) and (c) respectively. Average values obtained during the

Table 5.10 Average Coefficient of Volume Compressibility (m_v) Values (m^2/MN)

	Sample Ref.	Undisturbed Samples	Remoulded Samples 297-2426kN/m^2	Remoulded Samples 4675-34967kN/m^2
British Material				
London Clay 14m	LC14	0.009	0.415	0.013
London Clay 37m	LC37	0.003	0.282	0.011
Gault Clay	GC	0.007	0.258	0.012
Fuller's Earth (Redhill)	FE23	0.007	0.245	0.016
Weald Clay	WC	0.002	0.117	0.007
Kimmeridge Clay	KC	0.002	0.246	0.011
Oxford Clay 10m	OC10	0.005	0.124	0.011
Oxford Clay 44m	OC44	0.003	0.276	0.011
Fuller's Earth (Bath)	FE19	0.005	0.363	0.015
Lias Clay 10m	L10	0.002	0.280	0.013
Lias Clay 36m	L36	0.003	0.212	0.012
Keuper Marl	KM	-	0.126	0.008
Swallow Wood roof	SWR	-	0.228	0.012
Flockton Thin roof	FTR	-	0.189	0.012
Flockton Thin seat	FTS	-	0.246	0.012
Widdringham roof	WR	-	0.159	0.010
North American Materials				
Yazoo Clay	YC	0.020	0.435	0.016
Kincaid Shale 6m	K6	0.004	0.443	0.010
Kincaid Shale 8m	K8	0.004	0.383	0.009
Nacimiento Shale	N1	0.001	0.172	0.011
Nacimiento Shale	N2	0.001	0.200	0.010
Nacimiento Shale	N3	0.002	0.306	0.014
Fox Hills Shale	FOX	0.007	0.186	0.013
Dawson Shale	DS	0.003	0.326	0.014
Pierre Shale (Dakota)	PSD	0.005	0.534	0.017
Pierre Shale (Colorado)	PSC	0.002	0.258	0.010

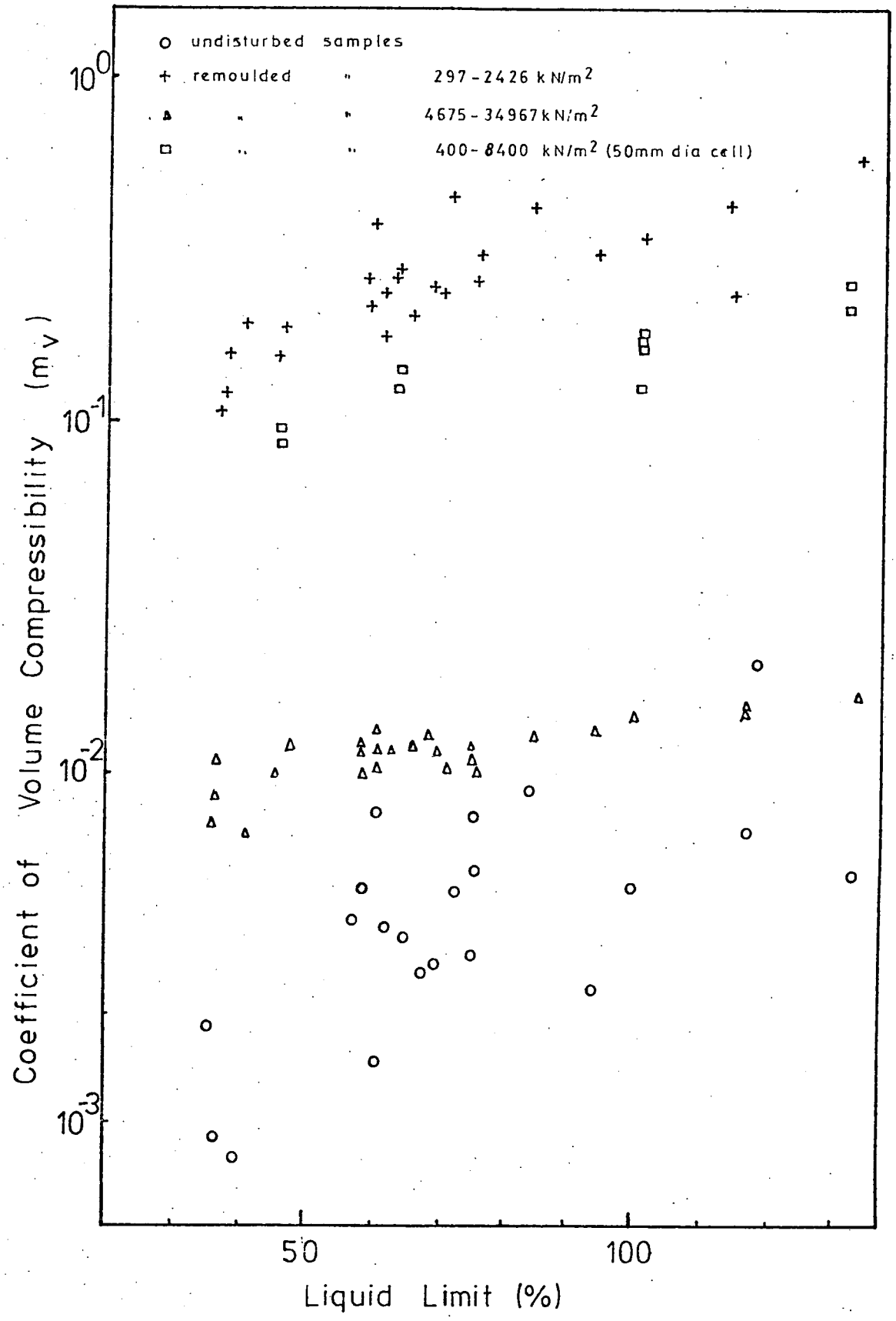

Figure 5.9. Variation of Coefficient of Volume Compressibility (m_v) with Liquid Limit.

Table 5.11 Consolidation Parameters from Low Pressure Tests (400 - 8400kN/m²)

		c_v (m^2/y)	C_c	C_s	k ($m/s * 10^{-10}$)	m_v (m^2/MN)
Pierre Shale (Dakota)	L.L.	0.07	0.859	0.252	0.0626	0.249
	0.50L.I.	0.13	0.757	0.209	0.0929	0.212
Fuller's Earth (Bath)	L.L.	0.07	0.664	0.187	0.0757	0.183
	0.75L.I.	0.07	0.647	0.161	0.0939	0.170
	0.50L.I.	0.05	0.650	0.158	0.0493	0.173
	0.25L.I.	0.04	0.509	0.140	0.0229	0.124
London Clay 37m	L.L.	0.72	0.410	0.107	0.4189	0.139
	0.50L.I.	0.35	0.374	0.096	0.1694	0.128
Widdringham roof	L.L.	8.12	0.253	0.068	2.1502	0.095
	0.50L.I.	2.56	0.268	0.093	0.7318	0.099

Figure 5.10. Variation of Consolidation Parameters with Applied Pressure.

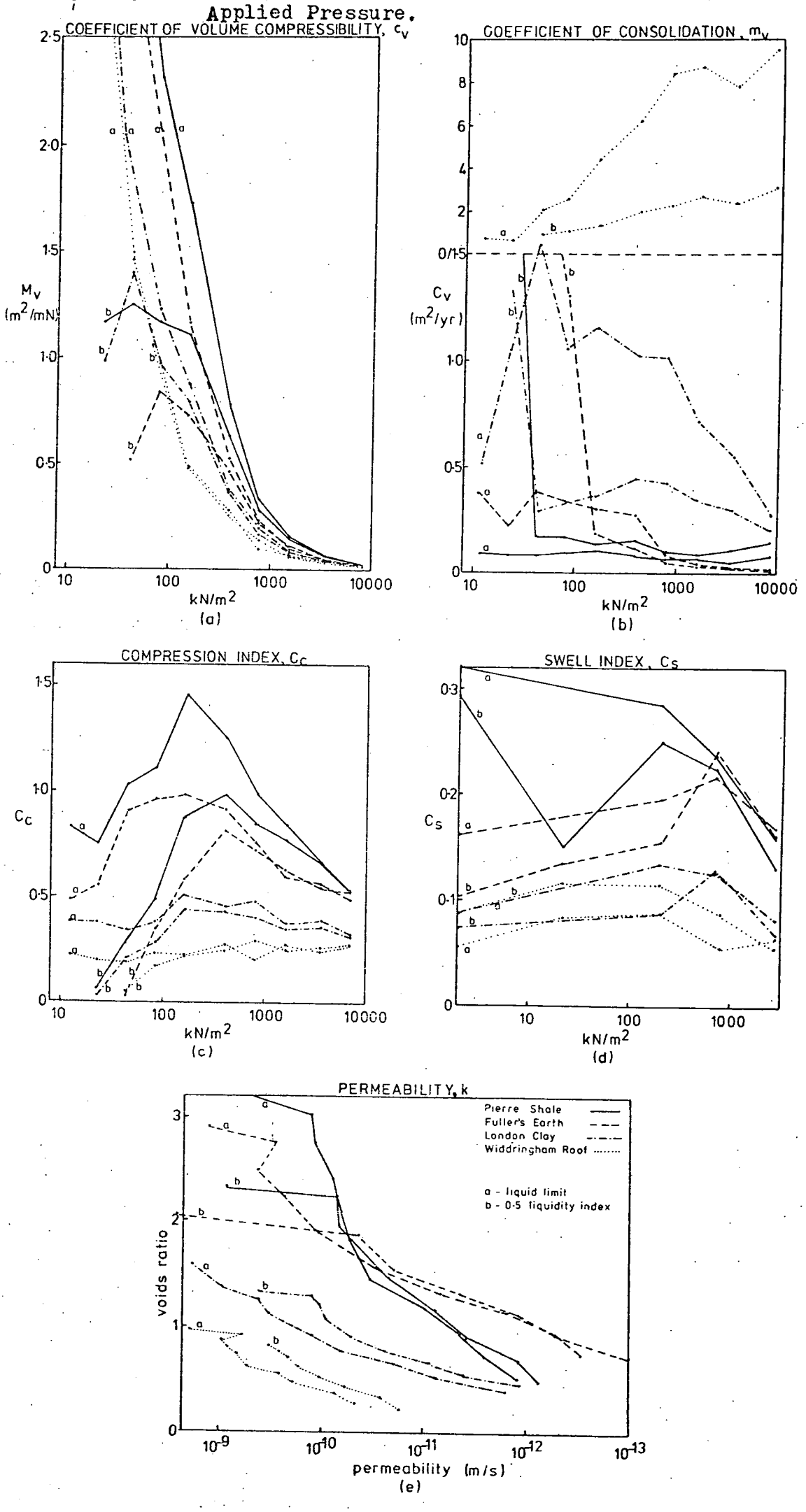

consolidation of remoulded clays in a conventional oedometer are presented in Table 5.11.

Volume compressibility decreases with increasing pressure in a manner illustrated in Figure 5.10a, whereby at any given pressure larger values are encountered in clays with higher liquid limits (also see Figure 5.9). The lower values of m_v encountered for the undisturbed materials (Fig.5.9) result because in many cases higher pressure ranges are required to consolidate the specimen beyond the preconsolidation load. The effect is further emphasised by the log-normal fit.

5.9.7 Swell Pressure

Swell pressure is the pressure required to prevent a clay from swelling in a given direction when it is allowed to saturate freely in a confined space. Yong et al (1963) suggest that a special measuring device is required to make accurate determinations because normal oedometers allow too much volume expansion. Nevertheless in the present study two sets of measurements (Appendix A.3.32) have been made using an oedometer, and the results of these are presented in Table 5.12.

A relationship between swell pressure and present depth of burial has been observed by Fleming et al (1970) and Figure 5.11 (based on independent measurement) shows that all of the British materials of Lias age and younger, and seven of the ten North American materials follow this trend. The British Carboniferous materials have much lower swell pressures than would be predicted from their present depths of burial using the aforementioned observation, (Fig.5.11). However, this probably reflects their indurated nature acting to reduce their swelling potential, as proposed by Yong and Warkentin, (1975). On the other hand, the Nacimiento Shales N1 and N2 and

Table 5.12 Swell Pressure of Samples Tested

	Per Independent Test (kN/m^2)	Per High Pressure Consolidation Tests (kN/m^2)
British Materials		
London Clay 14m	362.86	130.63
London Clay 37m	220.66	254.98
Gault Clay	288.33	166.72
Fuller's Earth (Redhill)	34.32	69.63
Weald Clay	289.31	148.09
Kimmeridge Clay	98.07	118.66
Oxford Clay 10m	118.66	117.68
Oxford Clay 44m	424.64	203.59
Fuller's Earth (Bath)	176.53	185.35
Lias Clay 10m	186.33	167.21
Lias Clay 36m	741.41	332.46
Swallow Wood roof	481.52	-
Flockton Thin roof	468.77	567.83
Flockton Thin seatearth	118.66	94.15
Widdrington roof	594.30	57.67
North American Materials		
Yazoo Clay	84.93	85.91
Kincaid 6m	117.68	131.41
Kincaid 8m	9.81	51.98
Nacimiento Shale	1422.01	398.48
Nacimiento Shale	1075.44	983.64
Nacimiento Shale	-	677.66
Fox Hills Shale	672.76	641.38
Dawson Shale	1188.61	623.14
Pierre Shale (Dakota)	211.83	127.69
Pierre Shale (Colorado)	188.29	72.96

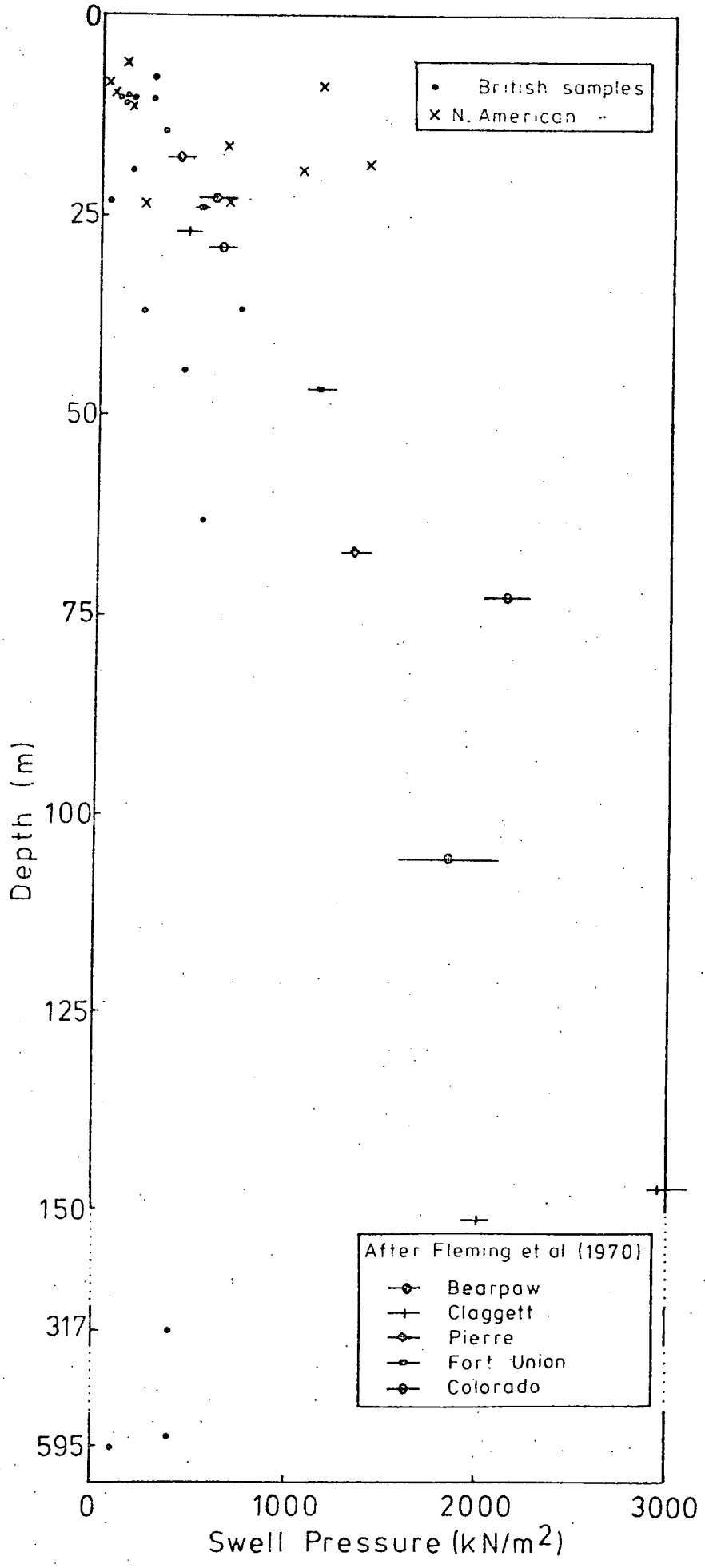

Figure 5.11. Relationship Between Swell Pressure and Depth of Burial.

the Dawson Shale have larger swell pressures than would normally be predicted from their current depths of burial. The writer is unsure why this should be but suggests that it could result from the random, flocculated nature of their clay particles (Table (4.5), endowing the material with a greater swelling potential.

In addition to depth dependence, Fleming et al (1970) suggest that a reduction of excess swell pressure at shallow depth might reflect the greater availability of water nearer the surface, so that materials tend to equilibrium under a different moisture environment. They further notice that the swell pressure of material from similar depths tends to be up to 30 per cent higher for those with the higher liquid limit, a fact that is not evident in the present study.

Ward et al (1959) found that the swell pressure of the London Clay measured parallel to the bedding was less than that measured normal to it. Fleming et al (1970) also notice this effect and cite ratios of 0.26 - 1.00 depending upon the material. This effect has, however, not been investigated in the current work.

5.10 An Investigation into the Presence of Diagenetic Bonding

In the present study an attempt has been made to identify the presence of diagenetic bonding by the use of the swelling characteristics obtained from the rebound curves. This method, unfortunately does not give any indication of the type of bonds present, although this matter is discussed further in Chapter 7 when slaking characteristics are considered. However, the relative roles of mineralogical composition and depth of burial are discussed, and in addition evidence is offered to substantiate Bjerrum's hypothesis regarding the destruction of bonds (Chapter 1.5.6).

For the purposes of the present exercise it has been assumed that when the undisturbed samples are consolidated, any diagenetic bonds present will be destroyed in proportion to their strength and the applied pressure, i.e. at the maximum pressure used (35000kN/m^2) weak bonds being almost completely destroyed and strong bonds retaining a proportion of their strength. This effect may, however, be somewhat affected by the variation in the relationships between the maximum consolidation pressure and the preconsolidation loads (which range from 1900 - 40000kN/m^2). Nevertheless, broad trends do emerge when the swell indices obtained from equivalent tests on undisturbed and remoulded material (in which all the bonding has been destroyed) are compared (see Table 5.7).

The statement regarding the progressive decrease of bond strength with applied pressure is supported by reference to one additional consolidation test performed on the unweathered Oxford Clay (sample 0C44) which has a preconsolidation load of 11000 - 14000kN/m^2. The swelling index of 0.071, obtained when the material was consolidated to a pressure of 35000kN/m^2 is seen to be significantly higher than that obtained when the material was consolidated to a pressure of 6245kN/m^2 (i.e. 0.044). This indicates that a larger proportion of the bonding had been destroyed during the test to the higher pressure. When the remoulded material was consolidated to a pressure of 35000kN/m^2, a swell index of 0.099 resulted. This value probably approaches the maximum value obtainable, since in this condition the material does not contain any original bonds.

Thirteen samples tested (marked by an asterisk in Table 5.7), all of which are very stiff and from below the depth of weathering, (using Bjerrum's 1967a depth spectrum), show a substantial increase in their

swell index value (ranging from 0.017 - 0.076) when their remoulded condition is considered. This implies that there is some sort of strong bonding present in the natural material. There does not however, appear to be any rigid trend relating the maximum depth of burial to the swell index because the mineralogical composition appears to play an important role. Nevertheless a crude trend can be depicted in the British materials (Fig.5.12) where illite and kaolinite form the major constituents. This ranges from the London Clay, sample L37, (maximum depth 450m) showing an increase in the swell index of 0.017, to the Oxford and Lias Clays, samples OC44 and L36 respectively (maximum depths 900 - 1050m), which show increases in their swell indices of 0.028 - 0.030, to the Carboniferous shales (maximum depth 3800m), which show increases in their swell indices of 0.032 - 0.060.

With regard to mineralogical composition, particularly large increases in swell index, equivalent to, and often greater than those observed in the Carboniferous shales, are noticed in certain younger fine-grained sediments where smectite is present in substantial quantities (see Fig.5.12) i.e. Fuller's Earth from Bath (sample FE19) - 0.076, Pierre Shale from Dakota (sample PSD) - 0.063, Nacimiento Shale No. 3 - 0.045, and the Pierre Shale from Colorado (sample PSC) - 0.042. The presence of granular material such as quartz and feldspar may also have a decisive effect by suppressing any bonds which may develop between clay minerals. The Nacimiento Shales Nos.1 and 2, which are unweathered and from the same horizons as the Nacimiento Shale No.3 (i.e. having a maximum depth of burial of 1500 - 1800m) contain moderate amounts of smectite and yet the presence of these minerals appears to have caused a lower bond strength (represented by an increase in the swell index of 0.025) to develop. This value is of the same

order as those of the Oxford and Lias Clays which have only been buried to between 900 - 1050m. The Dawson Shale, containing 49 per cent smectite, also shows a smaller increase of the swell index than would be expected. This again must be attributed to the granular content present (Fig.5.12).

Five samples tested, i.e. London Clay 14m (sample LC14), Kimmeridge Clay, Kincaid Shale 8m (sample K8), Weald Clay and Fuller's Earth from Redhill (sample FE23) have a swell index for the remoulded material which is almost coincident with that encountered for the material in the undisturbed condition. This implies that any bonds which may once have been present, have now been destroyed. All of these materials, with the exception of the Fuller's Earth (Redhill), are from within the zone of weathering according to Bjerrum (1967a), i.e. within 17 metres of the surface; consequently no diagenetic bonding would have been expected. The Fuller's Earth, however, is from 23m depth but as this specimen was sampled from a vertical section of a quarry, it is possible that stress release in the horizontal direction has lead to the destruction of any bonds that were originally present.

The remaining six specimens have a swell index value for the remoulded material which is significantly lower than that for the undisturbed material. Again, all but one of these (i.e. the Fox Hills Shale) are from within Bjerrum's zone of weathering. However, because the virgin compression curve of the undisturbed material in all cases is parallel to the curve obtained when the material is consolidated in the remoulded condition, it can only be assumed that some sort of metastable condition exists in the former and that a fundamental rearrangement of the constituents has occurred upon remoulding, leading to a reduction of the swelling properties. This is particularly noticeable in the Oxford Clay, where both the weathered

Figure 5.12. Relationship Between Diagenetic Bonding and Depth of Burial.

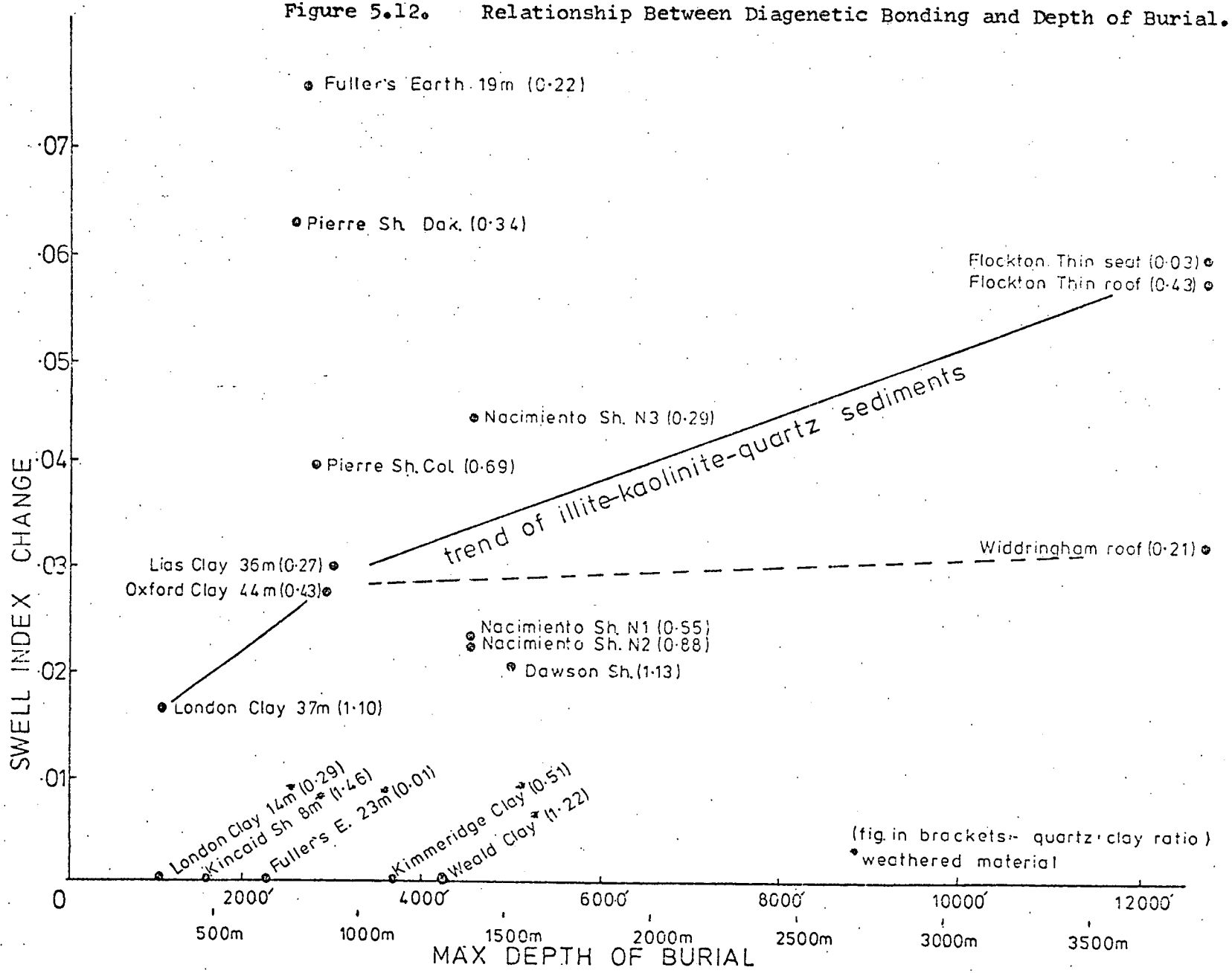

and unweathered materials have approximately the same mineralogical composition (Table 3.2). The former material which shows some signs of ice disturbance (Chapter 2) has significantly larger initial and final voids ratios than the latter, but upon remoulding, however, the final stress relieved voids ratio becomes similar to that of the unweathered sample. With regard to the Fox Hills Shale, which is apparently unweathered, the large amounts of visible organic matter (Chapter 2) could have a marked effect on the consolidation properties of the shale, (see Skempton,1970) especially as its size and distribution is radically altered upon remoulding. Nevertheless, the rebound behaviour of these six materials is consistent with their containing no significant degree of diagenetic bonding.

5.11 Strain Energy and Stress-Strain Relationships

The stress-strain relationships of a sediment during a consolidation cycle are principally dependent upon the initial condition of the materials (i.e. whether it is normally - or overconsolidated) and also upon the composition, which in turn imparts the physical attributes to the material. Consequently, the strain energy involved will be dependent on these factors. Therefore by performing a series of tests which investigates each of these factors separately, it is possible to consider their relative effects and contributions to the sediment.

Remoulded or normally-consolidated sediments have stress-strain relationships which take the form of that shown in Figure 5.13 (a), for which the strain energy, measured in mkN/m^3 (see Brooker, 1967), involved during the consolidation cycle can be divided into three categories:-

(i) The 'total strain energy' absorbed during the compression stage, represented by the area OAC.

(ii) The 'recoverable strain energy' represented by the area ABC which is attributed to elastic rebound (Morely, 1940), physico-chemical effects (Bolt, 1956) and capillarity (Terzaghi and Peck, 1948).

(iii) The 'non-recoverable strain energy' represented by area OAB which is attributed to sliding and reorientation effects and the crushing of the point contacts (or actual grains at high pressures). This area may be compared to the hysteresis loop obtained during the stress-strain cycle of a crystalline solid (Morely,1940), although in this case the energy is expended as heat within the material.

The interpretation of the stress-strain relationships presented by Brooker (1967) - see Chapter 1, is somewhat different from those currently employed, although in the light of conventional strain energy concepts (for example Morely, 1940), the writer considers that Brooker has misinterpreted the hysteresis loop of the stress-strain cycle. It is concluded that the area between the curves (Fig.5.13a) is wholly represented by the work dissipated during the consolidation cycle, as previously mentioned.

If the stress is reduced to zero at some point during the loading stage (i.e. D-E, Fig.5.13b), the non-recoverable strain energy is represented by the area ODE, and the residual strain is OE. However, when the stress is reapplied to the previous maximum pressure (point D) the resulting stress-strain curve is E-G, the strain at point G being slightly greater than that at point D, primarily because of a more effective state of packing. The hysteresis loop in this particular case is represented by a much smaller area (DEG). If several cycles of

Figure 5.13. Stress-Strain Relationships for One-Dimensional Consolidation.

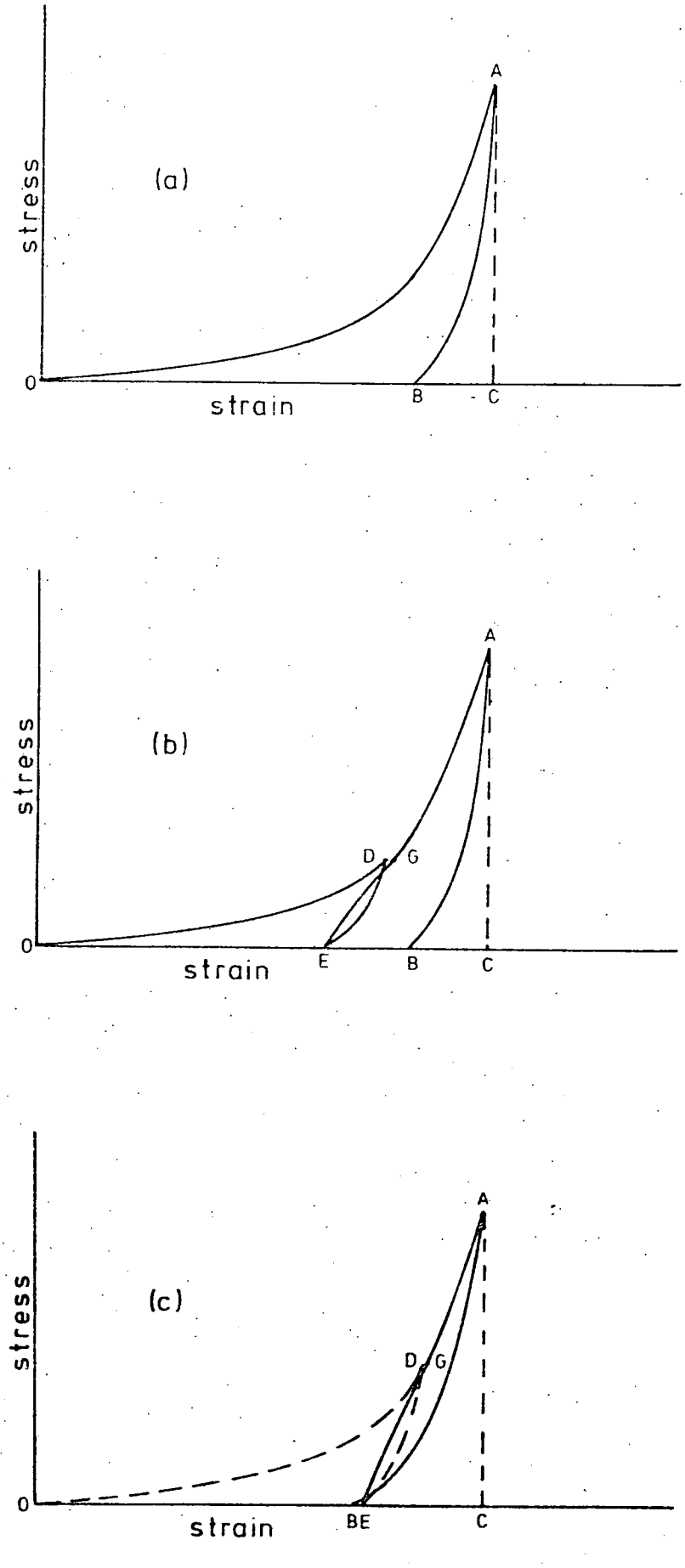

loading and unloading between a pressure equivalent to that at point G and zero are performed, then during the first few cycles (e.g. 10 - 50 for sand), small permanent increases in the strain will result. On subsequent cycles, a stable hysteresis loop will result involving little or no additional strain for each cycle (Lambe and Whitman, 1969). At this stage the particles have reached their most effective state of packing, where only a small amount of energy is absorbed during each cycle. Upon increasing the load to point A, the stress-strain curve will be essentially the same as if no unloading had taken place. However, upon unloading from point A, the stress-strain curve will follow the path AB to point B. Consequently the residual strain will increase from OE to OB, and the total hysteresis loop will increase to area OAB. The stress-strain cycle EAB (Fig5.13b) is equivalent to the consolidation cycle of a laboratory prepared overconsolidated shale with a preconsolidation load equal to G. However, as can be seen from the tests currently conducted, a naturally overconsolidated material usually rebounds to its original thickness or even swells beyond this point when the stress is removed (e.g. see Fig.5.13(c)). This is presumably because these materials have only been subjected to secondary compression and have often been held at depth for long periods of time. Consequently the particles have probably attained their most effective state of packing.

Stress-strain relationships for clays presently under consideration are presented in Figure 5.14.1 - 5.14.26. In cases where tests have been performed on the material in both the natural state and from a remoulded condition with the initial moisture content equal to the liquid limit, the curve with the least amount of strain represents the former condition; swell pressures and swelling beyond the original

thickness being duly accommodated. The resulting strain energies, calculated from the measured areas beneath the stress-strain curves using a polar planimeter, have been analysed in two ways, i.e. on a total volume basis (Tables 5.13 and 5.14) and on a unit weight basis (Tables 5.15 and 5.16).

For each method of analysis, significant relationships (Tables 5.18 and 5.19) which exist between the strain energy parameters themselves, or between the strain energy parameters and the mineralogy, Atterberg limits etc. have been deduced using a correlation matrix, involving 24 samples (results from the Keuper Marl and Swallow Wood roof being excluded because only remoulded tests were performed on these materials).

The geochemistry has not been included in the analysis because it is adequately reflected by the mineralogy.

Significant relationships obtained from tests performed on the remoulded materials should reflect, approximately, those relationships which occur during sedimentation and compaction of normally-consolidated clays, assuming that no drastic changes have taken place within the sediment. On the other hand, significant correlations obtained from tests performed on undisturbed material are affected by the state of the material (e.g. the variation of the preconsolidation load or hardness etc.), Nevertheless, broad trends do emerge which can be reconciled to the remoulded condition.

The results have also been reviewed in the light of work done by Brooker (1967) by reference to several additional tests carried out in a conventional oedometer on material remoulded at various moisture contents (Table 5.17 and Fig.5.15). Unfortunately, because the strain energy parameters are pressure and volume dependent, only values within each of these three groups are directly comparable

(see Test Procedures, Appendix A.3). Nevertheless, the resulting trends are universally comparable.

With regard to the total volume basis of analysis, the total compressional energy appears to be related to the compressibility of the minerals present. This is supported by a strong positive correlation with the plastic limit for the remoulded group and also by a strong positive correlation with the total expandable mineral content (including smectite content) for the undisturbed group (Table 5.18). The recoverable strain energy is dominantly controlled by the total expandable mineral content, and in particular the concentration of smectite. This is substantiated by strong positive correlations with these constituents and also with the Atterberg limits and clay-size components. In addition, the relationship is supported by an associated negative correlation between recoverable strain energy and quartz, kaolinite and illite (see Table 5.18).

The most significant feature with regard to the non-recoverable strain energy, is that is has a strong negative relationship with the liquid limit and plasticity index when the material is remoulded at the liquid limit, whereas a positive relationship is obtained for samples in the undisturbed condition.

This reversal of trends is also observed when the initial moisture content of the four remoulded clays, consolidated in the conventional oedometer, is reduced from the liquid limit to a liquidity index of 0.5 (Table 5.17 and Fig.5.16b). In addition, the total compressional energy also increases as the initial moisture content is lowered (Fig.5.16(c)) although a somewhat irregular trend is observed for the recoverable strain energy (Fig.5.16(a)).

From additional tests performed on the Fuller's Earth (Fig.5.16(g), (h) and (i)), it can be seen that as the initial moisture content is

reduced from the liquid limit to a liquidity index of 0.75 and then to 0.5, the non-recoverable strain energy, and also the total compressional and recoverable strain energies, increase rapidly in an almost linear manner. However, when the initial moisture content is at a liquidity index of 0.25 the non-recoverable strain energy has only increased very slightly.

Therefore, on a purely volumetric basis of analysis and in the light of present evidence it appears that the initial moisture content has a large effect on the strain energy, although the results in this form do not give a clear indication of why this is so. However, based on the results of 5 clays remoulded at a liquidity index of 0.5, Brooker(1967) concludes that the increase in strain energy between the loading and unloading curves (which he defines as the 'absorbed strain energy', see Chapter 1.5.6) with increasing plasticity, is related to the disintegration characteristics (slaking) of the material. In the present work this strain energy is deemed to be non-recoverable (e.g. Fig.5.13(a)).

When the data are considered on a unit dry weight basis, i.e. strain energy per gram, a new picture emerges which leads to the formation of a simple working model.

With regard to the remoulded samples, all three types of strain energy increase with increasing plasticity (Fig.5.17 (a),(b) and (c)); this being substantiated by strong positive correlations between the energies per gram and the Atterberg limits (Table 5.19). The undisturbed materials all of which have liquidity indices of zero or below, also produce a similar trend, (Fig.5.17 (d),(e) and (f)), although lower values of strain energy per gram are obtained. Another similar trend is also encountered for the materials

consolidated from the liquid limit in the conventional oedometer (Fig.5.16 (d),(e) and (f)). Furthermore, results from this series of tests indicate that the strain energy per gram for each material remains constant until the initial moisture content is reduced to a liquidity index of 0.5 (Table 5.17), although upon reducing the initial moisture content to a liquidity index of 0.25, a reduction in the strain energies per gram occurs (see Fuller's Earth, Table 5.17).

Therefore, it has been concluded that during the consolidation cycle of a clay, more non-recoverable energy per gram of dry solid is expended as the plasticity increases because initially high moisture contents allow larger relative displacements and reorientations of particles. This will result in larger volumetric strains. Consequently, a larger amount of total compressional strain energy is required, although there is usually a greater amount of associated recoverable strain energy caused by the presence of expandable minerals. If the initial moisture content is reduced, then the strain energies per gram of dry solid remain relatively constant until a liquidity index of 0.5 is reached. Below this value, less energy is expended because the denser state of packing restricts large displacements and reorientations of the minerals. As a consequence of this behaviour, the total compressional, recoverable and non-recoverable strain energies are reduced.

It is also interesting to note the effect of previous compaction on the three types of strain energy. As the degree of over-consolidation increases (Fig.5.18(a)), the amount of non-recoverable energy per gram decreases for undisturbed materials. At the same time the difference between this value and the amount of non-recoverable strain energy per gram expended during the consolidation of the remoulded material

Table 5.13 Total Strain Energy and Linear Strain for Undisturbed Samples

	Sample Ref.	Total Compression Energy (mkN/m³)	Recoverable Energy (mkN/m³)	Non-Recoverable Energy (mkN/m³)	Strain (%)
British Materials					
London Clay 14m	LC14	2456.1	668.8	1877.3	26.7
London Clay 37m	LC37	1955.5	633.6	1321.9	17.1
Gault Clay	GC	2913.7	754.8	2158.9	22.0
Fuller's Earth (Redhill)	FE23	3113.2	1494.0	1619.2	26.0
Weald Clay	WC	1032.5	297.2	735.3	8.8
Kimmeridge Clay	KC	1710.3	657.1	1053.2	19.2
Oxford Clay 10m	OC10	2862.9	754.8	2108.1	24.3
Oxford Clay 44m	OC44	2111.9	676.6	1435.3	15.5
Fuller's Earth (Bath)	FE19	2244.9	1055.9	1189.0	22.1
Lias Clay10m	L10	1654.3	664.9	989.4	20.1
Lias Clay36m	L36	1583.9	637.5	946.4	14.3
Keuper Marl	KM	-	-	-	-
Swallow Wood roof	SWR	-	-	-	-
Flockton Thin roof	FTR	598.4	242.5	355.9	5.6
Flockton Thin seat	FTS	762.6	281.6	481.0	8.2
Widdringham roof	WR	747.0	293.3	453.7	6.7
North American Materials					
Yazoo Clay	YC	3046.7	1204.6	1842.1	38.0
Kincaid Shale 6m	K6	2029.8	477.2	1552.6	20.4
Kincaid Shale 8m	K8	2147.2	265.9	1881.3	19.1
Nacimiento Shale	N1	637.5	320.7	316.8	5.4
Nacimiento Shale	N2	551.4	265.9	285.5	5.4
Nacimiento Shale	N3	1345.4	543.6	801.8	10.7
Fox Hills Shale	FOX	2948.9	817.4	2131.5	24.1
Dawson Shale	DS	1568.3	469.3	1099.0	11.8
Pierre Shale (Dakota)	PSD	2581.3	946.4	1634.9	21.8
Pierre Shale (Colorado)	PSC	864.3	359.8	504.5	8.7

Table 5.14 Total Strain Energy and Linear Strain for Remoulded Samples

	Sample Ref.	Total Compression Energy (mkN/m^3)	Recoverable Energy (mkN/m^3)	Non-Recoverable Energy (mkN/m^3)	Strain (%)
British Material					
London Clay 14m	LC14	1376.9	453.7	923.2	62.9
London Clay 37m	LC37	1482.2	453.6	1028.6	54.9
Gault Clay	GC	1642.6	477.2	1165.4	57.2
Fuller's Earth (Redhill)	FE23	1928.1	758.7	1169.4	60.6
Weald Clay	WC	1607.4	308.9	1298.5	36.2
Kimmeridge Clay	KC	1627.0	563.2	1063.8	56.3
Oxford Clay 10m	OC10	1583.9	383.3	1200.6	57.1
Oxford Clay 44m	OC44	1607.4	391.1	1216.3	54.0
Fuller's Earth (Bath)	FE19	1716.9	727.4	989.5	63.5
Lias Clay 10m	L10	1658.3	375.5	1282.8	56.5
Lias Clay 36m	L36	1744.3	508.4	1235.9	53.4
Keuper Marl	KM	1587.9	230.7	1357.2	39.1
Swallow Wood roof	SWR	1716.9	441.9	1275.0	53.8
Flockton Thin roof	FTR	1775.6	387.2	1388.4	50.2
Flockton Thin seat	FTS	1529.2	484.9	1044.3	54.5
Widdringham roof	WR	1646.5	332.4	1314.1	42.7
North American Material					
Yazoo Clay	YC	1505.8	629.7	876.1	68.44
Kincaid Shale 6m	K6	1325.8	402.8	923.0	57.1
Kincaid Shale 8m	K8	1353.2	219.0	1134.2	54.2
Nacimiento Shale	N1	1724.8	383.3	1341.5	44.2
Nacimiento Shale	N2	1673.9	308.9	1365.0	43.4
Nacimiento Shale	N3	1517.4	586.6	930.8	62.7
Fox Hills Shale	FOX	2108.0	590.6	1517.4	49.3
Dawson Shale	DS	1486.2	457.6	1028.6	57.5
Pierre Shale (Dakota)	PSD	1439.2	539.7	899.5	71.5
Pierre Shale (Colorado)	PSC	1454.9	379.4	1075.5	55.4

Table 5.15 Strain Energy (per gram dry weight) for Undisturbed Samples

	Sample Ref.	Total Compression Energy/gm (mkN/m³g)	Recoverable Energy/gm (mkN/m³g)	Non-Recoverable Energy/gm (mkN/m³g)
British Materials				
London Clay 14m	LC14	94.3	24.7	69.5
London Clay 37m	LC37	64.3	20.8	43.5
Gault Clay	GC	106.0	27.4	78.5
Fuller's Earth (Redhill)	FE23	142.3	68.3	74.0
Weald Clay	WC	25.0	7.2	17.8
Kimmeridge Clay	KC	52.4	20.1	32.3
Oxford Clay 10m	OC10	102.1	26.9	75.2
Oxford Clay 44m	OC44	70.8	22.6	48.1
Fuller's Earth (Bath)	FE19	93.3	43.9	49.4
Lias Clay 10m	L10	51.5	20.7	30.8
Lias Clay 36m	L36	46.5	18.7	27.8
Keuper Marl	KM	-	-	-
Swallow Wood roof	SWR	-	-	-
Flockton Thin roof	FTR	15.5	6.3	9.2
Flockton Thin seat	FTS	20.3	7.5	12.8
Widdringham roof	WR	19.8	7.8	12.0
North American Materials				
Yazoo Clay	YC	135.3	53.5	81.8
Kincaid Shale 6m	K6	65.5	15.4	50.1
Kincaid Shale 8m	K8	70.6	8.7	61.9
Nacimiento Shale	N1	15.5	7.8	7.7
Nacimiento Shale	N2	13.6	6.5	7.0
Nacimiento Shale	N3	41.5	16.7	24.7
Fox Hills Shale	FOX	125.0	34.6	90.3
Dawson Shale	DS	47.5	14.2	33.2
Pierre Shale (Dakota)	PSD	101.1	37.0	64.0
Pierre Shale (Colorado)	PSC	23.4	9.7	13.6

Table 5.16 Strain Energy (per gram dry weight) for Remoulded Samples

	Sample Ref.	Total Compression Energy/gm (mkN/m^3g)	Recoverable Energy/gm (mkN/m^3g)	Non-Recoverable Energy/gm (mkN/m^3g)
British Materials				
London Clay 14m	LC14	116.3	38.3	77.9
London Clay 37m	LC37	102.1	31.2	70.9
Gault Clay	GC	126.4	36.7	89.7
Fuller's Earth (Redhill)	FE23	203.2	79.9	123.2
Weald Clay	WC	65.2	12.5	52.6
Kimmeridge Clay	KC	118.0	40.8	77.1
Oxford Clay10m	OC10	122.7	29.6	93.0
Oxford Clay44m	OC44	110.9	26.9	83.9
Fuller's Earth (Bath)	FE19	171.1	72.5	98.6
Lias Clay 10m	L10	119.1	26.9	92.1
Lias Clay 36m	L36	120.1	35.0	85.1
Keuper Marl	KM	80.1	11.6	68.5
Swallow Wood roof	SWR	108.8	28.0	80.8
Flockton Thin roof	FTR	104.1	22.7	81.4
Flockton Thin seat	FTS	100.5	31.8	68.6
Widdringham roof	WR	92.0	18.5	73.4
North American Materials				
Yazoo Clay	YC	151.3	63.2	88.0
Kincaid Shale 6m	K6	99.4	30.2	69.2
Kincaid Shale 8m	K8	86.9	14.0	72.8
Nacimiento Shale	N1	94.7	21.0	73.6
Nacimiento Shale	N2	90.7	16.7	73.9
Nacimiento Shale	N3	134.7	52.1	82.6
Fox Hills Shale	FOX	147.8	41.4	106.4
Dawson Shale	DS	111.6	34.3	77.2
Pierre Shale (Dakota)	PSD	169.7	63.6	106.1
Pierre Shale (Colorado)	PSC	98.3	25.6	72.8

Table 5.17 Stress-Strain Behaviour of Four Clays Remoulded at Various Initial Moisture Contents

		Non-Recoverable Energy (mkN/m³)	Recoverable Energy (mkN/m³)	Total Compression Energy (mkN/m³)	Strain (%)
Total Strain Energy and Linear Strain					
Pierre Shale (Dakota)	L.L.	313.82	144.65	458.47	69.38
Pierre Shale (Dakota)	0.50L.I.	481.03	168.09	649.22	54.83
Fuller's Earth (Bath)	L.L.	305.97	150.53	456.61	59.99
Fuller's Earth (Bath)	0.75L.I.	364.70	218.04	582.74	53.83
Fuller's Earth (Bath)	0.50L.I.	416.50	223.90	640.43	45.64
Fuller's Earth (Bath)	0.25L.I.	421.41	235.64	657.04	35.44
London Clay 37m	L.L.	331.37	129.06	460.43	50.92
London Clay 37m	0.50L.I.	377.37	131.90	509.37	40.35
Widdringham roof	L.L.	345.10	109.44	454.65	39.96
Widdringham roof	0.50L.I.	386.19	142.69	528.89	34.51

		Non-Recoverable Energy (mkN/m³g)	Recoverable Energy (mkN/m³g)	Total Compression Energy (mkN/m³g)	Dry Weight (g)
Strain Energy Per Unit Gram of Dry Powder					
Pierre Shale (Dakota)	L.L.	14.52	6.69	21.22	21.604
Pierre Shale (Dakota)	0.50L.I.	15.67	5.47	21.15	30.692
Fuller's Earth (Bath)	L.L.	12.67	6.23	18.91	24.145
Fuller's Earth (Bath)	0.75L.I.	12.79	7.64	20.44	28.507
Fuller's Earth (Bath)	0.50L.I.	12.42	6.67	19.59	33.526
Fuller's Earth (Bath)	0.25L.I.	10.74	6.01	16.76	39.203
London Clay 37m	L.L.	8.95	3.48	12.44	37.007
London Clay 37m	0.50L.I.	8.47	2.96	11.44	44.525
Widdringham roof	L.L.	7.58	2.40	9.99	45.493
Widdringham roof	0.50L.I.	7.38	2.72	10.10	52.316

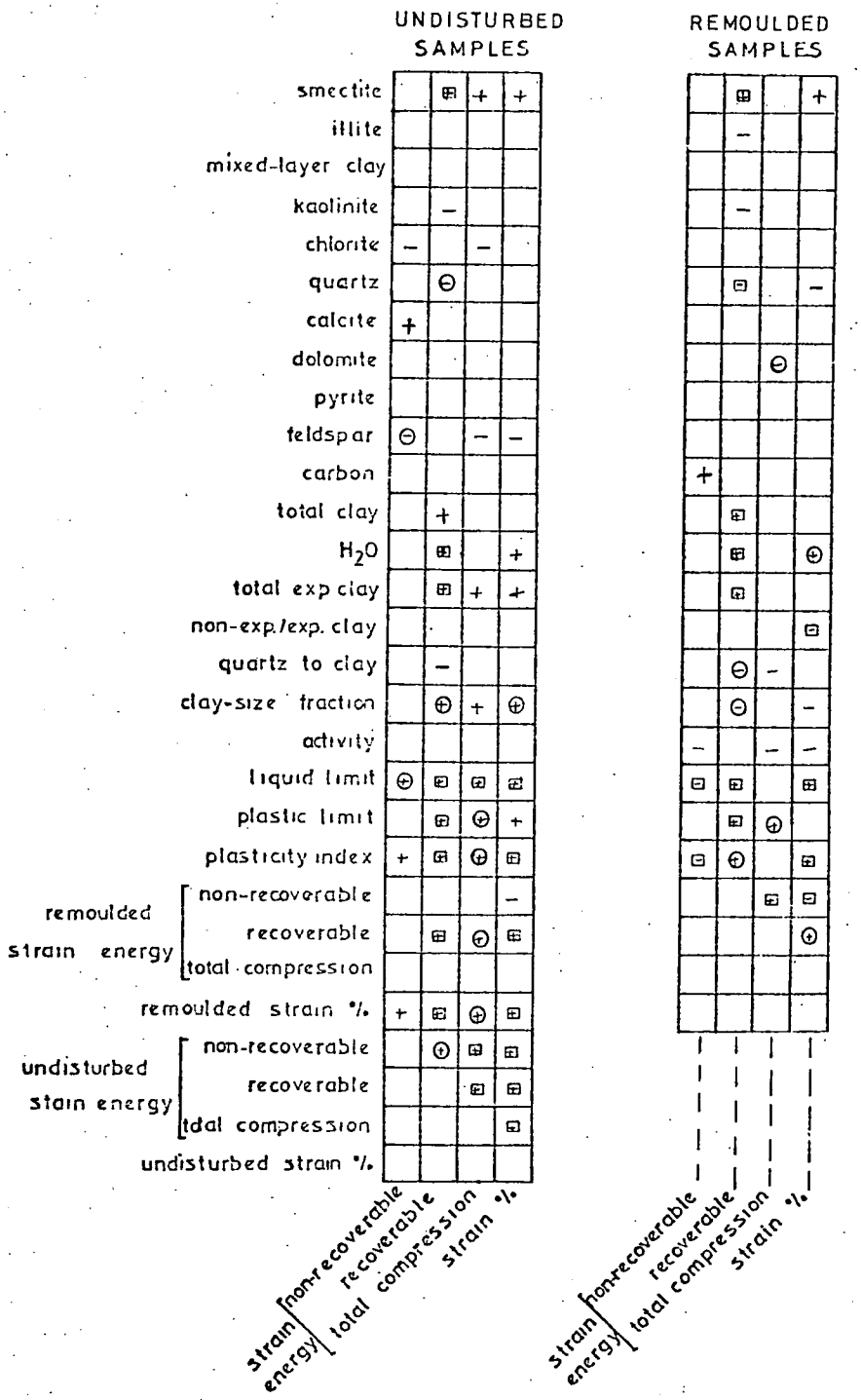

\+ - 95.0% - Probably Significant

⊖ ⊖ 99.0%

⊟ ⊟ 99.9% - Highly Significant

Table 5.18. Significant Correlations Associated with Strain Energy (Considered on a Total Volume Basis).

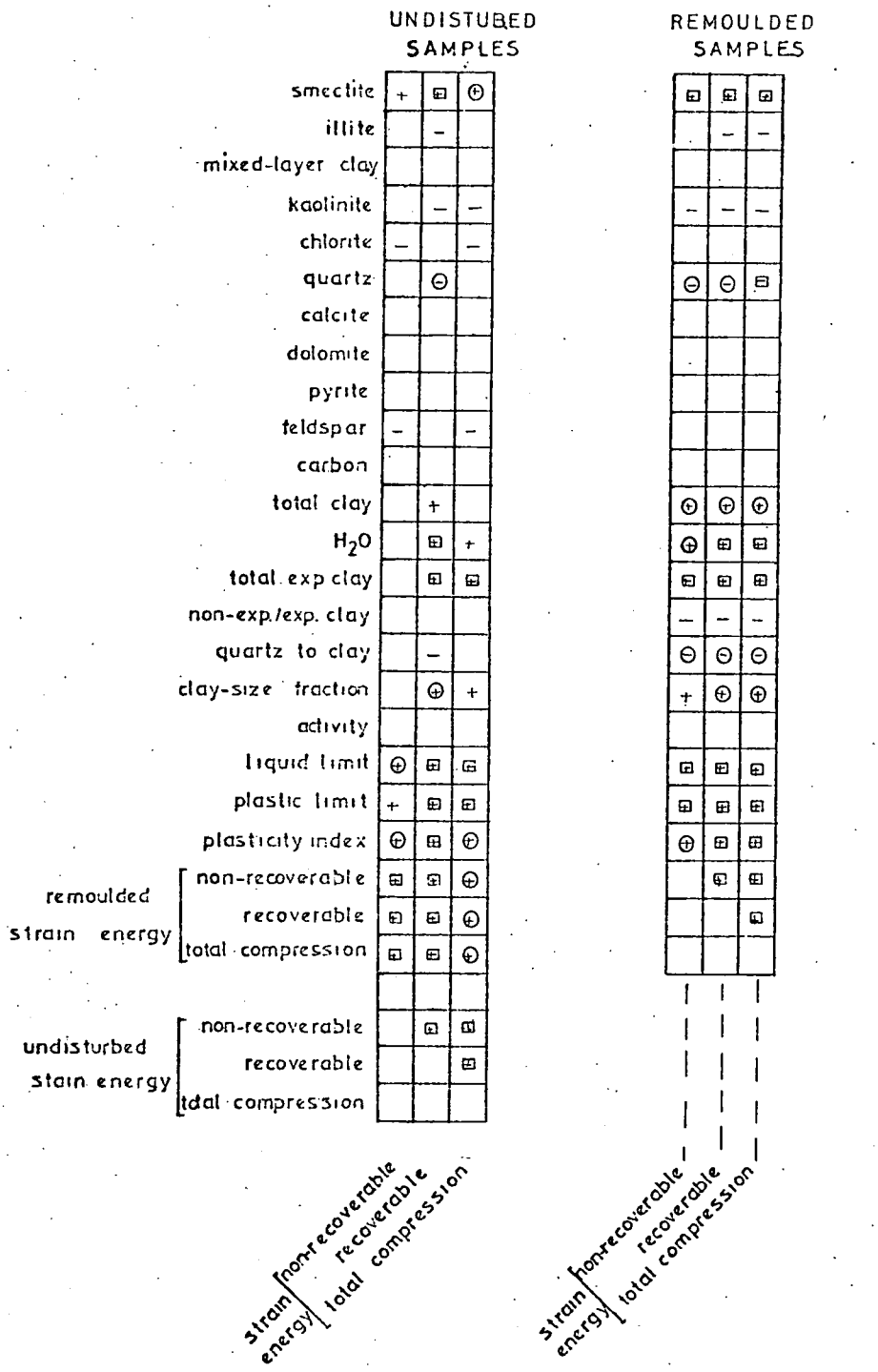

\+ − 95.0% - Probably Significant

⊕ ⊖ 99.0%

⊞ ⊟ 99.9% - Highly Significant

Table 5.19. Significant Correlations Associated with Strain Energy (Considered on a Unit Dry Weight Basis).

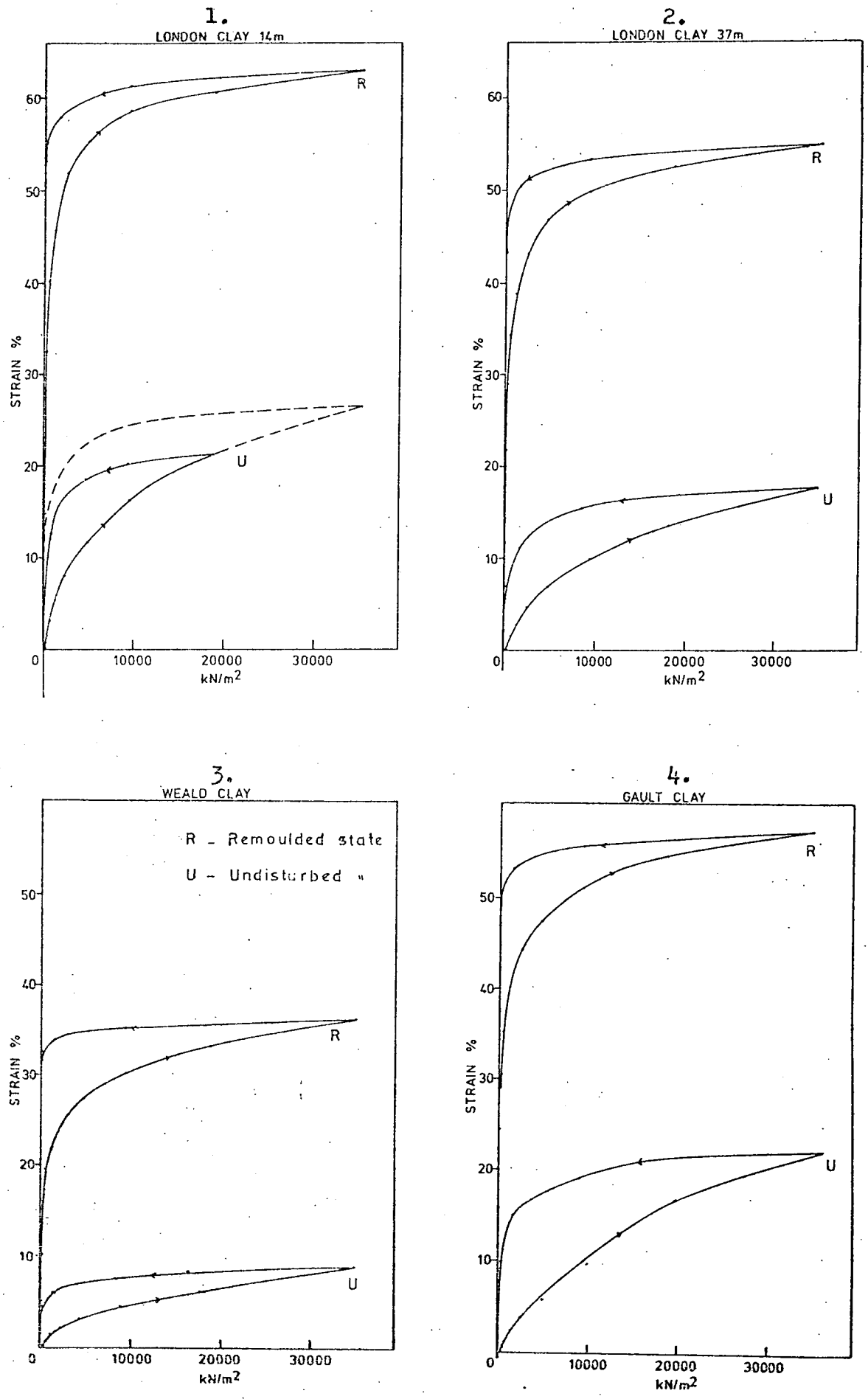

Figure 5.14. Stress - Strain Relationships for Samples Tested.

5.

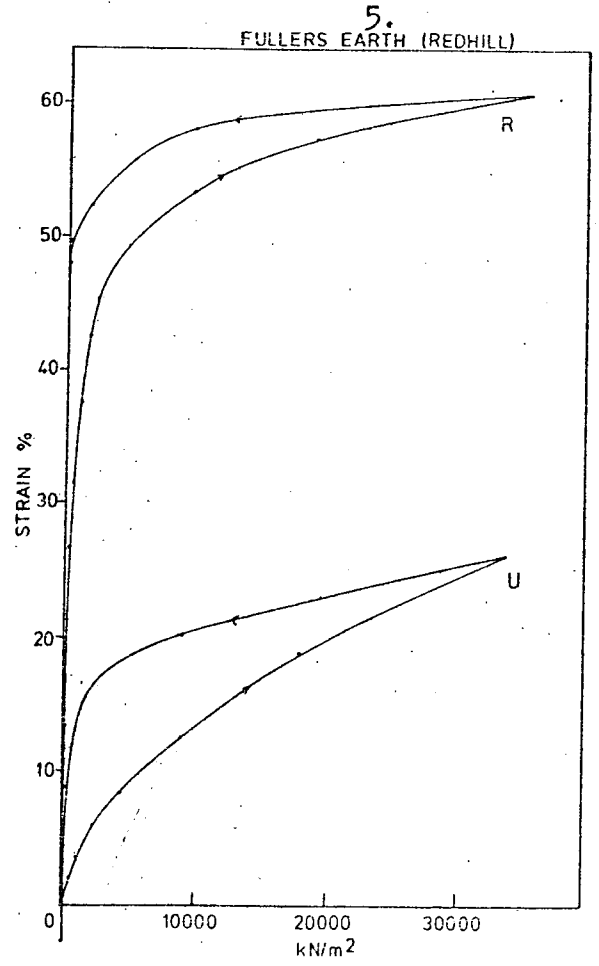

6.

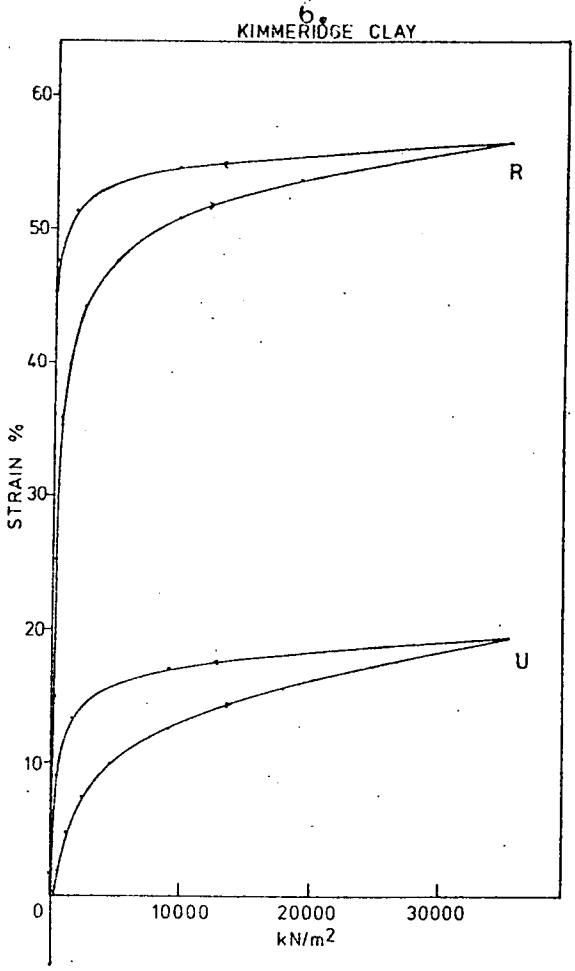

7.

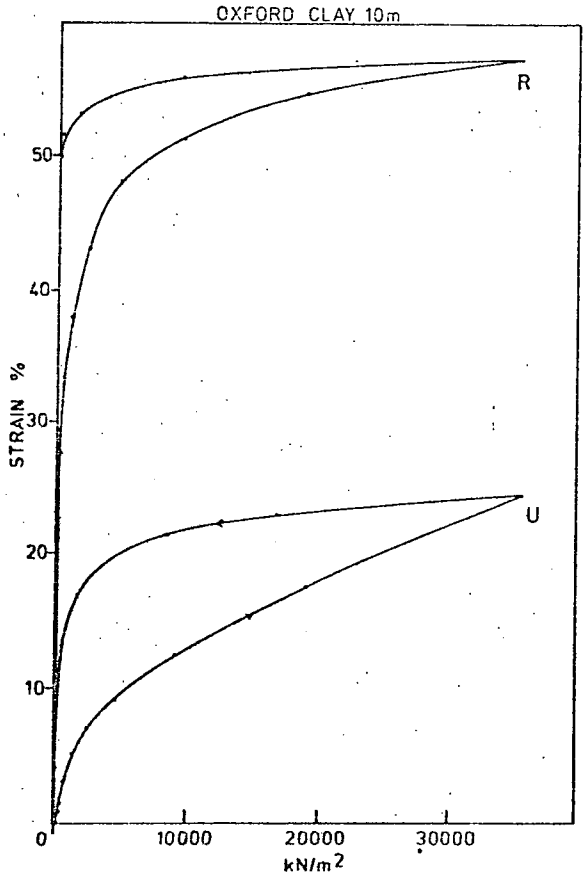

8.

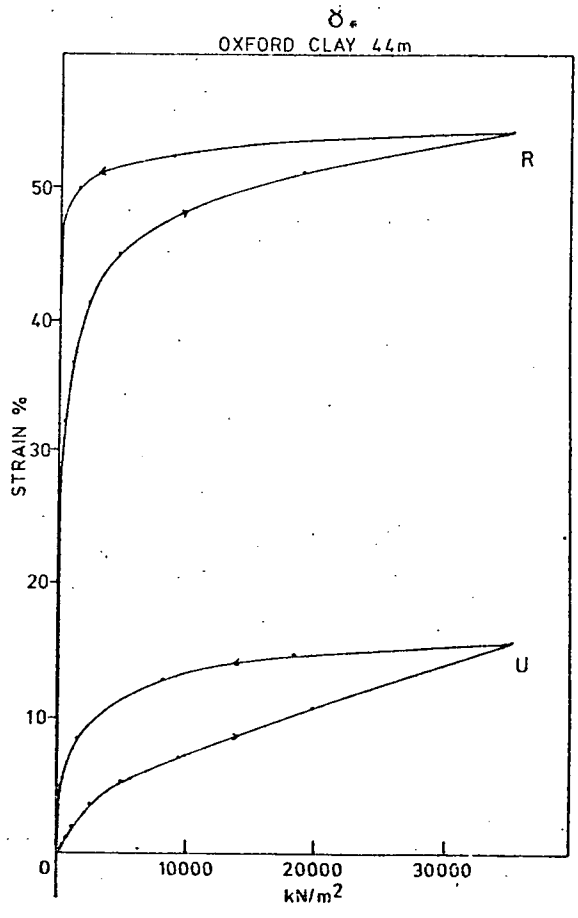

Figure 5.14. cont.

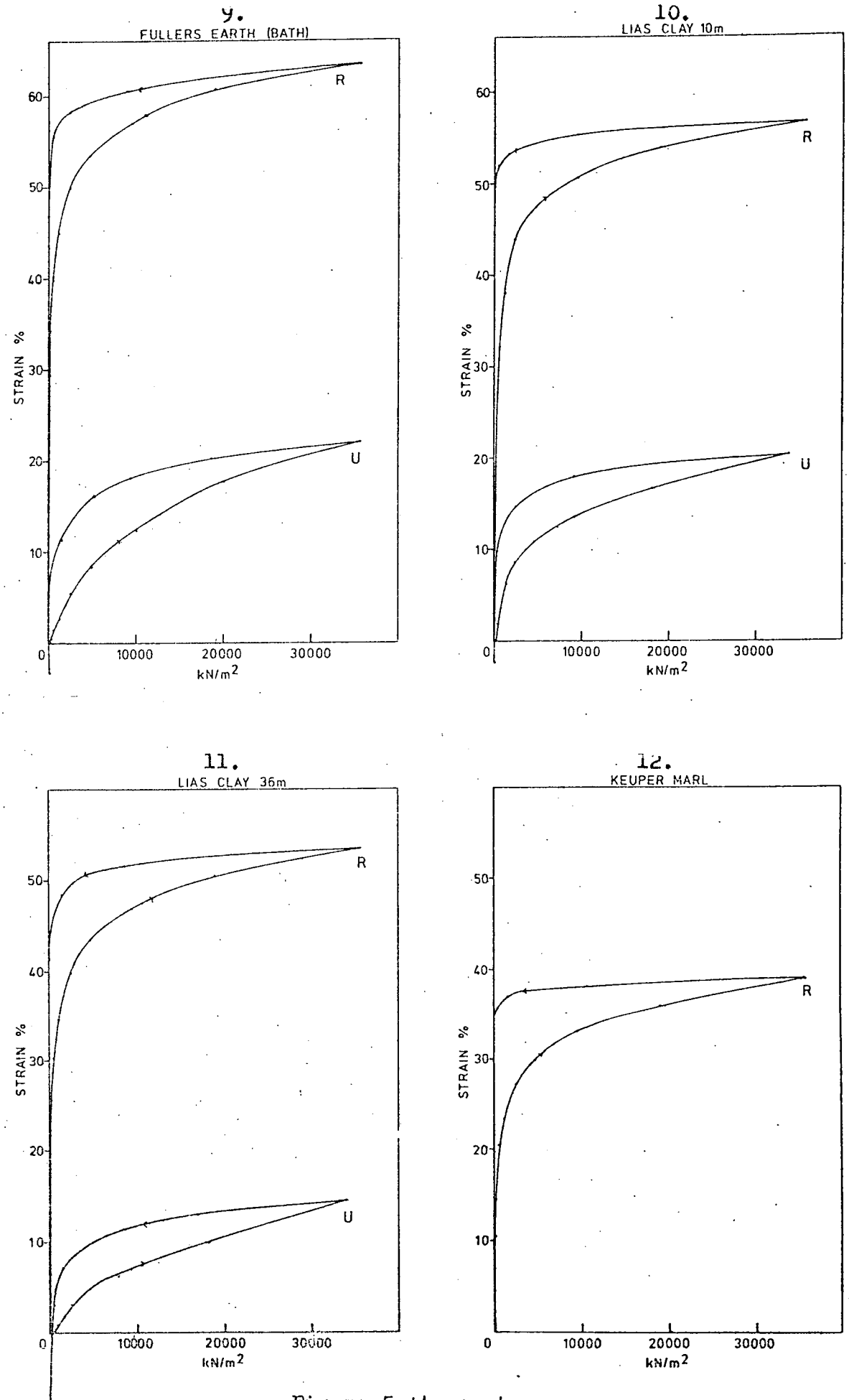

Figure 5.14. cont.

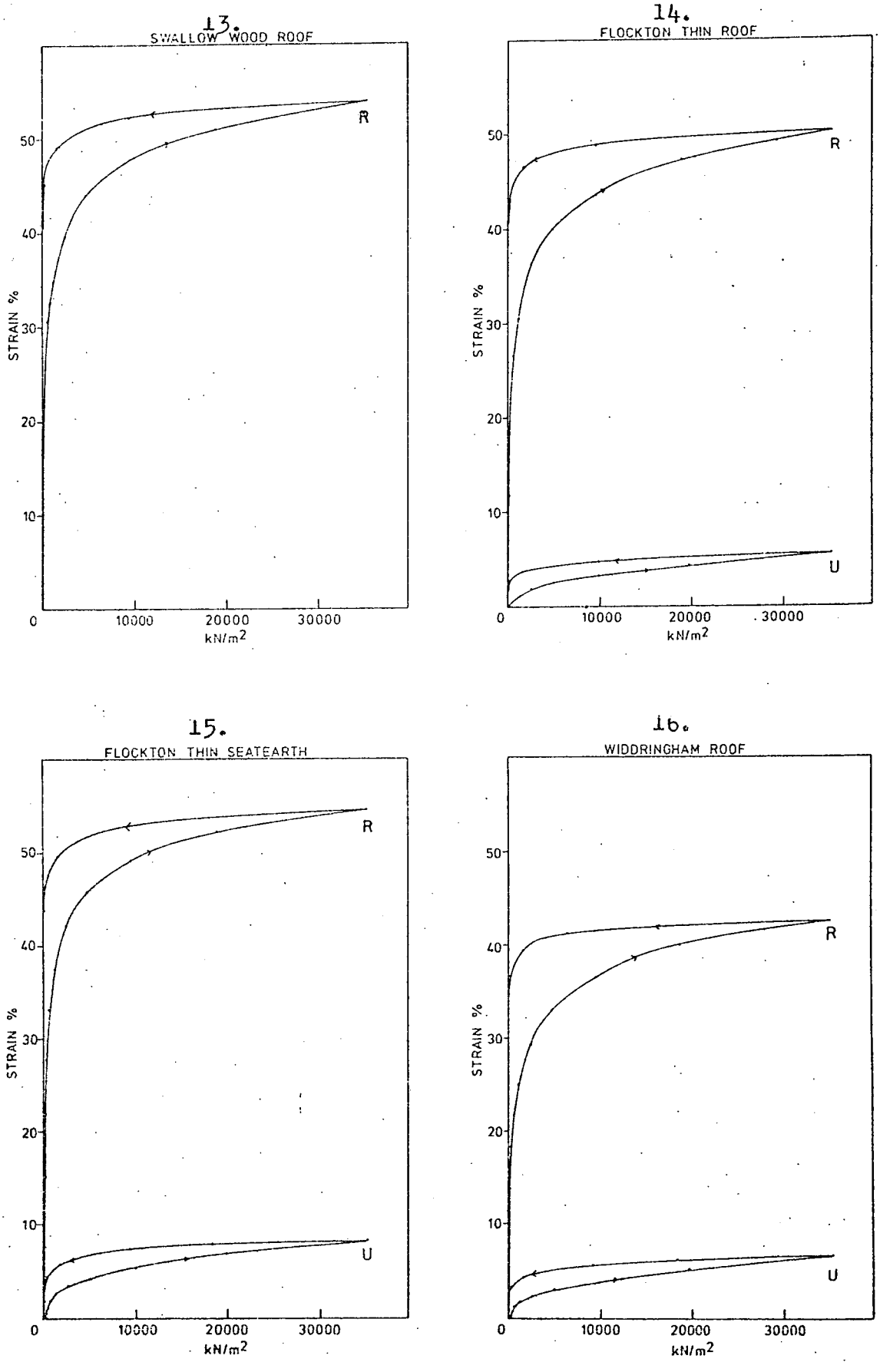

Figure 5.14. cont.

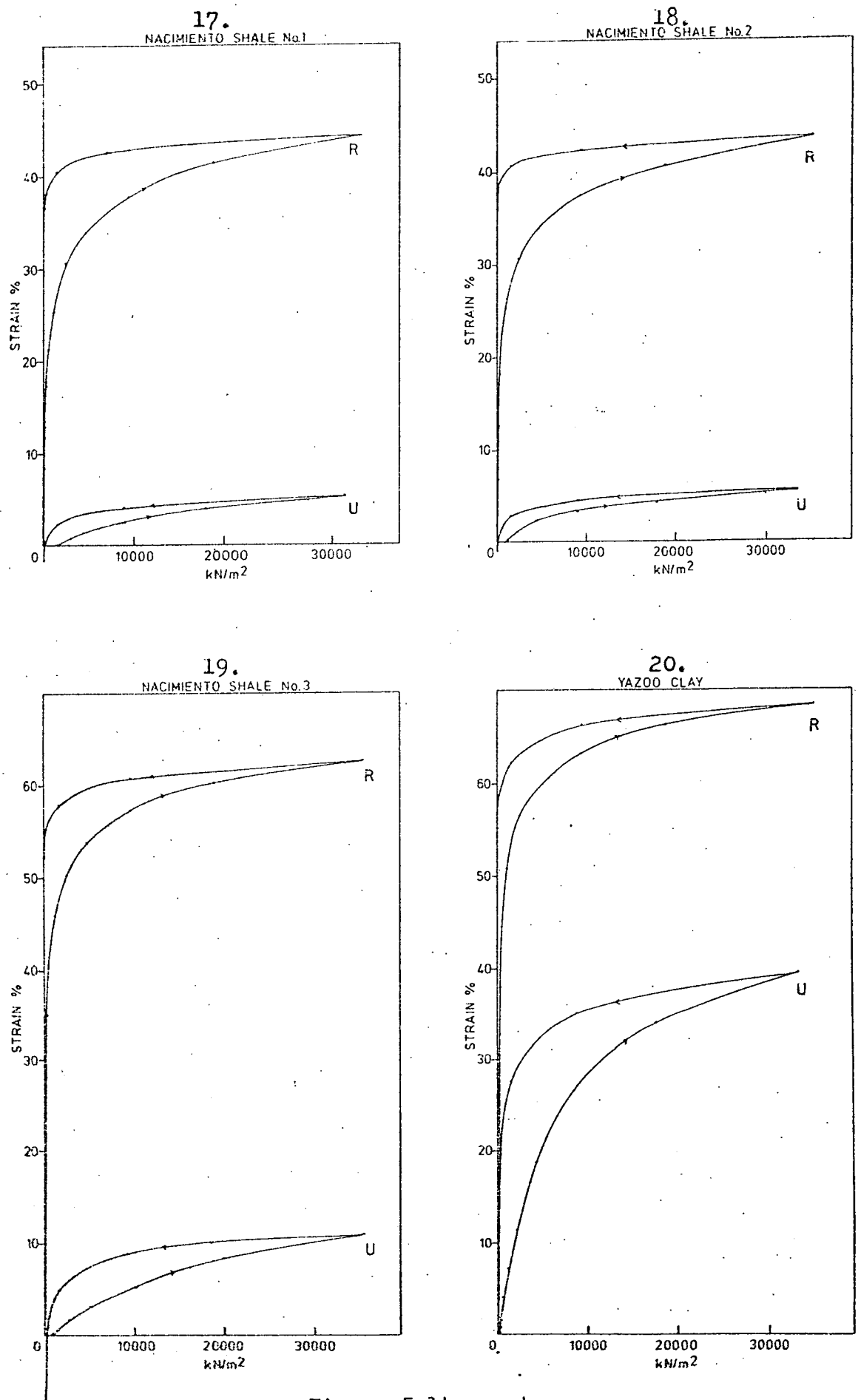

Figure 5.14. cont.

21.

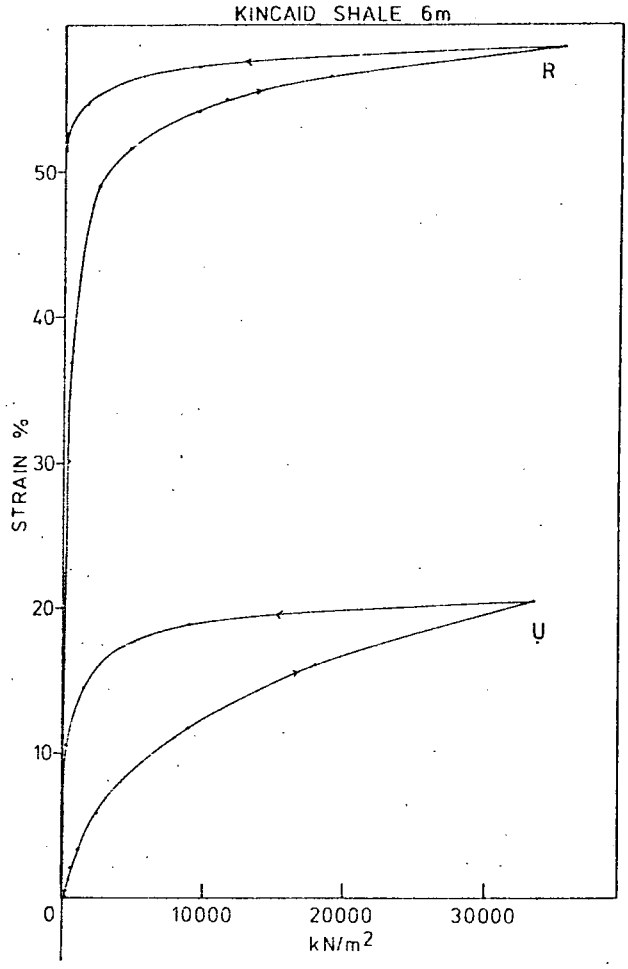

22.

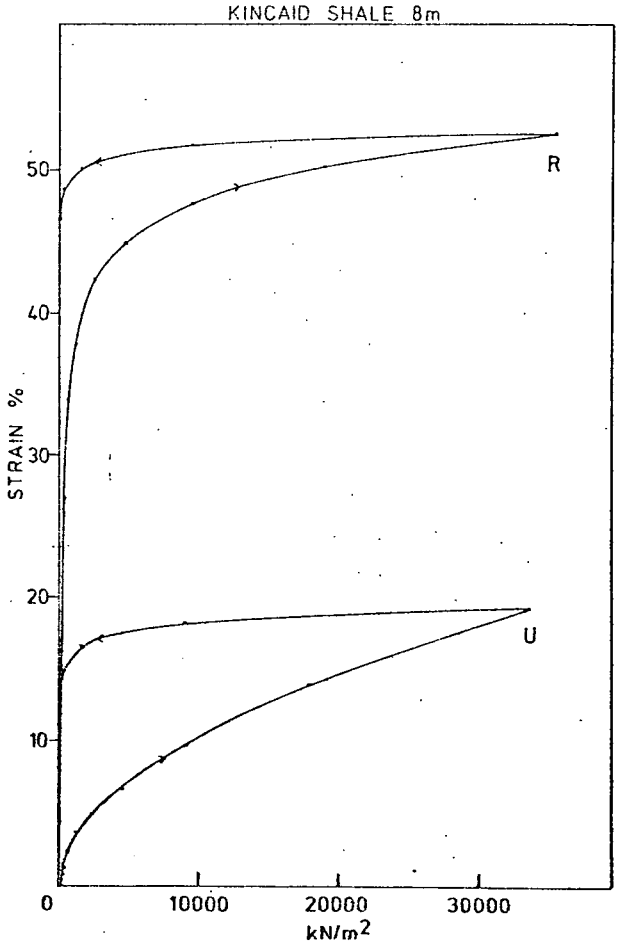

Figure 5.14. cont.

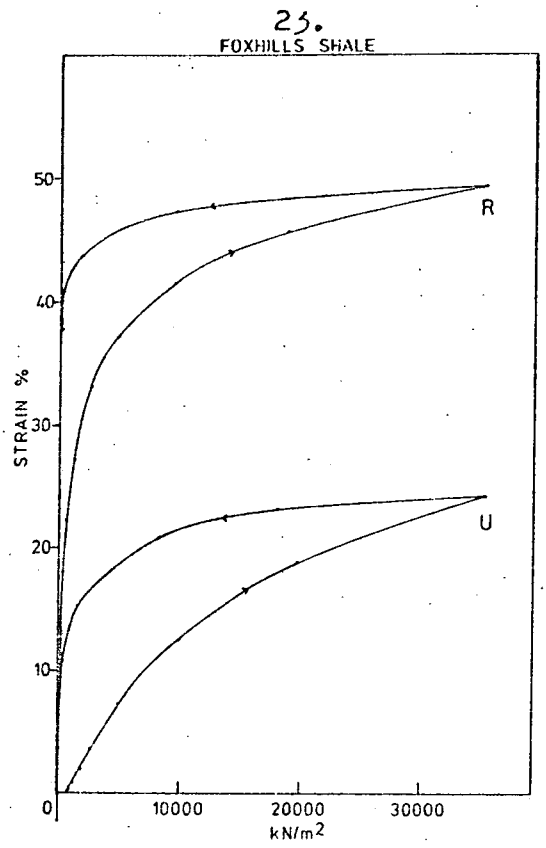

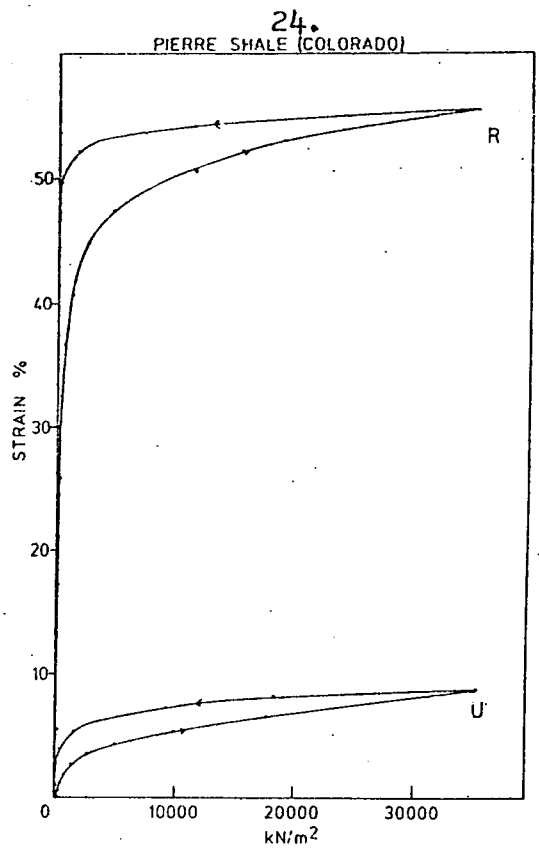

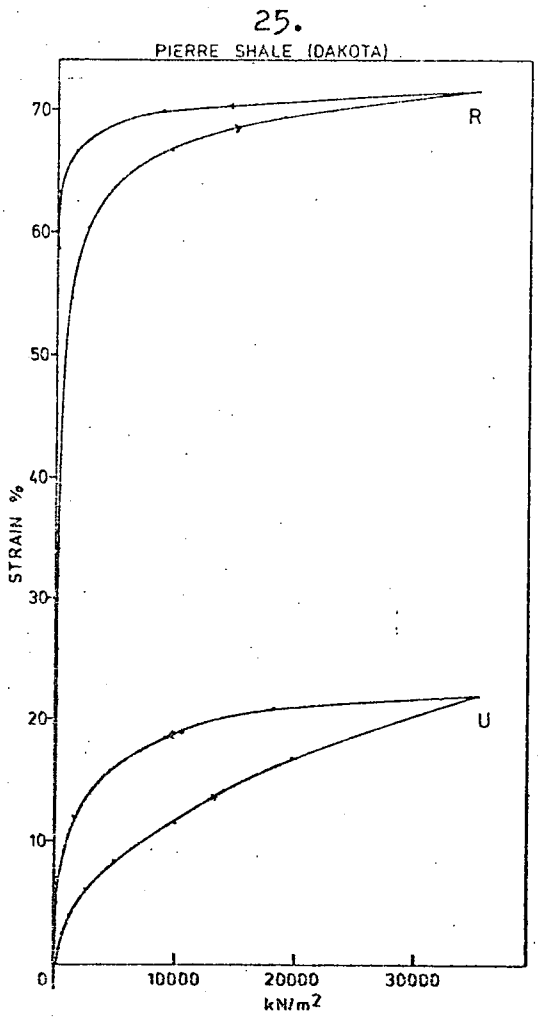

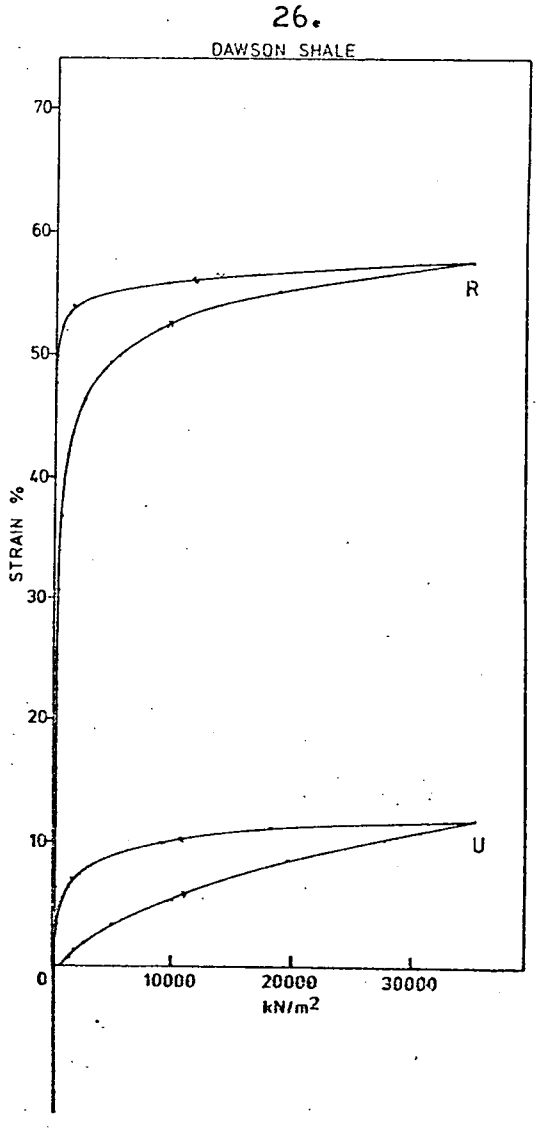

Figure 5.14. cont.

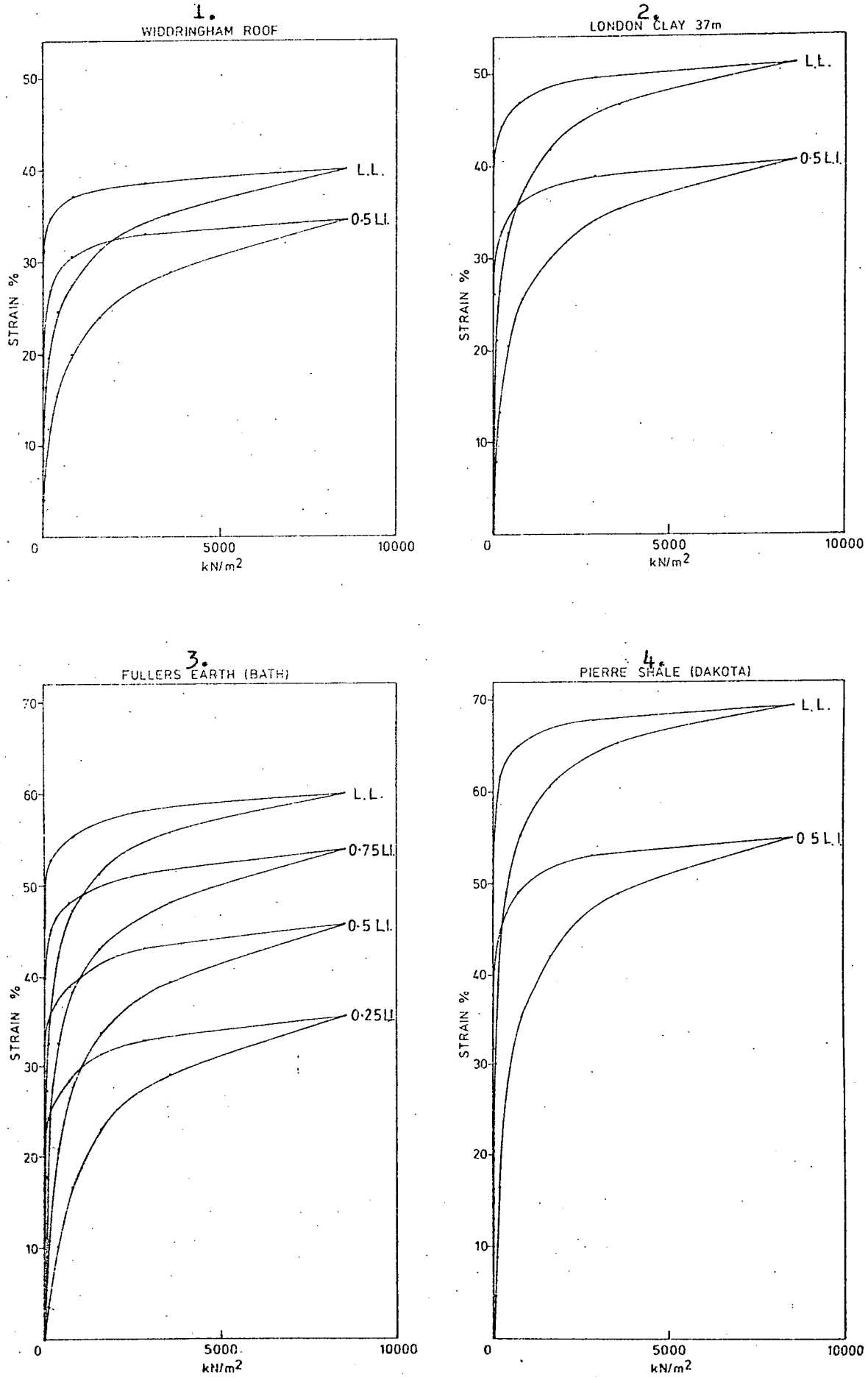

Figure 5.15. Stress - Strain Relationships for Four Clays Remoulded at Various Initial Moisture Contents.

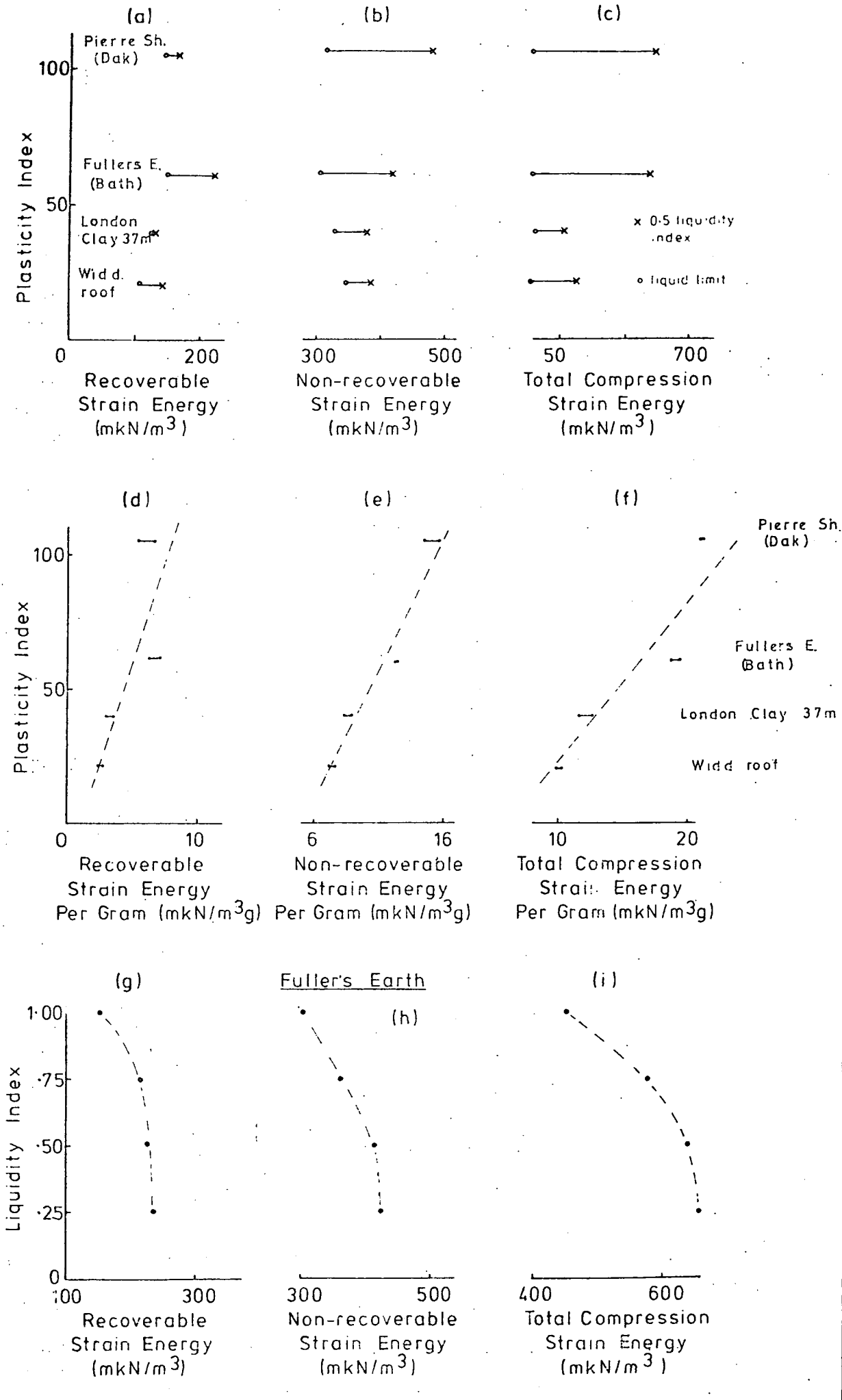

Figure 5.16. The Effect of Reducing the Initial Moisture Content upon Strain Energy.

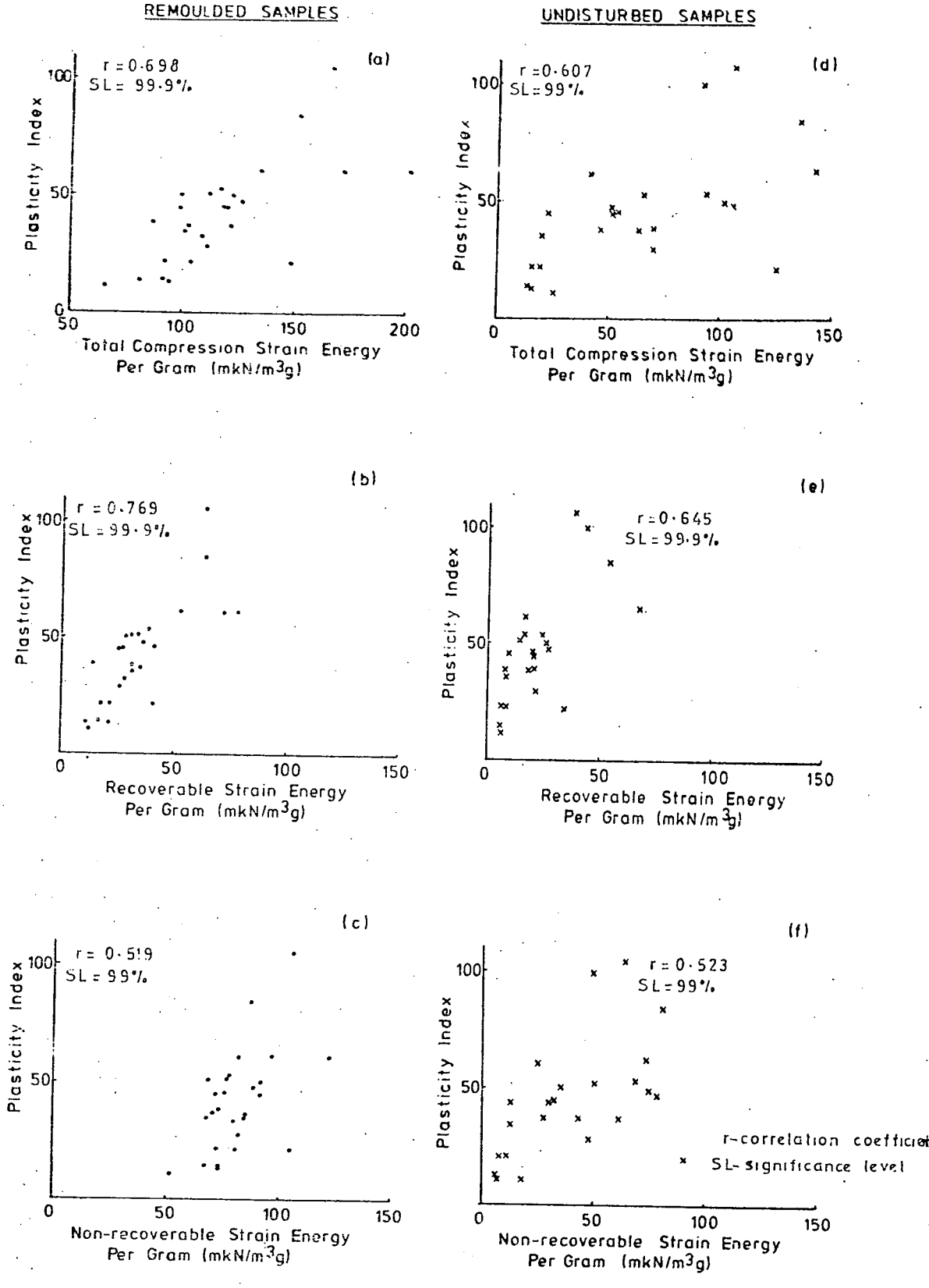

Figure 5.17. The Relationship Between Strain Energy (per gram dry weight) and Plasticity.

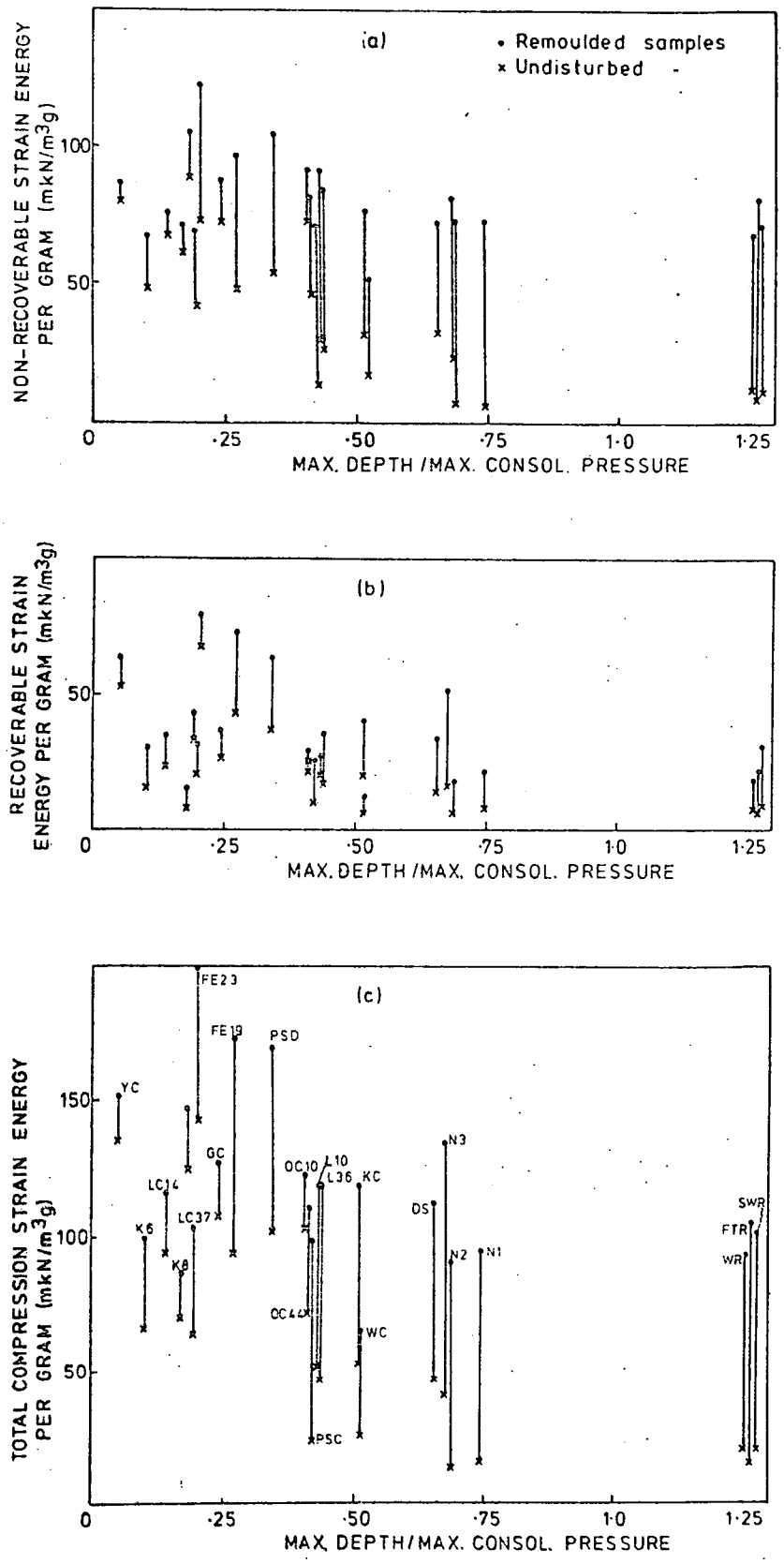

Figure 5.18. The Relationship Between Strain Energy and Maximum Depth of Burial.

increases until the ratio of maximum depth of burial to the maximum consolidation pressure reaches 0.4, after which the difference tends to remain constant. This is probably a function of compaction i.e. as the material becomes more compact the grains become more densely packed and do not have the same degrees of freedom as those in the loosely remoulded state. However, until the material has been buried to a depth of about 3500 feet (1050m)* there still appears to be a certain degree of freedom for adjustments within the materials, which is inferred from the fact that more non-recoverable strain energy per gram is expended in the less deeply buried samples. A similar trend is also noticed for the total compressional energy (Fig.5.18(c)), although the increase in the amount of recoverable strain energy appears to remain fairly constant over the compaction range (Fig.5.18(b)) and may be dependent on the amount of bonding present (Section 5.6).

5.12 Conclusions

1. The results obtained with the high pressure cell compare favourably with those of a conventional floating head oedometer and therefore can be used realistically for the basis of discussion.

2. A review of the consolidation parameters highlighted the following features:-

(a) The value of c_v decreases with increasing liquid limit but there is no significant difference between those values obtained from the tests performed on undisturbed materials and those from tests performed at both the high and low pressure range on the remoulded materials.

(b) In the low pressure range (297 - 2426kN/m^2) the compression index (C_c) agrees with previously derived equations. However, at higher pressures (2426 - 34967kN/m^2) the values conform to an equation which can be represented as:-

* Ratio of preconsolidation pressure to maximum consolidation pressure = 0.4

$$C_c = 0.004 (LL - 10\%)$$

(c) When identical pressure ranges are considered, the Swell Index values (C_s) of remoulded materials are sometimes greater than for the undisturbed counterparts; the differences being attributed to the presence of diagenetic bonding. A general increase in swell index also occurs when the maximum consolidation pressure is increased and this phenomenon may be associated with tighter packing of the clay particles.

(d) With regard to permeability, at similar pressures the value appears to be independent of the state of the material (i.e. undisturbed or remoulded). However, there is a general decrease with increasing liquid limit.

(e) The coefficient of volume compressibility (m_v) like C_c, decreases with increasing pressure, although at any given pressure, the larger values are associated with the higher liquid limits.

3. (a) Diagenetic bonding has been detected in unweathered material by the presence of reduced swell index values (compared with values obtained from the remoulded counterparts).

(b) The diagenetic bonding appears to be related to both mineralogy and maximum depth of burial. No relationship with the age of the material was positively confirmed. Where smectite is present as a major constituent, diagenetic bonds can be formed at depths between 900-1800m which show similar effects to those formed in shales with a more inert mineralogy which have been buried to depths probably up to 3800 m (e.g. British Carboniferous materials). Slaking tests (Chapter 7) indicate that diagenetic bonding in Carboniferous materials is in the nature of mineral-mineral welding whereas that present in the younger sediments may be more characteristic of cationic bonding.

(c) The diagenetic bonding present in the unweathered shales is still retained, but at a reduced level, even when the material is recompressed to pressures in excess of their preconsolidation loads.

(d) The results obtained are in accordance with Bjerrum's theory of diagenetic bonding.

4. (a) By considering the non-recoverable, recoverable and total compressional strain energy components in terms of energy per gram of dry solid, rather than on a total volume basis, a simple model has been put forward to explain the behaviour of clays during compaction, based on the state of packing and the ability of minerals to re-orientate under applied stress.

(b) In the light of the above observations, it would appear that Brooker's hypothesis regarding absorbed strain energy can be questioned.

(c) With regard to previous compaction, the difference between the amount of total compressional strain energy for remoulded and undisturbed materials, decreases until the ratio of maximum depth of burial to maximum consolidation pressure reaches a value of 0.4 (approximately equivalent to 1050m). After this, it remains relatively constant which probably reflects the state of packing of the material. A similar trend is also observed for the non-recoverable strain energy. However, the difference between the recoverable strain energy for undisturbed and remoulded materials remains relatively constant over the complete range and may be dependent upon the amount of diagenetic bonding present.

Chapter Six
Soil Suction Characteristics

6.1 Introduction

Having considered the effect of compaction upon the physical properties of clays and shales, it is now pertinent to investigate their behaviour in the near-surface zones and in particular at outcrop, where the engineering performance will vary the most.

As a consequence, in this Chapter the variation of moisture content with soil suction has been studied in the range of pF 0.3 to pF 4.6 for both the wetting and drying conditions. Experimental techniques are reported in Appendix A.4. Suction characteristics have subsequently been related to the nature of the material (in particular, the Atterberg limits and the mineralogical composition.

Surface area determinations (in m^2/g) on the materials studied have also been made by using the suction curves, and these have been related to the mineralogical composition and certain geotechnical properties.

In addition, evidence is presented of the effect of burial on the suction characteristics of certain shales studied.

6.2 The Relationship between Suction and Effective Pressure

The relationship existing in equation (2) for fully compressible soils can be rearranged to showsin terms of u and P, i.e.

$$s = u - P \quad \ldots\ldots\ldots\ldots\ldots\ldots \quad (26)$$

and in this form it is in the same format as the effective stress equation, i.e.

$$\sigma' = \sigma - u \quad \ldots\ldots\ldots\ldots\ldots\ldots \quad (27)$$

Equations (26) and (27) can be used to find the suction (s)

which combines with zero applied pressure to produce the same moisture content as P and u combined.

In laboratory one-dimensional consolidation experiements, the pore water pressure at the end of each loading increment is zero, hence

$$s = -\sigma \quad \ldots\ldots\ldots\ldots\ldots\ldots \quad (28)$$

The consolidation results from both the undisturbed tests and tests on the remoulded material have furthermore been superimposed (as a broken line) on the suction curves (Fig.5.1), by assuming numerical equality only, and in the cases where the desorption suction curve was obtained (see Appendix A.4.3), it can be observed that the compression legs from the former tests are seen to approximately coincide with these. Therefore, where the desorption curve was not obtained, the consolidation curve has been used to estimate the specific surface areas (Section 6.5) for this condition.

The sorption curve from oven dryness was obtained for all the materials tested. However, close agreement with the expansion legs of the consolidation curves can only be seen in a limited number of cases. In the remainder the final suction moisture content is significantly higher than that from the consolidation test. This may be explained by the fact that the initial condition of the material used for the two tests was not identical, i.e. the wetting suction test involved oven dried material (at 105°C), whereas the consolidation test involved material in the natural condition. Consequently, the oven drying may have enhanced the slaking properties of some of the materials, resulting in their having a higher final moisture content.

6.3 Experimental Methods for the Determination of the Relationship between Suction and Moisture Content

The principal methods used to determine the relationship between

soil suction and moisture content are listed in Table 6.1. Of these only the suction plate (Appendix A4.1) and the pressure membrane (Appendix A4.2) have been employed in this project.

The sorption balance has been used by the Road Research Laboratory for studying the suction/moisture content relationships of comparactively dry soils. In this method the sample is allowed to reach equilibrium with a known humidity; the suction being computed from the thermodynamic relationships between itself and the humidity (Croney and Coleman, 1948). The detailed shapes of the suction curves in the low humidity region have subsequently been used to indicate the mechanism of absorption in soils containing different clays minerals and as a consequence, the surface areas per unit mass are obtainable (see Section 6.5).

Freezing point and electrical methods do not appear to be readily applicable to undisturbed soils (Croney et al, 1958).

6.4 The Relationship of Suction to the Mineralogy and Present State of Overconsolidated Shales

By observing the suction-moisture content relationships (Fig.6.1) those of the Flockton Thin roof shale (Fig.6.1.11), Flockton Thin seatearth (Fig.6.1.12) and the Weald Clay (Fig.6.1.4) are characteristic of incompressible materials (c.f. the Chalk, Lewis and Croney, 1965). Common Carboniferous shales are also concluded to show a similar response (Taylor, 1978).

The initially long, vertical portions of the drying curve at relatively low suctions, observed for the roof shale and Weald Clay, indicate that considerable suction can be applied before the pores begin to empty; drainage appearing to begin, as noted by a change in slope of curves, at pF 3 for the former and pF 2.5 for the latter.

Table 6.1 Methods of Determining the Relationship between Soil Suction and Moisture Content *

	pF Range
Suction Plate or Pressure Plate	0 - 3
Pressure Membrane	0 - 6.2
Centrifuge	3 - 4.5
Freezing Point	3 - 4
Vacuum Desiccator or Sorption Balance	5 - 7
Calibrated Electrical Absorption Gauge	3 - 7

* (After Croney et al, 1958)

From these values to about pF 6 the materials show a steady decrease of moisture content with increasing suction. However, above pF 6 the curve once again steepens, indicating that nearly all the pores have been emptied. Unfortunately, because of complete disintegration upon initial saturation a drying curve for the seatearth was not obtained but may be assumed to follow a similar trend to that obtained for the two other materials.

The wetting curves show a similar trend to the drying curves, in that they have a steep portion at both high and low suctions separated by an area of relatively uniform gradient.

Where both wetting and drying curves were obtained, the materials show a considerable hysteresis and at any given suction the value of moisture content for the former condition is lower than that for the latter condition. The maximum hysteresis value of 1.6 per cent for the Weald Clay occurs at pF 3, whereas that for the roof shale (of about 1.3 per cent) occurs at pF 4.6; the higher suction probably reflecting differences in pore size distributions.

Non-coalescence of the two curves for the Weald Clay may result from differences in lithology of the samples used during testing, although entrapped air can also be responsible according to Childs (1969).

Regarding the saturation moisture content of materials, the Flockton Thin seatearth has a value of 9.6 per cent (Table 6.2) which is twice that of the roof shale. However, because both of these materials are relatively deficient in quartz, the higher value is probably a reflection of the large quantities of expandable minerals in the seatearth coupled with its much lower degree of preferred orientation (Table 4.5) endowing it with a greater slaking ability (Chapter 7). Moreover, since their mineralogical compositions are

similar to younger fully compressible soils containing a fairly inert mineralogy (e.g. Oxford Clay (OC44)), Lias Clay (L36)), a higher saturation moisture content would be anticipated (see Fig.6.2). Therefore it must be concluded that some form of mineral-mineral welding is present in the Carboniferous materials, preventing true expansion upon saturation. Further evidence for diagenetic bonding in Carboniferous materials with a welding nature is offered in Chapters 5 and 7.

The saturation moisture content of the Weald Clay is approximately the same as that observed for the seatearth (i.e. 9.7 - 11.1 per cent), but in this case is probably due to the silty-granular nature of the material since it is not shown to contain any diagenetic bonding, (Chapter 5.10). Philpot (1971) accounts for the difference in the saturation moisture contents of three Carboniferous shales on a bulk density basis, although as with the present Carboniferous materials it is possible that orientation and bonding effects may play an important role.

Suction-moisture content relationships which suggest an intermediate soil type are shown by the wetting curve of the Nacimiento Shale (N2). This material has a characteristically siltstone appearance in the undisturbed state and a liquid limit of 39 which suggests that it should exhibit suction characteristics similar to those of the Weald Clay. However, it can be seen from the suction-moisture content curve (Fig.6.1.16) that it has a maximum moisture content of 27.5 per cent, compared with 10 per cent for the Weald Clay. Moreover, it shows a pronounced sigmoidal shape at relatively low suctions (i.e. pF 0.5 to pF 3.5), followed by a steep linear section up to pF 7. The early curvature may be associated with a greater range of pore sizes than

Table 6.2 Recorded Saturation Moisture Contents

	Sample Ref.	Liquid Limit	Plastic Limit	Saturation Moisture Content
Incompressible Materials				
Weald Clay	WC	36	25	11.1
Flockton Thin roof	FTR	46	24	4.8
Flockton Thin seatearth	FTS	61	26	9.6
Partially Compressible Materials				
Nacimiento Shale	N2	39	14	27.5
Fully Compressible Materials				
London Clay 14m	LC14	84	53	41.7
London Clay 37m	LC37	63	38	35.2
Gault Clay	GC	75	48	35.6
Kimmeridge Clay	KC	70	46	27.0
Oxford Clay 10m	OC10	76	50	38.2
Oxford Clay 44m	OC44	58	29	27.5
Fuller's Earth (Bath)	FE19	100	61	55.0
Lias Clay 10m	L10	68	45	36.5
Lias Clay 36m	L36	65	37	25.7
Kincaid Shale	K6	72	53	22.5
Yazoo Clay	YC	117	85	43.0
Fox Hills Shale	FOX	61	21	35.2
Dawson Shale	DS	75	51	22.0
Pierre Shale (Dakota)	PSD	135	106	92.0

encountered in incompressible and fully compressible materials, and between pF 0.5 and pF 3.5 water enters the structure comparatively rapidly by filling the channels associated with the silty components. At higher suctions, above pF 3.5, the structure is comparatively devoid of water and that which remains is probably held in the structure and small pore spaces of the clay minerals. The relatively high saturation moisture content may also be associated with the presence of 15 per cent smectite, although unlike the Weald Clay, this material appears to have a far higher proportion of clay sized particles* (Table 3.17) which will substantially alter the pore space geometry.

The suction-moisture content relationships for the remaining materials tested (Figs. 6.1.1, 6.1.2, 6.1.3, 6.1.5, 6.1.6, 6.1.7, 6.1.8 6.1.9, 6.1.10, 6.1.13, 6.1.14, 6.1.15, 6.1.17, 6.1.18) are similar to those illustrated by Croney, Coleman and Black (1958) and may be described as those of fully compressible soils, which in general show a gradual decrease of moisture content with increasing suction. However, for complete analysis a shrinkage curve is also required but this was not undertaken in this project. Where both the wetting and drying curves were obtained, hysteresis occurs in a similar manner to that encountered in the incompressible materials, but usually to a greater extent, i.e. in the order of 2 - 9 per cent.

In general the value of the moisture content determined for the fully saturated condition (Table 6.2) increases with increasing plasticity and liquid limit (Fig.6.3), although observations of the behaviour of certain materials leads to a further possible relationship with diagenetic bonding. In particular it is noticed that the unweathered sample of Lias Clay (L36) has a much lower saturation moisture content than its weathered counterpart, even though both

* The writer is unsure of the validity of this value.

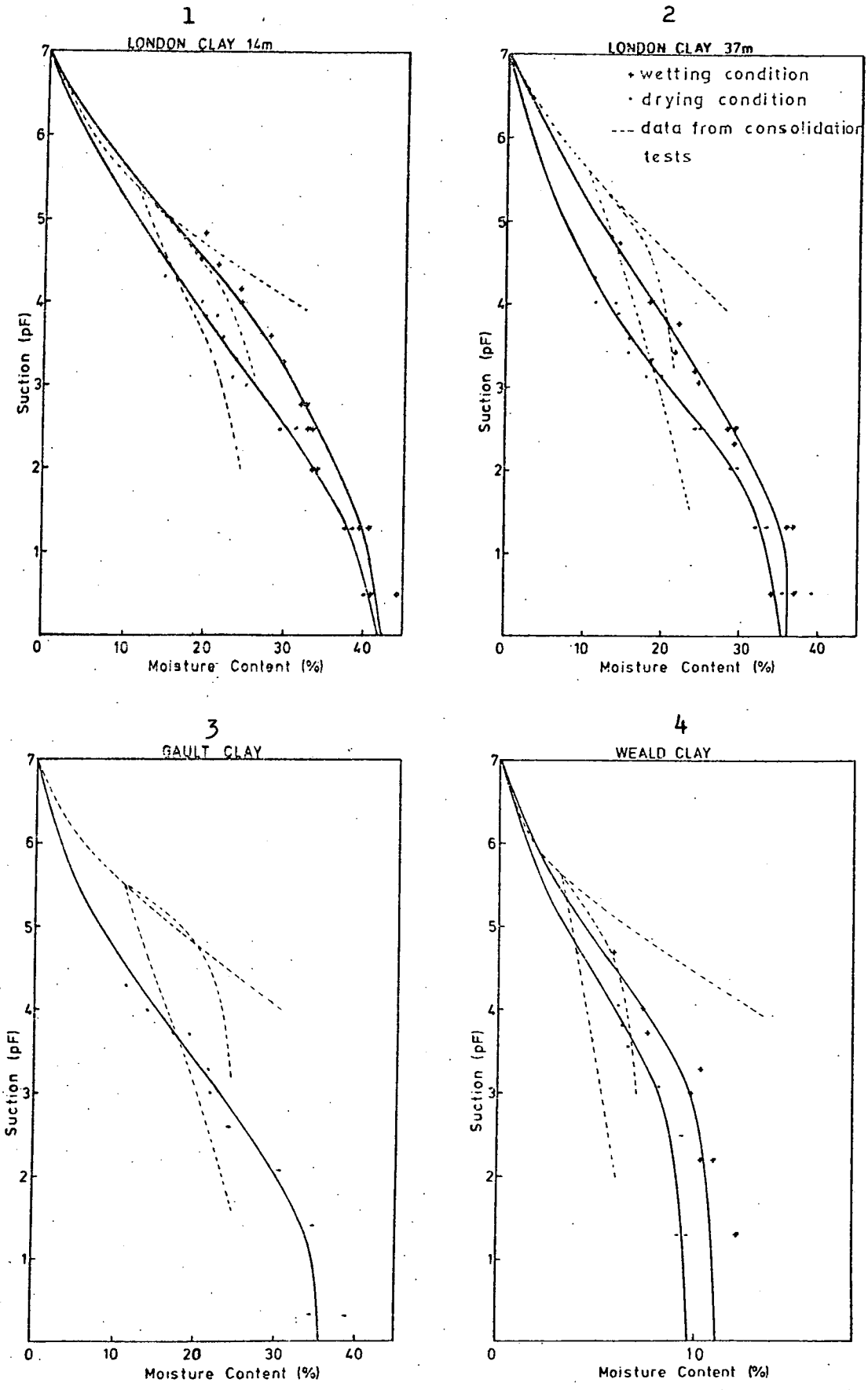

Figure 6.1. Suction - Moisture Content Relationships for Samples Studied.

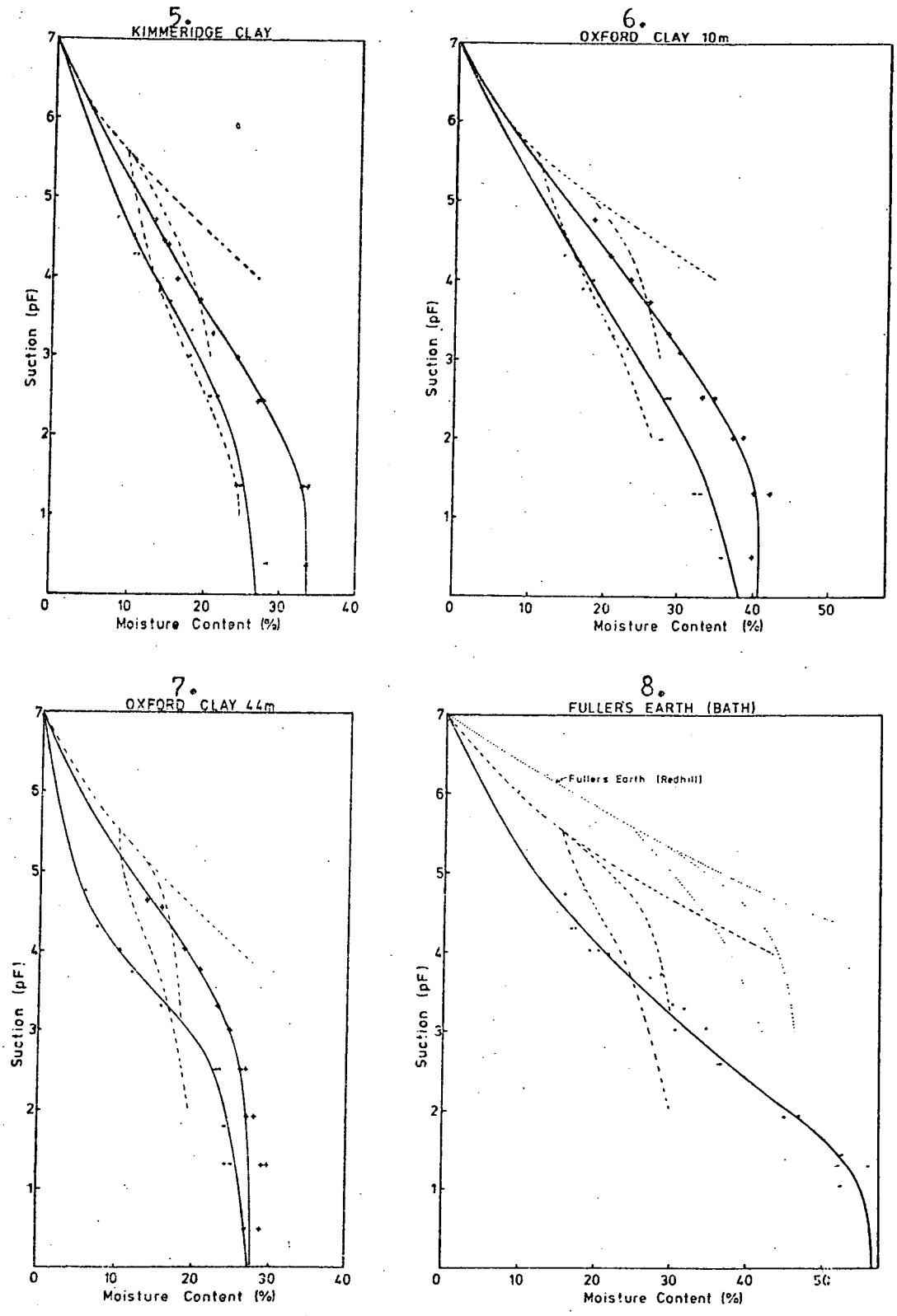

Figure 6.1. cont.

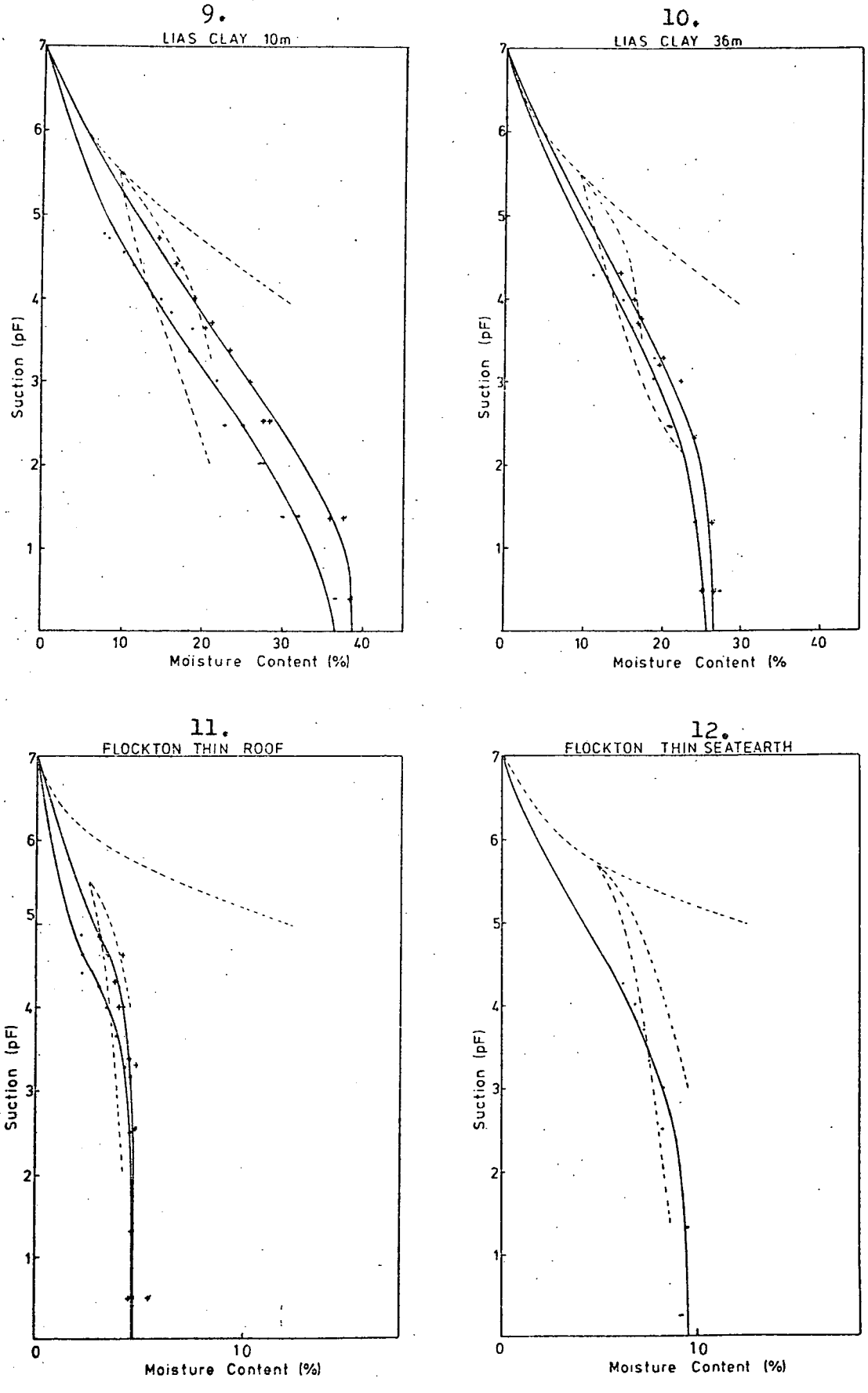

Figure 6.1. cont.

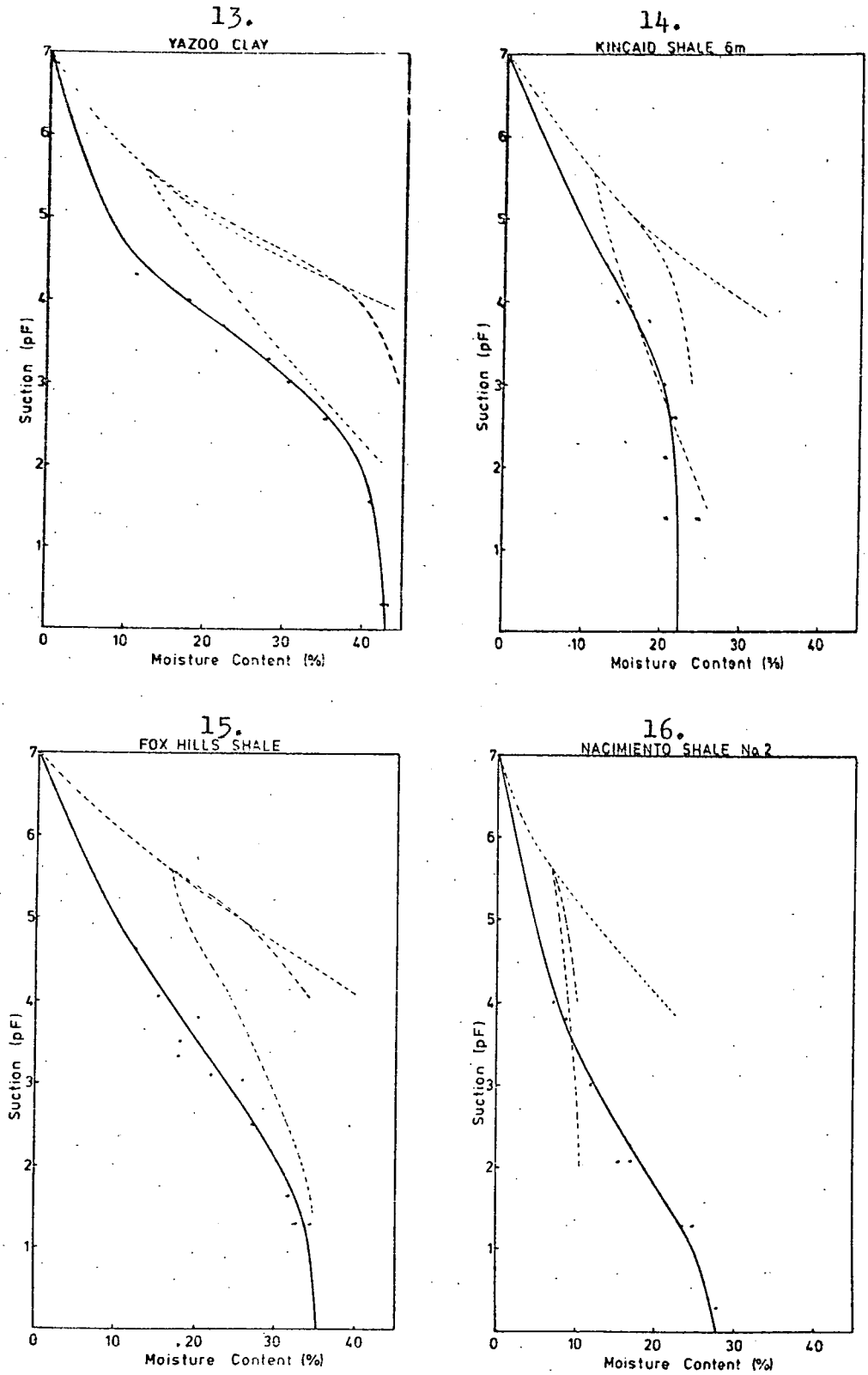

Figure 6.1. cont.

17.

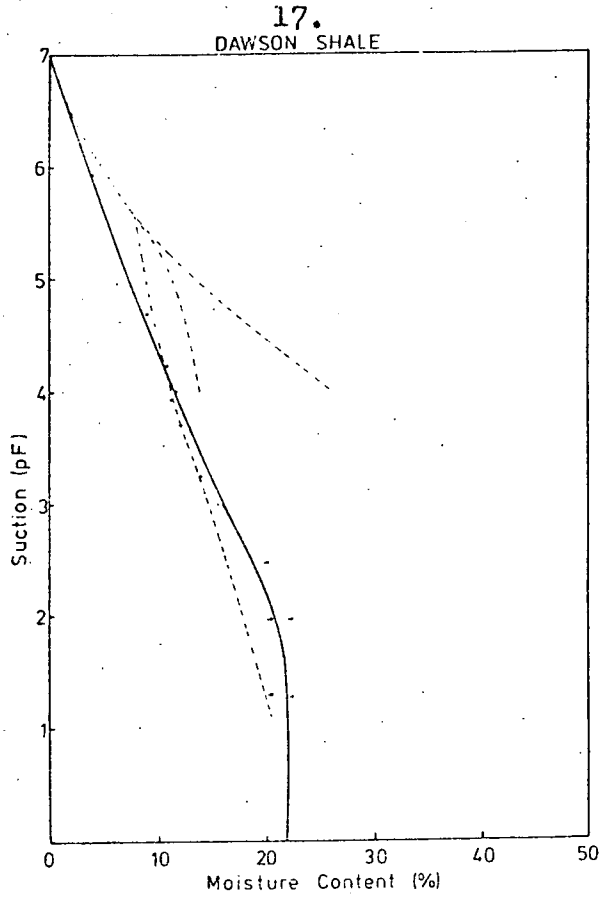

18.

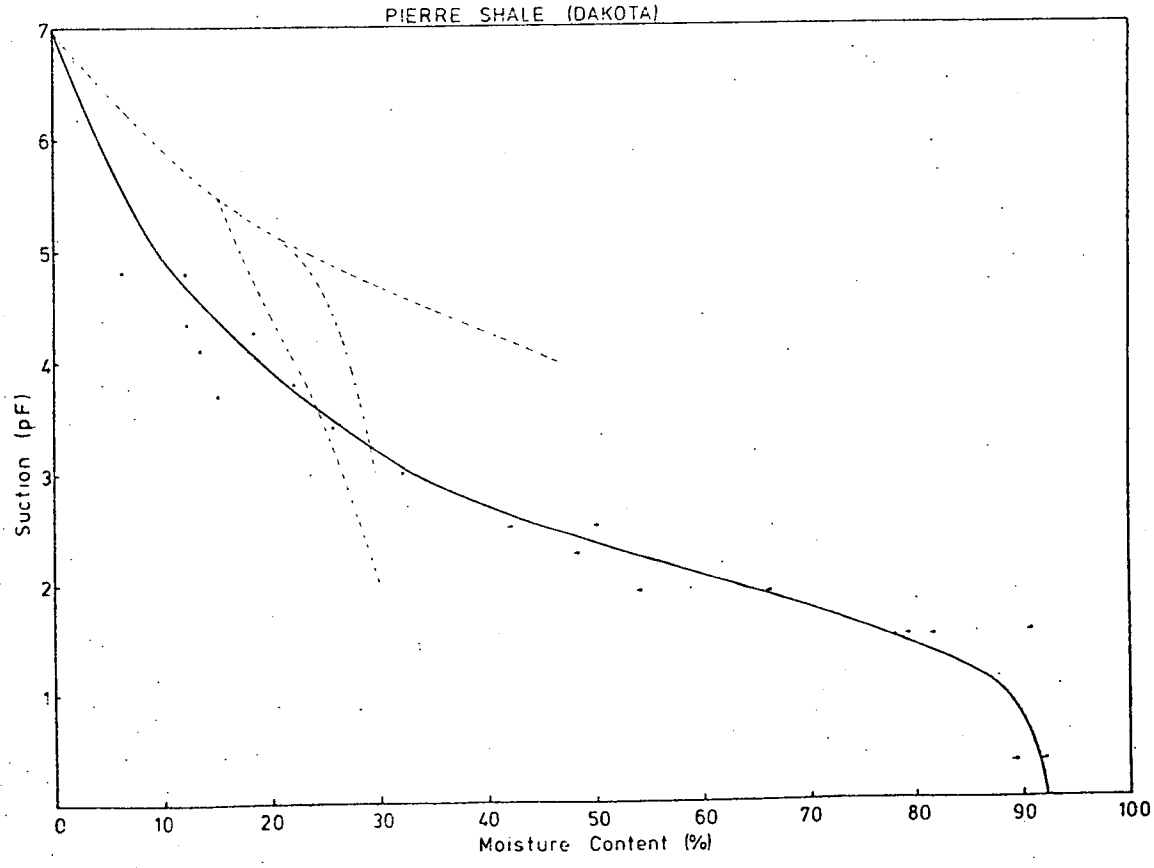

Figure 6.1. cont.

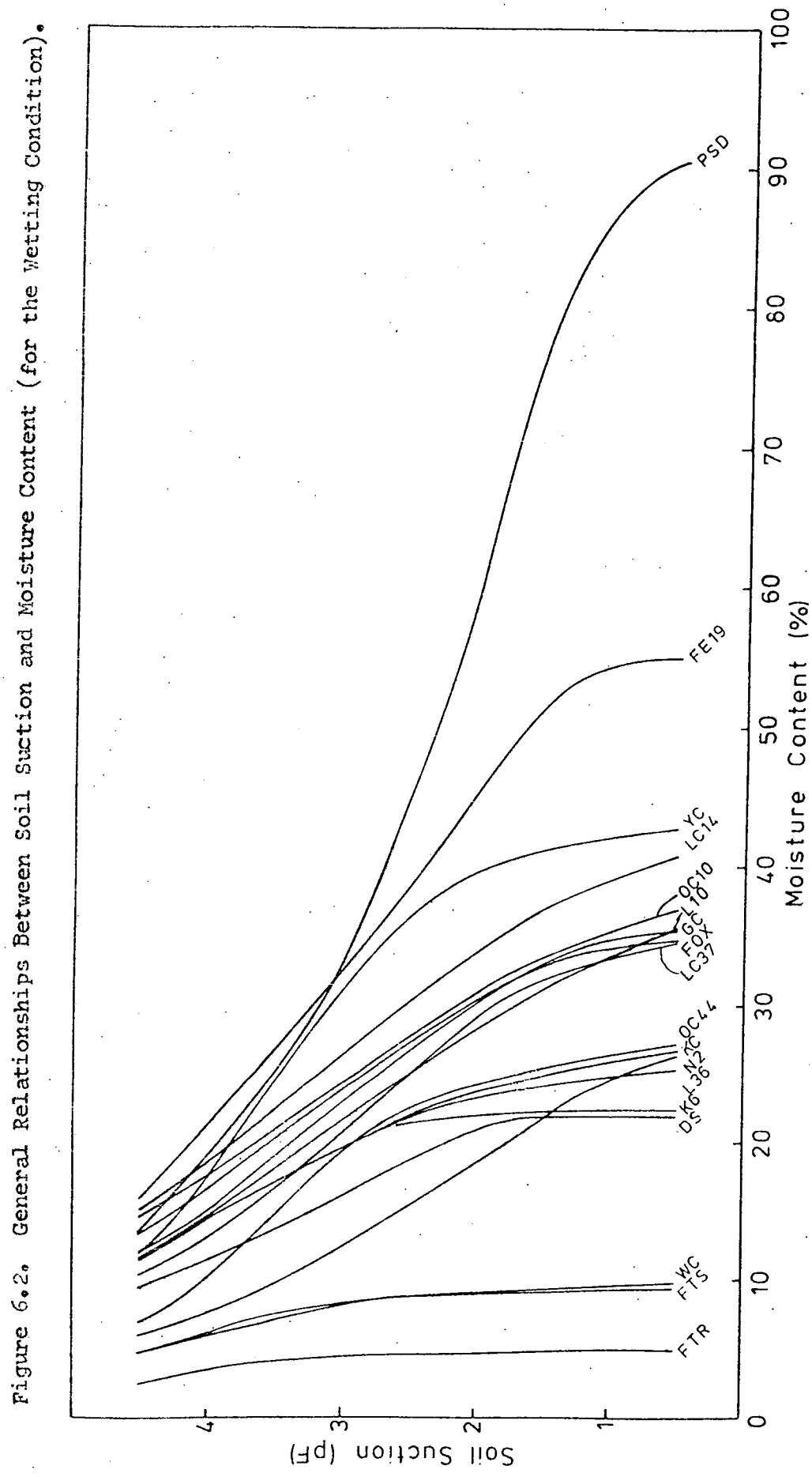

Figure 6.2. General Relationships Between Soil Suction and Moisture Content (for the Wetting Condition).

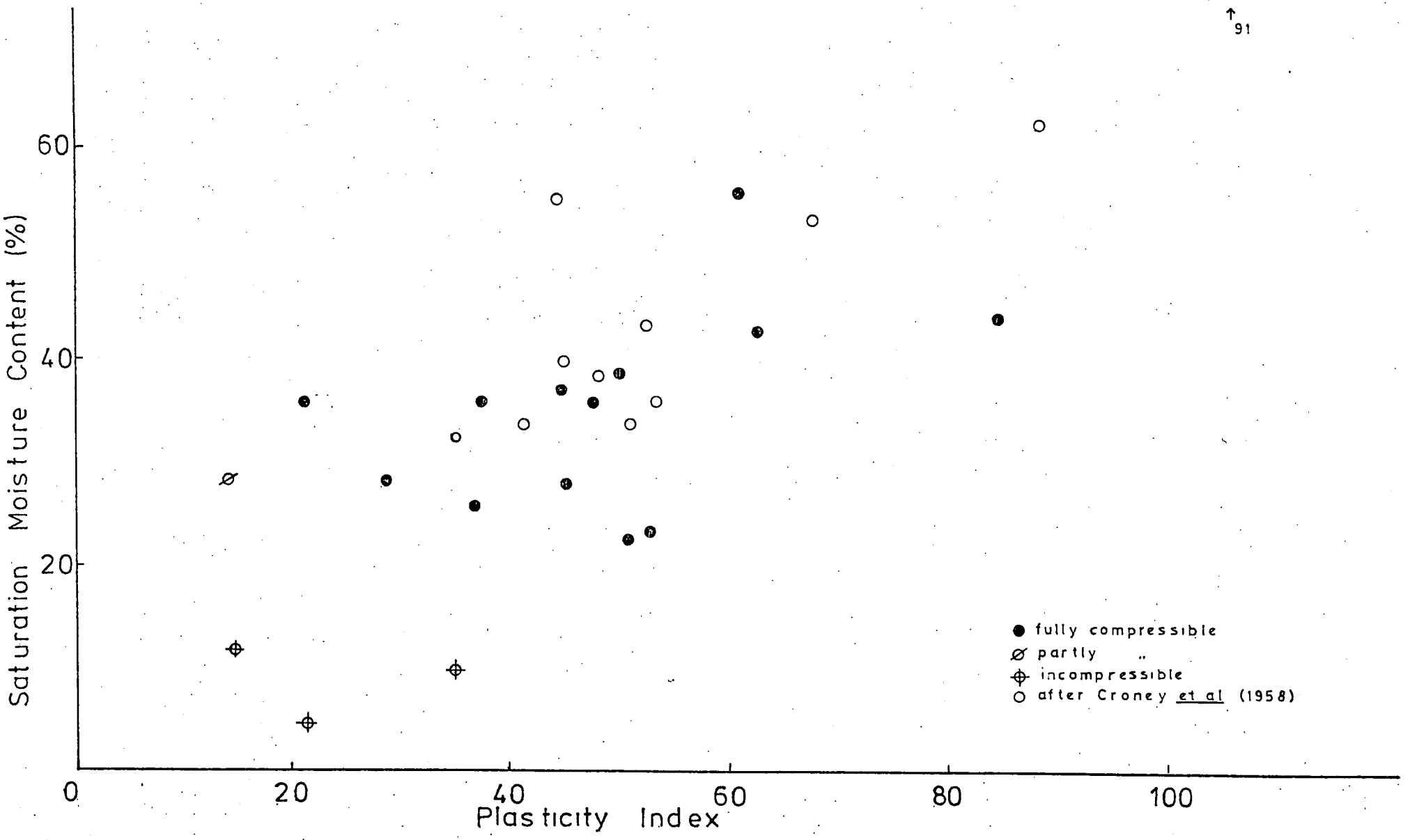

Figure 6.3. Relationship Between Saturation Moisture Content and Plasticity Index.

materials have almost identical mineralogical compositions (Table 3.2) and Atterberg limits (Table 3.16). A similar effect is observed in the Oxford Clay, although in this case it may be partially accounted for by slight differences in the aforementioned parameters. Furthermore for both of these clays, the weathered and unweathered samples appear to possess a similarly high degree of preferred orientation (e.g. by observing fissility in hand specimens and from orientation studies on the latter). Therefore it is possible that diagenetic bonding (postulated in Chapter 5.10) may be preventing true expansion in the unweathered material. Moreover, it is also concluded that the bonding is of a cationic nature, since static slaking tests (Chapter 7) suggest that mineral welding can be discounted. The low value of hysteresis encountered in the Lias Clay (L36) may also be associated with the presence of bonding.

The small differences observed in the curves for the London Clay may be entirely accounted for in terms of mineralogical variations.

6.5 Surface Area Determinations

The B.E.T. equation is designed for use in conjunction with the high range of suction (i.e. 5 - 6.9) therefore in the present work the sorption and desorption isotherms under these conditions have been obtained by extrapolating the suction moisture content relationships in the experimental range (i.e. pF 0.3 - 4.6). In addition where the desorption curve could not be obtained because of complete disintegration of the sample upon saturation (due to the presence of expandable minerals) the compression leg of the consolidation curve (which approximates to the drying condition) has been used for calculation purposes.

Table 6.3 Calculated Surface Areas (m^2/g)

	Sample Ref.	Drying Curve	Wetting Curve
British Material			
London Clay 14m	LC14	134.15	97.43
London Clay 37m	LC37	110.29	62.34
Gault Clay	GC	115.89 *	59.93
Fuller's Earth (Redhill)	FE23	332.54 *	-
Weald Clay	WC	34.93	27.14
Kimmeridge Clay	KC	100.40	73.43
Oxford Clay 10m	OC10	134.20	106.51
Oxford Clay 44m	OC44	95.44	33.31
Fuller's Earth (Bath)	FE19	183.68 *	107.09
Lias Clay 10m	L10	103.36	69.49
Lias Clay 36m	L36	96.41	77.09
Swallow Wood roof	SWR	-	-
Flockton Thin roof	FTR	26.43	13.41
Flockton Thin seat	FTS	58.14 *	33.89
Widdringham Roof	WR	-	-
North American Materials			
Yazoo Clay	YC	151.27 *	63.91
Kincaid Shale 6m	K6	154.25 *	90.83
Kincaid Shale 8m	K8	-	-
Nacimiento Shale	N1	-	-
Nacimiento Shale	N2	83.80 *	43.20
Nacimiento Shale	N3	176.99	-
Fox Hills Shale	FOX	218.69 *	88.10
Dawson Shale	DS	92.59 *	71.36
Pierre Shale (Dakota)	PSD	181.20 *	142.85
Pierre Shale (Colorado)	PSC	-	-

* Calculated from consolidation curve

Table 6.4 Clay Mineral Surface Areas (after Farrar and Coleman, 1967)

		Total Area	Ext. Area *
London Clay	Heathrow, Middex	91	56
London Clay	Uxbridge, "	96	60
London Clay	Eastry, Kent	97	51
Gault Clay	Dunton Green, Kent	80	48
Gault Clay	Steyning, Sussex	98	40
Gault Clay	Aylesbury, Bucks	133	50
Gault Clay	Shaveswood, Sussex	186	51
Weald Clay	N. Holmwood, Surrey	45	27
Weald Clay	Ditchling Common, Sussex	94	42
Kimmeridge Clay	Gillingham, Dorset	79	57
Kimmeridge Clay	Sunningwell, Berks	126	54
Oxford Clay	Waddesden, Bucks	41	32
Oxford Clay	Cumnor, Berks	88	39
Oxford Clay	Alconbury, Hunts	71	37
L.Lias Clay	Stonehouse, Gloucs.	65	29
L.Lias Clay	Shipton, Oxon	75	38
Keuper Marl	Elaby, Leics.	61	50
Marl in Keuper	Measham, Staffs.	34	28
U. Coal Measures	Kingbury, Leics.	38	28

* Calculated from the nitrogen isotherm using the B.E.T. equation.

Ca Montmorillonite	491	122
Ca Illite	95	84
Ca Kaolinite	23	18

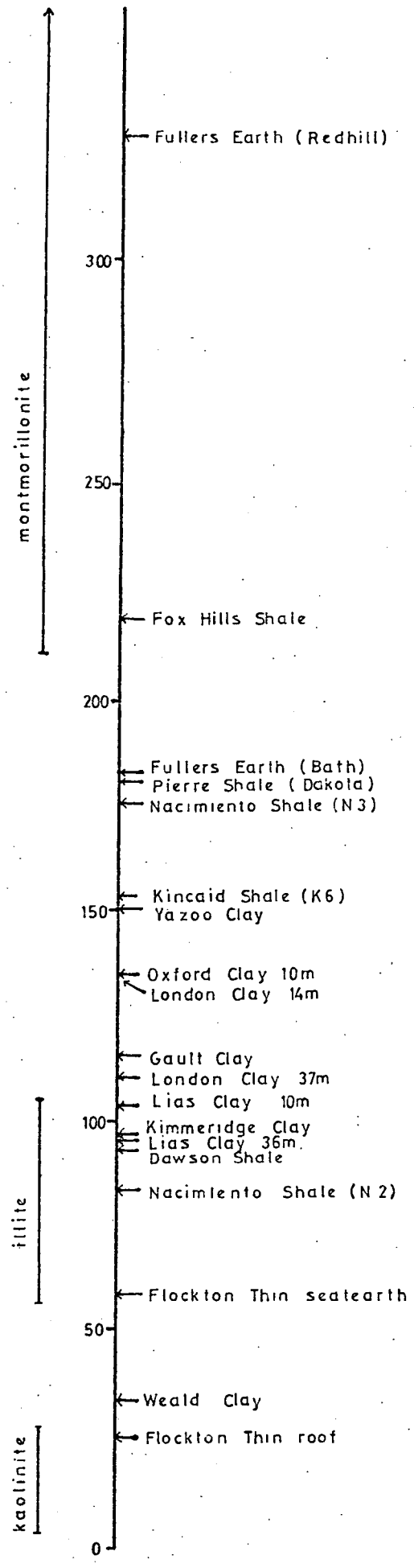

Figure 6.4. Calculated Surface Areas (in m^2/g) in Relation to those of Pure Clays.

Since the B.E.T. equation can be applied to both the sorption and desorption conditions, it follows that two values for the total surface area of each clay can be determined (Table 6.3). Farrar (1963) suggests that this could arise from slight differences in the molecular arrangements on the soil surface. If, on the other hand, the nitrogen absorption isotherm is studied, then when the B.E.T. equation is applied, only the external surface area is determined (see Table 6.4). However, for ease of identification, the following discussion is based on the total surface area calculated from the desorption curve, unless otherwise stated.

The range of surface areas encountered for the British materials studied in this project varies from 26.43m^2/g to 332.54m^2/g; the majority (8 out of 13) lying within the range of 95 - 135m^2/g, suggesting a dominance of illite (having a range of 67 - 105m^2/g) in these materials, (Fig.6.4). Farrar and Coleman (1967) also quote similar values for a similar sequence of clays from the British Isles (Table 6.4).

The Fuller's Earth from Bath (sample FE19) and Fuller's Earth from Redhill (sample FE23), yield total surface areas of 183.68m^2/g and 332.54m^2/g respectively. The latter value lies well within the published range of 210 - (?)1000m^2/g but the lower value shown by the former sample may be indicative of the relatively high proportion of other minerals present (Table 3.2). The writer also suggests, speculatively, that as this material is much older and has been buried more deeply, the chemistry may affect its re-expansion by the formation of rigid domains similar to those proposed by Alymore and Quirk (1959), although no supporting evidence can be offered for this statement. Nevertheless, since the surface areas of both shales occur towards the lower end of the smectite range, this indicates that Ca is the dominant exchangeable cation. Philpot (1971) quotes a value of

539m^2/g as the surface area of a sodium montmorillonite.

The three remaining British materials are all hard, incompressible materials which show low values for their surface areas. The recorded value for the Weald Clay of 39.93m^2/g may be attributed to the high quartz content of this material (Table 3.2), whereas the Flockton Thin roof and seatearth, having computed surface areas of 26.43 and 58.14m^2/g respectively consist mainly of illite, kaolinite, and mixed-layer clay. These values are consequently lower than would be anticipated for such sediments and it is suggested that their indurated nature may account for the reduction in the surface areas and small moisture uptake as shown from the suction curves. It is nevertheless interesting to note that the seatearth, containing a large amount of mixed-layer clay and practically no quartz (Table 3.2) has a significantly larger surface area than the roof shale, which it is suggested may be a reflection of its greater ability to slake upon immersion in water. Philpot (1971) also records low surface areas for Carboniferous materials containing large amounts of 10Å illite (plus kaolinite and quartz), e.g. High Hazels - 32m^2/g and the Park seatearth 19m^2/g, but he also records higher values (of 68 - 105m^2/g) where a large proportion of mixed-layer clay is present (i.e. in certain tonsteins).

The North American materials, being mainly smectite - quartz sediments with minor amounts of illite and kaolinite, have surface areas which are in general, larger than those of the British sediments and which range from 83.80m^2/g to 216.69m^2/g.

The Dawson Shale, Kincaid Shale (K6) and the Nacimiento Shale (N2) have particularly high granular contents (quartz + feldspar+ calcite) i.e. 53, 56 and 46 per cent respectively and yet their

surface areas are much larger than that encountered in the Weald Clay, which has a similar granular content. This phenomenon must be solely accounted for by the smectite content present in these materials (Table 3.2).

The remaining four materials tested (Table 6.3), having relatively low granular contents (Table 3.2), also show the dominance of smectite reflected in their surface areas; the values equating reasonably well with the calculated values for the Fuller's Earth (Redhill) when the concentrations are considered.

Conclusions

(1) Suction-moisture content relationships obtained from suction plate and pressure membrane experiments have indicated whether the shales tested possess incompressible, partly compressible or fully compressible soil characteristics.

(2) Suction-moisture content relationships for certain incompressible materials are inconsistent with their mineralogy but have been associated with the presence of diagenetic bonding. Similar observations, but of a lesser degree have also been made for certain fully compressible materials.

(3) With the exception of the Carboniferous materials, surface area determinations are consistent with mineralogical compositions. Those of the Carboniferous shales, are however, much lower than expected and are again attributed to the presence of strong bonding welding the particles together.

(4) In general, for fully compressible materials, the saturation moisture content increases with increasing plasticity and liquid limits.

Chapter Seven

Slaking Behaviour of Over consolidated Shales

7.1 Introduction

Upon entering the zone of weathering, compacted argillaceous sediments disintegrate at varying rates depending on the nature of the material. As a result of this, it is often essential for the engineering geologist to obtain a measure of the breakdown which may occur, especially when the rocks are at outcrop. Consequently several attempts have been made to classify shales from their slaking behaviour (e.g. Morgenstern and Eigenbrod, 1974; Franklin and Chandra 1972; Gamble, 1971), although at present no absolute classification has been obtained.

In the present work, two simple slaking tests (using water as the slaking medium) have been employed with a view to constructing a classification of the shales tested. One of these methods is based on a static test, the other upon the rate of disintegration to below a specified mesh size. In addition, the results are also seen to offer indirect evidence of the type of diagenetic bonding present within certain materials (see Chapter 5).

Finally, an indication of the possible erodability of the materials studied by the incidence of dispersion has been postulated by examination of the cations present in the pore water and on the exchange sites.

7.2 Slaking Tests

7.2.1. A Review of Previous Testing Procedures

A large number of tests to quantify the slaking behaviour of clays and shales, have been devised by engineers, concerned with the stability of clay masses, and soil scientists concerned with crumbs or aggregates.

A simple static descriptive test, used by such workers as Eno (1926), Mead (1936), Denisov and Reltov (1961), Brooker (1967) and Fleming et al (1970) involves immersing a specific amount of solid of known shape in a liquid for a given time and observing the disintegration by means of an arbitary numerical classification. This test has also been used to distinguish between compaction shales and cemented shales (Mead, 1936), to classify shales (Emerson, 1967) and to study fabric anisotropy (Hvorslev, 1960). The static test used by Taylor and Spears (1970) is a quantitative version of these methods.

The Public Roads Administration's original slaking test (Hogentogler, 1937) involves recording the time taken for a dried cylinder of soil to fall through a brass ring or coarse screen when completely immersed in water. Whereas the Public Roads Administration's alternative slaking test involves recording the change in apparent weight as a function of time of a specimen which is placed in a container attached to a balance and partly immersed in water. A similar type of test was used by Moriwaki (1974).

The Russian pedologists slaking test (Hogentogler, 1937) involves producing a soil specimen in a mould used for moulding tensile test specimens of cement mortar. After drying, it is completely coated in paraffin except for a $\frac{1}{4}$ inch band around the middle, and then suspended in water. The time taken for complete separation is referred to as the slaking time.

The falling drop test (McCalla, 1944) which is also a type of erosion test, is performed by allowing drops of distilled water, of known diameter, to fall a known distance on to a lump of material until it is also washed away through a screen.

In the single screen wet-sieving test (Bouyoucos, 1929) a known amount of graded aggregate is placed on a sieve of given size and after presoaking, the sieve is oscillated vertically in water at a known rate and stroke for a given length of time. The dried weight retained is subsequently recorded. In the multiple-screen wet-sieving test (Bouyoucos, 1935; Yoder, 1936;) a given amount of material is sieved through a series of screens, decreasing in size in descending order.

Franklin and Chandra (1972) and Gamble (1971) have used a slake durability test, modified from the N.C.B.'s 'end-over-end' test of the mid-1950's whereby the material is placed in a cylindrical drum made of standard 2mm mesh and which has its axis in the horizontal plane. After partial immersion in water the drum is rotated at a constant speed for a given time; the ratio of final to initial weight retained in the drum is the slaking durability index. Although this test has been adopted as an International Rock Mechanics Standard, it has serious defects in the case of argillaceous rocks. It is a dynamic attrition test, the prototype of which was introduced originally by the N.C.B. for performance simulation of coal washing plant. Moriwaki (1974) is critical of the results obtained using oven-dried shales. Morgenstern and Eigenbrod (1974) have devised a water absorption slaking test whereby a dried sample is cut into a perforated brass cylinder, open at both ends, and saturated by placing the sample on a wet filter paper. The increase in moisture content with each of a number of drying and wetting cycles is subsequently measured.

7.2.2. Present Test Procedures

(a) The shales under test, having previously been cut into a cylindrical shape measuring 1cm in height by 1cm in diameter,

and air dried for several weeks (shrinkages are presented in Table 4.1), were subjected to a slightly modified version of the Public Roads Alternative Slaking Test, (see Appendix A5.1). The rate and amount of disintegration of rock debris below mesh size B.S. No.36 were subsequently obtained. In addition, during each test, the slaking behaviour of each material was carefully noted.

(b) A purely static test, reported in Appendix A5.2 has been employed to measure the uptake of water after air-drying. The results of this have ultimately been reviewed in the light of the work of Morgenstern and Eigenbrod (1974).

7.3 Rate and Amount of Breakdown in Water

Tests to determine slaking behaviour were performed on all of the materials studied, except for the Keuper Marl, which by virtue of its nature (Chapter 2) could not be cut into a suitable shape for testing. Observations made during each test about the way in which breakdown occurred are presented in Table 7.1.

To define the rate of disintegration, two methods of presentation have been employed. Firstly the percentage of material passing through the mesh has been plotted directly as a function of the time (in minutes), and secondly the rate has been expressed in the form of a first order reaction from the expression:

$$\text{Log}_e \frac{M}{M_o - M} = kt \quad \ldots\ldots\ldots\ldots\ldots\ldots \quad (29)$$

where M_o is the original weight of material and M is the weight passing through the mesh at time t. According to Badger et al (1956) and Berkovitch et al (1959) if the material is homogeneous then the rate of disintegration below a given size will be proportional to the weight

still above that size. However, they point out that the surface area will also be an important factor; its ratio to the percentage of oversize material varying as disintegration proceeds.

When the results of the samples currently under discussion are reviewed in the light of the first method of presentation (Figs. 7.1 and 7.2) then it can be seen that there is a very large spread in the breakdown rates (Table 7.2). In a large number of instances an almost linear relationship between percentage passing and time is observed over the initial stages of the disintegration. Consequently the rates of disintegration have been split into three groups, i.e. rapid slaking (rate greater than 3.5% per min.), fast-medium slaking (rate 3.5 - 0.5% per min.) and slow slaking (rate less than 0.5% per min.), principally by reference to the behaviour of the British materials, although the same divisions appear quite satisfactory when the North American materials are considered.

Shales which fall into the rapid slaking catagory (i.e. 2 British and 6 American samples) predominantly contain large amounts of expandable clay minerals (principally smectite), causing some of these materials (e.g. the two Fuller's Earths and the Nacimiento Shale N3) to literally explode when immersed in water. Taylor and Spears (1970) report that certain British Coal measures strata containing large quantities of mixed-layer clay (e.g. Stafford Tonstein) are also explosive when immersed in water and the writer suggests that these materials would undoubtedly fall into the rapid slaking group.

From observations made during the tests (Table 7.1), materials falling within the rapid slaking group disintegrated by initially shedding tiny flakes and particles from the edges immediately after immersion, followed by a general slumping of the mass with associated loss of structure. The Dawson Shale did, however, retain some sort of structure

Table 7.1 Breakdown Observations of Shales Studied

British Materials

London Clay 14m London Clay 37m	Rapid flaking and dislodgement of particles from edges. General loss of shape.
Gault Clay	Rapid loss of structure into a pile of particles and flakes.
Fuller's Earth (Redhill)	Rapid disintegration and loss of structure.
Weald Clay	Slow slaking at edges and along planes of weakness.
Kimmeridge Clay	Rapid flaking and dislodgement of particles from edges. Loss of structure.
Oxford Clay 10m	Breaks along planes of weakness with associated disintegration into flakes and particles.
Oxford Clay 44m	Splits along bedding into fine laminae.
Fuller's Earth (Bath)	Rapid disintegration and loss of structure.
Lias Clay 10m	Slumped into mass of varied shaped flakes.
Lias Clay 36m	Split along bedding, plus small amount of flaking.
Swallow Wood roof	Splits along parallel planes into thick laminae
Flockton Thin roof	Splits along parallel planes into thick laminae.
Flockton Thin seatearth	Rapid slaking into large flakes and chips
Widdringham roof	Splits along parallel planes into thick laminae.

North American Material

Yazoo Clay	Rapid disintegration and loss of structure.
Kincaid Shale 6m	Rapid disintegration and loss of structure.
Kincaid Shale 8m	Slakes into small aggregates.
Nacimiento Shale N1	Attack along bedding with some disaggregation.
Nacimiento Shale N2	Initial attack along bedding followed by slow disintegration.
Nacimiento Shale N3	Rapid disintegration and loss of structure.
Fox Hills Shale	Rapid formation of chips and flakes, structure quickly lost.
Dawson Shale	Disintegration by flaking and particle dislodgement. Shape remains relatively intact.
Pierre Shale (Dakota)	Rapid disintegration and loss of structure.
Pierre Shale (Colorado)	Small aggregate and individual particle dislodgement from edge. Shape remains intact.

Table 7.2 Rate and Amount of Breakdown

British Materials	Sample Ref.	% Passing B.S. No.36 Mesh	Rate of Disintegration (% per minutes)
London Clay 14m	LC14	94	3.00
London Clay 37m	LC37	80	2.00
Gault Clay	GC	94	3.00
Fuller's Earth (Redhill)	FE23	100	19.00
Weald Clay	WC	22	0.15
Kimmeridge Clay	KC	91	2.50
Oxford Clay 10m	OC10	65	1.75
Oxford Clay 44m	OC44	0	0.00
Fuller's Earth (Bath)	FE19	99	13.00
Lias Clay 10m	L10	40	1.00
Lias Clay 36m	L36	5	0.25
Swallow Wood roof	SWR	0	0.00
Flockton Thin roof	FTR	0	0.00
Flockton Thin seat	FTS	6	0.23
Widdringham roof	WR	0	0.00
North American Materials			
Yazoo Clay	YC	94	8.00
Kincaid Shale 6m	K6	83	4.25
Kincaid Shale 8m	K8	70	1.50
Nacimiento Shale	N1	21	0.40
Nacimiento Shale	N2	82	0.35
Nacimiento Shale	N3	98	22.50
Fox Hills Shale	FOX	87	4.25
Dawson Shale	DS	87	3.75
Pierre Shale (Dakota)	PSD	97	5.50
Pierre Shale (Colorado)	PSC	96	1.50

during the early stages of the test. Typical examples of slumped masses are shown in Figure 7.3, where it can be observed that the Fuller's Earth (Bath) has disintegrated to a much finer state than the Pierre Shale from Dakota (which contains exchangable sodium cations in the smectite). For the group as a whole usually over 80% of the material disintegrates below mesh size, (Table 7.2).

Preferred orientation studies (Table 4.5) indicate that all of these materials, with the exception of the Yazoo Clay, have a randomly orientated structure. However, although the structure of the Yazoo Clay contains a high degree of preferred orientation, the writer considers that this is completely over-ridden by the nature of the mineralogy (Table 3.2).

In the fast-medium slaking group (which contains 7 British and 2 American samples), breakdown was observed to occur in number of ways. At the faster end of the group, the members slaked principally by flaking and dislodgement of particles from the edges, with an associated general loss of structure into small lumps, rather than slaking of the whole mass (like materials in the rapid slaking group). The Gault Clay, and to a certain extent, the Kincaid Shale (K8) disintegrated quite slowly at first, but after about 10 minutes, the rate rapidly increased. The writer surmises that slaking of these materials may have a certain critical pore-air pressure, (see Taylor & Spears, 1970) above which they are blown apart from within.

The Pierre Shale (Colorado) which disintegrated at a rate in the middle of the range (Fig. 7.2) retained its structure almost to the end of the test; slaking occurring by surface dislodgement of particles and small flakes at an almost constant rate.

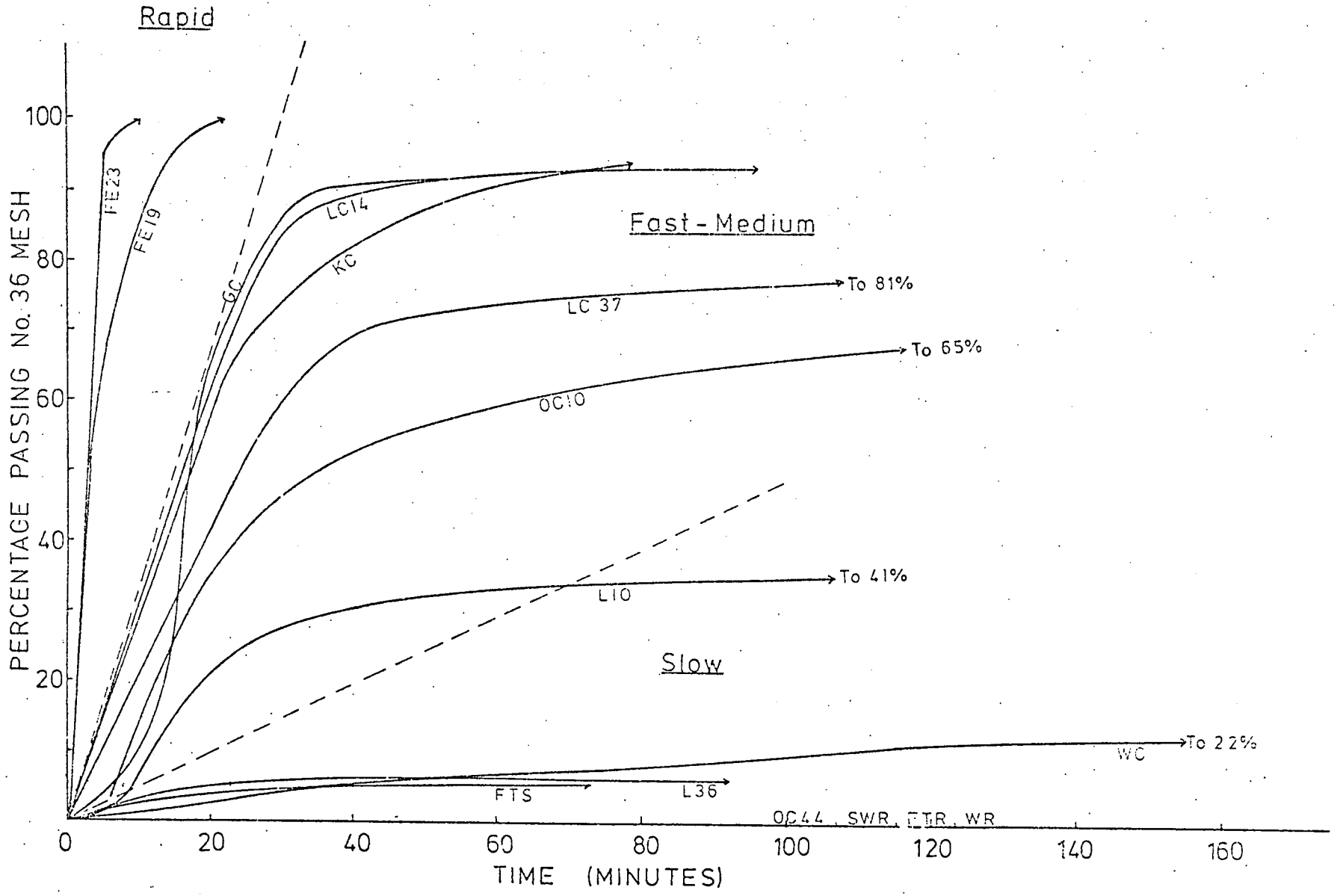

Figure 7.1. Breakdown - Time Relationships for the British Materials.

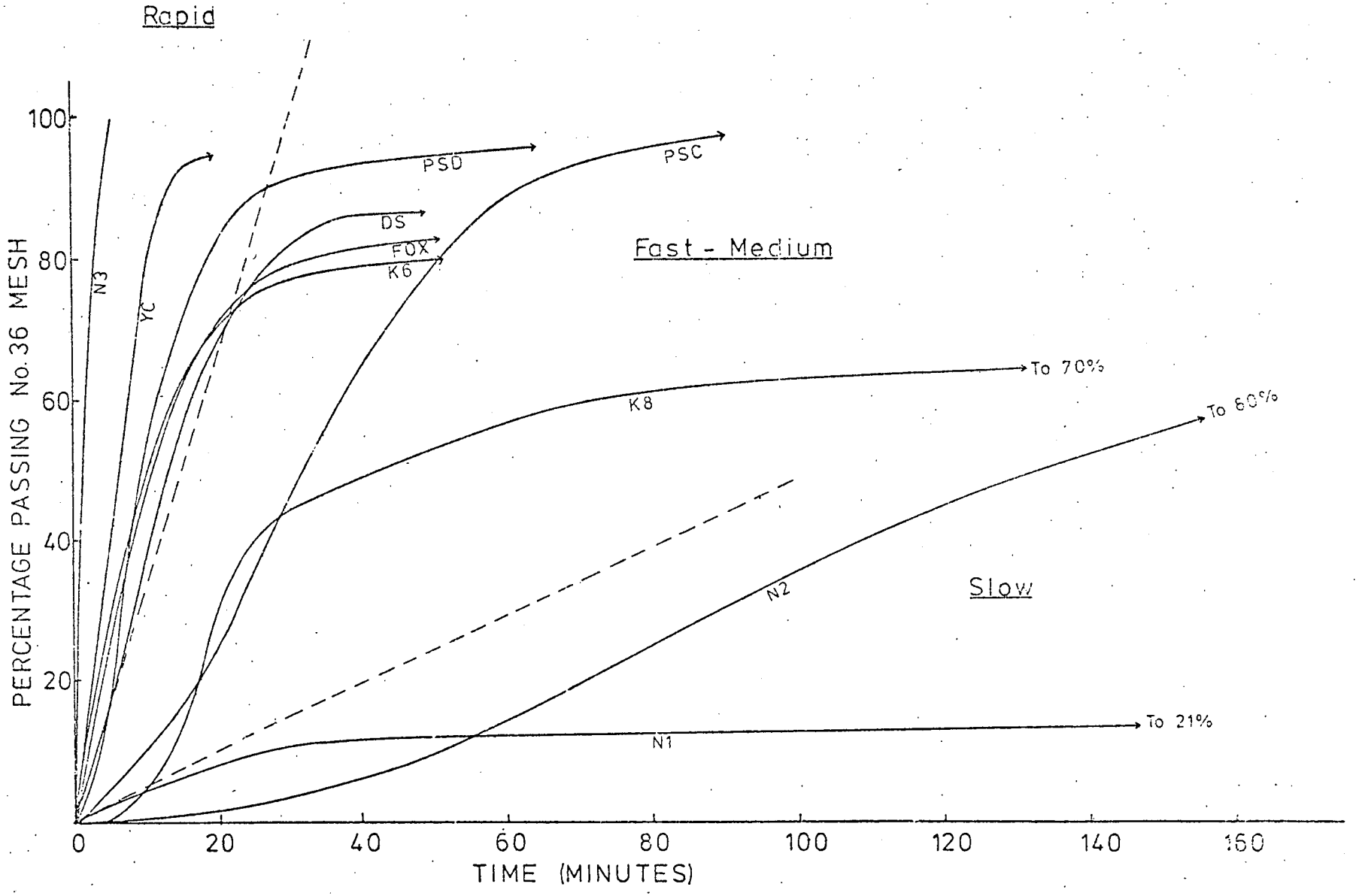

Figure 7.2. Breakdown - Time Relationships for the North American Materials.

At the slower end of the fast-medium range, the Oxford Clay (OC10) and Lias Clay (L10) started to disintegrate by splitting along planes of weakness, which usually coincided with the direction of bedding, followed by a slow dislodgement of particles and flakes.

The amount of observed breakdown below mesh size was also variable and ranged from between 90 - 100 per cent at the faster end to 45 per cent at the slower end of the group (Table 7.2).

With regard to preferred orientation, where quantitative results were obtained (Table 4.5) it appears that materials at the faster end of the range have very poorly orientated fabrics, but in general better than those materials in the rapid slaking group. Also, in a number of cases (e.g. the London Clay, Gault Clay, Pierre Shale and Kincaid Shale (K6)) smectite and expandable mixed-layer clays are present to a moderate degree which must aid the disintegration process. No orientation studies were performed on the Oxford Clay (OC10) and Lias Clay (L10), from the slower, end of the group. However, these materials, although quite soft, did tend to split along sub-parallel planes to the bedding and it can be subsequently postulated that they would have a better preferred orientation than those materials at the faster end of the range.

Materials falling within the slow breakdown group exhibit a wide range of behaviour. The Nacimiento Shales N1 and N2 are siltstone like materials (Chapter 2) and contain almost identical mineralogical compositions (Table 3.2). Slaking in both cases proceeded by attacking planes of weakness (parallel to the direction of bedding), followed by a slow disaggregation. However, at the end of the time alloted, over 82 per cent of sample N2 had passed through the mesh compared with 21 per cent for sample N1. Therefore, because both materials contain between 15 - 17 per cent smectite, which should aid breakdown, it can only be concluded that sample N1 is being held together by some form

of cementation or bonding, which although is comparatively weak (Chapter 5.10), is slightly stronger than that in sample N2. The end result of the slaking test on sample N1 is presented in Figure 7.5.

The Weald Clay, a quartz-rich sediment, also disintegrated slowly, principally by attacking planes of weakness. Ultimately 22 per cent passed through the mesh producing a similar end result to sample N1, (of irregular shaped chips - Fig. 7.4).

Of the six remaining samples in this group (all British) two exhibit minor breakdown below mesh size (i.e. the Lias Clay (L36) and the Flockton Thin seatearth), whereas four materials (i.e. the Oxford Clay (OC44), the Swallow Wood roof, the Flockton Thin roof and the Widdringham roof) did not disintegrate at all below the alloted mesh size in the given time. The seatearth, which contains a high proportion of mixed-layer clay and degraded kaolinite (Table 3.2) and which also has a randomly orientated structure (Table 4.5) was seen to breakdown into flakes and chips (larger than the mesh size) at a comparatively rapid rate; in fact the major part of the event took place within the first 10 - 15 minutes after immersion. However, these chips then remained as hard entities (Figure 7.10) for the remainder of the slaking period.

The slaking behaviour of the Oxford Clay (OC44), Lias Clay (L36), Swallow Wood roof, Flockton Thin roof and Widdringham roof, all of which contain a fairly inert mineralogy of illite - kaolinite - quartz (Table 3.2) is dominantly controlled by their highly preferred orientation of clay minerals, in that breakdown of the post-Carboniferous shales occurred by separation of the material into thin laminae parallel to the bedding (Figs. 7.6 and 7.7), although the Carboniferous sediments, being far more compacted, tended to split into thicker units (Figs. 7.8, 7.9, 7.11).

Figure 7.3. Typical Breakdown of Smectite-Rich Sediments.

Figure 7.4. Breakdown of the Weald Clay.

Figure 7.5. Breakdown of the Nacimiento Shale (N2).

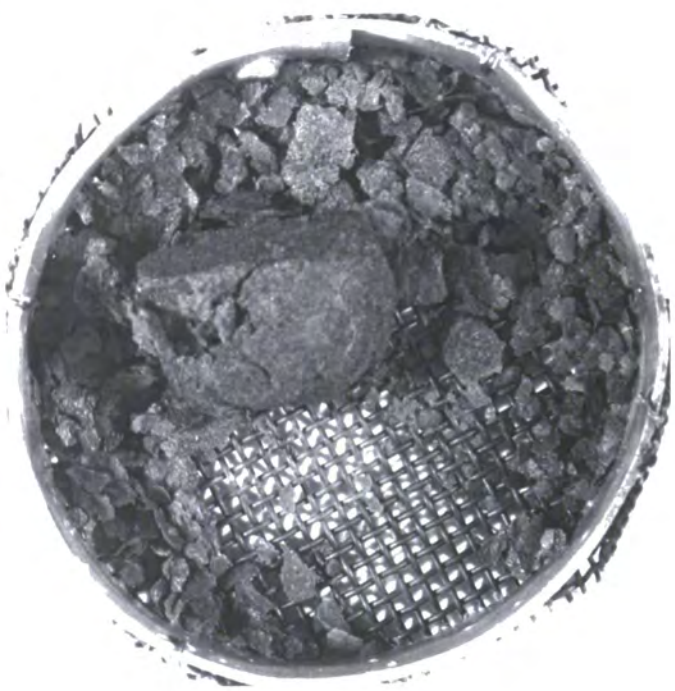

Figure 7.6. Breakdown of the Oxford Clay 44m

Figure 7.7. Breakdown of the Lias Clay 36m.

Figure 7.8. Breakdown of the Swallow Wood roof.

Figure 7.9. Breakdown of the Flockton Thin roof.

Figure 7.10. Breakdown of the Flockton Thin seat - earth.

Figure 7.11. Breakdown of the Widdringham roof.

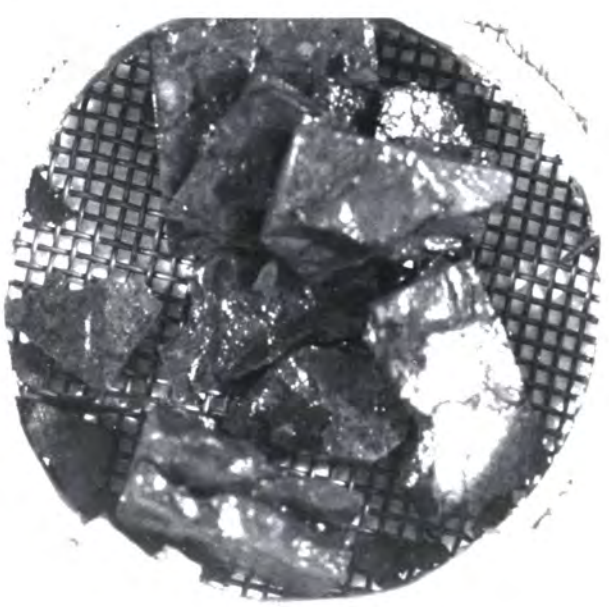

An interesting feature observed for the Oxford and Lias clays, was that their weathered equivalents (previously discussed) did partially disintegrate below mesh size. This must reflect the absence of bonding in these forms, coupled with a slightly disturbed fabric (seen in hand specimen but not quantitatively analysed).

In terms of first order reactions (Figs.7.12 and 7.13) four materials from the rapid slaking group (i.e. the two Fuller's Earths, the Nacimiento Shale N3, and the Yazoo Clay) yield an approximately linear relationship over their entire breakdown; only a very small amount of curvature occurring at the end of the process. The remainder of the materials from this group (Fig.7.13) only show a linear relationship for the first 20 - 25 minutes, followed by a gradual reduction in the amount of slaking until breakdown ceases. This may well be associated with micro-lithological changes whereby the more inert areas upon being exposed, take longer to breakdown. This is supported by the fact that a certain proportion did not pass through the sieve (Table 7.2). Berkovitch et al (1959) suggests that the initial rapid rate of disintegration of some Coal Measures shales is possibly caused by the fact that at the beginning of the test the surfaces of the pieces are rough and provide more area for attack until they become smooth and rounded. However, as the whole structure is destroyed, the writer considers this not to be the case in the present circumstances. Alternatively the end of the linear portion could mark the end of a particular breakdown process (e.g. breakage by entrapped air pressure or saturation of expandable minerals).

Within the remaining two groups, a non-linear response is predominantly observed. However, in two instances, i.e. the Pierre Shale (Colorado) and the Nacimiento Shale N2, an almost linear

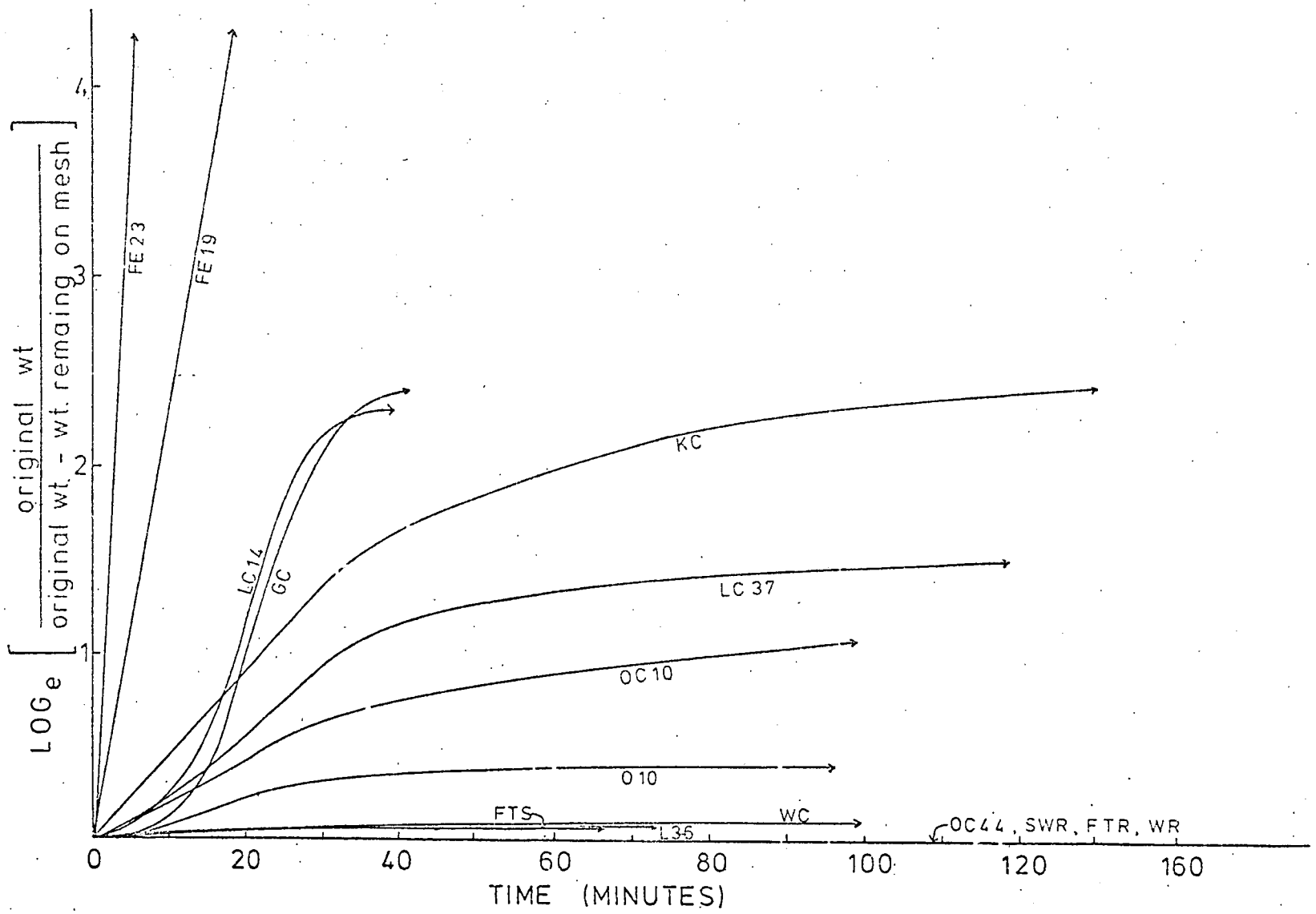

Figure 7.12. Disintegration of the British Materials According to a First Order Reaction.

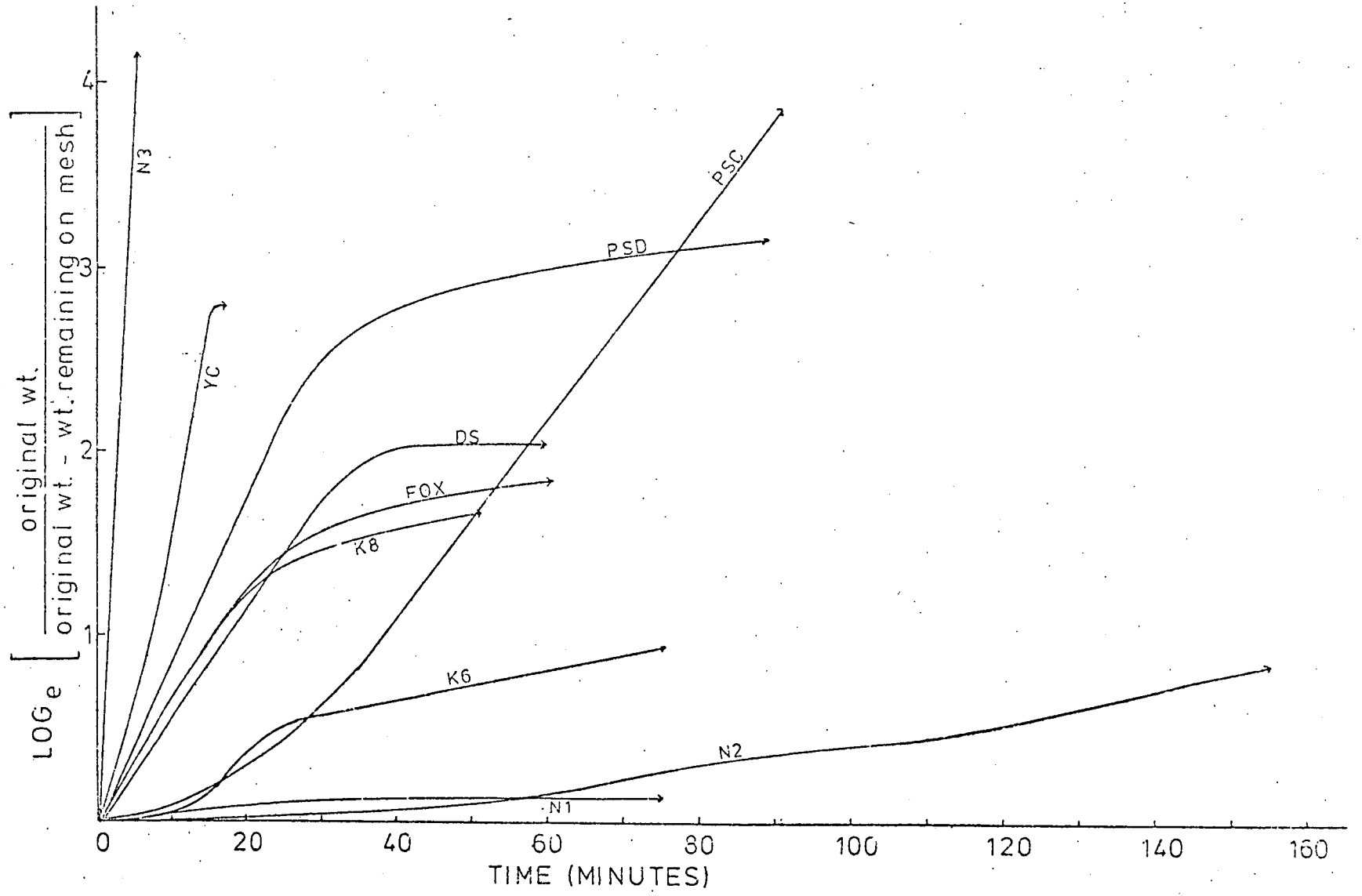

Figure 7.13 Disintegration of the North American Materials According to a First Order Reaction.

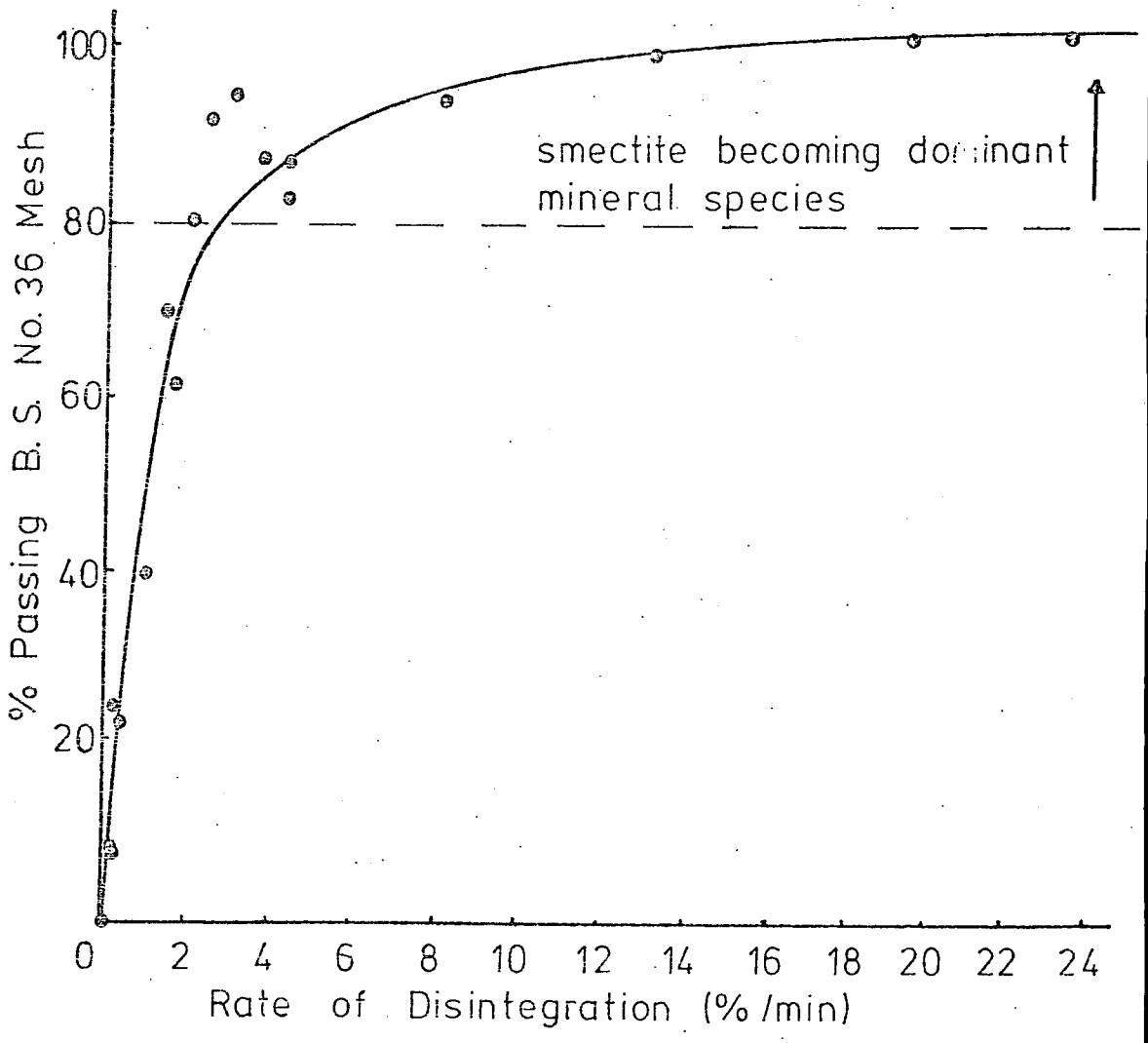

Figure 7.14. Relationship Between Percentage Breakdown and Rate of Disintegration.

relationship is indicated in the middle to later stages of the test.

As noted earlier, the amount of material disintegrating below mesh size No.36 in 24 hours (Table 7.2) is observed to increase as the rate of disintegration increases. However, this relationship is non-linear (Fig. 7.14) and appears to be dominantly controlled by the mineralogical composition (i.e. the higher percentage breakdowns being associated with the smectite concentration), although preferred orientation and amounts of induration are important factors in shales which show a small to moderate breakdown.

7.4 Uptake of Water upon Immersion

According to Morgenstern and Eigenbrod (1974) the maximum moisture content of shales retained in a brass ring, open at both ends, and with free access to water, increases with each drying-wetting cycle until the liquid limit of the material is reached. As a consequence of their results, they have erected a classification based upon the rate of change of liquidity index during the first drying-wetting cycle and the liquid limit of the material.

The uptake of water of the shales presently under consideration have been found by using the same basic technique (reported in Appendix A5.2) as Morgenstern and Eigenbrod, although in this case the materials were unconfined during the immersion. Nevertheless, with regard to classifying the materials, the writer considers that the results presented should be compatible with those of Morgenstern and Eigenbrod because, they allow free swelling from both ends of the confining ring. In addition, when considered in conjunction with suction and compaction studies (Chapter 8) the results give an indication of the type of bonding present in certain materials.

Table 7.3 Uptake of Water during Static Slaking

British Materials	Sample Ref.	Maximum Moisture Content (%)	Slaked Liquidity Index	Natural Liquidity Index	Change in Liquidty Index
London Clay 14m	LC14	82.38	0.98	-0.11	1.09
London Clay 37m	LC37	58.97	0.89	-0.13	1.02
Gault Clay	GC	Not sufficient material			
Fuller's Earth (Redhill)	FE23	142.28	1.39	-0.12	1.51
Weald Clay	WC	18.33	-0.63	-1.80	1.17
Kimmeridge Clay	KC	54.76	0.67	-0.11	0.78
Oxford Clay 10m	OC10	72.15	0.92	0.10	0.82
Oxford Clay 44m	OC44	51.84	0.79	-0.43	1.22
Fuller's Earth (Bath)	FE19	123.89	1.39	-0.09	1.48
Lias Clay 10m	L10	57.92	0.77	-0.08	0.85
Lias Clay 36m	L36	54.49	0.73	-0.35	1.08
Keuper Marl	KM	35.03	1.14		
Swallow Wood roof	SWR	13.25	-0.36	-0.66	0.30
Flockton Thin roof	FTR	9.46	-0.68	-0.97	0.29
Flockton Thin seat	FTS	25.80	0.00	-0.54	0.54
Widdringham roof	WR	13.31	-0.45	-0.84	0.39
North American Materials					
Yazoo Clay	YC	116.90	1.00	0.13	0.87
Kincaid Shale 6m	K6	60.04	0.77	-0.35	1.12
Kincaid Shale 8m	K8	39.59	0.51	0.00	0.51
Nacimiento Shale	N1	36.58	1.00	-1.34	2.34
Nacimiento Shale	N2	42.88	1.28	-1.35	2.63
Nacimiento Shale	N3	Not sufficient material			
Fox Hills Shale	FOX	Not sufficient material			
Dawson Shale	DS	64.76	0.80	-0.20	1.00
Pierre Shale (Dakota)	PSD	134.86	1.00	0.00	1.00
Pierre Shale (Colorado)	PSC	50.27	0.73	-0.18	0.91

For the majority of post-Carboniferous shales it can be seen (Fig.7.15) that the uptake of water during the test, approaches and often exceeds the liquid limit which would suggest that expansion of the structure is relatively unrestricted. Excess water held in the Fuller's Earths is probably a reflection of their low permeabilities, whilst the low values for the Kincaid Shale (K8) and the Weald Clay is a reflection of the coarse granular content.

The low values for the maximum moisture content (with respect to the liquid limit), Table 7.3, of the four Carboniferous materials must reflect their indurated and compact nature preventing expansion of the structure. It is however, anticipated that upon subsequent cycles, that their maximum moisture content will approach the liquid limit, as the rigid structure is gradually destroyed.

Changes in liquidity index (Table 7.3) are further presented according to the classification proposed by Morgenstern and Eigenbrod (1974) in Figure 7.16. However, because slaking in the present context is related to the uptake of water and not to degree of physical breakdown (as previously discussed) the two sets of results are not directly comparable. It is nevertheless, noted that shales which disintegrated at the rapid or fast-medium rates do fall within the fast and very fast rate of slaking catagories with respect to the change of liquidity index for medium-high slaking materials. The reverse situation does not however, apply because five materials i.e. the Oxford Clay (OC44), Lias Clay (L36), Weald Clay and the Nacimiento Shales (N1) and (N2) which disintegrate at a slow rate also fall within the fast and very fast rate of slaking catagories. This would suggest that these materials are fundamentally quite different from the Carboniferous shales in that, although they have

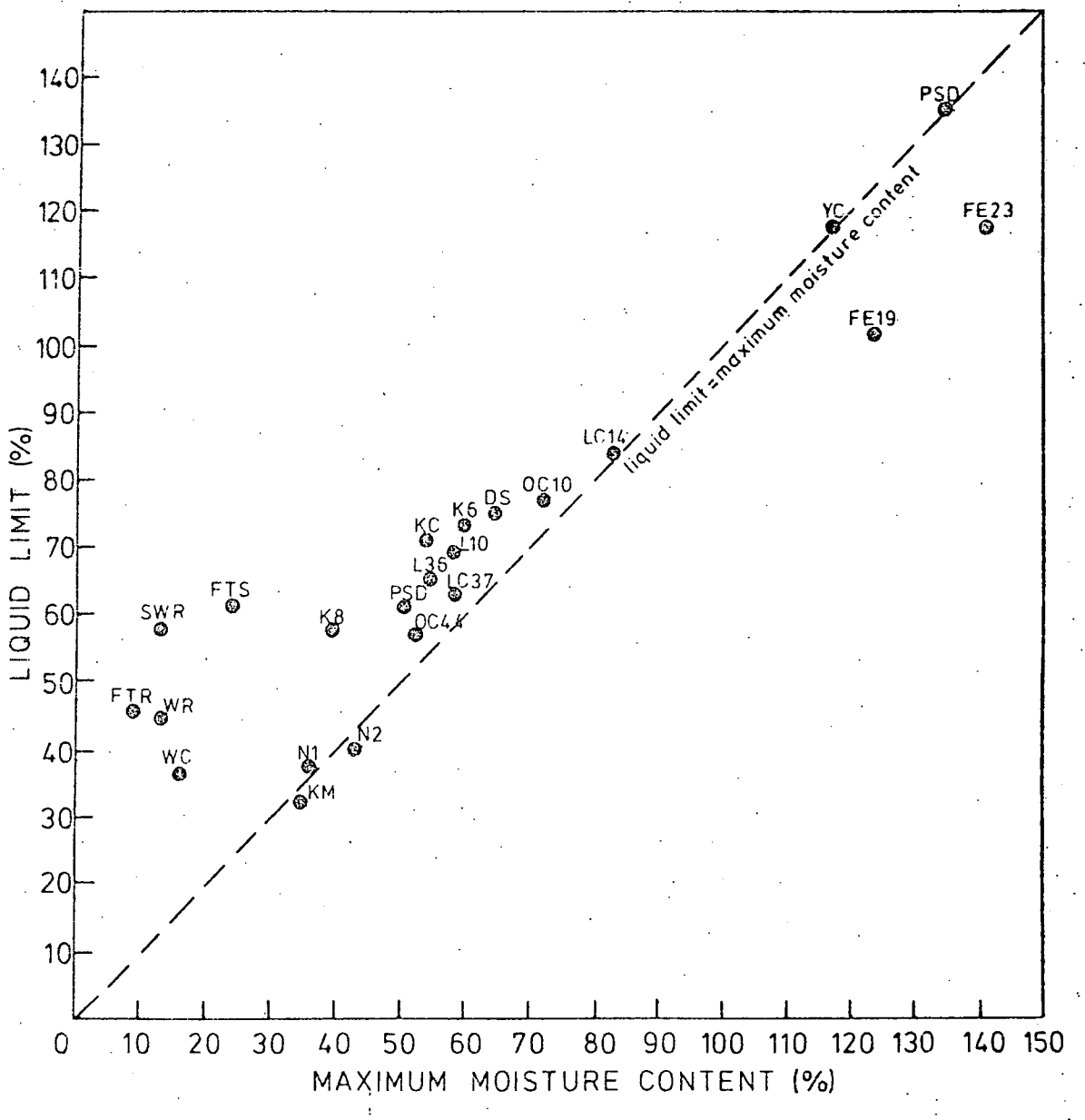

Figure 7.15. Relationship Between Maximum Moisture Content and Liquid Limit for the Uptake of Water During the First Drying - Wetting Cycle.

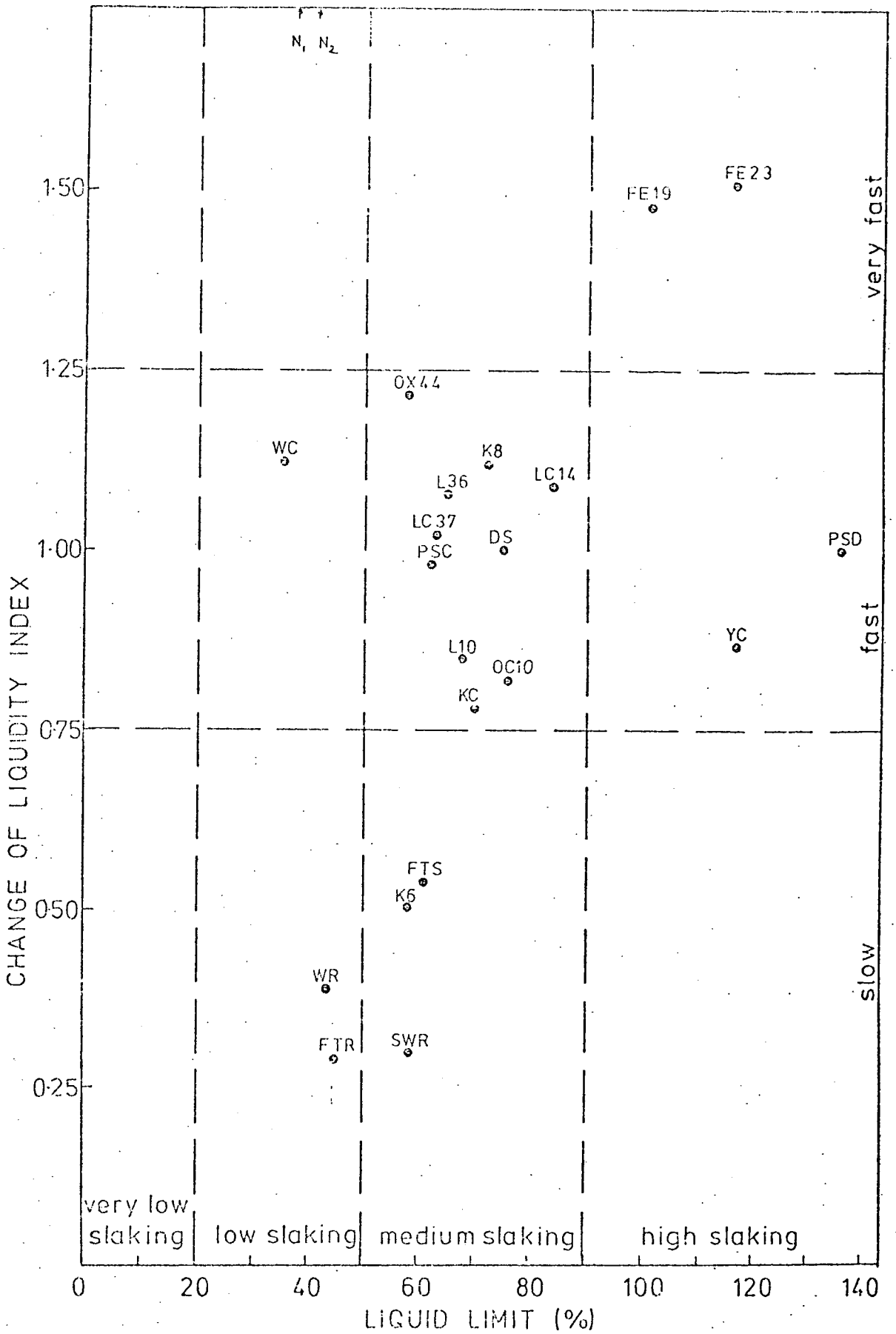

Figure 7.16. Classification of Shales Studied (Based on Morgenstern and Eigenbrod, 1974).

Table 7.4 Slaking under Vacuum

British Materials

	Sample Ref.	
London Clay 14m	LC14	Soft but intact
London Clay 37m	LC37	Soft but intact
Gault Clay	GC	Just slaked
Fuller's Earth (Redhill)	FE23	-
Weald Clay	WC	Intact
Kimmeridge Clay	KC	Soft but intact
Oxford Clay 10m	OC10	Soft but intact
Oxford Clay 44m	OC44	Soft but intact
Fuller's Earth (Bath)	FE19	Rapid slaking
Lias Clay 10m	L10	Soft but intact
Lias Clay 36m	L36	Soft but intact
Swallow Wood roof	SWR	-
Flockton Thin roof	FTR	Intact
Flockton Thin seat	FTS	Slaked
Widdringham roof	WR	-

North American Materials

Yazoo Clay	YC	Slaked
Kincaid Shale 6m	K6	Slaked
Kincaid Shale 8m	K8	Slaked
Nacimiento Shale	N1	-
Nacimiento Shale	N2	Slaked
Nacimiento Shale	N3	-
Fox Hills Shale	FOX	Slaked
Dawson Shale	DS	Slaked
Pierre Shale (Dakota)	PSD	Slaked
Pierre Shale (Colorado)	PSC	-

a similar hardness and/or preferred orientation, they possess a mineral skeleton with weaker adhering forces; a hypothesis which is further discussed in connection with diagenetic bonding in Chapter 8.

7.5 Slaking under Vacuum

No specific slaking tests under vacuum were performed. However, during the saturation of materials being prepared for suction tests (see Appendix A4.3) certain basic observations were noted (Table 7.4) which indicated that, on the whole, shales which contained large quantities of expandable clay minerals tended to disintegrate under vacuum, whilst those where illite and kaolinite were dominant remained intact but became very soft.

7.6 The Relationship between Exchangeable Cations, Water-Soluble Cations and the Possibility of Erosion

Recent research into the erodability of shales (from dams) in Australia and North America (e.g. Aitchison and Wood, 1965; Cole and Lewis, 1960; Sherard et al, 1972) has highlighted a strong correlation between the incidence of piping failure and clay chemistry, and in particular the concentration of sodium cations on the exchange sites and in the pore water. Indeed the effect of exchangeable cations and the electrolyte concentration with respect to flocculation and dispersion of pure clays has been extensively studied, (see Chapter 1.7.2).

Soil scientists express the concentration of sodium on the exchange sites in terms of the exchangeable sodium percentage (ESP), i.e.

$$ESP = \frac{Na}{CEC} * 100 \quad \ldots\ldots\ldots\ldots\ldots\ldots \quad (30)$$

where Na and CEC are in milliequivalents per 100 grams of clay. The concentration of sodium in the pore water is expressed in terms of

the sodium absorption ratio (SAR), i.e.

$$SAR = \frac{Na}{\frac{Ca + Mg}{2}} \quad \ldots\ldots\ldots\ldots\ldots (31)$$

where Na, Ca and Mg are the concentration of dissolved salts in milliequivalents per litre in the pore water at the liquid limit (or saturation extract of Sherard et al, 1972).

Richards, (1954) has shown a relationship between ESP and SAR (see Fig.7.17). Sherard et al, (1972) also observe this relationship in materials from failed clay dams. In the present study, the ESP (Table 7.5) and the SAR (Table 7.6), which has been recalculated from the cation concentration in the washings associated with ammonium acetate leaching (Appendix A1.3), do not show such a strong relationship as observed by the former workers; instead a more irregular response is noticed (Fig.7.17).

Sherard et al (1972) have also investigated the combined effect of percentage sodium and total soluble salts in the saturation extract upon the dispersing behaviour of clays (Fig.7.18). They conclude that sufficient data are available to suggest that strong erosion of clay dams by dispersion does not occur if the total salt concentration is greater than 15 milliequivalents per litre (implying a sodium percentage of between 50 - 60 per cent). On the other hand, agricultural scientists recognise that soils which have an ESP greater than 15 and low total salts in the pore water are highly dispersive.

Nevertheless, using Sherard et al's parameters the calculated values for the current shales (Table 7.6) suggest that in their present condition, all except the Nacimiento Shale N3 and the Flockton Thin seatearth would be resistant to erosion by dispersion (Fig.7.18). However, even these shales only fall within the transition zone and consequently would only be susceptible to low dispersion, although

Table 7.5 Exchangeable Sodium Values for Samples Studied

	Sample Ref.	ESP
British Materials		
London Clay 14m	LC14	1.36
London Clay 37m	LC37	1.36
Gault Clay	GC	10.97
Fuller's Earth (Redhill)	FE23	1.11
Weald Clay	WC	-
Kimmeridge Clay	KC	3.91
Oxford Clay 10m	OC10	7.53
Oxford Clay 44m	OC44	4.32
Fuller's Earth (Bath)	FE19	0.64
Lias Clay 10m	L10	6.00
Lias Clay 36m	L36	5.12
Keuper Marl	KM	-
Swallow Wood roof	SWR	24.40
Flockton Thin roof	FTR	22.70
Flockton Thin seat	FTS	56.66
Widdringham roof	WR	5.64
North Americal Materials		
Yazoo Clay	YC	0.90
Kincaid Shale 6m	K6	1.34
Kincaid Shale 8m	K8	2.65
Nacimiento Shale	N1	4.44
Nacimiento Shale	N2	3.55
Nacimiento Shale	N3	1.28
Fox Hills Shale	FOX	7.55
Dawson Shale	DS	1.09
Pierre Shale (Dakota)	PSD	13.46
Pierre Shale (Colorado)	PSC	2.11

Table 7.6 Concentration of Cations in the Pore Water (including Sodium Absorption Ratio)

British Materials	Cation Concentrations in m.eq/litre Na	K	Ca	Mg	Total	SAR	%Na
London Clay 14m	15	41	56	118	230	1.6	0.65%
London Clay 37m	47	40	38	93	218	5.8	21.5%
Gault Clay	9	36	176	67	288	0.8	3.0%
Fuller's Earth (Redhill)	3.5	7.5	102	19	132	0.4	2.6%
Weald Clay	-	-	-	-	-	-	-
Kimmeridge Clay	9.5	11	55	18	93.5	1.6	10.1%
Oxford Clay 10m	74	40	104	37	255	8.8	29%
Oxford Clay 44m	136	41	178	52	407	12.6	13.3%
Fuller's Earth (Bath)	3.5	11	89	24	127.5	0.5	2.7%
Lias Clay 10m	78	52	158	51	339	7.6	23.0%
Lias Clay 36m	137	35	130	34	340	15.1	40.3%
Swallow Wood roof	97	47	8	18	170	26.9	57.0%
Flockton Thin roof	180	37	11	24	252	43.0	71.4%
Flockton Thin seat	165	13	6	10	194	58.3	85.0%
Widdringham roof	55	17	15	17	54.5	1.4	10.1%
North American Materials							
Yazoo Clay	35	13	103	48	199	4.0	17.5%
Kincaid Shale 6m	17.5	6	150	14	187.5	2.1	9.3%
Kincaid Shale 8m	22	7	68.3	24	736	1.1	2.9%
Nacimiento Shale	110	9	20	20	159	24.5	69.1%
Nacimiento Shale	86	12	29	6	133	20.5	64.6%
Nacimiento Shale	30	11	19	8	68	8.1	44.1%
Fox Hills Shale	40	8	121	143	312	3.5	12.8%
Dawson Shale	48	50	103	47	248	5.5	16.1%
Pierre Shale (Dakota)	113	8	19	20	160	25.5	70.6%
Pierre Shale (Colorado)	225	24	34	50	333	34.7	67.5%

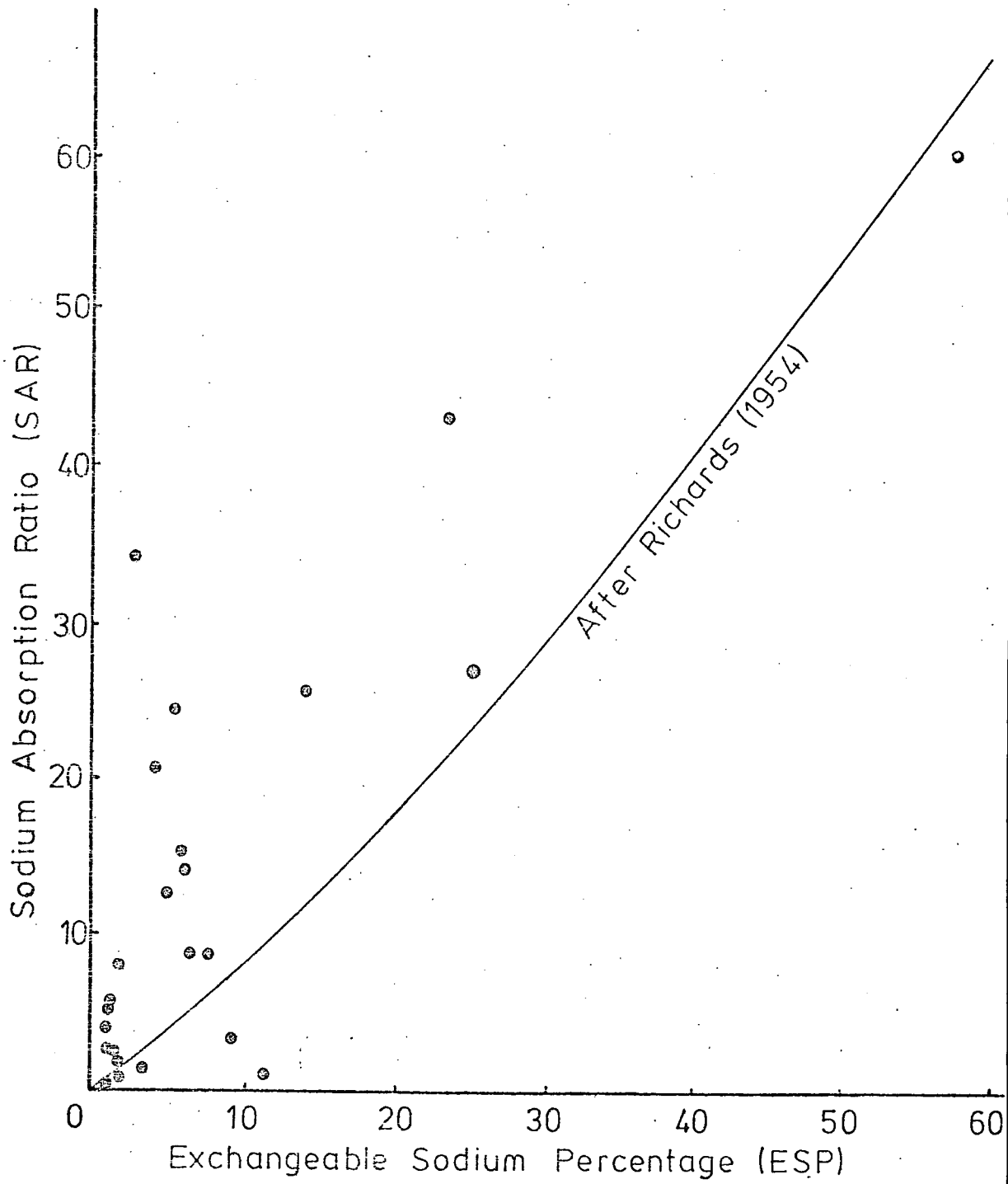

Figure 7.17. Relationship Between Exchangeable Sodium Percentage and Sodium Absorption Ratio.

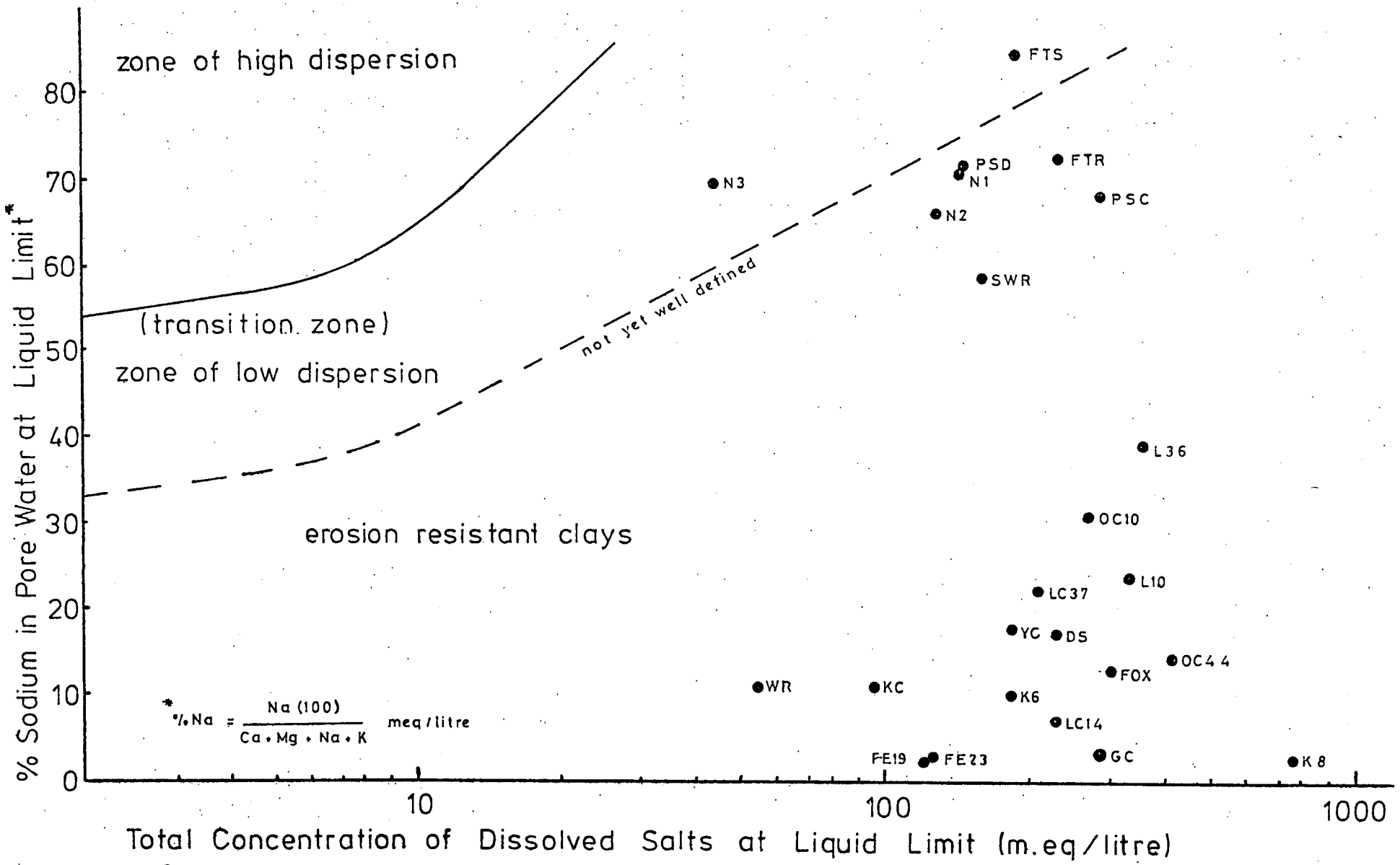

Figure 7.18. Relationship Between Percentage Sodium and Total Salt Concentration in Pore Water; Based on Sherard et al (1972).

the indurated nature of the seatearth would probably hold the material together to a certain extent. The writer does, however, consider that clays falling just below the proposed transition zone of Sherard et al (1972), may easily become dispersing to varying degrees if slight changes occur in the chemistry of the pore solution, (e.g. if a dilution of the salt concentration occurred).

7.7 Conclusions

(1) Two simple slaking tests, i.e. measuring the rate of disintegration below mesh size B.S. No.36 and the uptake of water during the first drying-wetting cycle, have been used to assess the breakdown characteristics of the shales studied.

(2) From the rate of disintegration test, a broad classification of breakdown into three groups has been made i.e. rapid (greater than 3.5% per minute), fast-medium (3.5 - 0.5% per minute) and slow (less than 0.5% per minute); disintegration being shown to be related to mineralogy, preferred orientation and the presence of diagenetic bonding.

(3) From the uptake of water during the first drying-wetting cycle, the shales have been classified according to the method adopted by Morgenstern and Eigenbrod (1974).

(4) By considering the breakdown behaviour of each shale during both tests, indirect evidence is offered for the type of bonding present in certain materials (see Chapter 8).

(5) It is considered that the majority of shales currently studied would be resistant to erosion by dispersion with their present pore water chemistry, although slight adjustments might make some of the shales moderately dispersive.

Chapter Eight
Summary and General Conclusions

The study of a random selection of overconsolidated, weak, argillaceous rocks from major formations in the United Kingdom and North America, has been used to establish relationships between depth of burial, geological age, mineralogical composition, interparticulate bonding, together with the subsequent response of the materials as a consequence of uplift and erosion.

The maximum depth of burial for each material has been investigated by up to three different methods depending upon the available data. Literary evidence, whilst being reasonably complete for the British materials is quite scant when the North American sample locations are considered. Nevertheless, even where complete data appear to be available, the method relies on the fact that recorded thicknesses have not been subjected to periods of widespread erosion (or non-deposition). Typical instances of intense erosion leading to reduced thicknesses of British strata in the areas of the sample localities are detected in the deposits above the London Clay (where up to 250m of sediments have been removed), the Chalk (where up to 360m of sediments have been removed) and above the Carboniferous deposits (where several thousands of metres of Permo-Trias deposits have been removed). According to North American stratigraphy, materials from the Rocky Mountains region have been subjected to rapid deposition and erosion of many thousands of meters of overlying sediments during the formation of these mountains in the Miocene Period. As a consequence, literary documentation of thicknesses in this region are often very incomplete or non-existent.

To overcome the shortcomings notedabove in the literary method, two geotechnical techniques were also employed to obtain a measure of the maximum depth of burial of the sediments studied. Where possible, the Casagrande construction was performed on the compression e-log P curve of the undisturbed specimens. However, as a consequence of the limiting pressure of the oedometer (i.e. 35000kN/m^2) the method could only be applied to materials buried to a maximum depth of between 2100m to 2500m. The use of the rebound characteristics from the undisturbed samples gave values which are consistent with those obtained by the other two methods in every instance except for the three Carboniferous roof shales, where exceptionally high values, in the order of two or three times the anticipated maximum, are recorded. However, it is considered that these results probably reflect the fact that certain Carboniferous sediments behave in a manner more akin to hard, indurated rocks, than to overconsolidated clays. A similar technique using the rebound characteristics from the remoulded material (proposed by Altschaefl and Harrison, 1959) has also been investigated. However, results from this project indicate that enhanced values for the maximum depth of burial are obtained when diagenetic bonding (see later) is present.

In general terms, strata from the British Isles appears to be less deeply buried than strata of equivalent age from the North American continent, although areas of similarly buried strata can be found. Rayner (1967) quotes that the maximum thicknesses of British strata to the base of the Jurassic occur in the Weald and Wessex basins and are of the order of 2400 - 3000m (i.e. 450 - 700m of Tertiary, 1200 - 1500m of Cretaceous, 1200 - 1500m Jurassic); thicker deposits may however, occur in the North Sea basin. Tertiary deposits, alone,

from the fringe basins of the Eastern Rockies are up to 3650m in thickness, whereas in the Mississippi Embayment, equivalent deposits of between 7600 - 9100m have been recorded. Cretaceous deposits in the Great Plains region form an eastwards sloping wedge ranging in thickness from 6000m against the Rocky Mountains, to 600m as the Appalachians are approached. In the Mississippi Embayment, Cretaceous sediments reach a total thickness of about 2150m.

These above mentioned thicknesses are, in general, reflected by the majority of samples tested in this present study (see Table 2.2). Here it can be seen that the maximum depths of burial of the British Jurassic deposits are of the order of 1000 - 1250m and even the oldest British specimens (from the Upper Carboniferous Period) have only been buried to a maximum depth of about 3800m, whereas certain North American specimens from the Late Cretaceous and Early Tertiary Periods yield maximum overburden thicknesses of up to 1550m. Nevertheless, three samples from the fringes of the Mississippi Embayment and one from the centre of the Great Plains show maximum overburdens which fall in line with recorded depths for British strata of equivalent age.

Consequently it has been concluded that, in general, overburden does not increase systematically with age, although on a local scale this may be true provided deposition is reasonably uninterrupted.

X-ray analysis has been used to identify the major clay mineral components (i.e. illite, kaolinite, montmorillonite, mixed-layer clay and chlorite) as well as other detrital and non-detrital minerals such as quartz, feldspar, calcite, dolomite and pyrite. Semi-quantitative analyses were performed using boehmite as an

internal standard (Griffin, 1954; Gibbs, 1967). However, estimates of the quantities of minerals which occurred as minor constituents of a limited number of samples, (e.g. chlorite and feldspar) were determined by spiking the relevant specimens with penninite and orthoclase respectively. Determination of water, carbon and carbon dioxide was by wet chemical methods; the major element analyses being by X-ray fluorescence.

From a detailed analysis of the mineralogy, major differences have been found in the relative abundances of mineral species present in the North American and British materials examined, and as a consequence it was anticipated that the engineering behaviour of each group would be markedly different. The results indicate that smectite (averaging 30 per cent) is the dominant clay mineral species present in the North American shales (Table 8.1) and its occurrence in the Late Cretaceous and Tertiary strata of the Western Interior of America is associated with the uplift of the Rocky Mountains. Some material underwent terrestial accumulation and transportation to the site of deposition (e.g. Dawson Shale and Nacimiento Shales), but the majority is probably the result of volcanic fallout (Tourtelot, 1962), (e.g. Pierre Shale and Fox Hills Shale). The occurrence of smectite in the British materials is limited to a small number of samples, although its presence has been recorded in the majority of post-Carboniferous strata (Perrin, 1971). Concentrated deposits of smectite, resulting from devitrification of volcanic fallout (Hallam and Sellwood, 1968), such as the Fuller's Earth, are comparatively rare in British strata although diluted deposits have been recorded elsewhere (Bradshaw, 1975). K-bentonite bands occurring in the Carboniferous Period are

also considered to be diagenetically altered volcanic ash deposits. Smectite occurring in the London and Gault Clays is considered to be of detrital origin because of the absence of nearby volcanic centres.

An investigation of the transformation of smectite to mixed-layer clay and illite (Powers, 1959 and 1967; Keller, 1963; Burst, 1959 and 1969; Weaver, 1959; Larsen and Chilingar, 1967) was made by recalculation of the structural formulae of this mineral from several samples where a simple mineralogy was identified. Smectites from both samples of Fuller's Earth (one of Upper Cretaceous age and the other of Middle Jurassic age) yield Si/Al ratios of 4.0 and 3.94 respectively, indicating that they are nearly pure montmorillonites, and since both materials have been buried to approximately the same depth (i.e. 760m) it would appear that any transformation which may occur is not related to geological age. However, according to Powers (1959) it may sometimes give this appearance because, in general, the older sediments have been more deeply buried. In fact Powers (1967) suggests that the transformation does not begin until 1000m of overburden is present. Recalculations of the smectites observed in the Nacimiento Shale (N3) and the Dawson Shale (buried to a maximum depth of about 1500m) reveal Si/Al ratios of 2.9 - 3.6 with an associated high potassium content indicating a beidellitic character, and probably reflect the first stages of the montmorillonite to illite transformation. A low Si/Al ratio is also recorded for the smectite in the Yazoo Clay. However, no conclusions could be drawn regarding this because the material is considered to be of secondary detrital origin; the smectite not resulting directly from volcanic fallout.

Therefore, from current observations, it has been concluded that depth of burial is the most important factor influencing the diagenetic alteration of smectite minerals.

Illite (averaging 23 per cent), closely followed by kaolinite (averaging 21 per cent) are the most common clay mineral species present in the British materials examined (Table 8.1). In the North American samples however, after smectite, kaolinite is the next most important clay mineral (averaging 19 per cent), whereas illite (averaging 8 per cent) only appears as a minor constituent. These minerals, in addition to chlorite, which only occurs in trace amounts in the British materials, are considered to be detrital in origin, especially since they represent stable mineral phases even under the influence of large temperatures and pressures.

Mixed-layer clay occurs to a varying degree in both groups of sediments, but as the material, currently identified, is closely related to the illite concentration, the larger amounts are found in the British materials. Absence of correlation with smectites, also noted by Bradshaw (1975) indicates that mixed-layer species present are detrital in origin and do not arise from the transformation of the aforesaid mineral. Attewell and Taylor (1973) do, however, record a relationship between mixed-layer clay and smectite when studying a series of North American strata.

Quartz is the dominant detrital non-clay mineral in both groups of materials. Moreover, it has a significantly higher concentration in the North American samples, i.e. 32 per cent compared with 22 per cent in the British materials, which reflects the higher rates of deposition. Feldspar species are also found in both groups,

Table 8.1. Average Mineralogical Compositions.

British Shales	Average (%)	Range (%)
Illite	23	0 - 54
Kaolinite	21	0 - 54
Mixed-layer Clay	13	0 - 45
Smectite	13*	0 - 99
Quartz plus other equant habit minerals	30	1 - 55
Carbonates	4	0.1 - 34
Pyrite	2	0.1 - 6
Carbon	1	0 - 4
North American Shales		
Illite	8	0 - 25
Kaolinite	19	5 - 31
Mixed-layer Clay	3	0 - 15
Smectite	31	8 - 54
Quartz plus other equant habit minerals	39	20 - 60
Carbonates	3	0.1 - 11
Pyrite	0.5	0.1 - 3.5
Carbon	1	0.1 - 3

* Distorted by extremely high concentrations in the Fuller's Earths.

but again their occurrence is far more frequent in the North American materials; being associated with the vulcanicity present during the Late Cretaceous and Tertiary Periods in the United States.

Non-detrital minerals, such as pyrite and carbonates occur throughout both groups of sediments, although the former is more common in the British materials. Carbonates generally reflecting marine conditions of deposition are often observed as fossil debris within the sediments.

Determination of exchangeable cations revealed that calcium and magnesium are the dominant species in both groups of shales, although exchangeable sodium is an important constituent of the Flockton Thin seatearth and the Pierre Shale from Dakota. Water-soluble cation concentrations show a certain amount of compatibility with the findings of Spears (1974) with regard to the palaeosalinity of ancient environments. This is especially so for the Carboniferous sediments and certain non-marine American shales, although no definite conclusions can be drawn from the remaining results.

However, by considering the pore water chemistry in conjunction with the exchange capacity, it has been concluded that in their present condition, the majority of clays studied would be resistant to erosion by dispersion. Nevertheless it is likely that a slight alteration in the pore water chemistry, e.g. by dilution, may lead to moderate dispersing properties of several materials (especially the Pierre and Nacimiento Shales). Possible dispersion of three Carboniferous sediments may be resisted by their indurated nature.

Preferred orientation studies play an important role in the understanding of the depositional and compaction histories of clayey

sediments. Consequently, quantitative evaluations of the orientations of clay minerals have been made using both optical and X-ray techniques. In addition, the general inter-relationships between the mineral species present have been examined using a scanning electron microscope. Moreover, no impregnation of the specimens was required to preserve the clay structure during drying because air-dried shrinkages were found on the whole, to be well within the limits accepted by other workers (e.g. Quigley and Thompson, 1966; Morgenstern and Tchalenko, 1967a).

In general, the degree of preferred orientation is not associated with depth of burial or geological age; a fact which is highlighted by the juxtaposition of the Flockton Thin seatearth (a specimen having a random orientation), against the Flockton Thin roof shale (which exhibits an almost perfect orientation). This phenomenon may arise from the domain concept (Aylmore and Quirk, 1960), whereby an increase in preferred orientation with depth is not required because the effect of compression is to increase the number of particles in each domain (Blackmore and Miller, 1961), which may still be randomly orientated in a flocculated sediment or parallel in a dispersed sediment. Shales exhibiting a preferred orientation predominantly contain the larger clay minerals of illite and kaolinite as the major clay species present, whereas with the exception of the Yazoo Clay, montmorillonite clays tend to retain a poor or random orientation irrespective of the depth of burial. (The Yazoo Clay is considered to have been laid down under slow conditions of sedimentation such that the montmorillonite acquired a high degree of preferred orientation, i.e. a purely detrital origin).

Furthermore, it has been observed that, in general, when illite and kaolinite occur together they are seen to exhibit the same degree of preferred orientation, although when montmorillonite is also present, evidence is offered to show that in certain shales (e.g. London Clay and Pierre Shale), a lower orientation is present in this mineral than in the other two. This would seem to confirm the statement of Meade (1961b), who suggests that illite and kaolinite, being much larger minerals, are subject to a certain amount of reorientation at some stage during compaction; montmorillonite only suffering expulsion of pore fluids.

Clay microstructure, as observed from S.E.M. photographs, is seen to mirror, in a general way, the degree of preferred orientation obtained by other indirect methods, i.e. dispersed turbostratic structures being shown by shales exhibiting a high preferred orientation, flocculated structures by those exhibiting a random orientation. However, as noted by Barden (1972), the structure of overconsolidated shales is not necessarily that which was in existence at the time of deposition, and consequently a dispersed turbostratic fabric observed in a natural clay may result from the collapse of an originally flocculated arrangement. In this respect, an interesting feature was noted in the reconsolidated sample of Lias Clay. Here partial alignment of illite and kaolinite particles has occurred even after rapid compression and rebound, which the writer considers may have occurred during the early stages of the test when the moisture content was high.

S.E.M. photographs of the Carboniferous materials indicate that these are unlike any of the younger sediments studied and are probably a reflection of their stress history causing a certain amount of alteration to the original sediment. Differences in behaviour of

these materials, compared to post-Carboniferous sediments are further noticed in the consolidation, suction and slaking test results.

Consolidation tests were performed in a specially constructed oedometer, using a maximum pressure of approximately 35000kN/m^2 (equivalent to an overburden of between 2100 - 2500m of sedimentation), on materials in both their natural state and in a remoulded condition from an initial moisture content equal to the liquid limit. The latter condition was chosen because it is considered to represent the state of the materials just below the liquid-solid interface and therefore consequent consolidation will give a general indication of the natural compaction.

An additional series of tests was performed on four remoulded clays to a pressure of 8400kN/m^2 in a conventional floating head oedometer to investigate the effect of variation in the initial moisture content. Moreover, since the parameters obtained from the high pressure tests were compatible with those from the conventional machine, it was concluded that a high degree of acceptability could be placed on the aforementioned results.

Current results show that the coefficient of consolidation (c_v) decreases with increasing liquid limit in accordance with the trend observed by Terzaghi and Peck (1948), but there is no significant difference between values obtained (beyond the preconsolidation load) for the tests performed on undisturbed materials and those from tests performed on remoulded materials.

With regard to the compression index (C_c), of those values in the low pressure range (297 - 2426kN/m^2), i.e. before the intermediate rebound stage for the remoulded materials, there is general agreement with equations previously determined (e.g. Terzaghi and Peck, 1948).

At higher pressures however, i.e. 2426 - 34967kN/m^2 for remoulded materials and values obtained beyond the preconsolidation load for natural materials, the compression index is better expressed by an equation of the form:-

$$C_c = 0.004 (LL - 10\%)$$

In addition, all values of compression index define one trend when equated to the average voids ratio which is similar to, but above that obtained by Komornik et al (1970). The coefficient of volume compressibility (m_v), like C_c, decreases with increasing pressure, although at any given pressure, the higher values are associated with the higher liquid limits.

The swell index (C_s) is, in general, seen to increase with liquid limit in accordance with previous findings (e.g. Lambe and Whitman, 1969). However, more important is the fact that the recorded swell index for undisturbed materials is often lower than that found in the remoulded counterpart. This phenomenon is concluded to be associated with the presence of diagenetic bonding and is accordingly discussed in this connection.

The permeability, at similar pressures, has been found to be independent of the state of the material but dependent upon the voids ratio. Consequently there is a general decrease associated with increasing liquid limit.

The stress - strain response has been reviewed in the light of conventional strain energy concepts (e.g. Morely, 1940) whereby the area under the stress - strain curve is represented by three conditions (i.e. the non-recoverable strain energy and the recoverable strain energy, which combined form the total strain energy for the cycle). Furthermore, the results have been analysed on a volumetric

basis (where no account is taken of the weight of solid) and on a unit dry weight basis.

The former method of analysis has also been employed by Brooker in his 1967 paper where, in consolidating five remoulded shales from a liquidity index of 0.5, he observes that the area between the loading and unloading curves (which he refers to as representing 'absorbed strain energy') increases as the plasticity increases. He goes on to relate this phenomenon to the disintegration properties of the materials. However, upon extending the range of initial remoulded moisture contents, it is noticed that the relationship obtained by Brooker does not always hold true, thus casting doubt on the hypothesis.

In the present study, a positive relationship between plasticity and the non-recoverable energy (i.e. the area between the loading and unloading curves) is noticed for materials consolidated in the natural condition and also remoulded materials consolidated in a conventional oedometer from a liquidity index of 0.5. However, this relationship becomes negative when the consolidation tests are performed on remoulded material starting from an initial moisture content equivalent to the liquid limit. Consequently it has been concluded that this method of analysis does not fully account for the process in operation, although it does indicate that the total compressional strain energy is related to the compressibility of the shales, whereas the recoverable strain energy is dominantly controlled by the total expandable mineral content and in particular, the smectite concentration.

By computing the energy components in terms of strain energy per unit weight of dry solid, a new picture emerges whereby, under similar initial conditions, all these values increase with increasing plasticity.

It has subsequently been concluded that, during the consolidation cycle, more non-recoverable strain energy is dissipated as the plasticity increases because initially higher moisture contents allow greater relative displacements and reorientation of particles, thus resulting in larger volumetric strains. Consequently a larger amount of total compressional strain energy is required, and because of the presence of more expandable minerals, there is usually a greater amount of recoverable strain energy.

It has also been observed that the strain energy portions (per unit dry weight) remain relatively constant as the initial moisture content is reduced from the liquid limit to a liquidity index of 0.5. However, below this value less energy is expended because the denser state of packing restricts large displacements o. reorientations, and as a consequence, the total compressional and recoverable strain energy components are also reduced.

Extending the study of strain energy to the effect of previous compaction, it has been observed that as the degree of overconsolidation increases, the amount of non-recoverable strain energy (per unit dry weight) decreases. Moreover, at the same time, the difference between this value and that obtained during the consolidation of material remoulded from the liquid limit also decreases until a maximum depth of burial of about 1050m is recorded, after which the difference remains relatively constant. This infers that until this depth is reached there is still some degree of freedom available for permanent movements within the material. Furthermore a similar trend is also observed for the total compressional strain energy, although the recoverable strain energy remains approximately constant and may be dependent upon the presence of bonding.

Consolidation tests have confirmed that strain energy may be retained in unweathered, heavily overconsolidated shales by the formation of diagenetic bonding, which in this instance, has been identified by the presence of a depressed swell index in these materials, compared with that obtained from their remoulded counterparts. Furthermore, materials obtained from the zone of weathering, cited by Bjerrum (1967a), i.e. less than 17m from the surface, are shown to be almost devoid of diagenetic bonding. These findings are especially supported by reference to the London, Oxford and Lias Clays where both weathered and unweathered specimens were examined. As a consequence the overall results are in excellent agreement with the hypothesis proposed by Bjerrum in 1967.

It has also been shown, by reference to one unweathered specimen, that this bonding can be progressively destroyed by applied pressure, although total destruction appears to require loads far in excess of the limiting pressure of the oedometer used. Furthermore, since the preconsolidation load is different for each specimen (i.e. ranging from $1400 - 40000 kN/m^2$) a slightly distorted picture may emerge when the spectrum of shales are considered although broad trends do emerge which relate to mineralogical variation and depth of burial.

A crude depth dependent relationship covering a range of 450m in the Tertiary sediments to 3800m in the Carboniferous sediments has been depicted where illite and kaolinite are the major mineral species. However, in clays where smectite is a major constituent, diagenetic bonds can be formed in sediments buried to only 900 - 1800m depth which result in the suppression of swell index values to a similar extent encountered in the Carboniferous sediments. On the other hand, a high proportion of quartz and other equant habit minerals

would seem to offset the above behaviour even where smectite is a major constituent.

Unfortunately, consolidation results do not offer any indication of the type of bonding present within the materials studied. Nevertheless, by considering the engineering behaviour prevalent in the near-surface zone in terms of suction and slaking characteristics, certain evidence is offered which suggests that the Carboniferous shales examined possess bonding in the form of mineral to mineral welding, whereas a dominantly weaker cationic form is probably present in younger materials.

The response of the materials to total immersion in water (i.e. slaking) has been investigated by two methods. Firstly by a simple static slaking test, measuring the uptake of water in terms of a change of liquidity index for the first drying - wetting cycle, and secondly by measuring the rate and amount of disintegration below mesh size B.S. No.36.

Soil suction characteristics, in the pF range 0.3 to 4.6, have been obtained using the suction plate and pressure membrane methods. A wetting curve, from oven dryness, was obtained for each material studied, although the drying condition could only be found in a limited number of cases because many samples, notably those which contained large quantities of expandable material, tended to disintegrate during the saturation process. However, a simple mathematical relationship between suction pressure and effective stress has led to a comparison of moisture retention during suction and consolidation experiments. Moreover, because of very close agreement in the high suction pressure range, the consolidation curve

has been used to calculate the specific surface areas when a drying curve was not obtained.

Current results indicate that the Carboniferous shales and the Weald Clay have suction - moisture content relationships resembling incompressible materials, whilst the Nacimiento Shale (N2) has intermediate characteristics. The remaining specimens appear to behave in accordance with fully compressible materials and also show a general increase in saturation moisture content with increasing plasticity.

However, it is observed that the Carboniferous materials have a broadly similar mineralogical composition (of illite - kaolinite - quartz) to certain younger, fully compressible materials (notably the Oxford and Lias Clays). They also have Atterberg limits which are of a similar order, although slightly lower than those of typical fully compressible materials. Consequently it would be anticipated that their suction curves would also be similar. Therefore since they show a very marked difference (i.e. their saturation moisture contents are 4 - 10 per cent compared with 20 - 30 per cent for similar fully compressible materials) see Figure 6.2, it must be concluded that they are prevented from behaving as true clays by the presence of some form of bonding which has a mineral to mineral welding nature. Surface area determinations for the Carboniferous sediments are also significantly lower than would be expected for the mineral suite present (i.e. 25 - 50 m^2/g compared with approximately 80 - 120m^2/g for similar overconsolidated clays or clay-shales).

The effect of diagenetic bonding (possibly coupled with the effect of a highly preferred orientation) is also inferred in certain illite - kaolinite rich fully compressible materials in that the uptake

of water at any given suction is significantly lower in unweathered materials than in their weathered counterparts. Furthermore, although swell index results indicate that the bonding present in these materials is generally about half as strong as in the Carboniferous sediments, evidence from static slaking tests suggests that it is of a significantly different nature. In these tests, the recorded changes in liquidity indices for the unweathered specimens (in the order of 0.9 - 1.1) do not show any marked variation from changes in the values recorded in unbonded shales, inferring that the bonds can be easily destroyed by free immersion in water, and may therefore be of a cationic nature. Changes in liquidity indices for the Carboniferous materials are generally less than half the aforementioned values, suggesting that these materials are substantially resisting the attack by water. Surface area determinations (Table 6.3) which are consistent with the mineralogical compositions also indicate the absence of a welding - type of bonding.

On the other hand, materials which contain strong bonding as indicated by compaction studies, but which also contain large quantities of expandable material (notably smectite), appear to show suction-moisture content relationships which are compatible with their mineralogy and related properties, and also disintegrate rapidly in water. Consequently, it has been concluded that bonding in these materials is of a cationic nature, readily destroyed by drying and resaturation. Furthermore, it is also postulated that it may be of a similar nature to that encountered in the previously mentioned sediments, although in the latter materials the effect may be stronger because of the orientated structure.

As a consequence of the slaking tests (previously discussed) an attempt has been made to classify the materials studied by various

methods suitable for engineering purposes. Firstly, the change in liquidity index has been related to the liquid limit in a manner first described by Morgenstern and Eigenbrod (1974). This classification as previously mentioned does indicate whether bonding of a welding nature is present, but does not depict materials which contain the weaker cationic form. Secondly, a new classification based on the initial rate of disintegration (below mesh size B.S. No.36) and relating more to structural and mineralogical composition has lead to a subdivision into three categories i.e. a rapid slaking group (disintegration greater than 3.5 per cent per minute), a fast - medium slaking group (disintegration between 0.5 - 3.5 per cent per minute) and a slow slaking group (disintegration less than 0.5 per cent per minute). The disintegration process in terms of a first order reaction is only shown by the very explosive materials within the rapid slaking group, although in general terms, no true first order process could be positively identified, indicating that more than one form of breakdown was operating.

Shales which fall within the rapid slaking group predominantly contain large quantities of expandable minerals (notably smectite). Preferred orientation studies indicate that materials in this group generally have a random structure, although a highly orientated structure is noted in the Yazoo Clay.

Breakdown in the fast-medium group is observed to occur in a number of ways, materials exhibiting the faster rates generally contain small to moderate quantities of expandable minerals (including some smectite) and possess a fairly random structure, although generally better orientated than those observed in the rapid slaking group. On the other hand, breakdown of materials having disintegration rates towards the slower end of the group usually starts by splitting along planes of weakness followed by slow disintegration. Observations

from hand specimens infers that their fabrics have a reasonable degree of orientation. Within the slow slaking group, materials having a highly preferred orientation show little, or no tendency towards breakdown, although splitting along planes of weakness does occur. On the other hand, slightly indurated quartz deficient, randomly orientated materials, (e.g. the seatearth) are observed to breakdown quite rapidly into large chips not small enough to pass through the mesh. Hard, silty materials (with liquid limits between 35 - 42 per cent), however, also breakdown into large chips, but at a slower rate, and in certain cases continued slow breakdown below mesh size occurs where smectite is present.

The amount of disintegration below mesh size, with certain exceptions, is observed to generally decrease as the rate of disintegration decreases. The range is from 80 - 100 per cent within the rapid group and faster end of the fast-medium group, to 45 per cent at the lower end of the latter, to zero per cent in the slow group.

Therefore, in conclusion, it has been shown from studies on a wide spectrum of 'shales' that the compaction history, coupled with the mineralogical composition have a decisive bearing on the behaviour of these materials, both at depth and in the near surface zone. A new interpretation of stress-strain response has been proposed as a result of these studies, and in addition the role of interparticulate bonding has been extensively studied with further evidence being offered to support Bjerrum's (1967a) hypothesis. Bonding studies have further indicated that, in general, materials examined of post-Carboniferous age contain mainly cationic forms, whereas a welding nature is indicated from sediments of the Carboniferous age. Furthermore, although simple slaking and suction experiments will depict the latter type of bonding, they generally fail to detect the

weaker cationic form, which may often be the cause of unforeseen engineering complications in the field. Consequently to investigate this phenomenon in full, it is suggested that consolidation tests (of a lesser magnitude than those currently used) should be performed on both undisturbed and remoulded material in addition to a simple static slaking test. Moreover, it is also suggested that materials containing 'strong bondings', according to Bjerrum (1967a) can be further sub-divided into those where a welding type bond is present and those where a cationic form is present; the latter being inherently the most dangerous from an engineering aspect.

References.

AITCHISON, G.D. & WOOD, C.C. (1965) 'Some interactions of compaction, permeability and post-constructional deflocculation affecting the probability of piping failure in small earth dams', 6th. Int. Conf. on Soil Mechs. & Fdn. Engng., Montreal, Vol. 11, pp.442.

ALLEN, P. (1959)'The Wealden environment: The Anglo-Paris Basin', Phil. Trans. R. Soc. Bull., 242, pp.283-346.

ALLING, H.L. (1945) 'Use of microlithologies as illustrated by some New York sedimentary rocks', Bull. Geol. Soc. Am., 56, pp.737-756.

ALTSCHAEFFL, A.G. & HARRISON, W. (1959) 'Estimation of a minimum depth of burial for a Pennsylvanian underclay', J. Sed. Pet., 29(2), pp.178-185.

AMERICAN GEOLOGICAL INSTITUTE. (1957) 'Glossary of geology and related sciences', Washington D.C.,p.325.

ARORA, H.S. (1969) 'Clay dispersion as influenced by chemical environment and mineralogical properties', Ph.D. Thesis, Univ. of California, Riverside.

ARKELL, W.J. (1947) 'The geology of the country around Weymouth, Swanage, Corfe and Lulworth', Memoirs of the Geol. Surv. of Great Britain.

ATHY, L.F. (1930) 'Density, porosity and compaction of sedimentary rocks', Am. Ass. Petrol. Geol. Bull., 14(1), pp.1-24.

ATTERBERG, A. (1911) 'On the investigation of the physical properties of soils and on the plasticity of clays', Int. Mitt. Fur. Bodenkunde, 1, pp.10-43.

ATTEWELL, P.B. & TAYLOR, R.K. (1970) 'Jointing in Robin Hood's Bay, North Yorkshire Coast, England', Int. J. Rock Mech. & Min. Sc., 8, pp.477-481.

ATTEWELL, P.B. & TAYLOR, R.K. (1973) 'Clay shale discontinous rock mass studies', Report to U.S. Army, No. DA-ERO-591-72-90005.

AUGHENBAUGH, N.B. (1974) 'Effects of moisture on shale', 23rd. Annual Soil Mech. & Fdn. Eng. Conf., Univ. of Kansas.

AYLMORE, L.A.G. & QUIRK, J.P. (1959) 'Swelling of clay-water systems', Nature, 183, pp.1752-1753.

AYLMORE, L.A.G. & QUIRK, J.P. (1960) 'Domain and turbostratic structure of clays', Nature, 187, pp.1046-1048.

BADGER, C.W., CUMMINGS, A.D. & WHITMORE, R.L. (1956) 'The disintegration of shales in water', J. Inst. Fuel, 29, pp.417-423.

BALDWIN, B. (1971) 'Ways of deciphering compacted sediments', J. Sed. Pet., 41, pp.293-301.

BALTZ, E.H. (1967) 'Stratigraphy and regional tectonic implications of part of the Upper Cretaceous and Tertiary rocks, East Central San Juan Basin - New Mexico', U.S.G.S. Prof. Paper 552.

BARDEN, L. (1965a) 'Consolidation of compacted and unsaturated clays', Geotechnique, 15, pp.267-286.

BARDEN, L. (1965b) 'Consolidation of clays with non-linear viscosity', Geotechnique, 15, pp.345-362.

BARDEN, L. (1972) 'The relation of soil structure to the engineering geology of clay soil', Quart. J. Engr. Geol., 5, pp.85-102.

BARDEN, L. & BERRY, P.L. (1965) 'Consolidation of normally-consolidated clay', Soil Mech. & Fdn. Div. J., A.S.C.E. Proc., 91, SM5, pp.15-35.

BARDEN, L. & SIDES, G.R. (1970) 'Engineering behaviour and the structure of compacted clay', Am. Soc. Civ. Eng. Proc., 96, SM4, pp.1171-1200.

BARDEN, L. & SIDES, G.R. (1971a) 'The microstructure of dispersed and flocculated samples of kaolinite, illite and montmorillonite', Can. Geotech. J., 8, pp.391-399.

BARDEN, L. & SIDES, G.R. (1971b) 'Sample disturbance in the investigation of clay micro-structure', Geotechnique, 21(3), pp.211-222.

BARSHAD, I. (1950) 'Effect of interlayer cations on expansion of the mica lattice', Am. Min., 35, pp.225-238.

BARSHAD, I. (1955) 'Adsorption and swelling properties of clay-water systems', Clays & Clay Technology, Dept. of Natural Resources, State of Calif. Bull., 169, pp.70-77.

BASS, N.W. & NORTHROP, S.A. (1963) 'Geology of Glenwood Springs Quadrangle & Vicinity, Northwestern Colorado', U.S.G.S. Bull., 1142-J.

BASTIANSEN, R., MOUM, J. & ROSENQUIST, I.Th. (1957) 'Some investigations of alum slate in construction', Publ. 22, Norwegian Geotechnical Inst., Oslo, pp.69.

BATES, T.F. (1947) 'Investigation of the micaceous minerals in slate', Am. Min., 32, pp.625-636.

BEALL, A. (1974) Personal communication to Rieke, H.H. and Chilingarian, G.V., Compaction of Argillaceous Sediments, Developments in Sedimentology, 16, Elsevier, Amsterdam.

BERKOVITCH, I., MANACKERMAN, M. & POTTER, N.M. (1959) 'The shale breakdown problem in coal washing. Part 1: Assessing the breakdown of shale in water', J. Inst. Fuel, 32, pp.579-589.

BISHOP, A.W., WEBB, D.L. & LEWIN, P.I. (1965) 'Undisturbed samples of London Clay from the Ashford Common shaft: Strength-effective stress relationships', Geotechnique, 15, pp.1-31.

BJERRUM, L. (1967a) 'Progressive failure in slopes of over-consolidated plastic clay and clay shales', Soil Mech. & Fdn. Div., A.S.C.E. Proc., SM5, 93, pp.1-49.

BJERRUM, L. (1967b) 'Engineering geology of Norwegian normally consolidated marine clays as related to settlements of buildings', Geotechnique, 17, pp.81-118.

BJERRUM, L. (1969) 'Closure to 'Progressive failure in slopes of overconsolidated plastic clay and clay shales' by L.Bjerrum', J. Soil Mech, & Fdn. Div., A.S.C.E. Proc., 95, SM5, p.1255.

BJERRUM, L. & LO, K.Y. (1963) 'Effect of aging on the shear-strength properties of a normally-consolidated clay', Geotechnique, 13, pp.147-157.

BJERRUM, L. & WU, H.T. (1960) 'Fundamental shear-strength properties of the Lilla Edet clay', Geotechnique, 10, pp.101-109.

BLACKMORE, A.V. & MILLER, R.D. (1961) 'Tachoid size and osmotic swelling in calcium montmorillonite', Soil Sci. Soc. Am. Proc., 25, pp.169-173.

BOLT, G.H. (1956) 'Physico-chemical analysis of the compressibility of pure clays', Geotechnique, 6(1), pp.86-93.

BOUYOUCOS, G.J. (1929) 'The ultimate structure of natural soils', Soil Sci., 28, pp.27-37.

BOUYOUCOS, G.J. (1935) 'Method of making mechanical analysis of the ultimate structure of soils', Soil Sci., 48, pp.481-485.

BRADLEY, W.F. (1945) 'Molecular associations between montmorillonite and some polyfunctional organic liquids', J. Am. Chem. Soc., 67, pp.975-981.

BRADLEY, W.F., GRIM, R.E. & CLARK, G.L. (1937) 'Behaviour of montmorillonite on wetting', Z. Kristallog., 97, pp.216-222.

BRADSHAW, M.J. (1975) 'Origin of montmorillonite bands in the Middle Jurassic of Eastern England', Earth and Planetary Science Letters, 26, pp.245-252.

BREWER, R. (1964) 'Fabric and mineral analysis of soils', New York: John Wiley.

BRINDLEY, G.W. (1961a) 'Quantitative analysis of clay mixtures', In: G. Brown Ed. The X-Ray Identification and Crystal Structures of Clay Minerals, Min. Soc. Monograph, London.

BRINDLEY, G.W. (1961b) 'Chlorite minerals', In: G. Brown Ed. The X-Ray Identification and Crystal Structures of Clay Minerals, Min. Soc. Monograph, London.

BRINDLEY, G.W. & ROBINSON, K. (1947) 'X-ray studies of some kaolinite fireclays', Trans. Brit. Ceram. Soc., 46, pp.49-62.

BRITISH STANDARDS 1377. (1967) 'Methods of testing soils by civil engineering', H.M.S.O.

BROOKER, E.W. (1967) 'Strain energy behaviour of overconsolidated soils', Can. Geotech. J., 2, pp.323-327.

BROWN, G. (1961) ' The X-ray identification and crystal structures of clay minerals', Min. Soc. Mono., London.

BROWN, R.W. (1943) 'Cretaceous-Tertiary boundary in the Denver basin Colorado', Bull. Geol. Soc. Am., 51(1), pp.65-8

BROWN, G. & FARROW, R. (1956) 'Vapour glycerolation', Clay Mins. Bull., 63, pp.44-45.

BRUNAUER, G., EMMETT, P.H. & TELLER, E. (1938) 'Adsorption of gases in multi-molecular layers', J. Am. Chem. Soc., 60, pp.309-319.

BRUNTON, G. (1955) 'Vapour glycolation', Am. Min., 40, p.124-126

BURNETT, A.D. & FOOKES, P.G. (1974) 'A regional engineering geological study of the London Clay in the London and Hampshire basins', Quart. J. Eng. Geol., 7(3), pp.257-295.

BURST, J.F. (1959) 'Post diagenetic clay mineral environment relationships in the Gulf Coast Eocene', Proc. of the 6th. Natl. Conf. Clay and Clay Min., pp.327-341.

BURST, J.F. (1969) 'Diagenesis of Gulf Coast sediments and its possible relation to petroleum migration', Am.Assoc. Petrol. Geol. Bull., 53(1), pp.73-93.

CASAGRANDE, A. (1932a) 'The structure of clay and its importance in foundation engineering', J. Boston Soc. Civ. Engrs., 19, pp.168-209.

CASAGRANDE, A. (1932b) 'Research on the Atterberg limits of soils', Public Roads, 13, pp.121-136.

CASAGRANDE, A. (1936) 'The determination of the preconsolidation load and its practical significance', Proc. 1st. Int. Conf. on Soil Mechanics, Harvard, 3, pp.60-64.

CASAGRANDE, A. (1948) 'Classification and identification of soils', Trans. Am. Soc. Civ. Engrs., 113, pp.901-930.

CASAGRANDE, A. (1949) 'Notes on swelling characteristics of clay shales', Harvard Univ., Cambridge, Mass., 16pp.

CHANDLER, R.J. (1971) 'Lias Clay: weathering processes and their effect on shear strength', Private Communication to Barden (1972), 'The relation of soil structure to the engineering geology of clay soil', Quart. J. Engr. Geol., 5, pp.85-102.

CHAPMAN, H.D. (1965) 'Cation exchange capacity', In: Methods of Soil Analysis, Part 2 (Ed. Black, C.A.), Am. Soc. Agronomy, 15, pp.771-1572.

CHATWIN, C.P. (1947) 'East Anglia and Adjoining Areas', British Regional Geology.

CHATWIN, C.P. (1948) 'Hampshire Basin and Adjoining Areas', British Regional Geology.

CHILDS, E.C. (1969) 'Introduction to the physical basis of soil water phenomena', J. Wiley and Sons Ltd.

CHILINGAR, G.V. & KNIGHT, L. (1960) 'Relationship between pressure and moisture content of kaolinite, illite and montmorillonite clays', Am. Assoc. Petrol. Geol. Bull., 44(1), pp. 101-106.

CHILINGARIAN, G.V. & RIEKE, H.H. (1968) 'Data on consolidation of finegrained sediments', J. Sed. Pet., 38, pp.811-816.

CLARK, F.W. (1924) 'Data on geochemistry', U.S.G.S. Bull., 770, p. 140.

CORNELL UNIVERSITY (1951) 'Final report on solidification research', Ithaca, N.Y.

COLE, D.C.H. & LEWIS, J.G. (1960) 'Piping failure of earth dams built of plastic materials in arid climates', 3rd. Australian-New Zealand Conf. on Soil Mech. & Fdn. Engrg., p.93.

COLEMAN, J.D. (1949) 'Soil thermodynamics and road engineering', Nature, 163, pp.143-145.

COLEMAN, J.D. (1959) 'An investigation of the pressure membrane method for measuring the suction properties of soil', Road Research Note RN/3464.

COLEMAN, J.D. & FARRAR, D.M. (1956) 'The measurement of the vapour pressure and surface area of soils', Road Research Note RN/2763.

COOLEY, M.F., HARSHBARGER, J.W., AKERS, J.P. & HARDT, W.F. (1969) 'Regional hydrogeology of the Navajo and Hopi Indian reservations, Arizona, New Mexico and Utah', U.S.G.S. Prof. Paper, 521-A.

CRAWFORD, C.B. (1964) 'Interpretation of the consolidation test', J. Soil Mech. & Fdn. Div. Proc., A.S.C.E., 90, SM5, pp.87-101.

CRONEY, D. & COLEMAN, J.D. (1948) 'Soil thermodynamics applied to the movement of moisture in road foundations', Proc. 7th. Int. Congr. Appl. Mech., 3, pp.163-177.

CRONEY, D. & COLEMAN, J.D. (1954) 'Soil structure in relation to soil suction', J. Soil Sci., 5, pp.75-84.

CRONEY, D. & COLEMAN, J.D. (1961) 'Pore pressure and suction in soil', In: Pore Pressure and Suction in Soils (London), pp.31-38

CRONEY, D., COLEMAN, J.D. & BLACK. W.P.M. (1958) 'The movement and distribution of water in soil in relation to highway design and performance', Highway Research Board Special Paper, 40, Washington D.C.

CRONEY, D., COLEMAN, J.D. & BRIDGE, P.M. (1952) 'The suction of moisture held in soils and other porous material', Road Research Tech. Paper, 24, H.M.S.O.

CUSHING, E.M., BOSWELL, E.H. & HOSMAN, R.L. (1964) 'General geology of the Mississippi Embayment', U.S.G.S. Prof. Paper, 448-B.

DAVIS, E.H. & RAYMOND, G.P. (1965) 'A non-linear theory of consolidation', Geotechnique, 15, pp.161-173.

DEERE, D.U. & GAMBLE, J.C. (1971) 'Durability-plasticity classification of shales and indurated clays', Proc. 22nd. Annual Highway Geology Symp., Univ. of Oklahoma, pp.37-52.

DENISOV, N.Y. & RELTOV, B.F. (1961) 'The influence of certain processes on the strength of soils', Proc. 5th. Int. Conf. on Soil Mech. and Fdn. Engrg., 1, pp.75-78.

DEO, P. (1972) 'Shales as embankment materials', Joint Highway Research Project, Purdue University and Indiana State Highway Commision.

DINES, H.G. & EDMUNDS, F.H. (1933) 'The geology of the country around Reigate and Dorking', Memoirs of the Geol. Surv. of Great Britain.

DREVER, J.I. (1971) 'Early diagenesis of clay minerals, Rio Ameco Basin, Mexico', J.Sed. Pet., 41, pp.982-995.

DUMBLETON, M.J. & WEST, G. (1970) 'The suction and strength of remoulded soils as affected by composition', Transport and Road Research Laboratory, Report LR 306.

DUNBAR, C.O. & WAAGE, K.M. (1969) 'Historical geology', J. Wiley and Sons.

DUTT, A.K. (1948) 'Mechanism of aggregation of clay minerals by soluble silicates', Soil Sci., 65, pp.309-319.

EDMUNDS, F.H. (1947) 'Central England', Brit. Regional. Geology.

ELGABALY, M.M. & ELGHAMRY, W.M. (1970) 'Water permeability and stability of kaolinite systems as influenced by adsorbed cation ratio', Soil Sci., 110, pp.107-110.

EMERSON, W.W. (1962) 'The swelling of Ca-montmorillonite due to water absorption - 2. Water uptake in the liquid phase', J. Soil Sci., 13, pp.40-45.

EMERSON, W.W. (1963) 'The swelling of sodium montmorillonite due to water absorption', Austral. J. Soil Res., 1, pp.129-143.

EMERSON, W.W. (1964) 'The slaking of soil crumbs as influenced by clay mineral composition', Austral. J. Soil Res., 2, pp.211-217.

EMERSON, W.W. (1967) 'A classification of soil aggregates based on their coherence in water', Austral. J. Soil Res., 5, 47-57.

EMERSON, W.W. (1968) 'The dispersion of clay from soil aggregates' Trans. 9th. Int. Cong. of Soil Sci., 1, Adelaide, Australia, pp.617-625.

ENO, F.H. (1926) 'The slaking test', Proc., Highway Research Board, 6, p.142.

FAIRBURN, P.E. & ROBERTSON, R.H.S. (1956) 'Liquid limit and dye adsorption', Min. Soc., London, Clay Mins. Bull., 3, pp.129-136.

FARRAR, D.M. (1963) 'The use of vapour pressure and moisture content measurement to deduce the internal and external surface areas of soil particles', J.Soil Sci., 14(2), pp.303-321.

FARRAR, D.M. & COLEMAN, J.D. (1967) 'The correlation of surface area with other properties of nineteen British clay soils', J.Soil Sci., 18(1), pp. 118-124.

FASSET, J.E. & HINDS, J.S. (1971) 'Geology and fuel resources of the Fruitland Formation and Kirkland Shale of the San Juan Basin, New Mexico and Colorado', U.S.G.S. Prof. Paper, 676.

FINK, D.H., NAKAYAMA, F.S. & McNEAL, B.L. (1971) 'Demixing of exchangeable cations in free-swelling bentonite clay', Soil Sci. Soc. Am. Proc., 35, pp.552-555.

FISHER, R.A. & YATES, F. (1974) 'Statistical tables for biological, agricultural and medical research', 6th Ed. London.

FLEMING, R.W., SPENCER, G.S. & BANKS, D.C. (1970) 'Empirical study of behaviour of clay shale slopes', U.S. Army Engs. Nuclear Cratering Group, Livermore, Calif., Tech. Report No. 15.

FOOKES, P.G. (1966) 'London Tertiary Sediments', Geotechnique, 16, pp.260-263.

FRANKLIN, J.A., BROCH, E. & WALTON, G. (1970) 'Logging the mechanical character of rock', Rock Mechs. Research Report D - 14, Imperial College, London.

FRANKLIN, J.A. & CHANDRA, R. (1972) 'The slake-durability test', Int. J. Rock Mech. Soc., 9, pp. 325-341.

GAMBLE, J.C. (1971) 'Durability-plasticity classification of shales and other argillaceous rocks', Ph.D. Thesis, Univ. of ILLinois.

GIBBS, R.J. (1967) 'Quantitative X-ray diffraction analysis using clay mineral standards extracted from the samples analysed', Clay Mins., 7,

GIBSON, R.E., ENGLAND, G.L. & HUSSEY, M.J.L. (1967) 'The theory of one-dimensional consolidation of saturated clays', Geotechnique, 17(3), pp.261-273

GIBSON, R.E. & LO. (1961) 'Theory of consolidation of saturated clays', Norwegian Geotechnical Inst. Pub., No. 4.

GILKES, R.J. & HODSON, E. (1971) 'Two mixed-layer mica-montmorillonite minerals from sedimentary rocks', Clay Mins, 9, pp.125-137.

GILLOT, J.E. (1969) 'Study of fabric of finegrained sediments with the scanning electron microscope', J. Sed. Pet., 39, pp. 90-105.

GILLOT, J.E. (1970) 'Fabric of Leda Clay investigated by electron optical and X-ray diffraction methods', Eng. Geol., 4, pp.133-153.

GIPSON, M. (1966) 'A study of the relations of depth, porosity, and clay mineral orientation in Pennsylvanian Shales', J. Sed. Pet., 36, pp.888-903.

GOLDSCHMIDT, V.M. (1954) 'In: 'Geochemistry', A Muir (Ed), Oxford Univ. Press, London, 730pp.

GRICE, R.H. (1968) 'The effect of temperature-humidity on the disintegration of non-expandable shales', Assoc. of Eng. Geol. Bull., 5(2), pp.69-77.

GRIFFIN, O.G. (1954) 'A new internal standard for quantitative X-ray analysis of shales and mine dust', Research Report No. 101, Safety in Mines Establishment, Ministry of Power, Sheffield.

GRIM, R.E. (1968) 'Clay mineralogy', International Series in Earth and Planetary Sciences, 2nd. Ed., McGraw-Hill.

HAIL, W.J. (1968) 'Geology of south-western North Park and Vicinity, Colorado', U.S.G.S. Bull., 1257.

HALLAM, A. & SELLWOOD, B.W. (1968) 'Origin of Fuller's Earth in the Mesozoic of southern England', Nature, 220, pp.1193-1195.

HAMROL, A. (1961) 'A quantitative classification of the weathering and weatherability of rocks', Proc. 5th, Conf. Soil Mech. & Fdn. Engrg., France, 2, pp.771-774.

HANSBO, S. (1960) 'Consolidation of clay with special reference to the influence of vertical sand drains', Swedish Geotech. Inst. Res. No. 18.

HEDBERG, H.D. (1936) 'Gravitational compaction of clays and shales', Am. J. Sci., 5th. Series, 31(184), pp. 241-287.

HENIN, S. (1938) 'A physical chemical study of the stability of soils', Monograph, National Centre of Agronomic Research, Paris.

HILPERT, L.S. (1969) 'Uranium resources of northwestern New Mexico', U.S.G.S. Prof. Paper, 603.

HINCKLEY, D.N. (1963) 'Variability in crystallinity values among the kaolin deposits of the coastal plain of Georgia and S. Carolina', Proc. 11th. Nat. Conf. on Clays and Clay Mins., Pergamon Press, pp. 229-235.

HOGENTOGLER, C.A. (1937) 'Engineering properties of soils', McGraw-Hill, New York.

HONEYBOURNE, D.B. (1951) 'Clay minerals in the Keuper Marl', Clay Mins. Bull., 1(5), pp.150-155.

HOUGH, R.K. (1957) 'Basic soils engineering', Ronald Press.

HVORSLEV, M.J. (1960) 'Physical components of the shear strength of saturated clays', A.S.C.E. Research Conf. on Shear Strength of Cohesive Soils, Boulder, Colorado, pp. 169-273.

INGLES, O.G. (1968) 'Soil chemistry relevant to the engineering behaviour of soils', In: Soil Mechanics-Selected Topics, I.K. Lee (Ed.); Butterworth, London, pp.1-57.

INGRAM, R.L. (1953) 'Fissility of mudrocks', Geol. Soc. Am. Bull., 64, pp. 869-878.

JACKSON, J.O. & FOOKES, P.G. (1974) 'The relationship of the estimated former depth of burial of the Lower Oxford Clay to some soil properties', Quart. J. Eng. Geol. 7(2), pp.137-179.

JOHNS, E.A., BURNETT, R.G. & CRAIG, C.L. (1963) 'Oahe Dam: Influence of shale on Oahe power structures design', J. Soil Mech. & Fdn. Div. Proc., A.S.C.E., 89, SM1, pp.95-113.

KAARSBERG, E.A. (1959) 'Introductory studies of natural and artificial argillaceous aggregates by sound propagation and X-ray diffraction methods', J. Geol., 67, pp.447-472.

KELLER, W.D. (1963) 'Diagenesis in clay minerals - a review', Clays and Clay Mins., 11, pp.136-157.

KEMPER, W.D. (1961) 'Movements of water as affected by free energy and pressure gradients', Soil Sci. Soc. Am. Proc., 25, pp.255-265.

KENNARD, M.F., KNILL, J.L. & VAUGHAN, P.R. (1967) 'The geotechnical properties and behaviour of Carboniferous shales at the Boulderhead Dam', Quart. J. Eng. Geol., 1(1), pp;3-24.

KENNEY, T.C., MOUM, J. & BERRE, T. (1967) 'An experimental study of bonds in natural clay', Geotechnical Conf. Proc., Oslo, pp.65-69.

KERR, P.F. & HAMILTON, P.K. (1949) 'Reference clay minerals', A.P.I. Research Project, No. 49.

KOMORNIK, A., ROHLICH, V. & WISEMAN, G. (1970) 'Overconsolidation by desiccation of coastal Late Quarternary clays in Israel', Sedimentology, 14, pp.125-140.

KRUMBEIN, W.C. (1947) 'Shales and their environmental significance', J. Sed. Pet., 17, pp.101-108.

LAMBE, T.W. (1953) 'The structure of inorganic soils', Am. Soc. Civ. Engrs. Proc., Separate No. 315.

LAMBE, T.W. (1958) 'The structure of compacted clay', J.Soil Mech & Fdn. Div. Proc., A.S.C.E., 84, SM2, pp.1-34.

LAMBE, T.W. & WHITMAN, R.V. (1969) 'Soil Mechanics', J. Wiley and Sons.

LANGER, K. (1936) 'Influence of speed of loading increment on the pressure voids ratio diagram of undisturbed soil samples', Proc. 1st. Int. Conf. on Soil Mech., Cambridge, Mass., 2, pp.116-118.

LARSEN, G. & CHILINGAR, G.V. (1967) (Ed.) 'Diagenesis in sediments', Elsevier, Amsterdam.

LARWOOD, G.P. & FUNNEL, B.M. (1970) 'The geology of Norfolk', Collection of papers to the Paramoudra Club 10th Anniversary, Headley Bros

LEGGETT, R.F. (1962) 'Geology and engineering', McGraw-Hill & Co., New York, p.48.

LEONARDS, G.A. & ALTSCHAEFFL? A.G. (1964) 'Compressibility of clay', J. Soil Mech. & Fdn. Div. Proc., A.S.C.E., 90, SM5, paper 4019, pp.143-155.

LEONARDS, G.A. & GIRAULT, P. (1961) 'A study of the one-dimensional consolidation test', Proc. 5th. Int. Conf. Soil Mech., 1, pp.213-221.

LEONARDS, G.A. & RAMAIH, B.L. (1959) 'Time effects in the consolidation of clays', Special Tech. Pub. No. 254, Am. Soc. for Testing Material, pp.116-130.

LEWIS, W.A. (1950) 'an investigation of the consolidation test for soils', Dept. of Scientific & Industrial Research, Road Research Laboratory, Note No. RN/1349/WAL.

LEWIS, W.A. & CRONEY, D. (1965) 'The properties of chalk in relation to road foundations and pavements', Paper 3 of Chalk in Earthworks and Foundations, Proc. of a symposium held at the Inst. of Civ. Engs.

LO, K.Y. (1961) 'Secondary compression of clays', J. Soil Mech. & Fdn. Div. Proc., A.S.C.E., Paper 2885, pp.61-87.

LOWE, J., JONAS, E. & OBRICIAN, V. (1969) 'Controlled gradient consolidation test', J. Soil & Fdn. Eng. Div., A.S.C.E., 95, pp.77-97.

MACEWAN, D.M.C. (1948) 'Adsorption of montmorillonite and its relation to surface area adsorption', Nature, 162, pp.935-935.

MACEWAN, D.M.C. (1954) 'Short range electrical forces between charged colloid particles', Nature, 174, pp.39-40.

MACEWAN, D.M.C. (1961) 'Montmorillonite minerals', In: G. Brown (Ed.), 'X-ray identification of crystal structures of clay minerals', Mem. Min. Soc. (London).

McCALLA, T.M. (1944) 'Water-drop method of determining stability of soil structure', Soil Sci., 58, pp.117-121.

MEAD, W.J. (1936) 'Engineering geology of damsites' Trans. 2nd. Int. Cong. on Large Dams, Washington D.C., 4, pp.171-192.

MEADE, R.H. (1961a) 'X-ray diffractometer methods for measuring preferred orientation in clays', U.S.G.S. Prof. Paper, 424B, pp.273-276.

MEADE, R.H. (1961b) 'Compaction of montmorillonite-rich sediments in Western Fresno County, California', U.S.G.S. Prof. Paper, 424, PD89-D91.

MEADE, R.H. (1964) 'Removal of water and rearrangement of particles during compaction of clayey sediments - review', U.S.G.S. Prof. Paper, 497B, B1-B23.

MEADE, R.H. (1966) 'Factors influencing the early stages of compaction of clays and sands - review', J. Sed. Pet., 36, 1085-1101.

MESRI, G. & OLSON, R.E. (1971) 'Mechanisms controlling the permeability of clays', Clays & Clay Mins., 19(3), pp.151-158.

MIELENZ, R.C. & KING, M.E. (1955) 'Physical-chemical properties and engineering performance of clays', Clays and Clay Tech. Bull., 169, Calif. State Div. of Mines, pp.196-254.

MILLER, J.G. & OULTON, T.D. (1970) 'Prototropy in kaolinite during percussive grinding', Clays and Clay Mins, 18.

MITCHELL, J.K. (1956) 'The fabric of natural clays and its relation to engineering properties', Highway Research Board Proc., 35, pp.693-713.

MITCHELL, J.K. (1960) 'The application of colloidal theory to the compressibility of clays', In: R.H. Parry (Ed.), 'Interparticulate forces in clay-water-electrolyte systems', C.S.I.R.O., Melbourne, pp.2.92-2.97.

MITCHELL, J.K. (1965) 'The slaking of Newton Dam Claystone', Consulting Report, p.18.

MITCHELL, J.K. (1973) 'Recent advances in the understanding of the influences of mineralogy and pore solution chemistry on the swelling and stability of clays', 3rd. Int. Conf. on Expansive Soils, Haifa, Israel.

MITCHELL, J.K., SINGH, A. & CAMPANELLA, R.G. (1969) 'Bonding, effective stresses, and strength of soils', J. Soil Mech. & Fdn. Div. Proc., A.S.C.E. 95, SM5, pp.1219-1246.

MONROE, W.H. (1954) 'Geology of the Jackson area, Mississippi', U.S.G.S. Bull., 986pp.

MOON, C.F. (1972) 'The microstructure of clay sediments', Earth Sci. Reviews, 8, pp.303-321.

MORGENSTERN, N.R. & EIGENBROD, K.D. (1974) 'Classification of argillaceous soils and rocks', J. of the Geotech. Eng. Div., A.S.C.E., 100, No. GT10, pp.1137-1156.

MORGENSTERN, N.R. & TCHALENKO, J.S. (1967a) 'The optical determination of preferred orientation in clays and its application to the study of microstructure in consolidated kaolin-1', Proc. Roy. Soc., A300, pp.218-234.

MORGENSTERN, N.R. & TCHALENKO, J.S. (1967b) 'The optical determination of preferred orientation in clays and its application to the study of microstructure in consolidated kaolin-2', Proc. Roy. Soc., A300, pp.235-250.

MORIWAKI, Y. (1974) 'Causes of slaking in argillaceous materials', Ph.D. Thesis, Univ. of Calif., Berkeley

MORLEY, A. (1940) 'Strength of materials', 9th. Ed., Longman Press.

MURAYAMA, S. & SHIBATA, T. (1959) 'On the secondary consolidation of clay', Proc. 2nd. Cong., Japanese Soc. for Testing Materials, Kyoto Univ., Kyoto, Japan, p.178.

MURRAY, H.H. & LYONS, S.C. (1956) 'Correlation of paper-coating quality with degree of crystal perfection of kaolinite', A. Swineford (Ed.), Clays & Clay Mins. pp.31-40.

NAGELSCHMIDT, G. (1938) 'Atomic arrangements of the montmorillonite group', Min. Mag., 25, pp.140-155.

NAKANO, R. (1967) 'On weathering and change of properties of Tertiary mudstone related to landslides', Soil & Fdn., 7, pp.1-14.

NEWLANDS, P.L. & ALLELY, B.H. (1960) 'A study of the consolidation characteristic of a clay', Geotechnique, 10(2), pp.62-74.

NICHOLLS, G.D. & LORING, D.H. (1960) 'Some chemical data on British Carboniferous sediments and their relationship to the clay mineralogy of these rocks', Clay Mins. Bull., 4, 198pp.

NORDQUIST, E.C. & BAUMAN, R.D. (1967) 'Stabilisation of expansive Mancos Shale', Proc. 3rd. Asian Conf. on Soil Mech. & Fdn. Engrg., Haifa, Israel, pp.107-110.

NORRISH, K. & QUIRK, J.P. (1954) 'Crystalline swelling of montmorillonite', Nature, 173, pp.255-257.

NORTHEY, R.D. (1956) 'Rapid consolidation tests for routine investigations', Proc. 2nd. Australia-New Zealand Conf. on Soil Mech., Christchurch, N.Z., pp.20-24.

O'BRIEN, N.R. (1964) 'Origin of Pennsylvanian underclays in the Illinois basin', Am. Geol. Soc. Bull., 75, pp.823-832.

O'BRIEN, N.R. (1968) 'Electron microscope study of a black shale fabric', Naturwiss., 55, pp.490-491.

ODOM, I.E. (1967) 'Clay fabric and its relation to structural properties in mid-continental Pennsylvanian sediments', J. Sed. Pet., 37, pp.610-623.

OLSEN, H.W. (1966) 'Darcy's law in saturated kaolinite' Water Resour., 2, pp.287-294.

OLSON, R.E. & MESRI, G. (1970) 'Mechanisms controlling the compressibility of clays', J. Soil Mech. & Fdn. Div. Proc., A.S.C.E., 96, SM6, pp.1863-1878.

OLSON, R.E. & MESRI, G. (1971) 'Consolidation characteristics of montmorillonite', Geotechnique, 21(4), pp.341-352.

OVERTON, H.L. & ZANIER, A.M. (1970) 'Hydratable shales and the salinity high enigma', Soc. Pet. Eng., Am. Inst. Min. Metal. Eng., 45th. Ann. Fall Meet., Huston, Texas, Paper No. 2989, 9pp.

PAYNE, T.G. (1942) 'Stratigraphical analysis and environmental reconstruction', Am. Assoc. Pet. Geol. Bull., 26, pp.1697-1770.

PERRIN, R.M.S. (1971) 'The clay mineralogy of the British sediments', Min. Soc. (Clay Mins. Group), London.

PETERSON, R. (1954) 'Studies of Bearpaw Shale at a damsite in Saskatctewan', A.S.C.E. Proc., No. 476, 80, 28pp.

PETERSON, R. (1958) 'Rebound in the Bearpaw Shale in western Canada', Geol. Soc. Am. Bull., 69, pp.1113-1123.

PETTIJOHN, F.J. (1957) 'Sedimentary rocks', Harper Bros., New York.

PHILPOT, K. (1971) 'Suction and swelling pressure of certain argillaceous material', M.Sc. Thesis, Univ. of Durham.

POWERS, M.C. (1959) 'Adjustment of clays to chemical change and the concept of equivalence level', Proc. 6th. Natl. Conf. Clays and Clay Mins., pp.309-326.

POWERS, M.C. (1967) 'Fluid-release mechanisms in compacting marine mudrocks and their importance in oil exploration', Am. Assoc. Pet. Geol. Bull., 51(7), pp.1240-1254.

PUSCH, R. (1966) 'Quickclay microstructure', Eng. Geol., 1, pp.433-443.

QUIGLEY, R.M. & THOMPSON, C.D. (1966) 'The fabric of anisotropically consolidated sensitve marine clay', Can. Geotech. J., 3, pp.61-73

RAYNER, D.H. (1967) 'The stratigraphy of the British Isles', Cambridge Univ. Press.

RAYNER, D.H. & HEMINGWAY, J.E. (1974) 'The geology and mineral resources of Yorkshire', S. Maney & Sons Ltd., Leeds.

REEVES, M.J. (1971) 'Geochemistry-mineralogy of British Carboniferous seatearths from northern coalfields', Ph.D. Thesis, Univ. of Durham.

RICHARDS, L.A. (1954) 'Diagnosis and improvement of saline and alkali soils', U.S. Dept. of Agriculture Handbook, No. 60, U.S. Govn. Printing Office, Washington D.C.

RIEKE, H.H. & CHILINGARIAN, G.V. (1974) 'Compaction of argillaceous sediments', In: Developments in Sedimentology, 16, Elsevier.

ROBINSON, C.S., MAPEL, W.J. & BERGENDAHL, M.L. (1964) 'Stratigraphy and structure of the northern and western flanks of the Black Hills uplift, Wyoming, Montana and S. Dakota', U.S.G.S. Prof. Paper, 404.

ROBERTSON, R.H.S. & WARD, R.M. (1950) 'The assay of pharmaceutical clays', J. Pharmacol., 3, pp.27-35.

ROSENQUIST, I.T. (1959) 'Physico-chemical properties of soils', Proc. Am. Soc. Civ. Eng., 85, SM2, pp.31-53.

ROSS, C.S. & HENDRICKS, S.B. (1945) 'Minerals of the montmorillonite group' U.S.G.S. Prof. Paper, 205B.

ROWELL, D.L. (1963) 'Effect of electrolyte concentration on the swelling of orientated aggregates of montmorillonite Soil Sci., 96, pp.368-374.

ROWELL, D.L., PAYNE, D. & AHMAD, N. (1969) 'The effect of the concentration and movement of solutions on the swelling, dispersion and movement of clay in saline and alkaline soils', J. Soil Sci., 20(1), pp.176-188.

RUSSAM, K. (1959) 'Climate and moisture conditions under road pavements', 2nd. Reg. African Conf. on Soil Mech. & Fdn. Engrg., Laurenco Marques.

RUSSEL, E.R. & MICKLE, J.L. (1970) 'Liquid limit by soil moisture tension', J. Soil Mech. & Fdn. Div. Proc., A.S.C.E. 96, pp.967-990.

SCHIFFMANN, R.L. (1958) 'Consolidation of soil under time - dependent loading and varying permeability', Proc. Highways Research Board, 37, pp.584-608.

SCHOFIELD, R.K. (1935) 'The pF of water in soil', Trans. 3rd. Int. Congr. Soil Sci., 2, pp.37-48.

SCHOFIELD, R.K. & SAMPSON, H.R. (1953) 'The deflocculation of kaolinite suspensions and the accompanying change over from positive to negative chloride adsorption', Clay Mins. Bull., 2, pp.45-51.

SCHOFIELD, R.K. & SAMPSON, H.R. (1954) 'Flocculations of kaolinite due to the attraction of oppositely charged crystal faces', Discussion of the Faraday Soc. No.18.

SCHULTZ, L.G. (1958) 'Petrology of underclays', Geol. Soc. Am. Bull., 69, pp.363-402.

SCHULTZ, L.G. (1964) 'Quantitative interpretation of mineralogical composition from X-ray and chemical data for the Pierre Shale', U.S.G.S. Prof. Paper, 391-C.

SEED, H.B., WOODWARD, R.J. & LUNDGREN, R. (1964) 'Clay mineralogical aspects of the Atterberg limits', J. Soil Mech. & Fdn. Div. Proc., A.S.C.E., SM4, pp.107-131.

SHAW, D.B. & WEAVER, C.E. (1965) 'The mineralogy and composition of shales', J. Sed. Pet., 35, 213-222.

SHAWE, D.R. (1970) 'Stratigraphy of Slick Rock district and vicinity, San Miguel and Dolores Counties, Colorado' U.S.G.S. Prof. Paper, 576-A.

SHERARD, J.L., DECKER, R.S. & RYKER, N.L. (1972) 'Piping in earth dams of dispersing clay', Proc. Speciality Conf. on 'Performance of Earth & Earth Supported Structures', 1, A.S.C.E., New York, pp.589-626.

SHERLOCK, R.L. (1947) 'London and Thames Valley', British Regional Geology.

SILLS, I.D., AYLMORE, L.A.G. & QUIRK, J.P. (1973) 'An analysis of pore size in illite-kaolinite mixtures', J. Soil Sci., 24(4), pp.480-490.

SKEMPTON, A.W. (1944) 'Notes on the compressibility of clays', Quart. J. Geol. Soc., London, 100, pp.119-135.

SKEMPTON, A.W. (1953) 'Soil mechanics in relation to geology', Proc. Yorks. Geol. Soc., 29, pp.33-62.

SKEMPTON, A.W. (1970) 'The consolidation of clays by gravitational compaction', Quart. J. Geol. Soc., London, 125(3), pp.373-411.

SLOANE, R.L. & KELL, T.F. (1966) 'The fabric of mechanically compacted kaolin clays and clay minerals', Proc. Natl. Conf. Clays and Clay Mins., Berkeley, Calif., 14, pp.289-296.

SMART, P. (1967) 'Particle arrangements in kaolin', Clays and Clay Mins., 15, pp.241-254.

SMART, P. (1969) 'Soil structure in the electron microscope', Proc. Int. Conf. Structure. Solid Mechs. Eng. Design Civ. Eng. Mater., Univ. of Southampton.

SMITH, J.E. & WAHLS, H.E. (1969) 'Consolidation under controlled rate of strain', J. Soil Mech. & Fdn. Div. Proc., A.S.C.E., 95, SM2, pp.519-539.

SORBY, H.C. (1908) 'On the application of quantitative methods to the study of structure and history of rocks', Quart. J. Geol. Soc., London, 64, pp.171-232.

SPEARS, D.A. (1964) 'The major element geochemistry of the Mansfield marine band in the Westphalian of Yorkshire', Geochim. & Cosmochim. Acta, 28, pp.1969-1979.

SPEARS, D.A. (1971) 'The mineralogy of the Stafford tonstein', Proc. Yorks. Geol. Soc., 38, pp.497-516.

SPEARS, D.A. (1973) 'Relationship between exchangeable cations and palaeosalinity', Geochim. & Cosmochim. Acta, 37, pp.77-85.

SPEARS, D.A. (1974) 'Relationship between water-soluble cations and palaeosalinity', Geochim. & Cosmochim. Acta, 38, pp.567-575.

SRIDHARAN, A. & VENKATAPPA ROA, G.V. (1973) 'Mechanisms controlling volume change of saturated clays and the role of effective stress concept', Geotechnique, 23, pp.359-382.

STRAHAN, A. & HOLMES, T. V., DEWEY, H., CUNNINGHAM, C.H., SIMMONS, W.C., KING, W.B.R. & WRAY, D.A. (1916) 'Thicknesses of strata', Memoirs of the Geological Survey of England and Wales.

TAN TJONG-KLE (1957) 'Secondary time effects and consolidation of clays', Academia Sinica, Inst. Civ. Eng. & Arch., Harbin, China.

TAYLOR, D.W. (1942) 'Research on consolidation of clays', Serial 82, Mass. Inst. of Tech.

TAYLOR, D.W. (1948) 'Fundamentals of soil mechanics', Wiley, New York.

TAYLOR, R.K. (1967) 'Methylene blue adsorption by finegrained sediments', J. Sed. Pet., 37(4), pp.1221-1230.

TAYLOR, R.K. (1971) 'The petrography of the Mansfield marine band cyclotherm at Tinsley Park, Sheffield', Proc. Yorks. Geol. Soc., 38, pp.299-328.

TAYLOR, R.K. (1978) 'Properties of mining waste with respect to foundations', In: F.G.Bell (Ed.), 'Foundation Engineering in Difficult Ground', Newnes-Butterworth, London, pp.175-203.

TAYLOR, R.K. & SPEARS, D.A. (1970) 'The breakdown of British Coal Measure rocks', Int. J. Rock Mech. Sci., 7, pp.481-501

TEODOROVICH, G.I. & CHERNOV, A.A. (1968) 'Character of changes with depth in productive deposits of Apsheron oil-gas bearing region', Sov. Geol., 4, pp.83-93.

TERZAGHI, K. (1923) 'Die berechnung der durchlassigkeitsziffer des tones aus den verlauf der hydrodynamischen spannungserscheinungen', Sitz. Akad. Wissen. Wien Math-naturw., Kl. 132, pp.105-124.

TERZAGHI, K. (1925) 'Erdbaumechanik auf bodenphysikalischer grundlage', Viennna Deuticke, Leipzig.

TERZAGHI, K. (1926) 'The mechanics of adsorption and of the swelling of gels', Colloidal Symposium Monograph, Chemical Catalog Co., Inc., New York.

TERZAGHI, K. (1929) 'Technisch-geologische beschreibung der bodenbeschaffenheit fur bautechnische zwecke', Chapter 9, Part A, Ingenieurgeologie by Redkich, K.A., Terzaghi, K., & Kemper, R., Wien und Berlin, Springer.

TERZAGHI, K. (1936) 'Stability of slopes in natural clay', Proc. 1st. Int. Conf. on Soil Mech. & Fdn. Eng., Boston, Mass., 1, p.161.

TERZAGHI, K. (1941) 'Undisturbed clay samples and undisturbed clays', J. Boston Soc. Civ. Eng., 28, pp.211-231.

TERZAGHI, K. (1946) ' Rock tunnelling with steel supports' Edited by Proctor and White, Commercial Shearing & Stamping Co., Youngstown. p.20.

TERZAGHI, K. & FROLICH, O.I. (1936) 'Theorie der setzung von tonschichten', Franz Deuticke, Leipzig.

TERZAGHI, K. & PECK, R.B. (1948 & 1967) 'Soil mechanics in engineering practice', J. Wiley & Sons, New York.

TCHALENKO, J.S. (1968) 'The microstructure of the London Clay', Quart. J. Eng. Geol., 1(3), pp.155-168.

TILL, R. & SPEARS, D.A. (1969) 'The determination of quartz in sedimentary rocks using an X-ray diffraction method', Clays & Clay Mins., 117, pp.323-327.

TOURTELOT, H.A. (1962) 'Preliminary investigation of the geologic setting and chemical composition of the Pierre Shale, Great Plains Region', U.S.G.S. Prof. Paper, 390.

TREWIN, N.H. (1968) 'Potassium bentonites in the Namurian of Staffordshire and Derbyshire', Proc. Yorks. Geol. Soc. 37(1), 37pp.

TROSTEL, L.J. & WYNNE, D.J. (1940) ' Determination of quartz (free silica) in refractory clays', J. Am. Ceram. Soc., 23, pp.18-22.

TSCHEBOTARIOFF, G. (1951) 'Soil mechanics, foundation and earth structures', McGraw-Hill, New York.

TWENHOFEL, W.H. (1936) 'Terminology of the finegrained mechanical sediments', Report of the Committee on Sedimentation Natl. Res. Council, pp.81-104.

UNDERWOOD, L.B. (1967) 'Classification and identification of shales' J. Soil Mech. & Fdn. Div. Proc., A.S.C.E., 93, SM6, pp.77-116.

UNDERWOOD, L.B., THORFINNSON, S.T. & BLACK, W.T. (1964) 'Rebound in redesign of Oahe dam hydraulic structures', J. Soil Mech. & Fdn. Div. Proc., A.S.C.E., 90, SM2, pp.65-86.

VAN EECKHOUT, E.M. (1976) 'The mechanism of strength reduction due to moisture in coal mine shales', Int. J. Rock Mech. Min. Sci. & Geochem. Abstracts, 13, pp.61-67.

VAN MOORT, J.C. (1971) 'A comparative study of the diagenetic alteration of clay minerals in Mesozoic shales from Papua, New Guinea and in Tertiary shales from Louisiana, USA', Clays and Clay Mins. 19(1), pp.1-20

VAN OLPHEN, H. (1963) 'An introduction to clay colloid chemistry', Wiley, New York.

VAN ZELST, T.W. (1948) 'An investigation of the factors affecting laboratory consolidation of clays', Proc. 2nd. Int. Conf. Soil Mech. & Fdn. Engrg., Rotterdam, 7, p.53.

VARNES, D.J. & SCOTT, G.R. (1967) 'General engineering geology of the U.S. Air Force Academy site, Colorado', U.S.G.S. Prof. Paper, 551.

VON ENGELHARDT, W. & GAIDA, K.H. (1963) 'Concentration changes of pore solutions during compaction of clay sediments',J. Sed. Pet., 33(4), pp.919-930.

WAIDELICH, W.C. (1958) 'Influence of liquid and clay mineral type on the consolidation of clay-liquid systems', In; Winterkorn (Ed.), 'Water and its conduction in soils', Highway Res. Board, Spec. Paper, 40, Natl. Acad. Sci.-Natl. Res. Council Publ., 629, pp.24-42.

WALKER, G.F. (1950) 'Vermiculite organic complexes', Nature, 116, p.695.

WALKER, G.F. (1957) 'Differentiation of vermiculites and smectites in clays', Clay Mins. Bull., 3, pp.154-163

WALKER, G.F. (1961) 'Vermiculite minerals' In: G. Brown (Ed.), 'X-ray identification and crystal structures of clay minerals', Min. Soc. Mono., London.

WARD, W.H., SAMMUALS, S.C. & BUTLER, M.E. (1959) 'Further studies of the properties of the London Clay', Geotechnique, 9, 33pp.

WARNER, D.L. (1964) 'An analysis of the influence of physical-chemical factors upon the consolidation of fine-grained sediments', Thesis, Univ. of Calif., Berkeley.

WEAVER, C.E. (1958a) 'Geologic interpretation of argillaceous sediments' Am. Assoc. Pet. Geol. Bull., 42,

WEAVER, C.E. (1958b) 'The effects and geological significance of potassium 'fixation' by expandable clay minerals derived from muscovite, biotite, chlorite and volcanic material', Am. Min., 43, pp.839-861.

WEAVER, C.E. (1959) 'The clay petrology of sediments' Clays and Clay Mins., 6th. Natl. Conf., pp.154-187.

WEAVER, C.E. & BECK, K.C. (1971) 'Clay water diagenesis during burial: how mud becomes gneiss', Geol. Soc. Am., Spec. Paper 134.

WEAVER, C.E. & POLLARD, L.D. (1973) 'The chemistry of the clay minerals', Developments in Sedimentology, 15, Elsevier.

WEBSTER'S DICTIONARY (1966) G. & C. Merriam & Co., Springfield, Mass., p.2085.

WEIMER, R.J. & LAND, C.B. (1975) 'Maestrichtian deltaic & interdeltaic sedimentation in the Rocky Mountain region of the United States', Geol. Assoc. Can., Spec. Paper No 13 Cretaceous System in the Western Interior of North America, pp.633-666.

WELLER, F.A. (1959) 'Compaction of sediments', Am. Assoc. Pet. Geol. Bull., 43(2), pp.273-310.

WELSH, F.B.A. & CROOKALL, R. (1935) 'Bristol and Gloucester', British Regional Geology.

WHITE, W.A. (1961) 'Colloid phenomena in sedimentation of argillaceous rocks', J. Sed. Pet., 31, pp.560-570.

WIJEYESEKERA, D.C. & De FREITAS, M.F. (1976) 'High pressure consolidation of kaolinite clay' Am. Assoc. Pet. Geol. Bull., 60(2), pp.293-299.

WILSON, V. (1948) 'E. Yorkshire and Lincolnshire' Brit. Reg. Geol

WINTERKORN, H.F. (1942) 'Mechanisms of water attack on dry cohesive soil', Soil Sci., 54, pp.259-273.

WISSA, A.E.Z. CHRISTIAN, J.T. & DAVIS, E.H. (1971) 'Consolidation at constant rate of strain', J. Soil Mech. & Fdn. Div. Proc., A.S.C.E., 97, SM10, Paper 8447, pp.1393-1413.

YAALON, D.H. (1962) 'Mineral composition of the average shale', Bull. Geol. Surv., 5, pp.31-36.

YODER, R.E. (1936) 'A direct method of aggregate analysis of soils and a study of the physical nature of erosion losses', J. Am. Soc. Agron., 28, pp.337-350.

YODER, H.S. & EUGESTER, H.P. (1955) 'Synthetic and natural muscovites', Geochim. & Cosmochim. Acta, 8, pp.225-280.

YONG, R.N., TAYLOR, L.O. & WARKENTIN, B.P. (1963) 'Swelling pressure of sodium montmorillonite at depressed temperatures', Natl. Conf. Clays and Clay Minerals Proc., 2, pp.268-281.

YONG, N.R. & WARKENTIN, B.P. (1975) 'Soil properties and behaviour', In: Developments in geotechnical engineering, 5.

Acknowledgements

I would like to thank the Natural Environment Reasearch Council for making a grant available to finance this project. My thanks also go to the following people and organisations for providing fresh material, without which this project would not have been possible:

Mr. M.H. Logan (U.S. Dept. of the Interior, Bureau of Reclamation) for providing all North American materials.

Dr. B. Hawkins (Bristol University) for providing Jurassic Fuller's Earth.

The Fuller's Earth Union for providing Cretaceous Fuller's Earth.

Mr. J.L. Horrell (London Brick Co.) for providing Oxford and Gault Clays.

London Brick Co. (Horsham) for providing Weald Clay.

Messrs T & C Hawksley (Chartered Civil Engineers) for providing Lias Clay.

Dr. G. Goosens (N.C.B., Doncaster) for providing the Flockton Thin and Swallow Wood Carboniferous shales.

Mr. G. Mockler (N.C.B. Opencast) for providing the Widdringham shale.

Dr. P.B. Attewell (Durham University) for providing the London Clay.

I would also like to thank Prof. G. Higginson (Durham University for his assistance with the interpretation of strain energy and Dr. G. Larwood (Durham University) for certain geological details.

Lastly, but by no means least, I would like to convey my thanks to my supervisor, Dr. R.K. Taylor, for complete support for the duration of this project.

APPENDIX

Appendix A.1.
Mineralogy & Geochemistry

A.1.1. Semi-Quantitative Mineralogical Analysis

A.1.1.1 Basis of Analysis

Semi-quantitative mineralogical analyses were performed on kaolinite, illite, montmorillonite, quartz, calcite, dolomite and pyrite using boehmite (Griffin, 1954; Gibbs, 1967) as an internal standard.

Boehmite was chosen as an internal standard because:-

(i) The mass absorption at the CoK_{α} wavelength is of the same order as those of the minerals encountered.

(ii) It does not interfere with any of the proposed analytical peaks.

(iii) It has strong intensities when only small quantities are present.

The 6.18Å reflection of boehmite was used for comparison with the 7Å reflection of kaolinite (Fig.A.1.1), 10Å reflection of illite (Fig.A.1.2), 15-17Å reflection of montmorillonite (Fig.A.1.3) 4.26Å reflection of quartz (Fig.A.1.4), 3.03Å reflection of calcite (Fig. A.1.5), 2.71Å reflection of pyrite (Fig.A.16), 2.88Å reflection of dolomite (Fig.A.1.7). The peaks chosen for the three clay minerals represent those of the relatively strong basal reflections. The 4.26Å reflection of quartz was chosen because it varies uniformly with the amount of quartz present in a range which is easily comparable with that of the boehmite reflection. Till and Spears (1969) produced a quartz (4.26Å) to boehmite (6.18Å) calibration curve by a method which involved destroying all the clay minerals present by ignition at 950°C. This method was used by these authors because the 4.5Å reflection of illite can overlap the 4.26Å

reflection of quartz near to the baseline. For calcite, dolomite and pyrite the peaks chosen were the strongest for each of the minerals.

A.1.1.2 Experimental Procedures

The experimental procedure adopted for X-ray diffraction work was as follows:- An air dried sample of clay was gently powdered in an agate mortar and pestle. Then 0.225 grams of the powder were thoroughly mixed with 0.025 grams of boehmite, i.e. making the boehmite 10 per cent by weight of the mixture. The mixture was smear-mounted on a glass microscope slide using acetone as the liquid medium and an X-ray trace was produced with a Phillips PW 1130 X-ray Diffractometer using iron-filtered cobalt K_α radiation at 60kW and 25mA, with divergent, scatter and receiving slits of 1°, I° and $0.I^\circ$ respectively. All the samples were run at a scanning speed of 1° of 2θ per minute, covering a range of 3° of 2θ to 50° of 2θ. The smear-mounted samples were then placed in a sealed vessel containing ethylene glycol and heated for a period of 12 hours at 50 - 60°C, after which, the slides were X-rayed again using the same conditions. The difference between the traces was used for identification of the expandable minerals.

A polar planimeter was used to measure the peak areas after a suitable baseline had been inserted. Placing of this baseline was found to be very subjective, but a standard method was adopted which entailed inserting a smooth curve at the foot of the background under the areas concerned. Quantitative assessment was found to be more accurate using the peak area (integrated intensity) than the peak heights because the latter depends on instrumental factors and on the crystalline nature of the material studied (Brown, 1961). i.e. crystals much smaller than one micron give appreciably broadened reflections

Figure A 1.1.

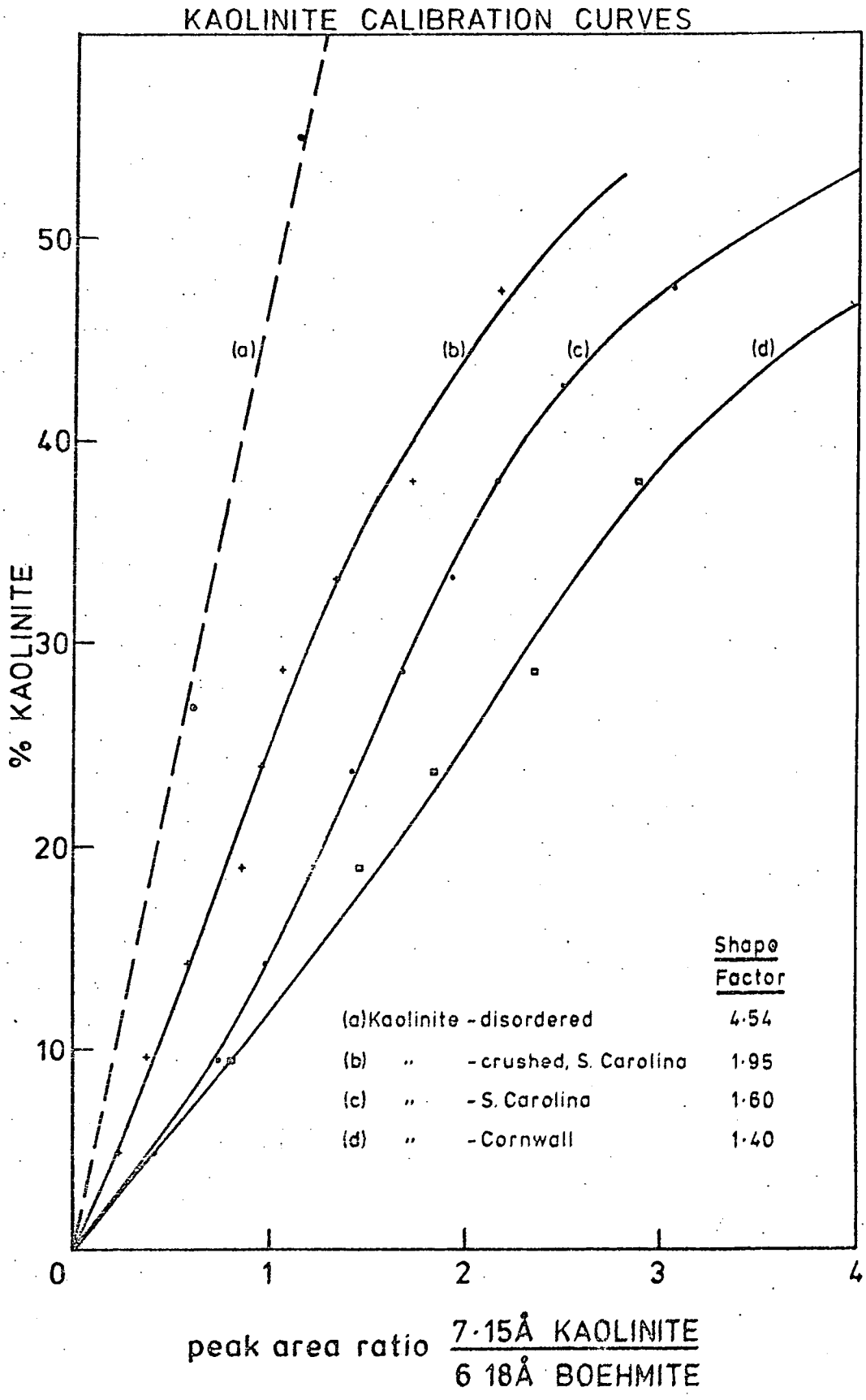
KAOLINITE CALIBRATION CURVES
% KAOLINITE
50
40
30
20
10
0
1
2
3
4
(a)
(b)
(c)
(d)
Shape Factor
(a)Kaolinite - disordered 4·54
(b) " - crushed, S. Carolina 1·95
(c) " - S. Carolina 1·60
(d) " - Cornwall 1·40
peak area ratio 7·15Å KAOLINITE / 6 18Å BOEHMITE

Figure A 1.2.

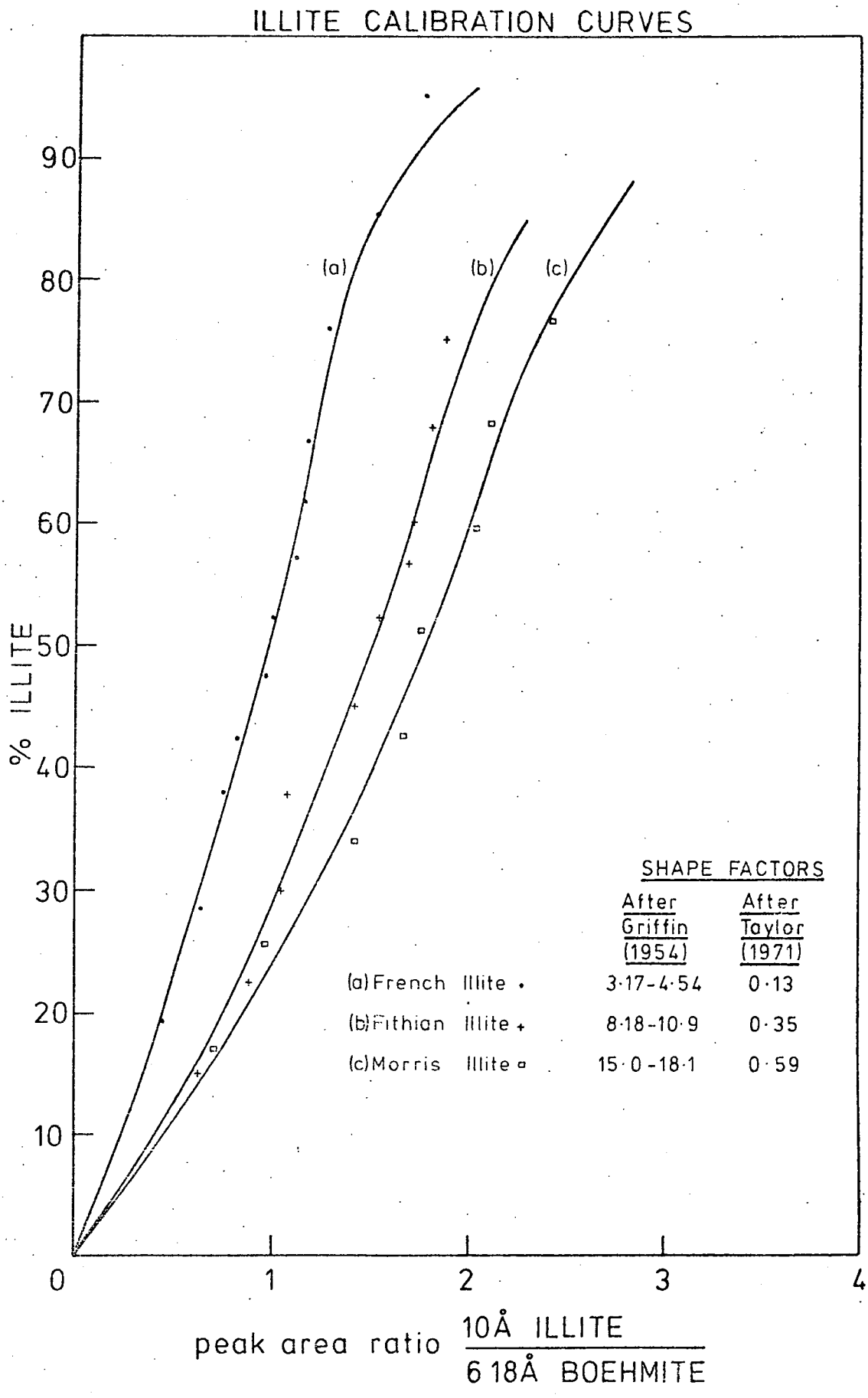
ILLITE CALIBRATION CURVES
% ILLITE
90
80
70
60
50
40
30
20
10
0
1
2
3
4
(a)
(b)
(c)
peak area ratio 10Å ILLITE / 6·18Å BOEHMITE
SHAPE FACTORS
After Griffin (1954)
After Taylor (1971)
(a) French Illite • 3·17-4·54 0·13
(b) Fithian Illite + 8·18-10·9 0·35
(c) Morris Illite ▫ 15·0-18·1 0·59

Figure A 1.3.

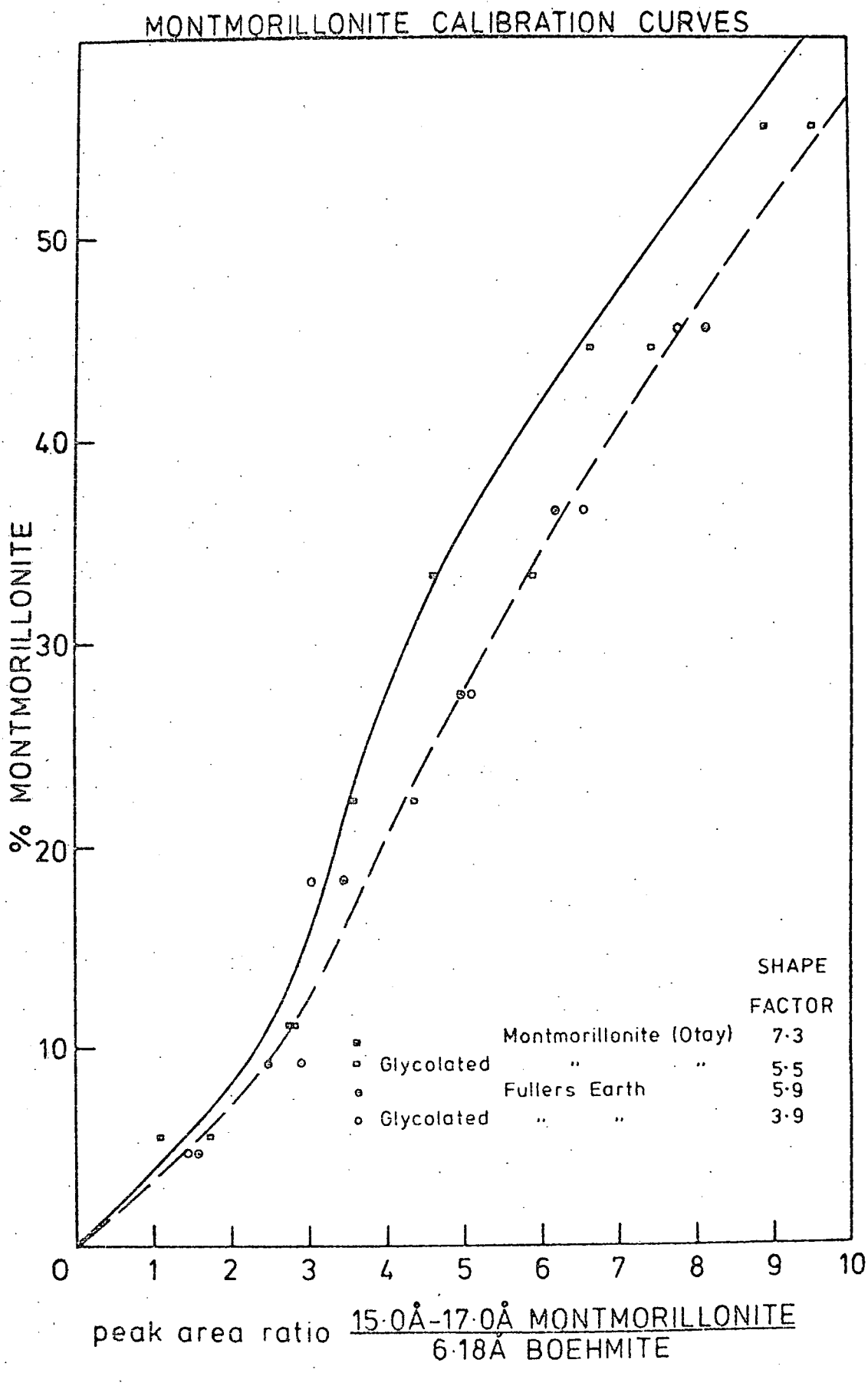
MONTMORILLONITE CALIBRATION CURVES
% MONTMORILLONITE
50
40
30
20
10
0
1
2
3
4
5
6
7
8
9
10
peak area ratio 15·0Å-17·0Å MONTMORILLONITE / 6·18Å BOEHMITE
SHAPE FACTOR
Montmorillonite (Otay) 7·3
Glycolated " " 5·5
Fullers Earth 5·9
Glycolated " " 3·9

Figure A 1.4.

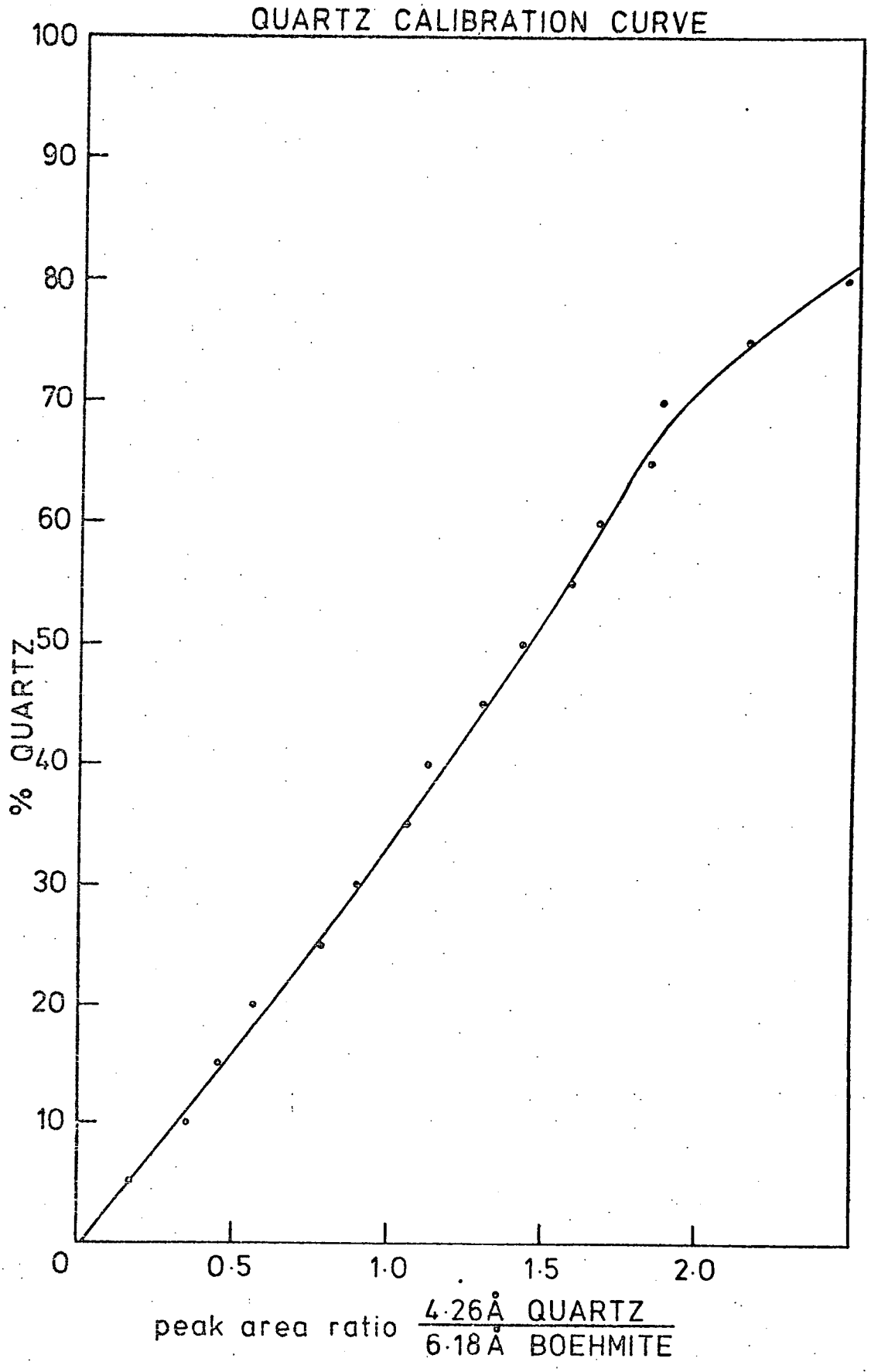
QUARTZ CALIBRATION CURVE
100
90
80
70
60
50
40
30
20
10
0
% QUARTZ
0·5
1·0
1·5
2·0
peak area ratio 4·26Å QUARTZ / 6·18Å BOEHMITE

Figure A 1.5.

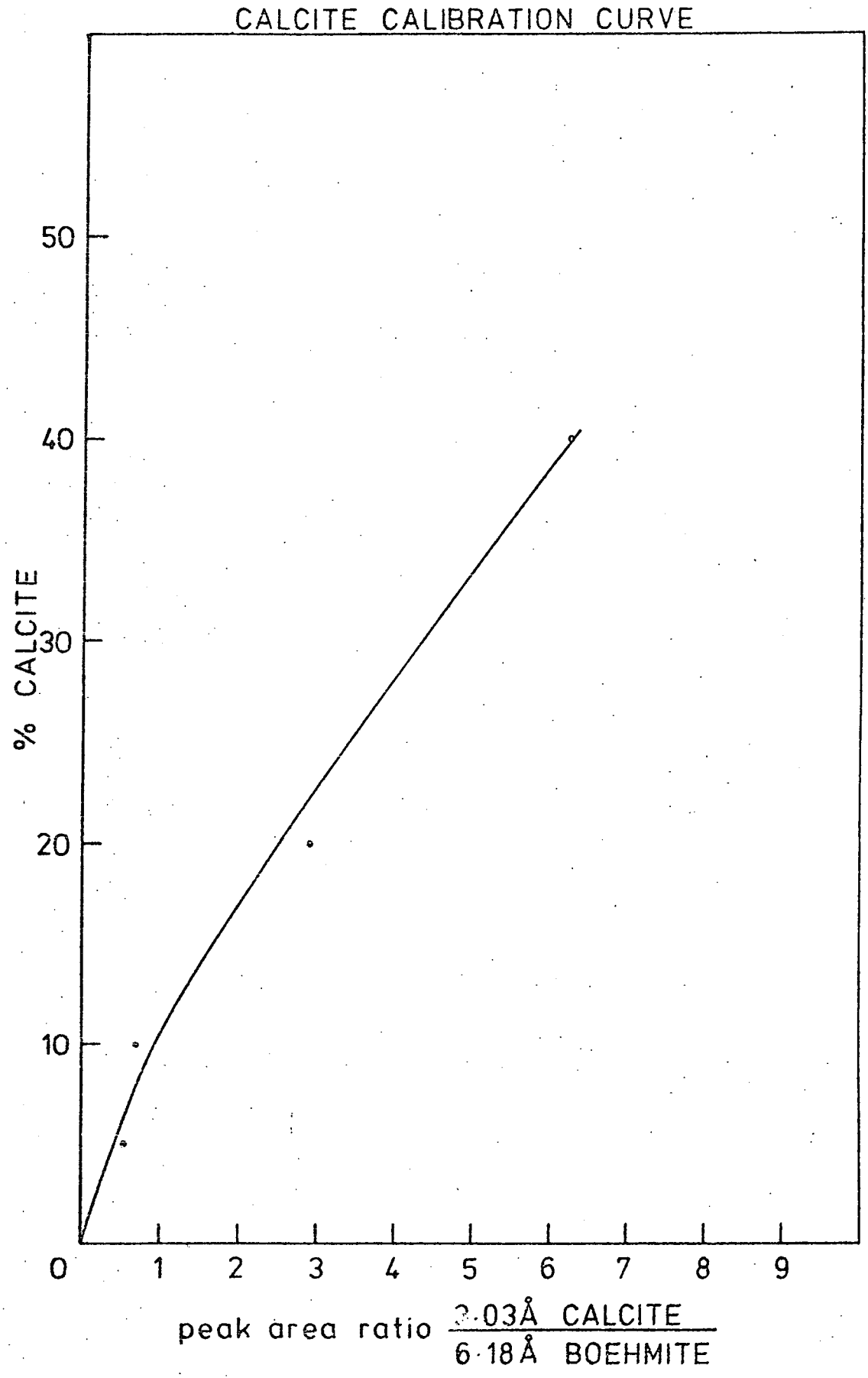
CALCITE CALIBRATION CURVE
% CALCITE
50
40
30
20
10
0
1
2
3
4
5
6
7
8
9
peak area ratio 3·03Å CALCITE / 6·18Å BOEHMITE

Figure A 1.6.

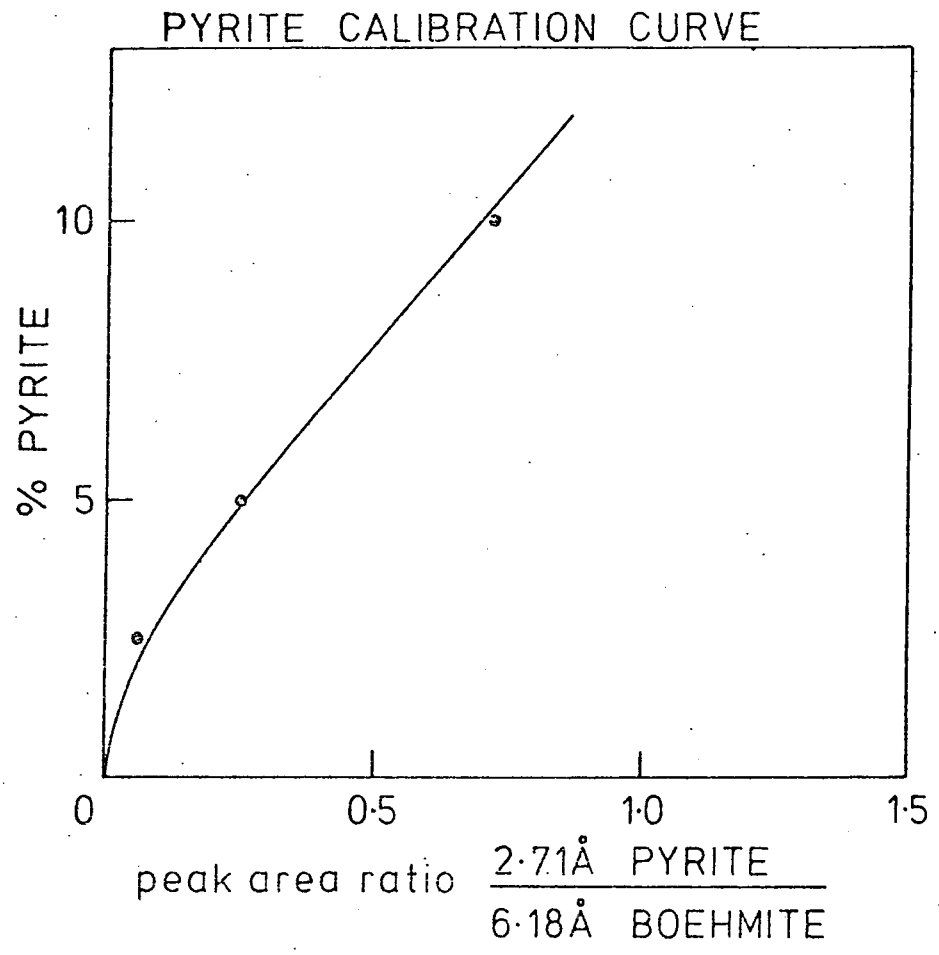

Figure A 1.7.

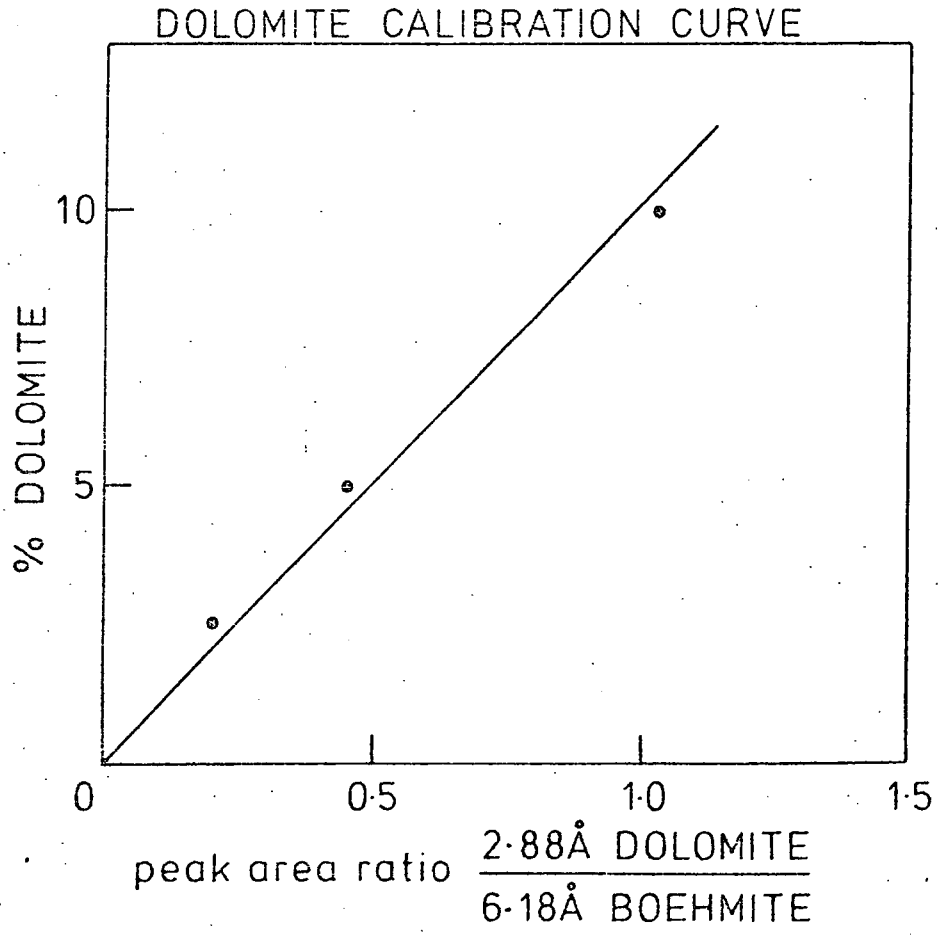

with correspondingly smaller peak heights. Reeves (1971) found that measurements of peak height multiplied by the width at half height gave reasonable results for quartz, kaolinite, illite and chlorite, but measurements of peak height gave only adequate results for kaolinite, quartz and chlorite, and very poor results for illites.

When chlorite was present its (002) 7Å reflection coincided with the 7Å reflection of kaolinite. This increased the area of the latter and led to enhanced kaolinite values. To overcome this difficulty, the relationship of the 7Å to the 14Å reflection, of chlorite, was determined experimentally using a penninite from Switzerland. The relationship is:-

$$\text{area 7Å peak} = 2.35 * \text{area 14Å peak}$$

A.1.2 Correction Procedures for Smectite Calculation

To calculate the smectite structural formulae, the following procedure has been adopted to correct geochemical analyses where kaolinite, feldspar and calcite are present.

(i) Kaolinite ($Al_2Si_2O_5(OH)_4$)

Formula = $Al_2O_3 \cdot 2SiO_2 \cdot 2H_2O$

or 46.54% SiO_2, 39.5% Al_2O_3, 13.96% H_2O

If kaolinite is x per cent of total (by weight), then subtract:

x×46.54% from total SiO_2

x×39.50% from total Al_2O_3

(ii) Feldspar ($K_2Al_2Si_3O_{8}$ - assuming potassium form is present)

Formula = K_2O, Al_2O_3, $6SiO_2$

or 16.92% K_2O, 18.31% Al_2O_3, 64.76% SiO_2

If feldspar is x per cent of total (by weight) then subtract:

x × 16.92% from total K_2O

x × 18.31% from total Al_2O_3

x × 64.76% from total SiO_2

(iii) Calcite ($CaCO_3$)

Formula = $CaO.\ CO_2$

or 56.03% CaO, 43.96% CO_2

If calcite is x per cent of total (by weight), then subtract:

x × 56.03% from the total CaO

x × 43.96% from the total CO_2

A.1.3 Cation Exchange Capacity

A.1.3.1 Leaching with Ammonium Acetate

Samples of air-dried clay were gently crushed to pass a B.S.200 mesh and 0.4 grams of the resulting powder were placed in each of two 50 millilitre centrifuge tubes. 20 millilitres of distilled water were then added and the mixture was mechanically shaken for 15 minutes. At the end of this period the suspension was centrifuged at 4500 r.p.m. until the resulting liquor became clear, at which stage it was decanted into a plastic stoppered bottle. This process was repeated 5 times and a total of 100 mils. of washings were collected.

Next, a solution of 1N ammonium acetate at pH 7 was added to the clay, mechanically shaken for 15 minutes and allowed to stand for a period of 12 hours, after which time it was centrifuged and decanted into a separate plastic stoppered bottle.

Analysis of Ca and Mg ions (by atomic absorption spectometry) and Na and K ions (by flame photmetry) was then carried out on the washings and acetate solutions.

A.1.3.1.1. Atomic Absorption

Ca and Mg cations were analysed by this method after the addition of one millilitre of 5 per cent w/v Lanthenum solution to nine

millilitres of each liquor (making the Lanthenum content about 1.0 per cent of the total, which was sufficient to prevent absorption effects by sulphates, phosphates, silicon etc.).

Standard solutions (also containing 5 per cent w/v Lanthenum) of 2, 5, 10, 25, 50 and 100ppm for Ca and Mg were previously prepared and used to calibrate the machine before and after the unknowns were analysed; the results being displayed via a pen recorder printout.

The concentration of the cations in the actual solutions was obtained by multiplying the recorded ppm's by a factor of 10/9. Conversion to milliequivalents per 100 grams of clay was accomplished by reference to the calculations set out in A.1.3.1.3.

A.1.3.1.2. Flame Photometer

Na and K cations were analysed by this method. Prior to analysing the unknown the photometer was calibrated with standard solutions of 2, 5, 10 and 25 ppm Na or K; the results being displayed by a galvonometer at the front of the machine.

Conversion to milliequivalents per 100 grams of clay was made by reference to the calculations set out in A.1.3.1.3.

A.1.3.1.3. Calculations

(i) General Calculation:

x ppm = x grms per 10^6 grms of solution,

x ppm per cc. (water) = $x/10^6$ grms/cc.

In y ccs of water, no. of grms of ions = $x \cdot y \cdot 10^{-6}$ grms.

If $x \cdot y \cdot 10^{-6}$ grms of ions are produced from z grms of clay,

then $\frac{x \cdot y \cdot 10^{-6}}{z}$ grms of ions are produced from 1grm of clay,

or $\frac{x \cdot y \cdot 10^{-6} \times 100}{z}$ grms are produced from 100 grms of clay,

By converting the above equation to equivalent weights:

$$C.E.C. = \frac{x * y * 10^{-6} * 100 * 1000}{z * Eq.wt.} \quad meg/100grms\ clay$$

(The above equation gives the same results whether the element or the oxide is considered).

(ii) C.E.C. Capacities:

Volume of acetate used = 40ccs.

Volume of washings used = 100ccs. (5 repeats of 20 ccs.)

Calcium (wt. = 40.08)

C.E.C. (acetate) = 0.4490 * ppm

C.E.C. (washings) = 1.2475 * ppm

Magnesium (wt. = 24)

C.E.C. (acetate) = 0.8223 * ppm

C.E.C. (washings) = 2.0558 * ppm

Sodium (wt. = 22.91)

C.E.C. (acetate) = 0.4364 * ppm

C.E.C. (washings) = 1.0912 * ppm

Potassium (wt. = 39.10)

C.E.C. (acetate) = 0.2557 * ppm

C.E.C. (washings) = 0.6393 * ppm

A.1.3.2. Methylene Blue ($C_{16}H_{18}N_3S.Cl.3H_2O$) Absorption

The method is based upon quantitative work on pure clays by Robertson and Ward (1951) which was quantified by Taylor (1967) and adopted for argillaceous rocks.

A 0.1 per cent stock solution of methylene blue was prepared. Twenty millilitres of distilled water was added to 0.2 - 0.5 grams of clay, which had passed a B.S.200 mesh and been heated at 380°C to remove organic matter by oxydation. Methylene blue was added to the suspension from a burette, mechanically shaken for $\frac{1}{2}$ - 1 hour,

centrifuged at 4500 r.p.m. and then visually examined for traces of blue colouration. If none was visible, the procedure was repeated, otherwise the contents were transferred to a 1 litre volumetric flask and made up to volume, the glassware being thoroughly cleaned with a rubber policeman. The flask was then gently agitated for one hour to ensure that all the excess dye had been washed from the clay and glassware.

The excess dye was determined photoelectrically from centrifuged samples of solution, using a Unicam SP 500 Spectrophotometer at an optimum wavelength of 655mu(Fig.A.1.8), and a comparative solution of 0.0001 per cent.

The procedure was repeated if the concentration of excess dye was greater than 6 - 8 per cent because the onset of physical absorption was demonstrated by Fairburn and Robertson (1956) at greater concentrations.

A typical calculation, as set out by Taylor (1967) is given below, assuming that the dye is 100 per cent pure.

A.1.3.2.1. General Calculation

Percentage dye initially	0.1
Excess dye (as a percentage of standard)	x
Excess dye (as a percentage of original)	$x/1000$ **
Percentage dye absorbed	$0.1 - x/1000$
Moisture content of dye	a ***
Purity of dye	100-a
Milliequivalent of dye (equivalent wt. of anhydrous dye = 0.3199)	0.3199
Volume of dye solution used	y
Dry weight of clay	z

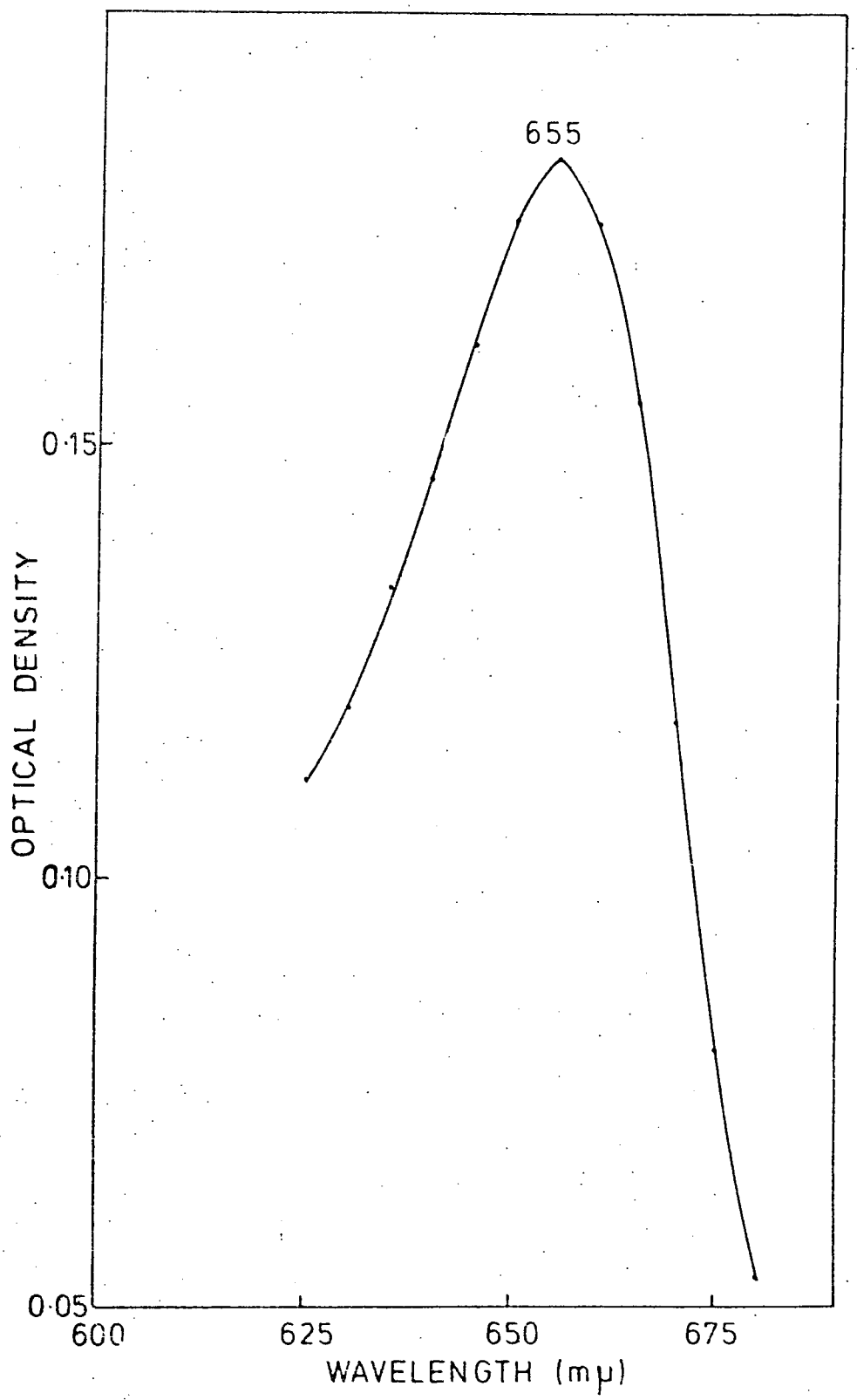

Figure A 1.8. Optimum Wavelength for Methylene Blue Absorption.

C.E.C. in milliequivalents per 100 grams of dry clay:

$$\frac{\text{(Percentage dye initially - Percentage excess dye) * Percentage purity}}{\frac{\text{Equivalent weight}}{1000} * \frac{100}{\text{Volume of dye}} * \text{Dry weight of clay}}$$

$$= \frac{(0.1 - x/1000)^{*} (100 - a) * y}{0.3199 * 100 * z}$$

** One cc of 0.1 per cent stock solution was diluted to 1000ccs.

*** For the present series of tests the water content was not measured and the purity has been taken at 100 per cent.

A.1.4 Wet Chemical Methods

A.1.4.1. Determination of Carbon Dioxide

0.5g. of rock powder were placed in a flask and 50 millilitres of orthophosphoric acid were added via a tap funnel. Gentle heat was then applied. Carbon dioxide gas given off was collected in U-tubes containing known weights of soda-lime.

$$\% CO_2 \text{ in sample} = \frac{x}{y} \times 100$$

where x = weight of CO_2 collected and y is the weight of rock powder.

A.1.4.2 Determination of Carbon

Upon completion of the experimental procedures to determine carbon dioxide, 3 grams of chromium trioxide were added. Upon boiling, any carbon present was oxidised to carbon dioxide, which was again collected in U-tubes containing known weights of soda-lime.

$$\% C \text{ in sample} = \% CO_2 \times 12/44$$

A.1.4.3. Determination of Total Water

A known weight of sample was heated at 1200°C for 15 minutes in an electric furnace. Any water evolving from the sample was flushed

from the furnace by a gentle stream of nitrogen gas and collected in U-tubes containing known weights of anhydrous calcium chloride.

$$\% H_2O \text{ in sample} = \frac{\text{increase in wt. of } CaCl_2}{\text{wt. of rock powder used}} \times 100$$

A.1.4.4 Determination of Loosely held Water

A known weight of air-dried sample was placed in a sintered glass bowl and heated overnight in a furnace at 105°C. The reduction in weight, expressed as a percentage, represents the loosely held water (see Table A.1.7).

Table A 1.1.

Structural Formula of Smectite in the Fuller's Earth (Redhill).

Impurities: 1% Quartz (i.e. combined silica = 54.14%)
0.6% Calcite (i.e. CaO = 3.10%)

	Wt (%)	Mol. Props.	Metal Atoms	O_2 Atoms	Metal Atoms per 11 O_2 Atoms.	
SiO_2	54.14	0.9009	0.9009	1.8018	4.0399	
Al_2O_3	12.53	0.1228	0.2456	0.3684	1.1013	
Fe_2O_3	7.20	0.0450	0.0900	0.1350	0.4035	
MgO	3.39	0.0841	0.0841	0.0841	0.3771	
CaO	3.10	0.0552	0.0552	0.0552	0.2475	factor =
Na_2O	0.24	0.0038	0.0076	0.0038	0.0340	4.4843
K_2O	0.45	0.0047	0.0094	0.0047	0.0421	
				2.4530		

Tetrahedral layer: Si - 4.0399
Middle layer: Al - 1.1013, Fe - 0.4035, Mg - 0.3771
Excess ions: Ca - 0.2475, Na - 0.0340, K - 0.0421

Table A 1.2.

Structural Formula of Smectite in the Fuller's Earth (Bath).

Impurities: 2% Calcite (i.e. CaO = 2.29%)
7% Feldspar (i.e. SiO_2 = 47.54%, K_2O = 0.44%, Al_2O_3=13.86%)

	Wt(%)	Mol. Props.	Metal Atoms	O_2 Atoms	Metal Atoms per 11 O_2 Atoms.	
SiO_2	47.54	0.7911	0.7911	1.5822	3.9433	
Al_2O_3	13.86	0.1359	0.2718	0.4077	1.3548	
Fe_2O_3	4.54	0.0284	0.0568	0.0852	0.2831	
MgO	3.20	0.0793	0.0793	0.0793	0.3952	
CaO	2.29	0.0408	0.0408	0.0408	0.2033	factor =
Na_2O	0.44	0.0070	0.0140	0.0070	0.0697	4.9845
K_2O	0.44	0.0046	0.0092	0.0046	0.0458	
				2.2068		

Tetrahedral layer: Si - 3.9433, Al - 0.0567
Middle layer: Al - 1.2981, Fe - 0.2831, Mg - 0.3952
Excess ions: Ca - 0.2033, Na - 0.0618, K - 0.0458

Table A 1.3.

Structural Formula of Smectite in the Nacimiento Shale (N3).

Impurities: 22.5% Quartz, 28% Kaolinite (i.e. SiO_2 = 22.65%, Al_2O_3=6.0%)
0.18% Calcite (i.e. CaO = 1.29%).

	Wt(%)	Mol. Props.	Metal Atoms	O_2 Atoms	Metal Atoms per 11 O_2 Atoms.	
SiO_2	22.65	0.3769	0.3769	0.7538	3.6189	
Al_2O_3	6.00	0.0588	0.1176	0.1764	1.1291	
Fe_2O_3	7.13	0.0446	0.0892	0.1338	0.8564	
MgO	1.27	0.0315	0.0315	0.0315	0.3024	
CaO	1.29	0.0230	0.0230	0.0230	0.2208	factor =
Na_2O	0.18	0.0029	0.0058	0.0029	0.0556	9.6019
K_2O	2.28	0.0242	0.0484	0.0242	0.4647	
				1.1456		

Tetrahedral layer: Si - 3.6189, Al - 0.3811
Middle layer: Al - 0.7480, Fe - 0.8564, Mg - 0.3024
Excess ions: Ca - 0.2208, Na - 0.0556, K - 0.4647

Table A 1.4.

Structural Formula of the Smectite in the Dawson Shale.

Impurities: 49% Quartz, 7% Kaolinite, 4% Feldspar (i.e. SiO_2 = 15.26%, Al_2O_3 = 10.82%, K_2O = 1.26%).

	Wt(%)	Mol. Props.	Metal Atoms	O_2 Atoms	Metal Atoms per 11 O_2 Atoms.	
SiO_2	15.26	0.2539	0.2539	0.5079	2.9059	
Al_2O_3	10.82	0.1061	0.2122	0.3183	2.4286	
Fe_2O_3	3.55	0.0222	0.0444	0.0666	0.5081	
MgO_3	1.45	0.0359	0.0359	0.0359	0.4108	
CaO	0.95	0.0169	0.0169	0.0169	0.1934	factor =
Na_2O	0.14	0.0022	0.0044	0.0022	0.0503	11.4452
K_2O	1.26	0.0133	0.0267	0.0133	0.3055	
				0.9611		

Tetrahedral layer: Si-2.9059, Al-1.0941
Middle layer: Al-1.3345, Fe-0.5081, Mg-0.1574
Excess ions: Mg-0.2534, Ca-0.1934, Na-0.0503, K-0.3055

Table A 1.5.

Structural Formula of the Smectite in the Yazoo Clay.

Impurities: 11.5% Quartz, 26% Kaolinite, (i.e. SiO_2=27.74%, Al_2O_3=10.27%) 5.81% Calcite (i.e. CaO = 0.31%).

	Wt(%)	Mol. Props.	Metal Atoms	O_2 Atoms	Metal Atoms per 11 O_2 Atoms.	
SiO_2	27.74	0.4616	0.4616	0.9232	3.8363	
Al_2O_3	7.33	0.0718	0.1436	0.2154	1.1934	
Fe_2O_3	5.50	0.0344	0.0688	0.1032	0.5717	
MgO_3	2.16	0.0535	0.0535	0.0535	0.4446	
CaO	0.31	0.0055	0.0055	0.0055	0.0457	factor =
Na_2O	0.25	0.0040	0.0080	0.0040	0.0664	8.3106
K_2O	1.78	0.0188	0.0376	0.0188	0.3124	
				1.3236		

Tetrahedral layer: Si-3.8363, Al-0.1637
Middle layer: Al-0.0297, Fe-0.5717, Mg-0.3986
Excess ions: Mg-0.0460, Ca-0.0457, Na-0.0664, k-0.3124

Table A 1.6.

Structural Formula of the Montmorillonite (Otay, California).

	Wt(%)	Mol. Props.	Metal Atoms	O_2 Atoms	Metal Atoms per 11 O_2 Atoms.	
SiO_2	56.06	0.9329	0.9329	1.8658	4.0450	
Al_2O_3	13.66	0.1339	0.2678	0.4017	1.1611	
Fe_2O_3	1.88	0.0117	0.0234	0.0351	0.1014	
MgO_3	7.61	0.1887	0.1887	0.1887	0.8182	
CaO	1.33	0.0237	0.0237	0.0237	0.1027	factor =
Na_2O	1.13	0.0182	0.0364	0.0182	0.1578	4.3360
K_2O	0.35	0.0037	0.0074	0.0037	0.0320	
				2.5369		

Tetrahedral layer: Si-4.0450
Middle layer: Al-1.1575, Fe-0.1011, Mg-0.7375
Excess ions: Mg-0.0807, Ca-0.1027, Na-0.1578, K-0.0320

Table A 1.7. Absorbed Water Content of Samples Studied.

British Materials	Sample Ref.	(%)
London Clay 14m	LC14	3.46
London Clay 37m	LC37	2.86
Gault Clay	GC	2.51
Fuller's Earth (Redhill)	FE23	15.54
Weald Clay	WC	1.31
Kimmeridge Clay	KC	1.82
Oxford Clay 10m	OC10	2.22
Oxford Clay 44m	OC44	3.52
Fuller's Earth (Bath)	FE19	12.43
Lias Clay 10m	L10	1.80
Lias Clay 36m	L36	2.01
Keuper Marl	KM	1.89
Swallow Wood roof	SWR	1.35
Flockton Thin roof	FTR	1.06
Flockton Thin seatearth	FTS	2.89
Widdringham roof	WR	1.08
North American Materials		
Yazoo Clay	YC	7.00
Kincaid Shale 6m	K6	3.34
Kincaid Shale 8m	K8	2.74
Nacimiento Shale	N1	3.33
Nacimiento Shale	N2	3.12
Nacimiento Shale	N3	7.14
Fox Hills Shale	FOX	5.27
Dawson Shale	DS	4.40
Pierre Shale (Dakota)	PSD	4.24
Pierre Shale (Colorado)	PSC	2.22

Table A 1.8.

Normalisation of Quartz + Carbonate + Feldspar : Expandable Clay : Non-Expandable Clay.

British Materials	Sample Ref.	Quartz + Carbonate + Feldspar	Expandable Clay	Non-Expandable Clay.
London Clay 14m	LC14	23.0	23.0	54.0
London Clay 37m	LC37	52.5	14.5	33.0
Gault Clay	GC	49.5	8.5	42.0
Fuller's Earth (Redhill)	FE23	1.0	99.0	0.0
Weald Clay	WC	55.0	1.0	44.0
Kimmeridge Clay	KC	34.0	26.5	39.5
Oxford Clay 10m	OC10	30.0	26.5	43.5
Oxford Clay 44m	OC44	40.0	15.5	44.5
Fuller's Earth (Bath)	FE19	18.0	82.0	0.0
Lias Clay 10m	L10	21.5	17.0	61.5
Lias Clay 36m	L36	21.0	17.5	61.5
Keuper Marl	KM	55.0	8.0	37.0
Swallow Wood roof	SWR	12.0	15.5	72.5
Flockton Thin roof	FTR	30.0	13.0	57.0
Flockton Thin seatearth	FTS	3.0	45.5	51.5
Widdringham roof	WR	17.5	9.5	73.0
North American Materials				
Yazoo Clay	YC	20.0	49.0	31.0
Kincaid Shale 6m	K6	59.0	13.5	27.5
Kincaid Shale 8m	K8	59.5	14.5	26.0
Nacimiento Shale	N1	35.5	18.5	46.0
Nacimiento Shale	N2	46.5	17.0	36.5
Nacimiento Shale	N3	22.5	49.5	28.0
Fox Hills Shale	FOX	31.0	55.5	13.5
Dawson Shale	DS	53.0	40.0	7.0
Pierre Shale (Dakota)	PSD	25.5	55.5	19.0
Pierre Shale (Colorado)	PSC	41.0	22.0	37.0

Table A 1.9.

Clay Mineral Normalisation.

	Sample Ref.	Kaolinite + Chlorite	Mica	Expandable Clay
British Materials				
London Clay 14m	LC14	25.5	44.5	30.0
London Clay 37m	LC37	22.5	47.5	30.0
Gault Clay	GC	38.0	45.5	16.5
Fuller's Earth (Redhill)	FE23	0.0	0.0	100.0
Weald Clay	WC	40.0	57.0	3.0
Kimmeridge Clay	KC	28.0	32.0	40.0
Oxford Clay 10m	OC10	30.5	32.0	37.5
Oxford Clay 44m	OC44	35.5	38.5	26.0
Fuller's Earth (Bath)	FE19	0.0	0.0	100.0
Lias Clay 10m	L10	46.0	32.0	22.0
Lias Clay 36m	L36	46.0	32.0	22.0
Keuper Marl	KM	9.0	73.0	18.0
Swallow Wood roof	SWR	20.5	62.0	17.5
Flockton Thin roof	FTR	28.5	53.0	18.5
Flockton Thin seatearth	FTS	37.0	16.0	47.0
Widdringham roof	WR	69.0	19.0	12.0
North American Materials				
Yazoo Clay	YC	39.0	0.0	61.0
Kincaid Shale 6m	K6	67.5	0.0	32.5
Kincaid Shale 8m	K8	64.0	0.0	36.0
Nacimiento Shale	N1	42.0	29.0	29.0
Nacimiento Shale	N2	39.0	29.0	32.0
Nacimiento Shale	N3	36.0	0.0	64.0
Fox Hills Shale	FOX	9.0	11.0	80.0
Dawson Shale	DS	14.5	0.0	85.5
Pierre Shale (Dakota)	PSD	7.0	19.0	74.0
Pierre Shale (Colorado)	PSC	20.0	42.0	38.0

Table A 1.10.

Ratio of Non-Expandable Clay to Expandable Clay and Ratio of Quartz to Clay.

	Sample Ref.	Ratio: Non-Expandable Clay to Expandable Clay	Ratio: Quartz to Clay
British Samples			
London Clay 14m	LC14	2.32	0.29
London Clay 37m	LC37	2.32	1.10
Gault Clay	GC	5.10	0.98
Fullers Earth (Redhill)	FE23	0.00	0.01
Weald Clay	WC	32.33	1.22
Kimmeridge Clay	KC	1.48	0.51
Oxford Clay 10m	OC10	1.67	0.43
Oxford Clay 44m	OC44	2.88	0.66
Fullers Earth (Bath)	FE19	0.00	0.22
Lias Clay 10m	L10	3.60	0.27
Lias Clay 36m	L36	3.50	0.27
Keuper Marl	KM	4.71	1.23
Swallow Wood roof	SWR	4.71	0.14
Flockton Thin roof	FTR	4.38	0.43
Flockton Thin seatearth	FTS	1.14	0.03
Widdringham roof	WR	7.65	0.21
North American Samples			
Yazoo Clay	YC	0.63	0.25
Kincaid Shale 6m	K6	2.08	1.45
Kincaid Shale 8m	K8	1.79	1.46
Nacimiento Shale	N1	2.44	0.55
Nacimiento Shale	N2	2.18	0.88
Nacimiento Shale	N3	0.57	0.29
Fox Hills Shale	FOX	0.24	0.45
Dawson Shale	DS	0.17	1.13
Pierre Shale (Dakota)	PSD	0.35	0.34
Pierre Shale (Colorado)	PSC	1.63	0.69

Appendix A.2

Clay Microstructure and Preferred Orientation

A.2.1. Optical Microscopy

A.2.1.1. Sample Preparation

The preparation of thin sections utilised a surface impregnation technique of the clay in its natural condition. Initially a piece of clay approximately 1.5 cms^3 was immersed in a 1:1 mixture of acetone and plasticraft and subjected to a vacuum of 760mm pressure for several minutes. It was then immersed in a mixture of plasticraft and hardener (2 drops per millilitre) and placed in an oven at approximately 40°C until hardening had occurred. At this point the clay was in a condition which prevented disintegration during the preparation stage.

An orientated slice of clay was then cut and polished flat, firstly with a medium abrasive and then a very fine abrasive using paraffin as the lubricating fluid. A 1:1 mixture of araldite AY105 and Versamid 140lAD was then applied to the polished surface and a glass slide placed on top. After the adhesive had hardened, the specimen was ground down to a thickness of 25 microns, after which a glass cover slip was applied.

A.2.1.2. Method of Analysis

Estimations of the degree of preferred orientation were made by reference to the ratio of maximum to minimum birefringence, using the technique adopted by Morgenstern and Tchalenko (1967a);(see Fig.A.2.1)

The method depends upon the fact that between crossed nicols, a clay particle will transmit zero light intensity when the direction of the optic axis coincides with the polarising direction and maximum intensity

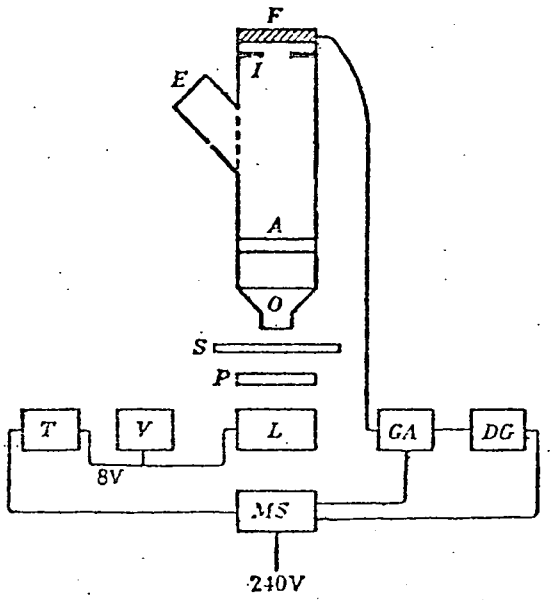

Diagrammatic sketch of microscope arrangement. *A*, analyser *DG*, display galvanometer; *E*, eyepiece; *F*, selenium photocell; *GA*, galvanometer amplifier; *I*, iris diaphragm; *L*, light source unit; *O*, objective; *P*, polarizer; *MS*, mains stabilizer; *S*, thin section; *T*, transformer; *V*, voltmeter.

Figure A 2.1. Apparatus used to determine Orientation Ratios by an Optical Method (After Morgenstern and Tchalenko, 1967a).

at 45° to these directions. When an aggregate is considered, the birefringence behaves in a similar manner, but will depend on the optical distribution of particles, although it will seldom be zero unless the particles are in perfect alignment.

The birefringence ratio has been calculated from slide areas of 0.33mm^2 (i.e. x 40 magnifications) and the resulting numerical value for the degree of preferred orientation was obtained by reference to the two dimensional model of Morgenstern and Tchalenko (1967a) see Fig. 4.1.

A.2.2 X-ray Diffraction

A.2.2.1. Sample Preparation

Air-dried, orientated samples were prepared by cutting strips of dry clay approximately 10mm wide by 20mm long in directions parallel to, and at right angles to the vertical direction. The large surfaces of the strips were ground flat with a medium abrasive (3CF) and finally polished flat with a very fine abrasive (F1000CF), using paraffin as the lubricating medium because water caused slaking of the material.

A.2.2.2. X-ray Analysis

The polished slices were placed in a Phillips PW 1130 X-ray Diffractometer and a trace was produced using the same conditions as those used for analysis of the mineralogy (see Appendix A.1).

After a suitable baseline had been inserted, also in the same manner as that used for the mineralogical analysis (see Appendix A1.), estimations of the peak intensities of the kaolinite 001 and 020 reflections, the illite 002 and 110 reflections and the montmorillonite 001 and 020 reflections were made by the following methods:-

(a) Measurement of the peak height above the baseline

(b) Measurement of the peak area with a polar planimeter

A.2.3. Sample Preparation for Electron Microscopy

The method of sample preparation giving the least structural disturbance of the particles present was adopted from Barden and Sides (1971b). This involved air-drying the clays, followed by fracturing a thin slice (5mm thick) in the particular direction to be studied, (in this case parallel to give a vertical section). The side opposite the fracture was then sandpapered down to produce a flat surface and the resulting block (5mm high by 10mm wide) was glued to an aluminium backing stub. Cleaning of the fractured surface was accomplished by peeling with adhesive tape between 50 - 100 times. Barden and Sides (1971b) found this to be very effective for removing all loose debris, leaving a surface which presented a clear picture of the structure. The stub was then coated, firstly with a thin layer of carbon and then with a thin layer of gold palladium to prevent charging of the particles by the scanning electron beam; both processes being performed in a vacuum.

Appendix A.3
Consolidation

A.3.1 General Procedures

All tests performed on undisturbed and remoulded material were carried out using a load increment ratio ($\Delta P/P$) of approximately unity, which was considered adequate to allow the consolidation process to proceed according to the Terzaghi theory.

The progress and amount of compression during each period of loading was recorded graphically against the square root of time from the beginning of the stage and consequently the value for T_{90}, used to calculate various consolidation parameters, was obtained in the usual manner described in most standard soils texts.

A.3.2 Tests on Undisturbed Material

Undisturbed material, orientated such that the bedding was perpendicular to the applied stress, was carefully cut to fit the oedometer cell, which had been previously lined with silicone grease; the resulting specimen being approximately 16mm high by 37mm in diameter. After being weighed and measured, the sample was placed in the oedometer and allowed to saturate for 24 hours. Initially a pressure of $20kN/m^2$ was applied to ensure that the lever arm was resting on the plunger.

Swelling was prevented during the saturation period by gradually applying loads to maintain a zero reading on the strain dial recording the specimen height. The resulting pressure at the end of the saturation period was known as the 'swell pressure'.

The specimen was then consolidated to the maximum pressure by approximately doubling the load every 24 hours and the subsequent unloading was performed in 4 or 5 stages, again over periods of 24 hours.

At the end of the unloading stages the sample was measured for thickness between two glass cover slides, reweighed wet, oven dried and then reweighed dry.

In addition to the above test, a specimen was placed in a conventional oedometer cell 20mm high by 50mm in diameter and an independent measurement was made of the swell pressure, free swell, wet and dry density and stress relieved voids ratio. This data, (Table A.3.64) was also used to confirm the initial voids ratio used in the consolidation test.

A.3.3 Tests on Remoulded Material

(i) Remoulding

To ensure that each sample retained the same mineralogical composition for this set of tests, the oven-dried materials from the tests on the undisturbed material were used.

Firstly each clay was slaked in distilled water for 2 - 3 days and then completely disintegrated in a mechanical stirrer until a smooth gel was obtained. After being oven-dried, this material was powdered to pass a B.S.200 mesh and made up to a moisture content equivalent to the liquid limit, which was assumed to approximate to the condition of the original sediment just below the sediment-water interface (Skempton, 1944).

(ii) Consolidation Tests from the Liquid Limit

The remoulded material was made up to an initial volume of 13mm in height by 37mm in diameter in a modified oedometer cell (see Fig.A.3.1), after which it was placed in the oedometer and a small load of 20kN/m^2 was applied to ensure that the lever arm was seated on top of the plunger. It was found necessary to use a smaller volume of material to accommodate the travel of the lever arm over the pressure range.

Incremental consolidation then proceeded to a pressure of 2426kN/m^2, after which the load was removed in three stages to allow rebound to occur. Subsequently the load was reapplied in three stages back up to 2426kN/m^2, and from this point normal incremental loading was resumed until a maximum pressure of 34967kN/m^2 was reached. The sample was finally unloaded in four stages, after which it was measured and reweighed in the same manner as described for the undisturbed tests.

(iii) Low Pressure Tests on Remoulded Material

Four clays covering a wide range of Atterberg limits, were consolidated in a conventional oedometer, with a 50mm diameter cell, to a maximum pressure of 8400kN/m^2. Initially all of the clays were remoulded as described above and were subsequently consolidated from initial moisture contents equal to their liquid limits and a liquidity index of 0.5. In addition, the Fuller's Earth was consolidated from initial moisture contents equal to liquidity indices of 0.75 and 0.25.

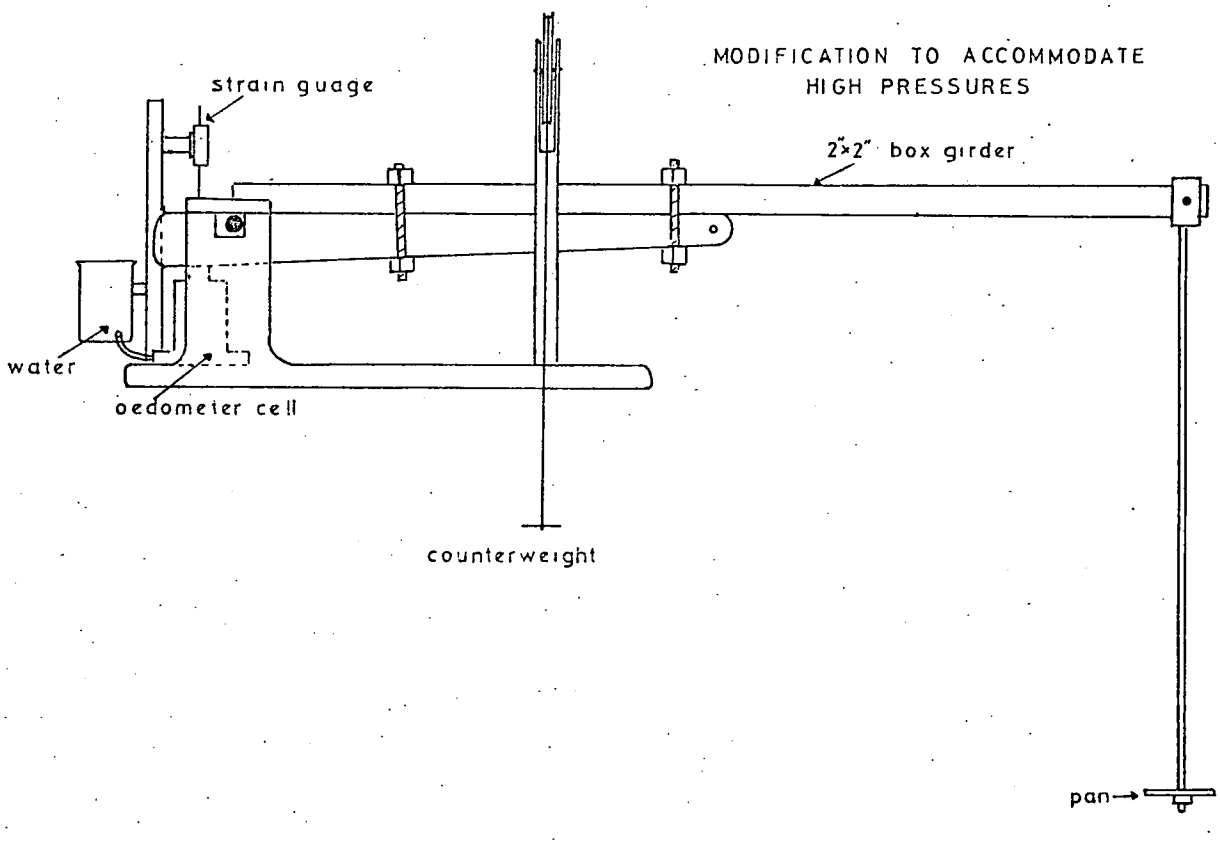

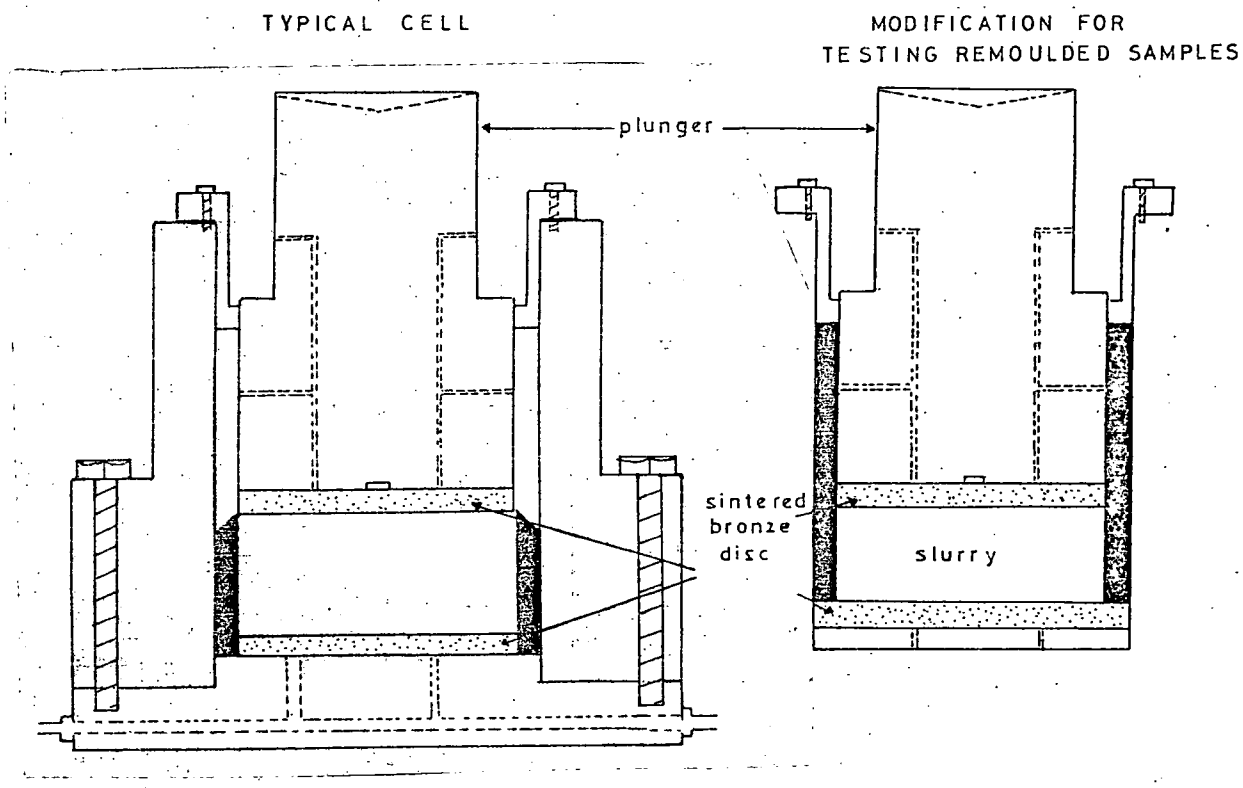

Figure A 3.1. High Pressure Oedometer with Modification for Remoulded Material.

Table A 3.1.

Consolidation Data - London Clay 14m (Undisturbed).

Initial m/c	= 28.21%	Final m/c	= 31.20%
Natural Bulk Density	= 2.07g/cm^3	Natural Dry Density	= 1.61g/cm^3
Final Bulk Density	= 2.01g/cm^3	Final Dry Density	= 1.53g/cm^3
Swell Percentage	= 5.22%	Swell Pressure	=130.63kN/m^2

Pressure (kN/m^2)	Voids R	Strain (%)	c_v (m^2/y)	m_v (m^2/MN)	k (m/s$*10^{-10}$)	C_c/C_s
130	0.718					
149	0.717	0.08	26.98	0.030	2.56227	-0.023
167	0.716	0.13	10.53	0.032	1.05620	-0.018
200	0.711	0.39	1.96	0.088	0.53648	-0.054
276	0.704	0.82	0.91	0.053	0.15185	-0.054
422	0.690	1.62	0.55	0.056	0.09594	-0.074
714	0.664	3.13	0.74	0.052	0.12089	-0.114
1297	0.625	5.41	0.60	0.040	0.07477	-0.150
2283	0.580	8.03	0.51	0.028	0.04441	-0.183
4799	0.515	11.79	0.48	0.016	0.02433	-0.200
9342	0.438	16.28	0.33	0.011	0.01144	-0.266
18663	0.349	21.45	0.23	0.006	0.00479	-0.306
9120	0.368	20.38				0.059
4560	0.398	18.58				0.102
912	0.499	12.72				0.144
3	0.808	-5.22				0.123

Table A 3.2

Consolidation Data - London Clay 14m (Remoulded).

Initial m/c	= 84.00%	Final m/c	= 23.06%
Initial Wet Density	= 1.44g/cm^3	Initial Dry Density	= 0.78g/cm^3
Final Bulk Density	= 2.06g/cm^3	Final Dry Density	= 1.67g/cm^3

Pressure (kN/m^2)	Voids R	Strain (%)	c_v (m^2/y)	m_v (m^2/MN)	k (m/s$*10^{-10}$)	C_c/C_s
20	2.530					
54	2.373	4.43	0.05	1.308	0.20276	-0.364
89	2.071	12.99	0.06	2.558	0.47581	-1.402
158	1.771	21.50	0.06	1.415	0.26333	-1.202
297	1.348	33.49	0.08	1.098	0.27236	-1.553
574	1.111	40.19	0.08	0.365	0.09036	-0.826
1128	0.917	45.68	0.12	0.126	0.04695	-0.661
2426	0.738	50.76	0.12	0.072	0.02676	-0.539
867	0.756	50.25				0.040
175	0.815	48.58				0.084
37	0.926	45.43				0.166
605	0.853	47.48	0.08	0.067	0.01654	-0.060
1214	0.783	49.48	0.16	0.062	0.03076	-0.233
2426	0.697	51.91	0.13	0.040	0.01603	-0.285
4675	0.593	54.87	0.14	0.027	0.01182	-0.366
9349	0.494	57.67	0.12	0.013	0.00494	-0.327
18697	0.392	60.55	0.12	0.007	0.00275	-0.338
34967	0.309	62.91	0.72	0.003	0.00817	-0.306
9347	0.367	61.27				0.101
1560	0.486	57.89				0.153
175	0.582	55.19				0.100
20	0.656	53.09				0.079

Table A 3.3

Consolidation Data - London Clay 37m (Undisturbed).

Initial m/c	= 19.71%	Final m/c	= 21.41%
Natural Bulk Density	= 2.06g/cm^3	Natural Dry Density	= 1.72g/cm^3
Final Bulk Density	= 2.05g/cm^3	Final Dry Density	= 1.69g/cm^3
Swell Percentage	= 2.05%	Swell Pressure	=254.98kN/m^2

Pressure (kN/m^2)	Voids R	Strain (%)	c_v (m^2/y)	m_v (m^2/MN)	k (m/s* 10^{-10})	C_c/C_s
255	0.578					
294	0.578	0.00	0.00	0.000	0.00000	0.000
331	0.578	0.00	0.00	0.000	0.00000	0.000
404	0.575	0.18	15.24	0.026	1.23030	-0.029
550	0.570	0.52	11.61	0.021	0.78259	-0.040
842	0.555	1.42	8.13	0.032	0.82463	-0.076
1431	0.536	2.65	1.55	0.021	0.09967	-0.084
2590	0.507	4.48	1.01	0.016	0.05100	-0.112
4925	0.474	6.60	0.72	0.009	0.02093	-0.120
9597	0.430	9.39	0.56	0.006	0.01108	-0.152
18244	0.372	13.05	0.35	0.004	0.00525	-0.207
35025	0.308	17.11	0.27	0.002	0.00241	-0.225
9120	0.342	14.98				0.057
1824	0.407	10.82				0.094
367	0.472	6.71				0.093
3	0.610	-2.05				0.061

Table A 3.4.

Consolidation Data - London Clay 37m (Remoulded).

Initial m/c	= 63.00%	Final m/c	= 20.16%
Initial Wet Density	= 1.64g/cm^3	Initial Dry Density	= 1.01g/cm^3
Final Bulk Density	= 2.11g/cm^3	Final Dry Density	= 1.76g/cm^3

Pressure (kN/m^2)	Voids R	Strain (%)	c_v (m^2/y)	m_v (m^2/MN)	k (m/s* 10^{-10})	C_c/C_s
20	1.700					
54	1.641	2.19	1.10	0.642	2.19161	-0.137
89	1.384	11.68	1.02	2.780	8.79140	-1.188
158	1.116	21.64	0.66	1.629	3.33333	-1.076
297	0.915	29.08	0.69	0.683	1.46173	-0.737
574	0.771	34.38	0.50	0.271	0.42077	-0.500
1128	0.652	38.82	0.40	0.121	0.15039	-0.408
2426	0.533	43.19	0.33	0.055	0.05672	-0.355
867	0.549	42.61				0.035
175	0.612	40.27				0.091
37	0.669	38.19				0.083
435	0.629	39.64	0.20	0.059	0.03696	-0.036
1214	0.569	41.89	0.36	0.047	0.05277	-0.136
2426	0.518	43.76	0.57	0.027	0.04738	-0.168
4675	0.433	46.91	0.26	0.025	0.02007	-0.298
9349	0.351	49.96	0.30	0.012	0.01138	-0.274
18697	0.282	52.51	0.21	0.005	0.00355	-0.228
34967	0.216	54.95	0.22	0.003	0.00215	-0.242
9347	0.257	53.42				0.072
1560	0.338	50.43				0.103
175	0.436	46.80				0.103
20	0.530	43.32				0.100

Table A 3.5.

Consolidation Data - Gault Clay (Undisturbed).

Initial m/c	= 26.29%	Final m/c	= 31.08%
Natural Bulk Density	= 2.06g/cm^3	Natural Dry Density	= 1.63g/cm^3
Final Bulk Density	= 2.12g/cm^3	Final Dry Density	= 1.62g/cm^3
Swell Percentage	= 0.70%	Swell Pressure	=166.72kN/m^2

Pressure (kN/m^2)	Voids R	Strain (%)	c_v (m^2/y)	m_v (m^2/MN)	k (m/s* 10^{-10})	C_c/C_s
166	0.662					
240	0.661	0.04	27.36	0.008	0.68693	-0.004
313	0.660	0.14	11.37	0.008	0.29068	-0.014
458	0.654	0.50	9.41	0.025	0.72715	-0.035
750	0.642	1.19	6.10	0.024	0.46984	-0.053
1371	0.623	2.34	4.78	0.018	0.27613	-0.073
2556	0.598	3.83	3.66	0.012	0.14747	-0.092
4928	0.569	5.61	2.50	0.007	0.06139	-0.104
9853	0.505	9.47	1.86	0.008	0.04871	-0.213
19703	0.385	16.65	0.54	0.008	0.01400	-0.397
35025	0.296	22.04	0.33	0.004	0.00451	-0.358
18241	0.311	21.13				0.053
9120	0.347	18.95				0.120
1824	0.414	14.93				0.095
366	0.498	9.89				0.120
2	0.674	-0.70				0.084

Table A 3.6.

Consolidation Data - Gault Clay (Remoulded).

Initial m/c	= 76.00%	Final m/c	= 20.17%
Initial Wet Density	= 1.58g/cm^3	Initial Dry Density	= 0.89g/cm^3
Final Bulk Density	= 2.12g/cm^3	Final Dry Density	= 1.76g/cm^3

Pressure (kN/m^2)	Voids R	Strain (%)	c_v (m^2/y)	m_v (m^2/MN)	k (m/s* 10^{-10})	C_c/C_s
20	2.013					
54	1.798	7.14	0.30	2.098	1.95183	-0.500
89	1.542	15.61	0.47	2.614	3.80875	-1.184
158	1.279	24.35	0.43	1.499	1.99876	-1.055
297	1.095	30.46	0.39	0.598	0.72304	-0.674
574	0.953	35.18	0.44	0.244	0.33376	-0.497
1128	0.806	40.03	0.69	0.136	0.29061	-0.498
2426	0.680	44.24	0.67	0.054	0.11163	-0.381
867	0.696	43.69				0.037
175	0.753	41.80				0.081
37	0.812	39.84				0.088
435	0.786	40.72	0.31	0.036	0.03401	-0.025
1214	0.720	42.90	0.73	0.048	0.10735	-0.147
2426	0.663	44.78	1.08	0.027	0.09154	-0.188
4675	0.579	47.58	0.77	0.023	0.05361	-0.295
9349	0.474	51.06	0.80	0.014	0.03528	-0.348
18697	0.366	54.64	0.59	0.008	0.01433	-0.358
34967	0.288	57.22	0.39	0.003	0.00437	-0.287
9347	0.329	55.89				0.070
1560	0.407	53.29				0.101
175	0.489	50.57				0.086
20	0.536	49.00				0.050

Table A 3.7.

Consolidation Data - Fullers Earth, Redhill (Undisturbed).

Initial m/c	= 48.85%	Final m/c	= 58.91%
Natural Bulk Density	= 1.81g/cm^3	Natural Dry Density	= 1.22g/cm^3
Final Bulk Density	= 1.88g/cm^3	Final Dry Density	= 1.18g/cm^3
Swell Percentage	= 2.74%	Swell Pressure	= 69.63kN/m^2

Pressure (kN/m^2)	Voids R	Strain (%)	c_v (m^2/y)	m_v (m^2/MN)	k (m/s* 10^{-10})	C_c/C_s
69	1.302					
134	1.297	0.21	25.20	0.032	2.61043	-0.017
200	1.290	0.49	39.19	0.046	5.60957	-0.037
331	1.283	0.82	8.62	0.023	0.62353	-0.035
594	1.259	1.83	24.59	0.039	3.04697	-0.091
1152	1.223	3.44	66.51	0.029	5.88842	-0.128
2302	1.171	5.69	15.97	0.020	1.00700	-0.172
4437	1.110	8.34	0.63	0.013	0.02570	-0.214
8873	1.014	12.49	0.33	0.010	0.01077	-0.317
17744	0.866	18.92	0.02	0.008	0.00059	-0.492
33185	0.702	26.04	0.01	0.005	0.00022	-0.602
8873	0.837	20.19				0.234
1481	0.955	15.08				0.151
331	1.100	8.75				0.223
2	1.365	-2.74				0.128

Table A 3.8.

Consolidation Data - Fullers Earth, Redhill (Remoulded).

Initial m/c	=117.00%	Final m/c	= 45.78%
Initial Wet Density	= 1.40g/cm^3	Initial Dry Density	= 0.66g/cm^3
Final Bulk Density	= 1.81g/cm^3	Final Dry Density	= 1.24g/cm^3

Pressure (kN/m^2)	Voids R	Strain (%)	c_v (m^2/y)	m_v (m^2/MN)	k (m/s* 10^{-10})	C_c/C_s
20	3.335					
54	3.083	5.82	0.83	1.709	4.39919	-0.587
89	2.753	13.42	0.83	2.309	5.94164	-1.529
158	2.409	21.36	1.04	1.328	4.28278	-1.378
297	2.181	26.61	0.75	0.495	1.15185	-0.834
574	1.969	31.51	0.39	0.240	0.29088	-0.743
1128	1.170	37.48	0.10	0.157	0.04881	-0.882
2426	1.400	44.62	0.02	0.088	0.00546	-0.931
867	1.430	43.93				0.067
175	1.506	42.19				0.109
37	1.578	40.54				0.106
435	1.566	40.81	0.06	0.011	0.00215	-0.011
1214	1.469	43.04	0.01	0.049	0.00150	-0.216
2426	1.367	45.40	0.01	0.034	0.00087	-0.340
4675	1.195	49.36	0.01	0.033	0.00056	-0.603
9349	1.025	53.29	0.01	0.017	0.00028	-0.566
18697	0.845	57.44	0.01	0.009	0.00023	-0.597
34967	0.707	60.62	0.01	0.004	0.00011	-0.506
9349	0.811	58.23				0.180
1560	1.065	52.37				0.329
175	1.176	49.79				0.117
20	1.259	47.89				0.087

Table A 3.9.

Consolidation Data - Weald Clay (Undisturbed).

Initial m/c	= 7.24%	Final m/c	= 11.97%
Natural Bulk Density	= 2.42g/cm^3	Natural Dry Density	= 2.26g/cm^3
Final Bulk Density	= 2.57g/cm^3	Final Dry Density	= 2.30g/cm^3
Swell Percentage	= 0.00%	Swell Pressure	=148.09kN/m^2

Pressure (kN/m^2)	Voids R	Strain (%)	c_v (m^2/y)	m_v (m^2/MN)	k (m/s 10^{-10})	C_c/C_s
148	0.189					
281	0.188	0.03	25.92	0.006	0.50812	-0.001
412	0.186	0.22	4.89	0.013	0.19480	-0.014
675	0.180	0.71	71.37	0.019	4.25886	-0.027
1234	0.170	1.51	15.01	0.015	0.70541	-0.036
2302	0.162	2.16	14.78	0.006	0.29333	-0.029
4437	0.151	3.09	14.55	0.004	0.19994	-0.039
8873	0.136	4.40	29.66	0.003	0.28234	-0.051
17744	0.117	6.02	28.77	0.001	0.17102	-0.063
34827	0.083	8.88	27.42	0.001	0.15367	-0.116
16429	0.090	8.26				0.022
8213	0.099	7.47				0.031
1481	0.117	6.00				0.023
331	0.134	4.59				0.026
2	0.170	1.57				0.017

Table 3.10.

Consolidation Data - Weald Clay (Remoulded).

Initial m/c	= 35.00%	Final m/c	= 35.00%
Initial Wet Density	= 2.12g/cm^3	Initial Dry Density	= 1.57g/cm^3
Final Bulk Density	= 2.61g/cm^3	Final Dry Density	= 2.29g/cm^3

Pressure (kN/m^2)	Voids R	Strain (%)	c_v (m^2/y)	m_v (m^2/MN)	k (m/s 10^{-10})	C_c/C_s
20	0.706					
54	0.618	5.19	0.14	1.517	0.65843	-0.206
89	0.532	10.19	0.39	1.518	1.83602	-0.396
158	0.475	13.56	0.67	0.539	1.11996	-0.230
297	0.422	16.67	0.98	0.266	0.80863	-0.194
574	0.373	19.50	1.77	0.124	0.68257	-0.169
1128	0.335	21.73	3.61	0.050	0.55907	-0.129
2426	0.284	24.72	7.81	0.030	0.71256	-0.153
867	0.289	24.46				0.010
175	0.304	23.58				0.021
37	0.322	22.51				0.027
435	0.308	23.35	3.80	0.027	0.31032	-0.013
1214	0.292	24.30	33.41	0.016	1.62634	-0.036
2426	0.277	25.18	11.74	0.009	0.34862	-0.050
4675	0.240	27.35	10.22	0.013	0.40817	-0.129
9349	0.192	30.13	10.52	0.007	0.23627	-0.158
18697	0.138	33.21	11.94	0.004	0.17605	-0.174
34967	0.088	36.21	10.91	0.002	0.09307	-0.187
9347	0.105	35.24				0.029
1560	0.127	33.92				0.029
175	0.151	32.52				0.025
20	0.169	31.47				0.019

Table A 3.11.

Consolidation Data - Kimmeridge Clay (Undisturbed).

Initial m/c	= 21.99%	Final m/c	= 29.28%
Natural Bulk Density	= 2.10g/cm^3	Natural Dry Density	= 1.72g/cm^3
Final Bulk Density	= 2.11g/cm^3	Final Dry Density	= 1.63g/cm^3
Swell Percentage	= 5.43%	Swell Pressure	=118.66kN/m^2

Pressure (kN/m^2)	Voids R	Strain (%)	c_v (m^2/y)	m_v (m^2/MN)	k (m/s 10^{-10})	C_c/C_s
118	0.555					
183	0.552	0.19	27.92	0.029	2.56895	-0.015
249	0.546	0.56	0.27	0.058	0.04902	-0.042
495	0.528	1.77	0.15	0.047	0.02200	-0.063
1152	0.482	4.67	0.09	0.045	0.01278	-0.123
2302	0.441	7.36	0.11	0.024	0.00820	-0.139
4437	0.403	9.78	0.15	0.012	0.00615	-0.132
8873	0.360	12.53	0.24	0.006	0.00519	-0.142
17744	0.314	15.52	0.31	0.003	0.00383	-0.154
33181	0.256	19.20	0.25	0.002	0.00225	-0.210
8873	0.291	16.98				0.060
1480	0.349	13.25				0.074
331	0.416	8.96				0.102
2	0.639	-5.43				0.109

Table A 3.12.

Consolidation Data - Kimmeridge Clay (Remoulded).

Initial m/c	= 70.00%	Final m/c	= 19.85%
Initial Wet Density	= 1.63g/cm^3	Initial Dry Density	= 0.96g/cm^3
Final Bulk Density	= 2.09g/cm^3	Final Dry Density	= 1.75g/cm^3

Pressure (kN/m^2)	Voids R	Strain (%)	c_v (m^2/y)	m_v (m^2/MN)	k (m/s 10^{-10})	C_c/C_s
20	1.796					
54	1.688	3.86	0.38	1.136	1.33829	-0.251
89	1.382	14.81	0.27	3.252	2.72238	-1.420
158	1.093	25.14	0.33	1.758	1.79879	-1.156
297	0.936	30.75	0.47	0.555	0.80957	-0.575
574	0.795	35.81	0.44	0.262	0.35863	-0.494
1128	0.681	39.87	0.48	0.114	0.17058	-0.387
2426	0.561	44.16	0.49	0.055	0.08354	-0.360
867	0.576	43.61				0.034
175	0.640	41.32				0.092
37	0.713	38.74				0.108
435	0.669	40.30	0.30	0.064	0.05942	-0.040
1214	0.601	42.73	0.45	0.053	0.07296	-0.152
2426	0.542	44.84	0.59	0.030	0.05561	-0.196
4675	0.465	47.58	0.54	0.022	0.03716	-0.269
9349	0.378	50.71	0.42	0.013	0.01744	-0.291
18697	0.298	53.58	0.40	0.006	0.00798	-0.266
34967	0.221	56.32	0.35	0.003	0.00413	-0.282
9347	0.270	54.56				0.086
1560	0.360	51.36				0.115
175	0.464	47.63				0.110
20	0.532	45.18				0.072

Table A 3.13.

Consolidation Data - Oxford Clay 10m (Undisturbed).

Initial m/c	= 27.64%	Final m/c	= 33.47%
Natural Bulk Density	= 1.88g/cm^3	Natural Dry Density	= 1.47g/cm^3
Final Bulk Density	= 1.95g/cm^3	Final Dry Density	= 1.46g/cm^3
Swell Percentage	= 0.81%	Swell Pressure	=117.68kN/m^2

Pressure (kN/m^2)	Voids R	Strain (%)	c_v (m^2/y)	m_v (m^2/MN)	k (m/s* 10^{-10})	C_c/C_s
117	0.690					
184	0.686	0.25	28.90	0.038	3.16488	-0.021
250	0.676	0.81	26.00	0.089	7.24323	-0.071
381	0.665	1.48	28.32	0.051	4.39847	-0.061
661	0.636	3.20	3.40	0.062	0.65563	-0.121
1238	0.603	5.15	1.94	0.035	0.21024	-0.121
2309	0.571	7.06	1.77	0.018	0.10227	-0.119
4451	0.537	9.05	1.94	0.010	0.06110	-0.118
8896	0.480	12.42	1.60	0.008	0.04198	-0.189
17796	0.387	17.92	0.58	0.007	0.01310	-0.309
34931	0.279	24.30	0.41	0.004	0.00605	-0.368
16475	0.304	22.82				0.076
8237	0.328	21.39				0.080
1482	0.404	16.93				0.101
329	0.488	11.96				0.128
2	0.701	-0.68				0.104

Table A 3.14.

Consolidation Data - Oxford Clay 10m (Remoulded).

Initial m/c	= 76.00%	Final m/c	= 20.23%
Initial Wet Density	= 1.48g/cm^3	Initial Dry Density	= 0.844g/cm^3
Final Bulk Density	= 2.02g/cm^3	Final Dry Density	= 1.69g/cm^3

Pressure (kN/m^2)	Voids R	Strain (%)	c_v (m^2/y)	m_v (m^2/MN)	k (m/s* 10^{-10})	C_c/C_s
20	1.949					
54	1.828	4.08	0.32	1.206	1.19713	-0.280
89	1.528	14.25	0.11	3.031	1.03354	-1.391
158	1.323	21.20	0.05	1.176	0.18216	-0.820
297	1.135	27.57	0.08	0.582	0.14439	-0.689
574	0.969	33.20	0.12	0.280	0.10441	-0.580
1128	0.834	37.80	0.17	0.123	0.06522	-0.462
2426	0.679	43.06	0.18	0.065	0.03633	-0.466
4675	0.567	46.84	0.13	0.030	0.01195	-0.391
867	0.605	45.57				0.051
175	0.656	43.82				0.074
37	0.715	41.85				0.087
867	0.674	43.23	0.07	0.028	0.00625	-0.029
2426	0.598	45.81	0.10	0.029	0.00909	-0.170
4675	0.530	48.10	0.10	0.019	0.00586	-0.238
9349	0.440	51.14	0.12	0.012	0.00468	-0.298
18697	0.336	54.67	0.08	0.008	0.00194	-0.345
34967	0.262	57.17	0.04	0.003	0.00054	-0.271
9349	0.303	55.81				0.070
1560	0.381	53.14				0.101
175	0.427	51.59				0.048
20	0.476	49.93				0.052

Table A 3.15.

Consolidation Data - Oxford Clay 44m (less than preconsolidation load)

Initial m/c	= 15.90%	Final m/c	= 15.90%
Natural Bulk Density	= 1.99g/cm^3	Natural Dry Density	= 1.72g/cm^3
Final Bulk Density	= 2.06g/cm^3	Final Dry Density	= 1.64g/cm^3
Swell Percentage	= 4.63%	Swell Pressure	=528.60kN/m^2

Pressure (kN/m^2)	Voids R	Strain (%)	c_v (m^2/y)	m_v (m^2/MN)	k (m/s 10^{-10})	C_c/C_s
528	0.470					
660	0.469	0.12	4.22	0.005	0.06741	-0.018
791	0.466	0.29	1.30	0.015	0.06282	-0.031
1234	0.455	1.06	3.10	0.017	0.16277	-0.059
2302	0.431	2.70	1.96	0.015	0.09384	-0.089
4437	0.404	4.48	2.56	0.008	0.07013	-0.091
6245	0.392	5.36	3.28	0.005	0.04806	-0.087
1480	0.416	3.73				0.038
331	0.449	1.44				0.051
2	0.538	-4.63				0.043

Table A 3.16.

Consolidation Data - Oxford Clay 44m (Undisturbed).

Initial m/c	= 18.20%	Final m/c	= 22.00%
Natural Bulk Density	= 2.04g/cm^3	Natural Dry Density	= 1.73g/cm^3
Final Bulk Density	= 2.04g/cm^3	Final Dry Density	= 1.68g/cm^2
Swell Percentage	= 3.05%	Swell Pressure	=203.59kN/m^2

Pressure (kN/m^2)	Voids R	Strain (%)	c_v (m^2/y)	m_v (m^2/MN)	k (m/s 10^{-10})	C_c/C_s
203	0.463					
276	0.462	0.02	28.68	0.009	0.83247	-0.002
349	0.461	0.15	12.72	0.029	1.16918	-0.018
495	0.456	0.45	1.82	0.023	0.13225	-0.029
787	0.447	1.10	1.85	0.021	0.12149	-0.047
1188	0.435	1.92	1.57	0.020	0.10065	-0.067
2556	0.410	3.60	1.31	0.012	0.05138	-0.074
4928	0.387	5.15	1.24	0.006	0.02619	-0.079
9853	0.360	7.03	1.01	0.004	0.01277	-0.091
19703	0.307	10.62	0.68	0.003	0.00849	-0.174
35025	0.235	15.56	0.49	0.003	0.00538	-0.289
18241	0.248	14.65				0.047
8208	0.275	12.84				0.076
1642	0.339	8.44				0.092
366	0.398	4.43				0.090
2	0.507	-3.05				0.052

Table A 3.17.

Consolidation Data - Oxford Clay 44m (Remoulded).

Initial m/c	= 57.00%	Final m/c	= 57.00%
Initial Wet Density	= 1.54g/cm^3	Initial Dry Density	= 0.98g/cm^3
Final Bulk Density	= 2.05g/cm^3	Final Dry Density	= 1.70g/cm^3

Pressure (kN/m^2)	Voids R	Strain (%)	c_v (m^2/y)	m_v (m^2/MN)	k (m/s 10^{-10})	C_c/C_s
20	1.580					
54	1.504	2.96	3.63	0.866	9.74953	-0.177
89	1.210	14.34	0.29	3.354	3.01586	-1.362
158	1.041	20.90	0.60	1.108	2.06135	-0.677
297	0.813	29.74	1.03	0.803	2.56614	-0.836
574	0.747	32.29	1.00	0.131	0.40745	-0.229
1128	0.633	36.72	1.20	0.117	0.43817	-0.390
2426	0.517	41.21	1.13	0.056	0.19170	-0.348
867	0.529	40.72				0.028
175	0.583	38.62				0.078
37	0.662	35.56				0.117
261	0.637	35.56	0.59	0.067	0.12281	-0.030
867	0.574	38.98	0.81	0.064	0.15949	-0.120
2426	0.502	41.78	2.08	0.029	0.18692	-0.161
4675	0.422	44.86	1.26	0.024	0.09377	-0.279
9349	0.345	47.85	0.94	0.011	0.03501	-0.256
18697	0.262	51.09	0.77	0.006	0.01644	-0.277
34967	0.186	54.03	0.63	0.003	0.00746	-0.279
8657	0.223	52.57				0.062
1560	0.292	49.92				0.092
175	0.384	46.36				0.096
37	0.482	42.54				0.147

Table A 3.18.

Consolidation Data - Fullers Earth, Bath (Undisturbed).

Initial m/c	= 32.98%	Final m/c	= 44.55%
Natural Bulk Density	= 1.99g/cm^3	Natural Dry Density	= 1.50g/cm^3
Final Bulk Density	= 2.10g/cm^3	Final Dry Density	= 1.45g/cm^3
Swell Percentage	= 3.36%	Swell Pressure	=185.35kN/m^2

Pressure (kN/m^2)	Voids R	Strain (%)	c_v (m^2/y)	m_v (m^2/MN)	k (m/s*10^{-10})	C_c/C_s
185	0.804					
331	0.803	0.07	24.70	0.004	0.29071	-0.004
477	0.795	0.47	3.93	0.030	0.37024	-0.045
769	0.777	1.48	9.46	0.034	1.00711	-0.087
1352	0.757	2.59	2.92	0.019	0.17474	-0.082
2556	0.706	5.41	0.95	0.024	0.07099	-0.184
4928	0.655	8.26	0.04	0.012	0.00150	-0.180
9853	0.582	12.29	0.03	0.009	0.00089	-0.241
19703	0.484	17.74	0.01	0.006	0.00035	-0.327
35022	0.404	22.16	0.01	0.003	0.00010	-0.319
18241	0.437	20.32				0.117
9120	0.478	18.06				0.135
1641	0.602	11.21				0.166
366	0.672	7.32				0.108
2	0.864	-3.36				0.093

Table A 3.19.

Consolidation Data - Fullers Earth, Bath (Remoulded).

Initial m/c	=105.00%	Final m/c	= 39.70%
Initial Wet Density	= 1.43g/cm^3	Initial Dry Density	= 0.69g/cm^3
Final Bulk Density	= 1.83g/cm^3	Final Dry Density	= 1.31g/cm^3

Pressure (kN/m^2)	Voids R	Strain (%)	c_v (m^2/y)	m_v (m^2/MN)	k (m/s*10^{-10})	C_c/C_s
20	2.895					
54	2.635	6.68	0.79	1.964	4.80817	-0.605
89	2.251	16.53	0.84	3.018	8.17851	-1.780
158	1.912	25.22	0.40	1.511	1.87390	-1.354
297	1.560	34.26	0.14	0.919	0.39887	-1.292
574	1.338	39.97	0.12	0.313	0.11644	-0.778
1128	1.145	44.92	0.05	0.149	0.02309	-0.656
2426	0.948	49.99	0.03	0.071	0.00653	-0.594
867	0.992	48.86				0.099
175	1.109	45.84				0.169
37	1.211	43.22				0.152
435	1.159	44.55	0.04	0.059	0.00720	-0.049
1214	1.039	47.63	0.04	0.071	0.00887	-0.269
2426	0.940	50.18	0.02	0.041	0.00244	-0.329
4675	0.809	53.56	0.02	0.031	0.00199	-0.461
9349	0.668	57.17	0.01	0.017	0.00078	-0.468
18697	0.528	60.76	0.01	0.009	0.00038	-0.463
34967	0.419	63.57	0.01	0.004	0.00015	-0.403
8657	0.532	60.65				0.188
1560	0.722	55.79				0.254
175	0.945	50.06				0.235
17	1.068	46.91				0.121

Table A 3.20.

Consolidation Data - Lias Clay 10m (Undisturbed).

Initial m/c	= 21.14%	Final m/c	= 26.78%
Natural Bulk Density	= 2.07g/cm^3	Natural Dry Density	= 1.71g/cm^3
Final Bulk Density	= 2.11g/cm^3	Final Dry Density	= 1.67g/cm^3
Swell Percentage	= 2.35%	Swell Pressure	=167.21kN/m^2

Pressure (kN/m^2)	Voids R	Strain (%)	c_v (m^2/y)	m_v (m^2/MN)	k (m/s 10^{-10})	C_c/C_s
167	0.562					
232	0.559	0.19	9.52	0.029	0.87201	-0.020
300	0.553	0.58	1.05	0.057	0.18553	-0.056
429	0.534	1.79	0.25	0.094	0.07350	-0.121
692	0.507	3.84	0.14	0.066	0.02903	-0.127
1231	0.468	6.03	0.13	0.049	0.02045	-0.159
2299	0.429	8.52	0.17	0.025	0.01329	-0.143
4437	0.394	10.74	0.22	0.011	0.00769	-0.114
8873	0.353	13.35	0.23	0.006	0.00479	-0.135
17743	0.304	16.52	0.43	0.004	0.00544	-0.165
33184	0.247	20.15	0.42	0.002	0.00368	-0.208
8875	0.283	17.86				0.062
1480	0.354	13.32				0.091
331	0.411	9.66				0.088
2	0.598	-2.35				0.091

Table A 3.21.

Consolidation Data - Lias Clay 10m (Remoulded).

Initial m/c	= 68.00%	Final m/c	= 17.79%
Initial Wet Density	= 1.52g/cm^3	Initial Dry Density	= 0.90g/cm^3
Final Bulk Density	= 2.12g/cm^3	Final Dry Density	= 1.80g/cm^3

Pressure (kN/m^2)	Voids R	Strain (%)	c_v (m^2/y)	m_v (m^2/MN)	k (m/s 10^{-10})	C_c/C_s
20	1.937					
54	1.835	3.48	0.13	1.021	0.41160	-0.237
89	1.562	12.76	0.12	2.751	1.02345	-1.264
158	1.383	18.87	0.16	1.012	0.50227	-0.718
297	1.196	25.21	0.06	0.581	0.10812	-0.582
574	0.993	32.15	0.10	0.331	0.10345	-0.713
1128	0.822	37.96	0.17	0.154	0.08161	-0.582
2426	0.690	42.45	0.18	0.056	0.03111	-0.396
867	0.693	42.33				0.007
175	0.743	40.63				0.072
37	0.799	38.75				0.082
605	0.756	40.20	0.13	0.042	0.01695	-0.035
1214	0.710	41.78	0.18	0.043	0.02408	-0.154
2426	0.648	43.88	0.30	0.030	0.02780	-0.205
4675	0.545	47.39	0.27	0.028	0.02420	-0.361
9349	0.456	50.43	0.19	0.012	0.00725	-0.296
18697	0.357	53.80	0.30	0.007	0.00717	-0.329
34967	0.277	56.52	0.30	0.003	0.00346	-0.294
9347	0.315	55.21				0.067
1560	0.374	53.21				0.075
175	0.411	51.95				0.039
20	0.479	49.63				0.072

Table A 3.22.

Consolidation Data - Lias Clay 36m (Undisturbed).

Initial m/c	= 17.01%	Final m/c	= 28.25%
Natural Bulk Density	= 2.12g/cm^3	Natural Dry Density	= 1.81g/cm^3
Final Bulk Density	= 2.14g/cm^3	Final Dry Density	= 1.67g/cm^2
Swell Percentage	= 8.70%	Swell Pressure	=332.46kN/m^2

Pressure (kN/m^2)	Voids R	Strain (%)	c_v (m^2/y)	m_v (m^2/MN)	($^k/_{s^*10}$ m/s)	C_c/C_s
332	0.459					
464	0.458	0.05	27.43	0.005	0.44152	-0.005
596	0.454	0.32	7.57	0.020	0.48776	-0.036
859	0.447	0.79	2.49	0.018	0.14128	-0.043
1485	0.432	1.80	1.16	0.016	0.05954	-0.062
2427	0.413	3.10	1.35	0.013	0.05614	-0.085
4451	0.389	4.78	1.50	0.008	0.03994	-0.096
8896	0.358	6.88	1.28	0.005	0.01993	-0.102
17796	0.316	9.79	1.11	0.003	0.01195	-0.141
33283	0.249	14.36	0.67	0.003	0.00682	-0.245
16475	0.271	12.85				0.072
8237	0.293	11.32				0.074
1482	0.355	7.07				0.083
329	0.413	3.12				0.088
2	0.586	-8.77				0.084

Table A 3.23.

Consolidation Data - Lias Clay 36m (Remoulded).

Initial m/c	= 65.00%	Final m/c	= 22.50%
Initial Wet Density	= 1.61g/cm^3	Initial Dry Density	= 0.97g/cm^3
Final Bulk Density	= 2.03g/cm^3	Final Dry Density	= 1.66g/cm^3

Pressure (kN/m^2)	Voids R	Strain (%)	c_v (m^2/y)	m_v (m^2/MN)	($^k/_{s^*10}$ m/s)	C_c/C_s
20	1.719					
54	1.542	6.51	0.27	1.914	1.60250	-0.412
89	1.334	14.18	0.41	2.338	2.97147	-0.967
158	1.154	20.76	0.78	1.117	2.70252	-0.716
297	1.021	25.67	0.83	0.457	1.17686	-0.490
574	0.896	30.27	1.04	0.223	0.71988	-0.437
1128	0.777	34.63	1.40	0.113	0.49164	-0.405
2426	0.643	39.58	1.32	0.058	0.23773	-0.404
867	0.658	39.03				0.033
175	0.728	36.43				0.103
37	0.811	33.39				0.123
261	0.781	34.50	0.75	0.074	0.17195	-0.036
867	0.707	37.22	1.08	0.069	0.22957	-0.142
2426	0.625	40.21	1.49	0.031	0.14231	-0.182
4675	0.539	43.41	1.13	0.024	0.08246	-0.305
9349	0.443	46.92	1.05	0.013	0.04458	-0.317
18697	0.346	50.50	0.81	0.007	0.01874	-0.323
34967	0.264	53.49	0.43	0.003	0.00516	-0.299
8657	0.316	51.59				0.085
1560	0.401	48.46				0.114
175	0.512	44.38				0.117
37	0.596	41.28				0.126

Table A 3.24.

Consolidation Data - Keuper Marl (Remoulded).

Initial m/c	= 33.00%	Final m/c	= 11.45%
Initial Wet Density	= 1.79g/cm^3	Initial Dry Density	= 1.35g/cm^3
Final Bulk Density	= 2.32g/cm^3	Final Dry Density	= 2.08g/cm^3

Pressure (kN/m^2)	Voids R	Strain (%)	c_v (m^2/y)	m_v (m^2/MN)	k (m/s 10^{-10})	C_c/C_s
20	1.042					
54	0.947	4.64	0.24	1.368	1.01800	-0.220
89	0.824	10.67	0.49	1.804	2.74173	-0.571
158	0.745	14.54	0.89	0.627	1.73186	-0.316
297	0.677	17.86	1.20	0.288	1.07371	-0.249
574	0.623	20.49	1.55	0.116	0.55854	-0.189
1128	0.563	23.43	5.04	0.067	1.04251	-0.204
2426	0.495	26.77	10.45	0.034	1.08582	-0.205
867	0.497	26.65				0.005
175	0.508	26.11				0.016
37	0.522	25.46				0.020
435	0.513	25.87	7.15	0.014	0.31037	-0.008
1214	0.502	26.45	10.16	0.009	0.29396	-0.026
2426	0.485	27.23	9.97	0.009	0.28860	-0.053
4675	0.430	29.93	9.50	0.016	0.48490	-0.193
9349	0.364	33.19	3.41	0.010	0.10433	-0.221
18697	0.304	36.14	9.82	0.004	0.14325	-0.200
34967	0.242	39.17	5.98	0.002	0.05545	-0.227
9347	0.262	38.15				0.036
1560	0.284	37.09				0.028
175	0.309	35.88				0.026
20	0.323	35.18				0.015

Table A 3.25.

Consolidation Data - Swallow Wood Roof (Remoulded).

Initial m/c	= 57.00%	Final m/c	= 20.52%
Initial Wet Density	= 1.65g/cm^3	Initial Dry Density	= 1.05g/cm^3
Final Bulk Density	= 2.14g/cm^3	Final Dry Density	= 1.77g/cm^3

Pressure (kN/m^2)	Voids R	Strain (%)	c_v (m^2/y)	m_v (m^2/MN)	$(\frac{k}{s}$ m/s* $10^{-10})$	C_c/C_s
20	1.609					
54	1.538	2.71	0.18	0.800	0.44663	-0.164
89	1.251	13.71	0.06	3.230	0.60090	-1.331
158	1.085	20.07	0.12	1.068	0.39754	-0.664
297	0.994	25.48	0.24	0.501	0.37263	-0.517
574	0.810	30.60	0.40	0.248	0.30852	-0.477
1128	0.710	34.80	0.60	0.108	0.20210	-0.373
2426	0.576	39.58	0.80	0.057	0.14041	-0.375
867	0.596	38.82				0.044
175	0.669	36.01				0.105
37	0.729	33.70				0.099
435	0.678	35.66	0.42	0.073	0.09558	-0.047
1214	0.606	38.42	0.91	0.055	0.15531	-0.161
2426	0.545	40.78	1.13	0.026	0.09175	-0.205
4675	0.462	43.96	0.82	0.024	0.06079	-0.291
9349	0.365	47.67	1.18	0.014	0.05193	-0.321
18697	0.281	50.90	1.13	0.006	0.02300	-0.289
34967	0.205	53.81	0.91	0.003	0.01020	-0.289
9347	0.247	52.20				0.073
1560	0.328	49.06				0.105
175	0.453	44.31				0.130
20	0.545	40.75				0.108

Table A 3.26.

Consolidation Data - Flockton Thin Roof (Undisturbed).

Initial m/c	= 2.80%	Final m/c	7.07%
Natural Bulk Density	= 2.48g/cm^3	Natural Dry Density	= 2.41g/cm^3
Final Bulk Density	= 2.63g/cm^3	Final Dry Density	= 2.46g/cm^3
Swell Percentage	= 0.00%	Swell Pressure	=567.83kN/m^2

Pressure (kN/m^2)	Voids R	Strain (%)	c_v (m^2/y)	m_v (m^2/MN)	k (m/s* 10^{-10})	C_c/C_s
567	0.137					
1279	0.126	1.01	49.30	0.014	2.07661	-0.032
2556	0.115	1.92	9.25	0.007	0.21956	-0.034
4929	0.109	2.47	7.20	0.002	0.05061	-0.022
9855	0.099	3.34	4.35	0.001	0.02468	-0.033
19708	0.089	4.23	2.35	0.001	0.00672	-0.034
35033	0.073	5.61	18.23	0.001	0.05417	-0.063
9855	0.083	4.73				0.018
1644	0.096	3.65				0.016
367	0.105	2.81				0.014
2	0.116	1.84				0.005

Table A 3.27.

Consolidation Data - Flockton Thin Roof (Remoulded).

Initial m/c	= 46.00%	Final m/c	= 15.08%
Initial Wet Density	= 1.67g/cm^3	Initial Dry Density	= 1.14g/cm^3
Final Bulk Density	= 2.21g/cm^3	Final Dry Density	= 1.92g/cm^3

Pressure (kN/m^2)	Voids R	Strain (%)	c_v (m^2/y)	m_v (m^2/MN)	k (m/s* 10^{-10})	C_c/C_s
20	1.404					
54	1.338	2.74	0.15	0.807	0.37544	-0.153
89	1.119	11.83	0.13	2.676	1.07852	-1.014
158	0.982	17.54	0.20	0.937	0.58094	-0.548
297	0.868	22.28	0.44	0.413	0.56441	-0.418
574	0.766	26.54	0.65	0.197	0.39721	-0.358
1128	0.671	30.48	0.96	0.097	0.28897	-0.323
2426	0.562	35.01	0.97	0.050	0.15113	-0.327
867	0.572	34.60				0.022
175	0.617	32.73				0.064
37	0.653	31.21				0.054
435	0.624	32.43	0.65	0.044	0.08798	-0.027
1214	0.577	34.40	1.48	0.037	0.17043	-0.107
2426	0.530	36.32	1.52	0.024	0.11589	-0.153
4675	0.445	39.88	1.39	0.025	0.10647	-0.300
9349	0.356	43.59	2.26	0.013	0.09231	-0.296
18697	0.268	47.22	1.43	0.007	0.03070	-0.290
34967	0.196	50.28	1.98	0.003	0.02177	-0.270
9347	0.229	48.85				0.060
1560	0.286	46.49				0.072
175	0.369	43.04				0.087
20	0.425	40.70				0.060

Table A 3.28.

Consolidation Data - Flockton Thin Seatearth (Undisturbed).

Initial m/c	= 6.80%	Final m/c	= 10.76%
Natural Bulk Density	= 2.27g/cm^3	Natural Dry Density	= 2.12g/cm^3
Final Bulk Density	= 2.39g/cm^3	Final Dry Density	= 2.16g/cm^2
Swell Percentage	= 0.00%	Swell Pressure	= 94.15kN/m^2

Pressure (kN/m^2)	Voids R	Strain (%)	c_v (m^2/y)	m_v (m^2/MN)	k (m/s* 10^{-10})	C_c/C_s
94	0.250					
239	0.244	0.51	46.69	0.033	4.79135	-0.015
385	0.237	1.05	10.23	0.038	1.22225	-0.032
677	0.226	1.89	17.25	0.030	1.62851	-0.042
1279	0.217	2.63	14.64	0.012	0.55342	-0.033
2556	0.207	3.47	23.33	0.006	0.46536	-0.035
4929	0.198	4.18	19.29	0.003	0.18790	-0.031
9855	0.184	5.29	18.93	0.002	0.13921	-0.046
19708	0.165	6.82	18.41	0.001	0.09294	-0.063
35033	0.147	8.26	13.10	0.001	0.04093	-0.071
18247	0.152	7.81				0.020
9125	0.160	7.17				0.026
1644	0.179	5.68				0.025
367	0.194	4.45				0.023
2	0.228	1.77				0.016

Table A 3.29.

Consolidation Data - Flockton Thin Seatearth (Remoulded).

Initial m/c	= 67.00%	Final m/c	= 17.94%
Initial Wet Density	= 1.72g/cm^3	Initial Dry Density	= 1.02g/cm^3
Final Bulk Density	= 2.13g/cm^3	Final Dry Density	= 1.81g/cm^3

Pressure (kN/m^2)	Voids R	Strain (%)	c_v (m^2/y)	m_v (m^2/MN)	k (m/s* 10^{-10})	C_c/C_s
20	1.609					
54	1.522	3.34	0.13	0.980	0.42117	-0.203
89	1.213	15.16	0.08	3.500	0.86811	-1.430
158	1.038	21.87	0.11	1.146	0.39080	-0.701
297	0.887	27.68	0.28	0.533	0.46262	-0.555
574	0.739	33.34	0.40	0.283	0.35117	-0.516
1128	0.632	37.45	0.56	0.111	0.19287	-0.365
2426	0.509	42.14	1.44	0.057	0.25491	-0.368
867	0.529	41.38				0.044
175	0.592	38.98				0.090
37	0.641	37.11				0.072
435	0.608	38.36	0.44	0.050	0.06823	-0.030
1214	0.548	40.65	0.69	0.048	0.10240	-0.134
2426	0.495	42.70	0.97	0.028	0.08490	-0.177
4675	0.411	45.91	0.62	0.025	0.04944	-0.293
9349	0.329	49.07	0.68	0.012	0.02711	-0.273
18697	0.247	52.20	0.52	0.006	0.01100	-0.271
34967	0.185	54.55	0.43	0.003	0.00420	-0.226
9347	0.230	52.83				0.078
1560	0.311	49.73				0.104
175	0.403	46.21				0.097
20	0.469	43.67				0.070

Table A 3.30.

Consolidation Data - Widdringham Roof (Undisturbed).

Initial m/c	= 3.94%	Final m/c	= 8.24%
Natural Bulk Density	= 2.32g/cm^3	Natural Dry Density	= 2.24g/cm^3
Final Bulk Density	= 2.49g/cm^3	Final Dry Density	= 2.31g/cm^3
Swell Percentage	= 0.00%	Swell Pressure	= 57.67kN/m^2

Pressure (kN/m^2)	Voids R	Strain (%)	c_v (m^2/y)	m_v (m^2/MN)	k (m/s* 10^{-10})	C_c/C_s
57	0.117					
203	0.112	0.42	22.37	0.029	2.02982	-0.008
349	0.108	0.76	74.63	0.024	5.70000	-0.015
641	0.102	1.33	54.33	0.019	3.12340	-0.024
1279	0.097	1.74	13.45	0.007	0.29653	-0.015
2556	0.090	2.37	5.91	0.005	0.09154	-0.023
4929	0.083	3.03	17.87	0.002	0.14992	-0.026
9855	0.073	3.89	70.38	0.001	0.40895	-0.032
19708	0.057	5.31	14.64	0.001	0.06862	-0.052
35033	0.041	6.76	24.00	0.001	0.07348	-0.064
18247	0.047	6.27				0.019
9125	0.054	5.65				0.023
1644	0.068	4.33				0.019
367	0.078	3.47				0.015
2	0.082	3.09				0.002

Table A3.31.

Consolidation Data - Widdringham Roof (Remoulded).

Initial m/c	= 43.00%	Final m/c	= 13.75%
Initial Wet Density	= 1.81g/cm^3	Initial Dry Density	= 1.26g/cm^3
Final Bulk Density	= 2.20g/cm^3	Final Dry Density	= 1.94g/cm^3

Pressure (kN/m^2)	Voids R	Strain (%)	c_v (m^2/y)	m_v (m^2/MN)	k (m/s* 10^{-10})	C_c/C_s
20	0.974					
54	0.875	5.00	2.43	1.475	11.11603	-0.230
89	0.778	9.90	2.80	1.478	12.82988	-0.448
158	0.699	13.92	7.95	0.643	15.86904	-0.318
297	0.611	18.37	10.06	0.372	11.62071	-0.321
574	0.546	21.66	10.05	0.145	4.53809	-0.227
1128	0.480	25.02	8.41	0.077	2.00908	-0.226
2426	0.395	29.31	10.18	0.044	1.39631	-0.254
867	0.405	28.83				0.021
175	0.435	27.27				0.044
37	0.465	25.78				0.043
261	0.451	26.47	9.45	0.042	1.24998	-0.016
867	0.423	27.91	12.70	0.032	1.25369	-0.054
2426	0.383	29.90	13.68	0.018	0.76466	-0.088
4675	0.320	33.09	11.25	0.020	0.70619	-0.221
9349	0.252	36.57	6.08	0.011	0.20777	-0.228
18697	0.183	40.05	5.44	0.006	0.09944	-0.228
34967	0.130	42.75	4.13	0.002	0.03529	-0.195
9347	0.154	41.51				0.042
1560	0.195	39.45				0.052
175	0.248	36.75				0.056
20	0.286	34.81				0.041

Table A 3.32.

Consolidation Data - Yazoo Clay (Undisturbed).

Initial m/c	= 46.24%	Final m/c	= 56.15%
Natural Bulk Density	= 1.80g/cm^3	Natural Dry Density	= 1.23g/cm^3
Final Bulk Density	= 1.88g/cm^3	Final Dry Density	= 1.20g/cm^3
Swell Percentage	= 2.28%	Swell Pressure	= 85.91kN/m^2

Pressure (kN/m^2)	Voids R	Strain (%)	c_v (m^2/y)	m_v (m^2/MN)	k (m/s* 10^{-10})	C_c/C_s
85	1.217					
150	1.209	0.33	4.94	0.055	0.85015	-0.029
215	1.195	0.96	8.95	0.097	2.70553	-0.090
347	1.174	1.93	2.49	0.072	0.55946	-0.103
610	1.125	4.11	0.14	0.085	0.03716	-0.197
1152	1.058	7.13	0.09	0.058	0.01623	-0.242
2302	0.966	11.30	0.10	0.039	0.01205	-0.307
4437	0.803	18.64	0.06	0.039	0.00722	-0.571
8873	0.616	27.06	0.03	0.023	0.00217	-0.620
17743	0.462	34.01	0.02	0.010	0.00066	-0.512
33181	0.342	39.44	0.01	0.005	0.00016	-0.442
8873	0.440	35.00				0.171
1480	0.605	27.57				0.212
331	0.766	20.34				0.246
2	1.267	-2.28				0.244

Table A 3.33.

Consolidation Data - Yazoo Clay (Remoulded).

Initial m/c	=117.00%	Final m/c	= 31.76%
Initial Wet Density	= 1.40g/cm^3	Initial Dry Density	= 0.65g/cm^3
Final Bulk Density	= 1.91g/cm^3	Final Dry Density	= 1.44g/cm^3

Pressure (kN/m^2)	Voids R	Strain (%)	c_v (m^2/y)	m_v (m^2/MN)	k (m/s* 10^{-10})	C_c/C_s
20	3.215					
54	2.969	5.84	0.15	1.716	0.78914	-0.578
89	2.461	17.90	0.10	3.656	1.13366	-2.358
158	2.069	27.20	0.09	1.641	0.45796	-1.569
297	1.606	38.18	0.10	1.085	0.33640	-1.699
574	1.342	44.45	0.11	0.365	0.12473	-0.923
1128	1.072	50.83	0.07	0.208	0.04517	-0.917
2426	0.853	56.04	0.05	0.081	0.01262	-0.659
867	0.905	54.81				0.115
175	1.041	51.57				0.197
37	1.147	49.06				0.157
435	1.087	50.49	0.04	0.069	0.00868	-0.056
1214	0.947	53.81	0.04	0.086	0.01061	-0.314
2426	0.832	56.54	0.04	0.049	0.00606	-0.382
4675	0.694	59.80	0.04	0.034	0.00419	-0.482
9349	0.549	63.25	0.04	0.018	0.00224	-0.483
18697	0.422	66.27	0.03	0.009	0.00100	-0.423
34967	0.330	68.44	0.03	0.004	0.00035	-0.336
9347	0.420	66.31				0.156
1560	0.589	62.29				0.218
175	0.743	58.65				0.162
20	0.886	55.26				0.152

Table A 3.34.

Consolidation Data - Kincaid Shale 6m (Undisturbed).

Initial m/c	= 21.00%	Final m/c	= 28.62%
Natural Bulk Density	= 1.98g/cm^3	Natural Dry Density	= 1.63g/cm^3
Final Bulk Density	= 2.02g/cm^3	Final Dry Density	= 1.57g/cm^3
Swell Percentage	= 4.27%	Swell Pressure	=131.41kN/m^2

Pressure (kN/m^2)	Voids R	Strain (%)	c_v (m^2/y)	m_v (m^2/MN)	k (m/s* 10^{-10})	C_c/C_s
131	0.654					
200	0.650	0.21	27.87	0.036	3.11851	-0.019
265	0.645	0.54	9.59	0.046	1.38596	-0.044
412	0.634	1.17	5.67	0.043	0.79956	-0.054
660	0.620	2.05	5.59	0.043	0.59868	-0.070
1152	0.598	3.35	26.44	0.027	2.26237	-0.089
2302	0.557	5.82	12.97	0.022	0.89703	-0.136
4437	0.516	8.30	2.51	0.012	0.09596	-0.144
8873	0.461	11.62	2.21	0.008	0.05603	-0.182
17743	0.387	16.10	0.63	0.005	0.01115	-0.246
33184	0.316	20.40	0.47	0.003	0.00482	-0.261
8873	0.343	18.80				0.046
1480	0.412	14.58				0.089
331	0.481	10.45				0.105
2	0.724	-4.27				0.118

Table A 3.35.

Consolidation Data - Kincaid Shale 6m (Remoulded).

Initial m/c	= 72.00%	Final m/c	= 17.04%
Initial Wet Density	= 1.53g/cm^3	Initial Dry Density	= 0.89g/cm^3
Final Bulk Density	= 2.15g/cm^3	Final Dry Density	= 1.83g/cm^3

Pressure (kN/m^2)	Voids R	Strain (%)	c_v (m^2/y)	m_v (m^2/MN)	k (m/s* 10^{-10})	C_c/C_s
20	2.037					
54	2.008	0.96	2.45	0.281	2.13419	-0.067
89	1.811	7.43	0.31	1.877	1.79821	-0.912
158	1.543	16.27	0.26	1.384	1.11367	-1.074
297	1.123	30.10	0.17	1.188	0.62610	-1.541
574	0.915	36.92	0.19	0.353	0.20800	-0.724
1128	0.731	42.99	0.19	0.173	0.10219	-0.628
2426	0.576	48.11	0.17	0.069	0.03636	-0.468
867	0.582	47.88				0.015
175	0.609	47.02				0.037
37	0.639	46.02				0.045
435	0.630	46.31	0.43	0.013	0.01808	-0.008
1214	0.593	47.54	0.22	0.029	0.01985	-0.084
2426	0.547	49.05	0.31	0.024	0.02282	-0.153
4675	0.469	51.61	0.17	0.022	0.01187	-0.273
9349	0.394	54.10	0.14	0.011	0.00498	-0.251
18697	0.321	56.48	0.12	0.006	0.00211	-0.240
34967	0.261	58.45	0.09	0.002	0.00078	-0.220
9347	0.302	57.13				0.070
1560	0.374	54.74				0.093
175	0.436	52.69				0.065
20	0.473	51.48				0.039

Table A 3.36.

Consolidation Data - Kincaid Shale 8m (Undisturbed).

Initial m/c	= 18.94%	Final m/c	= 23.00%
Natural Bulk Density	= 1.96g/cm^3	Natural Dry Density	= 1.65g/cm^3
Final Bulk Density	= 2.12g/cm^3	Final Dry Density	= 1.72g/cm^3
Swell Percentage	= 0.00%	Swell Pressure	= 51.98kN/m^2

Pressure (kN/m^2)	Voids R	Strain (%)	c_v (m^2/y)	m_v (m^2/MN)	k (m/s* 10^{-10})	C_c/C_s
52	0.613					
117	0.606	0.47	73.35	0.065	14.95138	-0.021
183	0.601	0.75	72.80	0.047	10.64566	-0.024
314	0.591	1.35	25.98	0.047	3.84005	-0.041
577	0.576	2.33	71.01	0.036	7.89125	-0.060
1152	0.552	3.77	17.31	0.026	1.42116	-0.077
2302	0.531	5.08	67.32	0.011	2.43547	-0.070
4437	0.505	6.69	29.01	0.007	0.71532	-0.091
8873	0.455	9.79	89.36	0.007	2.07465	-0.166
17743	0.388	13.93	57.25	0.005	0.92134	-0.222
33184	0.304	19.18	37.70	0.004	0.45814	-0.311
8873	0.321	18.11				0.030
1480	0.347	16.53				0.033
331	0.373	14.88				0.041
2	0.541	4.45				0.082

Table A 3.37.

Consolidation Data - Kincaid Shale 8m (Remoulded).

Initial m/c	= 59.00%	Final m/c	= 14.01%
Initial Wet Density	= 1.65g/cm^3	Initial Dry Density	= 1.04g/cm^3
Final Bulk Density	= 2.21g/cm^3	Final Dry Density	= 1.94g/cm^3

Pressure (kN/m^2)	Voids R	Strain (%)	c_v (m^2/y)	m_v (m^2/MN)	k (m/s* 10^{-10})	C_c/C_s
20	1.554					
54	1.531	0.88	3.07	0.264	2.52070	-0.052
89	1.445	4.25	1.09	0.970	3.28037	-0.399
158	1.180	14.64	0.52	1.572	2.53214	-1.061
297	0.867	26.89	0.36	1.032	1.25271	-1.148
574	0.688	33.90	0.44	0.346	0.47212	-0.625
1128	0.585	37.92	0.61	0.110	0.20825	-0.350
2426	0.490	41.65	0.69	0.046	0.09872	-0.286
867	0.492	41.59				0.003
175	0.498	41.34				0.009
37	0.511	40.84				0.019
435	0.509	40.90	6.77	0.002	0.06915	-0.001
1214	0.494	41.50	1.07	0.011	0.03683	-0.033
2426	0.472	42.36	2.26	0.012	0.08518	-0.073
4675	0.407	44.89	0.53	0.019	0.03228	-0.227
9349	0.338	47.61	0.89	0.010	0.03000	-0.230
18697	0.272	50.17	0.81	0.005	0.01347	-0.217
34967	0.214	52.45	0.26	0.002	0.00232	-0.214
9347	0.235	51.63				0.036
1560	0.274	50.09				0.050
175	0.309	48.75				0.036
20	0.367	46.45				0.062

Table A.3.38.

Consolidation Data - Nacimiento Shale, N1 (Undisturbed).

Initial m/c	= 7.19%	Final m/c	= 11.25%
Natural Bulk Density	= 2.28g/cm^3	Natural Dry Density	= 2.13g/cm^3
Final Bulk Density	= 2.32g/cm^3	Final Dry Density	= 2.09g/cm^3
Swell Percentage	= 1.75%	Swell Pressure	=398.48kN/m^2

Pressure (kN/m^2)	Voids R	Strain (%)	c_v (m^2/y)	m_v (m^2/MN)	$(m/s^{*}10^{-10})$	C_c/C_s
1398	0.263					
2959	0.253	0.74	28.85	0.005	0.45362	-0.029
4437	0.245	1.37	35.12	0.004	0.47023	-0.045
8873	0.230	2.59	27.92	0.002	0.23507	-0.051
17740	0.212	3.98	18.88	0.001	0.09659	-0.058
33184	0.194	5.42	9.13	0.001	0.02721	-0.067
8873	0.212	4.02				0.030
1480	0.234	2.29				0.028
331	0.257	0.47				0.035
2	0.285	-1.75				0.013

Table A 3.39.

Consolidation Data - Nacimiento Shale, N1 (Remoulded).

Initial m/c	= 37.00%	Final m/c	= 14.13%
Initial Wet Density	= 1.71g/cm^3	Initial Dry Density	= 1.24 g/cm^3
Final Bulk Density	= 2.24g/cm^3	Final Dry Density	= 1.96g/cm^3

Pressure (kN/m^2)	Voids R	Strain (%)	c_v (m^2/y)	m_v (m^2/MN)	$(m/s^{*}10^{-10})$	C_c/C_s
20	1.157					
54	1.113	2.05	1.19	0.599	2.21322	-0.102
89	0.977	8.33	1.28	1.838	7.29691	-0.629
158	0.880	12.85	2.36	0.711	5.20224	-0.389
297	0.782	17.35	3.33	0.375	3.87730	-0.356
574	0.696	21.34	3.71	0.174	2.00380	-0.300
1128	0.609	25.37	5.54	0.092	1.59021	-0.297
2426	0.509	30.03	4.93	0.048	0.73114	-0.302
867	0.519	29.61				0.020
175	0.544	28.38				0.038
37	0.573	27.08				0.042
435	0.555	27.87	4.32	0.028	0.37497	-0.016
1214	0.527	29.17	9.45	0.023	0.67712	-0.063
2426	0.495	30.66	11.22	0.017	0.60139	-0.107
4675	0.426	33.88	3.77	0.021	0.23980	-0.243
9349	0.340	37.85	3.38	0.013	0.13511	-0.284
18697	0.263	41.43	1.17	0.006	0.02226	-0.257
34967	0.203	44.20	0.26	0.002	0.00242	-0.219
9347	0.233	42.83				0.051
1560	0.282	40.55				0.063
175	0.337	38.02				0.057
20	0.368	36.55				0.034

Table A 3.40.

Consolidation Data - Nacimiento Shale, N2 (Undisturbed).

Initial m/c	= 5.85%	Final m/c	= 12.81%
Natural Bulk Density	= 2.22g/cm^3	Natural Dry Density	= 2.10g/cm^3
Final Bulk Density	= 2.34g/cm^3	Final Dry Density	= 2.08g/cm^3
Swell Percentage	= 0.91%	Swell Pressure	=983.64kN/m^2

Pressure (kN/m^2)	Voids R	Strain (%)	c_v (m^2/y)	m_v (m^2/MN)	k (m/s$*10^{-10}$)	C_c/C_s
983	0.270					
1234	0.267	0.24	35.62	0.009	1.03919	-0.030
2302	0.256	1.14	28.52	0.008	0.71870	-0.042
4437	0.241	2.32	56.99	0.005	0.98823	-0.052
8873	0.229	3.23	5.64	0.002	0.03811	-0.038
17740	0.218	4.10	18.64	0.001	0.05832	-0.037
33184	0.202	5.40	32.39	0.001	0.08538	-0.060
8873	0.214	4.44				0.021
1480	0.234	2.89				0.025
331	0.256	1.13				0.034
2	0.282	-0.91				0.012

Table A 3.41.

Consolidation Data - Nacimiento Shale, N2 (Remoulded).

Initial m/c	= 39.00%	Final m/c	= 13.53%
Initial Wet Density	= 1.75g/cm^3	Initial Dry Density	= 1.26g/cm^3
Final Bulk Density	= 2.24g/cm^3	Final Dry Density	= 1.97g/cm^3

Pressure (kN/m^2)	Voids R	Strain (%)	c_v (m^2/y)	m_v (m^2/MN)	k (m/s$*10^{-10}$)	C_c/C_s
20	1.112					
54	1.047	3.07	0.29	0.904	0.81376	-0.151
89	0.966	6.92	0.43	1.130	1.50703	-0.377
158	0.849	12.46	0.65	0.877	1.76763	-0.478
297	0.725	18.33	0.97	0.480	1.45079	-0.454
574	0.636	22.56	1.30	0.186	0.75067	-0.313
1128	0.555	26.38	1.34	0.089	0.37128	-0.275
2426	0.465	30.65	1.51	0.045	0.20874	-0.271
867	0.469	30.44				0.019
175	0.486	29.62				0.025
37	0.510	28.52				0.034
435	0.496	29.19	1.28	0.023	0.09152	-0.013
1214	0.476	30.10	2.83	0.017	0.15050	-0.043
2426	0.455	31.11	3.08	0.011	0.11205	-0.071
4675	0.396	33.91	0.93	0.018	0.05193	-0.207
9349	0.320	37.47	0.53	0.011	0.01911	-0.250
18697	0.255	40.59	0.39	0.005	0.00662	-0.219
34967	0.195	43.42	0.28	0.002	0.00261	-0.219
9347	0.219	42.28				0.041
1560	0.253	40.67				0.044
175	0.296	38.64				0.045
20	0.348	36.16				0.056

Table A 3.42.

Consolidation Data - Nacimiento Shale, N3 (Undisturbed).

Initial m/c	= 16.63%	Final m/c	= 25.74%
Natural Bulk Density	= 2.09g/cm^3	Natural Dry Density	= 1.79g/cm^3
Final Bulk Density	= 2.10g/cm^3	Final Dry Density	= 1.67g/cm^3
Swell Percentage	= 7.24%	Swell Pressure	=677.66kN/m^2

Pressure (kN/m^2)	Voids R	Strain (%)	c_v (m^2/y)	m_v (m^2/MN)	k (m/s* 10^{-10})	C_c/C_s
677	0.538					
750	0.538					
820	0.537	0.04	31.49	0.009	0.90673	-0.009
969	0.534	0.24	38.79	0.013	1.57521	-0.043
1279	0.531	0.49	38.62	0.006	0.75527	-0.032
2556	0.512	1.67	6.99	0.009	0.21050	-0.060
4927	0.490	3.09	1.97	0.006	0.03746	-0.077
9853	0.459	5.15	0.83	0.004	0.01086	-0.105
19703	0.412	8.21	0.04	0.003	0.00031	-0.156
35025	0.372	10.79	0.04	0.001	0.00023	-0.159
18241	0.384	9.99				0.043
9120	0.404	8.68				0.067
1641	0.464	4.82				0.079
366	0.506	2.08				0.065
2	0.649	-7.24				0.068

Table A 3.43.

Consolidation Data - Nacimiento Shale, N3 (Remoulded).

Initial m/c	= 93.00%	Final m/c	= 22.85%
Initial Wet Density	= 1.50g/cm^3	Initial Dry Density	= 0.77g/cm^3
Final Bulk Density	= 2.06g/cm^3	Final Dry Density	= 1.67g/cm^3

Pressure (kN/m^2)	Voids R	Strain (%)	c_v (m^2/y)	m_v (m^2/MN)	k (m/s* 10^{-10})	C_c/C_s
20	2.548					
54	2.443	2.97	1.62	0.870	4.37219	-0.245
89	1.890	18.55	0.68	4.589	9.67368	-2.564
158	1.550	28.13	0.60	1.705	3.17135	-1.360
297	1.302	35.11	0.44	0.699	0.95438	-0.909
574	1.108	40.60	0.68	0.304	0.64139	-0.681
1128	0.920	45.89	0.48	0.161	0.23957	-0.640
2426	0.764	50.28	0.28	0.062	0.05433	-0.467
867	0.789	49.57				0.056
175	0.857	47.66				0.097
37	0.916	45.99				0.088
435	0.881	46.99	0.16	0.045	0.02253	-0.033
1214	0.811	48.96	0.19	0.048	0.02813	-0.157
2426	0.746	50.79	0.24	0.030	0.02200	-0.216
4675	0.639	53.80	0.16	0.027	0.01358	-0.374
9349	0.514	57.32	0.19	0.016	0.00961	-0.415
18697	0.407	60.34	0.07	0.007	0.00162	-0.356
34967	0.321	62.76	0.06	0.003	0.00072	-0.316
9347	0.390	60.81				0.121
1560	0.496	57.83				0.135
175	0.588	55.25				0.096
37	0.643	53.69				0.083

Table A 3.44.

Consolidation Data - Fox Hills Shale (Undisturbed).

Initial m/c	= 30.78%	Final m/c	= 34.06%
Natural Bulk Density	= 1.77g/cm^3	Natural Dry Density	= 1.36g/cm^3
Final Bulk Density	= 1.78g/cm^3	Final Dry Density	= 1.32g/cm^2
Swell Percentage	= 2.31%	Swell Pressure	=641.38kN/m^2

Pressure (kN/m^2)	Voids R	Strain (%)	c_v (m^2/y)	m_v (m^2/MN)	k (m/s* 10^{-10})	C_c/C_s
641	0.885					
713	0.884	0.05				
787	0.884	0.05				
933	0.879	0.30	28.99	0.018	1.63359	-0.060
1224	0.867	0.93	28.74	0.021	1.95528	-0.100
1809	0.848	1.96	25.64	0.017	1.38508	-0.114
2611	0.816	3.64	8.47	0.021	0.56620	-0.198
4928	0.748	7.28	0.80	0.016	0.04007	-0.249
9853	0.649	12.51	0.13	0.011	0.00463	-0.328
19703	0.530	18.82	0.06	0.007	0.00136	-0.395
35025	0.430	24.12	0.11	0.004	0.00148	-0.399
18025	0.448	23.19				0.061
8208	0.492	20.85				0.128
1641	0.597	15.28				0.151
366	0.682	10.75				0.131
2	0.929	-2.31				0.117

Table A 3.45.

Consolidation Data - Fox Hills Shale (Remoulded).

Initial m/c	= 62.00%	Final m/c	= 62.00%
Initial Wet Density	= 1.56g/cm^3	Initial Dry Density	= 0.96g/cm^3
Final Bulk Density	= 1.96g/cm^3	Final Dry Density	= 1.55g/cm^3

Pressure (kN/m^2)	Voids R	Strain (%)	c_v (m^2/y)	m_v (m^2/MN)	k (m/s* 10^{-10})	C_c/C_s
20	1.659					
54	1.563	3.63	0.42	1.061	1.38253	-0.224
89	1.418	9.06	0.69	1.616	3.45746	-0.671
158	1.308	13.21	1.03	0.659	2.10519	-0.441
297	1.181	17.97	1.23	0.895	1.50948	-0.465
574	1.071	22.12	1.25	0.182	0.70557	-0.385
1128	0.940	27.04	0.98	0.114	0.34690	-0.445
2426	0.803	32.21	0.80	0.054	0.13495	-0.413
867	0.824	31.41				0.047
175	0.879	29.34				0.079
37	0.930	27.42				0.076
435	0.899	28.60	0.95	0.039	0.11768	-0.029
1214	0.843	30.68	0.91	0.037	0.10675	-0.124
2426	0.779	33.10	0.80	0.029	0.07103	-0.214
4675	0.671	37.17	0.36	0.027	0.03011	-0.380
9349	0.554	41.57	0.22	0.015	0.01024	-0.388
18697	0.444	45.70	0.09	0.007	0.00228	-0.365
34967	0.346	49.39	0.05	0.004	0.00071	-0.360
9347	0.403	47.24				0.100
1560	0.496	43.75				0.119
175	0.570	40.94				0.078
20	0.655	37.77				0.090

Table A 3.46.

Consolidation Data - Dawson Shale (Undisturbed).

Initial m/c	= 14.02%	Final m/c	= 25.32%
Natural Bulk Density	= 2.17g/cm^3	Natural Dry Density	= 1.91g/cm^3
Final Bulk Density	= 2.12g/cm^3	Final Dry Density	= 1.69g/cm^3
Swell Percentage	= 12.89%	Swell Pressure	=623.14kN/m^2

Pressure (kN/m^2)	Voids R	Strain (%)	c_v (m^2/y)	m_v (m^2/MN)	k (m/s* 10^{-10})	C_c/C_s
623	0.370					
732	0.369	0.10	8.86	0.007	0.18392	-0.019
914	0.365	0.35	35.34	0.016	1.75877	-0.035
1206	0.362	0.61	4.94	0.007	0.11526	-0.029
1827	0.352	1.32	1.00	0.011	0.03666	-0.054
2556	0.344	1.89	0.70	0.008	0.01761	-0.054
4928	0.324	3.37	0.40	0.006	0.00777	-0.071
9853	0.298	5.27	0.33	0.004	0.00407	-0.086
19704	0.252	8.59	0.07	0.003	0.00078	-0.151
35025	0.208	11.80	0.04	0.002	0.00028	-0.176
18241	0.217	11.14				0.032
9120	0.234	9.96				0.054
1644	0.274	6.98				0.055
367	0.324	3.36				0.076
2	0.547	-12.88				0.106

Table A 3.47.

Consolidation Data - Dawson Shale (Remoulded).

Initial m/c	= 75.00%	Final m/c	= 19.77%
Initial Wet Density	= 1.59g/cm^3	Initial Dry Density	= 0.91g/cm^3
Final Bulk Density	= 2.09g/cm^3	Final Dry Density	= 1.74g/cm^3

Pressure (kN/m^2)	Voids R	Strain (%)	c_v (m^2/y)	m_v (m^2/MN)	k (m/s* 10^{-10})	C_c/C_s
20	1.871					
54	1.809	2.16	1.25	0.635	2.46127	-0.144
89	1.519	12.27	0.56	2.949	5.12070	-1.347
158	1.231	22.29	0.35	1.656	1.79787	-1.150
297	0.988	30.75	0.29	0.783	0.70446	-0.892
574	0.813	36.85	0.23	0.317	0.22658	-0.612
1128	0.668	41.90	0.22	0.144	0.09841	-0.494
2426	0.540	46.36	0.16	0.063	0.02452	-0.384
867	0.554	45.86				0.032
175	0.612	43.83				0.084
37	0.667	41.93				0.081
435	0.634	43.07	0.12	0.049	0.01836	-0.030
1214	0.578	45.02	0.12	0.044	0.01692	-0.126
2426	0.530	46.72	0.16	0.025	0.01287	-0.161
4675	0.453	49.39	0.13	0.022	0.00934	-0.269
9349	0.365	52.45	0.07	0.013	0.00295	-0.292
18697	0.289	55.10	0.05	0.006	0.00097	-0.253
34967	0.219	57.54	0.06	0.003	0.00063	-0.257
9347	0.268	55.83				0.085
1560	0.321	53.97				0.069
175	0.437	49.93				0.122
20	0.500	47.74				0.067

Table A 3.48.

Consolidation Data - Pierre Shale, Dakota (Undisturbed).

Initial m/c	= 29.52%	Final m/c	= 36.53%
Natural Bulk Density	= 1.92g/cm^3	Natural Dry Density	= 1.48g/cm^3
Final Bulk Density	= 1.98g/cm^3	Final Dry Density	= 1.45g/cm^3
Swell Percentage	= 1.84%	Swell Pressure	=127.69kN/m^3

Pressure (kN/m^2)	Voids R	Strain (%)	c_v (m^2/y)	m_v (m^2/MN)	k (m/s* 10^{-10})	C_c/C_s
127	0.780					
203	0.776	0.17	28.52	0.029	2.61419	-0.015
276	0.769	0.57	21.44	0.054	3.58854	-0.053
422	0.756	1.34	21.19	0.050	3.30639	-0.073
732	0.736	2.42	3.27	0.036	0.37243	-0.081
1316	0.709	3.97	0.99	0.027	0.08175	-0.108
2556	0.674	5.93	0.27	0.016	0.01382	-0.121
4928	0.633	8.23	0.23	0.010	0.00737	-0.143
9853	0.579	11.29	0.21	0.006	0.00437	-0.181
19703	0.484	16.61	0.21	0.006	0.00227	-0.315
35025	0.390	21.87	0.08	0.004	0.00105	-0.374
18241	0.411	20.72				0.072
9120	0.454	18.31				0.142
1641	0.567	11.94				0.152
366	0.658	6.82				0.140
2	0.812	-1.84				0.073

Table A 3.49.

Consolidation Data - Pierre Shale, Dakota (Remoulded).

Initial m/c	=135.00%	Final m/c	= 35.51%
Initial Wet Density	= 1.34g/cm^3	Initial Dry Density	= 0.57g/cm^3
Final Bulk Density	= 1.87g/cm^3	Final Dry Density	= 1.38g/cm^3

Pressure (kN/m^2)	Voids R	Strain (%)	c_v (m^2/y)	m_v (m^2/MN)	k (m/s* 10^{-10})	C_c/C_s
20	3.616					
54	3.514	2.22	18.65	0.649	37.57473	-0.238
89	2.842	16.77	0.05	4.253	0.65921	-3.117
158	2.427	25.76	0.04	1.565	0.19412	-1.660
297	1.806	39.21	0.03	1.303	0.12120	-2.279
574	1.399	48.03	0.04	0.523	0.06498	-1.423
1128	1.101	54.48	0.04	0.224	0.02782	-1.015
2426	0.860	59.69	0.04	0.088	0.01099	-0.723
867	0.898	58.88				0.083
175	1.040	55.79				0.205
37	1.204	52.25				0.244
435	1.102	54.45	0.03	0.115	0.01079	-0.095
1214	0.935	58.07	0.03	0.106	0.01117	-0.375
2426	0.828	60.39	0.06	0.047	0.00844	-0.356
4675	0.678	63.65	0.04	0.038	0.00548	-0.527
9349	0.539	66.65	0.04	0.018	0.00229	-0.459
18697	0.414	69.37	0.05	0.009	0.00148	-0.417
34967	0.315	71.51	0.04	0.004	0.00060	-0.363
8657	0.393	69.83				0.128
1560	0.544	66.54				0.204
175	0.702	63.13				0.166
20	0.908	58.65				0.220

Table A 3.50.

Consolidation Data - Pierre Shale, Colorado (Undisturbed).

Initial m/c	= 13.04%	Final m/c	= 13.04%
Natural Bulk Density	= 2.39g/cm^3	Natural Dry Density	= 2.11g/cm^3
Final Bulk Density	= 2.32g/cm^3	Final Dry Density	= 2.13g/cm^3
Swell Percentage	= 0.00%	Swell Pressure	= 72.96kN/m^2

Pressure (kN/m^2)	Voids R	Strain (%)	c_v (m^2/y)	m_v (m^2/MN)	k (m/s*10^{-10})	C_c/C_s
72	0.262					
148	0.259	0.21	29.20	0.031	2.83134	-0.008
221	0.253	0.67	59.21	0.065	11.98283	-0.033
367	0.245	1.27	9.93	0.043	1.34616	-0.034
659	0.237	1.97	34.97	0.022	2.35558	-0.035
1279	0.227	2.75	6.97	0.013	0.28172	-0.034
2556	0.216	3.60	19.05	0.007	0.41458	-0.035
4929	0.206	4.37	13.76	0.003	0.14782	-0.034
9855	0.195	5.31	3.92	0.002	0.02250	-0.039
17518	0.178	6.60	17.97	0.002	0.10341	-0.065
35033	0.151	8.72	30.80	0.001	0.12494	-0.089
18247	0.158	8.22				0.022
9125	0.168	7.40				0.034
1644	0.193	5.43				0.033
367	0.210	4.07				0.026
2	0.247	1.11				0.018

Table A 3.51.

Consolidation Data - Pierre Shale, Colorado (Remoulded).

Initial m/c	= 62.00%	Final m/c	= 15.66%
Initial Wet Density	= 1.64g/cm^3	Initial Dry Density	= 1.01g/cm^3
Final Bulk Density	= 2.20g/cm^3	Final Dry Density	= 1.90g/cm^3

Pressure (kN/m^2)	Voids R	Strain (%)	c_v (m^2/y)	m_v (m^2/MN)	k (m/s*10^{-10})	C_c/C_s
20	1.628					
54	1.482	5.56	0.070	1.639	0.35456	-0.340
89	1.172	17.37	0.098	3.568	1.08415	-1.440
158	0.948	25.86	0.104	1.494	0.48181	-0.893
297	0.772	32.56	0.208	0.649	0.41913	-0.646
574	0.662	36.77	0.301	0.224	0.20915	-0.386
1128	0.559	40.70	0.340	0.111	0.11796	-0.352
2426	0.457	44.56	0.387	0.051	0.06044	-0.305
867	0.466	44.20				0.021
175	0.501	42.90				0.049
37	0.540	41.41				0.058
435	0.513	42.44	0.292	0.044	0.03947	-0.025
1214	0.479	43.72	0.580	0.029	0.05181	-0.075
2426	0.447	44.92	0.841	0.017	0.04640	-0.105
4675	0.380	47.48	0.359	0.021	0.02287	-0.235
9349	0.299	50.56	0.416	0.012	0.01657	-0.269
18697	0.235	53.02	0.339	0.005	0.00558	-0.215
34967	0.171	55.44	0.218	0.003	0.00209	-0.233
9347	0.203	54.22				0.055
1560	0.258	52.12				0.071
175	0.328	49.47				0.073
20	0.399	46.77				0.075

Table A 3.52.

Consolidation Data - London Clay 37m (Liquid Limit, 50mm Cell).

Initial m/c = 65.00% Final m/c = 28.46%
Initial Wet Density = 1.56g/cm^3 Initial Dry Density = 0.94g/cm^3
Final Bulk Density = 1.96g/cm^3 Final Dry Density = 1.53g/cm^3

Pressure (kN/m^2)	Voids R	Strain (%)	c_v (m^2/y)	m_v (m^2/MN)	k (m/s* 10^{-10})	C_c/C_s
2	1.875					
11	1.577	10.39	0.52	11.516	18.56525	-0.384
21	1.477	13.87	1.05	3.880	12.63095	-0.380
41	1.379	17.26	1.56	1.978	9.56657	-0.347
80	1.268	21.13	1.07	1.196	3.96835	-0.383
158	1.116	26.39	1.16	0.859	3.08976	-0.511
394	0.932	32.79	1.07	0.368	1.22218	-0.466
786	0.787	37.85	1.02	0.191	0.60539	-0.485
1571	0.674	41.78	0.72	0.080	0.17979	-0.375
3502	0.536	46.58	0.55	0.042	0.07278	-0.397
8365	0.411	50.92	0.28	0.016	0.01452	-0.329
2802	0.450	49.55				0.083
700	0.526	46.91				0.126
196	0.600	44.34				0.134
2	0.779	38.13				0.089

Table A 3.53.

Consolidation Data - London Clay 37m (0.5 Liquidity Index, 50mm Cell).

Initial m/c = 45.00% Final m/c = 27.42%
Initial Wet Density = 1.64g/cm^3 Initial Dry Density = 1.13g/cm^3
Final Bulk Density = 1.96g/cm^3 Final Dry Density = 1.53g/cm^3

Pressure (kN/m^2)	Voids R	Strain (%)	c_v (m^2/y)	m_v (m^2/MN)	k (m/s* 10^{-10})	C_c/C_s
2	1.392					
21	1.347	1.90	1.34	0.990	4.11305	-0.044
41	1.288	4.37	0.30	1.256	1.16893	-0.210
80	1.204	7.87	0.35	0.941	1.02138	-0.288
158	1.073	13.34	0.38	0.762	0.89765	-0.443
394	0.901	20.53	0.45	0.357	0.49044	-0.435
786	0.779	25.64	0.43	0.163	0.21823	-0.408
1571	0.675	30.00	0.35	0.074	0.08080	-0.346
3502	0.548	35.29	0.31	0.039	0.03773	-0.364
8404	0.427	40.35	0.20	0.016	0.00988	-0.319
2801	0.460	38.96				0.070
700	0.532	35.94				0.120
196	0.604	32.92				0.130
21	0.689	29.37				0.088
2	0.766	26.17				0.074

Table A 3.54.

Consolidation Data - Fullers Earth, Bath (Liquid Limit, 50mm Cell).

Initial m/c	=105.00%	Final m/c	= 52.25%
Initial Wet Density	= 1.26g/cm^3	Initial Dry Density	= 0.61g/cm^3
Final Bulk Density	= 1.71g/cm^3	Final Dry Density	= 1.12g/cm^3

Pressure (kN/m^2)	Voids R	Strain (%)	c_v (m^2/y)	m_v (m^2/MN)	k (m/s* 10^{-10})	C_c/C_s
2	3.400					
11	2.889	11.63	0.39	12.900	15.60098	-0.657
21	2.741	14.97	0.23	3.805	2.71339	-0.559
41	2.488	20.73	0.40	3.381	4.19299	-0.902
80	2.205	27.16	0.35	2.080	2.28722	-0.974
158	1.913	33.80	0.31	1.168	1.11224	-0.997
394	1.551	42.01	0.18	0.526	0.29382	-0.909
786	1.324	47.19	0.09	0.227	0.06333	-0.759
1571	1.144	51.28	0.05	0.098	0.01529	-0.598
3502	0.947	55.76	0.03	0.047	0.00445	-0.567
8406	0.760	59.99	0.03	0.019	0.00183	-0.489
2802	0.841	58.16				0.169
786	0.972	55.18				0.237
198	1.080	52.73				0.180
2	1.404	45.37				0.161

Table A 3.55.

Consolidation Data - Fullers Earth, Bath (0.75 Liquidity Index, 50mm Cell).

Initial m/c	= 89.00%	Final m/c	= 47.80%
Initial Wet Density	= 1.36g/cm^3	Initial Dry Density	= 0.72g/cm^3
Final Bulk Density	= 1.77g/cm^3	Final Dry Density	= 1.19g/cm^3

Pressure (kN/m^2)	Voids R	Strain (%)	c_v (m^2/y)	m_v (m^2/MN)	k (m/s* 10^{-10})	C_c/C_s
2	2.745					
21	2.460	7.62	0.87	3.805	10.26228	-0.274
41	2.321	11.34	0.42	2.086	2.61527	-0.496
80	2.089	17.54	0.49	1.791	2.72089	-0.799
158	1.850	23.92	0.33	0.991	1.01475	-0.808
394	1.534	32.34	0.25	0.469	0.36411	-0.799
786	1.320	38.07	0.11	0.215	0.07346	-0.715
1571	1.142	42.81	0.06	0.097	0.01817	-0.591
3502	0.945	48.06	0.07	0.047	0.01033	-0.565
8407	0.729	53.83	0.05	0.022	0.00350	-0.568
2802	0.816	51.52				0.181
700	0.947	48.01				0.218
196	1.060	45.00				0.204
21	1.178	41.85				0.123
2	1.262	39.61				0.081

Table A 3.56.

Consolidation Data - Fullers Earth, Bath (0.5 Liquidity Index, 50mm Cell).

Initial m/c = 74.00% Final m/c = 47.33%
Initial Wet Density = 1.47g/cm^3 Initial Dry Density = 0.84g/cm^3
Final Bulk Density = 1.74g/cm^3 Final Dry Density = 1.18g/cm^3

Pressure (kN/m^2)	Voids R	Strain (%)	c_v (m^2/y)	m_v (m^2/MN)	k (m/s 10^{-10})	C_c/C_s
2	2.205					
41	2.140	2.03	30.94	0.520	49.87727	-0.049
80	2.037	5.25	13.03	0.841	33.97417	-0.355
158	1.865	10.62	0.19	0.726	0.42766	-0.583
394	1.544	20.64	0.13	0.474	0.19132	-0.813
786	1.326	27.45	0.06	0.218	0.04065	-0.727
1571	1.134	33.42	0.03	0.105	0.00977	-0.636
3502	0.945	39.31	0.03	0.046	0.00426	-0.542
8408	0.742	45.64	0.01	0.021	0.00066	-0.534
2802	0.815	43.37				0.153
700	0.965	38.71				0.248
196	1.050	36.04				0.155
21	1.179	32.02				0.134
2	1.288	28.61				0.105

Table A 3.57.

Consolidation Data - Fullers Earth, Bath (0.25 Liquidity Index, 50mm Cell).

Initial m/c = 59.00% Final m/c = 45.92%
Initial Wet Density = 1.58g/cm^3 Initial Dry Density = 0.99g/cm^3
Final Bulk Density = 1.77g/cm^3 Final Dry Density = 1.21g/cm^3

Pressure (kN/m^2)	Voids R	Strain (%)	c_v (m^2/y)	m_v (m^2/MN)	k (m/s 10^{-10})	C_c/C_s
2	1.710					
21	1.697	0.51	22.57	0.251	17.66500	-0.013
41	1.690	0.75	20.88	0.129	8.34991	-0.023
80	1.670	1.50	67.91	0.190	40.13362	-0.070
158	1.617	3.43	16.52	0.254	13.03291	-0.177
394	1.440	9.99	0.07	0.286	0.06218	-0.450
786	1.268	16.32	0.06	0.179	0.03344	-0.572
1571	1.093	22.77	0.05	0.098	0.01523	-0.582
3502	0.929	28.82	0.02	0.040	0.00251	-0.472
8406	0.750	35.44	0.02	0.019	0.00118	-0.471
2802	0.281	32.79				0.151
700	0.949	28.10				0.211
196	1.028	25.18				0.143
21	1.131	21.36				0.108
2	1.223	17.98				0.088

Table A 3.58.

Consolidation Data - Widdringham Roof (Liquid Limit, 50mm Cell).

Initial m/c	= 43.00%	Final m/c	= 23.00%
Initial Wet Density	= 1.65g/cm^3	Initial Dry Density	= 1.15g/cm^3
Final Bulk Density	= 1.98g/cm^3	Final Dry Density	= 1.61g/cm^3

Pressure (kN/m^2)	Voids R	Strain (%)	c_v (m^2/y)	m_v (m^2/MN)	k (m/s 10^{-10})	C_c/C_s
2	1.150					
11	0.975	8.17	0.73	9.041	20.46640	-0.226
21	0.921	10.64	0.69	2.734	5.84840	-0.201
41	0.867	13.15	2.06	1.405	8.97565	-0.192
80	0.798	16.39	2.65	0.947	7.78480	-0.239
159	0.731	19.50	4.44	0.471	6.49235	-0.229
394	0.621	24.61	6.15	0.270	5.15542	-0.276
786	0.560	27.43	8.45	0.096	2.51461	-0.202
1571	0.478	31.28	8.70	0.066	1.80592	-0.274
3502	0.392	35.23	7.77	0.030	0.72582	-0.244
8408	0.291	39.96	9.54	0.018	0.54964	-0.267
2802	0.322	38.53				0.064
786	0.352	37.11				0.055
198	0.403	34.75				0.087
21	0.481	31.12				0.081
2	0.539	28.41				0.056

Table A 3.59.

Consolidation Data - Widdringham Roof (0.5 Liquidity Index, 50mm Cell).

Initial m/c	= 33.00%	Final m/c	= 27.18%
Initial Wet Density	= 1.74g/cm^3	Initial Dry Density	= 1.31g/cm^3
Final Bulk Density	= 1.98g/cm^3	Final Dry Density	= 1.56g/cm^3

Pressure (kN/m^2)	Voids R	Strain (%)	c_v (m^2/y)	m_v (m^2/MN)	k (m/s 10^{-10})	C_c/C_s
2	0.903					
41	0.825	4.07	0.96	1.051	3.12769	-0.058
80	0.774	6.76	1.15	0.693	2.49061	-0.175
159	0.709	10.18	1.38	0.463	1.98414	-0.222
394	0.610	15.41	2.09	0.246	1.59710	-0.250
786	0.522	19.99	2.35	0.139	1.01578	-0.290
1571	0.445	24.04	2.74	0.064	0.54741	-0.256
3504	0.354	28.87	2.44	0.032	0.24668	-0.264
8406	0.246	34.51	3.19	0.016	0.16090	-0.283
2802	0.273	33.09				0.056
786	0.322	30.54				0.088
198	0.391	26.90				0.115
21	0.503	21.01				0.116
2	0.596	16.15				0.089

Table A 3.60.

Consolidation Data - Pierre Shale, Dakota (Liquid Limit, 50mm Cell).

Initial m/c = 136.00% Final m/c = 58.21%
Initial Wet Density = 1.28g/cm^3 Initial Dry Density = 0.54g/cm^3
Final Bulk Density = 1.65g/cm^3 Final Dry Density = 1.05g/cm^3

Pressure (kN/m^2)	Voids R	Strain (%)	c_v (m^2/y)	m_v (m^2/MN)	k (m/s* 10^{-10})	C_c/C_s
2	3.866					
11	3.216	13.35	0.10	14.842	4.54832	-0.835
21	3.019	17.40	0.08	4.672	1.25882	-0.749
41	2.728	23.38	0.09	3.620	1.01006	-1.035
80	2.404	30.04	0.10	2.119	0.65689	-1.114
159	1.972	38.92	0.12	1.606	0.59759	-1.461
394	1.477	49.10	0.09	0.708	0.19773	-1.255
786	1.179	55.22	0.07	0.307	0.06659	-0.992
1571	0.925	60.43	0.07	0.148	0.03222	-0.843
3502	0.692	65.23	0.05	0.062	0.00971	-0.671
8365	0.490	69.38	0.09	0.024	0.00684	-0.533
2802	0.566	67.82				0.159
700	0.709	64.88				0.238
196	0.866	61.64				0.285
2	1.522	48.17				0.328

Table 3.61.

Consolidation Data - Pierre Shale, Dakota (0.5 Liquidity Index, 50mm Cell).

Initial m/c = 82.00% Final m/c = 50.98%
Initial Wet Density = 1.41g/cm^3 Initial Dry Density = 0.77g/cm^3
Final Bulk Density = 1.72g/cm^3 Final Dry Density = 1.13g/cm^3

Pressure (kN/m^2)	Voids R	Strain (%)	c_v (m^2/y)	m_v (m^2/MN)	k (m/s* 10^{-10})	C_c/C_s
2	2.397					
21	1.230	2.27	2.38	1.193	8.80197	-0.073
41	2.239	4.65	0.18	1.219	0.68069	-0.288
80	2.095	8.90	0.17	1.139	0.60075	-0.496
159	1.837	16.48	0.15	1.105	0.49066	-0.871
394	1.447	27.96	0.17	0.584	0.30828	-0.988
786	1.195	35.40	0.10	0.262	0.08144	-0.842
1571	0.964	42.20	0.10	0.134	0.04155	-0.768
3504	0.736	48.91	0.12	0.060	0.02236	-0.654
8365	0.533	54.86	0.15	0.024	0.01118	-0.534
2802	0.596	53.03				0.130
700	0.731	49.04				0.225
196	0.870	44.96				0.250
21	1.014	40.71				0.150
2	1.318	31.76				0.291

Table A 3.62.

Consolidation Data - London Clay 37m (Remoulded, Teflon Cell).

Initial m/c	= 65.00%	Final m/c	= 22.17%
Initial Wet Density	= 1.64g/cm^3	Initial Dry Density	= 0.99g/cm^3
Final Bulk Density	= 2.17g/cm^3	Final Dry Density	= 1.78g/cm^3

Pressure (kN/m^2)	Voids R	Strain (%)	c_v (m^2/y)	C_c/C_s
20	1.736			
54	1.713	0.81	1.88	-0.051
89	1.456	10.22	0.61	-1.195
158	1.208	19.29	0.65	-0.993
297	1.033	25.66	0.64	-0.639
574	0.884	31.11	0.54	-0.520
1128	0.743	36.29	0.47	-0.483
2426	0.615	40.94	0.45	-0.383
4675	0.511	44.75	0.52	-0.365
867	0.564	42.82		0.072
294	0.632	40.34		0.144
37	0.739	36.41		0.120
349	0.696	38.00	0.37	-0.045
1560	0.567	42.70	0.28	-0.197
4675	0.474	46.12	0.35	-0.196
9349	0.389	49.23	0.31	-0.282
18697	0.283	53.08	0.65	-0.350
34967	0.150	57.94	0.37	-0.488
17315	0.167	57.33		0.054
8659	0.185	56.67		0.060
1560	0.272	53.48		0.117
349	0.378	49.63		0.162
2	0.527	44.19		0.071

Table A 3.63.

Consolidation Data - Oxford Clay 44m (Remoulded, Teflon Cell).

Initial m/c	= 57.00%	Final m/c	= 22.40%
Initial Wet Density	= 1.66g/cm^3	Initial Dry Density	= 1.06g/cm^3
Final Bulk Density	= 2.05g/cm^3	Final Dry Density	= 1.67g/cm^3

Pressure (kN/m^2)	Voids R	Strain (%)	c_v (m^2/y)	C_c/C_s
20	1.389			
54	1.254	5.64	2.38	e0.313
89	1.120	11.27	1.93	-0.624
158	0.982	17.03	3.65	-0.550
297	0.870	21.70	4.29	-0.410
574	0.706	28.60	2.44	-0.576
1128	0.591	33.40	3.68	-0.390
2426	0.477	38.17	2.04	-0.343
867	0.504	37.05		0.059
209	0.570	34.30		0.106
37	0.646	31.10		0.102
258	0.616	32.34	1.60	-0.035
867	0.548	35.22	1.51	-0.130
2426	0.468	38.53	2.26	-0.177
4675	0.376	42.39	1.75	-0.323
9349	0.292	45.93	1.07	-0.280
18697	0.193	50.07	0.62	-0.328
34967	0.092	54.30	0.48	-0.372
17312	0.120	53.10		0.093
8657	0.153	51.72		0.109
1560	0.238	48.17		0.114
175	0.365	42.87		0.133
37	0.446	39.47		0.121
2	0.510	36.79		0.057

Sample Ref.	Voids Ratio	Voids Ratio (Sat)	M/C Init (%)	M/C Final (%)	Bulk Density (Nat) (gm/cm^3)	Dry Density (Dry) (gm/cm^3)	Swell Pressure (kn/m^2)	Swell Per Cent (%)	Deg Sat (Nat)	Deg Sat (Sat)
British Materials										
LC37	0.592	0.688	19.89	24.58	2.048	1.708	220.66	6.00	0.91	0.97
LC14	0.718	0.873	24.96	30.76	2.014	1.612	362.86	9.00	0.96	0.98
GC	0.682	0.722	24.48	27.05	2.005	1.611	288.33	2.36	0.97	1.02
FE23	1.311	1.312	45.86	46.32	1.768	1.212	34.32	0.05	0.98	0.99
WC	0.178	0.189	5.37	7.11	2.407	2.284	289.31	1.00	0.81	1.01
KC	0.540	0.608	19.27	22.77	2.076	1.740	98.07	4.42	0.96	1.00
OC10	0.775	0.811	30.93	33.79	1.837	1.403	118.66	2.03	0.99	1.04
OC44	0.439	0.552	16.67	22.85	2.051	1.758	424.64	7.82	0.96	1.05
FE19	0.932	0.991	32.83	36.64	1.856	1.397	176.53	3.02	0.95	1.00
L10	0.544	0.624	18.88	22.88	2.056	1.730	186.33	5.20	0.93	0.98
L36	0.461	0.571	15.12	21.00	2.088	1.814	741.41	7.56	0.87	0.97
SWR	0.112	0.120	3.07	4.08	2.549	2.474	481.52	0.74	0.76	0.94
FTR	0.114	0.125	2.52	3.70	2.530	2.468	468.77	0.93	0.61	0.82
FTS	0.246	0.262	6.81	8.81	2.280	2.134	118.66	1.29	0.74	0.89
WR	0.161	0.176	4.50	6.30	2.250	2.154	594.30	1.27	0.70	0.90
North American Materials										
YC	1.270	1.332	46.44	52.83	1.761	1.203	84.93	2.73	1.00	1.08
K6	0.627	0.675	19.92	24.05	1.998	1.666	117.68	2.95	0.86	0.97
K8	0.585	0.587	18.59	20.96	1.991	1.679	9.81	0.17	0.85	0.95
N1	0.207	0.256	6.55	9.81	2.375	2.229	1422.01	4.02	0.85	1.03
N2	0.237	0.270	6.11	9.66	2.290	2.158	1075.44	2.68	0.69	0.95
FOX	0.852	1.099	28.18	43.16	1.778	1.387	672.76	13.31	0.85	1.01
DS	0.379	0.445	13.58	18.50	2.158	1.900	1188.61	4.75	0.94	1.09
PSD	0.774	0.865	29.80	32.84	1.932	1.488	211.83	5.14	1.02	1.00
PSC	0.245	0.259	8.68	10.88	2.331	2.145	188.29	1.13	0.95	1.12

Appendix A.4

Soil Suction

A.4.1 The Suction Plate

A.4.1.1 Apparatus

This apparatus, consisting of a filter unit and a mercury manometer (Fig.A.4.1), enables a constant suction (ranging from a few centimeters of water to one atmosphere) to be applied to a soil specimen via a porous plate.

The filter unit is composed of demountable glassware which consists of a sintered-glass porous disc fused into the narrow end of a B40 cone. This in turn is fused, at its other end, to a B24 cone; the narrow end of which being attached to a glass tube of 5mm internal diameter. The sintered-glass porous plate, which must be in good contact with the specimen, is chosen so that the pore size in the external surface will not allow air to pass until a suction of one atmosphere (pF3) has been applied. To satisfy this condition, a maximum external pore size of 1.5 microns is required. However, in practice a No.5 plate (porosity of 2 microns) with an external reinforcement of No.3 porosity (30 microns) is used. The external reinforcement is required because it has been found that a No.5 plate alone allows air to pass through at suctions of between 50 - 75 centimeters of mercury (Croney, Coleman and Bridge, 1952). The filter unit is inserted by means of an air tight groud glass seal into a standard filter flask, which also contains sufficient air-free water to allow immersion of the glass tube at the end of the filter unit.

A negative pressure, measured by a mercury manometer, is applied to the sintered glass porous disc by evacuating the air space in the filter flasks. To minimise pressure fluctuations in the apparatus caused by changes in atmospheric pressure, a glass cap is fitted over the B40 cone by means of a groud glass seal. This in turn is connected

to the open end of the mercury manometer by a rubber tube.

The suction in terms of pF is determined from the following equation (Coleman, 1959):-

$$pF = \log_{10}(h + 13.54H)$$

where h is the height of the suction plate above the level of the water in the flask and H is the negative pressure (in cms) recorded by the manometer. A maximum suction of pF3 can be attained and the smallest suction which can be applied is when:-

$$pF = \log_{10}h$$

A.4.1.2 Test Procedure

Before the apparatus was assembled (Fig.A.4.2) the suction plates were cleaned with acetone and boiled in distilled water for 5 minutes to ensure complete saturation. Each piece of demountable glassware was then completely filled with de-aired water and inserted into the filter flask, which was also filled with de-aired water to a level above the end of the glass tubing. An air tight seal between the glassware was ensured by smearing the ground glassglass contacts with silicone grease.

A suction of between one centimeter and one atmosphere was then applied to the system by means of pipe (a) - see Figure A.4.1, and after equilibrium suction had been attained (usually within a few seconds), the samples were placed on the suction plates. The open ends of the manometer were then closed by placing the glass caps over the B40 cones.

The system was then left for up to 24 hours to allow the sample to attain equilibrium with the suction plate. The time taken for this depended upon the nature of the material, the height of the sample and the closeness of the contact with the suction plate. Croney, Coleman and Bridge (1952) found that only one day was required for samples one centimeter in height to reach equilibrium for any material, provided

there is good contact. However, in the present study a maximum thickness of 3mm was used, thus ensuring that 24 hours was adequate to reach equilibrium.

A position of constant temperature was required for the duration of the test because changes in temperature affect the pressure of the air and hence the suction at the surface of the plate.

Ideally, one specimen should have been used for each series of tests on a particular material, thus illuminating mineralogical and textural variations. However, this was rarely possible because certain samples (particularly those containing montmorillonite or large quantities of mixed-layer clay) tended to disintegrate either upon removal from the suction plate or upon saturation before the test commenced.

A.4.2 Pressure Membrane

A.4.2.1 Apparatus

In the pressure membrane apparatus (Fig.A.4.2), the sample is placed in contact with a cellulose semi-permeable membrane which in turn is in contact with free water at atmospheric pressure via a sintered bronze disc. Compressed air within the chamber provides a differential pressure between moisture in the sample and that in the membrane.

The pressure vessel consists of a closed cylinder which is split into two poritions. The lower unit contains the sintered bronze disc which is connected by outflow pipes to distilled water supplies, maintained at atmospheric pressure. The upper unit comprises the pressure chamber and consequently contains an inlet/outlet air value and a pressure guage. A rubber 'O' ring, coated with silicone grease is contained in a groove at the base of the upper unit and when the apparatus is assembled the ring sits on the outer edge of the semi-permeable membrane, which covers and overlaps the brass disc.

The two portions of the pressure vessel are held together by means of a steel yoke attached to a heavy base plate.

This apparatus was originally regarded as being usable over a pressure range of 0 - 100 atmospheres (pF0 - 5), but has been extended by the Road Research Laboratory to cover suctions of pF6.2.

The value of suction produced is determined from the equation:-

$$pF = 1,8477 + \log_{10} P$$

where P is the applied pressure in lb/sq.in. and 1,8477 is the conversion factor relating lb/in^2 to centimeters of water (Coleman, 1959).

A.4.2.2 Test Procedure

Initially the porous disc was saturated by boiling in distilled water. The semi-permeable membrane, which consisted of a cellulose sheet 0.004 inches thick in the dry condition, was then cut into a circular shape to fit the space provided. Upon its subsequent saturation the membrane expanded to a thickness of about 0.007 inches but also expanded anistropically in the direction of the sheet, hence retrimming was necessary.

The apparatus was then assembled (according to Figure A.4.2), without the sample being present, and pressurised to the required pressure for several minutes; the water reservoirs being disconnected.

Pressurisation of the cell was accomplished by firstly releasing the tap on the air cylinder and then carefully opening the value on the pressure vessel until the required pressure was reached, after which it was closed. This pre-test procedure removed excess water from the membrane thus preventing the ultimate moisture content from becoming too high in the wetting condition and also reduced the time required for the sample to reach equlibrium in the drying condition.

The apparatus was then dismantled, the sample placed on the membrane and then reassembled, this time with water reservoirs connected and bled until any entrapped air removed.

The experiment was left for about 12 - 24 hours to allow the sample to reach equilibrium moisture content with the membrane. Upon dismantling firstly the water reservoirs were disconnected and then the pressure was released as quickly as possible in a controlled manner by loosening the nut at the base of the pressure dial. The sample was removed as quickly as possible to prevent rewetting.

A.4.3 Sample Preparation

(a) For the Sorption Curve

The material was initially air-dried and cut into pieces approximately 10mm by 10mm by 3mm, which were sandpapered flat on one side. The specimens were then heated in an oven at 105°C for several hours, after which time they were ready for use in either of the pieces. of apparatus previously discussed.

(b) For the Desorption Curve

This preparation required complete saturation of the material with de-aired water. Initially, air-dried material was cut into tablets 10mm by 10mm by 3mm which were sandpapered flat on one side. These were placed in the apparatus shown in Figure A.4.3, which was evacuated for several hours via a pump attached to pipe (B). After de-airing (which was indicated by the absence of bubbles in the water) the specimens were saturated (still in the evacuated condition) by opening tap (A). Finally air was re-admitted via tap (B), after which the specimens were removed and quickly placed in the waiting apparatus.

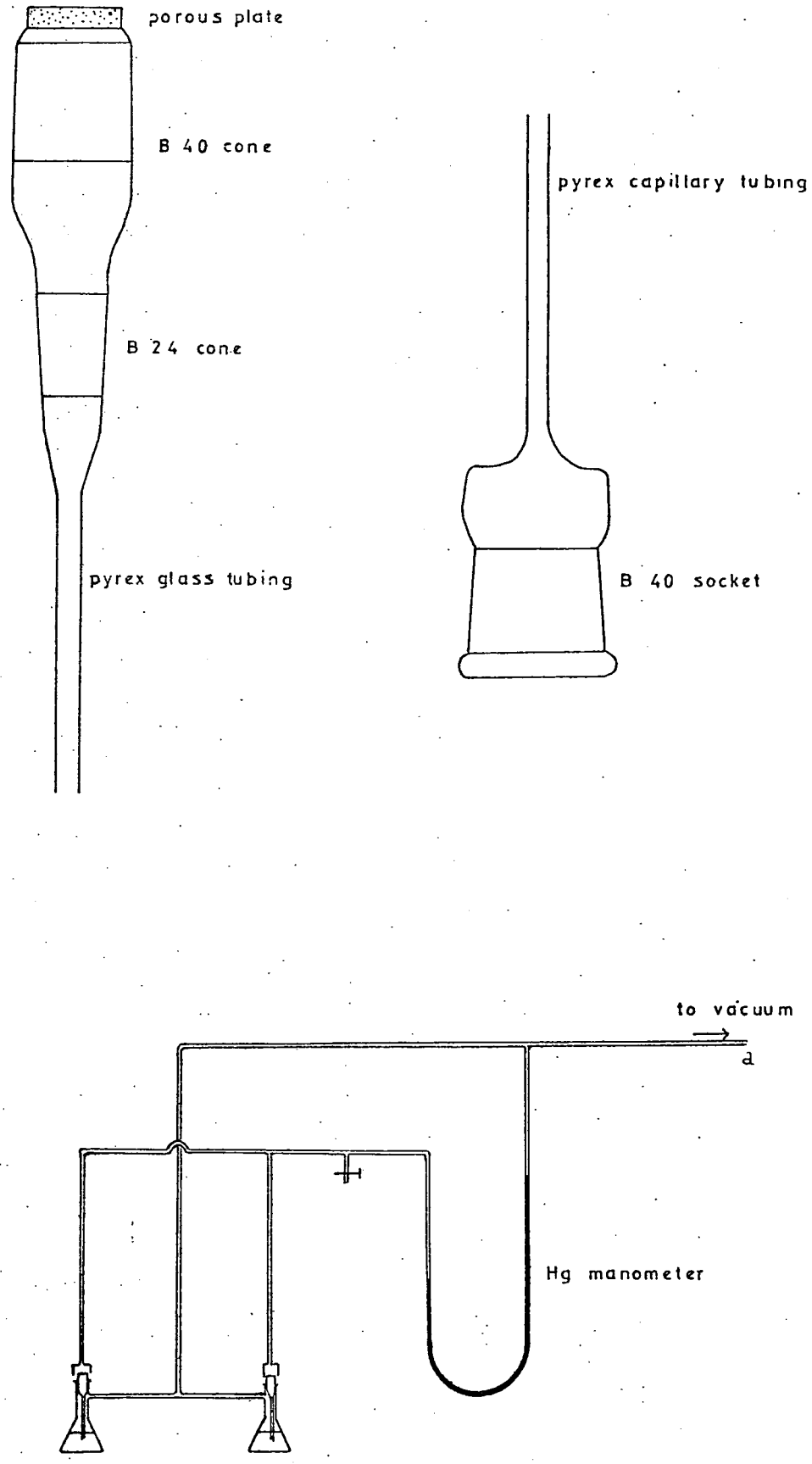

Figure A 4.1. Suction Plate Apparatus.

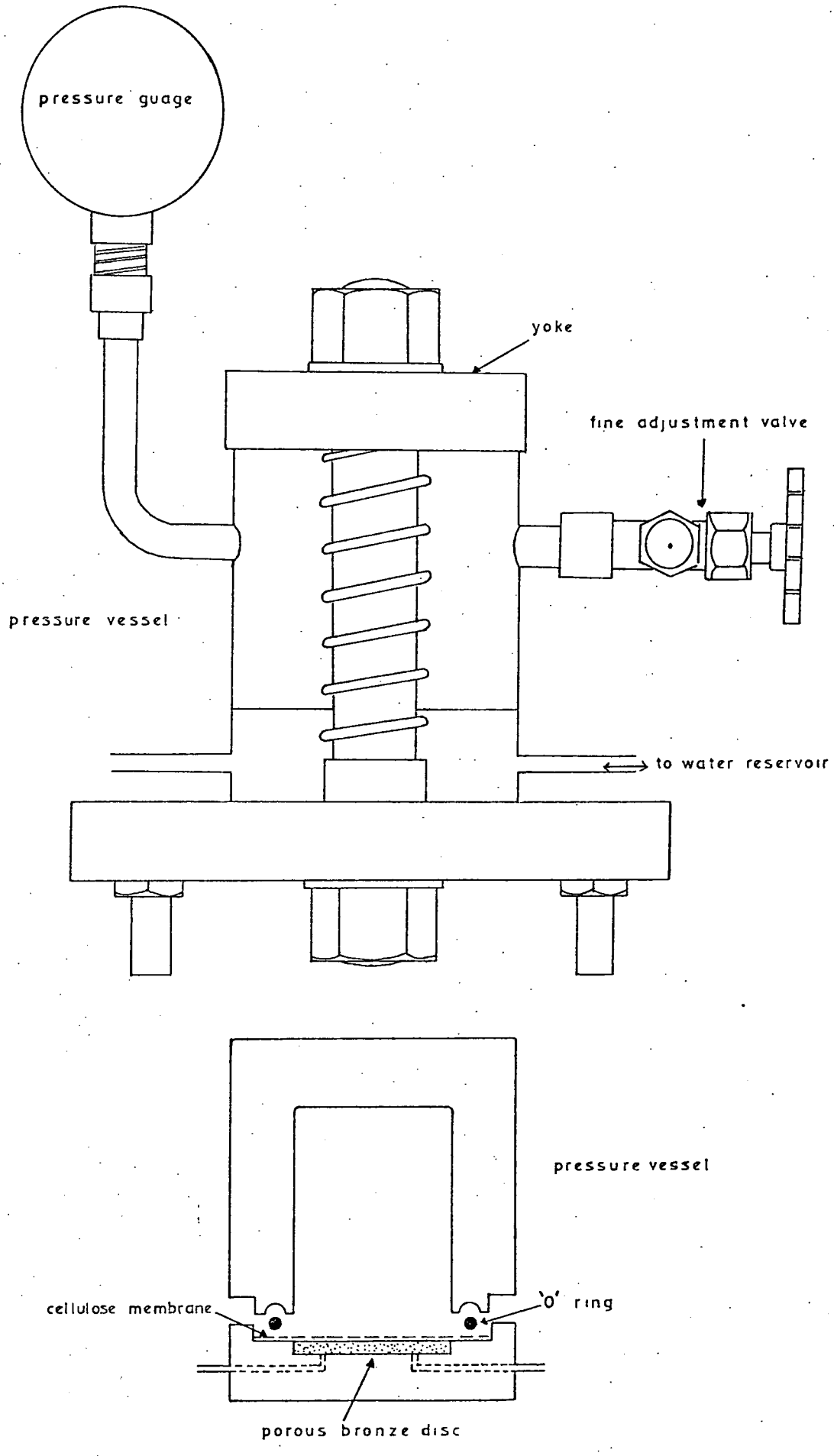

Figure A 4.2. Pressure Membrane Apparatus.

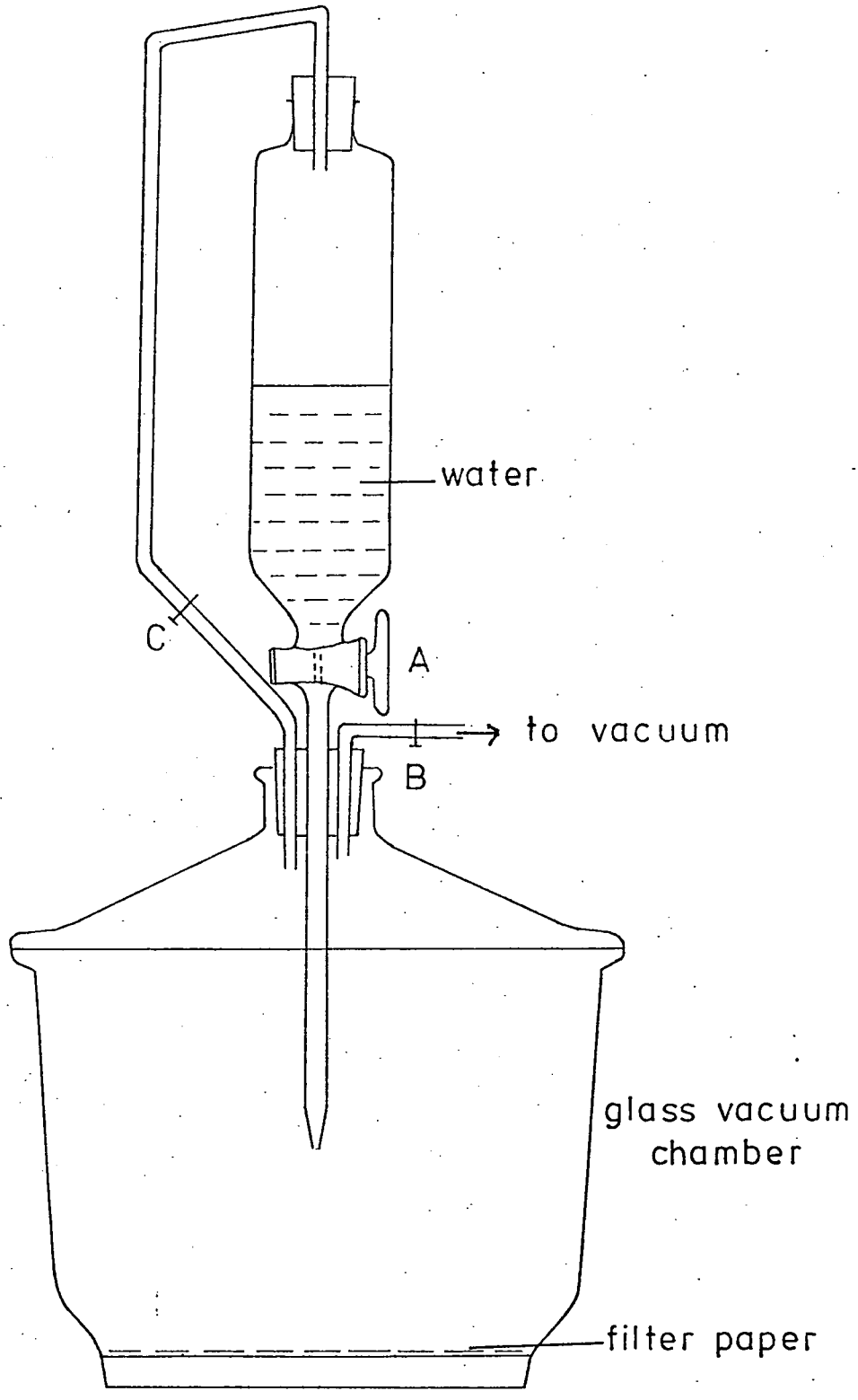

Figure A 4.3. Apparatus used for Saturating Suction Test Material.

Appendix A.5
Slaking Tests

A.5.1 Measurement of the Rate of Disintegration

A simple piece of apparatus (Hogentogler, 1937) was constructed using an obsolete beam balance (see Fig.A.5.1).

Initially the gauze cage (B.S.No.36) was suspended in distilled water and counterbalanced by the addition of weights to the pan. The cage was then removed from the water and a sample measuring 1cm in diameter by 1cm in height was placed in it. Re-immersion was accompanied by starting a laboratory clock and rapid rebalancing. After certain lengths of time (usually 1 min., 5 mins., 10 mins., 20 mins., 30 mins., 1 hr., etc.) the cage was gently agitated three times in a vertical direction to flush away material trapped by the wire mesh, and then the system was rebalanced. After a maximum period of about three days, material still remaining in the cage was balanced for a final time.

The amount of slaking at the given times of measurement was expressed as a percentage, by comparing the apparent weight at that time against the initial apparent weight of the material.

A.5.2 Measurement of the Uptake of Water during the Static Slaking Test

The apparatus used is presented in Figure A.5.2. Initially 30 - 50 grams of air-dried sample were placed inside the filter paper and subsequently saturated by allowing water to flow slowly into the funnel, in between the filter paper and glass. After immersion for 2 - 3 days, excess water was drained from the funnel, the retained moisture content being determined on a dry weight basis after oven drying at 105°C.

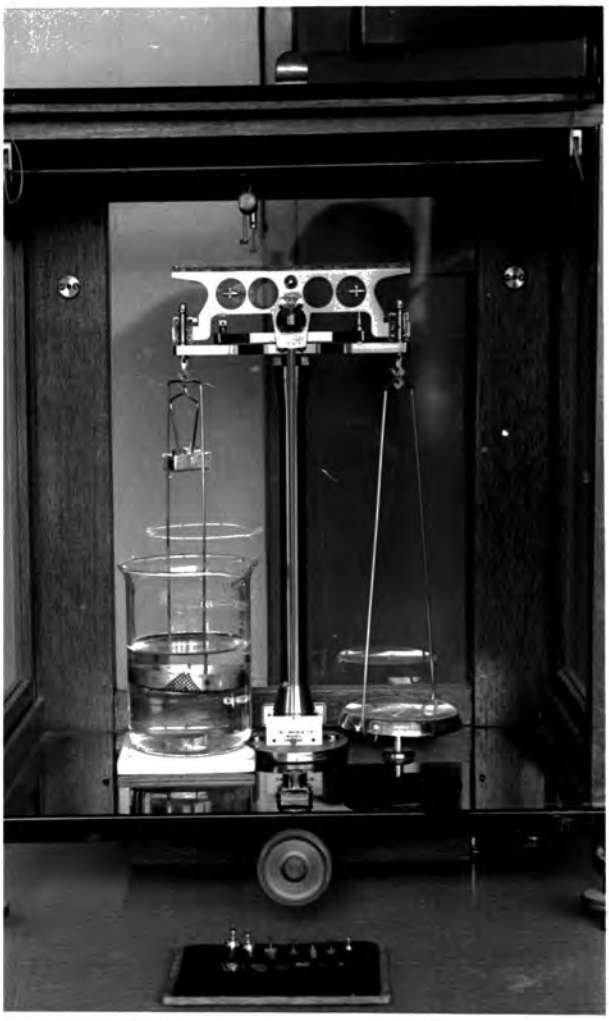

Figure A.5.1. Apparatus used to Determine Rate of Disintegration.

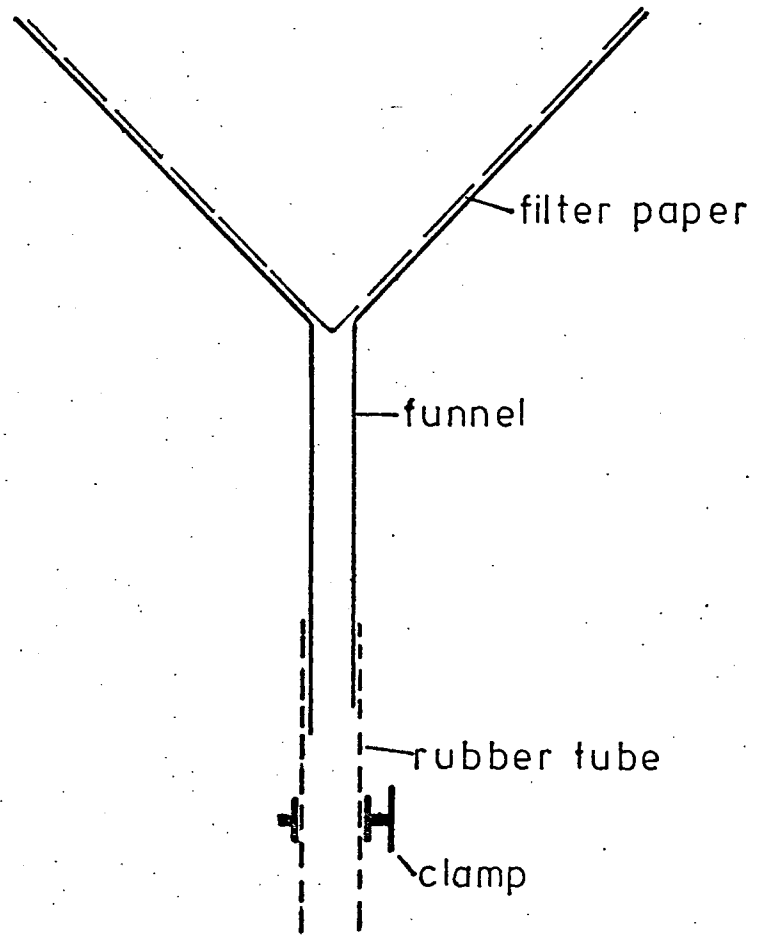

Figure A 5.2. Apparatus used for Static Slaking Test.